Geologic Studies in the Basin and Range–Colorado Plateau Transition in Southeastern Nevada, Southwestern Utah, and Northwestern Arizona, 1995

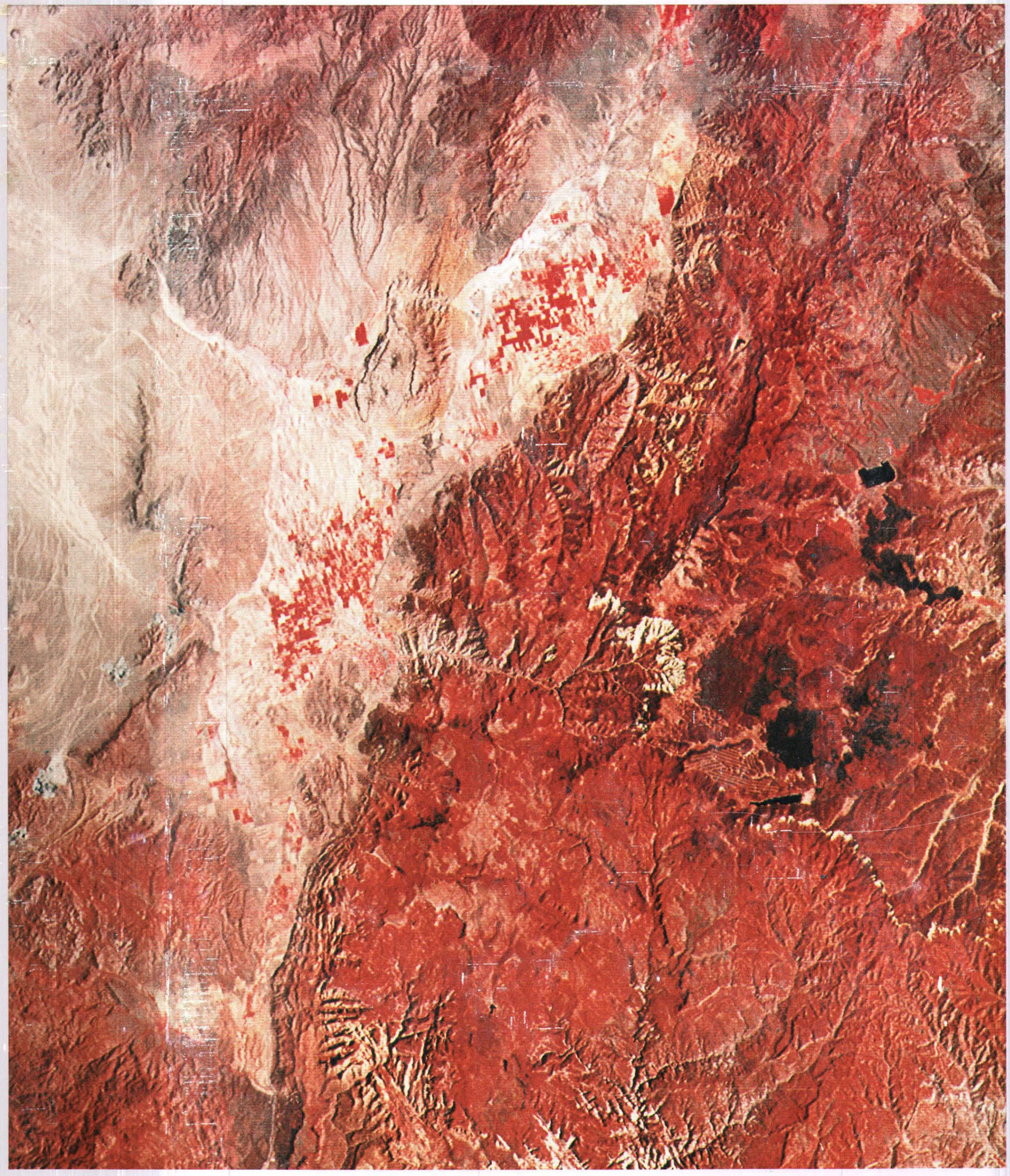

U.S. GEOLOGICAL SURVEY BULLETIN 2153

Cover. Infrared image of the eastern part of the BARCO area. The area extends from about lat. 38°10′ N., long 113°15′ W. in the northwest corner to about lat 37°15′ N., long 112°30′ W. in the southeast corner. The Parowan Valley (located near top of image) and Cedar City area (located south of Parowan Valley) show vegetated areas in red. The Hurricane Cliffs form a linear north-south pattern in the west half of the image along the western part of the Markagunt Plateau east of Cedar City, Utah. Black circular areas on the Markagunt Plateau are basaltic flows and cones. Light semicircle just west of flows is Cedar Breaks National Monument.

Geologic Studies in the Basin and Range–Colorado Plateau Transition in Southeastern Nevada, Southwestern Utah, and Northwestern Arizona, 1995

By Florian Maldonado *and* L. David Nealey, *Editors*

U.S. GEOLOGICAL SURVEY BULLETIN 2153

Chapter titles are listed on volume contents page

UNITED STATES GOVERNMENT PRINTING OFFICE, WASHINGTON : 1997

U.S. DEPARTMENT OF THE INTERIOR
BRUCE BABBITT, Secretary

U.S. GEOLOGICAL SURVEY
Gordon P. Eaton, Director

For sale by U.S. Geological Survey, Information Services
Box 25286, Federal Center
Denver, CO 80225

Library of Congress Cataloging-in-Publication Data

Geologic studies in the basin and range–Colorado Plateau transition in southeastern Nevada, southwestern Utah, and northwestern Arizona, 1995 / by Florian Maldonado and L. David Nealey, editors.
p. cm.—(U.S. Geological Survey bulletin ; 2153)
Includes bibliographical references (p. –).
Supt. of Docs. no. : I 19.3:B2153
1. Geology—Utah. 2. Geology—Nevada. 3. Geology—Arizona.
I. Maldonado, Florian. II. Nealey, L. David. III. Series.
QE75.B9 no. 2153
[QE169]
557.3 s—dc20
[557.92]

95–49016
CIP

CONTENTS

[Letters designate chapters]

Introduction

By Florian Maldonado *and* L. David Nealey

The U.S. Geological Survey's Basin and Range to Colorado Plateau Transition (BARCO) Study Unit was created to study the tectonic and magmatic evolution of the eastern part of the Basin and Range province and the western margin of the Colorado Plateaus province. The area includes the transition between the two provinces that will be referred to as the transition zone (fig. 1). The Study Unit began in 1988 and has been supported since 1992 by the National Geologic Mapping Program, as established by the National Geologic Mapping Act of 1992. One objective of the study is to compile existing geologic mapping of the BARCO area at a scale of 1:100,000. A group of eight 1:100,000 quadrangles, extending from the western margin of the Colorado Plateau to the eastern side of the Basin and Range province, contains the BARCO study area (fig. 2). A parallel objective of the study is to map previously unmapped areas, particularly near populated areas. This component of the BARCO study addresses a variety of societal and environmental issues, including earthquake, landslide, and volcanic hazards, and evaluates natural resource and hydrologic parameters related to the structural and stratigraphic framework of southeastern Nevada, southwestern Utah, and northwestern Arizona. Mapping in the BARCO area is being published as U.S. Geological Survey Open-File Reports, Geologic Quadrangle Maps (GQ maps), Miscellaneous Investigations Series Maps (I maps), and Miscellaneous Field Studies Maps (MF maps). Additionally, mapping is being published cooperatively by the Utah Geological Survey. Some mapping conducted at 1:100,000 scale is being compiled as quadrangle maps (30×60 minute maps). Other mapping is being conducted at scales of 1:12,000 to 1:24,000, in order to portray essential geologic and structural details needed to understand geologic problems. The status of mapping in the BARCO Study Unit at the end of 1993 is shown in figure 3.

The general geologic and geophysical framework of the BARCO study area was described by Scott and Swadley (1995) and Blank and Kucks (1989). Other summaries of the geology of the region are given in Eaton (1979; 1982), Anderson (1989), Hamilton (1989), Pakiser (1989), and Smith and others (1989). The general geology of the study area is therefore only briefly reviewed here.

The BARCO study area includes (1) that portion of the Basin and Range province in extreme southeastern Nevada and southwestern Utah; (2) the western margin of the Colorado Plateaus province in southwestern Utah; and (3) the transition zone between these two physiographic provinces (figs. 1 and 2) in southwestern Utah and northwestern Arizona. The Basin and Range province is characterized mainly by north- to northeast-trending mountain ranges separated by wide alluvial basins. This structural fabric resulted from intense east-west-directed extensional deformation in the Cenozoic. Significant magmatism in the Basin and Range resulted from the emplacement of crustal magma chambers associated with the "ignimbrite flareup" throughout the Cordilleran belt. In contrast, the Colorado Plateaus province has remained relatively stable structurally. Magmatism was mostly limited to the emplacement of relatively small cinder cones, domes, laccoliths, and lava flows along the margin of the Colorado Plateau. The transition between these two provinces contains features common to both, which represent various stages in the structural evolution. In the BARCO study area (fig. 1), the transition zone is bounded on the west by the Grand Wash-Gunlock fault zone in the Littlefield and St. George 1:100,000-scale quadrangles, and by the Hurricane fault in the Panguitch quadrangle (fig. 2). The eastern margin of the transition zone, for our purposes, is expressed by the Hurricane fault in the Littlefield quadrangle, by the Toroweap-Sevier fault in the Kanab quadrangle, and by the Paunsaugunt fault in the eastern part of the Panguitch quadrangle (fig. 2).

This is the second in a series of assembled reports describing the geology of the BARCO area. The first volume (U.S. Geological Survey Bulletin 2056, edited by Scott and Swadley, 1995) contains reports that describe mainly the geology of the western part of the BARCO study area. This volume contains reports that describe the geology in both the western and eastern parts of the area. The volume is composed of two parts.

The first part emphasizes the transition zone in southwestern Utah and northwestern Arizona. The papers describe several stratigraphic units (youngest to oldest) in the area

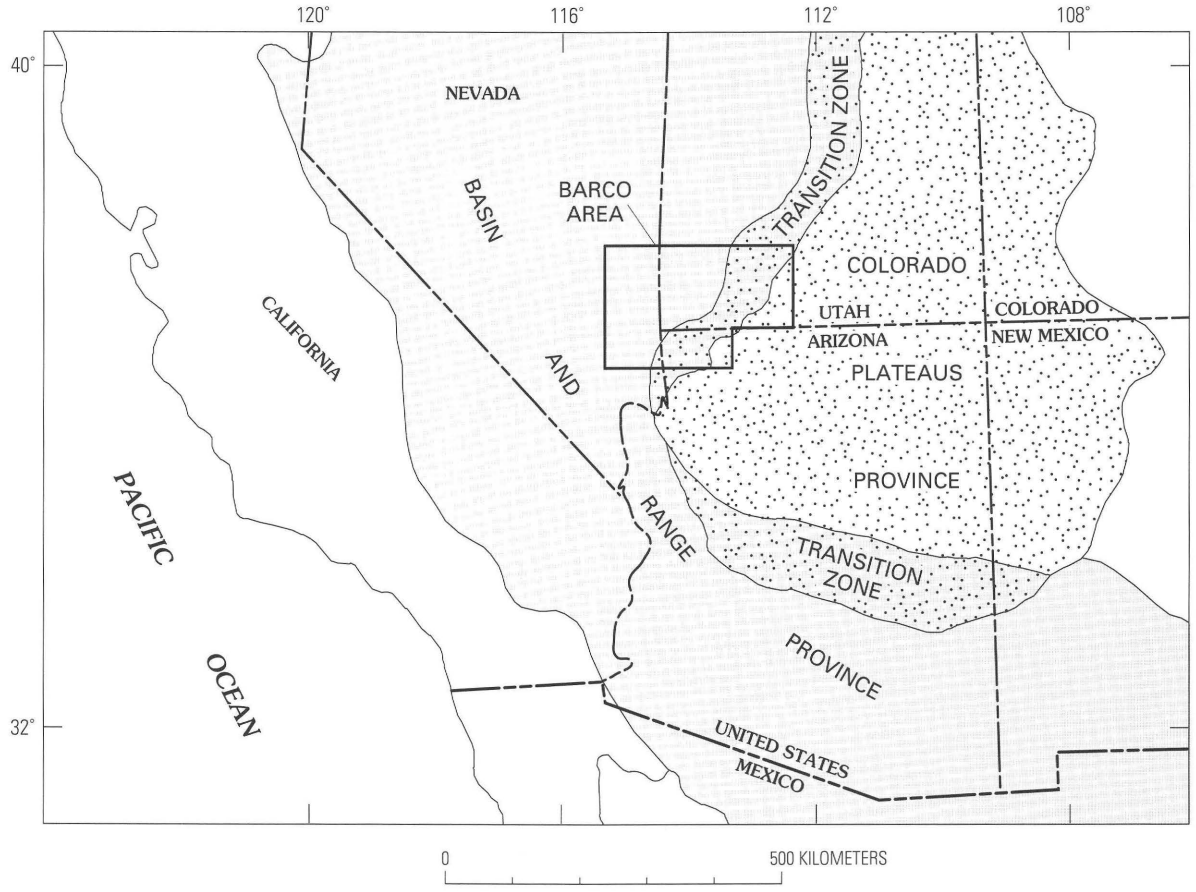

Figure 1. Regional map showing the BARCO Study Unit area, boundaries of the Basin and Range and Colorado Plateaus provinces, and transition zone between the provinces.

and then discuss the tectonic and basaltic magmatic evolution of the area. In chapter A, Sable and Maldonado reinstate the Tertiary Brian Head Formation as a formal unit after its abandonment in 1975. Locally, an informal Tertiary unit, the "variegated unit," underlies the Brian Head Formation. Feist and others (chapter B) discuss the environment of deposition and age of parts of this unit based on the presence of charophytes in the unit for the Sevier Plateau area. The Brian Head Formation and the variegated unit are underlain by the Tertiary Claron Formation. Bown and others (chapter C) describe hymenoptera and other insect trace fossils recovered from paleosols of the Claron Formation and discuss its paleoenvironments. The Claron Formation is underlain by the Paleocene Grand Castle Formation, a unit formalized by Goldstrand and Mullett (chapter D). The Tertiary units are underlain by a series of Cretaceous units; in chapter E, Nichols discusses the significance of palynomorphic data obtained from the Cretaceous Dakota Formation, Tropic Shale, and Straight Cliffs and Kaiparowits Formations, from the Markagunt Plateau and the area just east of the BARCO area in the northwestern part of the Kaiparowits Plateau. In chapter F, Billingsley describes the Permian clastic sedimentary sequence in northwestern Arizona.

The structure of the transition zone is more complex than previously thought. Maldonado and others (chapter G) discuss the complex evolution of Cenozoic low-angle normal and thrust faults and a system of anastomosing high-angle faults along the western front of the Markagunt Plateau. In chapter H, Sable and Maldonado outline the structural significance of breccias and megabreccia deposits that are widespread throughout the Markagunt Plateau. The evolution of basaltic magmas within the transition zone is also quite complex. Nealey and others (chapter I) present elemental and isotopic data for Quaternary basaltic rocks from the western margin of the Markagunt Plateau and Red Hills area and relate the volcanism to the tectonic evolution of the transition zone. Mattox (chapter J) examines the origin of Cenozoic basaltic rocks in the adjacent parts of the transition zone and high plateaus. Nusbaum and others (chapter K) evaluate the importance of mantle sources in the origin of basaltic rocks of the St. George area southeast of the Markagunt Plateau.

The second part of this volume contains reports on the Basin and Range province. Topics include igneous rocks in southwestern Utah and tectonic evolution of structures in southeastern Nevada. McKee and others (chapter L) discuss

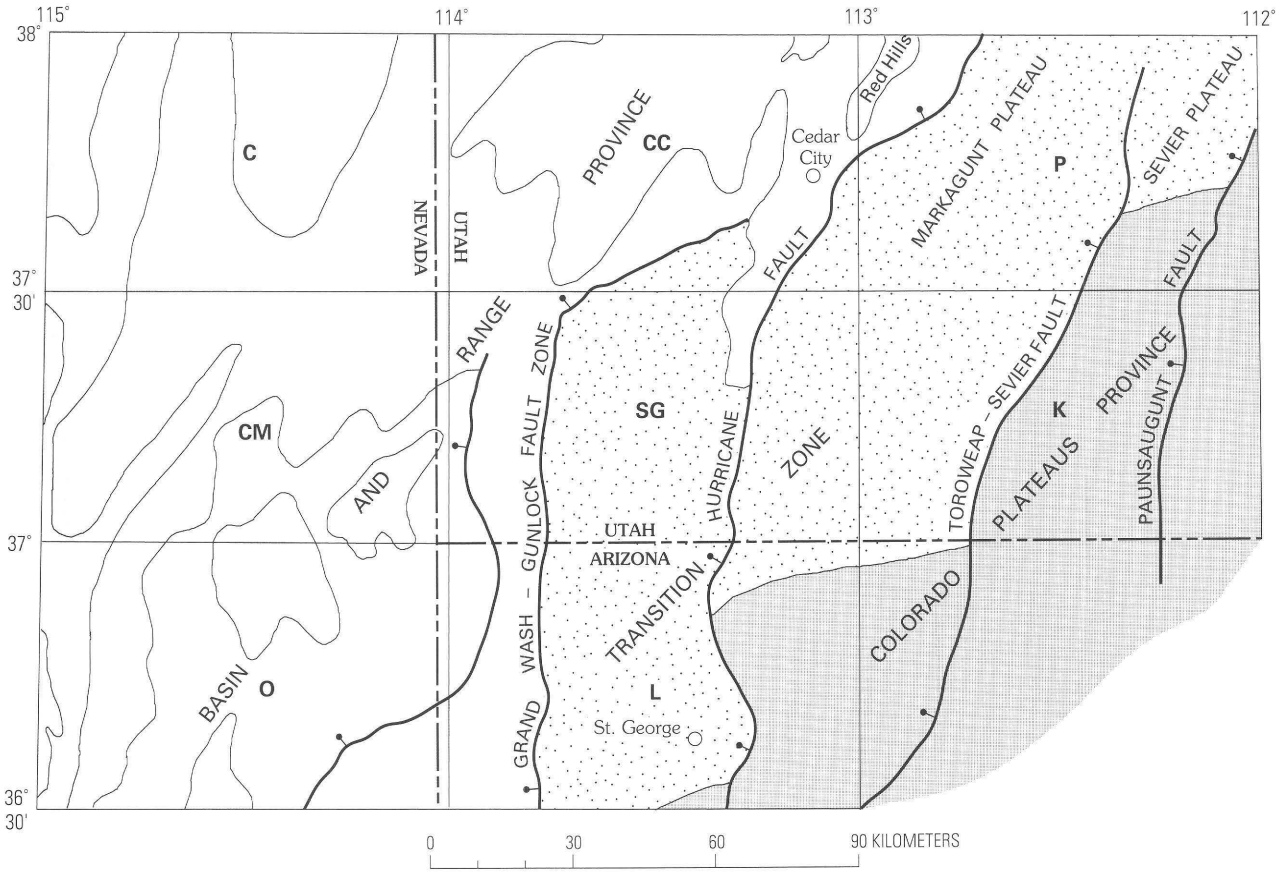

Figure 2. Map of BARCO Study Unit area showing locations of the eight 30×60 minute quadrangles (1:100,000); C, Caliente; CM, Clover Mountains; O, Overton; CC, Cedar City; SG, St. George; L, Littlefield; P, Panguitch; K, Kanab. Basin and Range province shown by lightly shaded ranges and unshaded basins; transition zone shown by a stipple pattern; Colorado Plateaus province shown by a medium shade. Heavy line, fault; bar and ball on downthrown side.

the relation between Tertiary intrusive and extrusive igneous rocks from the Bull Valley and Pine Valley Mountains located west of the Markagunt Plateau. They present K-Ar ages obtained from these rocks and discuss their significance. Byron (chapter M) identifies contractional features along the Pahranagat shear system in southeastern Nevada (Clover Mountain quadrangle) that are interpreted to be coeval with regional extension. Burke and Axen, in chapter N, discuss the tectonic history of several episodes of Tertiary extensional faulting in the Chief Range area, eastern Nevada (Caliente quadrangle), and describe the evolution of their geometry.

The affiliations of several authors of reports in this volume clearly indicate that BARCO is not solely a USGS project. In fact, the Survey's study group has encouraged all interested researchers to become active participants in the project since its inception. As a result, numerous current and former geology students and university faculty members and volunteers have provided field and laboratory support to the Survey's small staff of geologists working on this project. We thank all these individuals for their support and interest in furthering an understanding of the evolution of the Basin and Range–Colorado Plateau transition zone.

REFERENCES CITED

Anderson, R.E., 1989, Tectonic evolution of the Intermontane System; Basin and Range, Colorado Plateau, and High Lava Plains, *in* Pakiser, L.C., and Mooney, W.D., eds., Geophysical framework of the Continental United States: Geological Society of America Memoir 172, p. 163–176.

Blank, H.R., Jr., and Kucks, R.P., 1989, Preliminary aeromagnetic, gravity, and generalized geologic maps of the USGS Basin and Range–Colorado Plateau transition zone study area in southwestern Utah, southeastern Nevada, and northwestern Arizona: U.S. Geological Survey Open-File Report 89-432, 16 p., map scale 1:250,000.

Eaton, G.P., 1979, Regional geophysics, Cenozoic tectonics, and geologic resources of the Basin and Range province and adjoining regions, *in* Newman, G.W., and Goode, H.D., eds., Basin and Range Symposium and Great Basin Field Conference: Rocky Mountain Association of Geologists, Denver, Colo., and Utah Geological Association, Salt Lake City, p. 11–39.

———1982, Basin and Range province—Origin and tectonic significance: Annual Review of Earth and Planetary Sciences, v. 10, p. 409–440.

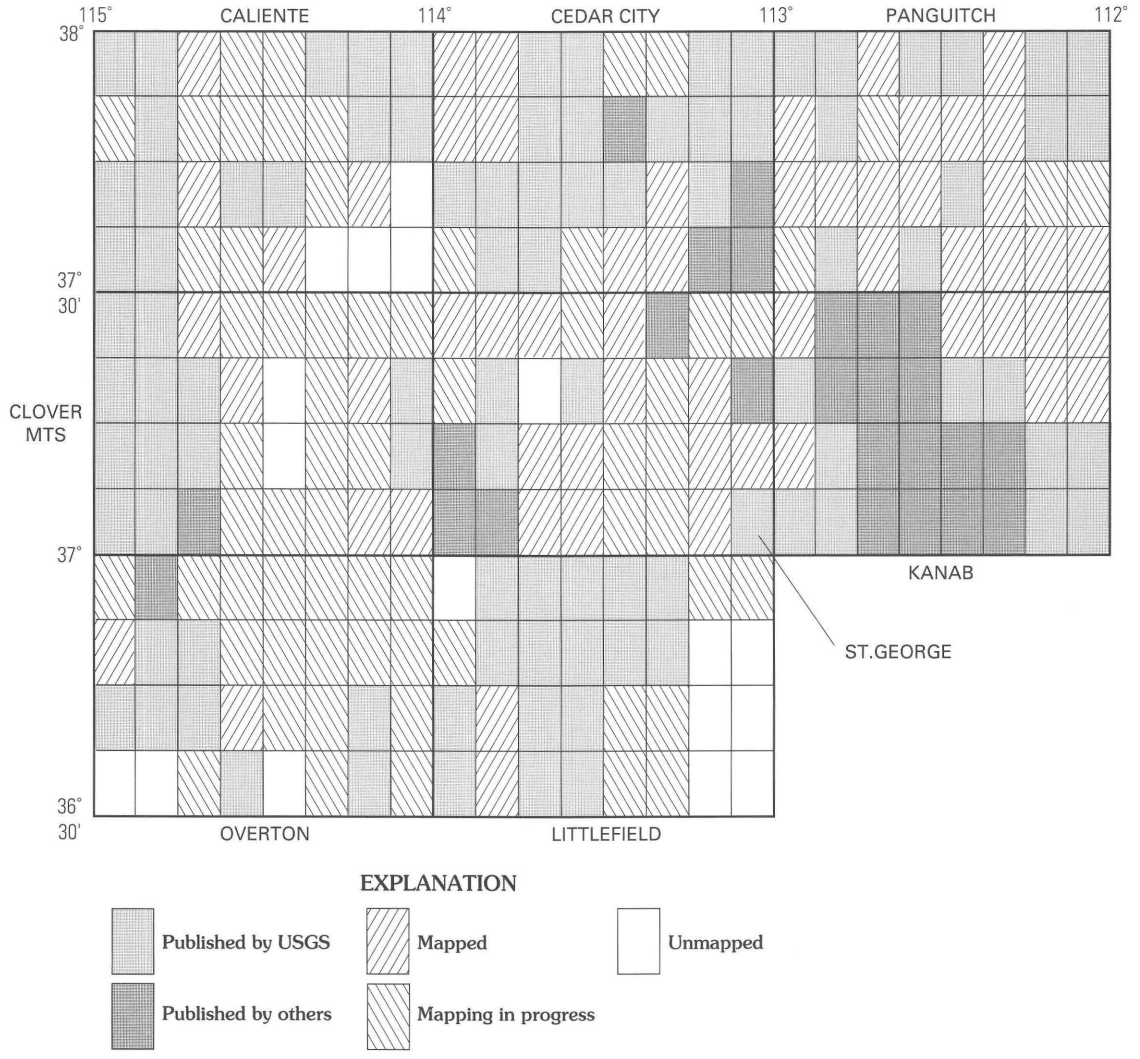

Figure 3. Status of 7.5-minute (1:24,000) quadrangle geologic mapping in the BARCO Study Unit at the end of 1993. The eight 30×60 minute quadrangles of the Study Unit are named on the margin.

Hamilton, W.B., 1989, Crustal geologic processes of the United States, *in* Pakiser, L.C., and Mooney, W.D., eds., Geophysical framework of the Continental United States: Geological Society of America Memoir 172, p. 743–781.

Pakiser, L.C., 1989, Geophysics of the intermontane system, *in* Pakiser, L.C., and Mooney, W.D., eds., Geophysical framework of the Continental United States: Geological Society of America Memoir 172, p. 235–247.

Scott, R.B., and Swadley, W C, 1995, Introduction, *in* Scott, R.B., and Swadley, W C, eds., Geologic studies in the Basin and Range–Colorado Plateau transition in southeastern Nevada, southwestern Utah, and northwestern Arizona, 1992: U.S. Geological Survey Bulletin 2056, p. 1–4.

Smith, R.B., Nagy, W.C., (Smith) Julander, K.A., Viveiros, J.J., Barker, C.A., and Gants, D.G., 1989, Geophysical and tectonic framework of the eastern Basin and Range–Colorado Plateau–Rocky Mountain transition, *in* Pakiser, L.C., and Mooney, W.D., eds., Geophysical framework of the Continental United States: Geological Society of America Memoir 172, p. 205–233.

The Brian Head Formation (Revised) and Selected Tertiary Sedimentary Rock Units, Markagunt Plateau and Adjacent Areas, Southwestern Utah

By Edward G. Sable *and* Florian Maldonado

GEOLOGIC STUDIES IN THE BASIN AND RANGE–COLORADO PLATEAU TRANSITION IN SOUTHEASTERN NEVADA, SOUTHWESTERN UTAH, AND NORTHWESTERN ARIZONA, 1995

U.S. GEOLOGICAL SURVEY BULLETIN 2153–A

UNITED STATES GOVERNMENT PRINTING OFFICE, WASHINGTON : 1997

CONTENTS

FIGURES

The Brian Head Formation (Revised) and Selected Tertiary Sedimentary Rock Units, Markagunt Plateau and Adjacent Areas, Southwestern Utah

By Edward G. Sable *and* Florian Maldonado

ABSTRACT

The name Brian Head Formation is herein revised after its reinstatement in 1993; the original formational boundaries are redefined, and its significance as the earliest widespread Tertiary volcaniclastic unit in the region is emphasized. The name applies to a distinctive succession of fluvial and lacustrine sedimentary rocks, mostly tuffaceous sandstone, claystone, clay, and conglomerate, lesser nontuffaceous clastic rocks, and locally volcanic rocks. The unit is as much as 220 meters thick on the Markagunt Plateau, southwestern Utah, and is present in adjoining areas such as the Red Hills and the Sevier Plateau. The formation comprises three informal units (ascending): (1) sandstone and conglomerate unit, consisting of nontuffaceous varicolored lithic arenite, rudite, claystone, and limestone; (2) gray volcaniclastic unit, characterized by tuffaceous sandstone and clay, and lesser amounts of limestone and chalcedony, and (3) volcanic unit, locally present, that includes volcanic mudflow breccia, volcanic autoclastic breccia, mafic lava flows, immature sandstone and conglomerate, and ash-flow and ash-fall(?) tuffs. The age of the Brian Head is probably late Eocene to middle Oligocene. It overlies, with apparent paraconformity, both the white and the red members of the Claron Formation (Paleocene and Eocene). A regional low-angle unconformity also may underlie the gray volcaniclastic unit. Autochthonous units that directly overlie the Brian Head are ash-flow tuffs of the Needles Range Group, the Isom Formation, alluvial facies of the Mount Dutton Formation, and the 20 Ma tuffaceous and the sedimentary strata of Limerock Canyon unit of Kurlich (1990). Allochthonous rocks overlying the Brian Head have been incorporated in megabreccia units of Miocene age that were decoupled by gravity-sliding or low-angle faulting.

Recent mapping has further delimited the distribution and stratigraphic position of other Tertiary sedimentary rock units of the region, especially those that contain strata similar to those of the Brian Head Formation. The Claron Formation is bracketed by the Brian Head Formation, as revised here, and the underlying Grand Castle Formation. Several tuffaceous sedimentary rock units lithologically similar to but younger than the Brian Head Formation include the Bear Valley Formation (upper Oligocene), the mudflow and lava-flow breccia and tuffaceous sandstone unit (Oligocene), other largely mudflow breccia units probably of the Mount Dutton Formation (Oligocene and Miocene), and the strata of the Limerock Canyon unit (lower Miocene). In structurally complex areas these lithologically similar units present serious and locally seemingly insurmountable problems of proper identification and correlation.

INTRODUCTION

The main purpose of this report is to revise the Brian Head Formation, a middle Tertiary stratigraphic unit exposed in and near the Markagunt Plateau, and to discuss its lithologic characteristics, distribution, geologic relationships, and historic significance. We also briefly review current information relating to selected Tertiary sedimentary rock units of the region that has resulted from recent mapping and topical studies.

The High Plateaus of southwestern Utah include, from west to east, the Markagunt, Paunsaugunt, Sevier, and Table Cliff Plateaus, and several other named plateaus (fig. 1) that lie within the structural transition zone between the Basin and Range and Colorado Plateaus provinces. This report deals mainly with selected Tertiary sedimentary rock units of the Markagunt Plateau, and to a lesser extent includes those in adjacent areas such as the Red Hills in the easternmost part of the Basin and Range province, and those in the Paunsaugunt, southern Sevier, and Table Cliff Plateaus, east of the Markagunt. The east-west extent of the Markagunt Plateau is from the Hurricane Cliffs eastward to the Sevier River valley, and the north-south extent from the vicinity of Cedar City northward to about lat. 38°00' N. (fig. 2).

The name Brian Head Formation was introduced by Gregory (1944), abandoned three decades later by Anderson and Rowley (1975), and reinstated in 1993. The abandonment was largely due to the inclusion of regional volcanic units that were subsequently formally named, to the miscorrelation of Brian Head strata with units of similar lithology

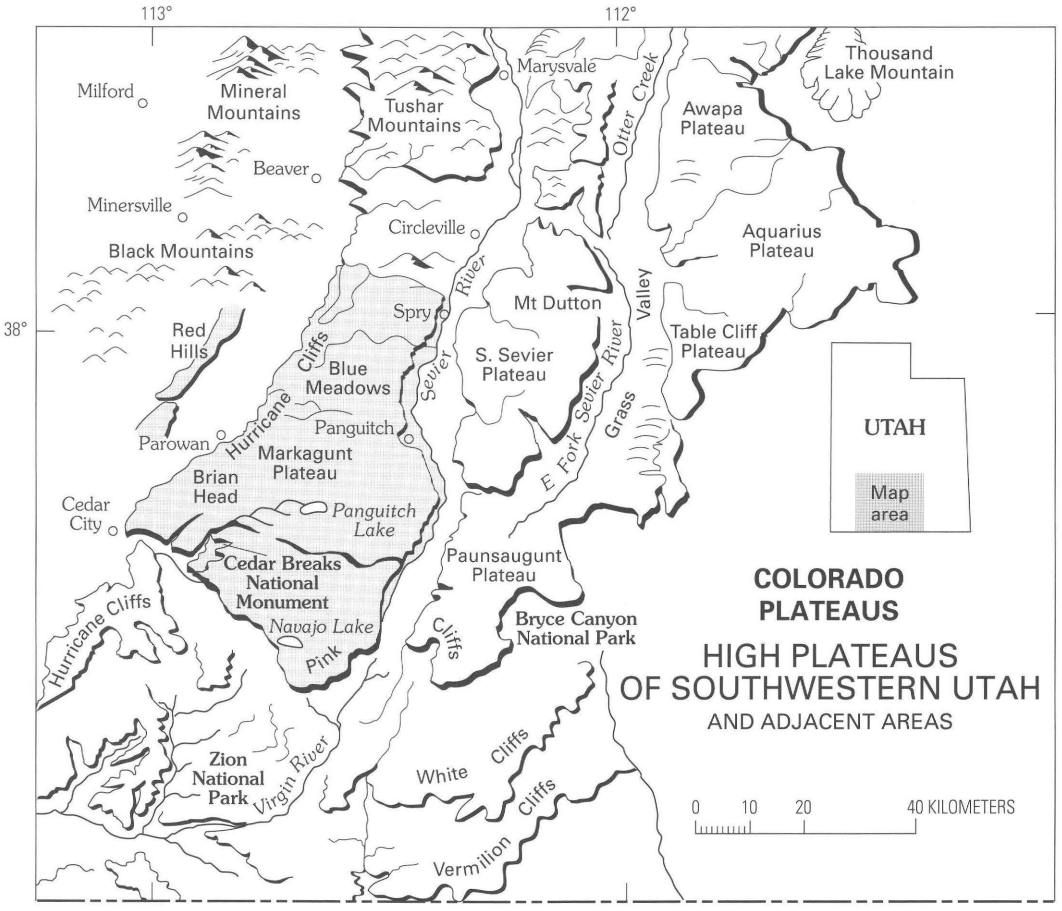

Figure 1. Index map of southwestern Utah. (Modified from Anderson and Rowley, 1975.)

but disparate ages, and to the inconsistent placement of boundaries of the unit in the High Plateaus region. The reinstated stratigraphic interval of the Brian Head (Anderson, 1993) was defined in a more restricted sense than that first published in 1944. Identification of the unit is difficult in many places because it is overlain by both autochthonous and allochthonous units, and an exposed section may not represent the entire stratigraphic interval of the formation because of low-angle displacement surfaces within the unit. Regional disconformities are interpreted to lie at the base of and within the formation. The correlation chart (fig. 3) illustrates the development of stratigraphic terminology relating to the Brian Head Formation and other lower Tertiary units of southwestern Utah.

NOMENCLATURAL HISTORY

The name Brian Head Formation was first used and described for strata at Brian Head peak by Gregory (1944), who further discussed its component lithologies, distribution, correlation, and inferred age in ensuing reports (1945, 1949, 1950) (fig. 3). Threet (1952a, b) discussed problems relating to the Brian Head and suggested restriction, redefinition, or abandonment, in that order. Anderson (1965) mapped most of the Brian Head Formation interval as part of the upper gray member of the Claron Formation, a name first introduced by Leith and Harder (1908). Anderson (1971, p. 1181–1182) criticized Gregory's usage on the basis of (1) Gregory's inconsistent and unclear use of the Brian Head as a mapping entity, (2) the inclusion in the original unit of regional ash-fall tuff units that subsequently were formally named, and (3) in part, the lack of conformity to the 1970 Code of Stratigraphic Nomenclature. Later, Judy (1974) noted that Gregory's reconnaissance maps failed in part to delineate the Brian Head, even in its type area.

Anderson and Rowley (1975) formally abandoned the names Brian Head Formation and Wasatch Formation in the region (fig. 3). Their specific reasons for elimination of the Brian Head name were (1) the inclusion by Gregory of units in the Brian Head that later were recognized as

Figure 2 (facing page). Map of Markagunt Plateau and adjoining areas. Base from U.S. Geological Survey 1:100,000 Panguitch (1980). Contour interval 1,000 feet. Triangle, described section and reference locality.

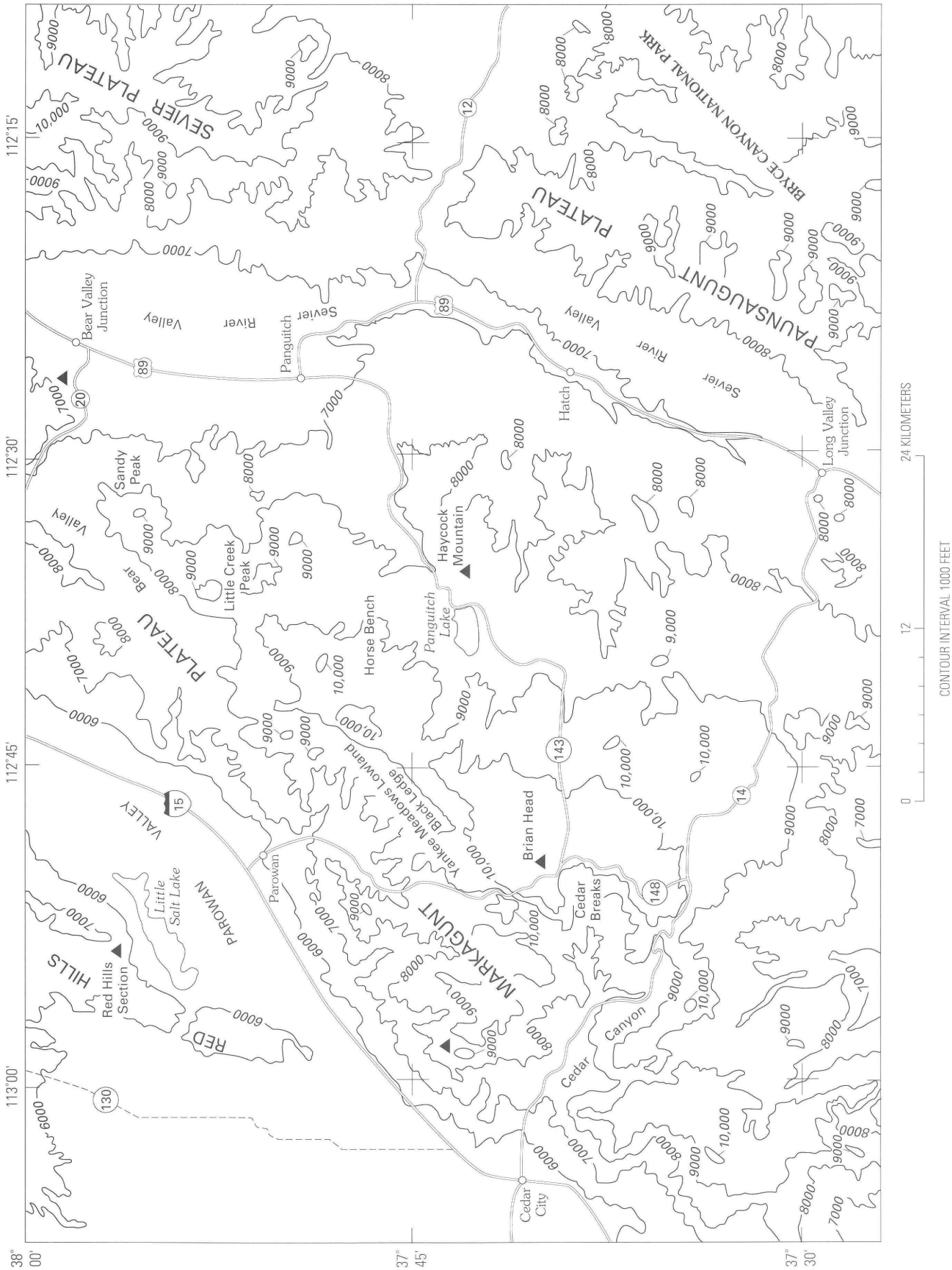
112°15'
112°30'
112°45'
113°00'
38° 00'
37° 45'
37° 30'
SEVIER PLATEAU
PAUNSAUGUNT PLATEAU
BRYCE CANYON NATIONAL PARK
Bear Valley Junction
Sevier River Valley
Panguitch
Hatch
Long Valley Junction
Sandy Peak
Little Creek Peak
Haycock Mountain
Panguitch Lake
Horse Bench
Bear Valley
PLATEAU
Yankee Meadows Lowland
Black Ledge
Brian Head
Parowan
VALLEY
PAROWAN HILLS
Red Hills Section
Little Salt Lake
RED
MARKAGUNT
Cedar Breaks
Cedar Canyon
Cedar City
89
20
15
130
143
14
148
12
0
12
24 KILOMETERS
CONTOUR INTERVAL 1000 FEET

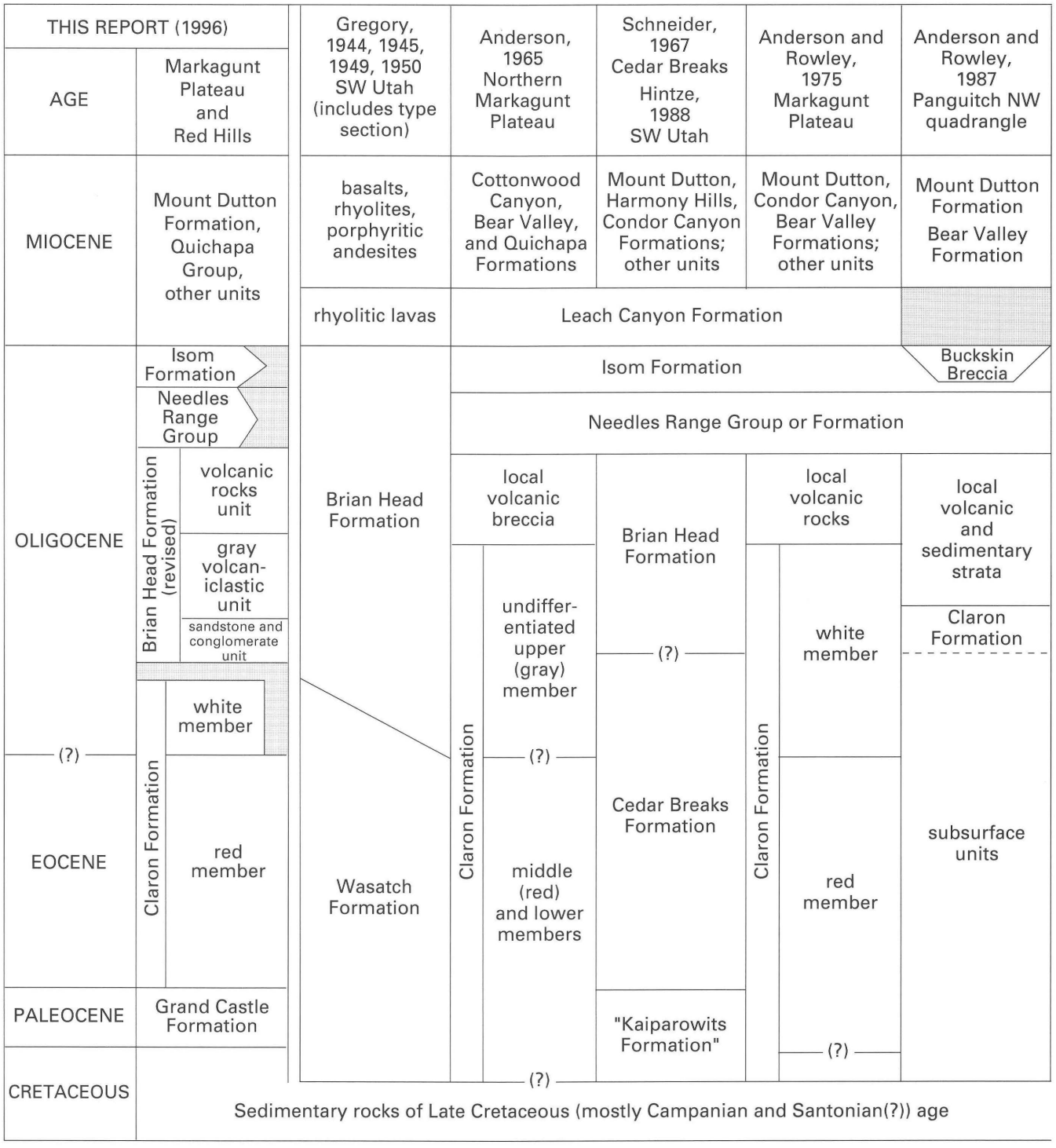

Figure 3 (above and facing page). Correlation chart of selected Tertiary rock units in Markagunt Plateau and adjoining areas relative to Brian Head Formation (revised). Missing unit intervals shaded. Query, approximate or uncertain placement of unit boundaries relative to those of this report. Systemic boundaries apply to column of this report.

Sable and Hereford, 1990 Kanab 1/2° × 1° quadrangle		Maldonado and Williams, 1993a Parowan Gap quadrangle (Red Hills)		Kurlich, 1990 Sable unpub Eastern Markagunt Plateau		Rowley, 1968 Rowley and others, 1987 Southern Sevier Plateau		Bowers, 1990 Bryce Canyon area		Bowers, 1972 Table Cliff Plateau		Anderson, 1993 Northern Markagunt Plateau	
Quaternary erosion		Mount Dutton Formation Quichapa Group Bear Valley Formation		Limerock Canyon Formation		Mount Dutton Formation		Quaternary erosion		volcanic rocks		Markagunt Megabreccia, "Haycock Mountain Tuff", Mount Dutton, Leach Canyon, Bear Valley, Isom Formations; Needles Range Group	
		Isom Formation				Needles Range Group						"locally derived volcanic strata"	
		Needles Range Group								(?)			
		sedimentary and volcanic rocks of Red Hills		Brian Head Formation		Claron Formation	white member			white tuffaceous sandstone unit		Brian Head Formation (restricted)	
Claron Formation	upper unit							conglomerate at Boat Mesa		Wasatch Formation	variegated sandstone member		
	white limestone unit	Claron Formation	not present	Claron Formation	white member			Claron Formation	white limestone member		white limestone member	Claron Formation	"white" member
	lower unit		lower part		red member		red member		pink limestone member		pink limestone member		"red" member
		conglomerate of Parowan Gap						not present		Pine Hollow Formation		not described	
										Canaan Peak Formation			
							(?)						
Sedimentary rocks of Late Cretaceous (mostly Campanian and Santonian(?)) age													

regionally widespread ash-flow tuff units of the Needles Range Group and Isom Formation (fig. 4); (2) the inclusion in the original Brian Head of sedimentary rock units that are lithologically similar but not coeval, such as the later named Bear Valley Formation (Anderson, 1971) and other units; and (3) the inconsistent or unclear inclusion or exclusion of prominent, cliffy white limestone units, the now white member (informal unit) of the Claron Formation, in the basal Brian Head. Anderson and Rowley (1975, p. 11–13) reassigned the Wasatch–Brian Head stratigraphic interval to the Claron Formation. Their Claron consisted of a red member and an overlying white member that included tuffaceous sedimentary rocks of the former Brian Head Formation as well as the distinctive cliff-forming white limestone beds. They defined the top of the Claron as "below the base of the lowest overlying lava flow, mudflow breccia, or ash-flow tuff." The base of the Claron was expressed more enigmatically, presumably because of the lack of regional correlation information. Anderson (1965) had mapped the approximate Brian Head interval as an "undifferentiated uppermost member" of the Claron. More recently, these rocks were mapped separately from the Claron as "local sedimentary and volcanic strata" (Anderson and Rowley, 1987; Anderson and others, 1987), or as "sedimentary and volcanic rocks of the Red Hills" (Maldonado and Williams, 1993a, b; Maldonado and others, 1990, 1992). In the Red Hills, these rocks underlie tuffs of the Needles Range Group and include, in addition to sedimentary rocks, local ash-flow and ash-fall(?) tuff beds (see "Red Hills Section" in this report).

Despite nomenclatural changes, usage of the name Brian Head has persisted in some published reports and has appeared regularly in informal correspondence of geologists working on the stratigraphy of the region. Anderson (1993, p. 5–6) reinstated the name Brian Head Formation for "rocks that paraconformably overlie the Claron Formation and most commonly underlie the Needles Range Group or, where it is missing, the Isom Formation; or elsewhere underlie other volcanic strata, including ash-flow tuff, lava, flow breccia, and lahar, but not airfall tuff; or cap the local section." Although he defined the lower contact in general terms, he clearly excluded rocks that he referred to as "locally derived volcanic strata that in places overlie these sedimentary strata" from the upper boundary zone. He implied that these volcanic strata constitute a separate unit or units.

ACKNOWLEDGMENTS

We acknowledge valuable discussion on regional aspects of the Brian Head Formation with J.J. Anderson, formerly of Kent State University, and D.W. Moore and H.R. Blank, Jr., of the U.S. Geological Survey. Technical reviews were by D.W. Moore and W C Swadley, nomenclatural review and clarification by T.W. Judkins, text editing by L.M. Carter, and text word processing by L.A. Heinicke, all of the U.S. Geological Survey.

DEFINITION AND DISTRIBUTION

The Brian Head Formation (revised) as defined here includes a heterogeneous assemblage of lower Tertiary dominantly volcaniclastic fluvial, lacustrine, and tuffaceous strata that paraconformably overlies units of the Claron Formation. In an autochthonous succession the Brian Head underlies welded ash-flow tuffs of the Needles Range Group, or where the Needles Range is absent, tuffs of the Isom Formation, or volcanically derived breccias and sedimentary rocks, such as those of the Mount Dutton Formation or the tuffaceous and sedimentary strata of Limerock Canyon unit of Kurlich (1990). The Brian Head consists of tuffaceous and nontuffaceous sandstone and conglomerate, limestone replaced in part by varicolored chalcedony, and minor ash-flow and air-fall tuff; locally the uppermost part consists of autoclastic flow breccia, mudflow breccia, and lava flows. The formation records the earliest extensive Tertiary volcanic activity in the region. The type section is at Brian Head (peak) (figs. 5 and 6) in the Brian Head 7.5-minute quadrangle; the base of the section is exposed 1 km north of Cedar Breaks National Monument. In the Red Hills, the Brian Head was mapped as the informal "sedimentary and volcanic rocks of the Red Hills" by Maldonado and Williams (1993a, b).

In most structurally undisturbed sections on the Markagunt Plateau, the Brian Head Formation (fig. 3) lies between an underlying distinctive white limestone unit and overlying volcanically derived units. The limestone unit is the uppermost bed of the white member of the Claron Formation (the upper of two relatively thick (more than 5 m) widespread "white" limestone beds of the member (Moore and others, 1994)). Where the white member is absent, the Brian Head rests on beds of the red member of the Claron. The upper boundary of the Brian Head Formation, where structurally undisturbed, is placed at the base of ash-flow tuffs of the Needles Range Group or Isom Formation, and locally beneath rocks of the Mount Dutton Formation, Limerock Canyon unit of Kurlich (1990) (see "Other Tertiary Sedimentary Rock Units"), or younger Tertiary and Quaternary units. As such, this boundary includes units that Anderson (1993) excluded from the Brian Head. We believe it necessary to include them, however, in order to establish a regionally distinctive top. The upper part of the Brian Head as defined here is too variable to be useful in regional lithostratigraphic correlations. The volcanic and volcanically derived rocks in the upper unit of the Brian Head have not been correlated with certainty beyond local areas. Conversely, the most consistent boundary markers for the top of the Brian Head Formation are the overlying ash-flow tuffs of the Needles Range Group or of the Isom Formation, which are distinctive and regionally persistent. Moreover, our definition of the lower and upper boundaries satisfies the criterion of mappability to a greater extent than previous boundary placements. The above relationships are

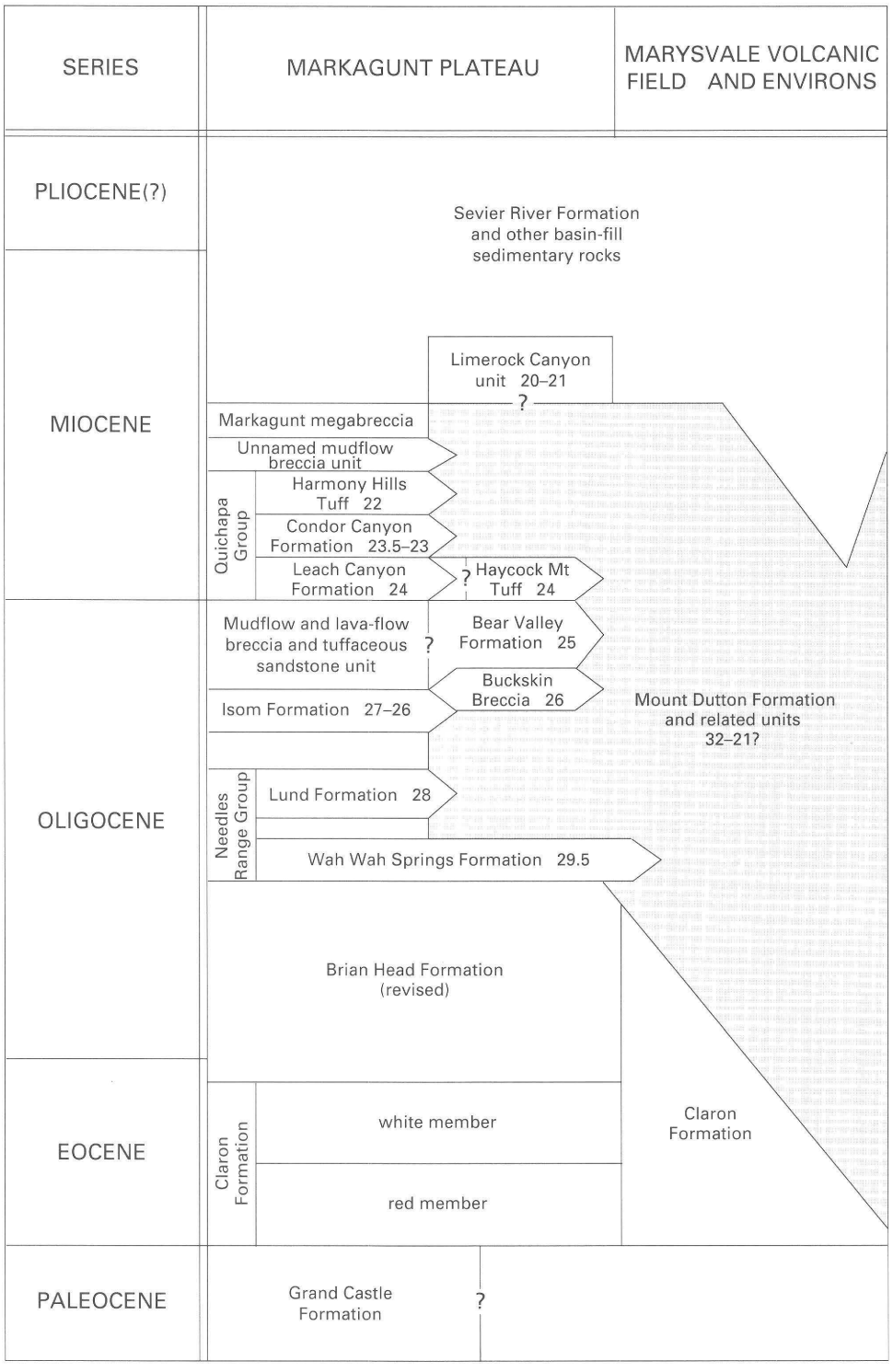

Figure 4. Stratigraphic column showing selected Tertiary units of Markagunt Plateau and adjoining areas. Numbers refer to isotopic ages rounded to nearest half million years. (Modified from Rowley and others, 1994.)


F16
49021
176
32
N
Brian Head
(Town)
Brian Head
(Peak)
Tu
Tlc
Ti
Tbhv
Tcw
Tbhs
Tcr
143
Cedar Breaks National Monument
0
1
2 KILOMETERS

Figure 6. Brian Head peak, looking northeast. Lowlands underlain by sandstone and conglomerate unit of Brian Head Formation; light-hued slopes expose gray volcaniclastic unit of Brian Head Formation; dark rocks on west side of peak are Isom Formation tuffs and unnamed volcanic rocks; Leach Canyon Formation felsic tuff caps peak.

autochthonous rock unit relationships; allochthonous rock units overlying the Brian Head Formation are the Markagunt megabreccia of Anderson (1993) and other megabreccia units such as that overlying the Red Hills shear zone, a zone of low-angle decoupling in or above the Brian Head Formation (Maldonado, 1995) (see Sable and Maldonado, this volume, chapter H).

Delimiting the specific regional extent of the Brian Head Formation (revised) will require more work because lithologically similar but younger units are sporadically exposed on the Markagunt Plateau and adjoining areas (see section, "Other Tertiary Sedimentary Rock Units"). They include the Bear Valley Formation (Anderson, 1971) and equivalents, the "tuffaceous and sedimentary rocks of Limerock Canyon" (Kurlich, 1990; Kurlich and Anderson, 1991), and other clastic and tuffaceous rocks which probably are part of the Mount Dutton Formation or part of younger Tertiary units. From west to east, however, known Brian Head rocks are present in the Red Hills and along the western margin of the Markagunt Plateau from the town of Parowan southwestward and nearly to Cedar City in the hills north of Cedar Canyon (fig. 2). Eastward from the Cedar Breaks–Brian Head area, the formation is poorly exposed but can be traced as an autochthonous unit 22 km to southeast of Panguitch Lake. Parts of the high Markagunt Plateau west of Panguitch Lake are covered by basalt of late Cenozoic age, and tracing the Brian Head Formation is tenuous in these areas. At Panguitch Lake, the Brian Head and younger units, such as the Isom Formation, are overridden by the main body of the allochthonous Markagunt megabreccia (Anderson, 1993) along a low-angle structural detachment. The Brian Head Formation can be traced from Haycock Mountain, east of Panguitch Lake, eastward to the vicinity of the town of Hatch, and thence in intermittent exposures, southwards along the eastern margin of the Markagunt Plateau to the Long Valley Junction area. At Hatch, a unit originally believed to be coeval with the Brian Head unconformably overlies a thin succession of Brian Head strata. This unit, the tuffaceous and sedimentary rocks of Limerock Canyon (Kurlich, 1990), is now known to be more than 10 million years younger than the Brian Head (see section, "Other Tertiary Sedimentary Rock Units"). East of the Markagunt Plateau, in the Paunsaugunt Plateau and the southern Sevier Plateau, as much as 260 m of lithologically similar strata is interpreted to be correlative with the Brian Head; these strata lie above the white member of the Claron Formation and underlie mudflow breccia and lahar deposits of the Mount Dutton Formation. Locally, these strata lie below rocks mapped as the Wah Wah Springs Formation of

Figure 5 (facing page). Aerial photograph showing location of Brian Head Formation type section traverse (arrows) and apparent overlap relationship of gray volcaniclastic unit on sandstone and conglomerate unit. Tlc, Leach Canyon Formation; Tu, unnamed lava and boulder agglomerate unit, the "mudflow and lava-flow breccia and sedimentary rocks" unit of Maldonado and Moore (1995); Ti, Isom Formation; Tbhv, gray volcaniclastic unit of Brian Head Formation; Tbhs, sandstone and conglomerate unit of Brian Head Formation; Tcw, white member of Claron Formation; Tcr, red member of Claron Formation; co, colluvium. Contact dashed where inferred.

the Needles Range Group (Rowley and others, 1987), which strongly suggests that the entire interval is correlative with the Brian Head Formation. Farther northeast in the Table Cliff region (fig. 1), Bowers (1972) reported a white tuffaceous sandstone unit overlying the Wasatch (present Claron) Formation. The Wasatch, as described by Bowers, consists of (in descending order) the variegated sandstone, white limestone, and pink limestone members. The white tuffaceous sandstone unit and the variegated sandstone member of the Wasatch are here provisionally correlated with the gray volcaniclastic rocks unit and sandstone and conglomerate unit, respectively, of the Brian Head Formation (revised) (fig. 3).

LITHOLOGY AND THICKNESS

The Brian Head Formation is here subdivided into three informal units (ascending): the sandstone and conglomerate unit, the gray volcaniclastic unit, and the volcanic rocks unit. Regional paraconformities or low-angle unconformities are interpreted to underlie both the sandstone and conglomerate unit and the gray volcaniclastic unit. The volcanic rocks unit appears to be of local and sporadic occurrence; regional correlation of the unit has not been achieved.

SANDSTONE AND CONGLOMERATE UNIT

This unit is rarely exposed, but commonly weathers to easily recognized red and brown soil and rubble. Good partial exposures are present at locations at the northern part of and north of Cedar Breaks National Monument. There the unit overlies the upper ledge-forming "white" limestone of the white member of the Claron Formation. It is a nontuffaceous, varicolored unit of reddish-brown, pink, and reddish-orange hues. At the type section, sandstone and granule- to pebble-conglomerate are submature lithic arenites and rudites with fine-grained clastic, in part silicified matrix containing subangular to subround clasts of gray and black chert, gray and pink quartzite, light-gray milky quartz, and abundant angular to subangular grains of pink and gray micritic to silty limestone identical to that in the underlying Claron Formation. Siltstone, claystone, and thin beds of micritic limestone constitute about 60 percent of the basal part of the unit; sandstone and conglomerate are more common in the upper part. Exposures farther east, south of Panguitch Lake (fig. 2), contain less conglomerate. The unit is about 30 m thick in the type area, and about 40 m near Panguitch Lake. It is absent or very thin in the Red Hills and in the westernmost and easternmost Markagunt Plateau. No age indicators have been found in the unit in the study area, but because of its stratigraphic position the sandstone and conglomerate unit is provisionally correlated with the finer grained variegated sandstone member of the Wasatch (Claron) Formation of Bowers (1972, p. B27–B28) of the Table Cliff Plateau region, 50 km northeast of the Markagunt Plateau. Preliminary determinations of a vertebrate fauna by J.G. Eaton (University of Utah, oral commun., June 1994) suggest a late Eocene age for the variegated sandstone member in the southern Sevier Plateau, less than 20 km east of the Markagunt.

GRAY VOLCANICLASTIC UNIT

The extensive and distinctive strata of the gray volcaniclastic unit constitute the largest volume of the Brian Head Formation. The unit has been mapped from the Red Hills eastward to the vicinity of Hatch, about 40 km, thence southward for about 8 km (fig. 2). No complete section of this unit is exposed on the Markagunt Plateau; its outcrops are commonly slumped or covered by clayey debris and highly plastic mudflow deposits. Dominant rock types are clayey, tuffaceous sandstone, conglomeratic sandstone, and claystone and clay of grayish, greenish-gray, and yellowish-gray hues. The sandstone is a lithic arenite, commonly of bimodal grain-size distribution and salt-and-pepper texture, is immature to submature, and consists of about 30 percent plagioclase (mostly oligoclase-andesine), 20 percent rounded calcite, 20 percent quartz, 15 percent sanidine, 5–10 percent volcanic rock fragments, and 5–10 percent fresh-appearing biotite and hornblende. Pebbles in the lower part of the unit consist largely of subrounded quartzite, organic limestone of Paleozoic age, and chert in a clayey, calcareous matrix. The pebbles and cobbles in the upper part of the unit, however, are dominantly moderately to highly welded ash-flow tuffs of mafic to felsic composition that do not resemble known tuffs of the region. Bioturbation is intense in some sandstones; root casts, worm(?) tubes, and small-scale penecontemporaneous slump of the bedding are common. Fluvial crossbedding is uncommon, having been obliterated in many beds by bioturbation and soft-sediment deformation preserved as convolute bedding. Other lithic components of the unit are ledge-forming light-gray to white micritic to sandy limestone beds as much as 2 m thick that are in part replaced by distinctive chalcedony that is amoeboid, lenticular, and in part brecciated and recemented. The chalcedony is of striking brown, red, gray, blue, yellow, orange, and black hues. Some chalcedony is highly brecciated and recemented by silica; some is suitable for lapidary use, but most is highly fractured. Geochemical analysis of chalcedony in the Brian Head Formation was reported by Maldonado (1995). Minor components of the unit are thin sandy ash-fall(?) tuff beds.

VOLCANIC ROCKS UNIT

The volcanic rocks unit is the most heterogeneous and the most poorly understood succession of the Brian Head Formation. Either it consists of scattered different but roughly contemporaneous rock facies or it was variably

eroded before emplacement of younger Tertiary units. Lithologies characteristic of this unit are mudflow breccia, immature lithic arenite, conglomerate containing pebbles to large boulders of volcanic rocks of felsic, intermediate, and mafic compositions, monolithologic autoclastic(?) breccia, mafic lava characterized by augite phenocrysts, and minor, but locally thick ash-flow tuff. Exposures of the unit are generally in steep-sided cliff- and ledge-dominated slopes such as those in the Red Hills (reference section 1), on the south slope of Haycock Mountain, and at a structural dome near Bear Valley Junction (Anderson and Rowley, 1987). The mudflow breccia and mudstone-matrix-supported conglomerate and conglomeratic sandstone contain many subround pebble- to boulder-sized clasts as much as 2 m in diameter and angular slabs as much as 20 m long, almost exclusively of ash-flow tuffs. Some of these tuff clasts and slabs are petrographically similar to tuffs of the Wah Wah Springs Formation of the Needles Range Group, the Baldhills Tuff Member of the Isom Formation, and the Bauers Tuff Member of the Condor Canyon Formation. At least one moderately welded, highly lenticular ash-flow tuff is present in the Red Hills (Maldonado and Williams, 1993 a, b). The tuff is dated at about 33–34 Ma (see section, "Age of the Brian Head Formation"). Sandstone and conglomerate matrix in the unit is a volcanic wacke locally containing abundant dark glass shards. Monolithologic autoclastic or volcanic mudflow breccia directly underlying the Needles Range Group tuff at the Bear Valley Junction dome, 15 km north of Panguitch, was included in a unit informally named "local volcanic and sedimentary strata" by Anderson and Rowley (1987) that also includes latite and trachyandesite lavas and ash-flow tuff. The volcanic rocks unit is not present at the type section of the Brian Head Formation, but is about 100 m thick in the Red Hills (reference section 1).

Some conglomerate beds contain pebble- to boulder-sized clasts of rocks that are also petrographically similar to tuffs in the Needles Range Group, Isom Formation, and Condor Canyon Formation (for example, in reference section 1 and reference locality 2), but are provisionally considered to be in the volcanic rocks unit of the Brian Head. The identity of the clasts remains enigmatic; if the clasts are from the above units, the enclosing strata are clearly younger than the Brian Head. In the Red Hills, however, the conglomerates underlie an ash-flow tuff dated at about 33–34 Ma that lies below rocks of the Needles Range Group (Maldonado, 1995; L.W. Snee, U.S. Geological Survey, written commun., February 1994). The geologic map of the Parowan Gap quadrangle (Maldonado and Williams, 1993a) that delineates the tuff also shows a low-angle structural discontinuity (Red Hills shear zone) at the base of overlying Needles Range rocks of reference section 1, but as explained in their map text, the discontinuity may not specifically coincide with the mapped contact; in this vicinity it lies within the lower 110 m of the reference section.

LOWER CONTACT

The basal contact of the Brian Head Formation with underlying units of the Claron Formation is rarely exposed. Over much of the area the abrupt change from the red clastics of the sandstone and conglomerate unit of the Brian Head to the limestone beds of the Claron white member is easily mapped. This relationship extends from Cedar Breaks eastward to the vicinity of Panguitch Lake. Farther east, in and south of the vicinity of Hatch, the middle gray volcaniclastic unit of the Brian Head overlies the Claron white member, and the contact is placed at the first appearance of volcanic constituents such as fresh-appearing biotite. Still farther northeast, in the southern Sevier Plateau, the variegated sandstone member of the Wasatch (Claron) (Bowers, 1972), which we correlate with the Brian Head sandstone and conglomerate unit, is widespread; its contact with the Claron white member is also distinctive and easily mapped on the basis of color contrast and slope- versus cliff-forming character.

Anderson and Kurlich (1989) reported a paraconformity at the base of beds now included in the Brian Head Formation, but what unit of the Brian Head they referred to is not clear. We suggest, mainly on the basis of the presence of the different underlying Claron members, that a disconformity representing erosion on a bevelled surface of east-dipping Claron strata lies at the base of the sandstone and conglomerate unit. The abundance of Claron-derived limestone clasts in the sandstone and conglomerate unit also suggests that an erosional interval preceded deposition of these basal Brian Head strata.

North and west of the Brian Head type section, the white member of the Claron Formation is only locally present; it is absent farther west in the northern Red Hills. At locations where the white member is absent, the gray volcaniclastic unit directly overlies the Claron red member in what we interpret to be an unconformable relationship because the sandstone and conglomerate unit is also absent. One of the very few exposures of the basal contact of the Brian Head Formation is along the West Fork of Braffits Creek (reference locality 1 of this report), where tuffaceous conglomerate and sandstone of the gray volcaniclastic unit overlie the Claron red member. At the Brian Head type section, the base of the gray volcaniclastic unit overlaps the underlying sandstone and conglomerate unit (fig. 5). This relationship, however, may in reality represent slump and slide deposits of Quaternary age rather than an intra-Tertiary erosional and depositional feature. The absence of the sandstone and conglomerate unit in some areas, such as those near Hatch and in the Red Hills, however, also suggests that an unconformity is present at the base of the gray volcaniclastic unit.

UPPER CONTACT

The upper contact of the Brian Head Formation with structurally autochthonous ash-flow tuffs of the Needles Range Group or Isom Formation is generally marked by a distinct lithologic change from clastic sedimentary rocks to superjacent resistant vitrophyres or welded tuffs. Good exposures of sedimentary rocks underlying tuff of the Needles Range Group can be seen along the upper part of Lowder Creek 3 km east of Brian Head (peak) in the Brian Head 7.5-minute quadrangle. Volcanic breccia, here included in the Brian Head Formation, underlies rocks of the Needles Range Group at the Bear Valley Junction dome (Anderson and Rowley, 1987), and a similar relationship west of Bear Valley was reported by Anderson and others (1987). At outcrop scale, the contact of the Brian Head with Needles Range or Isom tuffs appears to be conformable, but the absence of Needles Range rocks in many places may represent either an erosional interval before emplacement of Isom Formation rocks or nonemplacement of Needles Range tuffs. In some places, thinning or absence of the Needles Range is the result of low-angle structural displacement, along either the Red Hills shear zone or the base of other allochthonous bodies of rock. The otherwise extensive distribution of Needles Range tuffs and the time interval of several million years between deposition of the Brian Head and emplacement of Isom rocks, however, suggest that an erosional hiatus separates the two units.

THICKNESS

Few reliable thicknesses of the Brian Head Formation have been measured in the study area because of poor exposures and real or inferred structural and mass-movement complications. Measured and estimated thicknesses range from about 200 m in the western part of the Markagunt Plateau to incomplete sections of about 30 m near Hatch, along the plateau's eastern margin. The interval between the Claron Formation and Needles Range Group at Bear Valley Junction dome is 230 m thick (Anderson and Rowley, 1987); similarly, the interval in the Red Hills is more than 200 m thick (Maldonado and Williams, 1993a, b). A 290-m-thick section in the Casto Creek drainage, southernmost Sevier Plateau, was described by Rowley (1968), who assigned the rocks to the white member of the Claron Formation. We correlate the approximately upper 260 m of that section with the Brian Head and propose that the lower 30 m is part of the white member of the Claron. Farther north at Adams Head peak, Sevier Plateau, as much as 165 m of comparable strata, mapped as the Claron white member, lies below ash-flow tuff of the Needles Range Group (Rowley and others, 1987), thus indicating that these strata are Brian Head equivalents. Much of the strata in the Sevier Plateau exposures is highly pumiceous, and conglomerate clasts are almost entirely of volcanic rocks of unknown derivation.

STRATIGRAPHIC SECTIONS AND LOCALITIES

The Brian Head Formation is almost everywhere a poorly exposed unit owing to poor cementation and an expansive clay mineral fraction. Poorly resistant tuffaceous sandstone and clay weather to low to moderate slopes that are largely well vegetated or colluvium covered. These beds are exposed mostly in actively downcutting drainages. The more resistant beds such as limestone, limestone partly or wholly replaced by chalcedony, and to lesser extent, poorly to moderately welded tuff, crop out sporadically on slopes and in stream beds. Some roadcuts provide good exposures of the unit, but many are obscured by slumping. In wet weather, gumbo-like clay makes even improved unpaved roads impassable for most vehicles. Soil creep is common on hillsides, and at times, highway travel is obstructed by small earthflows and landslides within the gray volcaniclastic unit. Some slump and slide features occur at stratigraphic horizons where the rocks may have been comminuted by differential movement associated with low-angle faulting, such as along the Red Hills shear zone of Maldonado and others (1992; also see Maldonado, 1995).

Two measured and described sections are shown herein; they are the type section of the Brian Head Formation at Brian Head (peak) and the Red Hills reference section, 30 km north of the type section (fig. 2). The type section is provisionally considered to be an undisturbed section, but it does not contain the uppermost, volcanic rocks unit. If the zone of abundant chalcedony (units 6 to 8) represents silicification along the Red Hills shear zone as suggested by Maldonado (1995), some beds in this interval may be missing or attenuated. The Red Hills section is incomplete because the base of the formation is below ground level and because the Red Hills shear zone is suspected to occur in the upper part of the section.

BRIAN HEAD FORMATION TYPE SECTION

Brian Head (peak), Brian Head 7.5-minute quadrangle. Contiguous quarters of secs. 11, 12, 13, and 14, T. 36 S., R. 9 W., Iron County, Utah. The section, about 220 m thick, is exposed in mostly rubble covered slopes and in gullies and bedrock ledges from the top of cliffs of the uppermost limestone bed of the Claron Formation (white member) below the junction of Utah State Highway 143 and the road to Brian Head (peak) to cliff- and ledge-forming tuffs of the Isom Formation in the upper part of the peak (fig. 6). Reddish-brown sandstone and conglomerate and minor limestone in roadcuts and drainage ditch cuts form the basal unit of the formation, and they are overlain by mostly volcanic arenite containing minor limestone, pink tuff and conglomerate beds, and abundant chalcedony. Units 1–5 represent the sandstone and conglomerate unit division of the formation, and units 6–34 the gray volcaniclastic unit. The volcanic rocks unit is not present. This was the type area of the original Brian Head Formation of Gregory.

[*Measured by E.G. Sable and Michael Hill, May 22, 1992*]

Thickness (meters)

Leach Canyon Formation (Oligocene) of Quichapa Group (in part):

Narrows Tuff Member:

40. Tuff, grayish-red to brownish-gray; weathers pale red, dense, massive, lithic and crystal poor; crystals are about 25 percent quartz, 20 percent sanidine, 45 percent plagioclase, 5 percent biotite, and 5 percent red lithic fragments ..... 13+
39. Basal vitrophyre, brownish-gray to dark-gray, massive; contains probable sanidine and plagioclase phenocrysts ..... 6±

Unnamed unit:

38. Partly covered by rubble and talus of aphanitic dark-gray, platy-weathering lava(?) ..... 8±
37. Boulder agglomerate; contains clasts of brick-red and black aphanitic volcanic rock, basalt(?), obsidian, scoria, and vitrophyre. Elsewhere in places, this unit also contains clasts of Needles Range Group and Isom Formation (Maldonado and Moore, 1993) 21.3

Isom Formation (Oligocene):

36. "Tuff lava," medium-dark-gray, aphanitic, nonporphyritic, dense; contains conspicuous elongate vesicles. A few angular, cobble- to small boulder-sized fragments of Needles Range Group tuff present as slope litter 15.2
35. Rubble, mostly tuff lava; dark-reddish-brown clay at base 12.7

Brian Head Formation (middle Oligocene to upper Eocene?):

Gray volcaniclastic unit:

34. Mostly covered; rubble of aphanitic siliceous rock, mottled black and white, probably a thin bed. Minor chalcedony float 4.1
33. Chalcedony, light-gray to brownish-gray; minor light-gray limestone rubble, forms ledge 0.5
32. Rubble slope; clay, comminuted siltstone and sandstone, and white limestone partly replaced by gray chalcedony 15.3
31. Rubble, ash-fall(?) tuff, white, chalky ..... 0.3±
30. Rubble, sandy clay, gray 5.4
29. Rubble and ledges of tuffaceous sandstone, thin ash-fall tuff, and brown, plastic sandy clay. Includes thin resistant ledge of limestone partly replaced by grayish-brown chalcedony; sandstone is light gray to olive gray, fine to coarse grained, salt-and-pepper texture; unit capped by 3 cm of white chalcedony 14.3
28. Sandstone, light-gray to dark-olive-gray, tuffaceous; bimodal with fine to granule-sized grains; interbedded with two ash-fall(?) tuff beds in lower 0.6 m of unit. Upper tuff is light brown, clayey, soft, in part with channeled upper surface; lower tuff 1 cm thick, pale red, contains possible black biotite 1.8
27. Covered; sandy soil 1.6
26. Sandstone, gray, tuffaceous, contains borings or root casts 0.9
25. Covered; sandstone float 2.8
24. Limestone, very light gray, thin-bedded, sandy; partly replaced by white chalcedony ..... <0.3
23. Rubble, sandstone 4.4
22. Sandstone, gray, very fine grained, calcareous; borings or root casts 0.5

Thickness (meters)

Brian Head Formation Type Section—Continued

21. Sandstone, medium- to light-gray, fine-grained; exhibits salt-and-pepper texture; friable to moderately indurated, weathers in irregular shapes; contains pits, probably root molds, and convolute bedding 1.5
20. Covered; low-angle slope with gray clay and silty clay heavings 7.9
19. Limestone, very light gray, aphanitic; forms resistant ledge ..... <0.3
18. Limestone, yellowish-gray; weathers white; partly replaced by gray chalcedony; forms ledge 0.3
17. Rubble from unit 18 on low-angle slope; much gray clay 5.1
16. Limestone, medium-light-gray, crystalline to silty; "stockwork" fracture 0.3
15. Covered. Much gray clay in soil 1.6
14. Limestone, light-gray, partly replaced by translucent gray, blue, red, and black chalcedony; forms bench 0.3
13. Partly covered; rubble of clay and limestone 6.3
12. Rubble. Clay and clayey siltstone, olive-gray; minor very light gray limestone as chips and thin limestone bed at top 7.9
11. Covered 3.2
10. Dolomitic(?) limestone and chalcedony; limestone very light gray to white to moderate pink; micritic, exhibits irregular fracture; in part brecciated and recemented with pink calcite cement; contains calcite-filled vugs, pisolite-like structures and possible shell fragments. Replacement chalcedony occurs mostly in lower 0.3 m; moderate reddish brown, black, dusky blue, and gray; in part brecciated and recemented with silica; forms prominent bench 1.8
9. Rubble covered. Lower one-half of unit is clay or clayey siltstone, light-olive-gray, plastic, and minor fine-grained sandstone. Upper part contains very light gray limestone and minor chalcedony 34.9
8. Chalcedony, varicolored red, yellow, orange, gray; massive; forms ledge-like bench ..... 1.0±

Section below mostly covered; section intervals calculated from altimeter survey and by hand level; measurements are approximate, were made directly to southeast of section described above down to headwater drainage of Mammoth Creek; includes minor gully exposures.

7. Mostly rubble and vegetation cover. Interval includes olive-gray sandy clay, very light gray limestone chips, and concentrated float of rounded pebbles as much as 6 cm in diameter of red and pink aphanitic felsic ash-flow tuff and lesser amounts of gray intermediate tuff or lava. Includes dark, carbonaceous-appearing soil 12.2
6. Rubble and vegetation cover. Float of olive-gray to gray medium to coarse sand of salt-and-pepper texture in plastic mud matrix. Scattered large chalcedony blocks as much as 2 m in width. Mud probably bentonitic 51.8

Note: See Maldonado (1995) for chemical analysis of chalcedony samples from southwest side of Brian Head peak.

Section below measured immediately south of State Highway 143, 300 m north of Mammoth Summit road to Brian Head peak; measured uphill from limestone cliffs of white member of Claron Formation.

Sandstone and conglomerate unit:

Brian Head Formation Type Section—Continued

		Thickness (meters)
5.	Mostly vegetation cover. Scattered hillside rubble and road-cut exposures; light-olive gray to reddish-brown sandstone, conglomeratic sandstone, and conglomerate; conglomeratic rocks contain rounded pebbles of gray and black chert, varicolored quartzite, and angular clasts of pink to gray micritic limestone	25.9
4.	Rubble of silty limestone, pink, very finely crystalline; weathers reddish brown; irregularly fractured	<0.3
3.	Soil, reddish-brown	1.2
2.	Claystone, gray	1.2
1.	Clay, gray, plastic	0.3
	Approximate total thickness, Brian Head Formation:	177.6

Claron Formation, white member. Limestone, very light gray, weathers yellowish orange, in two cliff-forming units separated by varicolored claystone, sandstone, conglomerate, and limestone. Not measured; 2 km to south of above section, total thickness of white member is about 70 m.

RED HILLS SECTION

Reference section 1. Red Hills, Parowan Gap quadrangle, NW$^1/_4$ and NE$^1/_4$ of SE$^1/_4$, sec. 8, T. 33 S., R. 9 W., Iron County, Utah. Section occurs in steep, southwest-facing slopes, gullies, and ledges of a prominent unnamed hill. Along strike to the north, upper part of section contains a fairly prominent pink ash-flow tuff.

[Measured by E.G. Sable and Michael Hill, May 20, 1992]

		Thickness (meters)
Needles Range Group (Oligocene) (part):		
34.	Rubble. Low slope. Needles Range Group tuff overlain by cliffs of same rocks to hilltop. Estimated thickness	<15
33.	Vitrophyre, medium-gray, foliated; contains probable plagioclase phenocrysts	0.9
32.	Talus of Needles Range Group tuff	3.0
Brian Head Formation (part):		
Volcanic rocks unit:		
31.	Conglomerate, grayish-green to reddish-brown, iron-stained, grain-supported, poorly sorted, moderately indurated; contains clasts of large variety of tuff and lava, mostly subangular to round, 20–70 cm diameter; lithologies range from pink felsic to andesitic to basaltic rocks. Minor interbedded planar-bedded sandstone; ledge-forming unit	5.2
30.	Sandstone, dusky-red; as small ledges and talus	1.5
29.	Conglomeratic sandstone, bright-green to grayish-green, rusty-weathering; pebble- to large cobble-sized volcanic rock clasts	1.5
28.	Mostly debris covered. Conglomeratic sandstone in basal part is grayish orange pink. Upper part is a steep talus slope of conglomeratic sandstone debris. This covered interval may conceal pink ash-flow tuff elsewhere as much as 60 m thick reported by Maldonado and Williams (1993a) as a bed in their "sedimentary and volcanic rocks of Red Hills" (present Brian Head Formation) unit	13.7

Red Hills Section—Continued

		Thickness (meters)
27.	Cobble to boulder conglomerate, with subangular to rounded clasts as much as 0.8 m in diameter; clast- and matrix-supported; coarsens upwards. Clasts entirely of volcanic ash-flow tuff, mostly red felsic aphanitic rock of unknown origin; a few clasts of ash-flow tuff resemble those of Needles Range Group and Isom Formation	3.8
26.	Talus of sandstone, gray, clayey, tuffaceous; contains scattered pebbles and cobbles	6.1
25.	Conglomeratic sandstone and sandstone, pale-green to grayish-green, probably tuffaceous, moderately resistant; vivid green hues at clast boundaries. Clasts as large as 0.6×0.2 m in diameter composed of felsic aphanitic rocks with glassy feldspar; a few clasts of ash-flow tuffs that resemble those of Needles Range Group and Isom Formation	9.5
24.	Conglomerate and breccia, grayish-green, friable, very immature; fine- to medium-grained sandstone matrix; probably a mudflow	2.7
23.	Sandstone and conglomeratic sandstone, grayish-green; clasts are matrix-supported; unit moderately resistant	4.6
22.	Talus, sandstone and clay, gray to grayish-green	4.3
21.	Conglomeratic sandstone, gray to pale-green; contains volcanic tuff and quartzite clasts as much as 5 cm in diameter	0.9
20.	Tuffaceous sandstone and clay, gray; includes a 0.3-m-thick resistant conglomerate ledge; forms slope	4.9
19.	Conglomerate, conglomeratic sandstone, and breccia, pale-yellowish-brown, blocky to massive, resistant cliff- and ledge-former. Basal 0.2 m is conglomerate with clasts as much as 3 cm in diameter; bedding ranges from planar to very low angle crossbeds; contains angular to subround clasts of volcanic ash-flow tuffs. Resistant unit	5.5
18.	Rubble slope; clayey sandstone and sand	1.8
17.	Rubble of ash-fall(?) tuff, moderate-orange-pink to moderate-pink, chalky, soft; appears to be a lens that thickens southward	1.2±
16.	Sandstone and conglomeratic sandstone grading upwards into breccia; clasts entirely of volcanic tuff; resistant ledge	1.2
15.	Sandstone, poorly resistant, slope former	1.5
14.	Sandstone, planar-bedded, moderately crossbedded; ledge-former	0.3
13.	Sandstone and conglomeratic sandstone, tuffaceous; salt-and-pepper texture; possible zeolitic matrix; in part crossbedded; resistant unit	1.4
12.	Conglomerate, similar to unit 10; clasts include Paleozoic limestone in tuffaceous sandy matrix	0.6
11.	Sandstone, gray, fine- to medium-grained, moderately resistant	1.2
10.	Conglomerate with rounded to subangular clasts 1–10 cm in diameter of volcanic tuffs (dominant), chert, red and pink quartzite; grades into unit 11	0.9
9.	Conglomeratic sandstone similar to unit 5 with basal 0.4-m-thick conglomerate, yellowish-gray to very light gray, tuffaceous, bimodal grain size distribution; conglomerate clasts 1–8 cm in diameter of volcanic rocks in medium to coarse sand matrix; weathers to rounded bosses	3.8
8.	Sandstone similar to unit 6	1.6

	Thickness (meters)
Red Hills Section—Continued	
7. Breccia and conglomerate, pinkish-gray; clasts less than 1 cm in diameter of a variety of volcanic tuffs in mudstone matrix; very resistant	0.2
6. Sandstone similar to unit 2, tuffaceous; high clay or zeolite content	6.4
5. Conglomerate and sandstone, gray, medium- to coarse-grained, matrix-supported; contains 70 percent well-rounded clasts 1–15 cm in diameter of volcanic ash-flow tuff, including medium-gray olivine-bearing lava, pink felsic crystal tuff containing biotite and hornblende grains, grayish-green vitric tuff with quartz, feldspar, bright-green ferromagnesian mineral, and maroon aphanitic to finely crystalline rock with green matrix; grades into overlying unit	1.2
Gray volcaniclastic unit (part):	
4. Tuffaceous sandstone, very light gray, coarse-grained; thickens southeastwards	0.3
3. Tuffaceous sandstone, claystone, and white ash-fall(?) tuff in basal 3 cm of unit and as lenses within unit	0.2–0.3
2. Tuffaceous sandstone and conglomeratic sandstone, yellowish-gray, coarse-grained to very fine grained; minor dusky-green very thin clay(?) laminae; salt-and-pepper texture; contains pebbles of light-gray ash-flow tuff containing brown biotite and minor pink felsic rock; moderately resistant slope former	5.7
Section below is largely covered by rubble but contains a few ledgy exposures.	
1. Rubble of tuffaceous sandstone, clay, conglomerate, and mudflow breccia; sandstone is very light gray to olive gray, contains very fine to medium grains of biotite and white feldspar in zeolitic(?) and calcareous matrix; weathers flaggy to platy; generally moderately to well indurated; unit forms low-angle slope; conglomerate contains well-rounded to subangular pebbles, cobbles, and boulders as much as 0.7 m diameter similar in composition to Needles Range Group ash-flow tuffs, andesitic or basaltic lavas, chert, and quartzite. Mudflow breccia contains clasts similar to those described above	110+
Base of formation not exposed.	
Total exposed thickness of Brian Head Formation:	203+

REFERENCE LOCALITIES

In addition to the type and reference sections described, three reference localities (fig. 2) are briefly described here:

Reference locality 1. West Fork of Braffits Creek, Summit quadrangle, $NW^1/_4NE^1/_4$ sec. 15, T. 35 S., R. 10 W., Iron County, Utah. High cutbanks along east side of creek below small waterfall. This is one of the few known exposures of the basal contact of the Brian Head Formation. More than 15 m of the gray volcaniclastic unit, tuffaceous sandstone and conglomerate containing rounded quartzite, chert, and limestone clasts, overlies about 10 m of the red member of the Claron Formation. More than 100 m of tuffaceous sandstone, conglomerate, chalcedony, and limestone overlies the basal beds of the Brian Head in limited, mostly slumped exposures.

Reference locality 2. Haycock Mountain, Haycock Mountain quadrangle. $NW^1/_4NE^1/_4$ sec. 1, T. 36 S., R. 7 W., and $SE^1/_4SE^1/_4$ sec. 36, T. 35 S., R. 7 W., Garfield County, Utah. Exposures in south-facing slopes and cliffs on south side of Haycock Mountain. Lower part of section, more than 122 m thick, contains volcanic arenites, thin limestone beds, and chalcedony of the gray volcaniclastic unit that overlie rubble and discontinuous outcrops of the sandstone and conglomerate unit, about 40 m thick. Upper part of section, interpreted to be the volcanic rocks unit, is more than 30 m thick, and consists of mostly sandstone and conglomerate containing clasts of rocks resembling ash-flow tuffs of Needles Range Group, Isom Formation, and Condor Canyon Formation. This upper part is provisionally included in the Brian Head Formation, and is overlain (in ascending order) by rubble of allochthonous(?) porphyritic pyroxene-phenocryst lava, Baldhills Tuff Member of Isom Formation, and Haycock Mountain Tuff of Anderson (1993).

Reference locality 3. Bear Valley Junction dome, Panguitch NW quadrangle, secs. 5, 6, and 7, T. 33 S., R. 5 W., Garfield County, Utah. Section of the Brian Head Formation about 230 m thick occurs as west- to north-dipping strata on the northwest flank of the domal structure. According to Anderson and Rowley (1987), the section consists of tuffaceous sandstone and siltstone and volcanic mudflow breccia complexly interbedded with several kinds of lava as well as ash-flow tuff. The lavas are porphyritic latite and trachyandesite, and the tuff is a hornblende-sanidine vitric-crystal welded tuff. The top of the section is marked by a massive (>30 m), medium-gray, monolithologic volcanic autoclastic(?) flow breccia; it is overlain by Needles Range ash-flow tuff.

AGE OF THE BRIAN HEAD FORMATION

The Brian Head Formation is here provisionally considered to be late Eocene to middle Oligocene age. Although the age of some ash-flow tuff in the volcanic rocks unit is reasonably well established at about 32–34 Ma (middle Oligocene), those for the lower and middle units are less well constrained. Two radiometric ages have been reported from rocks known or interpreted to be in the upper part of the Brian Head Formation (revised) or in probable coeval strata. A 31.9±0.5 Ma K-Ar age from an ash-flow tuff in beds apparently equivalent to the upper Brian Head Formation in the Bear Valley area was reported by Fleck and others (1975), and a K-Ar age of 34.2±2.1 Ma on plagioclase was obtained from a sample of ash-flow tuff 3.5 km north of the Red Hills section, mapped by Maldonado and Williams (1993) (H.H. Mehnert, written commun., January 1992). Subsequent $^{40}Ar/^{39}Ar$ ages of the same Red Hills sample are

33.00±0.13 Ma on plagioclase and 33.70±0.14 Ma on biotite (L.W. Snee, written commun., February 1994). ($^{40}Ar/^{39}Ar$ determinations of apparent age and error factors are based on 2 sigma.)

Two samples of ash-flow tuff of the Wah Wah Springs Formation of the Needles Range Group directly overlying the Brian Head Formation along Lowder Creek, 3.2 km east of Brian Head peak, gave K-Ar ages of 30.4±3.1 and 32.4±3.4 Ma on biotite and 30.4±1.1 and 29.1±1.0 Ma on hornblende respectively (H.H. Mehnert, oral commun., January 1987; reported in Rowley and others, 1994, p. 10). (Parameters for age determinations of the Wah Wah Springs Formation are given in Rowley and others, 1994.)

No fossils of unequivocal age have been found to 1995 in the Brian Head on the Markagunt Plateau or Red Hills; Gregory (1945, 1949, 1951) assigned the formation to the Miocene. Feist and others (this volume, chapter B) report a maximum age of middle Eocene for charophytes from the basal part of the Brian Head in the southern Sevier Plateau. On the basis of palynomorphs, Goldstrand (1990) assigned the underlying Claron Formation a Paleocene and Eocene age in the Pine Valley Mountains, about 50 km southwest of the Markagunt Plateau, but he believed the basal beds to be time transgressive in an easterly direction. Eaton (1995) assigned Bowers' (1972) variegated sandstone member of the Wasatch (Claron) Formation a late Eocene age based on preliminary identification of vertebrate remains.[1]

DEPOSITIONAL ENVIRONMENTS AND SOURCES

The Brian Head Formation marks the earliest major pulse of Tertiary volcanism affecting the Markagunt Plateau and surrounding areas, as shown by abundant swelling clays and fresh biotite in volcanic arenites and claystones, as well as the presence of ash-flow tuffs and highly pumiceous ash-fall tuffs in these nonmarine rocks. Crossbedding and other current indicators in the clastic sedimentary rocks indicate a fluvial origin; local contorted bedding suggests penecontemporaneous aqueous slump features. Limestone locally contains abundant root casts, suggesting a marshy pond or lake environment favorable to calcium carbonate accumulation. Fauna reported by Gregory (1944, 1949, 1950) are sparse continental gastropod and pelecypod remains, suggesting lacustrine conditions. Sandstones and conglomerates appear to be discrete but lensing units that do not show features of extensive lateral distribution such as would be expected in braided stream deposits; thus, we infer that they represent deposits of separate ephemeral streams incised in a landscape of low relief. The well-rounded clasts of Precambrian(?) and Paleozoic rocks in conglomerates of the Brian Head do not necessarily indicate the presence of bedrock of those ages in the source areas, because identical well-rounded clasts are found in Upper Cretaceous and lower Tertiary (Claron and Grand Castle Formations) rocks of the region. Our opinion is that these well-rounded clasts represent recycled resistates from these older strata, possibly from uplifted areas along the Sevier orogenic belt west of the plateaus region. Chalcedony masses are amoeboid to irregular and are clearly replacements of limestone, and to a lesser degree tuff, possibly by ground-water (hydrothermal?) percolation of silica-rich solutions. Some limestone is highly brecciated and recemented by calcite; some chalcedony also exhibits a brecciated texture recemented by silica. If the brecciation is related, then replacement by silica postdated limestone deposition and lithification. Maldonado (1995) has suggested that some of the chalcedony may be the result of selective replacement along the Red Hills shear zone.

About 34 Ma, voluminous andesitic to rhyolitic volcanism associated with caldera complexes in southeastern Nevada and southern Utah (for example, Monroe Peak, Indian Peak, Marysvale) became a dominant source of deposition in southwestern Utah. The 33–34 Ma ash-flow tuff unit of the Brian Head Formation in the Red Hills, a discontinuous unit as much as 60 m thick (Maldonado and Williams, 1993a), may represent one of these regional tuff units. Air-fall(?) tuff units may be the distal parts of pyroclastic eruptions from calderas in Nevada or southern Utah. One or two thin felsic air-fall(?) tuff units are present at various locations on the Markagunt Plateau, and ash-flow tuff has been mapped in limited areas there. Volcanic sources for these tuffs may have lain to the west, north, or northeast. The apparent eastward or southward gross fining of sedimentary rocks in the Brian Head may suggest western or northern sources. The Brian Head thins eastward in the eastern Markagunt Plateau (Sable, unpub. mapping, 1994). The thinning, however, may not be depositional, but the result of erosion prior to the deposition of the overlying much younger strata of the Limerock Canyon unit near Hatch. Rowley and others (1994, p. 10) suggested a northeastern source, the Marysvale volcanic field, for rocks of the Brian Head. The volcanic rocks unit of the Brian Head contains ash-flow tuffs, lava flows, and mudflow breccias in its northern and eastern exposures; thus volcanic centers north or northeast of the Markagunt Plateau or local vents may have been sources for these rocks. In addition, the thick pyroclastic Brian Head equivalents in the southern Sevier Plateau contain clasts whose compositions do not resemble known volcanic tuffs from the western Great Basin. Thus, volcanic sources may have been bidirectional prior to emplacement of Needles Range Group rocks, and interfingering of volcanic and sedimentary materials from the two sources may have continued from middle Oligocene into early Miocene time.

[1]After completion of this report, a $^{40}Ar/^{39}Ar$ mean age determination of 34.99±0.22 Ma was reported from fresh-appearing biotite in a tuffaceous sandstone about 20 m above the base of the formation (Lisa Peters, New Mexico Geochronological Laboratory, written commun., September 3, 1996). Location: roadcut west side of U.S. Highway 89, lat 37°35′14″ N., long 112°28′12″ W. Volcaniclastic unit: errors reported at two sigma confidence level; decay constant and isotopic abundances are those suggested by Steiger and Jäger (1977, Earth and Planetary Science Letter 36, p. 359–362).

OTHER TERTIARY SEDIMENTARY ROCK UNITS

In addition to the Brian Head Formation, other units of dominantly sedimentary Tertiary rocks are exposed in the Markagunt Plateau and other areas of southwestern Utah. Some of these units contain lithologic components that, to the time of this writing, are indistinguishable from those of the Brian Head, and have therefore been correlated with the formation. The following brief discussions of some of these units afford an overview of recent and current developments during mapping and topical studies in this region. Besides inclusion of published material, unpublished data and interpretations derived from mapping and age determinations since Gregory's early work are also presented. The units, generally from older to younger, include the Claron Formation (Leith and Harder, 1908; first used on the Markagunt Plateau by Anderson, 1965), the Bear Valley Formation (Anderson, 1971), mudflow and lava-flow breccia and tuffaceous sandstone unit (Maldonado and Moore, 1995), alluvial facies rocks of the Mount Dutton Formation (Anderson and Rowley, 1975), tuffaceous and sedimentary strata of Limerock Canyon (Kurlich, 1990), and several local or uncorrelated, apparently discontinuous successions of fluvial and gravity-emplaced strata.

CLARON FORMATION

Many authors have reviewed and discussed the stratigraphic history of nomenclature of the Claron (formerly Wasatch) Formation, including resumés by Bowers (1972), Anderson and Rowley (1975), and most recently, Rowley and others (1994). Regional topical studies of the Claron in the plateaus of southwestern Utah and adjacent areas have been conducted; chief among these are those by Schneider (1967), who called the unit the Cedar Breaks Formation, Mullett and others (1988a, b), Mullett (1989), and Taylor (1993). This section presents evidence relating to the upper, lower, and intra-unit lithostratigraphic boundaries that have been recognized in mapping on the Markagunt Plateau and Red Hills by us and by D.W. Moore (Moore and others, 1994). These studies include reexamination of previously described Claron exposures and boundary contacts, especially as they relate to the Brian Head Formation, and older Tertiary units that have in the past been generally included in the lowermost Claron (Cashion, 1967; Sable and Hereford, 1990) or with underlying Cretaceous units.

Our field examination of stratigraphic sections reported by previous authors coupled with our review of literature related to the Claron (Wasatch) Formation indicates considerable variation in the placement of Claron unit contacts. Some of our interpretations (see correlation chart, fig. 3) are tentative because many earlier reports, although they describe lithologic criteria used to identify the Claron units, do not specify contact criteria or indicate by descriptive language that different criteria are used in different areas; thus those reports not only are lithologically inconsistent, but also put forth confusing time-stratigraphic relationships.

On the Markagunt Plateau and at least in parts of the southern Sevier and Paunsaugunt Plateaus, the Claron Formation has been generally considered to comprise two units, a lower red or pink member containing fluvial sandstone, conglomerate, siltstone, mudstone, and sandy to argillaceous to relatively pure lacustrine limestone characterized by red, orange, and pink hues; and an upper white to gray member characterized by relatively pure, cliff-forming "white" limestone in the lower part and by tuffaceous sandstone, clay, mudstone, and minor interbedded tuff in the upper part. Some workers have subdivided the upper white to gray member into a lower white limestone unit and an upper gray tuffaceous unit—the gray volcaniclastic unit of the Brian Head Formation of this report. The base of the Claron, generally at the base of red-hued strata, has been mapped, in some cases, to include (or in others, to exclude) conglomerate, sandstone, and shale that are probably equivalent to the Canaan Peak (Upper Cretaceous and Paleocene?), Grand Castle (Paleocene), and Pine Hollow (Paleocene? and Eocene) Formations (Goldstrand and Mullett, this volume, chapter D). For mapping purposes, the base of a red cliff-forming bed of sandstone and calcareous siltstone more than 17 m thick at Cedar Breaks is considered to correspond to the base of the Claron Formation, mainly on the criterion of color. The red hues, however, in the cementing agents, may be the result of secondary staining. Without such staining, the basal bed might be considered as the uppermost bed of the Grand Castle Formation, which it lithologically resembles.

Recent mapping has also revealed the presence of as much as 30 m of intermittently exposed Canaan Peak orthoquartzitic sandstone and Pine Hollow variegated shale (Bowers, 1972) underlying the Claron Formation along the "Pink Cliffs" from Long Valley Junction nearly to Navajo Lake (fig. 2). These lithologic units were previously included in an undivided Cretaceous rock unit by Cashion (1967) and in the basal Claron Formation by Sable and Hereford (1990). In cliffs south of the lake, however, Claron beds rest on Cretaceous sandstone and mudstone of probable Santonian age (Nichols, this volume, chapter E), and lithologically similar but undated strata underlie the Claron along State Highway 14 south of Cedar Breaks National Monument. Within and north of the monument, however, gray sandstone and conglomerate of the Grand Castle Formation (Goldstrand, 1990; Goldstrand and Mullett, this volume, chapter D) underlie basal Claron strata. These three lower Tertiary units are also absent in the Bryce Canyon area, Paunsaugunt Plateau, although a discontinuous conglomerate bed, a possible Grand Castle equivalent, was mapped in the basal Claron Formation there (Bowers, 1990).

The red member of the Claron is a widespread unit; it extends along the western margin and throughout the higher parts of the Markagunt Plateau and adjacent areas. It is as much as 370 m thick in the Red Hills (Threet, 1952a, b), is 400 m thick at Cedar Breaks (our interpretation of Schneider's 1967 data), and is about 244 m thick to the northeast in the Table Cliff Plateau region (Bowers, 1972) (fig. 1).

The white member of the Claron is generally composed of basal and upper distinctive "white" limestone units separated by sandy mudstone or by a succession of mudstone, sandstone, and conglomerate. Regionally, the relationships of the three units of the white member are not yet well understood, as indicated by Moore and others (1994, p. 4). The white member of the Claron is absent in the northern Red Hills; only sporadically present and thin along the western margin of the Markagunt Plateau and possibly the southern Red Hills (Maldonado and Sable, unpub. mapping); about 58–69 m thick at Cedar Breaks (Schneider, 1967; Moore and others, 1994); 26 m thick in the southeastern Markagunt Plateau (Moore and others, 1994); and it averages 168 m thick in the Table Cliff region (Bowers, 1972).

Bowers (1972, p. B27–B28) included in his Wasatch (Claron) Formation an uppermost, variegated sandstone member containing a sporadically occurring distinctive conglomerate characterized by clasts of black chert and light-hued limestone and quartzite overlain by varicolored sandstone, siltstone, and mudstone, including in the northern Table Cliff region, white and gray, "salt-and-pepper" sandstones "that appear to be slightly tuffaceous" in the upper part. The unit is about 80–90 m thick in the Table Cliff Plateau region. Schneider (1967, p. 185–186) included a similar but coarser grained succession about 33 m thick in the uppermost part of his Cedar Breaks Formation (Paleocene and Eocene). According to Schneider, scarce to abundant mica zones, not found by later investigators (Rowley and others, 1994), occur in these beds, and the section is overlain by the "light grays" of the Brian Head Formation. In this report, the variegated sandstone member of Bowers and the upper 33 m of Schneider's Cedar Breaks Formation are provisionally considered to be correlative and are included in the Brian Head Formation. No definitive age evidence has been obtained from the 33-m-thick section, but a late Eocene age is suggested by J.G. Eaton (oral commun., June 1994) based on vertebrate fossils, and by Feist and others (this volume, chapter B) for charophytes in the variegated sandstone member exposed on the Sevier Plateau.

BEAR VALLEY FORMATION, LIMEROCK CANYON UNIT, OTHER UNITS

The simplistic view visualized by early workers that sections of dominantly gray, tuffaceous "salt-and-pepper" sandstone, conglomerate, and associated tuffs exposed in the study region all represented the Brian Head Formation has been undermined by recognition of similar, but distinctly younger clastic sedimentary units such as the Oligocene Bear Valley Formation (Anderson, 1971). This unit contains zeolitic sandstone of eolian and fluvial origin, conglomerate, mudflow breccias, and thin tuff beds. Locally more than 300 m thick, it is dated at about 24.5 Ma (Rowley and others, 1994) and was apparently deposited in local grabens in the northern Markagunt Plateau.

An informal "mudflow and lava-flow breccia and tuffaceous sandstone unit as much as 150 m thick" (Maldonado and Moore, 1995), overlying the Isom Formation, is sporadically exposed along the western front of the Markagunt Plateau and has been recognized as far east as the Panguitch Lake area. The unit contains tuffaceous sandstone similar to that in the Brian Head Formation, along with mudflow breccia that locally contains megaclasts of the 26–27 Ma Baldhills Tuff Member of the Isom Formation and of the 28–30 Ma Needles Range Group. Its stratigraphic position is the same as that of the Bear Valley Formation and it is provisionally correlated with that unit.

Another unit that was incorrectly correlated with the Brian Head Formation is exposed near the town of Hatch in the eastern Markagunt Plateau. This unit was mapped by Kurlich (1990) and informally named "tuffaceous sedimentary strata of Limerock Canyon." The type sections of this unit, according to Kurlich, comprise 76 m of mostly gray, green, white, and bluish-white volcanic wacke and lesser amounts of calcareous, in part silicified, mudstone, tuffaceous siltstone, ash-fall tuff, and tuffaceous conglomerate containing predominant igneous clasts, in contrast to the metamorphic and sedimentary rock clasts dominant in basal Brian Head strata. As mapped by Kurlich, the Limerock Canyon unit directly overlies the white member of the Claron Formation, and contains varicolored chalcedony and dominantly calcareous strata in its lower part that are identical to those in the gray volcaniclastic unit of the Brian Head Formation. Thus, based on lithologic similarities and apparently similar stratigraphic position, the Limerock Canyon was considered to correlate with the Brian Head. However, radiometric ages show clearly that this correlation is invalid.

The Limerock Canyon unit is younger than the Brian Head by more than 10 million years, although their component lithologies are similar. K-Ar age determinations of samples of two poorly welded tuffs from the upper part of the Limerock Canyon unit, along Limestone Creek west of Hatch, yielded ages of 20.2±1.4 and 21.5±0.6 Ma on biotite and 19.8±0.8 and 21.0±1.0 Ma on sanidine (H.H. Mehnert, written commun., January 1992). $^{40}Ar/^{39}Ar$ determinations of a tuff between the two previously dated tuffs in the same stratigraphic section yielded an age of 20.48±0.8 Ma on biotite and 21.0±1.0 Ma on sanidine (L.W. Snee, written commun., 1994).

Further examination of the Limerock Canyon unit and mapping just west of the Hatch area (Sable, unpub. data, 1994) indicate that about 45 m of Limerock Canyon strata unconformably overlies a thin (about 30 m) succession of

Brian Head gray volcaniclastic unit strata that in turn overlies the white member of the Claron Formation. We suggest that the Limerock Canyon unit may be the basal part of extensive alluvial deposits that have been mapped as valley-fill gravels in the eastern Markagunt Plateau (Kurlich, 1990; Moore and others, 1994). Salt-and-pepper sandstone and conglomerate interbedded with coarser valley-fill gravels along the Sevier River 2.5 km north of Hatch closely resemble Limerock Canyon rocks. Work continues on this perplexing problem.

Recent mapping has confirmed the presence of apparently discontinuous thin (less than 15 m) units of tuffaceous sandstone and mudflow breccia between tuffs of the Needles Range Group and the Isom Formation at several locations in the western Markagunt Plateau; these are generally mapped with the Needles Range rocks. Other tuffaceous sandstone and conglomeratic sandstone units of uncertain correlation occur within the Markagunt megabreccia near Panguitch Lake. These contain clasts of ash-flow tuffs, some of which are compositionally identical to the Bauers Tuff Member of the Condor Canyon Formation (23.5–23 Ma). Locally the units underlie mudflow breccias interpreted to be part of the Mount Dutton Formation.

SUMMARY AND CONCLUSIONS

Revival and revision of the Brian Head Formation as a distinctive mappable unit remove it from the underlying Claron Formation with which it had been combined. Brian Head strata, of late Eocene to middle Oligocene age, show evidence of the earliest widespread Tertiary volcanic activity in the region, a precursor to the emplacement of the very widespread Great Basin ash-flow sheets and the voluminous volcanically derived material from the Marysvale volcanic field.

Regionally, the Brian Head Formation occupies the stratigraphic interval between the underlying white member of the Claron Formation and several overlying units, the Needles Range Group, Isom Formation, Mount Dutton Formation, Limerock Canyon unit, and late Tertiary valley-fill fluvial sediments. Along western margins of the Markagunt Plateau and in the northern Red Hills, the Brian Head overlies the older, red member of the Claron Formation, providing evidence for a regional disconformity at the base of the Brian Head. The basal sandstone and conglomerate unit of the formation, containing nontuffaceous sedimentary strata, is provisionally correlated with the variegated sandstone member of the Claron (Wasatch) Formation of the southern Sevier and Table Cliff Plateaus. The base of the middle, gray volcaniclastic unit, characterized by widespread tuffaceous rocks, is also suspected to coincide with a low-angle regional disconformity. The upper, volcanic rock unit is not everywhere present, due either to discontinuous deposition or emplacement or to erosion prior to deposition of overlying units.

Other dominantly sedimentary rock units of Tertiary age which contain strata that resemble those of the Brian Head Formation are relatively thin units between ash-flow tuff sheets of Great Basin origin, the 24 Ma Bear Valley Formation and probable equivalents, and the 20 Ma Limerock Canyon unit. In areas of poor exposure or structural complexity within the Markagunt Plateau correct recognition of such units is extremely difficult.

REFERENCES CITED

Anderson, J.J., 1965, Geology of northern Markagunt Plateau, Utah: Austin, Texas, University of Texas Ph. D. dissertation, 193 p.

———1971, Geology of the southwestern High Plateaus of Utah—Bear Valley Formation, an Oligocene-Miocene volcanic arenite: Geological Society of America Bulletin, v. 82, p. 1179–1205.

———1993, The Markagunt megabreccia—Large Miocene gravity slides mantling the northern Markagunt Plateau, southwestern Utah: Utah Geological Survey Miscellaneous Publication 93–2, 37 p.

Anderson, J.J., Iivari, T.A., and Rowley, P.D., 1987, Geologic map of the Little Creek Peak quadrangle, Garfield and Iron Counties, Utah: Utah Geological and Mineral Survey Map 104, scale 1:24,000.

Anderson, J.J., and Kurlich, R.A., III, 1989, Post-Claron Formation, pre-regional ash-flow tuff early Tertiary stratigraphy of the southern High Plateaus of Utah: Geological Society of America Abstracts with Programs, v. 21, no. 5, p. 50.

Anderson, J.J., and Rowley, P.D., 1975, Cenozoic geology of southwestern High Plateaus of Utah, *in* Anderson, J.J., Rowley, P.D., Fleck, R.V., and Nairn, A.E.M., Cenozoic geology of southwestern High Plateaus of Utah: Geological Society of America Special Paper 160, p. 1–51.

———1987, Geologic map of the Panguitch NW quadrangle, Iron and Garfield Counties, Utah: Utah Geological and Mineral Survey Map 103, scale 1:24,000.

Bowers, W.E., 1972, The Canaan Peak, Pine Hollow, and Wasatch Formations in the Table Cliff region, Garfield County, Utah: U.S. Geological Survey Bulletin 1331–B, 39 p.

———1990, Geologic map of Bryce Canyon National Park and vicinity, southwestern Utah: U.S. Geological Survey Miscellaneous Investigations Series Map I–2108, scale 1:24,000.

Cashion, W.B., 1967, Geologic map of the south flank of the Markagunt Plateau, northwest Kane County, Utah: U.S. Geological Survey Coal Investigations Map C–49, scale 1:62,500.

Eaton, J.G., 1995, A late Eocene fauna from undescribed strata overlying the Claron Formation, Sevier Plateau, southwestern Utah: Geological Society of America Bulletin, v. 107, p. 10.

Fleck, R.J., Anderson, J.J., and Rowley, P.D., 1975, Chronology of mid-Tertiary volcanism in High Plateaus region of Utah, *in* Anderson, J.J., Rowley, P.D., Fleck, R.J., and Nairn, A.E.M., Cenozoic geology of southwestern High Plateaus of Utah: Geological Society of America Special Paper 160, p. 53–61.

Goldstrand, P.M., 1990, Stratigraphy and paleogeography of Late Cretaceous and Paleogene rocks of southwest Utah: Utah Geological and Mineral Survey Miscellaneous Publication 90–2, 58 p.

Gregory, H.E., 1944, Geologic observations in the upper Sevier River Valley, Utah: American Journal of Science, v. 242, p. 577–607.

———1945, Post-Wasatch Tertiary formations in southwestern Utah: Journal of Geology, v. 53, p. 105–115.

———1949, Geologic and geographic reconnaissance of eastern Markagunt Plateau, Utah: Geological Society of America Bulletin, v. 60, p. 969–998.

———1950, Geology of eastern Iron County, Utah: Utah Geological and Mineralogical Survey Bulletin 37, 153 p.

———1951, The geology and geography of the Paunsaugunt region, Utah: U.S. Geological Survey Professional Paper 226, 116 p.

Hintze, L.F., 1988, Geologic history of Utah: Brigham Young University Geology Studies, Special Publication 7, 202 p.

Judy, J.R., 1974, Geologic evolution of the west-central Markagunt Plateau, Utah: Kent, Ohio, Kent State University M.S. thesis, 120 p.

Kurlich, R.A., III, 1990, Geology of the Hatch 7.5-minute quadrangle, Garfield County, southwestern Utah: Kent, Ohio, Kent State University M.S. thesis, 154 p.

Kurlich, R.A., III, and Anderson, J.J., 1991, Preliminary geologic map of the Hatch 7.5-minute quadrangle, Garfield County, southwestern Utah: U.S. Geological Survey Open-File Report 91–37, 7 p., scale 1:24,000.

Leith, C.K., and Harder, E.C., 1908, The iron ores of the Iron Springs district, southern Utah: U.S. Geological Survey Bulletin 338, 102 p.

Maldonado, Florian, 1995, Decoupling of mid-Tertiary rocks, Red Hills–western Markagunt Plateau, southwestern Utah, chapter I *in* Scott, R.B., and Swadley W C, eds., Geologic studies in the Basin and Range–Colorado Plateau transition in southeastern Nevada, southwestern Utah, and northwestern Arizona, 1992: U.S. Geological Survey Bulletin 2056, p. 233–254.

Maldonado, Florian, and Moore, R.C., 1990, Shallow detachment of mid-Tertiary rocks, Red Hills (Basin and Range), with implications for a regional detachment zone in the adjacent Markagunt Plateau (Colorado Plateau), southwest Utah: Geological Society of America Abstracts with Programs, v. 22, no. 3, p. 63.

———1992, Evidence for a Tertiary low-angle shear zone, Red Hills, with implications for a regional shear zone in the adjacent Colorado Plateau, *in* Harty, K.M., ed., Engineering & environmental geology of southwestern Utah: Utah Geological Association Publication 21, 1992 Field Symposium, p. 315–323.

———1995, Geology of the Parowan quadrangle, Iron County, Utah: U.S. Geological Survey Geologic Quadrangle Map GQ-1762, scale 1:24,000.

Maldonado, Florian, and Williams, V.S., 1993a, Geologic map of the Parowan Gap quadrangle, Iron County, Utah: U.S. Geological Survey Geologic Quadrangle Map GQ–1712, scale 1:24,000.

———1993b, Geologic map of the Paragonah quadrangle, Iron County, Utah: U.S. Geological Survey Geologic Quadrangle Map GQ–1713, scale 1:24,000.

Moore, D.W., Nealey, L.D., and Sable, E.G., 1994, Preliminary report, measured sections, and map of the geology of the Asay Bench quadrangle, Garfield and Kane Counties, Utah: U.S. Geological Survey Open-File Report 94–10, scale 1:24,000.

Mullett, D.J., 1989, Interpreting the early Tertiary Claron Formation of southern Utah: Geological Society of America Abstracts with Programs, v. 21, no. 5, p. 120.

Mullett, D.J., Wells, N.A., and Anderson, J.J., 1988a, Early Cenozoic deposition in the Cedar-Bryce depocenter—Certainties, uncertainties, and comparisons with other Flagstaff–Green River Basins: Geological Society of America Abstracts with Programs, v. 20, no. 3, p. 217.

———1988b, Unusually intense pedogenic modification of the Paleocene-Eocene Claron Formation of southwestern Utah: Geological Society of America Abstracts with Programs, v. 20, no. 5, p. 382.

Rowley, P.D., 1968, Geology of the southern Sevier Plateau, Utah: Austin, Texas, University of Texas Ph. D. dissertation, 385 p.

Rowley, P.D., Hereford, Richard, and Williams, V.S., 1987, Geologic map of the Adams Head–Johns Valley area, southern Sevier Plateau, Garfield County, Utah: U.S. Geological Survey Miscellaneous Investigations Series Map I–1798, scale 1:50,000.

Rowley, P.D., Mehnert, H.H., Naeser, C.W., Snee, L.W., Cunningham, C.G., Steven, T.A., Anderson, J.J., Sable, E.G., and Anderson, R.E., 1994, Isotopic ages and stratigraphy of Cenozoic rocks of the Marysvale volcanic field and adjacent areas, west-central Utah: U.S. Geological Survey Bulletin 2071, 35 p.

Sable, E.G., and Hereford, Richard, 1990, Preliminary geologic map of the Kanab 30×60-minute quadrangle, Utah and Arizona: U.S. Geological Survey Open-File Report 90–542, scale 1:100,000.

Schneider, M.C., 1967, Early Tertiary continental sediments of central and south-central Utah: Brigham Young University Geology Studies, v. 14, p. 143–194.

Taylor, W.J., 1993, Stratigraphic and lithologic analysis of the Claron Formation in southwestern Utah: Utah Geological Survey Miscellaneous Investigations Publication 93–1, 52 p.

Threet, R.L., 1952a, Geology of the Red Hills Area, Iron County, Utah: Seattle, Wash., University of Washington Ph. D. dissertation 7310, 107 p.

———1952b, Some problems of the Brian Head (Tertiary) Formation in southwestern Utah: Geological Society of America Bulletin, v. 63, no. 11, p. 1386.

Significance of Charophytes from the Lower Tertiary Variegated and Volcaniclastic Units, Brian Head Formation, Casto Canyon Area, Southern Sevier Plateau, Southwestern Utah

By Monique Feist, Jeffrey G. Eaton, Elisabeth M. Brouwers, *and* Florian Maldonado

GEOLOGIC STUDIES IN THE BASIN AND RANGE–COLORADO PLATEAU TRANSITION IN SOUTHEASTERN NEVADA, SOUTHWESTERN UTAH, AND NORTHWESTERN ARIZONA, 1995

U.S. GEOLOGICAL SURVEY BULLETIN 2153–B

UNITED STATES GOVERNMENT PRINTING OFFICE, WASHINGTON : 1997

CONTENTS

PLATE

FIGURES

Significance of Charophytes from the Lower Tertiary Variegated and Volcaniclastic Units, Brian Head Formation, Casto Canyon Area, Southern Sevier Plateau, Southwestern Utah

By Monique Feist,[1] Jeffrey G. Eaton,[2] Elisabeth M. Brouwers, *and* Florian Maldonado

ABSTRACT

Sparse charophyte gyrogonites representing the new combination *Stephanochara* aff. *Stephanochara vera* (Hu and Zeng) are described from the variegated and volcaniclastic units of the Paleogene Brian Head Formation in the Casto Canyon quadrangle. Based on documented ages of the charophyte species in the People's Republic of China, we infer that the basal part of the Brian Head Formation has a maximum age of middle Eocene.

INTRODUCTION

Specific ages, original depositional environments, and correlation of lower Tertiary sedimentary rocks exposed in southwestern Utah have been difficult to evaluate because of discontinuous exposures, facies changes, and post-depositional diagenetic alteration of sediments. In this report, we focus on nonmarine deposits of the Brian Head and Claron Formations exposed in the 7.5-minute Casto Canyon quadrangle, southern Sevier Plateau (figs. 1 and 2). Cretaceous and Paleocene nonmarine sedimentary rocks underlie these Paleogene units, and Oligocene and younger volcanic rocks overlie them.

This report documents a sparse, low-diversity charophyte flora collected from the variegated unit, considered to be the basal part of the Brian Head Formation, and from overlying volcaniclastic sediments of the Brian Head Formation. During reconnaissance field work in 1994 we identified several localities, in addition to those reported here, which contain nonmarine ostracodes and charophytes from Upper Cretaceous strata of the Kaipairowits Plateau and from the Paleogene Brian Head Formation. During 1995 we plan to further examine and collect the sedimentary rocks and fossils of the Claron and Brian Head Formations in order to better understand the paleoenvironmental and diagenetic history of southwestern Utah during the Eocene and Oligocene. Jeffrey G. Eaton (Utah Museum of Natural History, Salt Lake City, Utah) and Thomas M. Bown (U.S. Geological Survey, Denver, Colorado) have identified initial collections of abundant and diverse ichnofossil (trace fossil) assemblages from the Claron Formation (see Bown and others, this volume), which have yielded information on the paleoclimate and paleoenvironment of these units. The ichnofossil collections will also be supplemented during 1995 field work.

GEOLOGIC SETTING

Beginning in the latest part of the Cretaceous and ending during the Paleogene, the Sevier foreland basin in Utah and Nevada was deformed during the Laramide orogeny, producing a geographically complex province of basement-cored and thrust-bounded uplifts separated by numerous, isolated, internally drained basins (Dickinson and others, 1986; Goldstrand, 1992, 1994). Our study area is within the eastern part of the structural transition zone that separates the Basin and Range province from the Colorado Plateaus province. Upper Cretaceous and lower Tertiary nonmarine sedimentary rocks predominate in the four uplifted plateaus shown in figure 1 (the Markagunt, Paunsaugunt, Table Cliff, and Kaiparowits Plateaus).

Active upwarping was still occurring in the southern Markagunt and Paunsaugunt Plateaus during the early Paleocene, as evidenced by pinching out and absence of the Grand Castle Formation (Goldstrand, 1994). This stage of uplift and erosion is also evidenced by conglomerates of the Canaan Peak Formation that were reworked into the basal

[1] Institut des Sciences de l'Evolution, Université de Montpellier, 34095 Montpellier Cedex 05, France.

[2] Utah Museum of Natural History, The University of Utah, Salt Lake City, Utah 84112.

part of the Claron Formation. Sandstones and conglomerates of the basal Claron Formation represent sediments deposited in a broad basin that developed in the Pine Valley Mountains area, the southern Paunsaugunt Plateau, and the Markagunt Plateau, beginning in late Paleocene time and continuing into the Eocene. Overlap of anticlinal structures by the Claron Formation indicates the time of cessation of the Laramide orogeny, estimated to be about 50 Ma (Goldstrand, 1991).

Sedimentary strata in the basal part of the Claron Formation in southwestern Utah represent deposition in internally drained basins that developed between Laramide uplifted areas. From early Paleocene to middle Eocene time, fluvial and lacustrine deposition occurred in the Claron intermontane basins, with marginal lacustrine shorelines transgressing northeastward (Goldstrand, 1994). Alluvial, fluvial, and restricted lacustrine environments prevailed during the Paleocene and early Eocene.

The Brian Head Formation, overlying the Claron Formation, provides a record of the earliest extensive post-Laramide volcanism in southwestern Utah. The Brian Head is a complex unit that consists predominantly of fluvial strata and to a lesser extent lacustrine-derived and volcanic rocks. The upper part of the Brian Head Formation consists of mudflow breccia, sandstone, conglomerate, minor mafic rocks, and ash-flow tuff. The contact between the Brian Head and overlying, structurally autochthonous ash-flow tuff of the Needles Range Group is sharp (Sable and Maldonado, this volume, chapter A). However, in the Red Hills–western Markagunt Plateau area, the upper contact of the Brian Head is suggested to be structural in nature (Maldonado and others, 1992; Maldonado, 1995).

A period of volcanic activity and sediment deposition marks Oligocene and Miocene time in southwestern Utah and adjacent parts of southeastern Nevada. Ash-flow tuffs, alluvial sediments, and tuffaceous sedimentary rocks are present in units younger than the Brian Head Formation. These units include the Needles Range Group, Isom Formation, Mount Dutton Formation, Leach Canyon Formation, and Limerock Canyon rock units.

STRATIGRAPHY

CLARON FORMATION

The Claron Formation was defined by Leith and Harder (1908) in the Iron Springs mining district, 100 km west of our study area. No type section was designated and no measured section was published, although it seems likely that Leith and Harder were referring to an outcrop at Mount Claron east of Iron Mountain (SW sec. 27, T. 36 S., R. 13 W., Desert Mound 7.5-minute quadrangle). The description by

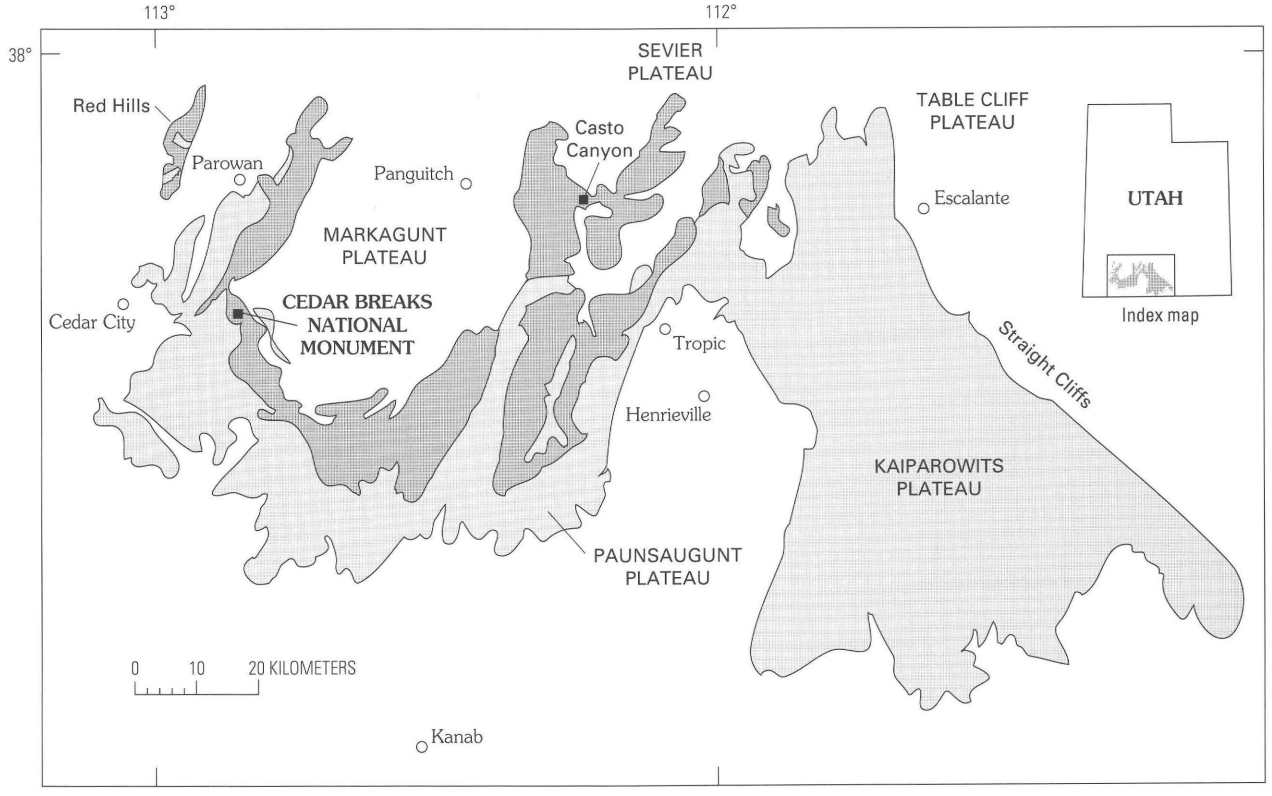

Figure 1. Localities and distribution of generalized sedimentary and volcaniclastic rocks of the study area. Light shade, undifferentiated Cretaceous outcrops; darker shade, lower Tertiary exposures.

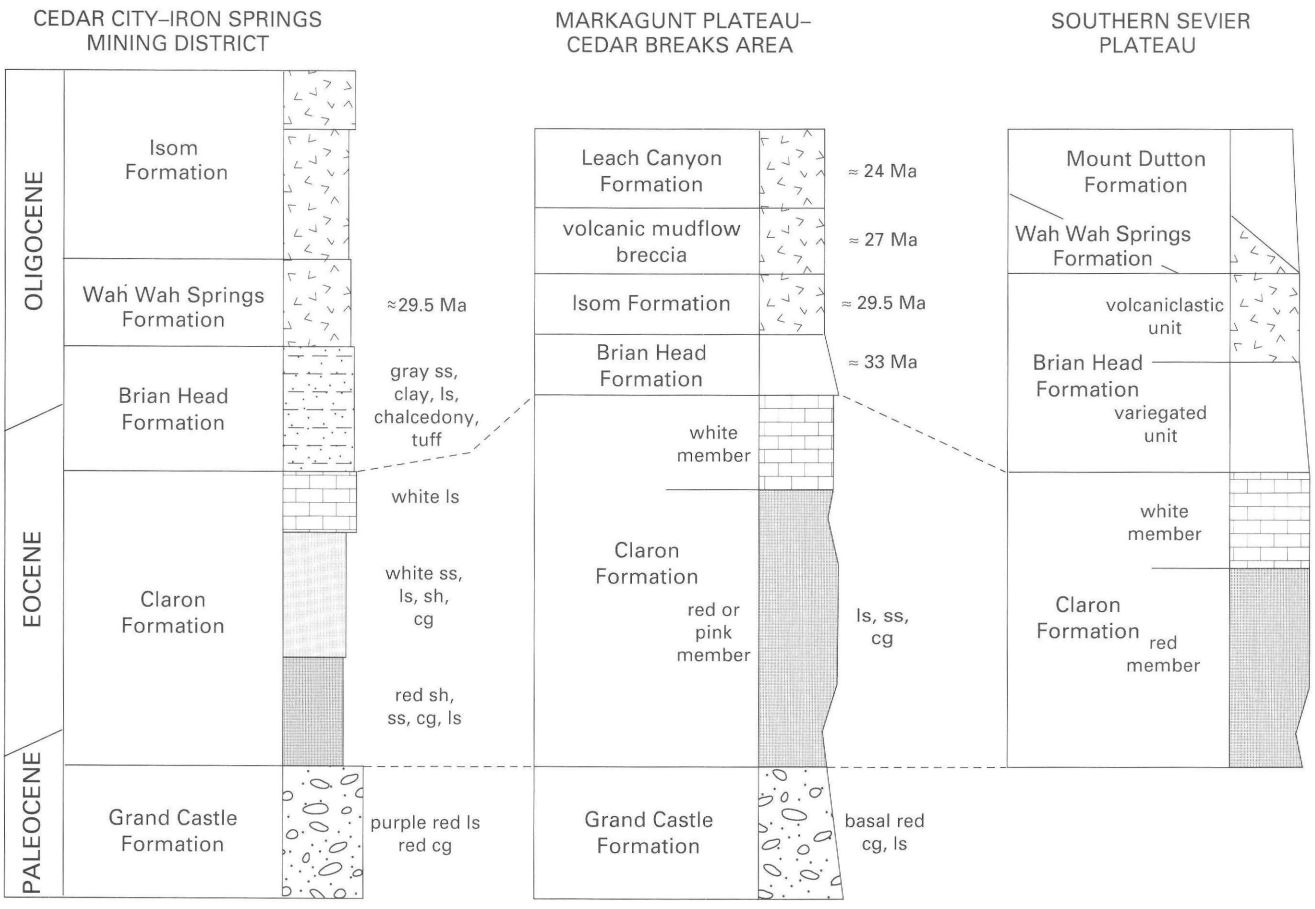

Figure 2. Schematic diagram of stratigraphic sequence in western part of study area near Cedar City–Iron Springs mining district, along west side of Markagunt Plateau near Cedar Breaks National Monument, and in southern part of Sevier Plateau.

Leith and Harder refers to a unit that consists mostly of limestone about 300 m in thickness. The name Claron was extended eastward to the plateau region by Mackin (1954, 1960), Cook (1957, 1965), and Averitt (1967). Other names proposed for the pink and white limestone include the Cedar Breaks Formation (Schneider, 1967), the informal Bryce Canyon beds (McFall, 1955), and Wasatch Formation (Bowers, 1972). Anderson and Rowley (1975) combined the rocks previously assigned to Brian Head and Wasatch Formations in southwestern Utah into the Claron Formation.

In southwestern Utah, the name Claron Formation was applied by Robison (1966) to a sequence of red and white limestones cropping out in the southwest margin of the Sevier Plateau. Robison divided the unit into a lower, pink member about 300 m thick and an upper, white member at least 200 m thick. Bowers (1972) used the term Wasatch Formation (originally named for lacustrine and fluvial sediments in central and northeastern Utah) for lower Tertiary rocks east of the Sevier and Paunsaugunt Plateaus, in the Table Cliff region. He divided beds previously assigned to the lowermost part of the Wasatch into two new formations, the Canaan Peak and the Pine Hollow. Bowers redefined the "Wasatch Formation" in the Table Cliff area to include the pink limestone member and the white limestone member, and he added an uppermost "variegated sandstone member." Bowers (1990) recognized the term Claron Formation in his report on the geology of Bryce Canyon. The variegated sandstone member, which we here call the "variegated unit," has previously been correlated with the lower part of the redefined Brian Head Formation. Sable and Maldonado (this volume) correlate the variegated unit with the basal sandstone and conglomerate unit of the Brian Head Formation described from the Markagunt Plateau, west of our study area (fig. 1).

Strata of the Claron Formation have been interpreted to represent fluvial and lacustrine deposition in the internally drained basins that were flanked by Laramide uplifted areas. Mullett and others (1988) and Mullett (1989) described much of the Claron as having been altered by pedogenic processes. Bown and others (this volume, chapter C) describe ichnofossils developed on these paleosols. Diagenetic alteration of the original lithology by pedogenesis has probably destroyed most of the original fluvial and lacustrine invertebrate fossils; only a few nonmarine gastropods have been recovered, in contrast to the very fossiliferous Wasatch Formation to the north.

The Claron Formation directly underlies the variegated unit of the Brian Head Formation. Any age determinations for the Claron Formation therefore provide maximum age constraints for the overlying Brian Head Formation. Most suggestions for the age of the Claron have been based on stratigraphic position, but scattered paleontological data provide some relative ages. Schneider (1967) suggested a Paleocene to earliest Eocene age for the lower Claron (his lower Cedar Breaks Formation) based on a correlation with the Flagstaff Limestone. Nonmarine gastropods collected from the Claron Formation include *Viviparus trochiformis*, *Goniobasis* sp., and *Physa* sp. (Eaton *in* Goldstrand, 1994); these taxa occur in the Paleocene to Eocene Flagstaff Limestone of central Utah. Goldstrand (1991) and Goldstrand and others (1993) reported a late Paleocene age for the lower part of the Claron Formation in the Pine Valley Mountains based on the palynomorph flora. Goldstrand (1994) suggested a middle Eocene age for the basal Claron Formation in the Table Cliff Plateau area based on fission-track analyses from the upper part of the underlying Pine Hollow Formation. This suggests a time-transgressive younging of the basal beds of the Claron Formation from west to east. Goldstrand (1994) noted that preliminary mammalian fossil ages from an overlying mudstone unit northwest of Table Cliff Plateau indicate that the upper Claron is no younger than latest Eocene (data of J.G. Eaton).

BRIAN HEAD FORMATION

The name Brian Head Formation was first used by Gregory (1945) for volcaniclastic rocks on the Markagunt Plateau. The name was abandoned by Anderson and Rowley (1975) because of confusion over what Gregory had intended to include within the formation. The name Brian Head Formation (restricted) was reintroduced as a useful genetic and stratigraphic unit by Anderson (1993), and the formation is described in detail by Sable and Maldonado (this volume). For the purposes of this report, we divide the Brian Head Formation into the informal "variegated" and "volcaniclastic" units.

VARIEGATED UNIT

Bowers (1972, p. B27) assigned a sequence "of interbedded red, pink, and purplish-gray very fine grained friable sandstone, siltstone, mudstone, and limy mudstone and gray to white fine- to medium-grained sandstone and calcareous sandstone" to the "variegated sandstone member" of the Wasatch Formation. Bowers suggested a range of 100–200 m for the thickness of the unit on the Table Cliff Plateau. He described a conglomerate (the "conglomerate at Boat Mesa"; Bowers, 1990) occurring between the Claron and Sevier Formations that is as much as 30 m thick and that contains conspicuous black chert pebbles. Gregory (1945) correlated these beds with his Brian Head Formation. This conglomerate is well developed along the southwest margin of the Sevier Plateau, where it forms the sharply defined top of the white limestone cliffs, which are made up of the upper white member of the Claron Formation. The conglomerate matrix is a white carbonate mudstone containing matrix-supported chert pebbles. The conglomerate is not genetically part of the Claron Formation, but it is difficult to map separately from the white limestone member. The term "sandstone" has been omitted from the original member name of Bowers (1972) in this report because the variegated unit is comprised dominantly of finer grained sediments. Because the variegated unit is distinct from other lithologies of the Brian Head Formation and because the Brian Head was not clearly described until this volume (Sable and Maldonado), we informally refer to these sediments as the variegated unit of the Brian Head Formation.

The variegated unit ranges from 16 to 38 m thick in the Casto Canyon 7.5-minute quadrangle, located along the southwest margin of the Sevier Plateau (fig. 1); this is the region where Rowley (1968) measured 290 m of strata that he called upper Claron Formation. Sixteen meters of the variegated unit was measured by Eaton at $SW^1/_4$ $SW^1/_4$ $SW^1/_4$ sec. 29, T. 34 S., R. 4 W., along the east side of Hancock Canyon, and 38 m was measured 2 miles (≈3.2 km) to the northwest in the $SE^1/_4$ sec. 13, T. 34 S., R. 4 W., in a tributary of the South Fork of Limekiln Creek. The variegated unit is lithologically the most similar to the Wasatch Formation of any Wasatch-equivalent units in southwestern Utah to which that name has been applied. The variegated unit consists of gray mudstones, yellow-gray mottled mudstones, deep red siltstones, orange mudstones, and relatively rare gray-brown sandstones. A thin (few centimeters), gray, carbonate bed containing gastropods and bivalve fragments is locally present. Several horizons have yielded vertebrate remains, including mammals, turtles, crocodiles, and fish; these vertebrates are presently under study by Eaton and Hutchison (1995 and work in progress).

The variegated unit is clearly thinner on the western Sevier Plateau than in the Table Cliff Plateau area and is absent on the eastern Markagunt Plateau, where the volcaniclastic unit overlies the white member of the Claron Formation. Sable and Maldonado (this volume) have redefined the Brian Head Formation on the Markagunt Plateau and subdivided it into three informal units: the lower sandstone and conglomerate unit, the gray volcaniclastic rocks unit, and the upper volcanic rocks unit. Sable and Maldonado suggest that the variegated unit may be equivalent to the sandstone and conglomerate unit of the Brian Head Formation.

The variegated unit is lithologically distinct from the underlying cliffs of the upper white member of the Claron and from the overlying volcaniclastic sediments of the Brian Head Formation.

The age of the variegated unit is not well constrained. Bowers (1972) suggested an Eocene age for the unit based on stratigraphic position. Since then, the unit has not been referred to in the literature, so no other age estimates are available. A complex assemblage of vertebrate fossils of late Eocene age from the variegated unit has been reported by Eaton and Hutchison (1995).

VOLCANICLASTIC UNIT

Overlying the variegated unit is a thick sequence (more than 300 m) dominated by volcaniclastic sediments, which are lithologically almost identical and probably coeval with the middle part of the Brian Head Formation, the gray volcaniclastic rocks unit described from the Markagunt Plateau by Sable and Maldonado (this volume). The overall color of the volcaniclastic unit is gray, but layers of bright green, orange, and lavender are present. Lithologies include thick bentonitic mudstones and sandstones. Rare conglomerates contain Paleozoic chert, quartzite, and igneous rock pebbles and cobbles. Volcaniclastic chalcedony lenses are characteristic of the unit. The volcaniclastic unit is well exposed on southwest-facing slopes in the NW sec. 29, T. 34 S., R. 4 W., Casto Canyon 7.5-minute quadrangle.

Until recently, no fossils had been reported from the volcaniclastic unit of the Brian Head Formation. Fossil turtles, mammals, and fish (under study by Eaton and Hutchison, 1995) have been recovered from locality JGE 9202, located stratigraphically low in the volcaniclastic unit (fig. 3). Eaton and Hutchison (1995) have reported a late Eocene vertebrate fauna from this unit.

Minimum age constraints for the volcaniclastic unit are based on two isotopic dates reported from ash-flow tuffs in the upper volcanic rocks unit of the Brian Head Formation and from an overlying tuff of the Needles Range Group.

Maximum age constraints are based on several isotopic dates in Brian Head equivalent units. An ash-flow tuff mapped in a Brian Head equivalent unit by Anderson and others (1990) in the Bear Valley area gave a K-Ar date of 31.9 $\pm$ 0.5 Ma (Fleck and others, 1975). Three isotopic dates were derived from a single ash-flow tuff interbedded with Brian Head equivalent units in the Red Hills (Maldonado and Williams, 1993): (1) a K-Ar date of 34.2 $\pm$ 2.1 Ma on plagioclase (H.H. Mehnert, written commun., 1992); (2) a $^{40}Ar/^{39}Ar$ date of 33.00 $\pm$ 0.13 Ma on plagioclase (L.W. Snee, written commun., 1994); and (3) a $^{40}Ar/^{39}Ar$ date of 33.70 $\pm$ 0.14 Ma on biotite (L.W. Snee, written commun., 1994).

YOUNGER VOLCANIC ROCKS

In the study area, the volcaniclastic unit is overlain by mudflow and lahar breccias of the Mount Dutton Formation. An age range of 26–21 Ma was published by Anderson and Rowley (1975) for the formation; recently Rowley and others (1994) have expanded the age range to 32–21 Ma. Locally, where the Mount Dutton Formation is missing, the volcaniclastic unit is overlain by the Wah Wah Springs Formation of the Needles Range Group (Rowley and others, 1994). The Wah Wah Springs Formation is a dacite ash-flow tuff that has been dated as 29.5 Ma by Best and Grant (1987), and as 29.1–32.4 Ma based on K/Ar by H.H. Mehnert (written commun., 1987) as reported in Rowley and others (1994).

CHAROPHYTE LOCALITIES

During screen washing for micro-vertebrates, several dozen charophyte gyrogonites were recovered from two sedimentary horizons in the Brian Head Formation (fig. 3). Charophytes from the lower variegated unit were recovered by Eaton in June 1992 (field number 9201) along the east margin of a line between the SW and NW quadrants of section 5, T. 35 S., R. 4 W., Casto Canyon 7.5-minute quadrangle, Garfield County, Utah (fig. 2). The locality is on the west side of Tent Hollow, the southernmost outcrops of gray siltstones above the south tributary to Casto Creek. The locality is a few meters above a pebble conglomerate bed containing chert and quartzite clasts in a carbonate matrix, interpreted to be just above the top of the white member of the Claron Formation. The locality is thus a few meters above the base, or stratigraphically very low, in the variegated unit.

Charophytes from the upper volcaniclastic unit of the Brian Head Formation were discovered by Eaton in June 1992 (field number JGE 9202) approximately at the NW SE NW section 29, T. 34 S., R. 4 W., Casto Canyon 7.5-minute quadrangle, Garfield County, Utah. The locality is on the west side of the easternmost amphitheater on the east margin of the Casto Canyon quadrangle. Charophytes were recovered from a greenish-gray bentonitic layer interbedded with whitish-gray siltstones near the top of a drab gray silty section that underlies a prominent lavender-colored layer, which in turn underlies a distinctive orange-colored sequence. The conglomeratic bed referred to in the preceding paragraph and the variegated unit are both present in the drainage (E$^1/_2$NE SE sec. 30) leading to the locality. The beds are relatively flat lying and the sampled horizon is no more than 37 m above the top of the variegated unit, within the lower part of the volcaniclastic unit.

CHAROPHYTE ANALYSIS

TAXONOMY

Order CHARALES

Family CHARACEAE

Subfamily CHAROIDEAE

Genus *STEPHANOCHARA* Grambast

The species occurring in the variegated and volcaniclastic units of the Brian Head Formation is very similar to *Eotectochara vera* Hu and Zeng, 1982. Following the generic criteria established by Feist and Grambast-Fessard (1982, 1991), the genus described as *Eotectochara* Hu and Zeng (1982) is characterized by gyrogonites that possess prominent apical nodules surrounded by a periapical groove, and lacking a noticeable reduction of the cellular width and thick basal plate; this falls within the definition of *Stephanochara* Grambast. We assign the three species formerly included in *Eotectochara* into *Stephanochara*:

Genus *STEPHANOCHARA* Grambast, 1959=*EOTECTOCHARA* Hu and Zeng, 1982, Beijing Geological Memoirs (2) 1, p. 562.

Stephanochara hunanensis n. comb.=*Eotectochara hunanensis* Hu and Zeng, 1982, Beijing Geological Memoirs (2) 1, p. 562, pl. 372, figs. 1–7.

Stephanochara vera n. comb.=*Eotectochara vera* Hu and Zeng, 1982, Beijing Geological Memoirs (2) 1, p. 563, pl. 372, figs. 8–15.

Stephanochara yuanshuiensis n. comb.=*Eotectochara yuanshuiensis* Hu and Zeng, 1982, Beijing Geological Memoirs (2) 1, p. 563, pl. 372, figs. 16–19.

***STEPHANOCHARA* aff. *S. VERA* (Hu and Zeng) n. comb.**

Plate 1, figures 1–8

Material.—Thirty-two specimens from the variegated unit and 16 specimens from the volcaniclastic unit, both from the lower part of the Brian Head Formation.

Description.—The gyrogonites are pear shaped with a convex apex and salient base. The apical ends of the spiral cells bear prominent rounded nodules; at the periphery of the apex, the width of the spirals is not modified, but their thickness is strongly reduced. The basal ends of the spiral are thickened, forming a funnel-shaped basal opening. The basal plate is simple, pentahedral, as large as thick. The spiral surface bears a medium crest, either continuous or divided into tubercles of variable size. The medium crest persists to the apex.

Dimensions. (based on 32 specimens from sample JGE 9201):

	Convolutions	*Length (micrometers)*	*Width (micrometers)*	*Isopolarity index*
Maximum	11	1,100	950	136
Minimum	9	930	750	111
Average	10	997	829	120

Affinities.—Based on the characters of the apex and the base of the gyrogonite, the species from the Brian Head Formation is related to *Stephanochara.* Among the species referred to this genus, it shows the most resemblance to *Stephanochara vera* (Hu and Zeng) new combination, previously reported from the Hunan Province of southern People's Republic of China (Hu and Zeng, 1982, 1985). The gyrogonite shape, with the upper part rounded and the base tapered, and the dimensions are similar. The American form differs in having better developed ornamentation of the spiral cells and a slightly larger gyrogonite width (750–950 µm versus 714–867 µm for the samples from Hunan). These slight differences do not justify the distinction of a new species, and we therefore consider the species from Utah as *affinis* to *S. vera.* The great geographic distance between the two localities or a slight difference in age could explain these morphological variations.

POSITION OF *STEPHANOCHARA* AFF. *S. VERA* AMONG EARLY TERTIARY CHAROPHYTE FLORAS OF NORTH AMERICA

Among the few reports describing Tertiary charophytes from North America, only *"Tectochara" matura* Holifield is similar to *Stephanochara* aff. *S. vera.* The thick basal plate and the prominent apical nodules, surrounded by a periapical groove with a slight reduction of cellular width, are similar in both species. *"Tectochara" matura* differs by being much larger in size and by its weakly developed ornamentation. The characters of the apex and base show that *"T." matura* should be referred to *Stephanochara.* However, revision of this species is beyond the scope of this report.

Holifield (1964) reported *"Tectochara" matura* from the Paleocene Flagstaff Member of the Green River Formation in San Pete County, Utah. The specimen illustrated on plate 1, figure 9 was recently collected by Feist in East Colton, Utah, from a coeval horizon with Holifield's Flagstaff locality; the East Colton locality has also yielded the Nitelloideae charophyte *Tolypella pecki* (Feist and Brouwers, 1990).

PALEOECOLOGY

The Brian Head Formation has yielded a single species of *Stephanochara* that is very closely related to *S. vera* Hu and Zeng, an Eocene charophyte species described from the Hunan region in China. It is on the basis of this species that we interpret the paleoenvironments prevailing during deposition of the Brian Head Formation.

A considerable amount of information is available on the ecology of extant charophytes (Wood, 1965 and references therein). In contrast, little has been published on the

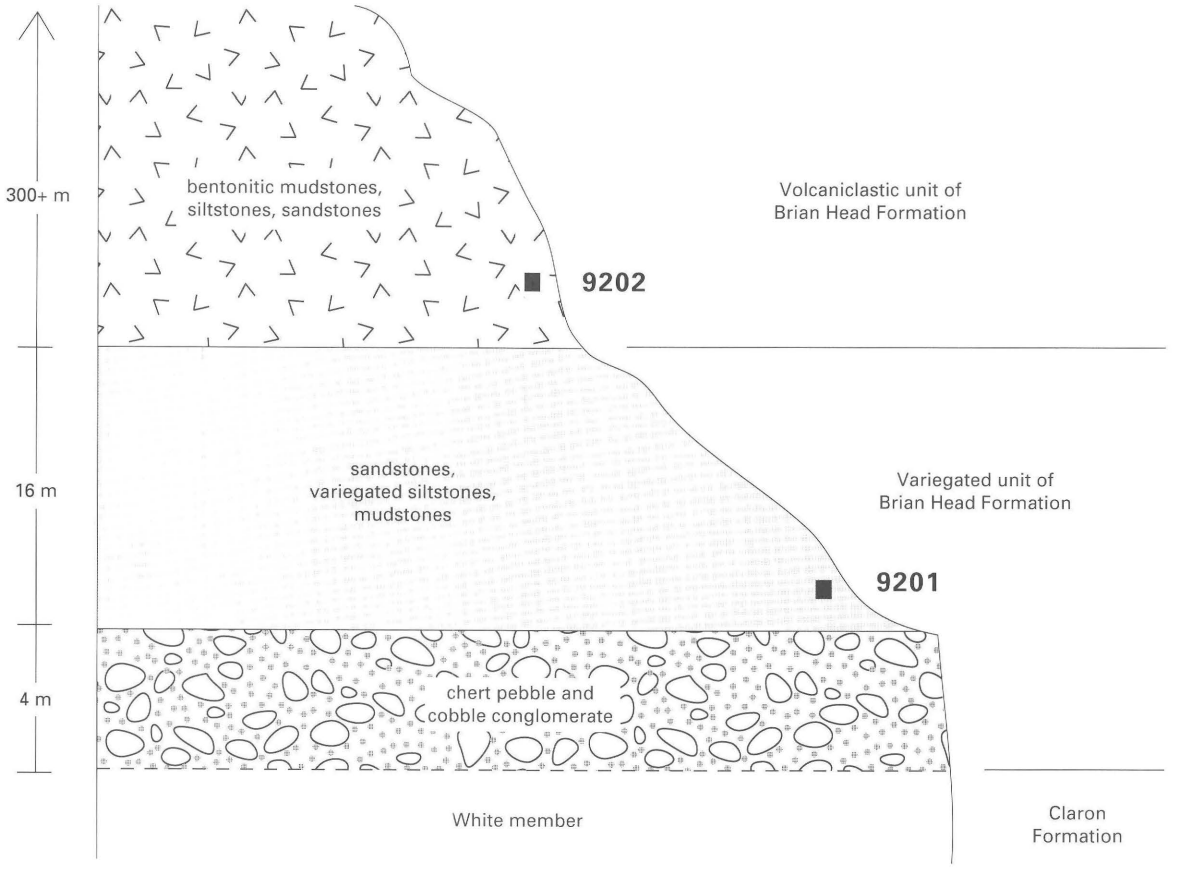

Figure 3. Schematic of lithologic sequence in Casto Canyon 7.5-minute quadrangle, showing relative stratigraphic position of the two charophyte samples collected by Eaton within the variegated and volcaniclastic units of the Brian Head Formation.

paleoecology of fossil forms with the exception of recent studies (Tambareau and others, 1991; Schudack, 1993; Soulie-Maersche, 1993; Lucas and Kietzke, 1994). The ecology of extant and fossil forms is similar, so we will reference extant ecology in our interpretations.

Most living charophyte species grow in quiet, clear water with a high pH. They are superficially fixed on a substratum which may be mud, sand, or silt-covered peat and sand (Moore, 1986). The climate, hardness, and salinity of water are the most obvious factors affecting their distribution (Corillion, 1975).

Climate.—The great majority of extant calcified species producing calcified and thus fossilizable oogonia are found in temperate and intertropical zones, and the fossil record shows the same general distribution. It has been shown that analysis of charophyte data, and even of lacustrine deposits in general, does not allow for direct extrapolation to paleoclimatology (Soulie-Maersche, 1993; Gasse and others, 1987).

Hardness.—In extant forms, 15 to 200 mg/liter of calcium carbonate is necessary for the calciphilous species (Corillion, 1975). In the Brian Head Formation, *Stephanochara* aff. *S. vera* lived under these conditions, as suggested by the carbonate matrix of the variegated unit (JGE locality 9201), which has yielded the greatest number of specimens. The species is clearly less abundant in the overlying volcaniclastic unit (JGE locality 9202), which does not contain a high percentage of carbonates.

Salinity.—Another aspect of charophyte ecology is tolerance to salinity. Some species are entirely lacustrine and others are restricted to polyhaline biotopes, but most species can support wide ranges of salinity (up to 70 ppt; Burne and others, 1980). Similar data were obtained in the early Eocene of Cabardes (southern France), where the composition of the charophyte assemblages varied according to salinity; the salinity ranges were determined by analysis of the associated ostracode faunas (Tambareau and others, 1991). In the Hanshou Formation of the Dongting Basin (Hunan Province, People's Republic of China), *Stephanochara vera* is associated with representatives of the genus *Lamprothamnium* (*"Obtusochara"* in Hu and Zeng, 1985), which is recognized to be the most polyhaline charophyte genus (Burne and others, 1980; Soulie-Maersche, 1993). In a recent paper, Lucas and Kietzke (1994) reported *Lamprothamnium* and *Chara* from Pliocene saline deposits in the Monticella Point Maar of Sierra County, N. Mex. The occurrence of the inferred polyhaline species *Stephanochara* aff. *S. vera* suggests that the Brian Head Formation was deposited at least partly in water with somewhat elevated salinity.

AGE DETERMINATION

The Brian Head Formation has yielded only one species of charophyte. The sample processing techniques that we used in the field were designed to recover micro-vertebrate material, and therefore probably only large charophyte specimens and species were retained on the coarse screen mesh. We cannot exclude the possibility that small charophyte species such as *Tolypella*, a better understood genus that would provide more detailed age and paleoenvironmental data, may be recovered in future collections.

In the People's Republic of China, *Stephanochara vera* has been reported from Assemblages 8 and 9 of the Hunan Province (Hu and Zeng, 1982, 1985), extending from the late Paleocene to the middle Eocene. *Stephanochara hunanensis* (Hu and Zeng) n. comb. occupies a similar age range; this species was also formerly referred to the genus *Eotectochara*. According to Tang and Di (1991), Assemblage 5 of Qaidam Basin (Qinghai Province, northern People's Republic of China), which represents Assemblage 9 of the Hunan Province (containing *S. vera*), does not extend into the upper Eocene.

We do not suggest restricting the age of the Brian Head Formation based solely on one charophyte taxon that does not correspond exactly to the type species. We believe that the similarities between the American and Chinese representatives of *Stephanochara vera* indicate that they are contemporaneous or of very similar ages. The presence of *S.* aff. *vera* supports, but does more finely constrain, the relative ages derived from the vertebrate and invertebrate fauna.

The charophyte data suggest that the variegated and volcaniclastic units of the Brian Head Formation are no younger than middle Eocene. The maximum age for the Brian Head Formation is thus middle Eocene, based on the charophytes and on nonmarine mollusks and palynomorphs from the underlying Claron Formation (Goldstrand and others, 1993; Goldstrand, 1994). Preliminary analyses of the vertebrate fauna by Eaton and Hutchison (1995) suggest a late Eocene age for the variegated unit and the lower part of the volcaniclastic unit of the Brian Head Formation.

REFERENCES CITED

Anderson, J.J., 1993, The Markagunt megabreccia—Large Miocene gravity slides mantling the northern Markagunt Plateau, southwestern Utah: Utah Geological Survey Miscellaneous Publication 93–2, 37 p.

Anderson, J.J. and Rowley, P.D., 1975, Cenozoic stratigraphy of the southwestern High Plateaus of Utah, *in* Anderson, J.J., Rowley, P.D., Fleck, R.J., and Nairn, A.E.M., eds., Cenozoic geology of southwestern High Plateaus of Utah: Geological Society of America Special Paper 160, p. 1–52.

Anderson, J.J., Rowley, P.D., Machette, M.N., Decatur, S.H., and Mehnert, H.H., 1990, Geologic map of the Nevershine Hollow area, eastern Black Mountains, southern Tushar Mountains, and northern Markagunt Plateau, Beaver and Iron Counties, Utah: U.S. Geological Survey Miscellaneous Investigations Series Map I–1999, scale 1:50,000.

Averitt, Paul, 1967, Geologic map of the Kanarraville Quadrangle, Iron County, Utah: U.S. Geological Survey Geologic Quadrangle Map GQ–694, scale 1:24,000.

Best, M.G., and Grant, S.K., 1987, Stratigraphy of the volcanic Oligocene Needles Range Group in southwestern Utah and eastern Nevada, chapter A *in* Oligocene and Miocene volcanic rocks in the central Pioche-Marysvale igneous belt, western Utah and eastern Nevada: U.S. Geological Survey Professional Paper 1433, p. 1–28.

Bowers, W.E., 1972, The Canaan Peak, Pine Hollow, and Wasatch Formations in the Table Cliff region, Garfield County, Utah: U.S. Geological Survey Bulletin 1331–B, 39 p.

———1990, Geologic map of Bryce Canyon National Park and vicinity, southwestern Utah: U.S. Geological Survey Miscellaneous Investigations Series Map I–2108, scale 1:24,000.

Burne, R.V., Bauld, J., and De Deckker, P., 1980, Saline lake charophytes and their geological significance: Journal of Sedimentary Petrology, v. 50, p. 281–293.

Cook, E.F., 1957, Geology of the Pine Valley Mountains, Utah: Utah Geological and Mineralogical Survey Bulletin 58, 111 p.

———1965, Stratigraphy of Tertiary volcanic rocks in eastern Nevada: Nevada Bureau of Mines Report 11, 61 p.

Corillion, R., 1975, Flore des charophytes (Characees) du Massif Armoricain et des contrees voisines d'Europe occidentale, *in* Jouve, ed., Flore et vegetation du Massif Armoricain, Volume IV: Paris, p. 1–216.

Dickinson, W.R., Lawton, T.F., and Inman, K.F., 1986, Sandstone detrital modes, central Utah foreland regions—Stratigraphic record of Cretaceous-Paleocene tectonic evolution: Journal of Sedimentary Petrology, v. 56, p. 276–293.

Eaton, J.G., and Hutchison, J.H., 1995, A late Eocene fauna from undescribed strata overlying the Claron Formation, Sevier Plateau, southwestern Utah: Rocky Mountain Section, Geological Society of America Abstracts with Programs.

Feist, Monique, and Brouwers, E.M., 1990, A new *Tolypella* from the Ocean Point dinosaur locality, North Slope, Alaska, and the Late Cretaceous to Paleocene Nitelloid charophytes: U.S. Geological Survey Bulletin 1990–F, 7 p.

Feist, Monique, and Grambast-Fessard, N., 1982, Cle de determination pour les genres de charophytes: Paleobiologie continentale, v. 13, no. 2, p. 1–28.

———1991, The genus concept in Charophyta, evidence from Palaeozoic to Recent, *in* Riding, R., ed., Calcareous algae and stromatolites: New York, Springer-Verlag, p. 189–203.

Fleck, R.J., Anderson, J.J., and Rowley, P.D., 1975, Chronology of mid-Tertiary volcanism in high plateaus region of Utah, *in* Anderson, J.J., Rowley, P.D., Fleck, R.J., and Nairn, A.E.M., eds., Cenozoic geology of southwestern High Plateaus of Utah: Geological Society of America Special Paper 160, p. 53–62.

Gasse, F., Fontes, J.C., Plaziat, J.C., Carbonnel, P., Karczmarska, I., De Deckker, P., Soulie-Maersche, I., Callot, Y., and Dupeuble, P.A., 1987, Biological remains, geochemistry, and stable isotopes for the reconstruction of environmental and hydrological changes in the Holocene lakes from north Sahara: Palaeogeography, Palaeoclimatology, Palaeoecology, v. 60, p. 1–46.

Goldstrand, P.M., 1991, Stratigraphy and paleogeography of Late Cretaceous and early Tertiary rocks of southwest Utah: Utah

Geological and Mineral Survey Miscellaneous Publication MP 90–2, 58 p.

———1992, Evolution of Late Cretaceous and Early Tertiary basins of southwest Utah based on clastic petrology: Journal of Sedimentary Petrology, v. 62, no. 3, p. 495–507.

———1994, Tectonic development of Upper Cretaceous to Eocene strata of southwestern Utah: Geological Society of America Bulletin, v. 106, no. 1, p. 145–154.

Goldstrand, P.M., Trexler, J.H., Kowallis, B.J., and Eaton, J.G., 1993, Late Cretaceous to early Tertiary tectonostratigraphy of southwestern Utah, *in* Morales, M., ed., Aspects of Mesozoic geology and paleontology of the Colorado Plateau: Museum of Northern Arizona Bulletin 59, p. 181–188.

Gregory, H.E., 1945, Post-Wasatch Tertiary formations in southwestern Utah: Journal of Geology, v. 53, no. 2, p. 105–115.

Holifield, R.R., 1964, Lower Tertiary Charophyta of North America: Columbia, Mo., University of Missouri M.S. thesis, 130 p.

Hu, Jimin, and Zeng, Demin, 1982, The paleontological atlas of Hunan: Geological Publishing House, Beijing, Geological Memoirs, Serie 2, v. 1, p. 543-595, pls. 359–394. [In Chinese.]

_____1985, Charophyte assemblages of the Cretaceous to Paleogene in Hunan Province: Oil and Gas Geology, v. 12, p. 409–418, pl. 1. [In Chinese, English abstract.]

Leith, G.K., and Harder, E.C., 1908, The iron ores of the Iron Springs district, southern Utah: U.S. Geological Survey Bulletin 338, 102 p.

Lucas, S.G., and Kietzke, K.K., 1994, Pliocene microfossils from the Monticello Point maar, Sierra County, New Mexico: New Mexico Geology, v. 16, no. 3, p. 41–48.

Mackin, J.H., 1954, Geology and iron ore deposits of the Granite Mountain area, Iron County, Utah: U.S. Geological Survey Mineral Investigation Field Studies Map MF-14, scale 1:12,000.

———1960, Structural significance of Tertiary volcanic rocks in southwestern Utah: American Journal of Science, v. 258, no. 2, p. 81–131.

Maldonado, Florian, 1995, Decoupling of mid-Tertiary rocks, Red Hills-western Markagunt Plateau, southwestern Utah, chapter I *in* Scott, R.B., and Swadley, W C, eds., Geologic studies in the Basin and Range–Colorado Plateau transition in southeastern Nevada, southwestern Utah, and northwestern Arizona: U.S. Geological Survey Bulletin 2056, p. 233–254.

Maldonado, Florian, Sable, E.G., and Anderson, J.J., 1992, Evidence for a Tertiary low-angle shear zone, Red Hills, Utah, with implications for a regional shear zone in the adjacent Colorado Plateau, *in* Engineering and environmental geology of southwestern Utah: Utah Geological Association Publication 21, 1992 Field symposium, p. 315–323.

Maldonado, Florian, and Williams, V.S., 1993, Geologic map of the Parowan Gap Quadrangle, Iron County, Utah: U.S. Geological Survey Geologic Quadrangle Map GQ–1712, scale 1:24,000.

McFall, C.C., 1955, Geology of the Escalante-Boulder area, Garfield County, Utah: New Haven, Conn., Yale University Ph. D. thesis, 180 p.

Moore, J.A., 1986, Charophytes of Great Britain and Ireland: Botanical Society of the British Isles, Handbook No. 5, 140 p.

Mullett, D.J., 1989, Interpreting the early Tertiary Claron Formation of southern Utah: Geological Society of America Abstracts with Programs, v. 2, no. 5, p. 120.

Mullett, D.J., Wells, N.A., and Anderson, J.J., 1988, Unusually intense pedogenic modification of the Paleocene-Eocene Claron Formation of southwestern Utah: Geological Society of America Abstracts with Programs, v. 20, no. 3, p. 217.

Robison, R.A., 1966, Geology and coal reserves of the Tropic area, Garfield County, Utah: Utah Geological and Mineralogical Survey Special Studies 18, 47 p.

Rowley, P.D., 1968, Geology of the southern Sevier Plateau, Utah: Austin, Texas, University of Texas Ph. D. dissertation, 385 p.

Rowley, P.D., Mehnert, H.H., Naeser, C.W., Snee, L.W., Cunningham, C.G., Steven, T.A., Anderson, J.J., Sable, E.G., and Anderson, R.E., 1994, Isotopic ages and stratigraphy of Cenozoic rocks of the Marysvale volcanic field and adjacent areas, west-central Utah: U.S. Geological Survey Bulletin 2071, 75 p.

Schneider, M.C., 1967, Early Tertiary continental sediments of central and south-central Utah: Brigham Young University Geology Studies, v. 14, p. 143–194.

Schudack, M., 1993, Moglichkeiten palokologisher Aussagen mit Hilfe von fossilien Charophyten: Festschrift Prof. W. Krutzsch, Museum fur Naturkunde, Berlin, p. 39–58.

Soulie-Maersche, I., 1993, Apport des charophytes fossiles a la recherche de changements climatiques abrupts: Bulletin de la Societe geologique de France, v. 164, no. 1, p. 123–130.

Tambareau, Y., Gruas-Cavagnetto, C., Feist, Monique, and Vilatte, J., 1991, Flores et faunes continentales llerdiennes du versant sud de la Montagne Noire et de la Montagne d'Alaric: Revue de Micropaleontologie, v. 34, no. 1, p. 69–89.

Tang, I., and Di, H., 1991, Fossil charophytes from Qaidam Basin, Qinghai: Scientific and Technical Documents, 220 p., 79 pls., Publishing House, Beijing. [In Chinese, English abridged version.]

Wood, R.D., 1965, A revision of the Characeae, Volume 1, Cramer, ed.: Weinheim, 904 p.

PLATE 1

[Figures 1–6, ×50; figure 7, ×100; figure 8, ×50; figure 9, ×40]

Figures 1–8. *Stephanochara* aff. *S. vera* (Hu and Zeng) n. comb. Brian Head Formation, Utah.
1, 2, 3, 6. Lateral views showing variations of shape and ornamentation.
4. Basal view.
5. Apical view.
7. Axial longitudinal section showing the basal plate.
8. Axial longitudinal section, general view.

9. *"Tectochara" matura* Holifield. Flagstaff Member, Green River Formation, East Colton, Utah. Lateral view.

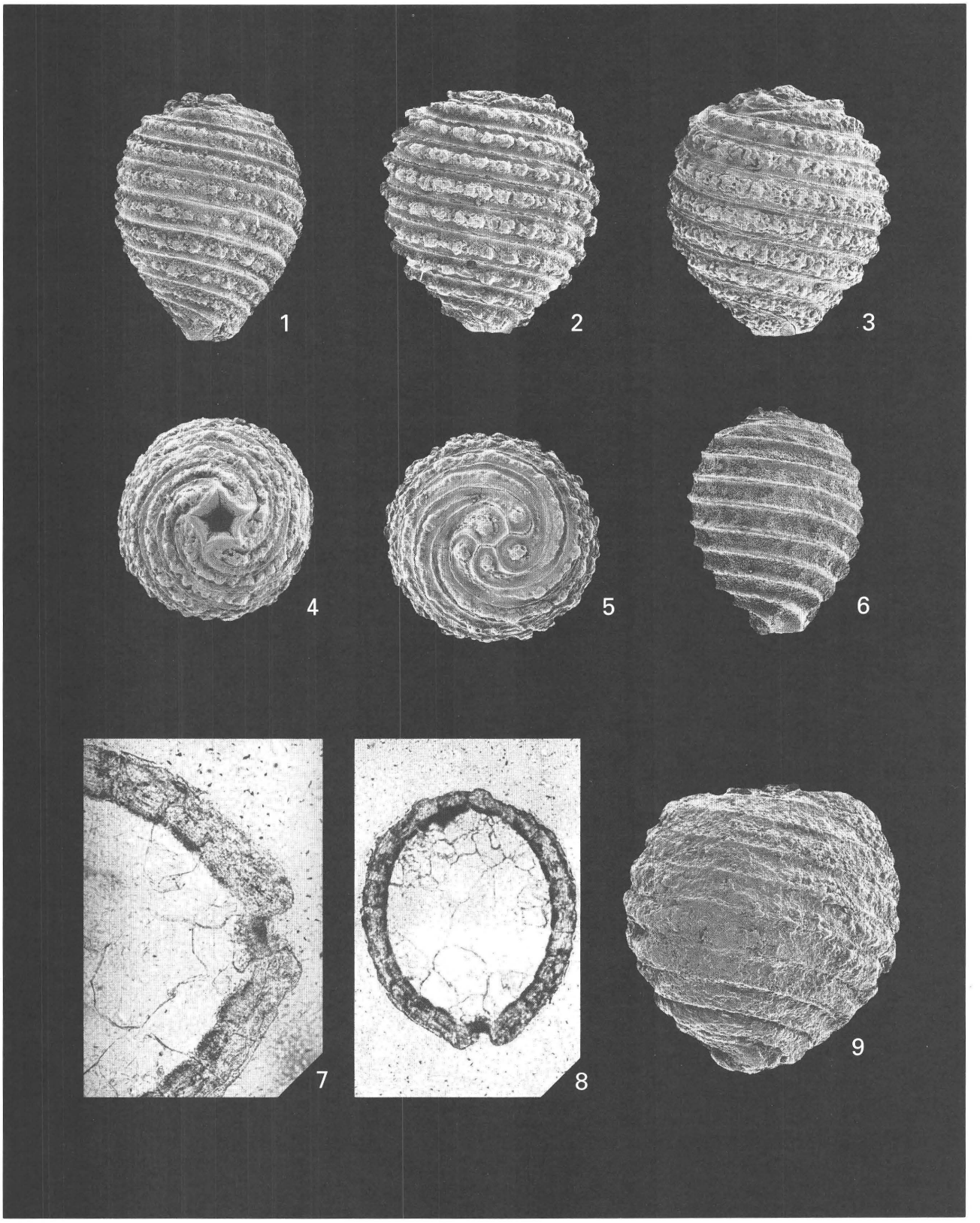

STEPHANOCHARA aff. *S. VERA* AND *"TECTOCHARA" MATURA*

Trace Fossils of Hymenoptera and Other Insects, and Paleoenvironments of the Claron Formation (Paleocene and Eocene), Southwestern Utah

By Thomas M. Bown, Stephen T. Hasiotis, Jorge F. Genise, Florian Maldonado, *and* Elisabeth M. Brouwers

GEOLOGIC STUDIES IN THE BASIN AND RANGE–COLORADO PLATEAU TRANSITION IN SOUTHEASTERN NEVADA, SOUTHWESTERN UTAH, AND NORTHWESTERN ARIZONA, 1995

U.S. GEOLOGICAL SURVEY BULLETIN 2153–C

UNITED STATES GOVERNMENT PRINTING OFFICE, WASHINGTON : 1997

CONTENTS

FIGURES

Trace Fossils of Hymenoptera and Other Insects, and Paleoenvironments of the Claron Formation (Paleocene and Eocene), Southwestern Utah

By Thomas M. Bown,[1] Stephen T. Hasiotis,[2] Jorge F. Genise,[3] Florian Maldonado, *and* Elisabeth M. Brouwers

ABSTRACT

About 650 hymenopteran trace fossils recently recovered from paleosols of the Paleocene and Eocene Claron Formation of southwestern Utah include a partial nest of an ant (Formicidae) and the larval cells and cocoons of bees (Sphecoidea) and wasps (Vespoidea). *Parowanichnus formicoides*, ichnogen. and ichnosp. nov., is the second described fossil ant nest and consists of superposed chambers and horizontal galleries that are connected by vertical shafts, resulting in a lattice-like nest architecture. The traces of digging bees include two varieties of cells (cf. *Celliforma* sp.) and cocoons, and the digger wasps are represented by a few cells and four sizes of cocoons, some of which appear to have been parasitized by other hymenopterans or dipterans. The new ichnogenus *Eatonichnus* is named to accommodate *Xenohelix*? *utahensis* Gilliland & LaRocque from the Colter Formation of central Utah, and a new species, *E. claronensis*, is described from the Claron Formation. *Eatonichnus* is probably a nest constructed of mud, possibly by an unknown dung beetle.

The new ichnofauna indicates that environments in southwestern Utah during development of ichnofossil-rich Claron paleosols were characterized by moderate plant growth and moist soils that underwent periodic (perhaps seasonal) episodes of drying.

GEOLOGIC SETTING AND INTRODUCTION

The Claron Formation was defined by Leith and Harder (1908) for sedimentary rocks exposed in the Iron Springs mining district, southwest of the Red Hills in southwestern Utah (fig. 1). Mackin (1960) informally divided the Claron Formation into a lower red member and an upper gray member (fig. 2). The gray member has been referred to more frequently in the literature as the white member. The red member consists predominantly of poorly to moderately resistant sandstone that is intercalated with variegated mudstone, limestone, and pebble conglomerate believed to be of mixed fluvial and lacustrine origin. The overlying white member is well developed to absent; for example, it is present in the southern part of the Red Hills area, but is absent in the northern part of that area. The white member is characterized by cliff-forming white limestone and varying proportions of mudstone, sandstone, and conglomerate. Mullett and others (1988) and Mullett (1989) have described various degrees of alteration of Claron sediments by pedogenesis.

The Claron Formation is late Paleocene and Eocene in age (Goldstrand, 1994), and is extensively developed throughout most of the Colorado Plateaus province, in parts of the Basin and Range province, and in the transition zone between these two provinces (High Plateaus subprovince, of which the area of fig. 1 is a small part). The formation is approximately 370 m thick (Threet, 1952a; Maldonado and Williams, 1993), but is as much as 435 m at Cedar Breaks National Monument where both members are fully developed and well exposed (Schneider, 1967).

The Claron Formation is underlain by the Grand Castle Formation and is overlain by the Brian Head Formation (fig. 2). The Grand Castle Formation is Paleocene in age and consists of about 275 m of conglomerate and sandstone. It is accorded formal unit status and described elsewhere in this volume (Goldstrand and Mullett, this volume, chapter D). The previously abandoned Brian Head Formation (Threet, 1952b; Anderson, 1971) was formally reinstated as a valid unit (Anderson, 1993) and revised (Sable and Maldonado, this volume, chapter A). The Brian Head Formation is late Eocene to middle Oligocene in age and as much as 300 m thick; it consists mainly of tuffaceous sandstone, sandstone, mudflow breccia, and pebble-to-boulder conglomerate, with lesser amounts of limestone, calcareous shale, lenses of chalcedony, and ash-flow and ash-fall tuffs. An ash-flow tuff

[1]Present address: Boulder, CO 80303.

[2]University of Colorado, Boulder, CO 80309, and U.S. Geological Survey.

[3]Museo Argentino Ciencias Naturales, 1405 Buenos Aires, Argentina.

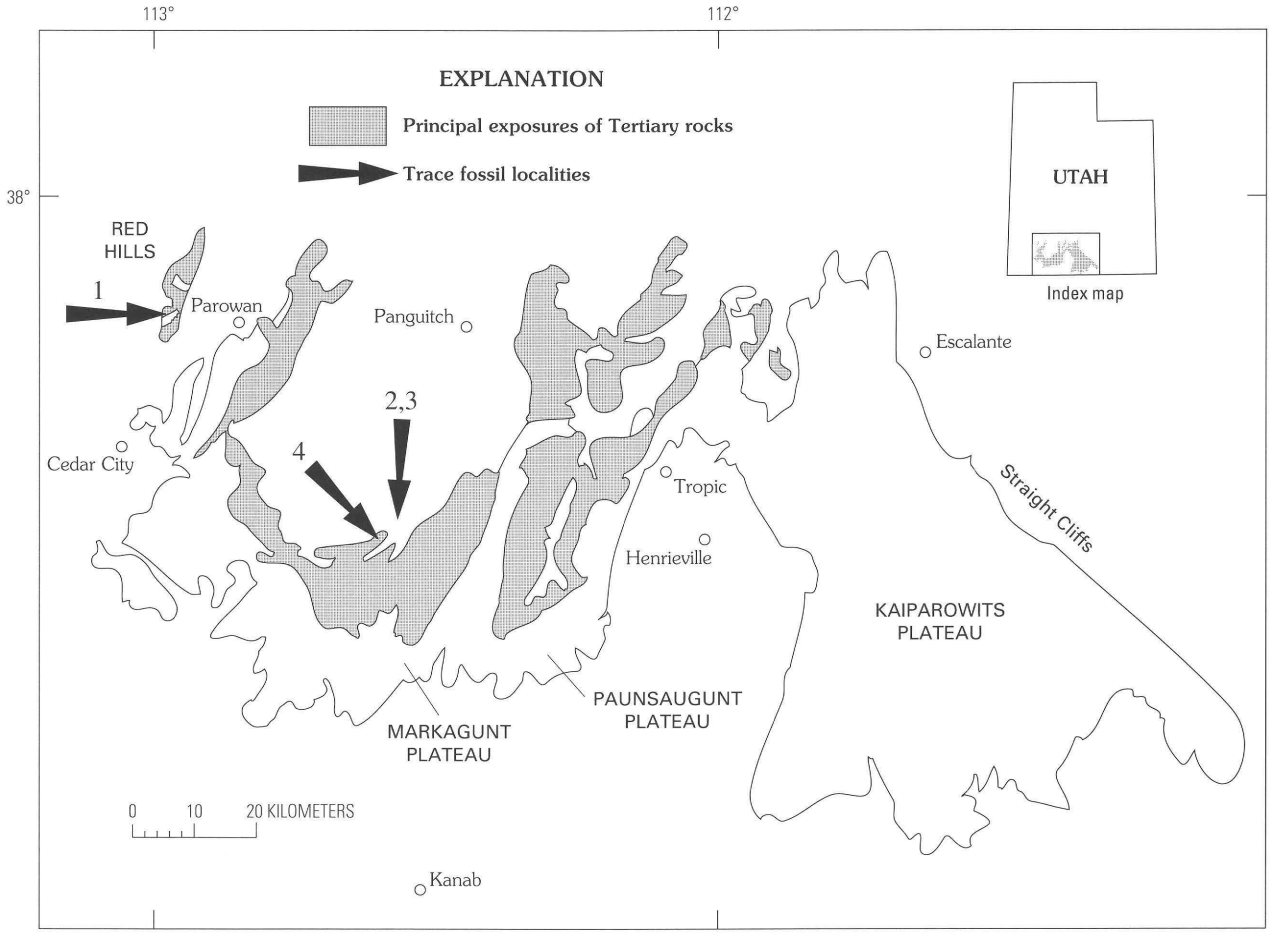

Figure 1. Map showing location of trace fossil localities in the Claron Formation of southwestern Utah. 1, Locality TMB U94-3, site of *Parowanichnus formicoides* (uppermost part of lower red member of Claron Formation); 2, Locality 94-EB-21 (lower red member of Claron Formation); 3, Locality 94-EB-22 and 94-EB-23 (upper part of lower member of Claron Formation); 4, Locality JGE 94-06 (lower part of upper member of Claron Formation). Modified from D.J. Nichols (this volume, chapter E).

present in the northern Red Hills in the upper part of the Brian Head Formation (termed the sedimentary and volcanic rocks of the Red Hills) has been dated at 34–33 Ma (Maldonado and Williams, 1993; Maldonado, 1995).

In the Sevier Plateau west of the study area and locally on the Markagunt Plateau (fig. 1), a unit termed the "variegated unit" by Bowers (1972) overlies the Claron Formation and underlies the Brian Head Formation. This unit is composed of variegated sandstone and mudstone and is discussed further by Feist and others (this volume, chapter B).

Field studies of the Claron Formation over many years by Jeffrey G. Eaton and reconnaissance examination of Claron exposures in 1994 by F.M., E.M.B., and T.M.B. resulted in the discovery and collection of numerous trace fossils of insects from four localities. The majority of these specimens appear to be of hymenopteran origin, and include the subterranean part of the nest of an ant (Formicidae), and numerous brood cells and cocoons of burrowing wasps and bees and their probable parasites.

The insect trace fossils of the Claron Formation occur in sandstones, mudstones, and volcaniclastic mudstones, all of which have undergone significant but varying degrees of pedogenetic alteration. As in the Upper Cretaceous Asencio Formation of Uruguay (Genise and Bown, 1996), the trace fossils are abundant and generally well preserved, and undoubtedly record numerous generations of insect nest-building activity.

ACKNOWLEDGMENTS

We are grateful to R.F. Dubiel and P.A. Holroyd for reviews of the manuscript, to K.C. McKinney for photography of specimens, and to P.A. Holroyd for preparing figures 1, 2, and 7. The holotype and paratypes of *Eatonichnus utahensis* were graciously made available to us by D.M. Gnidovec of the Orton Geological Museum of The Ohio State University. Field work in Utah was greatly facilitated by the efforts of J.G. Eaton and E. Fisher, and we are grateful for much valuable discussion concerning bee and wasp nests with J. Rozen, C. Michener, and H. Evans.

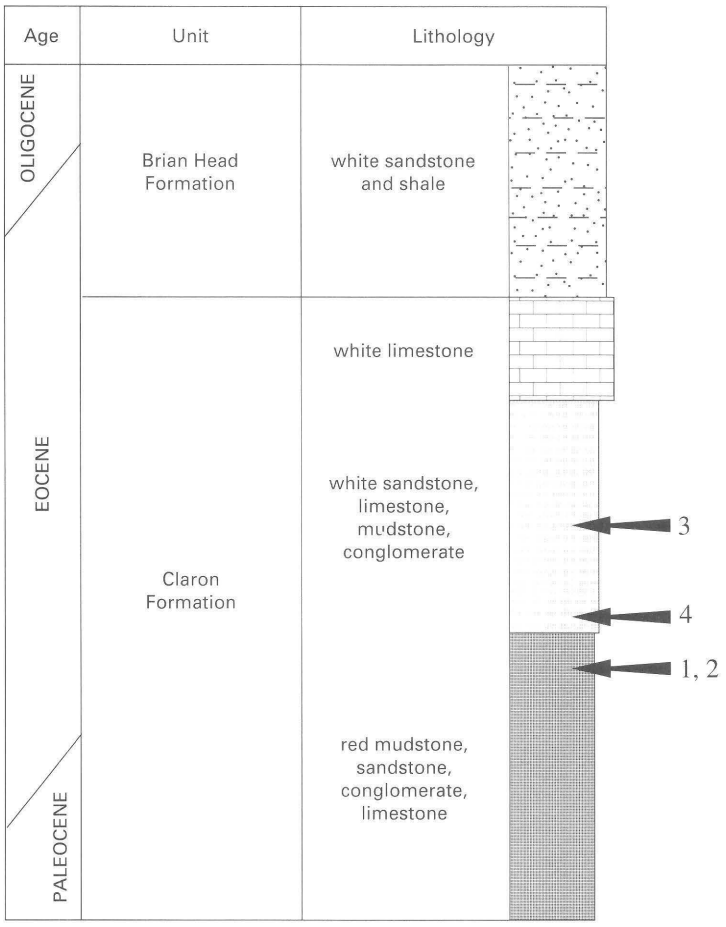

Figure 2. Generalized section of lower Tertiary rocks in the Markagunt Plateau region, showing approximate stratigraphic positions of trace fossil localities 1–4. Modified from Feist and others (this volume, chapter B).

SYSTEMATIC ICHNOLOGY

HYMENOPTERA

FORMICIDAE (ANT TRACES)

PAROWANICHNUS, ichnogenus nov.

Type Ichnospecies.—Parowanichnus formicoides, ichnospecies nov.; type and only known ichnospecies.

Diagnosis.—Parowanichnus differs from *Attaichnus* Laza (the only other described fossil formicid nest) in having (1) a much smaller total nest volume; (2) much smaller and less densely packed chambers; (3) chambers oblate to hemispherical rather than globular; (4) galleries essentially of one basic size—smaller than in *Attaichnus*; (5) galleries providing access equally to top, sides, and bottom of chambers; and (6) a gallery network that is crudely trellate in plan, forming a gridlike lattice with descending shaft galleries and lateral tunnel galleries set more-or-less perpendicular to one another. Resembles *Attaichnus* in having irregular walls on the insides of chambers.

Etymology.—Parowan, a village near the type locality; and Gr. *ichnos*, track or trace.

PAROWANICHNUS FORMICOIDES, ichnospecies nov.

(Figs. 4, 5)

Holotype.—Natural cross section of central part of subterranean nest and peripheral gallery system, in outcrop (figs. 4, 5).

Hypodigm.—The type only.

Locality and Distribution.—Locality TMB-U94-3 (fig. 3; locality 1, fig. 1); uppermost part of lower member of Claron Formation, southern Red Hills, center of $NW^1/_4$ section 27, T. 34 S., R. 10 W., Iron County, Utah. Type locality only.

Diagnosis.—Only known ichnospecies; same as for ichnogenus.

Etymology.—L. *formica*, ant; and Gr. *eides*, like.

Description and Discussion.—The type and only specimen of *Parowanichnus formicoides* is exposed in a weathered natural cross section on a small cliff face (fig. 3). The specimen consists of more than 100 chambers and numerous interconnecting galleries (figs. 4, 5) that comprise the subterranean part of a nest measuring approximately 1.0 m in height and about 3.3 m across its widest diameter. Irregular outcrop weathering at the type locality indicates that the central part of the nest continues into the rock at least 0.5 m

Figure 3. Type locality of *Parowanichnus formicoides* in the southern part of the Red Hills, about 13 km west of Parowan, Iron County, Utah. Upper arrow shows contact between upper and lower members of Claron Formation, and lower arrow depicts exposure with type specimen in place.

beyond the plane of best exposure. A system of small galleries connecting much larger chambers indicates that *Parowanichnus* is a trace fossil of social insect origin. The presence of unlined galleries taken in conjunction with the relative simplicity of the unlined chambers and overall nest organization suggests (with a few exceptions) that the tracemaker was an ant (Hymenoptera, Formicidae) and not a termite (Isoptera).

The chambers (fig. 4) have one elongate dimension, are wider than they are tall, and exhibit irregularly shaped internal walls. The walls are not reinforced with fine sediment or excreta, as occurs in the termite ichnofossil *Syntermesichnus* and many other termite nests (Bown and Laza, 1990). Chambers range from 10 to 50 mm in diameter and appear to have been constructed by the simple enlargement of galleries.

The galleries range from 4 to 12 mm wide and 2 to 4 mm in height. They are generally arranged horizontally, side by side, with vertical tiers distal to the periphery of the nest (fig. 4*A*), whereas near the nest center they comprise a labyrinthine swarm around the chambers (fig. 4*B*).

Attaichnus kuenzelii (Laza, 1982) is the only other described trace known to us that represents a fossil ant nest. Though possibly also constructed by an attine ant, *Parowanichnus formicoides* has a much smaller nest volume and differs from *Attaichnus* in several other important architectural attributes. The globular chambers in *Attaichnus* range in diameter from 140 to 170 mm, dwarfing the oblate to hemispherical, 10–50 mm chambers of *Parowanichnus*. The galleries of *Parowanichnus* are also smaller, with the largest (4–12 mm) corresponding in size to the smallest in *Attaichnus* (5–9 mm). Galleries may enter any part of the chamber in *Parowanichnus*, although the majority of access is from the side. This arrangement contrasts significantly with that in *Attaichnus*, in which the galleries invariably enter the chambers from the bottom.

Perhaps most importantly, nest organization is very different in the two traces. *Attaichnus* is characterized by a dense network of chambers and galleries that are bunched together, and the spatial relationships of the galleries and chambers lack geometric organization. In contrast, *Parowanichnus* is a more diffuse structure in which the chambers and galleries radiate away from the center of the nest and gradually decline in number. The galleries tend to be arranged parallel and perpendicular to one another, forming a boxwork of tiered galleries and chambers (fig. 4*A*) that extends up to a few meters distal to the nest center.

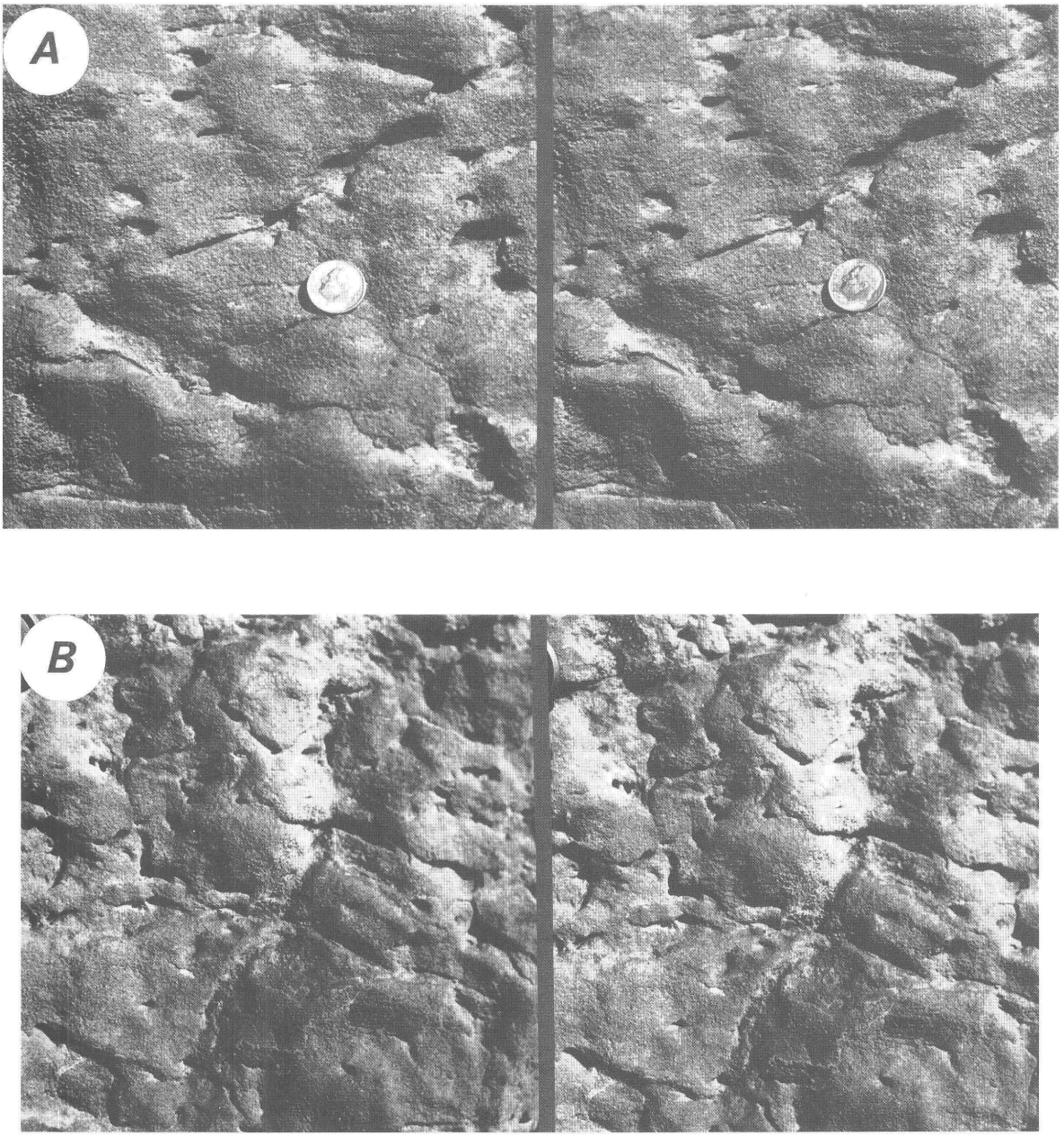

Figure 4. Type specimen of *Parowanichnus formicoides*; stereopairs. *A*, Natural cross section of weathered nest showing trellate arrangement of low, elongate chambers and interconnecting galleries at periphery of nest. *B*, Natural cross section showing greater density of galleries and chambers in heart of nest. Scale (coin diameter=1.75 cm) same in both *A* and *B*.

Excavated ant nests consist of a subterranean network of galleries connecting chambers (rooms) that are utilized for brood-raising, nursery caretaking, granaries and, in a few species, fungus-gardening. Of the nearly 300 genera and about 8,800 known species of ants (Hölldobler and Wilson, 1990), the nest architectures are well known for only a handful of species that excavate their nests in soil. None of these closely resembles the complete nest baüplan seen in *Parowanichnus formicoides*.

Ants excavate two basic types of nests: those consisting of a shallow maze of horizontal tunnels (for example, *Lasius alienus* and *Tetramorium caespitum*); and those dominated by vertical shafts (for example, many species of *Formica, Prenolepis*, and *Pogonomyrmex*; Sudd, 1967). In general, shallow nests with numerous horizontal galleries are typical of humid soils, and deeper nests dominated by vertical shafts are more commonly built by ants occupying drier regions. *Parowanichnus* is a relatively shallow nest (about 1.0–1.5 m) dominated by horizontal galleries. The short vertical shafts

connecting different levels of tiered galleries and chambers, however, might reflect that the nest was constructed in sediment that was subject to periodic drying.

Tiered chambers such as those seen in *Parowanichnus* are built by certain species of *Atta, Pogonomyrmex, Tetramorium,* and *Formica* as well as other ant genera (Talbot and Kennedy, 1940; Brian and Downing, 1956; Sudd and Franks, 1987), but these nests exhibit neither tiered galleries nor the network of perpendicularly intersecting excavations of *Parowanichnus*. Tiered galleries with perpendicular shafts occur in soil nests of the primitive Australian wood ant *Myrmecia dispar* (von Frisch, 1974), and tiered galleries and chambers are known in the honey-ant *Myrmecocystus melliger* from the western United States (McCook, 1882; Gregg, 1963). *Parowanichnus* does not resemble the nest of any fungus-cultivating ant (Wheeler, 1907, 1910; Stahel and Geijskes, 1939; Moser, 1963; Hölldobler and Wilson, 1990).

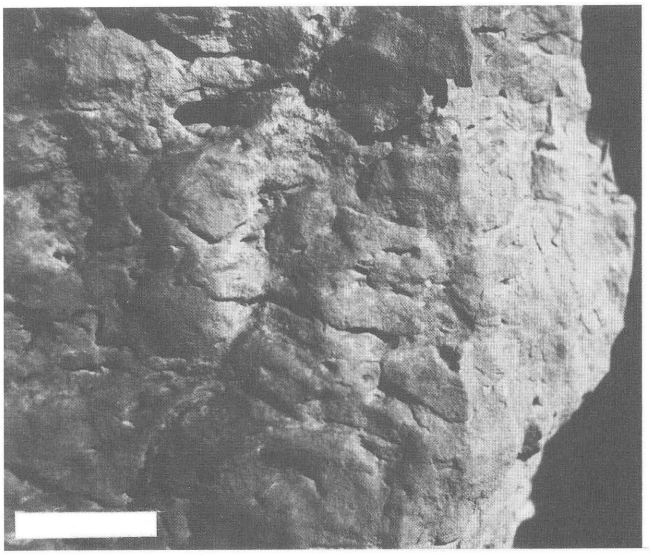

Figure 5. Type specimen of *Parowanichnus formicoides*, showing different levels of low, tiered chambers. Bar is 5 cm.

APIDAE (BEE TRACES)

cf. *CELLIFORMA* sp. Brown, 1934

(Fig. 6*B*)

Material.—22 complete and fragmentary cells.

Localities.—J.G. Eaton locality 89-32, $SE^1/_4NW^1/_4$ section 2, T. 36 S., R. 3 W., Garfield County, Utah. Upper part of lower member of Claron Formation. E.M. Brouwers localities 94-EB-22 (locality 3, fig. 1), $NE^1/_4NW^1/_4SW^1/_4NW^1/_4$ section 29, T. 37 S., R. 6 W.; and 94-EB-23 (locality 3, fig. 1), $NW^1/_4SE^1/_4NE^1/_4$ section 30, T. 37 S., R. 6 W., Garfield County, Utah. Top of lower member of Claron Formation.

Description and Discussion.—Two distinct types of structures from the Claron Formation, fossil cells and cocoons, record the activity of bees and wasps, respectively. Cells are excavated chambers where the eggs and food provisions for the developing young are stored. Cells are constructed by both bees and wasps, and fossil cells resemble the ends of burrows that have enlarged terminations. Cocoons, on the other hand, are constructed by mature larvae and may be either spun of body secretions or built out of earth and saliva (Evans, 1957, 1963; Zahradník, 1991).

In the Claron fossils, only one type of cell is preserved, and it has smooth surfaces and rounded terminations (fig. 6*B*). In all specimens, the cell is broader than the entrance burrow that leads to it. In contrast to the behavior of wasps, most bees line their cell walls with secretions, thus reinforcing the walls and causing them to be very smooth. It is also common that this strengthening of the cell wall is extended into the proximal part of the burrow, resulting in what is commonly good preservation of the proximal part of the burrow as well as the enlarged cell (fig. 6*B*). No burrowing wasps are known to harden either their cell walls or their burrows (J. Rozen, written commun., 1994).

Claron fossil bee cells occur as solitary cells and are not formed into combs; therefore, they are excluded from ichnogenera *Uruguay* (Roselli, 1938) and *Rosellichnus* (Genise and Bown, 1996) and probably belong in *Celliforma* (Brown, 1934). Retallack (1984, p. 585) rediagnosed this ichnogenus, restricting it to only those forms with "polished and smooth" cell walls. A revision of the ichnospecies of *Celliforma* is beyond the scope of this contribution, but would be necessary to determine if the Claron bee traces belong in a new ichnospecies of *Celliforma.*

VESPOIDEA AND (OR) SPHECIDAE (WASP TRACES)

(Figs. 6*A*, *C-E*; 8*A*, *B*)

Material.—612 complete and partial cocoons.

Localities.—E.M. Brouwers localities 94-EB-22 (locality 3, fig. 1), $NE^1/_4NW^1/_4SW^1/_4NW^1/_4$ section 29, T. 37 S., R. 6 W.; and 94-EB-23 (locality 3, fig. 1), $NW^1/_4SE^1/_4NE^1/_4$ section 30, T. 37 S., R. 6 W., Garfield County, Utah. Top of lower member of Claron Formation; 20 m above J.G. Eaton locality JGE 89-32, $SE^1/_4NW^1/_4$ section 2, T. 36 S., R. 3 W., Garfield County, Utah. Upper part of lower member of Claron Formation.

Description and Discussion.—In contrast to cells, cocoons are ovoid to spindle-shaped structures that were constructed within the cells by mature larvae. They are

Figure 6 (facing page). Cells of unknown bees (*B*) and cocoons of unknown wasps (*A, C–E*) from the Claron Formation. *A*, Five rugose wasp cocoons with pointed terminations. *B*, Four smooth bee cells with rounded terminations. *C*, Four naturally eroded wasp cells, each exhibiting an internal Group III cocoon. *D*, Large, complete Group I wasp cocoon. *E*, Naturally eroded Group II wasp cocoon, showing associated Group III (large arrow) and Group IV (small arrow) cocoons. Note parallel-ridged bioglyph on surface of largest (Group II) cocoon. Bars are 1.0 cm; upper bar is scale for *A–D*, lower bar is scale for *E*. *E* is a stereophotograph.

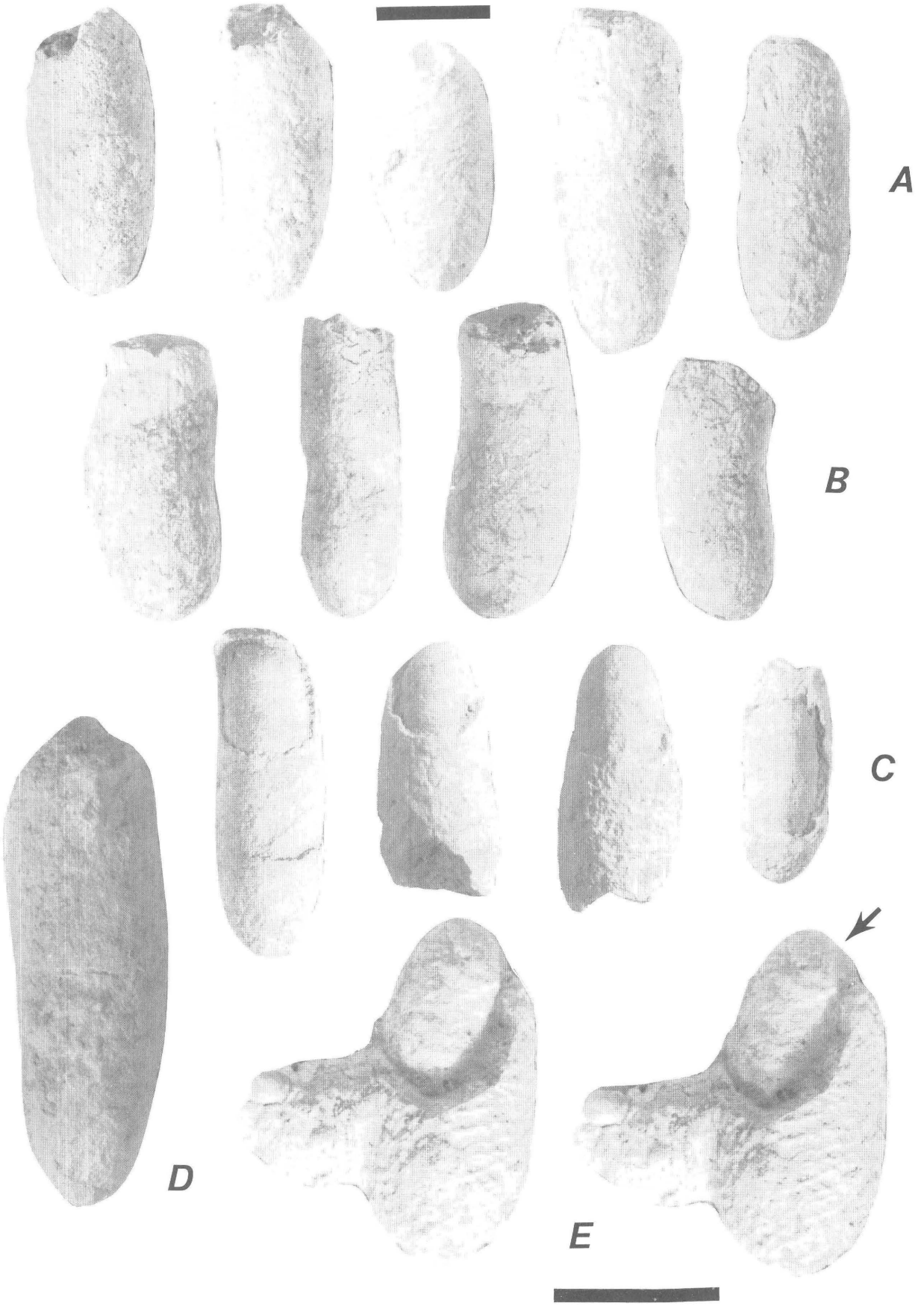
A
B
C
D
E

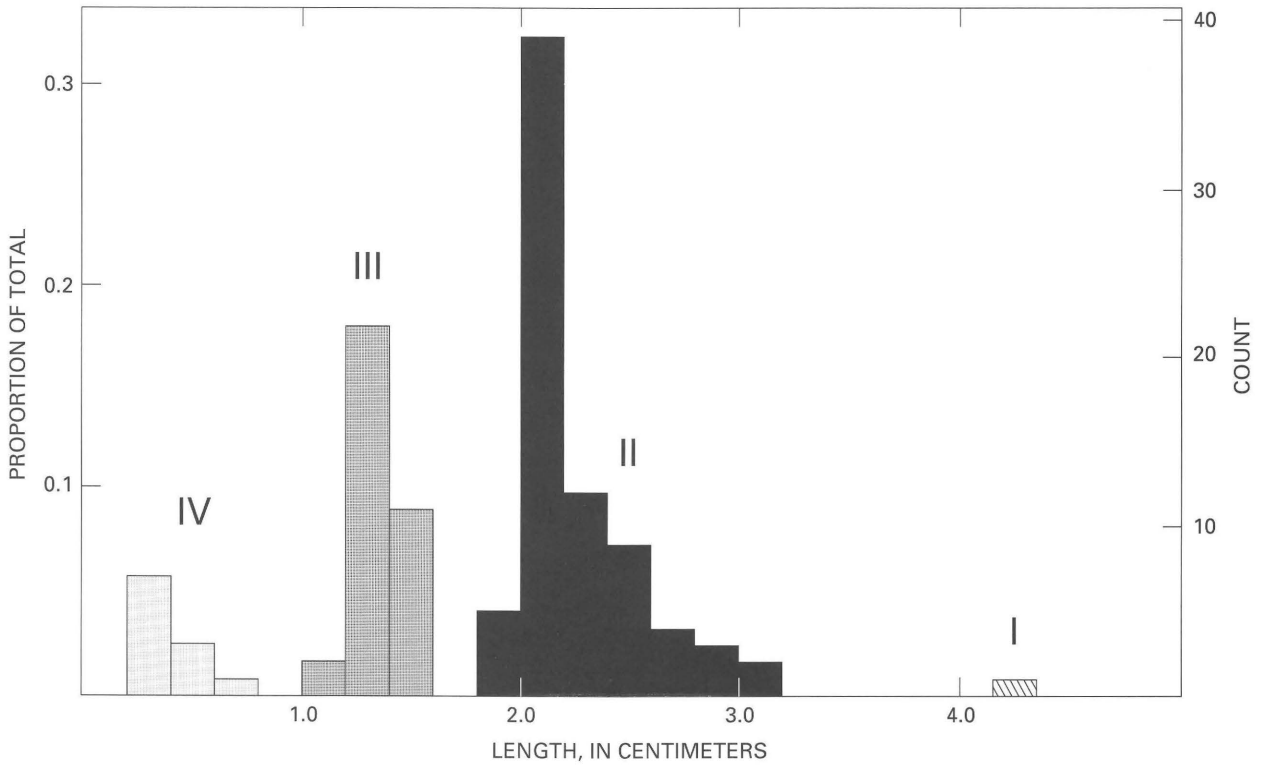

Figure 7. Histogram depicting four size groups (Groups I–IV, in text) of fossil cocoons from the Claron Formation.

closed structures that, aside from the large pores on some wasp cocoons, do not have openings into the cell or into the entrance burrow during the time of larval development. All trace fossils of wasps from the Claron Formation consist of cocoons (figs. 6*A*, *C–E*; 8*A,B*) and four fragments of cell walls (fig. 6*C*).

The lengths of the cocoons fall into four distinct sizes, termed Group I (largest) through Group IV (smallest, see fig. 7). The collection consists of but two examples of the largest (Group I) cocoon. The only complete specimen (fig. 6*D*) is 4.32 cm in length; it has a conical top and narrows to a gently rounded base. Although its surface is relatively smooth, it exhibits no bioglyph to suggest that it might have been woven as opposed to constructed of earth. Group II cocoons (figs. 6*E*, 8*A*) range from 1.8 to 3.2 cm in length and are spindle shaped. A few specimens preserve an external bioglyph consisting of faint parallel ridges oriented circumferentially around the short diameter of the cocoon (fig. 6*E*). This pattern suggests that Group II cocoons might have been woven by the larvae. Group III cocoons (fig. 6*E*, 8*B*) range from 1.05 to 1.60 cm in length and have an ovate shape. Their surfaces are very smooth but lack any perceptible bioglyph. Group IV cocoons (fig. 6*E*) range from 0.35 to 0.75 cm in length. Like Group III cocoons, they are ovoid in shape and have a smooth exterior with no trace of a bioglyph.

The presence of four distinct size ranges of cocoons from the Claron Formation suggests that four different wasps might be represented in the ichnofauna. However, three Group II cocoons contain Group III cocoons *inside* them, and Group IV cocoons *only occur inside* both Group I and Group II cocoons. This curious relationship introduces the likelihood that some if not all Group III and Group IV cocoons are those of wasp parasites that entered the original

Figure 8 (facing page). Cocoons of wasps (*A, B*), and holotype and paratypes of *Eatonichnus utahensis* (*C–F*). *A* and *B* are from the Claron Formation, and *B–F* are from the Colter Formation, Utah. *A*, Six large Group II wasp cocoons, showing perforations made by exiting adults or wasp parasites. *B*, Nine small Group III wasp cocoons, showing perforations made by exiting adults or wasp parasites. *C, D*, OM 20201, holotype of *Eatonichnus utahensis* in external view (*C*) and in polished longitudinal cross section (*D*). Note raised vertical bioglyph on whorls (*C*), and packed oblique (top) and partially meniscate vertical burrow fill in interior (*D*). *E*, OM 20203, paratype of *Eatonichnus utahensis*, showing distinctive whorls and raised spiral bioglyph. *F*, *Eatonichnus utahensis*; polished transverse section of OM 20204, paratype, showing filled central burrow. Note feathery pattern of cross section of whorls, tangential to periphery of internal burrow. Bars are 1.0 cm; top bar is scale for *A* and *B*, bottom bar is scale for *C–F*.

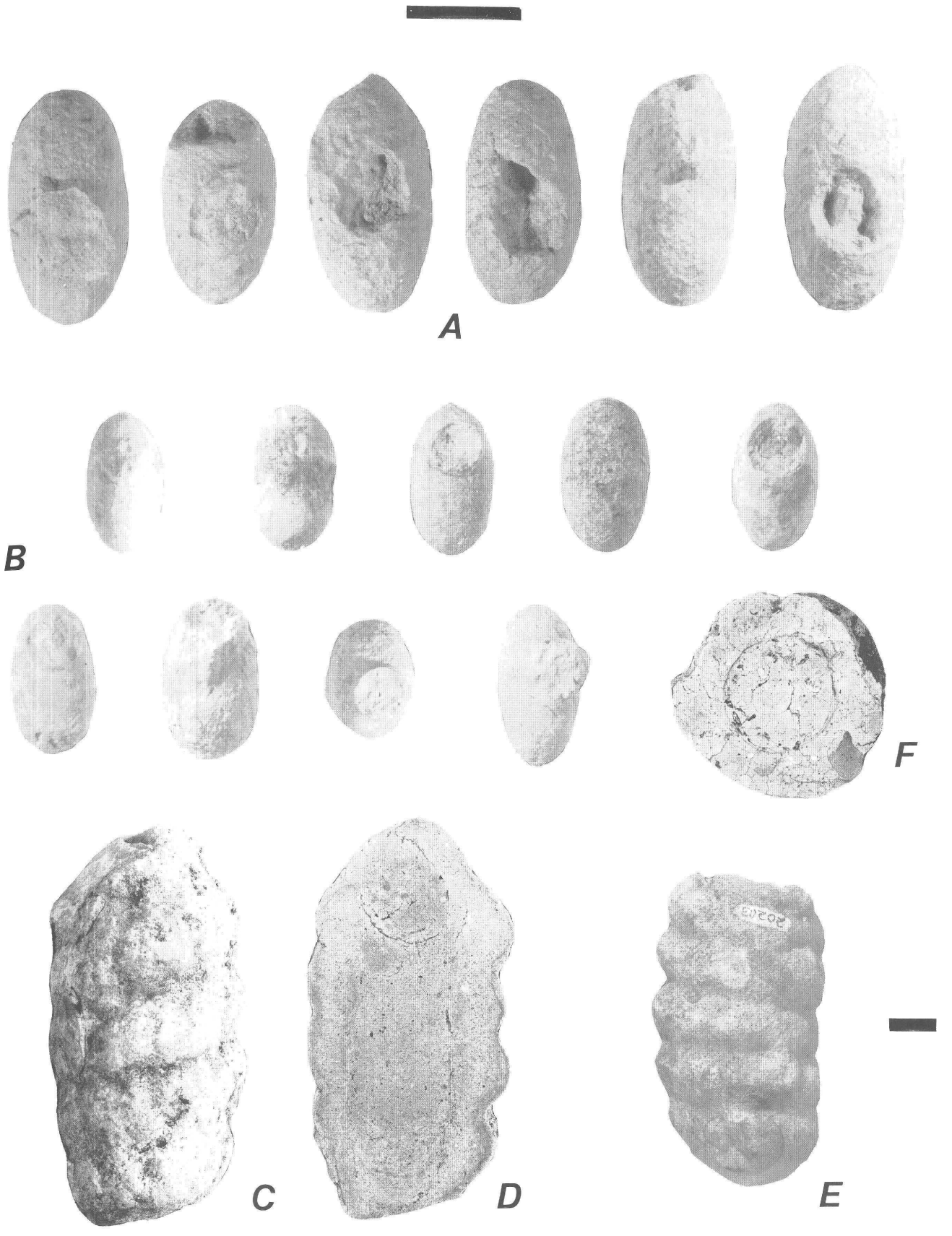
A
B
F
C
D
E

cells during provisioning and before closure, invaded the cocoon, and then laid eggs on the developing larvae. Several kinds of wasp parasites of this kind are known, including other wasps (which then construct their own cocoons), and rhipiphorid beetles and ichneumonid hymenopterans (which do not). Some miltogrammine dipterans are also known to pupate in wasp cocoons. The fact that Group IV cocoons were found *only* within larger cocoons argues strongly that its constructor was a wasp parasite.

Nearly all Group II and Group III cocoons (but no Group I or Group IV cocoons) are breached by round or oblong holes (fig. 8*A, B*). The diameter of these holes ranges from 30 to 50 percent of the length of the long axis of the cocoon, and the holes were probably chewed through the cocoon walls by parasites, because the adult wasp invariably emerges from one end of the cocoon.

TRACE FOSSILS OF UNCERTAIN ORIGIN (COLEOPTERA?)

EATONICHNUS, ichnogenus nov.

Type Ichnospecies.—Xenohelix? utahensis (Gilliland and LaRocque, 1952, p. 502).

Included Ichnospecies.—The type ichnospecies and *E. claronensis*, ichnospecies nov. (infra).

Diagnosis.—Closely appressed whorls tightly spiraled around a central cylindrical cavity and converging terminally, forming a closed, spindle-shaped helix. Helices sinistral or dextral with whorls inclined away from the transverse axis. Whorl diameter remains constant in size along helix and is invariably greater than the diameter of the central cavity. Central cavity fill closely packed, with or without menisci. Differs from *Monesichnus* Roselli in having the central cylindrical cavity surrounded by helical whorls. Differs from *Gyrolithes* De Saporta (incl. *Xenohelix* Mansfield) and *Daimonelix* Barbour in (1) having constructed rather than excavated whorls; (2) having closely appressed whorls forming a closed, rather than an open helix; (3) having whorls converge at both terminations along the long axis; and (4) having a packed central longitudinal cavity enclosed by the whorls of the helix. Differs from *Elipsoideichnus* Roselli and *Ichnogyrus* Bown & Kraus in having central longitudinal cavity.

Etymology.—For Dr. Jeffrey G. Eaton, collector of the holotype of *E. claronensis*, and in recognition of his many important contributions to the geology and paleontology of the Cretaceous and Tertiary of Utah.

EATONICHNUS UTAHENSIS (Gilliland and LaRocque, 1952)

(Figs. 8*C–F*, 9*A*)

Holotype.—The Ohio State University Orton Geological Museum (OM) 20201 (fig. 8*C, D*).

Diagnosis.—Eatonichnus utahensis differs from *E. claronensis* (infra), its closest morphological counterpart, in (1) its 200 percent larger size; (2) having whorls more greatly inclined from the transverse axis; (3) having meniscate fill in the central cavity; and (4) having a bioglyph composed of parallel ribbing that occurs in rows on the external surface of the whorls.

Hypodigm.—The holotype and four paratypes: UO 20202, 20203 (fig. 8*E*), 20204 (fig. 8*F*), 20205; possibly also U.S. Geological Survey (USGS) 26755 (fig. 9*A*) and 26756.

Type Locality.—"West end of Bald Knoll Canyon, section 26, Township 20 S., Range 1-1/2 W. (Salt Lake Meridian), Sevier County, Utah***" (Gilliland and LaRocque, 1952, p. 502). Lower part of upper part of what is probably Colter Formation.

Distribution.—The type locality and possibly also about 20 m above J.G. Eaton locality JGE 89-32; $SE^1/_4NW^1/_4$ section 2, T. 36 S., R. 3 W., Garfield County, Utah. Lower part of upper part of Colter Formation and upper part of lower member of Claron Formation.

Description.—The only known material of *Eatonichnus utahensis* consists of the holotype specimen and four paratypes from the type locality in the Colter Formation near Salina, Utah, and possibly two specimens from the Claron Formation. The type materials were collected from float (Gilliland and LaRocque, 1952), and it cannot be determined if this trace fossil occurs singly or in groups. Of the type materials, only the paratype OM 20202 preserves the terminal convergence of whorls at both ends of the helix and exhibits the spindle-like shape of the complete structure (Gilliland and LaRocque, 1952, Plate 59, figs. 4 and 5). The length of the long axis of this specimen is 100 mm and the trace possesses eight complete whorls (whorl diameter=12.5 mm). The whorls are coiled sinistrally and are inclined approximately 22° to the transverse plane of the specimen. Unfortunately, the external vertical bioglyph

---

Figure 9 (facing page). *Eatonichnus* (*A–I*), and indeterminate trace fossils (*J–L*) from the Claron Formation. *A*, *Eatonichnus* sp., cf. *E. utahensis*, USGS 26755, fragment of specimen in top (left), side (center), and polished section along long axis (right). Note burrow in top and burrow meniscae in sectioned views, and faint bioglyph in side view. *B–I*, *Eatonichnus claronensis*, n. sp.; showing UMNH IP 2241, holotype (*B*), paratypes (*D, E*), external bioglyph (*B, D, F, H*), natural sections of central burrow (*C, E, I*), and polished section exhibiting central burrow (*G*). *J–L*, cf. *Eatonichnus* sp., showing side and top views of two specimens (*K* and *L*), and polished transverse section (*J*). Scales are 1.0 cm; use top scale for *A*, middle scale for *B–I*, and bottom scale for *J–L*.

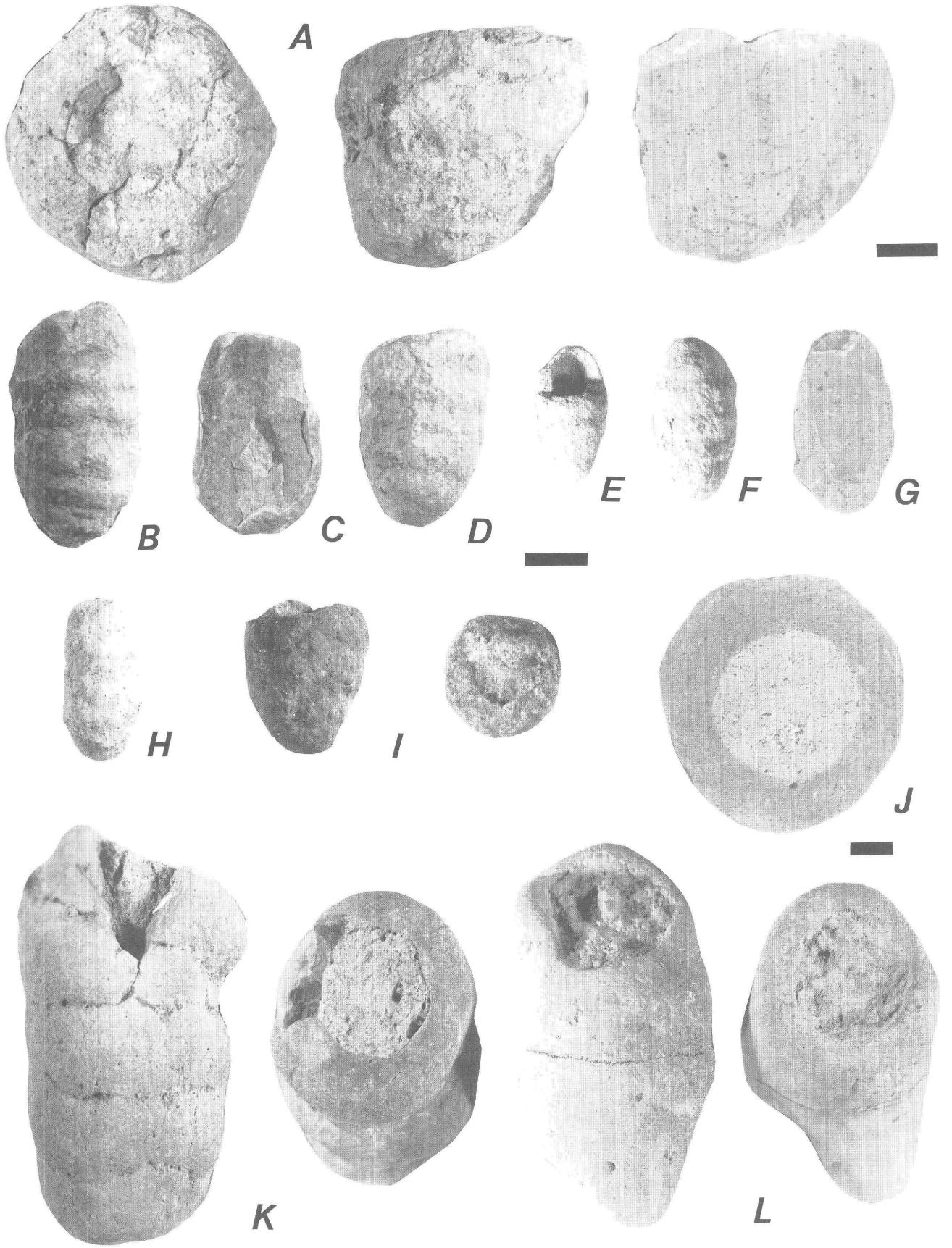
A
B
C
D
E
F
G
H
I
J
K
L

on the whorls is concealed by matrix. The specimen has been longitudinally sectioned and polished and exhibits a filled longitudinal cavity running the length of the specimen. This cavity is 22 mm in width and is nearly twice as broad as the diameter of the external whorls. The medial part of the cavity is 13.5 mm in diameter, and its fill exhibits tight, longitudinally stacked meniscae.

The holotype OM 20201 is 80 mm in length and possesses five complete whorls (whorl diameter=16.0 mm). The whorls are coiled dextrally and are inclined 15° to the transverse plane of the specimen. The external bioglyph on the whorls is well preserved (fig. 8*C*) and consists of a subtle vertical ribbing. The holotype has been sectioned along its longitudinal axis and polished, and it also exhibits a filled longitudinal cavity extending the length of the specimen (fig. 8*D*). This cavity is 21 mm in diameter, contrasting with the smaller whorl diameter of 16.5 mm, and is tightly packed with sediment that is meniscate in its lower third. At the extremity of the cavity opposite that with the meniscate fill, another cavity penetrates the fill of the longitudinal cavity (fig. 8*D*). This cavity has a diameter of 16.5 mm (equal to the whorl diameter) and is inclined 30° to the long axis of the longitudinal cavity.

The paratype OM 20203 (fig. 8*E*) is 72.5 mm long and has six complete whorls (whorl diameter=about 12 mm). The whorls are coiled sinistrally and are inclined at 12° to the transverse plane of the specimen. The whorls exhibit a faint vertically ribbed bioglyph, but this feature is best preserved in the holotype. The longitudinal cavity is exposed in cross section on the broken termination and has a diameter of 23 mm.

OM 20204 (fig. 8*F*) and 20205 are broken specimens that have been sectioned and polished in the transverse plane. Although the whorls are the most obvious external feature of *Eatonichnus*, their internal expression is considerably subdued as seen in cut and polished sections. In transverse section (fig. 8*F*), they appear only as a rind around the central cavity; however, close inspection reveals an obscure, feathery texture that is inclined and tangential to the periphery of the central cavity. In the polished longitudinal section of OM 20202 (not visible in the holotype), the margins of the whorls are sharply defined and whorl interiors show a pattern of irregular, nested crescents. This texture is unlike the packed meniscate fill of the central cavities and is so subtle that we have been unable to reproduce it photographically.

USGS 26755 (fig. 9*A*) and 26756 may represent poorly preserved specimens of *Eatonichnus utahensis* from the Claron Formation. Both are incomplete. USGS 26755 is 37 mm long and preserves three whorls (whorl diameter=12.3 mm), and has a meniscate central cavity with a diameter of 23.4 mm. USGS 26756 consists of four preserved whorls, is 38.2 mm long (whorl diameter=9.5 mm), and has a nonmeniscate central cavity with a diameter of 19 mm. More material is necessary to ascertain the degree of detailed morphological similarity between these specimens and *E. utahensis*; however, they are clearly much too large to belong to the new ichnospecies described next.

***EATONICHNUS CLARONENSIS*, ichnospecies nov.**

(Fig. 9*B-I*)

Holotype.—Utah Museum of Natural History (UMNH) IP 2241 (fig. 9*B*). Collected by J.G. Eaton.

Diagnosis.—*Eatonichnus claronensis* differs from *E. utahensis*, its closest morphological counterpart, in (1) being only 25–30 percent as large, (2) having whorls less inclined from the horizontal, (3) lacking meniscate fill in the central longitudinal cavity, and (4) lacking ribbed bioglyph on the external surface of the whorls.

Hypodigm.—UMNH-IP 2242 (paratype, fig. 9*D*), 2243 (paratype, fig. 9*E*); U.S. Geological Survey (USGS) 26759 (fig. 9*C*), 26760 (fig. 9*F*), 26761 (fig. 9*G*), 26762 (fig. 9*H*), 26763 (fig. 9*I*).

Etymology.—After the Claron Formation, source of all known specimens.

Type Locality.—About 20 m above J.G. Eaton locality JGE 89-32; $SE^1/_4NW^1/_4$ section 2, T. 36 S., R. 3 W., Garfield County, Utah. Upper part of lower member of Claron Formation.

Distribution.—The type locality and E.M. Brouwers locality 94-EB-21 (locality 2, fig. 1), $NE^1/_4SE^1/_4NE^1/_4$ section 30, T. 37 S., R. 6 W., Garfield County, Utah. Upper part of lower member of Claron Formation.

Description.—Fourteen specimens of *Eatonichnus claronensis* were collected from float at the two localities, and one specimen was obtained in place at the type locality. Matrix obscures details of coiling in most specimens; however, four were determined to be coiled dextrally and three sinistrally. The specimens average one whorl every 4.0 to 6.5 mm, and the whorl diameter ranges from 60 to 70 percent of the diameter of the central longitudinal cavity.

UMNH IP-2241, the holotype (fig. 9*B*), is the only complete specimen, and exhibits the distinctive spindle shape of *Eatonichnus*, resulting from closure of the whorls at both terminations. The holotype is 29 mm in length and possesses six complete whorls (whorl diameter=about 4.8 mm). The whorls are coiled dextrally and are inclined about 8° with respect to the transverse plane of the specimen. The specimen has not been sectioned, and its exterior reveals no evidence of the central cavity that is evident in natural or artificial cross sections of all other specimens.

The paratype UMNH IP-2242 (fig. 9*D*) is broken in the transverse plane. This specimen is 25.2 mm long and reveals all or part of five whorls (whorl diameter=about 5 mm). The whorls are coiled dextrally and are inclined at about 10° to the transverse plane of the specimen. Natural transverse breakage reveals a cross section of the internal cavity, which has a diameter of 9.8 mm.

The paratype UMNH IP-2243 (fig. 9*E*) is also naturally broken across the transverse axis and offers the best information about the morphology of the central longitudinal cavity. This specimen is 24 mm in length and retains five complete whorls (whorl diameter=4.8 mm) that are dextrally coiled at

about 12° to the transverse plane. Natural weathering has partially excavated the central cavity, showing it to be a smooth-sided feature having walls that are gently contoured convergently toward the terminations, reflecting the spindle form of the exterior of the trace. All other specimens of *Eatonichnus claronensis* conform to the morphology of the type sample in preserved parts of their structure.

EATONICHNUS sp.

(Fig. 9*J–L*)

Material.—Six fragmentary specimens preserving the middle portions of the trace and weathered natural transverse sections of the filled central cavity (fig. 9*J–L*). Collected by J.G. Eaton.

Locality.—J.G. Eaton locality JGE 94-06 (locality 4, fig. 1), $NE^1/_4NE^1/_4NW^1/_4$ section 23, T. 38 S., R. 7 W., Kane County, Utah. Lower part of upper member of Claron Formation.

Description.—Though all are fragmentary, specimens of *Eatonichnus* sp. are quite large, measuring up to 86 mm along the long axis and 44 mm transversely. In OM 20201, the nearly complete holotype of *Eatonichnus utahensis*, the length is 80 mm, and in the complete paratype OM 20203, it is 72.5 mm. All the specimens at hand have been naturally breached by weathering across the transverse plane; the longest specimen is breached near a termination (fig. 9*K*, bottom of left figure). The widest part of this specimen is at the other broken end, suggesting that if this trace was originally spindle shaped like *Eatonichnus*, its length would be at least 160 mm—nearly twice as great as in *E. utahensis*. The surfaces of all the specimens of *Eatonichnus* sp. are eroded such that the sides are nearly smooth (fig. 9*K, L*). Nonetheless, these surfaces in the five best preserved specimens show evidence of either sinistral (four examples) or dextral (one example) helical coiling. Transverse (fig. 9*J*) and longitudinal natural and cut sections reveal a large, uncomplicated central cavity, its fill lacking meniscae. The most complete specimen possesses five complete whorls and is 86 mm long (whorl diameter=17.2 mm), with a central cavity diameter of 22.5 mm.

Helically coiled, contacting whorls enclosing a filled central cavity with a diameter greater than whorl diameter are the signal diagnostic characters of *Eatonichnus*. The above specimens almost certainly belong in that ichnogenus; however, recovery of more and better material of *Eatonichnus* sp. is desirable to ascertain (1) if this form possessed a vertically arranged bioglyph like that in *E. utahensis*; (2) if the complete traces are spindle shaped; and (3) the size of the complete structure.

DISCUSSION OF *EATONICHNUS*

Since its original description in 1952, "*Xenohelix*? *utahensis*" has remained one of the most enigmatic of all continental trace fossils. Contrasted by its authors, Gilliland and LaRocque, with both of the helical traces known to them (*Xenohelix* Mansfield=*Gyrolithes* De Saporta, and *Daimonelix* Barbour), as well as with gastropods and spiral coprolites, those authors cogently concluded that the morphology of this trace is unlike that of any other ichnogenera with helical form. Though "*Xenohelix*? *utahensis*" has a complex morphology and is known from excellent specimens, it has continued to defy classification, and no reasonable behavioral explanation of its mode of construction nor identification of its trace-maker has ever been proposed. We present a new description of the type and paratype materials, offer an emended diagnosis, and propose the new ichnogeneric name *Eatonichnus* for this unique form. No new material of *Eatonichnus utahensis* is positively known; however, the new ichnofossil *E. claronensis*, ichnospecies nov., is quite similar and (1) offers clarification of the probable paleoenvironment of *Eatonichnus*; (2) provides some additional details regarding its probable mode of construction; and (3) suggests information about the nature of the trace-maker.

Examination of both species of *Eatonichnus* demonstrates that all known specimens possess a consistent and unique trace fossil morphology. The trace has a central cylindrical cavity that is enclosed in a structure with a helical external architecture that converges toward the terminations, forming a spindle. The whorls of the helix invariably have a lesser diameter than the central burrow. The presence or absence of a raised bioglyph on the whorls, variability in the nature of sediment packing in the central cylindrical cavity, and the variation in size among individual specimens are attributed to ichnospecific distinctions among *E. utahensis*, *E. claronensis*, and *Eatonichnus* sp. Aside from sharing a general helical form, the ichnogeneric attributes of *Eatonichnus* clearly do not at all resemble those of *Daimonelix* (Schultz, 1942; Martin and Bennett, 1977), or *Gyrolithes*, or the various forms attributed to its widely used junior synonym, *Xenohelix* (Mansfield, 1927, 1930; Häntzschel, 1962; Kilpper, 1962; Keij, 1965). In all the latter forms, the whorls neither contact each other nor converge at the terminations of the helix (that is, the helices are open). *Ichnogyrus* (Bown and Kraus, 1983) and an unnamed mammal burrow from the upper Eocene of Egypt (Bown, 1982, fig. 13E) are helical burrows with the whorls in contact; however, neither form has an enclosed central cavity and both lack the spindle form with terminally convergent helices. The Upper Cretaceous Uruguayan traces *Elipsoideichnus* and *Monesichnus* (Roselli, 1987) differ from *Eatonichnus* in lacking a central cylindrical cavity and lacking an external helix, respectively.

Although they offered no solution as to its origin, Gilliland and LaRocque (1952) questionably referred *Eatonichnus* to *Xenohelix* (=*Gyrolithes*), thus implying that it might be a trace of burrow origin. Meniscate packing of the internal longitudinal structure in *Eatonichnus utahensis* leaves little doubt that this part of the structure in all cases represents a packed cavity, but not necessarily a burrow. If the remainder of the known surficial and internal morphology of

Eatonichnus is taken into account, it is difficult to reconcile production of the whole trace fossil to any single type of behavior. If it is considered that the entire structure (whorls, whorl ornamentation—where present, convergence of whorls at terminations, and large internal longitudinal cavity) was produced by the burrowing of a single organism, a number of problems become apparent. Whereas the whorls might have been produced by an organism burrowing in a circular motion at an inclination to the horizontal (Toots, 1963), the whorl diameters in *Eatonichnus* are invariably smaller than the diameters of the associated internal cavities. Moreover, the sediment comprising the whorls is not meniscate but, where well preserved, appears instead to be layered—a circumstance suggesting that the whorls and the central cavity might have been produced by two distinct types of behavior. This idea is also supported by observations that (1) the whorls (so explicit on the exteriors of the specimens) are not obvious in cut sections, and (2) the whorls converge toward the center of the long axis at both terminations of the structure, forming a helix that is closed at both ends.

We suggest that *Eatonichnus* may be a subterranean nest that was constructed of masticated mud and silt particles taken from the sediment of the host soil. Such constructions (**aedificichnia** of Bown and Ratcliffe, 1988) have exceptional preservation potential (Genise and Bown, 1994; Hasiotis and others, 1994) and therefore, like *Eatonichnus*, generally occur as discrete, full three-dimensional-relief trace fossils that are readily separable from host matrices.

The external aspect and size, as well as the shape and size of the central cavity and the meniscate filling, suggest that *Eatonichnus* might be the nest of an unidentified type of dung beetle that constructed nests similar in some aspects to those of *Phaneina*. Among Scarabaeinae, tunnels with helicoidal pattern are known only in *Eucranium* (Monteresino); it is unknown, to our knowledge, for any other kind of underground insect nest. Although some wasps and bees construct helical nests, they are aerial and very different from *Eatonichnus*. The meniscate fill of the central cavity is recorded in some extant and fossil scarabaeid nests; for example, the trace fossils *Scaphichnium hamatum* (Bown and Kraus, 1983; Hasiotis and others, 1993), and *Monesichnus ameghinoi* (Roselli, 1987; Genise and others, submitted manuscript). The whorls with a vertical bioglyph are reminiscent of the juxtaposed arched mud cells of *Chubutolithes gaimanensis* (Genise and Bown, 1990); however, the internal structures of *Eatonichnus* and *Chubutolithes* are completely different.

New studies in progress by two of us (J.F.G. and T.M.B.) suggest that both *Monesichnus* and *Eatonichnus* might be constructions of dung beetles.

SUMMARY: PALEOENVIRONMENTS OF THE CLARON FORMATION

Insect trace fossils can be sensitive indicators of paleoclimate to the extent that their morphology directly reflects a general group adaptation to environmental circumstance, or is characteristic of a group whose environmental distribution, within certain constraints, is known. The constructor of *Parowanichnus formicoides* was almost certainly an ant; however, the internal morphologies of the nests of most living species of ants are unknown. Most ants prefer to dig in a slightly moist substrate (Hölldobler and Wilson, 1990), and the construction of closely nested, tiered galleries and chambers within a meter of the ancient ground surface in *Parowanichnus* suggests a relatively high water table. Conversely, the vertical shafts connecting concentrations of tiered chambers and galleries, though relatively shallow, suggest that the water table might have fallen at times. This combination of features would reflect adaptation to a climate with inequable, perhaps seasonal rainfall.

Digging bees and wasps have achieved their greatest diversity and are the most abundant in well-drained semiarid to subhumid regions, in which insect food for their larvae abounds and where there is adequate dry soil in which to nest (Malyshev, 1935; Evans, 1957, 1963; Evans and Eberhard, 1970). Solitary bees prefer bare, dry soil that is exposed to the sun (Batra, 1984). The abundance and variety of traces of subterranean bees and wasps in Claron paleosols (at least six different kinds) strongly argue for a mesic regime (wetter than semiarid and drier than subhumid), with a lesser rather than a greater density of ground vegetation (Genise and Bown, 1994, 1996). This interpretation is consistent with that of alternating wet and dry seasons that is suggested by the morphology of the ant nest *Parowanichnus*.

The paleoenvironmental significance of ichnospecies of the new trace fossil *Eatonichnus* is uncertain. The only known occurrences of the ichnogenus are in the Colter and Claron Formations of Utah, units that have been tentatively correlated in part by Schneider (1967), and both believed to be in part fluvial and in part lacustrine origin.

REFERENCES CITED

Anderson, J.J., 1971, Geology of the southwestern High Plateaus of Utah—Bear Valley Formation, an Oligocene-Miocene volcanic arenite: Geological Society of America Bulletin, v. 82, p. 1179–1205.

———1993, The Markagunt megabreccia—Large Miocene gravity slides mantling the northern Markagunt Plateau, southwestern Utah: Utah Geological Survey Miscellaneous Publication 93-2.

Batra, S.W.T., 1984, Solitary bees: Scientific American, February, p. 120–127.

Bowers, W.E., 1972, The Canaan Peak, Pine Hollow, and Wasatch Formations in the Table Cliff region, Garfield County, Utah: U.S. Geological Survey Bulletin 1331–B, 39 p.

Bown, T.M., 1982, Ichnofossils and rhizoliths of the nearshore fluvial Jebel Qatrani Formation (Oligocene), Fayum Province, Egypt: Palaeogeography, Palaeoclimatology, Palaeoecology, v. 40, p. 255–309.

Bown, T.M., and Kraus, M.J., 1983, Ichnofossils of the alluvial Willwood Formation (lower Eocene), Bighorn Basin, northwest Wyoming, U.S.A.: Palaeogeography, Palaeoclimatology, Palaeoecology, v. 43, p. 95–128.

Bown, T.M., and Laza, J.H., 1990, A Miocene termite nest from southern Argentina and its paleoclimatological implications: Ichnos, v. 1, p. 73–79.

Bown, T.M., and Ratcliffe, B.C., 1988, The origin of *Chubutolithes* [Ihering], ichnofossils from the Eocene and Oligocene of Chubut Province, Argentina: Journal of Paleontology, v. 62, p. 163–167.

Brian, M.V., and Downing, B.M., 1956, The nests of some British ants: Proceedings of the Tenth International Congress of Entomology, v. 2, p. 539–540.

Brown, R.W., 1934, *Celliforma spirifer*, the fossil larval chambers of mining bees: Journal of the Washington Academy of Sciences, v. 24, p. 532–539.

Evans, H.E., 1957, Studies on the comparative ethology of digger wasps of the genus *Bembix*. Ithaca, N.Y., Cornell Studies in Entomology; Ithaca, Comstock.

———1963, Wasp farm: Ithaca, N.Y., Cornell University Press, 178 p.

Evans, H.E., and Eberhard, M.J.W. 1970, The wasps: Ann Arbor, Mich., University of Michigan Press, 265 p.

Genise, J.F., and Bown, T.M., 1990, The constructor of the trace fossil *Chubutolithes*: Journal of Paleontology, v. 64, p. 482–483.

———1994, New Miocene scarabaeid and hymenopterous nests and early Miocene (Santacrucian) paleoenvironments, Patagonian Argentina: Ichnos, v. 3, p. 107–117.

———1996, *Uruguay* Roselli, 1938, and *Rosellichnus*, n. ichnogenus, two ichnogenera for clusters of fossil bee cells: Ichnos, v. 4, p. 199–217.

Gilliland, W.N., and LaRocque, A., 1952, A new *Xenohelix*? from the Paleocene of Utah: Journal of Paleontology, v. 26, p. 501–504.

Goldstrand, P.M., 1994, Tectonic development of Upper Cretaceous to Eocene strata of southwestern Utah: Geological Society of America Bulletin, v. 106, p. 145–154.

Gregg, R.E., 1963, The ants of Colorado, with reference to their ecology, taxonomy, and geographic distribution: Boulder, Colo., University of Colorado Press, 718 p.

Häntzschel, W., 1962, Treatise on invertebrate paleontology, Part W—Trace fossils and problematica: New York, p. 177–245.

Hasiotis, S.T., Aslan, Andres, and Bown, T.M., 1993, Origin, architecture, and paleoecology of the early Eocene continental ichnofossil *Scaphichnium hamatum*—Integration of ichnology and paleopedology: Ichnos, v. 3, p. 1–9.

Hasiotis, S.T., Bown, T.M., and Abston, Carl, 1994, Photoglossary of marine and continental ichnofossils: U.S. Geological Survey Digital Data Series, DDS–23 (CD-ROM Disc).

Hölldobler, B., and Wilson, E.O., 1990, The ants: Cambridge, Mass., Belknap, 732 p.

Keij, A.J., 1965, Miocene trace fossils from Borneo: Paläontologischichte Zeitschrift, v. 39, p. 220–228.

Kilpper, K., 1962, *Xenohelix* Mansfield 1927 aus der miozänen Niederrheinischen Braunkohlenformation: Paläontologischichte Zeitschrift, v. 36, p. 55–58.

Laza, J.F., 1982, Signos de actividad atribuibles a *Atta* (Myrmicidae, Hymenoptera) en el Mioceno de la provincia de La Pampa, República Argentina—Significación paleozoogeográfica: Ameghiniana, v. 19, p. 109–124.

Leith, G.K., and Harder, E.C., 1908, The iron ores of the Iron Springs district, southern Utah: U.S. Geological Survey Bulletin 338, 102 p.

Mackin, J.H., 1960, Structural significance of Tertiary volcanic rocks in southwestern Utah: American Journal of Science, v. 258, p. 81–131.

Maldonado, Florian, 1995, Decoupling of mid-Tertiary rocks, Red Hills–western Markagunt Plateau, southwestern Utah, chapter I *in* Scott, R.B., and Swadley, W C, eds., Geologic studies in the Basin and Range–Colorado Plateau transition in southeastern Nevada, southwestern Utah, and northwestern Arizona, 1992: U.S. Geological Survey Bulletin 2056, p. 233–254.

Maldonado, Florian, and Williams, V.S., 1993, Geologic map of the Parowan Gap quadrangle, Iron County, Utah: U.S. Geological Survey Geologic Quadrangle Map GQ–1712, scale 1:24,000.

Malyshev, S.I., 1935, The nesting habits of solitary bees: Eos, v. 11, p. 200–309.

Mansfield, W.C., 1927, Some peculiar fossil forms from Maryland: Proceedings of the U.S. National Museum, v. 71, p. 1–9.

———1930, Some peculiar spiral fossil forms from California and Mexico: Proceedings of the U.S. National Museum, v. 77, p. 1–2.

Martin, L.D., and Bennett, D.K., 1977, The burrows of the Miocene beaver *Palaeocastor*, western Nebraska, U.S.A.: Palaeogeography, Palaeoclimatology, Palaeoecology, v. 22, p. 173–193.

McCook, H.C., 1882, The honey ants of the garden of the gods, and the occident of the American plains: Philadelphia, J.B. Lippincott, 188 p.

Moser, J.C., 1963, Contents and structure of *Atta texana* nest in summer: Annals of the Entomological Society of America, v. 56, p. 286–291.

Mullett, D.J., 1989, Interpreting the early Tertiary Claron Formation of southern Utah: Geological Society of America Abstracts with Programs, v. 21, p. 120.

Mullett, D.J., Wells, N.A., and Anderson, J.J., 1988, Unusually intense pedogenic modification of the Paleocene-Eocene Claron Formation of southwestern Utah: Geological Society of America Abstracts with Programs, v. 20, p. 217.

Retallack, G.J., 1984, Trace fossils of burrowing beetles and bees in an Oligocene paleosol, Badlands National Park, South Dakota: Journal of Paleontology, v. 58, p. 571–592.

Roselli, F.L., 1938, Apuntes de geología y paleontología uruguayas y sobre insectos del cretáceo del Uruguay y el descubrimiento de admirables instintos constructivos de esa época: Boletín Sociedad Ciencias Naturales "Kraglievich-Fontana" (Nueva Palmira, Uruguay), v. 1, p. 29–96.

———1987, Paleoicnología—Nídos de insectos fósiles de la cubertura mesozóica del Uruguay: Publicaciónes del Museo Municipal de Nueva Palmira, vol. 1, p. 1–56.

Schneider, D.C., 1967, Early Tertiary continental sediments of central and south-central Utah: Brigham Young University Geology Studies, v. 14, p. 143–194.

Schultz, C.B., 1942, A review of the *Daimonelix* problem: Nebraska University Studies, Science and Technology, v. 2, p. 1–30.

Stahel, G., and Geijskes, D.C., 1939, Ueber den Bau der Nester von *Atta cephalotes* L. und *Atta sexdens* L. (Hym., Formicidae): Revue de Entomología, v. 10, p. 27–78.

Sudd, J.H., 1967, An introduction to the behaviour of ants: London, Edward Arnold, 200 p.

Sudd, J.H., and Franks, N.R., 1987, The behavioural ecology of ants: New York, Chapman and Hall, 206 p.

Talbot, M., and Kennedy, C.H., 1940, The slave-making ant *Formica sanguinea subintegra* Emery, its raids, nuptial flights, and nest structure: Annals of the Entomological Society of America, v. 33, p. 560–577.

Threet, R.L., 1952a, Geology of the Red Hills area, Iron County, Utah: Seattle, Wash., University of Washington Ph. D. dissertation, 107 p.

———1952b, Some problems of the Brian Head (Tertiary): Geological Society of America Abstracts with Programs, v. 63, p. 1386.

Toots, Heinrich, 1963, Helical burrows as fossil movement patterns: Contributions to Geology, v. 2, p. 129–134.

von Frisch, K., 1974, Animal architecture: New York, Harcourt Brace Jovanovich, 192 p.

Wheeler, W.M., 1907, Fungus-growing ants of North America: American Museum of Natural History Bulletin, v. 23, p. 727–799.

———1910, Ants: New York, Columbia, 663 p.

Zahradník, J., 1991, Bees, wasps, and ants—A field guide to the world's Hymenoptera: London, Hamlyn, 192 p.

The Paleocene Grand Castle Formation—A New Formation on the Markagunt Plateau of Southwestern Utah

By Patrick M. Goldstrand *and* Douglas J. Mullett

GEOLOGIC STUDIES IN THE BASIN AND RANGE–COLORADO PLATEAU TRANSITION IN SOUTHEASTERN NEVADA, SOUTHWESTERN UTAH, AND NORTHWESTERN ARIZONA, 1995

U.S. GEOLOGICAL SURVEY BULLETIN 2153–D

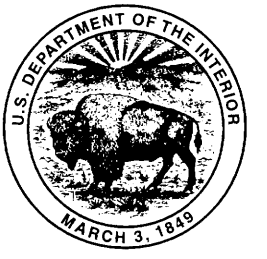

UNITED STATES GOVERNMENT PRINTING OFFICE, WASHINGTON : 1997

CONTENTS

FIGURES

The Paleocene Grand Castle Formation—A New Formation on the Markagunt Plateau of Southwestern Utah

By Patrick M. Goldstrand[1] *and* Douglas J. Mullett[2]

ABSTRACT

Recent geologic studies in southwestern Utah have defined a new formation, the Grand Castle Formation. The Paleocene Grand Castle Formation unconformably overlies the Upper Cretaceous Iron Springs Formation and is overlain by the Paleocene to Eocene Claron Formation. Previously, the Grand Castle was considered the basal part of the Claron Formation on the Markagunt Plateau. Lithologically similar strata of the Grand Castle are present on the Table Cliff Plateau (mapped as the upper part of the Upper Cretaceous to lower Paleocene Canaan Peak Formation) and are unconformably overlain and separated from the Claron Formation by the Paleocene(?) to Eocene(?) Pine Hollow Formation. The Grand Castle is considered to be Paleocene in age; it grades upward into possible upper Paleocene strata of the Claron Formation on the Markagunt Plateau, and lithologically similar strata to the Grand Castle on the Table Cliff Plateau are both underlain and overlain by lower Paleocene strata.

The Grand Castle Formation consists of as much as 230 meters of boulder to pebble conglomerate and sandstone deposited in a braided fluvial environment. Precambrian quartzite and Paleozoic carbonate clasts, in conjunction with east to south-southeast paleoflow indicators, suggest a source from the Wah Wah, Blue Mountain, and Iron Springs thrust sheets of southwestern Utah. The Grand Castle conglomerates unconformably overlie the easternmost, and presumably youngest, thrust fault attributed to the Sevier orogeny, indicating that the formation postdates the Sevier orogeny. Eastward, on the Table Cliff Plateau, correlative strata to the Grand Castle are tilted by folds attributed to the Laramide orogeny, indicating that the Grand Castle, in part, was deposited before extensive Laramide deformation. Thus, the Grand Castle provides a tectonostratigraphic record between the Sevier orogeny and extensive partitioning of the foreland basin during Laramide orogeny for southwestern Utah.

[1]Geological Sciences Dept., MS 172, University of Nevada, Reno, NV 89557.

[2]Ford Motor Company, 15201 Century Dr., Suite 608, Dearborn, MI 48120.

INTRODUCTION

Episodes of thrust faulting (Sevier orogeny) in southern California, southern Nevada, and western Utah controlled the patterns of sedimentation in central and eastern Utah during Cretaceous time, with sediment being shed eastward into the foreland basin (fig. 1; Spieker, 1946, 1949; Armstrong and Oriel, 1965; Armstrong, 1968; Fouch and others, 1983; Lawton, 1983; DeCelles, 1988). Beginning in latest Cretaceous and continuing into Paleogene time, basement-cored uplifts (Laramide orogeny) partitioned the Sevier foreland basin into internally drained, intermontane basins (fig. 1; Chapin and Cather, 1981; Dickinson and others, 1986, 1988; Franczyk and others, 1992).

Exposures of Upper Cretaceous to lower Tertiary rocks in southwestern Utah are important because they document the temporal and spatial basin development of the southern extension of the Sevier and Laramide orogenies. Of particular geologic interest is the recognition of a Paleocene formation that provides important evidence for the tectonic and paleogeographic development in southern Utah between the Sevier and Laramide orogenies. This report describes the stratigraphy, petrology, and facies in the Grand Castle Formation (new name), a conglomerate and sandstone unit as much as 230 m thick that lies between Upper Cretaceous foreland basin deposits and lower Tertiary intermontane deposits in southwestern Utah.

The Grand Castle Formation is named for exposures along the flanks of Grand Castle, a towering topographic feature southeast of the town of Parowan (fig. 2). This formation is lithologically distinctive from the underlying and overlying formations: it unconformably overlies foreland-basin sandstones and grades upward into intermontane mudstones and carbonate rocks. Because the Sevier thrust faults are truncated by the Grand Castle Formation, the formation must postdate the Sevier orogeny. However, lithologically identical strata to those of the Grand Castle Formation are present to the east in the Table Cliff Plateau and are interpreted to be correlative to the Grand Castle. These correlative strata in the Table Cliff Plateau are folded and overlain by Laramide basinal deposits, suggesting that, in part, rocks of the Grand Castle Formation were deposited before extensive partitioning of the foreland basin during the Laramide orogeny.

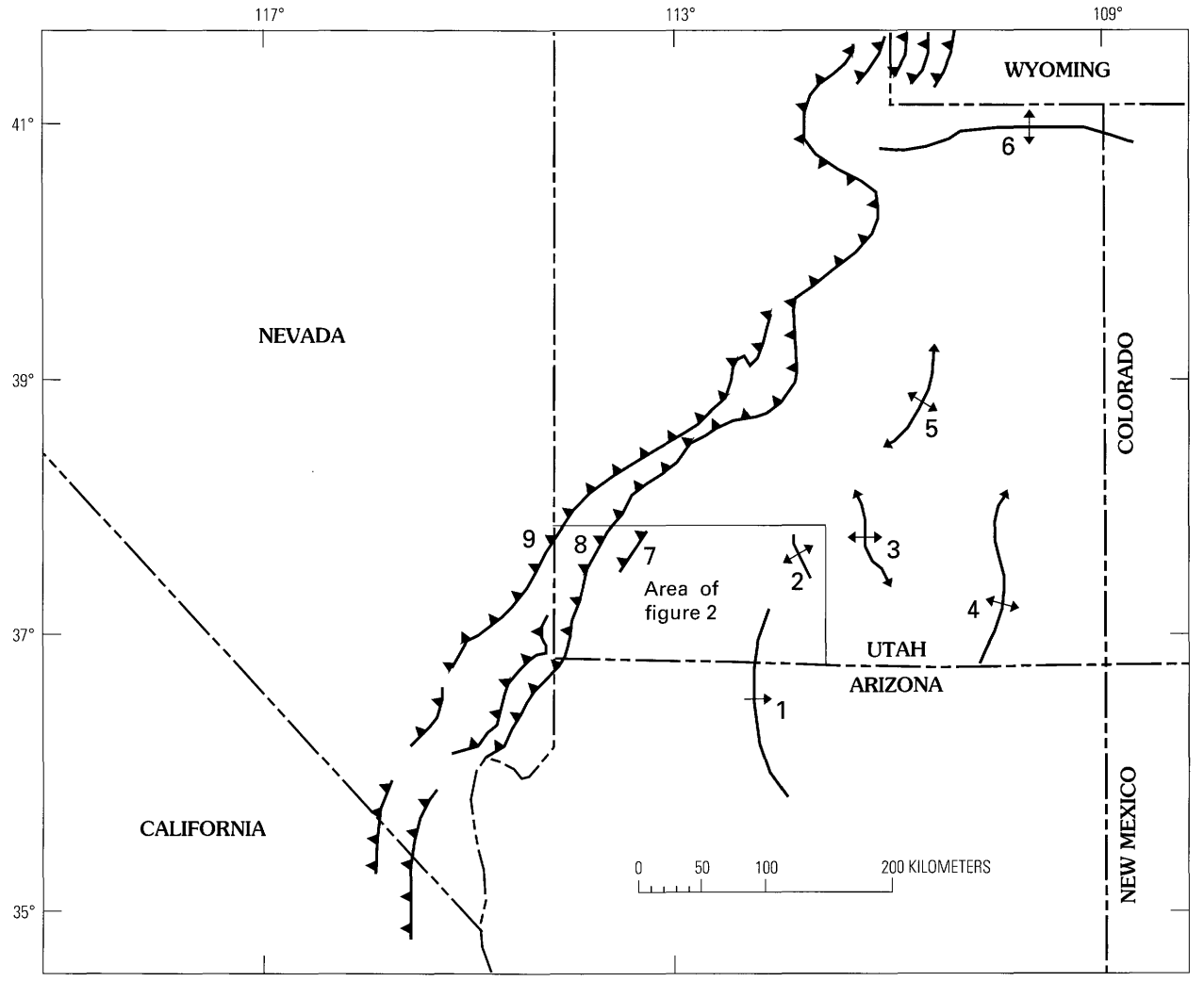

Figure 1. Paleotectonic map for Utah, northern Arizona, southern Nevada, and southeastern California showing positions of Sevier and Laramide structures in relation to the study area. Laramide structures: 1, Kaibab monocline; 2, Johns Valley anticline and Table Cliff syncline; 3, Circle Cliffs uplift; 4, Monument Upwarp; 5, San Rafael Swell; 6, Uinta Mountains. Arrows show dip and plunge of structures. Sevier structures: 7, Iron Springs thrust; 8, Blue Mountain thrust; 9, Wah Wah thrust (modified from Cross, 1986). Sawteeth on upthrust block.

ACKNOWLEDGMENTS

This research was part of P.M. Goldstrand's doctoral dissertation completed at the University of Nevada-Reno under direction of J.H. Trexler, Jr., and doctoral research in progress by D.J. Mullett through Kent State University under direction of N.A. Wells. Partial support for this research was provided through grants by Sigma Xi, Shell Oil, the Geological Society of America, and the Utah Geological and Mineral Survey to P.M. Goldstrand. We wish to thank J.J. Anderson, J.G. Eaton, K.L. Franczyk, L.F. Hintze, and T.F. Lawton for their helpful discussions, and E.A. Johnson and E.G. Sable of the U.S. Geological Survey for their review of this report.

PREVIOUS WORK AND STRATIGRAPHIC CORRELATIONS

The Grand Castle Formation has previously been included in the basal part of the Claron Formation (Reeside and Bassler, 1922; Thomas and Taylor, 1946; Gregory, 1950a, 1950b, 1951; Bissell, 1952; Cook, 1957, 1960; Threet, 1963) in the Markagunt Plateau (figs. 2, 3). Moore (1982) and Hilton (1984) distinguished this conglomeratic unit from the Claron Formation in their investigations of the west-central part of the Markagunt Plateau and called it the Beehive unit. Goldstrand (1991, 1992, 1994) and Maldonado and Moore (1993) referred to this unit informally as the "Grand Castle formation."

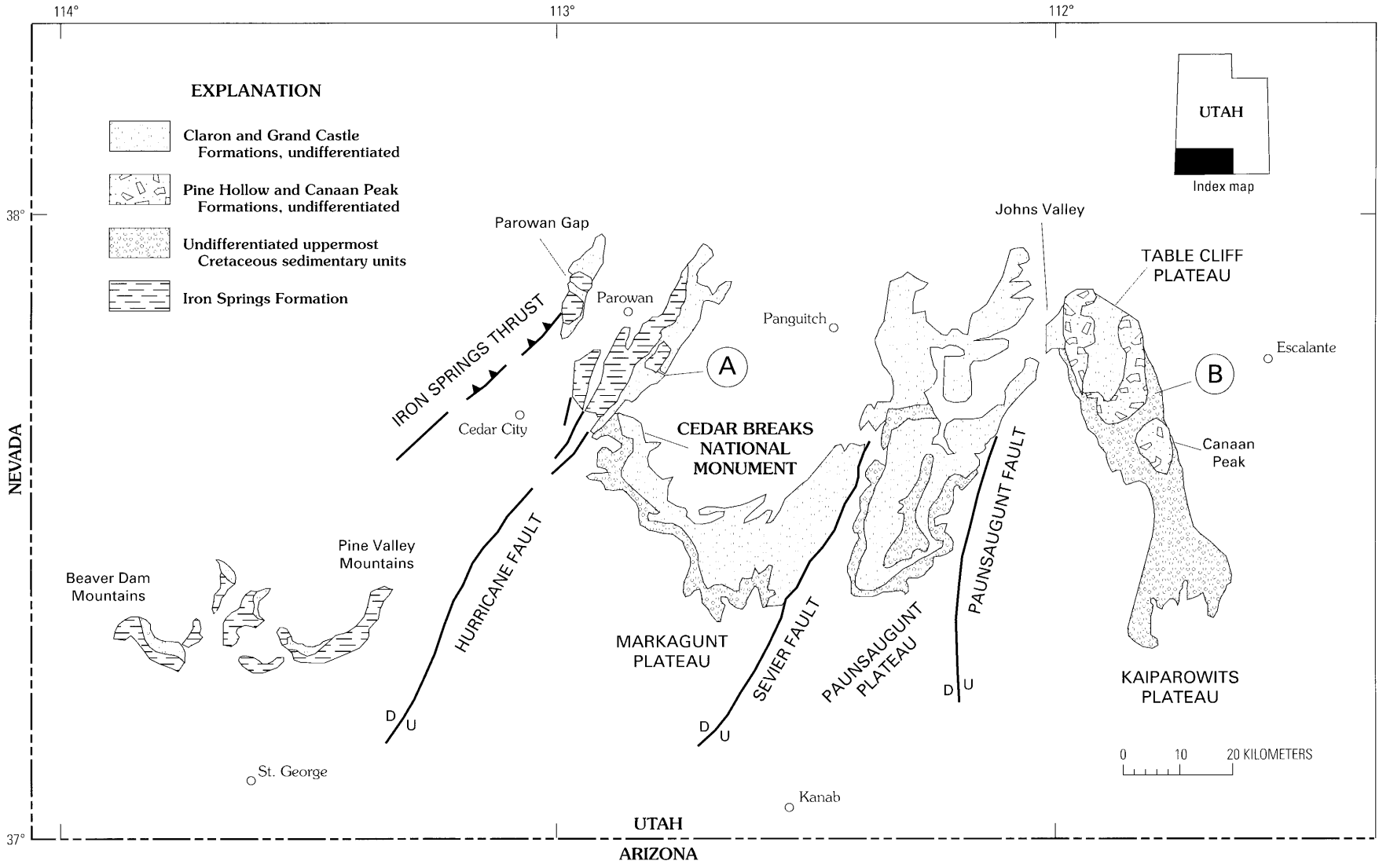

Figure 2. Generalized geologic map of Upper Cretaceous to Eocene strata of southwestern Utah (modified from Hintze, 1963). A, location of Grand Castle type section, B, Table Cliff area. On faults, U, upthrown side; D, downthrown side; sawteeth on upthrust block.

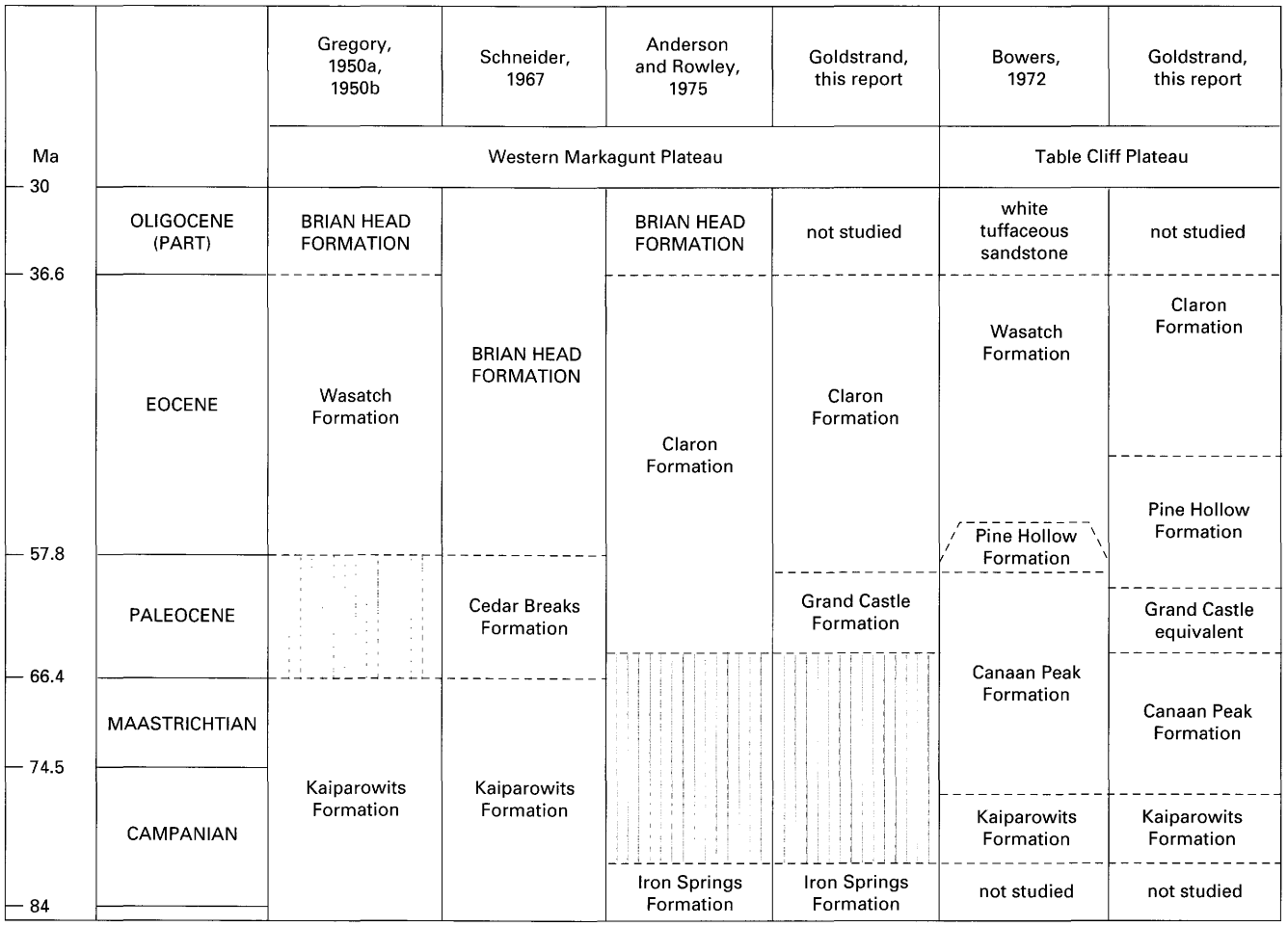

Figure 3. Correlation diagram of Upper Cretaceous and lower Tertiary formations presented in this report, and correlations with existing reports for the western Markagunt and Table Cliff Plateaus. Dashed boundary, exact age uncertain; vertical line pattern, erosional hiatus.

The Claron Formation of Leith and Harder (1908), which overlies the Grand Castle Formation, is exposed throughout the study area (fig. 2). This formation has been previously referred to as the Claron Formation, Wasatch Formation, and Cedar Breaks Formation by different workers (fig. 3). The use of Wasatch Formation has been questioned (Robison, 1966; Schneider, 1967; Anderson and Rowley, 1975) because of differences in lithology and age from the type Wasatch Formation (Hayden, 1869) in northern Utah and Wyoming, whereas the use of Cedar Breaks Formation (Schneider, 1967) has not gained wide acceptance.

Compositionally and texturally the Grand Castle Formation differs significantly from the Claron Formation and is designated a separate lithostratigraphic formation. The Claron Formation consists of as much as 640 m of pink to white limestone and calcareous sandstone and shale (Gregory, 1950a, 1950b; Bowers, 1972; Hackman and Wyant, 1973; Sargent and Hansen, 1982). In contrast, the Grand Castle consists of as much as 230 m of pebble to boulder conglomerate and sandstone. Calcareous beds are noticeably absent within the Grand Castle.

At Table Cliff Plateau, a compositionally identical conglomerate to that of the Grand Castle Formation is present in the upper part of the upper Campanian to lower Paleocene Canaan Peak Formation. Bowers (1972) first noted an upward compositional change in the conglomerate clasts, from dominantly quartzite and felsic volcanic clasts in the lower Canaan Peak to predominantly quartzite and limestone clasts in the upper part of the formation. Goldstrand (1991, p. 25–31) noted the compositional similarities between the Grand Castle conglomerates in the western Markagunt Plateau and those in the uppermost part of the Canaan Peak Formation at Table Cliff Plateau. The similarities in clast compositions between the Grand Castle conglomerate in the Markagunt Plateau and the conglomerate in the uppermost Canaan Peak Formation suggest that they are correlative (Goldstrand, 1991, 1992).

STRATIGRAPHY

The Grand Castle Formation unconformably overlies Cretaceous and Jurassic rocks and is overlain by the lower Tertiary Claron Formation in the Markagunt Plateau and Parowan Gap region. Along the Markagunt Plateau and the eastern part of Parowan Gap, the contact between the underlying Iron Springs and Grand Castle Formations is erosional and is placed at the abrupt change from sandstone of the Iron Springs to conglomerate of the Grand Castle. In the western part of Parowan Gap, the contact between the Grand Castle conglomerate and fine-grained Cretaceous and Jurassic strata is marked by a distinct angular unconformity.

The contact between the Grand Castle and overlying Claron Formations is either gradational or abrupt. Where the upper contact appears gradational, the contact is placed where red, calcareous sandstone and siltstone beds (of the Claron Formation) contribute greater than 50 percent of the lithology. At the type section (fig. 4, section 2), this contact is marked by an abrupt change from gray conglomerate to red, calcareous sandstone. In the Cedar Breaks National Monument area, 25 km south of the type section (figs. 2, 4), the upper part of the Grand Castle consists of white, quartz-rich sandstone. Here, the contact between the Grand Castle and Claron Formations is placed at a slope break, where white slope-forming Grand Castle (noncalcareous) sandstone is overlain by red, cliff-forming calcareous sandstone and siltstone of the Claron Formation.

At its type section, the Grand Castle Formation has been divided into three informal members: a lower conglomerate, a middle sandstone, and an upper conglomerate (fig. 5; and see Type Section). The lower conglomerate member forms gray "hoodoo" or steep, cone-shaped topography, whereas the upper conglomerate member forms red, massive cliffs. The middle sandstone member forms white, steplike slopes.

The three members of the Grand Castle Formation vary laterally in thickness along the Markagunt Plateau. South from the type area, in the Cedar Breaks National Monument area, the upper and lower conglomerate members thin and pinch out, and the middle sandstone member thickens correspondingly before it pinches out south of the monument (fig. 6). In the Parowan Gap area (fig. 4) the middle sandstone is not present, and it is uncertain which conglomerate member directly overlies the Iron Springs Formation and older Mesozoic strata. The steep cliff expression of the Grand Castle in Parowan Gap may indicate that only the upper conglomerate member is present in this area.

LITHOLOGY

Lithologies within the upper and lower conglomerate members of the Grand Castle Formation are similar and are therefore described together.

UPPER AND LOWER CONGLOMERATE MEMBERS

The coarse-grained rocks of the Grand Castle Formation are predominantly composed of structureless to crudely bedded conglomerate but include lesser amounts of planar and trough-crossbedded conglomerate. Individual beds are generally 0.3–0.9 m thick but rarely are as much as 3 m thick. Amalgamated complexes dominate and are as thick as 11 m. Beds are normally graded; boulder to pebble conglomerate grades upward and laterally into horizontally stratified sandstone. Medium- to coarse-grained, horizontally stratified sandstone lenses are common within the structureless to crudely bedded conglomerate. Lower bounding surfaces of individual complexes are eroded and channelled. Planar-crossbedded conglomerate is present as individual 1-m-thick beds or more commonly as amalgamated stacks of as many as three beds that are normally graded. The conglomerate commonly is overlain by lenses of trough and planar cross-stratified sandstone. Planar-crossbedded conglomerate commonly overlies structureless to crudely bedded conglomerate or, more rarely, trough-crossbedded conglomerate. Trough-crossbedded conglomerate is present in amalgamated beds as much as 8 m thick consisting of individual beds 1.5–2 m thick. The trough-crossbedded conglomerate commonly is overlain by structureless to crudely bedded conglomerate or by lenses of horizontally stratified sandstone.

A distinctive 1.4- to 2.5-m-thick pink marker unit of structureless and matrix-supported conglomeratic mudstone and sandstone is present in the upper conglomerate member at the type section and at surrounding outcrops. This unit consists of two beds: a 1- to 2-m-thick boulder-cobble conglomerate supported in a fine-grained sandstone matrix, and an overlying 0.4-m-thick pebbly mudstone (see Type Section). The pebbly mudstone, which contains fossil plant fragments and petrified wood, is overlain by a discontinuous bed of laminated very fine grained sandstone and siltstone.

MIDDLE SANDSTONE MEMBER

The middle sandstone member differs texturally from the lower and upper conglomerate members. With the exception of rare intraclasts of mudstone, the middle member is composed exclusively of very fine grained to fine-grained sandstone. The member contains horizontally stratified, planar and trough cross-stratified, and ripple-laminated sandstone. Convolute beds and associated dish structures are also abundant. The horizontally stratified sandstone contains beds that are generally 20–50 cm thick and fine upward into siltstone. Stacked sequences of horizontally stratified beds range in thickness from 1 to 3.5 m. The horizontally stratified sandstone generally overlies trough and planar cross-stratified sandstone. Trough cross-stratified sandstone is present in cosets as much as 4.5 m

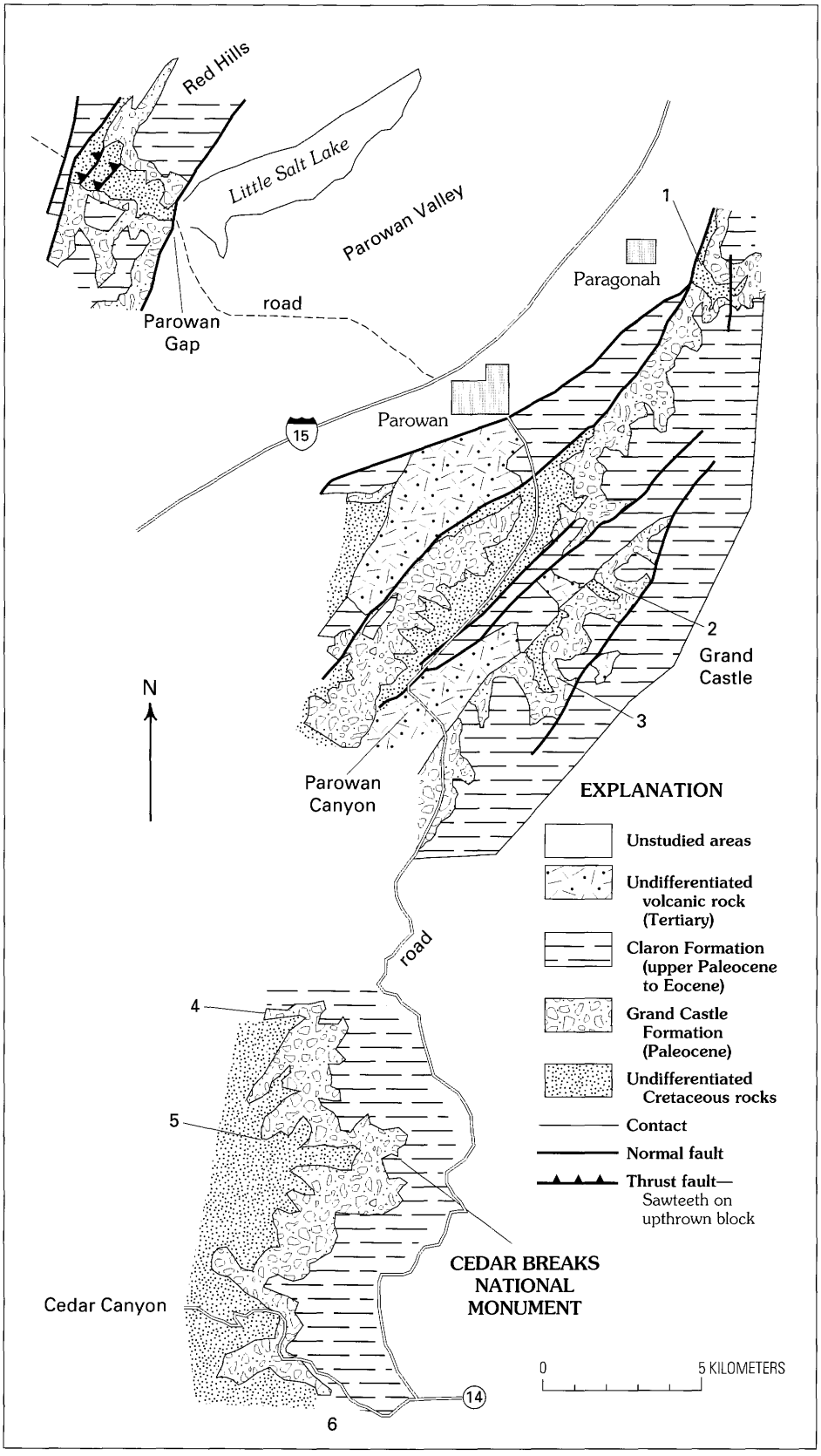

Figure 4. Generalized geologic map of the Parowan Gap and western Markagunt Plateau region of southwestern Utah. Numbers designate location of measured sections shown in figure 6. Data modified from Threet (1963), Moore (1982), Goldstrand (1991), Maldonado and Moore (1993), and Maldonado and Williams (1993).

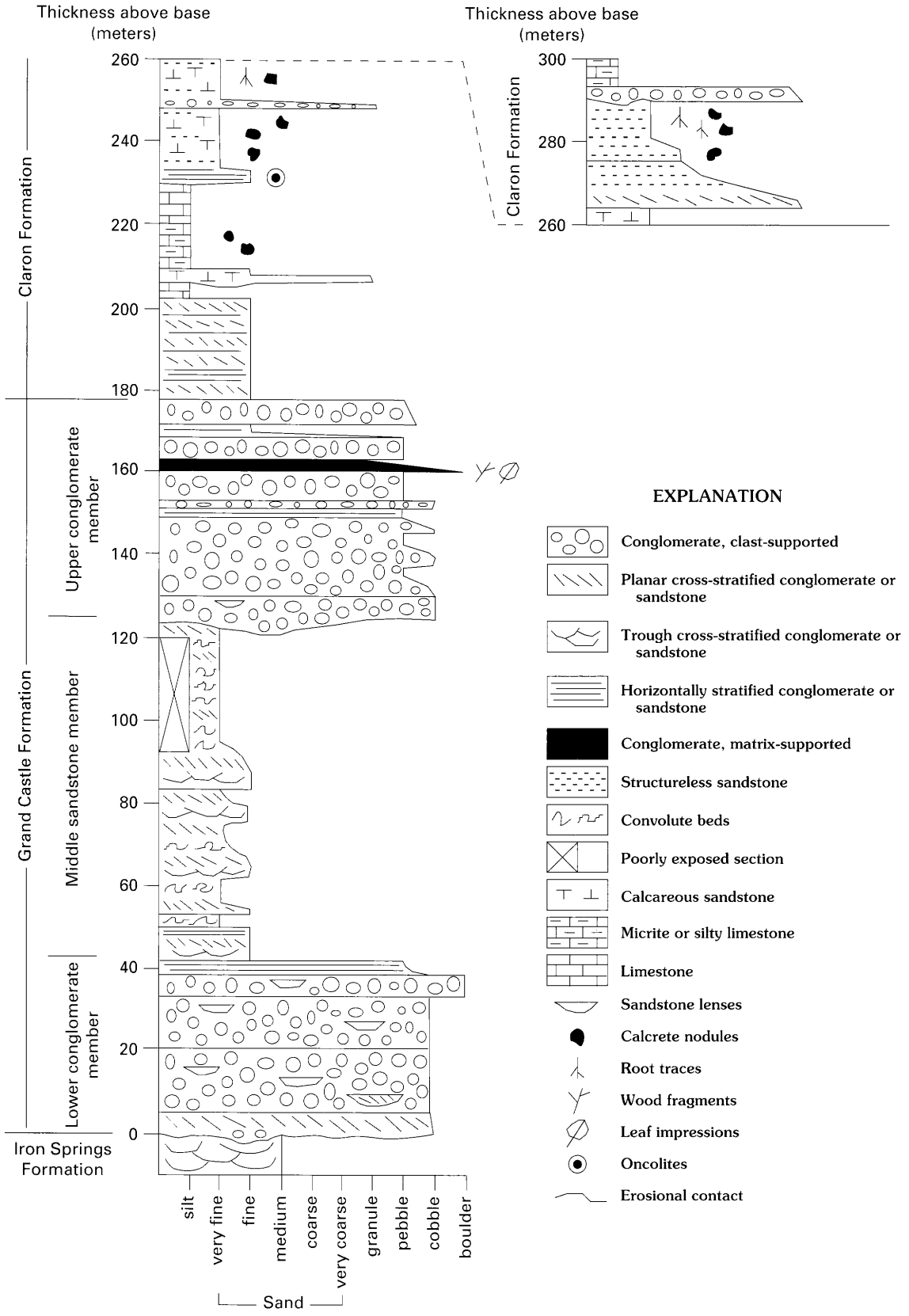

Figure 5. Generalized geologic column of the type section of the Grand Castle Formation and part of overlying Claron Formation, southwestern Utah. Location of measured section shown in figure 4 (section 2). See Type Section for detailed description (from Goldstrand, 1991).

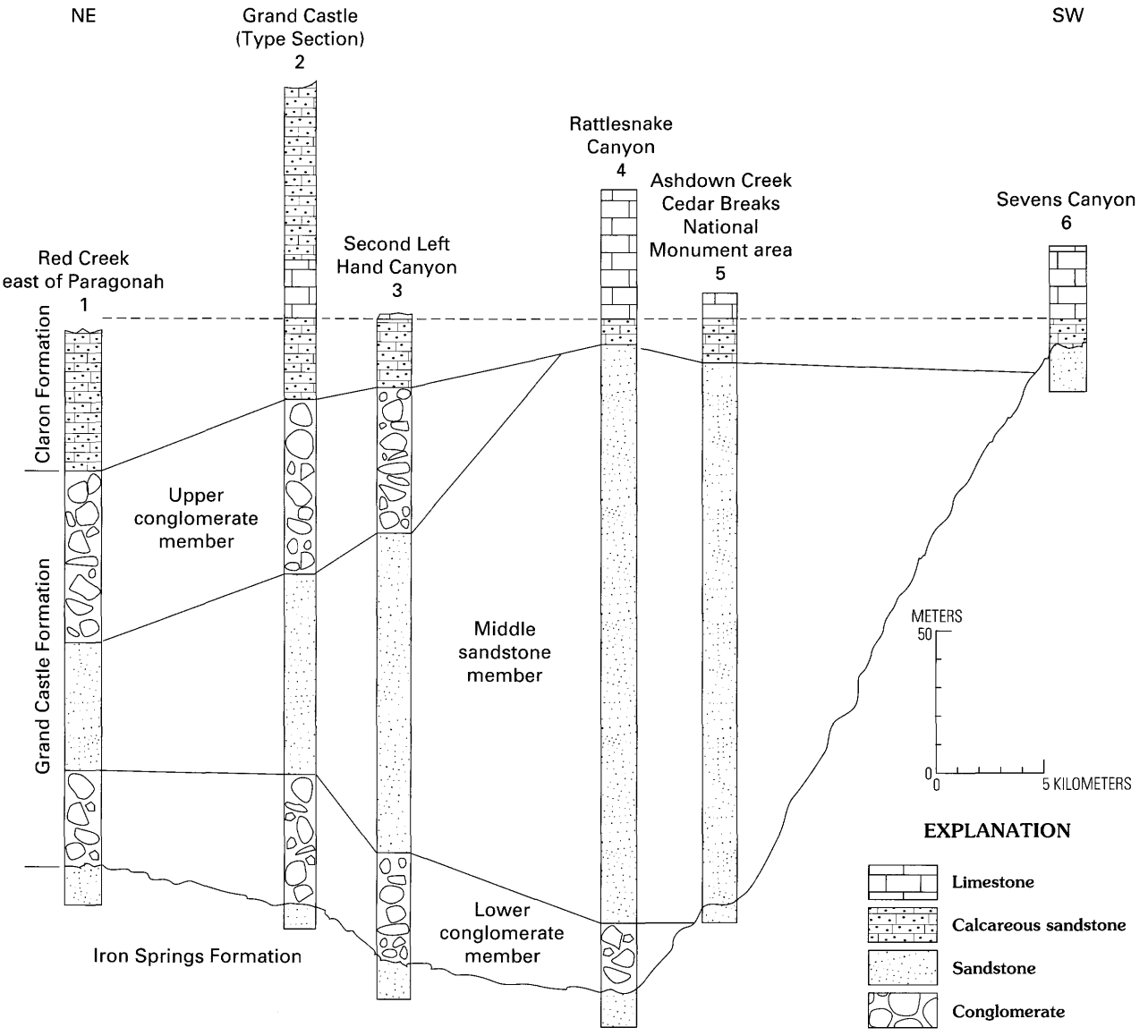

Figure 6. Generalized sections of the Grand Castle Formation and lower part of Claron Formation, western Markagunt Plateau (see fig. 4 for locations). Horizontal datum at lowest continuous limestone unit within the Claron Formation (from Goldstrand, 1991).

thick; single-trough sets are as much as 1 m thick and 3 m wide. These sandstones have sharp basal contacts and both gradational and erosional upper bounding surfaces. The trough cross-stratified sandstone is overlain by planar cross-stratified or horizontally stratified sandstone. Planar cross-stratified sandstones are commonly interbedded with horizontally stratified sandstone and siltstone lenses 10–20 cm thick. Planar cross-stratified sandstone beds range from 0.5 to 1.5 m in thickness. Ripple-laminated sandstone beds are less than 20 cm thick and are present above horizontally stratified and cross-stratified beds.

Log casts and carbonized wood debris are abundant in the middle sandstone member of the Grand Castle Formation. Broad-leafed plant impressions and root traces are locally abundant. Horizontal and vertical burrows are rare.

Paleocurrent data from the Grand Castle Formation are highly variable but generally indicate paleoflow to the southeast (fig. 7). Pebble imbrication in the lower and upper conglomerate members indicate an east to south-southeast paleoflow. Paleocurrent measurements of trough crossbed axes indicate a southeasterly paleoflow direction for the middle sandstone member.

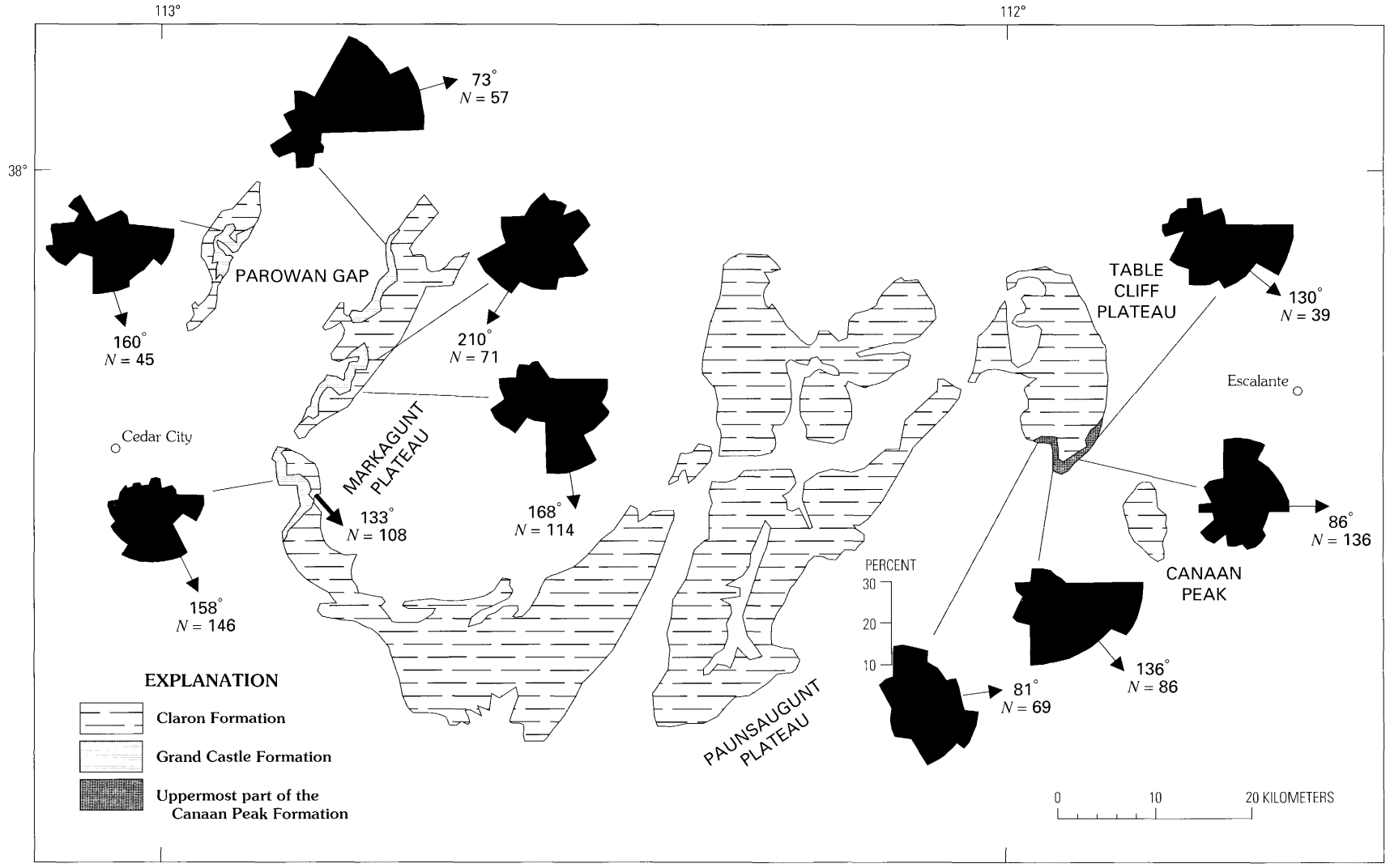

Figure 7. Paleocurrent data for the Grand Castle Formation and uppermost part of the Canaan Peak Formation. Rose diagrams show pebble-imbrication measurements; arrow denotes mean paleocurrent direction for each diagram. Heavy arrow (below Markagunt Plateau) indicates mean paleocurrent direction determined from trough-crossbed axes measurements from the middle member of the Grand Castle Formation; *N*, number of measurements.

TYPE SECTION OF THE GRAND CASTLE FORMATION

Composite section of the Grand Castle Formation and lower part of the Claron Formation measured by Jacob staff: Lower conglomerate and middle sandstone members located at west side of Grand Castle, First Left Hand Canyon, NE$^1/_4$ sec. 6, T. 35 S., R. 8 W., Parowan 7.5-minute quadrangle, Iron County, Utah. Upper conglomerate member and the overlying Claron Formation located above prospect pit on south side of Grand Castle at NW$^1/_4$NE$^1/_4$ sec. 8, T. 35 S., R. 8 W., Parowan 7.5-minute quadrangle, Iron County, Utah. Measured by P.M. Goldstrand in July 1988.

		Thickness (meters)	*Cumulative thickness (meters)*
Claron Formation (lower part only):			
33.	Limestone, silty, red, forms steep slopes	5	5
32.	Conglomerate, cobble- to boulder-size clasts, gray, structureless, channelized, with sandstone matrix; capped by discontinuous, white, very fine grained sandstone that grades laterally into sandy micrite and limestone. Clasts include quartzite 52 percent, gray limestone 36 percent, dolostone 5 percent, silicified limestone 3 percent, kaolinite 1 percent, other rock types 2 percent	4	9
31.	Sandstone, purple, very fine grained, structureless; contains calcrete nodules near the top and root traces 2–3 cm in diameter and as much as 1 m long; beds 0.5–1 m thick	8	17
30.	Sandstone, purple, very fine grained, calcareous; contains calcrete nodules	14.5	31.5
29.	Conglomerate; cobble-size clasts, channelized; grades upward into overlying sandstone	1.5	33
28.	Conglomerate; cobble- to pebble-size clasts, planar crossbedding; fines upward to sandstone. Clasts include quartzite, gray limestone, dolostone, and silicified limestone	2.5	35.5
27.	Sandstone, red, very fine grained, calcareous; contains calcrete nodules and calcite-filled root traces near top of unit and 0.5-m-thick pebble conglomerate at base. Sharp basal contact	11.5	47
26.	Sandstone, red to purple, very fine grained to fine-grained; exhibits crude horizontal stratification, beds are 0.5–1 m thick; contains algal and oncolitic rip-up clasts, grades upward to abundant calcrete nodules overlain by 0.5-m-thick red limestone at top of unit; forms steep slopes	19	66
25.	Limestone, purple, mottled; beds 0.5–1.5 m thick	9.5	75.5
24.	Limestone with interbedded silty micrite laminae, purple, yellow, light-gray; nodular layers common; forms massive cliffs	8	83.5
23.	Sandstone, red, fine-grained, structureless, calcareous; contains horizontal calcite-filled fractures; a 0.5-m-thick basal conglomerate, containing rip-up clasts of underlying unit, rests on erosional surface	6.5	90
Claron Formation —Continued			
22.	Limestone, red, yellow, and pink, silty, nodular	3	93
21.	Sandstone, red; contains amalgamated beds (20–70 cm thick) with scour channels and planar cross-stratification	13	106
20.	Sandstone, gray to pink, calcareous, thick-bedded; exhibits horizontal stratification and planar cross-stratification. Sharp basal contact	5.5	111.5
	Partial thickness for Claron Formation		111.5
Grand Castle Formation:			
Upper conglomerate member:			
19.	Conglomerate, pebble- to cobble-size clasts, stained red; some interbedded thick sandstone lenses	4.5	4.5
18.	Sandstone, gray, fine-grained; scour bases commonly contain pebbly sandstone throughout; exhibits horizontal stratification	3	7.5
17.	Conglomerate; pebble-size clasts, structureless; interbedded lenses of fine-grained sandstone with horizontal stratification. Clasts are: quartzite 44 percent, gray limestone 34 percent, silicified limestone 12 percent, dolostone 6 percent, kaolinite 1 percent, other rock types 3 percent	9.5	17
16.	Pebbly mudstone, white to pink, structureless, matrix supported; black siltstone and laminated very fine grained sandstone lenses at top of unit; very well indurated and forms a pink marker bed within overall gray cliffs; contains fossil plant fragments; petrified wood present, and Late Cretaceous palynomorphs that have possibly been reworked	0.4	17.4
15.	Conglomerate; boulder- to cobble-size clasts; pink, structureless; matrix supported in fine-grained sandstone	2	19.4
14.	Conglomerate; cobble-size clasts, gray; crude horizontal bedding; some pebble lenses at top grade laterally into horizontally stratified sandstone	3	22.4
13.	Pebbly sandstone, tan; exhibits horizontal bedding; fills a channel; cobble and boulder conglomerate at base and fines upward into horizontal stratified sandstone	4.5	26.9
12.	Conglomerate; cobble- to pebble-size clasts poorly sorted; in crude beds 30–90 cm thick that are thicker upward; overlain by lenses of medium-grained sandstone with planar cross-stratification	19	45.9
11.	Conglomerate; cobble-size clasts; gray, crudely bedded; beds grade upward into pebble conglomerate and medium- to coarse-grained sandstone lenses that are planar laminated; sharp basal contact with as much as 2 m of relief. Clasts include quartzite 46 percent, gray limestone 28 percent, silicified limestone 12 percent, kaolinite 9 percent, dolostone 3 percent, other rock types 2 percent	10	55.9

		Thickness (meters)	Cumulative thickness (meters)
Grand Castle Formation —Continued			
Middle sandstone member:			
10.	Sandstone, very light gray, very fine grained to fine-grained, quartz-rich, horizontal stratification, planar and trough cross-stratification; contains abundant convolute beds; forms slope	43	98.9
9.	Sandstone, tan to orange (iron-stained), very fine grained to fine-grained; exhibits convolute lamination and planar and trough cross-stratification	30	128.9
8.	Sandstone, very light gray, coarse-grained; exhibits convoluted bedding and trough cross-stratification; some dewatering structures; overlain by very fine grained ripple-laminated sandstone	3.5	132.4
7.	Sandstone, light-gray, yellow, and tan, fine-grained; exhibits convolute bedding, planar and trough cross-stratification, and horizontal stratification; sharp basal contact	8	140.4
Lower conglomerate member:			
6.	Conglomerate; pebble-size clasts; crude horizontal bedding; coarse-grained sandstone lenses abundant. Clasts include quartzite 63 percent, gray limestone 29 percent, kaolinite 7 percent, other rock types 1 percent	2.5	142.9
5.	Conglomerate; boulder-size clasts; structureless; horizontally stratified coarse- to medium-grained sandstone lenses common	4.5	147.4
4.	Conglomerate; cobble-size clasts; mostly structureless but some planar crossbeds; abundant sandstone lenses; forms hoodoos and cone-shaped cliffs	13	160.4
3.	Conglomerate; cobble-size clasts, gray; structureless to crude beds 1 m thick with sharp basal contacts; commonly overlain by lenses of planar cross-stratified sandstone; forms hoodoos and cone-shaped cliffs	16	176.4
2.	Conglomerate; cobble- to boulder-size clasts, gray; planar crossbedded to structureless; contains abundant sandstone lenses; sharp basal contact; forms hoodoos and cone-shaped cliffs. Clasts include quartzite 78 percent, gray limestone 22 percent	5	181.4
Total thickness of the Grand Castle Formation			181.4
Iron Springs Formation (part):			
1.	Sandstone, brown to tan, medium- to coarse-grained; convolute bedding common, trough cross-stratified	10+	10+

SANDSTONE AND CONGLOMERATE COMPOSITIONS

Sandstones of the Grand Castle Formation are sublitharenites and litharenites (see Folk, 1974). Grains are mostly fine to very fine, nonundulose, monocrystalline quartz (Goldstrand, 1992). The grains are well rounded, commonly have abraded quartz overgrowths, and have a frosted surface texture. The major lithic types are silicified carbonate and carbonate rock fragments. Grains of microspar and pseudospar are most common, but micrite grains are locally abundant (Goldstrand, 1992). Dolomite crystals and pseudomorphs are commonly preserved in the silicified carbonate grains. Other sedimentary lithic grains include quartzite with zircon and feldspar subgrains and foliated quartzite with muscovite subgrains.

Clasts in the Grand Castle Formation consist of quartzite, gray limestone, tan silicified carbonate, dark-gray dolostone, and minor white kaolinite (Goldstrand, 1992). Quartzite clasts are mostly red, purple, and tan and are banded and cross-laminated similar to strata in the Late Proterozoic and Lower Cambrian Prospect Mountain Quartzite. Paleozoic fossils are common in the silicified carbonate and limestone clasts and include the sponge *Chaetetes* sp.?, rugose corals, bryozoans, crinoid columnals, brachiopods, and fusulinid foraminifera; the fusulinid foraminifera suggest partial source from upper Paleozoic strata. Minor amounts of dolostone clasts are present within the upper part of the Grand Castle Formation. Clasts of kaolinite are restricted to the type section area.

AGE

The age of the Grand Castle Formation is not precisely constrained because of a lack of fossils and radiometrically datable material. Correlative strata in the uppermost part of the Canaan Peak Formation at Table Cliff Plateau apparently are early Paleocene in age. Early Paleocene palynomorphs have been collected from mudstone in the Canaan Peak Formation underlying conglomerate lithologically identical to that of the Grand Castle Formation. Early Paleocene palynomorphs have also been collected from the overlying lower part of the Pine Hollow Formation (Goldstrand, 1991, p. 36–38), although they might have been reworked from the underlying Canaan Peak Formation (Goldstrand, 1994). Thus, at Table Cliff Plateau, strata lithologically identical and apparently correlative to the Grand Castle Formation are stratigraphically bounded by lower Paleocene rocks.

The Grand Castle Formation (on the Markagunt Plateau) appears to grade upward into the Claron Formation and may be as young as late Paleocene in age. Late Paleocene palynomorphs have been collected from the basal Claron Formation in the Pine Valley Mountains (fig. 2; Goldstrand,

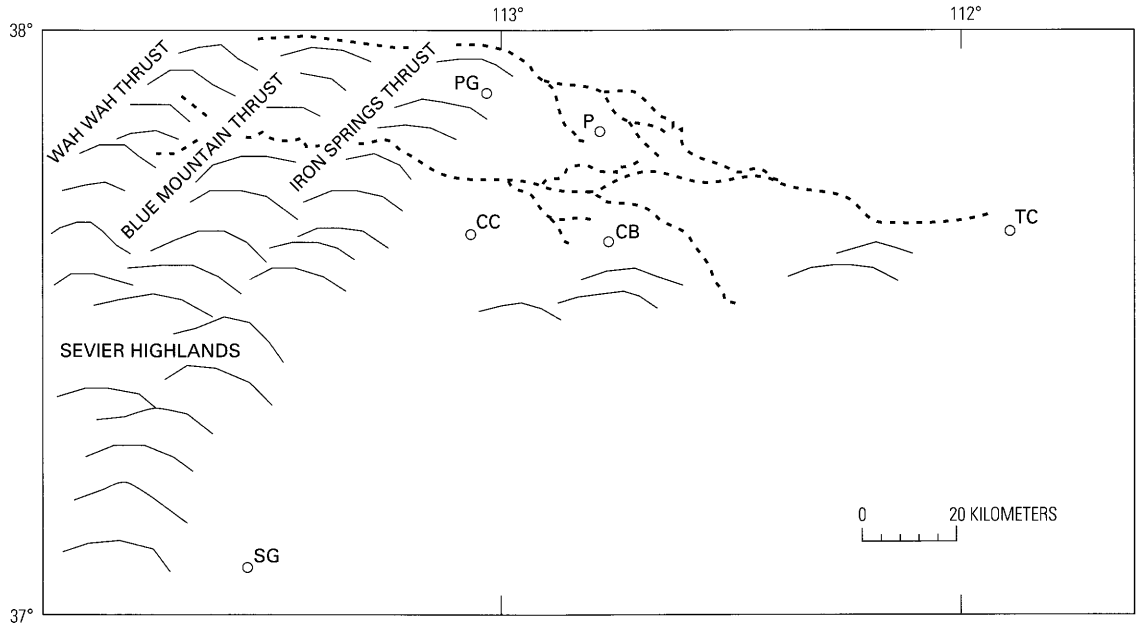

A

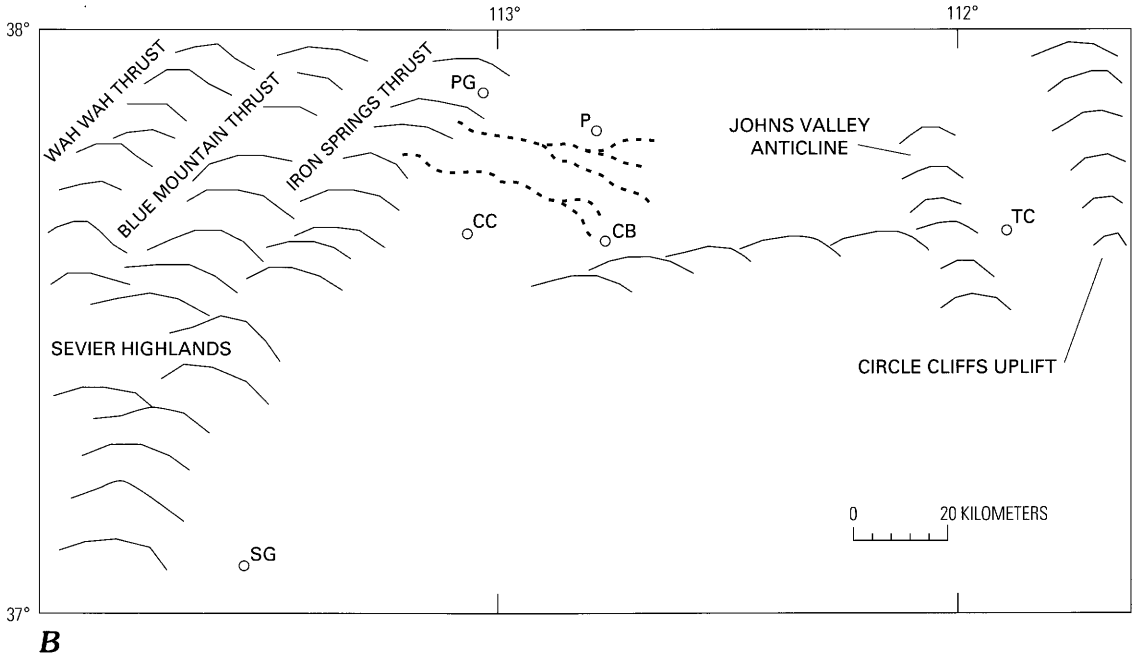

B

1991, p. 50). Assuming that the basal Claron is temporally equivalent from the Pine Valley Mountains northeastward to the western Markagunt Plateau (a distance of approximately 78 km), the Grand Castle on the Markagunt Plateau may be as young as late Paleocene.

Preservation of palynomorphs in the Grand Castle Formation has apparently been inhibited because of oxidation of the entire formation. Only one bed, a 0.4-m-thick very poorly sorted and matrix-supported pebbly mudstone, has provided palynomorph fossils. A Late Cretaceous (possibly Santonian) palynomorph age was determined from this bed (D.J. Nichols, written commun., 1991). As noted following, we believe that this bed is a debris-flow deposit derived from Late Cretaceous rocks, and that the Santonian-age palynomorphs were recycled into the Grand Castle Formation.

DEPOSITIONAL AND TECTONIC INTERPRETATIONS

The lower and upper conglomerate members of the Grand Castle Formation were deposited in a gravelly braided river, whereas the middle sandstone member formed in a sandy braided fluvial environment. In the lower and upper

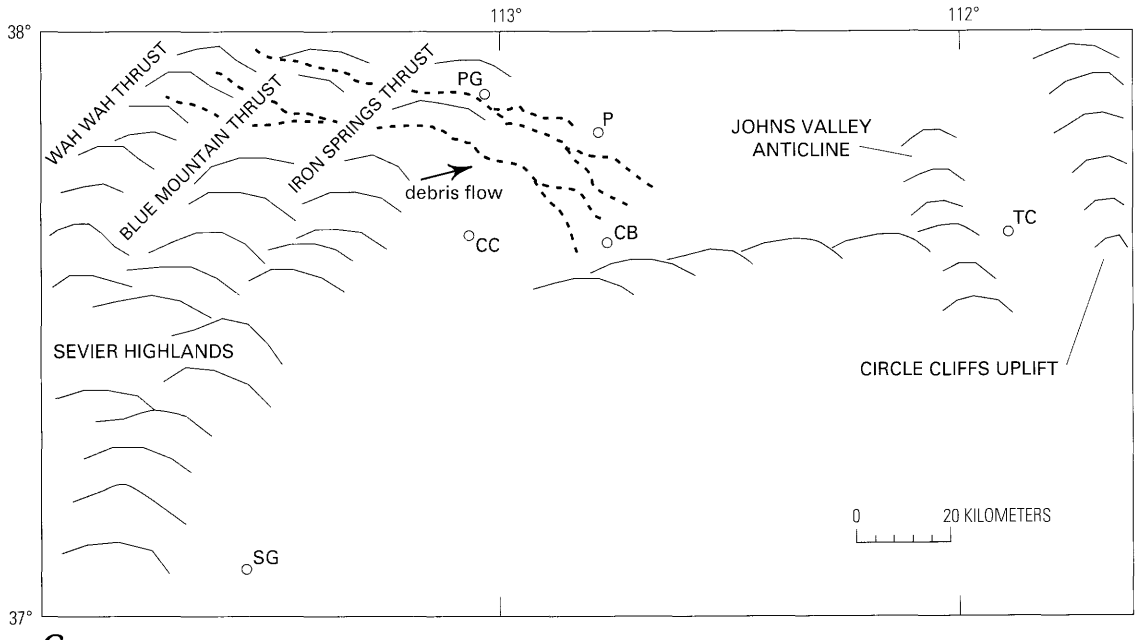

Figure 8 (above and facing page). Diagrammatic reconstructions of major tectonic features in southwestern Utah during the Paleocene. *A*, During deposition of the lower conglomerate member of the Grand Castle Formation with sediment transport from the Wah Wah and Blue Mountain thrust sheets. *B*, During deposition of the middle sandstone member, showing fluvial systems tranporting sediment possibly derived from upper plate of the Iron Springs thrust. *C*, During deposition of the upper conglomerate member with sediment transport from the Wah Wah and Blue Mountain thrust sheets. Northeast-directed debris flow (arrow) in the upper member may have been derived from Iron Springs thrust sheet. Short-dashed lines diagrammatically show possible braided fluvial system locations. CB, Cedar Breaks National Monument; CC, Cedar City; P, Parowan; PG, Parowan Gap; SG, St. George; TC, Table Cliff Plateau.

members, the structureless to crudely bedded conglomerate probably represents longitudinal bars developed during high-flow periods. Trough- and planar-crossbedded conglomerate may represent sinuous and straight-crested bars, respectively. Horizontally stratified sandstone lenses probably represent upper planar-bed flow across the bar tops as water depths decreased during waning flow.

Although most of the Grand Castle conglomerates are clast supported, one matrix-supported bed is present in the upper conglomerate member. This bed may represent emplacement of one or more debris flows into the upper Grand Castle fluvial system. The laminated sandstone and siltstone overlying this bed may indicate minor reworking of the upper part of the debris-flow deposit.

Within the middle sandstone member, planar cross-stratified sandstone probably represents sandy transverse bars, and trough cross-stratified sandstone probably represents lunate dunes that migrated within the channels. The overlying horizontally stratified sandstone represents planar-bed flow and modification of the bars and dunes during lower-flow periods. Convoluted bedding and dish structures indicate rapid deposition and subsequent dewatering of the sands.

The change in succeeding depositional systems, from gravelly braided (lower conglomerate member) to sandy braided (middle sandstone member), to still younger gravelly braided (upper conglomerate member) fluvial systems, may be a result of several factors, such as changes in tectonics, climate, or source area. The sandstone within the lower and upper conglomerates contains quartz, silicified carbonate, and carbonate lithic grains. Sandstone grain sizes in the conglomerate members range from very fine to granule. In contrast, the middle sandstone member is almost totally composed of well-rounded, very fine grained to fine-grained, monocrystalline quartz.

Goldstrand (1992) proposed that compositional differences between the gravelly fluvial deposits (lower and upper conglomerate members) and sandy fluvial deposits (middle sandstone member) were a result of differences in source areas. Southeasterly paleocurrents and the preponderance of upper Precambrian quartzite and Paleozoic carbonate clasts suggest that the source for the upper and lower conglomerate members was strata in the upper plates of the Wah Wah and Blue Mountain thrust sheets west of the study area (figs. 1, 8*A–C*; Goldstrand, 1992). The proposed source for the middle sandstone member is the Lower Jurassic eolian deposits of the Navajo Sandstone, based on the restricted fine-grain

size, quartzose composition, frosted surface textures, and abraded quartz overgrowths. The Navajo Sandstone is exposed in the lower plate of the Blue Mountain thrust and in the upper plate of the Iron Springs thrust at Parowan Gap (fig. 1; Threet, 1963; Miller, 1966). Thus, during deposition of the lower and upper conglomerate members, braided rivers had source areas in the Precambrian and Paleozoic rocks of the Sevier highlands. During the deposition of the middle sandstone member, sediment was derived from the Navajo Sandstone, suggesting that braided rivers either were incised into the lower plate of the Blue Mountain thrust or were derived from the Iron Springs thrust (fig. 8*B*). The absence of the middle member in the Parowan Gap area may indicate that this region was topographically positive during deposition of the middle sandstone member and also that the Navajo Sandstone in the upper plate of the Iron Springs thrust is a more plausible source area than the lower plate of the Blue Mountain thrust (fig. 8*B*).

A possible geographical connection between rocks of the Grand Castle Formation on the Markagunt Plateau and lithologically identical rocks to the east in the uppermost part of the Canaan Peak Formation in Table Cliff Plateau is now buried beneath younger volcanic rocks north of the Markagunt and Paunsaugunt Plateaus. At Table Cliff Plateau, paleocurrents in conglomerate of the uppermost part of the Canaan Peak Formation are to the east and southeast (fig. 7). If this conglomerate represents the distal part of an easterly thinning clastic wedge, a thick conglomeratic sequence may lie below the northern Paunsaugunt and northeastern Markagunt Plateaus (fig. 2).

The absence of the Grand Castle Formation on the Paunsaugunt Plateau and southward thinning of the formation on the southern Markagunt Plateau help to define the Grand Castle basin geometry. Stratigraphic thicknesses of the formation in the Markagunt Plateau and Parowan Gap region indicate that the depocenter was approximately 15 km south of Parowan (fig. 9). The southern basin margin may have been about 5 km south of the present southern boundary of Cedar Breaks National Monument (fig. 6). However, thin conglomeratic units identical in lithology to that of the Grand Castle are present in the southeastern part of the Markagunt Plateau (E.G. Sable, written commun., 1994), indicating that some Grand Castle conglomerate traversed the southeastern part of the Markagunt Plateau. The northern basin margin has not been identified due to the cover of Tertiary volcanic rocks and disruption along the Hurricane fault zone, but stratigraphic thinning to the north (Hilton, 1984; Goldstrand, 1991, p. 120) suggests that the Grand Castle Formation does not extend north much beyond Parowan. In Parowan Gap, the lower(?) conglomerate and middle sandstone members are absent, which may indicate that a positive topographic feature existed in the area before deposition of the upper member of the Grand Castle Formation (fig. 8).

Along Parowan Gap, the upper(?) member of the Grand Castle Formation unconformably overlies a fault-propagation fold and thrust within the Iron Springs Formation. During the Cretaceous, thrusting in Utah associated with the Sevier orogeny propagated eastward (Armstrong, 1968), and the thrust structures exposed in Parowan Gap are believed to be the easternmost and youngest thrust faults of the Sevier orogeny. Thus, the Grand Castle Formation postdates the Sevier orogeny.

A debris-flow deposit within the upper conglomerate member of the Grand Castle that contains Santonian(?) palynomorphs indicates that Upper Cretaceous rocks were exposed during deposition of the upper conglomerate member. Although the Grand Castle Formation overlies a fault-propagation fold in the Iron Springs Formation in the Parowan Gap area, surface and subsurface mapping to the southwest (Mackin and others, 1976; Mackin and Rowley, 1976; Van Kooten, 1988) indicates that this same fold-and-thrust structure is overlain by calcareous sandstone of the Claron Formation. We propose here that debris flows may have been derived from this structural feature southwest of the Parowan area, and that the structure formed a positive topographic feature throughout deposition of the Grand Castle Formation. Eventually, this source area was eroded and buried by sediments of the Claron Formation during late Paleocene or early Eocene time.

At Table Cliff Plateau, structural and stratigraphic relations indicate that the conglomerate in the upper part of the Canaan Peak Formation, correlative with the Grand Castle Formation, predates the Laramide orogeny. The conglomerate is tilted along the east limb of the Johns Valley anticline and is overlain by the Pine Hollow Formation. Bowers (1972) and Goldstrand (1994) have interpreted the rocks of the Pine Hollow Formation as having been deposited during the Laramide orogeny. Thus, strata correlative with the Grand Castle predate the Laramide orogeny in this region.

Stratigraphic evidence suggests that the geometry of the depositional basin may have been controlled by upwarping in the northern part of the Paunsaugunt Plateau and southern part of the Markagunt Plateau. The pinch-out and absence of the Grand Castle Formation in the southern part of the Markagunt and the Paunsaugunt Plateaus suggest upwarping and erosion in these regions. A southwest-trending anticlinal structure appears to project into the southern Markagunt Plateau from the northern Paunsaugunt Plateau, and may have formed the southern boundary of the Grand Castle depositional basin (Goldstrand, 1994).

However, as noted previously, conglomerates lithologically identical to those of the Grand Castle are present on the southeastern part of the Markagunt Plateau (fig. 2). The presence of this conglomerate may indicate that the proposed upwarp, in the southeastern Markagunt Plateau, had not fully developed prior to the initial deposition of the Grand Castle. This upwarp may also have been a relatively lower topographic feature on the southeastern Markagunt Plateau with respect to the southwestern part of the plateau (near Cedar Breaks National Monument), thus allowing distal fluvial conglomerate to be deposited farther to the southeast.

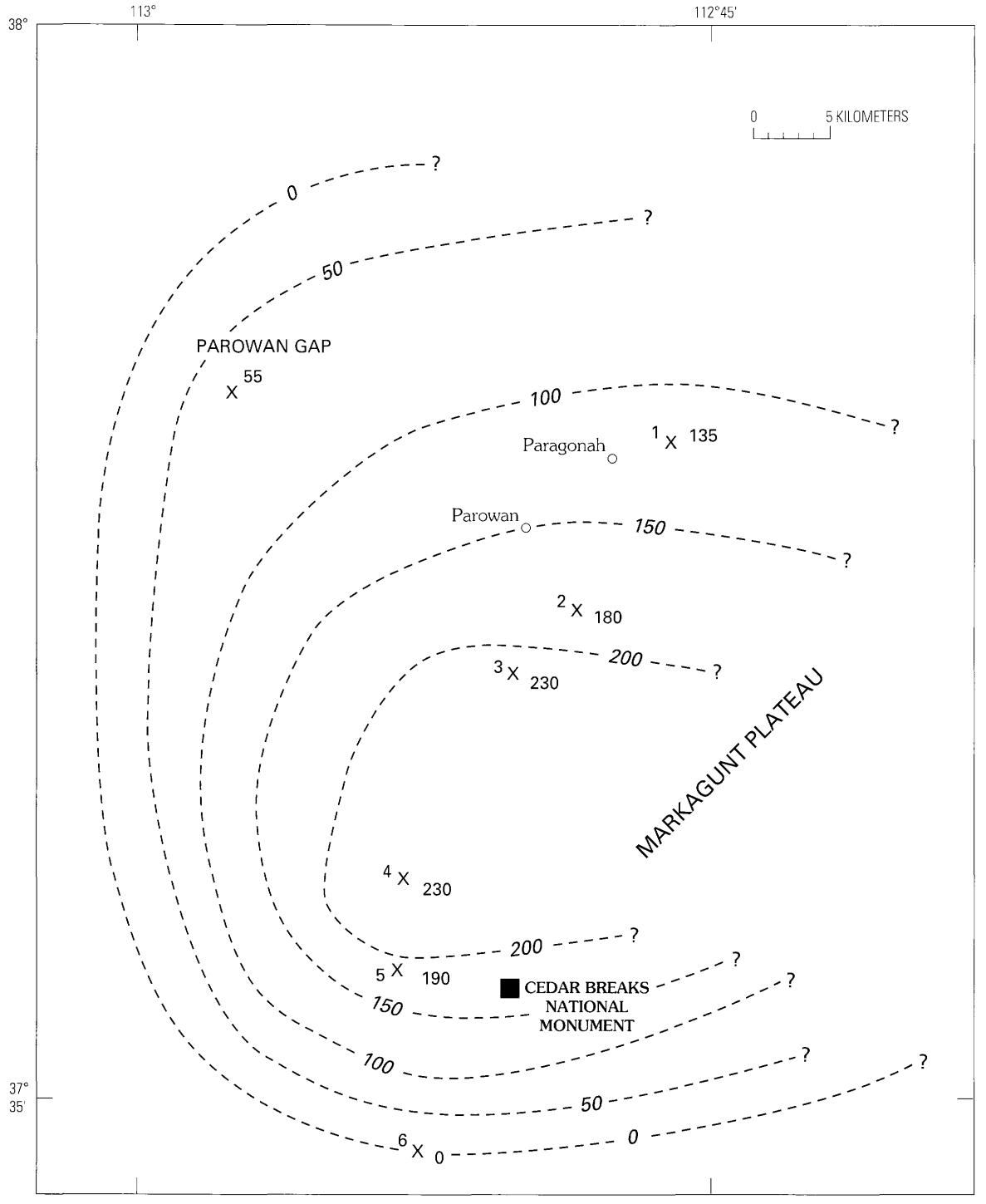

Figure 9. Isopach map of the Grand Castle Formation in the western Markagunt Plateau and Parowan Gap area, queried where extent uncertain. Location of numbered measured sections 1–6 shown in figure 4; corresponding thickness of Grand Castle Formation given in meters. Data for the 55 m of Grand Castle Formation measured in Parowan Gap from Goldstrand (1991). Contour interval 50 m.

SUMMARY

A sequence of conglomerate and sandstone previously mapped as the basal part of the Claron Formation in the Markagunt Plateau and Parowan Gap areas is herein formally named the Grand Castle Formation. The Grand Castle differs significantly from the Claron both compositionally and texturally. In contrast to the fine-grained carbonate rock and calcareous sandstone and shale of the Claron Formation, the Grand Castle Formation consists of siliciclastic conglomerate and sandstone. The contact between the Grand Castle and Claron Formations is placed at the boundary where red, calcareous sandstone and siltstone of the Claron Formation become dominant. The contact of the Grand Castle with the underlying Upper Cretaceous Iron Springs Formation, in the Markagunt Plateau and eastern part of Parowan Gap, is marked by an abrupt change from sandstone of the Iron Springs to conglomerate of the Grand Castle. In the western part of Parowan Gap, conglomerate of the Grand Castle Formation overlies fine-grained lithologies of various Cretaceous and Jurassic units with angular discordance.

The Grand Castle Formation is believed to be Paleocene in age. Along the western Markagunt Plateau, the Grand Castle grades upward into possible upper Paleocene strata of the Claron Formation. Strata believed to be correlative with the Grand Castle are present in the Table Cliff Plateau and are stratigraphically overlain and underlain by lower Paleocene units.

The Grand Castle represents a Paleocene braided fluvial system, the sediments of which were derived from the inactive Wah Wah, Blue Mountain, and Iron Springs thrust sheets of the Sevier thrust belt. Grand Castle conglomerates overlie the easternmost and youngest Sevier thrust faults, indicating that the formation postdates the Sevier orogeny. Deposition of the conglomerate and sandstone that compose the Grand Castle Formation was controlled initially by Laramide upwarping within the Sevier foreland basin around a depocenter south of the town of Parowan. Continued Laramide deformation in the Table Cliff Plateau area tilted conglomerate correlative with the Grand Castle prior to deposition of the intermontane deposits of the Pine Hollow Formation. Thus, strata of the Grand Castle Formation and its equivalents appear to have been deposited after the Sevier orogeny and before extensive partitioning of the foreland basin during Laramide orogeny.

REFERENCES CITED

Anderson, J.J., and Rowley, P.D., 1975, Cenozoic stratigraphy of southwestern High Plateaus of Utah, *in* Anderson, J.J., Rowley, P.D., Fleck, R.J., and Nairn, A.E.M., Cenozoic geology of southwestern High Plateaus of Utah: Geological Society of America Special Paper 160, p. 1–51.

Armstrong, F.C., and Oriel, S.S., 1965, Tectonic development of Idaho-Wyoming thrust belt: America Association of Petroleum Geologists Bulletin, v. 49, p. 1847–1866.

Armstrong, R.L., 1968, Sevier orogenic belt in Nevada and Utah: Geological Society of America Bulletin, v. 79, no. 4, p. 429–458.

Bissell, H.F., 1952, Geology of the Cretaceous and Tertiary sedimentary rocks of the Utah-Arizona-Nevada corner: Utah Geological Society Guidebook to the Geology of Utah 7, p. 69–78.

Bowers, W.E., 1972, The Canaan Peak, Pine Hollow, and Wasatch Formations in the Table Cliff region, Garfield County, Utah: U.S. Geological Survey Bulletin 1331–B, 39 p.

Chapin, C.E., and Cather, S.M., 1981, Eocene tectonics and sedimentation in the Colorado Plateau–Rocky Mountain area, *in* Dickinson, W.R., and Payne, W.D., eds., Relations of tectonics to ore deposits in the southern Cordillera: Arizona Geological Society Digest, v. 14, p. 173–198.

Cook, E.F., 1957, Geology of the Pine Valley Mountains, Utah: Utah Geological and Mineral Survey Bulletin 58, 111 p.

———1960, Geological atlas of Utah–Washington County: Utah Geological and Mineral Survey Bulletin 70, 119 p.

Cross, T.A., 1986, Tectonic controls of foreland basin subsidence and Laramide style deformation, western United States, *in* Allen, P.A. and Homewood, P.W.G., eds., Foreland basins: International Association of Sedimentologists Special Publication 8, p. 15–39.

DeCelles, P.G., 1988, Lithologic provenance modeling applied to the Late Cretaceous synorogenic Echo Canyon conglomerate, Utah—A case of multiple source areas: Geology, v. 16, p. 1039–1043.

Dickinson, W.R., Lawton, T.F., and Inman, K.F., 1986, Sandstone detrital modes, central Utah foreland region—Stratigraphic record of Cretaceous-Paleocene tectonic evolution: Journal of Sedimentary Petrology, v. 56, p. 276–293.

Dickinson, W.R., Klute, M.A., Hayes, M.J., Janecke, S.U., Lundin, E.R., McKittrick, M.A., and Olivares, M.D., 1988, Paleogeographic and paleotectonic setting of Laramide sedimentary basins in the central Rocky Mountain region: Geological Society of America Bulletin, v. 100, p. 1023–1039.

Folk, R.L., 1974, Petrology of sedimentary rocks: Austin, Texas, Hemphill's Book Store, 170 p.

Fouch, T.D., Lawton, T.F., Nichols, D.J., Cashion, W.B., and Cobban, W.A., 1983, Patterns and timing of synorogenic sedimentation in Upper Cretaceous rocks of central and northeast Utah, *in* Reynolds, M.W., and Dolly, E.D., eds., Mesozoic paleogeography of the west-central United States: Society of Economic Paleontologists and Mineralogists, Rocky Mountain Paleogeography Symposium 2, p. 305–328.

Franczyk, K.J., Fouch, T.D., Johnson, R.C., Molenaar, C.M., and Cobban, W.A., 1992, Cretaceous and Tertiary paleogeographic reconstructions for the Uinta–Piceance Basin study area: U.S. Geological Survey Bulletin 1787–Q, 37 p.

Goldstrand, P.M., 1991, Tectonostratigraphy, petrology, and paleogeography of Upper Cretaceous to Eocene rocks of southwest Utah: Reno, Nev., University of Nevada Ph. D. dissertation, 205 p.

———1992, Evolution of Late Cretaceous and Early Tertiary basins of southwest Utah based on clastic petrology: Journal of Sedimentary Petrology, v. 62, no. 3, p. 495–507.

———1994, Tectonic development of Upper Cretaceous to Eocene strata of southwest Utah: Geological Society of America Bulletin, v. 106, p. 145–154.

Gregory, H.E., 1950a, Geology and geography of the Zion Park region, Utah: U.S. Geological Survey Professional Paper 220, 200 p.

———1950b, Geology of eastern Iron County, Utah: Utah Geological and Mineral Survey Bulletin 37, 153 p.

———1951, The geology and geography of the Paunsaugunt region, Utah: U.S. Geological Survey Professional Paper 226, 116 p.

Hackman, R.J., and Wyant, D.G., 1973, Geology, structure, and uranium deposits of the Escalante quadrangle, Utah and Arizona: U.S. Geological Survey Miscellaneous Geologic Investigations Series Map I–744, scale 1:250,000.

Hayden, F.V., 1869, Preliminary field report (3rd ann.) of the United States Geological Survey of Colorado and New Mexico: Washington, U.S. Government Printing Office, 155 p.

Hintze, L.F., 1963, Geologic map of southwestern Utah: Utah Geological and Mineral Survey, scale 1:250,000.

Hilton, D.A., 1984, The petrology, sedimentology, and stratigraphy of the Late Cretaceous(?) and early Tertiary sedimentary rocks of southwest Markagunt Plateau, Utah: Kent, Ohio, Kent State University M.S. thesis, 137 p.

Lawton, T.F., 1983, Late Cretaceous fluvial systems and the age of foreland uplifts in central Utah, *in* Lowell, J.D., Rocky Mountain Foreland Basin and Uplift: Rocky Mountain Association of Geologists Symposium, p. 181–199.

Leith, C.K., and Harder, E.C., 1908, The iron ore of the Iron Springs district, southern Utah: U.S. Geological Survey Bulletin 338, 102 p.

Mackin, J.H., Nelson, W.H., and Rowley, P.D., 1976, Geologic map of the Cedar City NW quadrangle, Iron County, Utah: U.S. Geological Survey Geologic Quadrangle Map GQ–1295, scale 1:24,000.

Mackin, J.H., and Rowley, P.D., 1976, Geologic map of the Three Peaks quadrangle, Iron County, Utah: U.S. Geological Survey Geologic Quadrangle Map GQ–1297, scale 1:24,000.

Maldonado, Florian, and Moore, R.C., 1993, Preliminary geologic map of the Parowan quadrangle, Iron County, Utah: U.S. Geological Survey Open-File Report 93-3, scale 1:24,000.

Maldonado, Florian, and Williams, V.S., 1993, Geologic map of the Parowan Gap quadrangle, Iron County, Utah: U.S. Geological Survey Geological quadrangle Map GQ–1712, scale 1:24,000.

Miller, G.M., 1966, Structure and stratigraphy of southern part of the Wah Wah Mountains, southwest Utah: America Association of Petroleum Geologists Bulletin, v. 50, p. 858–900.

Moore, R.C., 1982, The geology of a portion of the west-central Markagunt Plateau, southwestern Utah: Kent, Ohio, Kent State University M.S. thesis, 72 p.

Reeside, J.B., Jr., and Bassler, Harvey, 1922, Stratigraphic sections in Utah and Arizona: U.S. Geological Survey Professional Paper 129, p. 53–77.

Robison, R.A., 1966, Geology and coal resources of the Tropic area, Garfield County: Utah Geologic and Mineral Survey Special Study 18, 62 p.

Sargent, K.A., and Hansen, D.E., 1982, Bedrock geologic map of the Kaiparowits coal-basin area, Utah: U.S. Geological Survey Miscellaneous Geologic Investigations Map I–1033-I, scale 1:125,000.

Schneider, M.C., 1967, Early Tertiary continental sediments of central and south-central Utah: Brigham Young University Geology Studies, v. 14, p. 143–194.

Spieker, E.M., 1946, Late Mesozoic and Early Cenozoic history of central Utah: U.S. Geological Survey Professional Paper 205–D, p. 117–161.

———1949, The transition between the Colorado Plateaus and the Great Basin in central Utah: Utah Geological Society Guidebook to the Geology of Utah 4, 106 p.

Thomas, H.E., and Taylor, G.H., 1946, Geology and groundwater resources of Cedar City and Parowan Valley, Iron County, Utah: U.S. Geological Survey Water-Supply Paper 993, 210 p.

Threet, R.L., 1963, Geology of the Parowan Gap area, Iron County, Utah: Intermountain Association of Petroleum Geologists, Guidebook to the geology of southwest Utah, p. 136–145.

Van Kooten, G.K., 1988, Structure and hydrocarbon potential beneath the Iron Springs laccolith, southwestern Utah: Geological Society of America Bulletin, v. 100, no. 10, p. 1541–1549.

Palynology and Ages of Some Upper Cretaceous Formations in the Markagunt and Northwestern Kaiparowits Plateaus, Southwestern Utah

By Douglas J. Nichols

GEOLOGIC STUDIES IN THE BASIN AND RANGE–COLORADO PLATEAU TRANSITION IN SOUTHEASTERN NEVADA, SOUTHWESTERN UTAH, AND NORTHWESTERN ARIZONA, 1995

U.S. GEOLOGICAL SURVEY BULLETIN 2153–E

Interpretations of the biostratigraphic significance of palynomorphs including spores, pollen, freshwater algal cysts, dinoflagellate cysts, and microforams recovered from the Upper Cretaceous Dakota, Straight Cliffs, and Kaiparowits(?) Formations

UNITED STATES GOVERNMENT PRINTING OFFICE, WASHINGTON : 1997

CONTENTS

PLATES

[Plates follow references cited]

FIGURES

Palynology and Ages of Some Upper Cretaceous Formations in the Markagunt and Northwestern Kaiparowits Plateaus, Southwestern Utah

By Douglas J. Nichols

ABSTRACT

Upper Cretaceous formations in the Markagunt and northwestern Kaiparowits Plateaus, southwestern Utah, yielded assemblages of marine and nonmarine palynomorphs that provide data on the geologic age of the formations and therefore are of potential use in regional geologic mapping. The study area is in and adjacent to the map area of the U.S. Geological Survey's Basin and Range–Colorado Plateau Transition (BARCO) Study Unit, which is discussed in the Introduction to this volume. Palynomorphs were recovered from the Dakota Formation, the Straight Cliffs Formation, and the Kaiparowits(?) Formation, units that range in age from Cenomanian to Santonian.

In the study area the palynoflora of the Dakota Formation includes 35 taxa of fossil palynomorphs including pollen, spores, and dinocysts; this assemblage is no older than Cenomanian. The palynoflora of the lower unit of the Straight Cliffs Formation in the study area includes about 15 taxa of pollen and spores, all of which are present also in the upper unit of the Straight Cliffs, and 7 or more dinocyst taxa, which are not present in the upper unit. This assemblage is not age-definitive, but falls within a palynostratigraphic zone of Cenomanian through Turonian age. The palynoflora of the upper unit of the Straight Cliffs Formation includes about 45 taxa of pollen and spores and no dinocysts. Several species in this assemblage indicate an age of early Coniacian. The palynoflora of the Kaiparowits(?) Formation in the study area includes about 40 taxa of pollen and spores (and no dinocysts). This assemblage is characteristic of a palynostratigraphic zone of mid-Coniacian through Santonian age; the Kaiparowits(?) Formation is most likely Santonian in age. Palynology indicates that the Kaiparowits(?) Formation in the Markagunt Plateau is older than the typical Kaiparowits Formation (Campanian) in the southern Kaiparowits Plateau.

INTRODUCTION

This report summarizes results of analyses of palynologic samples collected in the Markagunt and northwestern Kaiparowits Plateaus, in and adjoining the study area of the USGS Basin and Range–Colorado Plateau Transition (BARCO) Study Unit in southwestern Utah (fig. 1). Samples were collected to provide data on the palynostratigraphic ages of Cretaceous rock units in the study area to assist in mapping being conducted by personnel associated with the BARCO project, specifically in the Cedar City and Panguitch 30×60-minute quadrangles. Results also contribute to compilation of a palynological database for Mesozoic rocks of the region. Data in this report include sample localities and units sampled, age determinations, and lists of palynomorphs present. Photomicrographic illustrations are provided for common and (or) stratigraphically important spores, pollen, and dinocysts.

Samples were collected from several measured sections and a few isolated outcrops in the study area. Units sampled are: the Dakota Formation, including beds possibly transitional with the overlying Tropic Shale; the Straight Cliffs Formation, which in the study area is informally divided into a lower and an upper unit; and a formation of uncertain relation to the Kaiparowits Formation in its type area in the Kaiparowits Plateau that is referred to as the Kaiparowits(?) Formation. Samples were collected also from a unit of uncertain stratigraphic assignment thought to be either the Kaiparowits(?) Formation or the Wahweap Formation; it correlates palynostratigraphically with the Kaiparowits(?) Formation.

PREVIOUS WORK

In addition to earlier studies that established the framework for nomenclature of Cretaceous units in the Kaiparowits Plateau (Gregory and Moore, 1931) and the Markagunt Plateau (Gregory, 1950), more recent reports on the stratigraphy of the area include those by Peterson and Waldrop (1965), Robison (1966), and Peterson (1969). Studies on

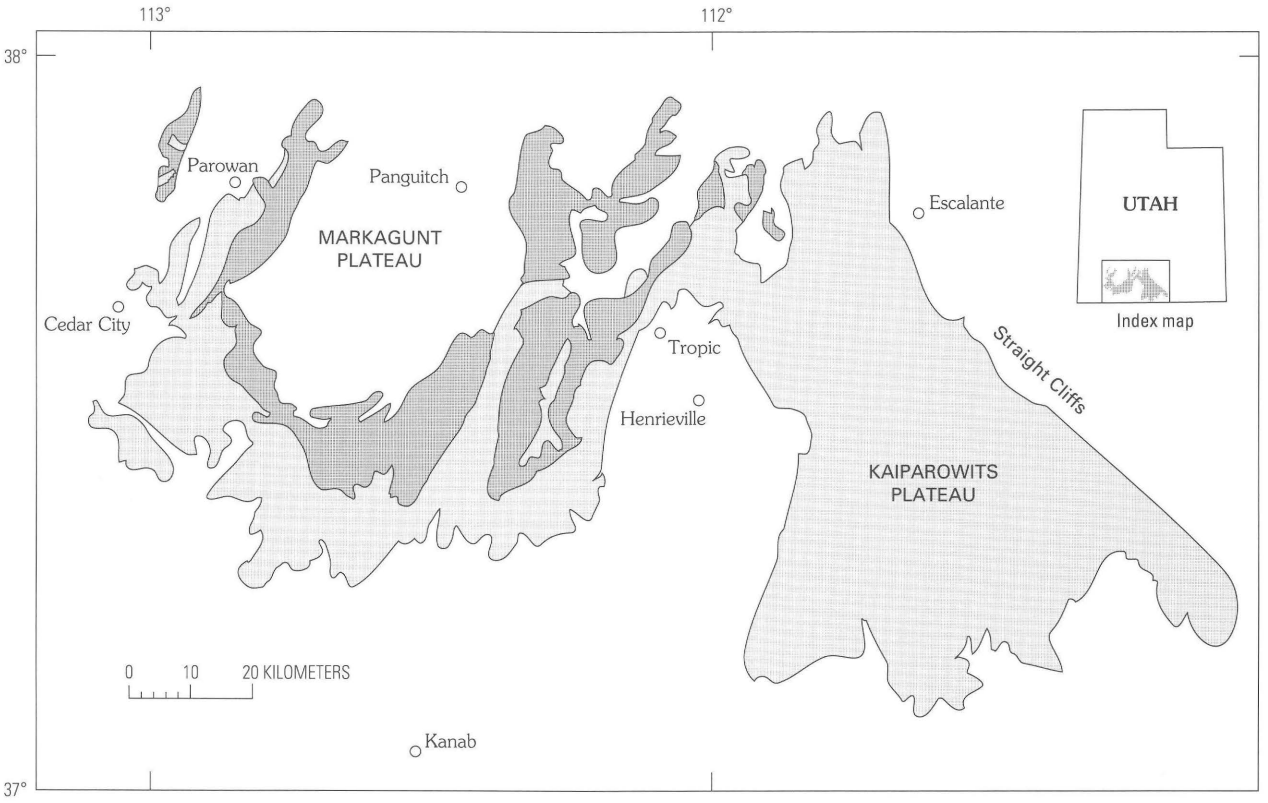

Figure 1. Generalized geology of the study area, modified from Goldstrand and others (1993); light shade, undifferentiated Cretaceous rocks; dark shade, overlying Tertiary rocks. Samples discussed in this report were collected from the Markagunt Plateau and northwestern part of the Kaiparowits Plateau.

stratigraphy, depositional environments, and tectonic implications of the Cretaceous rocks of the area were completed still more recently by Moir (1974) and Gustason (1989). Sable and Hereford (1990) first used the name Kaiparowits(?) Formation in the Markagunt Plateau to refer to the unit that is a major focus of the present palynological study. Most recently, Eaton (1991) summarized the biostratigraphic framework of the Upper Cretaceous of the Kaiparowits Plateau, and Goldstrand and others (1993) summarized Late Cretaceous to early Tertiary tectonostratigraphy of the region. Eaton's report includes some palynological data; Goldstrand and others made use of palynological age determinations but presented no data.

A few previous studies of the palynology of the Upper Cretaceous rocks of the region have been published. Lohrengel (1969) conducted a palynological study on the Kaiparowits Formation in its type area and purported to have determined its age. Agasie (1969) described and illustrated the palynoflora of the Dakota Formation in northeastern Arizona; his taxonomy is useful in the present study. Orlansky (1971) described and illustrated palynomorphs from the Straight Cliffs Formation near Henrieville, Utah, and May (1972) illustrated some palynomorphs from a coal field in the Straight Cliffs Formation in the northeastern part of the Kaiparowits Plateau. Bowers (1972) published some palynological data and interpretations of R.H. Tschudy (USGS) that concern the Kaiparowits and Canaan Peak Formations in the northern Kaiparowits Plateau and Table Cliff Plateau. May and Traverse (1973) reported on the palynology of the Dakota Formation near Bryce Canyon National Park, and May (1975) described a species of pollen said to be useful as a guide fossil for the Cenomanian of the region. am Ende (1991) utilized palynology in a study of depositional environments of the Dakota Formation at the southern edge of the Kaiparowits Plateau. Eaton (1991) reviewed previously published palynological data from the Kaiparowits Formation; they indicate that this unit is stratigraphically older than Lohrengel (1969) had concluded. Farabee (1991) restudied the palynology of the Kaiparowits Formation in its type area, reaffirming Eaton's conclusion about its age. Finally, Nichols (1994) published a revised palynostratigraphic zonation of the Upper Cretaceous of the Rocky Mountain region that is applicable to the study area.

STRATIGRAPHY

The stratigraphic units investigated in the present study are (from oldest to youngest) the Dakota Formation, Tropic Shale, Straight Cliffs Formation, Wahweap Formation, and Kaiparowits(?) Formation (fig. 2). All are Late Cretaceous, ranging from Cenomanian to Santonian in age. Brief discussions of the stratigraphy of each of these units follow; more detailed information is presented in the references previously cited.

The Dakota Formation consists of sandstone, mudstone, carbonaceous shale, and coal. It represents continental deposits marginal to the Cretaceous seaway. In some places in the study area, the Dakota is not clearly distinguishable from the overlying marine Tropic Shale, and Gustason (1989) presented evidence for intertonguing of these units.

The Tropic Shale, which represents shoreface and offshore marine deposits interbedded with lagoonal and mire deposits, is poorly exposed in most places. Samples collected in this study from an interval designated Dakota Formation–Tropic Shale (undivided) in the Clear Creek Mountain quadrangle, in the southwestern part of the study area, may include part of the Tropic Shale (E.G. Sable, written commun., 1992). Otherwise, the Tropic Shale was not sampled in the present study.

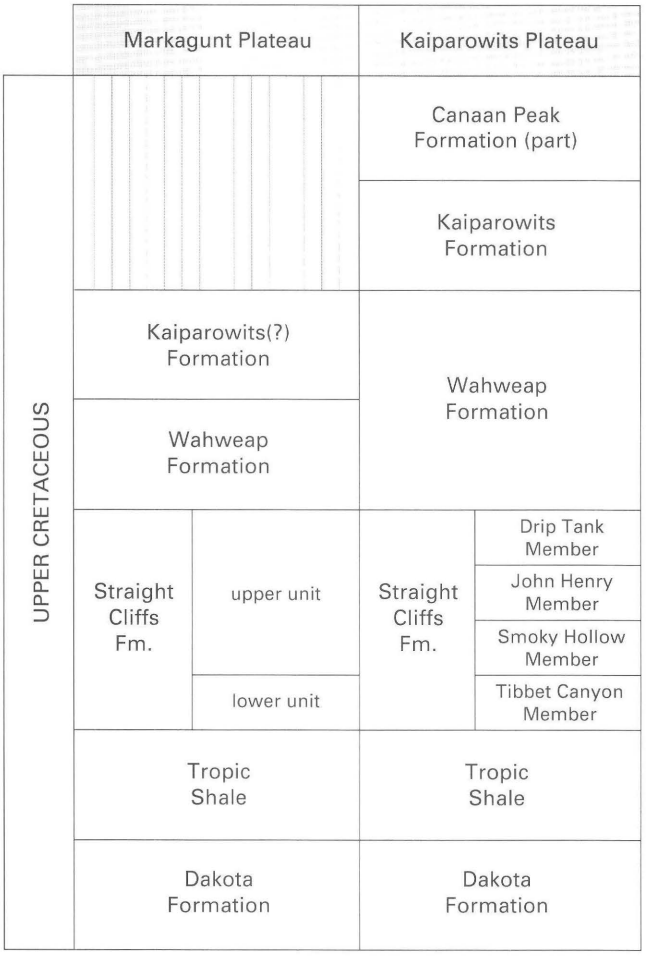

Figure 2. Nomenclature and generalized lithostratigraphic correlation of Upper Cretaceous formations in the study area. Actual relative thicknesses of units are not implied; vertical line pattern, hiatus.

The nonmarine Straight Cliffs Formation overlies and intertongues with the Tropic Shale. The Straight Cliffs is composed of sandstone, mudstone, carbonaceous mudstone, carbonaceous shale, limestone, and coal. In its type area in the Kaiparowits Plateau, the Straight Cliffs Formation is divided into four formally defined members (Peterson, 1969), but in the Markagunt Plateau, it is divided into two informal units (Sable and Hereford, 1990); see figure 3. The lower unit of the Straight Cliffs Formation is predominantly sandstone and is about 570 ft (174 m) thick. (Measurements in feet are original data of previous workers.) It forms the Gray Cliffs of the "Grand Staircase," a regional steplike geomorphologic feature on the southern flanks of the Markagunt and Kaiparowits Plateaus. The lower unit in the Markagunt Plateau–Cedar Canyon area is the lithostratigraphic equivalent of the Tibbet Canyon Member of the Straight Cliffs Formation of the Kaiparowits Plateau (Peterson, 1969). However, the lower unit of the Straight Cliffs in the Cedar Canyon area may be partly older than the Tibbet Canyon Member of the Kaiparowits Plateau. The upper unit of the Straight Cliffs in the Markagunt Plateau is composed of interbedded shale and sandstone and includes carbonaceous and coaly beds; it is about 1,450 ft (442 m) thick. It is lithostratigraphically equivalent to the Smoky Hollow and John Henry Members of the Straight Cliffs Formation in the Kaiparowits Plateau. The lower part of the upper unit evidently is not as young as the John Henry Member, based on results from the present study; the upper part of the upper unit was not dated in this study.

The Wahweap Formation overlies the Straight Cliffs Formation. It consists of interbedded sandstone, mudstone, and shale of nonmarine origin. It was not sampled in this study. However, a unit of uncertain stratigraphic assignment was sampled at one locality that appeared to be either the Wahweap or the Kaiparowits(?) Formation. The significance of this unit is discussed in the section, "Age Determinations and Correlations."

The presence of the Kaiparowits Formation (Gregory and Moore, 1931) in the study area is a matter of some dispute. A unit overlying the Wahweap and underlying the Claron Formation (Tertiary) at some places is lithologically similar to the Kaiparowits Formation in its type area in the southern Kaiparowits Plateau. In the study area, this unit is about 350 ft (105 m) thick south of Navajo Lake (fig. 4), but in places it appears to be absent. The age of this unit has been uncertain; it has been thought to be either Cretaceous or Tertiary. Results of palynological analyses of samples of this unit reported here establish its age as Cretaceous, but this alone is not an adequate basis for recognition of the

Kaiparowits Formation, a lithostratigraphic unit, in the study area. In this report, the name "Kaiparowits(?)" is used to refer to this disputed unit, following the usage of Sable and Hereford (1990). Ultimately the Kaiparowits(?) Formation of the Markagunt Plateau is concluded to be stratigraphically older than the Kaiparowits Formation in its type area in the eastern Kaiparowits Plateau.

Other units in the study area were evaluated in the field for their potential for yielding palynomorphs. They were not sampled because the rock types—sandstone or conglomerate—were deemed unsuitable (palynomorphs generally are not deposited in high-energy depositional environments in which sand or gravel is deposited). The units for which it is not possible to make palynological age determinations are (1) undifferentiated sandstone in the Pine Knoll area, southeast of Navajo Lake, that is transitional in appearance between Wahweap and Kaiparowits(?) Formations; (2) conglomeratic sandstone possibly equivalent to the Canaan Peak Formation, in the Pine Knoll area; and (3) sandstone and conglomerate in Parowan Canyon in the Markagunt Plateau. The ages of these units remain problems probably not subject to solution on the basis of palynological analysis. However, some problematic information pertaining to unit (3) is discussed in the section, "Age Determinations and Correlations."

SAMPLE LOCALITIES

Sample localities are listed by number within groups representing the stratigraphic units sampled. Four-digit numbers preceded by the letter "D" are U.S. Geological Survey paleobotany locality numbers registered in the Denver palynological laboratory. Letters following the four-digit numbers, if any, are used to distinguish multiple samples collected from a measured section at a single locality. These locality and sample numbers also identify microscope slides, unmounted fossil material (residues), and unprocessed splits of samples archived at the Denver laboratory. Geographic and cultural features mentioned in locality descriptions are shown in figure 4.

DAKOTA FORMATION

D7623.—Dakota Formation exposed in road cuts and natural exposures along county road below and above control point 6757; sec. 3, T. 40 S., R. 9 W., Kane County, Utah; Clear Creek Mountain 7.5-minute quadrangle; lat 37°21'31"–37°21'39" N., long 112°50'13"–112°50'25" W. Primary reference section for Dakota Formation in this study; measured section may include Tropic Shale in uppermost beds (not sampled). Sampled by E.G. Sable; positions of samples given as stratigraphic distance below base of the Straight Cliffs Formation.

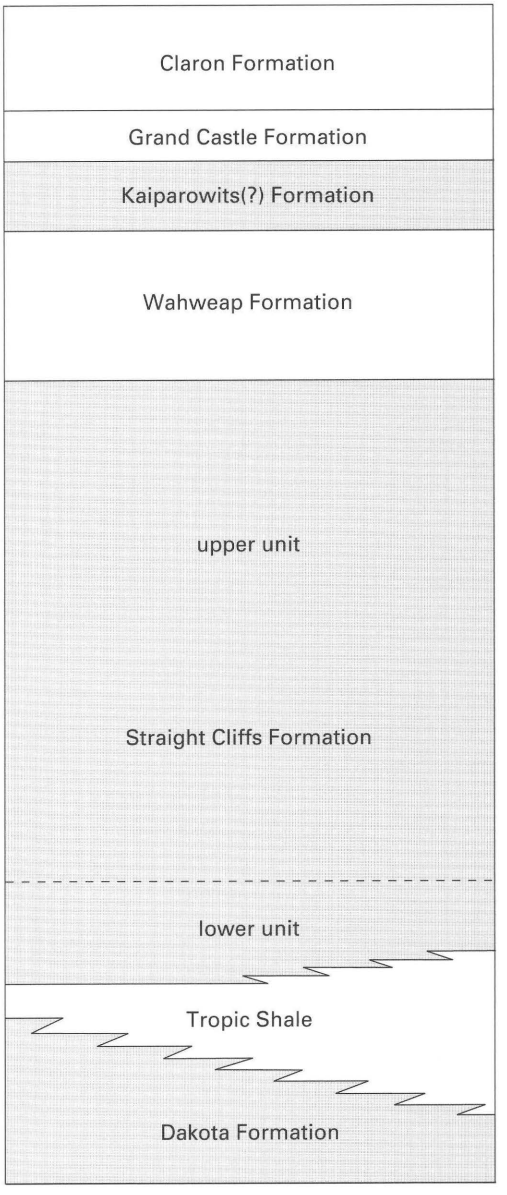

Figure 3. Stratigraphic relationships of formations in the Markagunt Plateau mentioned or discussed in detail in the text (modified from Sable and Hereford, 1990). Shading indicates units sampled for palynology in the present study. Grand Castle Formation is a new name (Goldstrand and Mullett, this volume, chapter D).

Straight Cliffs Formation (lower unit).

Dakota Formation:

–295 ft (–89.9 m)	(barren sample)
–518 ft (–157.9 m)	D7623-H, -I
–532 ft (–162.2 m)	D7623-F, -G
–544 ft (–165.8 m)	D7623-D, -E
–922 ft (–281.0 m)	D7623-C
–961 ft (–292.9 m)	D7623-B
–1,027 ft (–313.0 m)	D7623-A

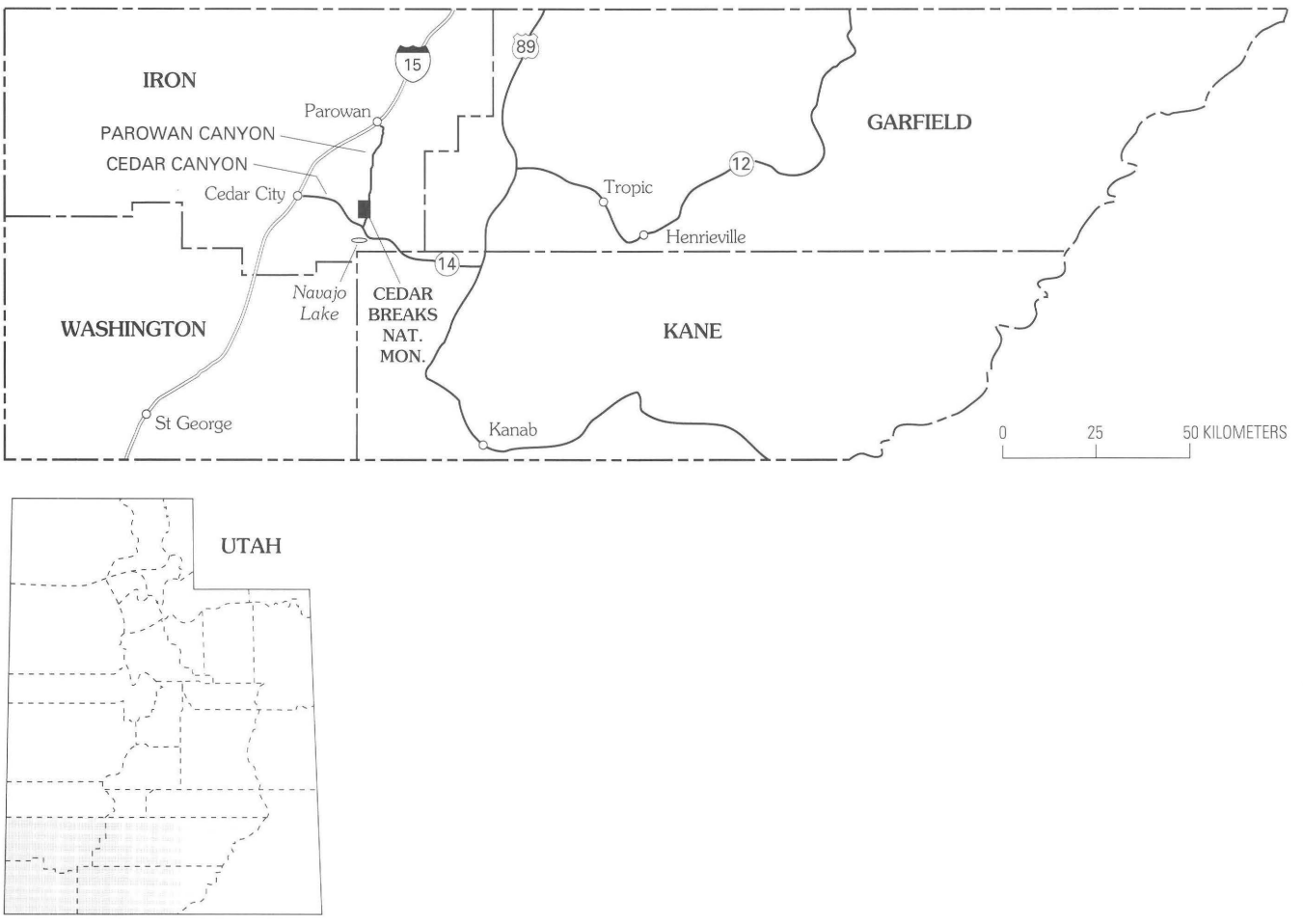

Figure 4. Geographic and cultural features mentioned in descriptions of sample localities, part of southwestern Utah.

D7621-A.—Dakota Formation exposed along north side of State Highway 12, east of Henrieville; sec. 8, T. 37 S., R. 1 W., Garfield County, Utah; Henrieville 7.5-minute quadrangle; lat 37°35'50" N., long 111°55'43" W. Sample collected by E.G. Sable about 4.5 ft (1.4 m) above base of measured section that includes 220 ft (67 m) of mudstone, sandstone, and carbonaceous shale below the Tropic Shale.

D7624-A.—Dakota Formation exposed in road cut along State Highway 14 in Cedar Canyon; sec. 36, T. 36 S., R. 10 W., Iron County, Utah; Flanigan Arch 7.5-minute quadrangle; lat 37°36'31"–37°37'34" N., long 112°55'48" W. Sample collected by E.G. Sable 181.0 ft (55.2 m) below base of the Straight Cliffs Formation.

D7826.—Dakota Formation exposed along State Highway 14 in Cedar Canyon; $SE^1/_4SE^1/_4$ sec. 26, T. 36 S., R. 10 W., Iron County, Utah; Flanigan Arch 7.5-minute quadrangle; lat 37°37'45" N., long 112°56'40" W. Sample collected by D.J. Nichols and E.G. Sable, probably from upper coal zone of the middle member of the Dakota Formation of Gustason (1989).

D7831.—Uppermost part of the Dakota Formation as mapped by Averitt and Threet (1973) exposed along Kolob Reservoir Road; $SW^1/_4SW^1/_4$ sec. 25, T. 36 N., R. 11 W., Iron County, Utah; Cedar City 7.5-minute quadrangle; lat 37°37'45" N., long 113°01'58" W. Two samples collected by D.J. Nichols and E.G. Sable from about the same stratigraphic level, about 18 ft (5.5 m) below base of Straight Cliffs Formation; sample D7831-A is coal and sample D7831-B is carbonaceous shale.

STRAIGHT CLIFFS FORMATION (LOWER UNIT)

D7624.—Lower unit of Straight Cliffs Formation exposed in road cuts along State Highway 14 in Cedar Canyon; sec. 36, T. 36 S., R. 10 W., Iron County, Utah; Flanigan Arch 7.5-minute quadrangle; lat 37°36'31"–37°37'34" N., long 112°55'48" W. Section measured and sampled by E.G. Sable, as follows:

Straight Cliffs Formation:

sandstone, coquina	16.0 ft (4.9 m)	
carbonaceous shale	1.5 ft (0.5 m)	D7624-E
sandstone	276.0 ft (84.1 m)	
carbonaceous shale	0.5 ft (0.2 m)	D7624-D
sandstone	252.0 ft (76.8 m)	
carbonaceous shale, coal	0.5 ft (0.2 m)	D7624-C
sandstone	15.0 ft (4.6 m)	
coaly shale, coal	0.5 ft (0.2 m)	D7624-B
sandstone	55.0 ft (16.8 m)	

Tropic Shale:

shale, sandstone	158.0 ft (48.1 m)	
shale, limestone, coquina	18.0 ft (5.5 m)	

D7827.—Lower unit of the Straight Cliffs Formation exposed along State Highway 14 in Cedar Canyon; $SW^1/_4$ sec. 36, T. 36 S., R. 10 W., Iron County, Utah; Webster Flat 7.5-minute quadrangle; lat 37°36'29" N., long 112°56'05" W. Sample collected by D.J. Nichols and E.G. Sable from coal seam about 55 ft (17 m) above base of lower unit of the formation, just above first sandstone cycle; same bed as sample D7624-B (which was barren).

D7829.—Lower unit of Straight Cliffs Formation exposed along State Highway 14 in Cedar Canyon; $NE^1/_4$ $NW^1/_4$ sec. 21, T. 37 S., R. 10 W., Iron County, Utah; Webster Flat 7.5-minute quadrangle; lat 37°36'05" N., long 112°56'55" W. Sample collected by D.J. Nichols and E.G. Sable about 16 ft (5 m) below mappable top of thick sandstone units in the lower unit of the formation.

STRAIGHT CLIFFS FORMATION (UPPER UNIT)

D7621.—Straight Cliffs Formation exposed along north side of State Highway 12, east of Henrieville; sec. 8, T. 37 S., R. 1 W., Garfield County, Utah; Henrieville 7.5-minute quadrangle; lat 37°35'50" N., long 111°55'43" W. Reference section in this study for the upper unit of the Straight Cliffs Formation in the Henrieville-Tropic area. Sampled by E.G. Sable from sections published by Robison (1966, p. 14–23), as follows:

Wahweap Formation.

Straight Cliffs Formation:

Drip Tank Member equivalent:

conglomerate, sandstone	523 ft (159.4 m)	

upper unit (John Henry and Smoky Hollow Members equivalent):

mudstone, sandstone	33 ft (10 m)	
mudstone	101 ft (30.8 m)	D7621-G
mudstone, sandstone	392 ft (119.5 m)	
carbonaceous mudstone, coal	24 ft (7.3 m)	D7621-E, -F
sandstone, mudstone	107 ft (32.6 m)	
white sandstone, conglomerate	66 ft (20.1 m)	
mudstone, sandstone	125 ft (38.1 m)	
carbonaceous mudstone, coal	9 ft (2.7 m)	D7621-B, -C,-D

lower unit (Tibbet Canyon Member equivalent):

sandstone	115 ft (35.1 m)	

Tropic Shale:

shale	690 ft (210 m)	

Dakota Formation.

D7830.—Upper unit of the Straight Cliffs Formation exposed along Urie Creek on the Markagunt Plateau; $NW^1/_4NW^1/_4$ sec. 16, T. 37 S., R. 10 W., Iron County, Utah; Webster Flat 7.5-minute quadrangle; lat 37°35'18" N., long 113°00'43" W. Samples collected by D.J. Nichols and E.G. Sable, as follows: base of section is about 160 ft (50 m) above the top of the lower unit of the formation, probably in the John Henry Member equivalent; sample D7830-A=carbonaceous shale from first coaly horizon above creek level; sample D7830-B=carbonaceous shale 11 ft (3.4 m) above D7830-A; sample D7830-C=coal from 6-inch-thick bed about 23 ft (7 m) above D7830-B.

KAIPAROWITS(?) FORMATION

D7622.— Kaiparowits(?) Formation in cirque-like outcrop at headwaters of unnamed draw south of Navajo Lake; sec. 13, T. 38 S., R. 9 W., Kane County, Utah; Navajo Lake 7.5-minute quadrangle; lat 37°30'32" N., long 112°47'39" W. Section measured and sampled by E.G. Sable, as follows:

Claron Formation.

Kaiparowits(?) Formation:

sandstone	51 ft (15.5 m)	
shale	28 ft (8.5 m)	(barren sample)
sandstone	131 ft (39.9 m)	
shale	8 ft (2.4 m)	D7622-B
sandstone	25 ft (7.6 m)	
shale	0 ft (3.1 m)	D7622-A
sandstone, shale	90 ft (27.4 m)	
shale	5 ft (1.5 m)	(barren sample)

D7626.—Kaiparowits(?) Formation exposed in road cut on east side of U.S. Highway 89; sec. 36, T. 39 S., R. 7 W., Kane County, Utah; Long Valley Junction 7.5-minute quadrangle; lat 37°22'30" N., long 112°35'30" W. Sample collected by E.G. Sable about 500 ft (150 m) below base of Claron Formation.

D7843.—Kaiparowits(?) Formation exposed in stream cut at Cascade Falls; $SE^1/_4SE^1/_4$ sec. 17, T. 38 S., R. 8 W., Kane County, Utah; Navajo Lake 7.5-minute quadrangle; lat 37°30'15" N., long 112°45'30" W. Sample collected by D.W. Moore about 95 m below the base of the Claron Formation.

D7625.— Kaiparowits(?) Formation or Wahweap Formation (stratigraphic assignment uncertain) exposed in cirque-like amphitheater on west side of Blowhard Mountain and in road cuts along State Highway 14; sec. 16 and 21, T. 37 S., R. 9 W., Iron County, Utah; Navajo Lake and Webster Flat 7.5-minute quadrangles; lat 37°34'57" N., long 113°52'20" W. Section measured and sampled by E.G. Sable, as follows:

Claron Formation.

Kaiparowits(?) or Wahweap Formation:

sandstone, shale	78 ft (23.8 m)	
carbonaceous siltstone, shale	1 ft (0.3 m)	D7625-A
sandstone	60 ft (18.3 m)	
sandstone, shale	250 ft (76.2 m)	
carbonaceous shale, sandstone	2–3 ft (0.6–0.9 m)	D7625-B

PALYNOLOGY

SAMPLE PROCESSING AND ANALYSIS

All samples were processed following standard procedures described by Doher (1980). Two slides were prepared from each maceration residue. The slides, unmounted residues, and unprocessed splits of samples are archived in the USGS palynological laboratory in Denver, Colo. All archived materials are filed by their respective locality numbers.

Slides were scanned and identifications of all species identified were recorded. Specimen counts were not made, but where certain species were found to be especially numerous and thus to characterize an assemblage, special note was made of their abundance. Some taxonomic identifications are preliminary, pending the outcome of detailed studies in progress; many are to the genus level only. Based on these records, palynofloral lists were compiled for each stratigraphic unit. Age determinations and correlations (discussed later) are based on the total palynoflora of each unit in the study area as it is represented in these lists. Stratigraphically important and commonly occurring species of palynomorphs are illustrated in plates 1–4.

PALYNOFLORA OF THE DAKOTA FORMATION

Bryophyte and pteridophyte spores
- *Appendicisporites potomacensis* Brenner (pl. 2, fig. 1)
- *Appendicisporites* spp.
- *Camarozonosporites ambigens* (Fradkina) Playford
- *Cicatricosisporites* spp. (pl. 2, fig. 9)
- *Cyathidites* sp.
- *Deltoidospora minor* (Couper) Pocock
- *Gleicheniidites senonicus* Ross emend. Skarby (pl. 1, fig. 11)
- *Klukisporites* sp. (pl. 1, figs. 13–14)
- *Laevigatosporites* sp. (pl. 1, fig. 1)
- *Lygodiumsporites* sp. 1 (pl. 1, fig. 6)
- *Microreticulatisporites* sp.
- *Stereisporites* spp.
- *Triporoletes novomexicanus* (Anderson) Srivastava

Gymnosperm pollen
- *Corollina torosa* (Reissinger) Klaus emend. Cornet & Traverse
- *Ephedripites* sp. D
- *Pityosporites* spp.
- *Quadripollis krempii* Drugg
- *Taxodiaceaepollenites hiatus* (Potonié) Kremp

Angiosperm pollen
- *Cupuliferoidaepollenites minutus* (Brenner) Singh
- *Foveotricolporites* sp. (pl. 3, figs. 12–13)
- *Liliacidites* sp.
- *Nyssapollenites albertensis* Singh (pl. 3, figs. 7–10)
- *Nyssapollenites* spp.
- *Stephanocolpites* sp. cf. *S. tectorius* Hedlund
- *Tricolpites* spp. (pl. 3, figs. 4–5)

Marine dinocysts
- *Palaeohystrichophora infusorioides* Deflandre (pl. 4, fig. 8)
- dinocysts, unidentified

The palynoflora of the Dakota Formation in the study area is dominated by nonmarine pollen and spore taxa but includes some marine dinocysts. About 35 species in 22 genera were recorded from a total of 14 samples analyzed from five localities in the Markagunt and northwestern Kaiparowits Plateaus. Specimens of fern spores representing more than a dozen species are the most common fossils in assemblages from these Dakota samples. Species of gymnosperm pollen displaying a wide range of morphology are present but not markedly abundant. Species of angiosperm pollen include monosulcate, tricolpate, tetracolpate, and tricolporate types; no triporate pollen is present in the Dakota palynoflora.

Palaeohystrichophora infusorioides Deflandre is the only dinocyst species positively identified in the samples studied, although a few other poorly preserved specimens were observed. The dinocysts are indicative of marine

influence in the depositional environment. Dinocysts are present in assemblages from within the upper 165 m of the Dakota Formation at locality D7623, an interval that may be transitional with the marine Tropic Shale (E.G. Sable, written commun., 1992; see also Gustason, 1989).

The gymnosperm pollen taxa identified have little paleoecologic or biostratigraphic significance because of their long stratigraphic ranges and their low numbers in these samples. The spore taxa similarly have long stratigraphic ranges. The angiosperm pollen taxa identified have greater biostratigraphic significance than either the spores or the gymnosperm pollen, even at a high taxonomic level. For example, the presence of tricolporates (especially species of the genus *Nyssapollenites*), together with the absence of triporates, is characteristic of assemblages of Cenomanian age in the Rocky Mountain region. A tetracolpate species from the Dakota Formation in the Markagunt Plateau identified as *Stephanocolpites* sp. cf. *S. tectorius* Hedlund closely resembles a specimen from the Dakota Formation in Arizona identified as *S. tectorius* by Agasie (1969, pl. 4, figs. 9–10) except that it is smaller than Agasie's specimen. It is the only species recorded in the present study that is unique to the palynoflora of the Dakota Formation. It was present in a single sample from locality D7621, in the northwestern Kaiparowits Plateau; it was poorly preserved and is not illustrated here.

The palynoflora of the Dakota Formation in southern Utah and northern Arizona is known from previous studies by Agasie (1969), May (1972), May and Traverse (1973), and am Ende (1991). Agasie described and illustrated 39 species (28 genera) of palynomorphs from the Black Mesa basin of Arizona, mostly spores but including tricolpate and tricolporate pollen clearly of Cenomanian aspect. May (1972) illustrated assemblages from three coal fields in Dakota rocks of southern Utah, including the Kolob coal field of the Markagunt Plateau. May's assemblages include some marine dinocysts (from the Henry Mountains coal field), but primarily consist of nonmarine pollen and spores. May (1972) and May and Traverse (1973) illustrated but did not identify the distinctive pollen tetrad *Artiopollis indivisus* Agasie, which had been described and named by Agasie (1969) and which was said to be a useful guide fossil for the Cenomanian of the area. May (1975) later described another distinctive Cenomanian guide fossil from the Dakota Formation, *Dichastopollenites reticulatus* May, stating that this palynomorph was present at most of his localities in Utah and also at Agasie's locality in Arizona. Neither of these species was found in samples of the Dakota Formation analyzed in the present study. The palynology of the Dakota Formation at the southern edge of the Kaiparowits Plateau was investigated by am Ende (1991) in her study of the depositional environments of the formation. She reported the occurrence of 84 species and discussed their relative abundance as major groups (bryophyte and pteridophyte spores, gymnosperm pollen, and angiosperm pollen). In contrast with previous studies of the Dakota palynoflora (and the present study), am Ende found that diversity was greatest in the angiosperm pollen. She noted that most angiosperm pollen specimens in her samples were tricolpate forms (about 62 percent of the species identified and 81 percent of the specimens counted). In addition to the tricolpates, she identified monosulcate and tricolporate forms, but no triporates.

May's (1972) report of triporate pollen from a supposed Dakota sample from the Kaiparowits coal field in the Seep Flat quadrangle casts serious doubt on the sampled bed's having been correctly identified as the Dakota Formation. Rocks of Dakota (Cenomanian) age in the southern Utah–northern Arizona region lack triporate pollen, as reaffirmed in subsequent studies, including the present one. Furthermore, the assemblage illustrated by May from the Seep Flat quadrangle lacks the Cenomanian guide fossils named herein.

PALYNOFLORA OF THE LOWER UNIT OF THE STRAIGHT CLIFFS FORMATION

Bryophyte and pteridophyte spores
- *Cicatricosisporites* sp.
- *Cyathidites* sp.
- *Laevigatosporites haardtii* (Potonié & Venitz) Thomson & Pflug
- *Stereisporites* spp.

Gymnosperm pollen
- *Corollina torosa* (Reissinger) Klaus emend. Cornet & Traverse
- *Pityosporites* spp.
- *Taxodiaceaepollenites hiatus* (Potonié) Kremp

Angiosperm pollen
- *Nyssapollenites* spp.
- *Retitrescolpites* sp. (pl. 3, fig. 6)
- *Tricolpites* spp.

Marine dinocysts
- *Alterbidinium* sp. (pl. 4, fig. 10)
- *Cleistosphaeridium* sp.
- *Cyclonephelium* sp.
- *Isabelidinium*? sp. (pl. 4, fig. 9)
- *Odontochitina operculata* (Wetzel) Deflandre & Cookson
- *Oligosphaeridium* sp. (pl. 4, fig. 12)
- *Palaeohystrichophora infusorioides* Deflandre (pl. 4, fig. 11)
- dinocysts, unidentified
- microforams (pl. 4, fig. 13)

The palynoflora of the lower unit of the Straight Cliffs Formation (Tibbet Canyon Member equivalent) in the study area includes seven or more species of marine dinoflagellate cysts and microforams—the chitinous inner linings of tests of marine foraminifers. The dinocyst assemblage is more diverse than that recorded from the marine facies of the Dakota Formation in this study. Thus, there is ample evidence of occasional marine influence in the depositional

environment of the lower unit of the Straight Cliffs Formation in the study area. These indicators of marine facies were not observed in samples from the upper unit of the formation. The assemblage of terrestrial spores and pollen from the lower unit is less diverse than that recorded from either the Dakota Formation or the upper unit of the Straight Cliffs Formation. About 15 species in 10 genera were recorded from a total of six samples analyzed, all from the Markagunt Plateau. Because several of these samples yielded only sparse assemblages, the palynoflora of the lower unit cannot be said to be well known in the study area.

The Straight Cliffs Formation in the northwestern Kaiparowits Plateau near Henrieville, Utah, was the subject of a previous study by Orlansky (1971). He also reported dinocysts from the lower part of the formation (the informal lower member of Peterson and Waldrop, 1965), and noted that these marine palynomorphs are restricted to this part of the formation. Although the palynoflora from this interval described by Orlansky (1971) is considerably more diverse than that recorded in the present study, it also excludes biostratigraphically important triporate species.

PALYNOFLORA OF THE UPPER UNIT OF THE STRAIGHT CLIFFS FORMATION

Bryophyte and pteridophyte spores
- *Appendicisporites* spp.
- *Camarozonosporites ambigens* (Fradkina) Playford
- *Cicatricosisporites augustus* Singh (pl. 2, figs. 2–4)
- *Cicatricosisporites australiensis* (Cookson) Potonié (pl. 2, figs. 5–6)
- *Cicatricosisporites imbricatus* (Markova) Singh (pl. 2, fig. 9)
- *Cicatricosisporites* spp.
- *Cyathidites* sp. cf. *C. diaphana* (Wilson & Webster) Nichols & Brown (pl. 1, figs. 2–3)
- *Cyathidites* sp.
- *Deltoidospora minor* (Couper) Pocock (pl. 1, figs. 4–5)
- *Echinatisporis varispinosus* (Pocock) Srivastava
- *Foraminisporis wonthaggiensis* (Cookson & Dettmann) Dettmann
- *Gleicheniidites senonicus* Ross emend. Skarby
- *Klukisporites* sp. (pl. 1, fig. 12)
- *Laevigatosporites haardtii* (Potonié & Venitz) Thomson & Pflug
- *Lygodiumsporites* sp. 2 (pl. 1, fig. 7)
- *Microreticulatisporites* sp.
- *Ornamentifera* sp.
- *Reticuloidosporites pseudomurii* Elsik
- *Stereisporites* spp.
- *Triporoletes* sp. (pl. 1, fig. 10)

Gymnosperm pollen
- *Araucariacites australis* Cookson ex Couper (pl. 2, fig. 13)
- *Callialasporites dampieri* (Balme) Dev emend. Norris (pl. 2, fig. 10)
- *Corollina torosa* (Reissinger) Klaus emend. Cornet & Traverse (pl. 2, figs. 15–16)
- *Cycadopites* sp.
- *Ephedripites* sp. D (pl. 2, figs. 11–12)
- *Pityosporites* spp.
- *Taxodiaceaepollenites hiatus* (Potonié) Kremp (pl. 2, fig. 14)
- *Vitreisporites pallidus* (Reissinger) Nilsson

Angiosperm pollen
- *Arecipites* sp. (pl. 3, figs. 1–2)
- *Complexiopollis* sp. 1 (pl. 4, fig. 7)
- *Cupuliferoidaepollenites minutus* (Brenner) Singh
- *Foveotricolporites johnhenryensis* (pl. 3, fig. 14)
- *Liliacidites* sp. (pl. 3, fig. 3)
- *Nyssapollenites albertensis* Singh
- *Plicapollis* sp. cf. *P. rusticus* Tschudy
- *Pseudoplicapollis triradiata* Jameossanaie (pl. 4, figs. 5–6)
- *Rhoipites* sp. (pl. 3, figs. 15–16)
- *Tricolpites* spp.

Freshwater algal cysts
- *Schizophacus* sp. cf. *S. laevigatus* (Stanley) Nichols & Brown

The palynoflora of the upper unit of the Straight Cliffs Formation (Smoky Hollow and John Henry Members equivalent) in the study area includes about 45 species in 35 genera. The palynofloral list was compiled from a total of nine samples analyzed from two localities, one each in the Markagunt and northwestern Kaiparowits Plateaus. The palynoflora, which includes spores, pollen, and freshwater algae, but no marine dinocysts, is considerably more diverse than that from the lower unit of the Straight Cliffs Formation. More than twice the numbers of both gymnosperm and angiosperm pollen species are present in the upper unit than in the lower unit, and in the upper unit, the number of species of bryophyte and pteridophyte spores is about equal to that of species of gymnosperm and angiosperm pollen combined. Angiosperm pollen includes monosulcate, tricolpate, tricolporate, and triporate types. Species of triporate pollen in the palynoflora of the upper unit of the Straight Cliffs Formation have the most biostratigraphic significance, as discussed later.

As mentioned, the Straight Cliffs Formation in the northwestern Kaiparowits Plateau near Henrieville, Utah, was the subject of a previous study by Orlansky (1971). He described and illustrated 124 palynomorph species from 20 samples. Many of the same species were recorded in the present study, but some names applied differ because of subsequent changes in palynological taxonomy and nomenclature. Locality D7621 of the present study is essentially the

same as that from which Orlansky collected his samples, although he sampled in greater detail. Despite differences in palynological nomenclature, Orlansky's study is of considerable value in determining the age relations of the upper unit of the Straight Cliffs Formation, especially because of the greater density of his sampling.

May (1972) illustrated some specimens from the Straight Cliffs Formation in Carcass Canyon in the eastern part of the Kaiparowits Plateau. His assemblage was from the John Henry Member in the Kaiparowits Plateau coal field.

The John Henry Member of the Straight Cliffs Formation in the subsurface of the central part of the Kaiparowits Plateau was extensively sampled by Nichols (1995). In total, 55 taxa from the formation were identified in that study, and the biostratigraphically significant ones were illustrated and discussed.

PALYNOFLORA OF THE KAIPAROWITS(?) FORMATION

Bryophyte and pteridophyte spores
- *Aequitriradites spinulosus* (Cookson & Dettmann) Cookson & Dettmann
- *Appendicisporites* spp.
- *Camarozonosporites ambigens* (Fradkina) Playford
- *Cicatricosisporites* spp.
- *Cyathidites* sp. cf. *C. diaphana* (Wilson & Webster) Nichols & Brown
- *Cyathidites* sp.
- *Deltoidospora minor* (Couper) Pocock
- *Echinatisporis varispinosus* (Pocock) Srivastava
- *Foraminisporis wonthaggiensis* (Cookson & Dettmann) Dettmann
- *Ghoshispora* sp.
- *Laevigatosporites haardtii* (Potonié & Venitz) Thomson & Pflug
- *Lygodiumsporites* sp. 3
- *Microreticulatisporites* sp.
- *Reticuloidosporites pseudomurii* Elsik
- *Triporoletes novomexicanus* (Anderson) Srivastava (pl. 1, figs. 8–9)

Gymnosperm pollen
- *Araucariacites australis* Cookson ex Couper
- *Corollina torosa* (Reissinger) Klaus emend. Cornet & Traverse
- *Ephedripites* sp. D
- *Pityosporites* spp.
- *Quadripollis krempii* Drugg
- *Taxodiaceaepollenites hiatus* (Potonié) Kremp

Angiosperm pollen
- *Arecipites* sp.
- *Complexiopollis*? sp. 2
- *Cupanieidites* spp.
- *Foveotricolporites* sp.
- *Inaperturotetradites scabratus* Tschudy
- *Liliacidites* sp.
- *Nyssapollenites* spp.
- *Proteacidites* spp. (pl. 4, figs. 1–4)
- *Pseudoplicapollis triradiata* Jameossanaie
- *Rhoipites* sp.
- *Tricolpites* spp.

Freshwater algal cysts
- *Schizophacus* sp. cf. *S. laevigatus* (Stanley) Nichols & Brown

The palynoflora of the Kaiparowits(?) Formation in the Markagunt Plateau includes about 40 species in 32 genera. The palynofloral list was compiled from a total of six productive samples analyzed from four localities in the Markagunt Plateau. The list includes pteridophyte spores, gymnosperm and angiosperm pollen, and freshwater algal cysts. Although pteridophyte spores are the most numerous palynomorph taxa recorded from the formation, proportionally there are more different kinds of angiosperm pollen in this unit than in the other Cretaceous formations in the study area. Angiosperm pollen taxa include monosulcate, tricolpate, tricolporate, syncolporate, and triporate types, and an unusual inaperturate tetrad; significantly, triprojectate types are absent.

Among the palynomorph species recorded in the palynoflora of the Kaiparowits(?) Formation, only a few have not been recorded also in the other Cretaceous formations in the study area. They are the spores *Aequitriradites spinulosus* (Cookson & Dettmann) Cookson & Dettmann, *Ghoshispora* sp., and *Lygodiumsporites* sp. 3, and the angiosperm pollen *Complexiopollis*? sp. 2, *Cupanieidites* spp., *Inaperturotetradites scabratus* Tschudy, and *Proteacidites* spp. *Aequitriradites spinulosus* is known from the Straight Cliffs Formation in the central part of the Kaiparowits Plateau (Nichols, 1995), but the others serve to distinguish the palynoflora of the Kaiparowits(?) Formation from those of other units in the region. *Inaperturotetradites scabratus* was originally described from the Judith River Formation (Campanian) in Montana by Tschudy (1973); its record of occurrence in the Kaiparowits(?) Formation extends the known geographic and stratigraphic range of this species. All productive samples from the Kaiparowits(?) Formation in the Markagunt Plateau contain pollen of the triporate genus *Proteacidites*. This genus has great palynostratigraphic utility in the Rocky Mountain region.

The palynoflora of the Kaiparowits Formation of the northwestern Kaiparowits Plateau was the subject of a previous study by Lohrengel (1969). He described and illustrated 80 species (41 genera) of palynomorphs. Aside from his more extensive palynofloral list, the most important difference between Lohrengel's results and those of the present study is his report of the occurrence of species of the triprojectate genus *Aquilapollenites* in his samples. In the present study, no specimens of *Aquilapollenites* or other triprojectate pollen were found in samples of the Kaiparowits(?) Formation in the Markagunt Plateau. Lohrengel (1969) also reported species of the triporate genus *Proteacidites* in his samples. These two palynomorph genera are especially important in age determination and correlation.

AGE DETERMINATIONS AND CORRELATIONS

DAKOTA FORMATION

Two species present in the palynoflora of the Dakota Formation, and the assemblages with which they are associated, are indicative of the age of this unit, and a third tends to substantiate the inferred age. The taxa are the marine dinocyst species *Palaeohystrichophora infusorioides* Deflandre, the tricolporate angiosperm species *Nyssapollenites albertensis* Singh, and the tetracolpate angiosperm pollen species here identified as *Stephanocolpites* sp. cf. *S. tectorius* Hedlund. *Palaeohystrichophora infusorioides* ranges no lower than the mid-Cenomanian in the Western Interior of North America (Nichols and Jacobson, 1982; Singh, 1983), and *Nyssapollenites albertensis* defines the *Nyssapollenites albertensis* Interval Zone of mid-Cenomanian through mid-Coniacian age (Nichols, 1994). *Stephanocolpites tectorius* was previously described from the Cenomanian of Oklahoma (Hedlund, 1966) and Arizona (Agasie, 1969).

Previous palynological studies concur in dating the Dakota Formation in or near the study area as Cenomanian (May and Traverse, 1973; May, 1975; am Ende, 1991). Palynologic age determinations for the Dakota Formation in the study area are confirmed by those based on mollusks and vertebrates, as summarized by Eaton (1991) and am Ende (1991).

LOWER UNIT OF THE STRAIGHT CLIFFS FORMATION

Palynomorph taxa identified from the lower unit of the Straight Cliffs Formation have long stratigraphic ranges and are of little use in age determination. Angiosperm pollen taxa identified are either tricolpate or tricolporate; no triporate species are present. The presence of tricolporates together with the absence of triporates indicates that the lower unit of the Straight Cliffs in the Markagunt Plateau is within the *Nyssapollenites albertensis* Interval Zone (Nichols, 1994). Thus, an age of Cenomanian through Turonian is indicated. From its stratigraphic position above the Dakota Formation (Cenomanian) and below the Coniacian-Santonian upper unit of the Straight Cliffs Formation, a Turonian age can be inferred for the lower unit of the Straight Cliffs Formation. This unit is the lithostratigraphic equivalent of the Tibbet Canyon Member of the Straight Cliffs Formation in the Kaiparowits Plateau. In that area the Tibbet Canyon Member has been dated as middle Turonian (Peterson, 1969; Eaton, 1991) on the basis of its molluscan fauna.

UPPER UNIT OF THE STRAIGHT CLIFFS FORMATION

Several species of triporate angiosperm pollen have value in determining the age of the upper unit of the Straight Cliffs Formation in the study area. The triporate angiosperm pollen species *Pseudoplicapollis triradiata* Jameossanaie is present in the stratigraphically highest productive sample collected from the measured section at locality D7621, near Henrieville, Utah. This sample is from within the interval between 422 and 446 ft (128.6 and 135.9 m) above the base of the Straight Cliffs Formation. Orlansky (1971) also reported this morphologically distinctive species (as *Cupanieidites* sp. B) in a sample he collected 345 ft (105 m) above the base of the formation at or near the same locality. The complete stratigraphic range of this species has not been determined, but it is present also in the John Henry Member of the Straight Cliffs Formation in the central part of the Kaiparowits Plateau, within an interval interpreted to be of mid-Coniacian through Santonian age (Nichols, 1995). Its presence suggests, but does not prove, that the upper unit of the Straight Cliffs Formation in the northwestern part of the Kaiparowits Plateau is Coniacian or younger (Santonian) in age.

A species of the triporate genus *Plicapollis* (possibly synonymous with *P. rusticus* Tschudy) also is present in the assemblage from the stratigraphically highest productive sample at locality D7621. *Plicapollis rusticus* is common in the John Henry Member in the central part of the Kaiparowits Plateau (Nichols, 1995). The presence of this species in the upper unit of the formation near Henrieville would tend to confirm the Coniacian age determination for this interval in the northwestern part of the plateau.

Of greater potential biostratigraphic significance in rocks of Late Cretaceous age are species of the triporate angiosperm pollen genus *Proteacidites*. *Proteacidites* is a guide to the Senonian (Coniacian through Maastrichtian) in the Rocky Mountain region (Nichols and Jacobson, 1982; Nichols, 1994). *Proteacidites* occurs together with *Plicapollis rusticus* and *Pseudoplicapollis triradiata* in the John Henry Member of the Straight Cliffs Formation in the central part of the Kaiparowits Plateau (Nichols, 1995), and there it is used to recognize the *Proteacidites retusus* Interval Zone. In the present study, no samples from the upper unit of the Straight Cliffs Formation were found to contain *Proteacidites* (with the possible exception of a single poorly preserved specimen questionably assigned to the genus that was recorded in sample D7621-F). However, the assemblage from Orlansky's (1971) sample that contained *Pseudoplicapollis triradiata* also contained *Proteacidites*, as did another of his samples about 95 ft (29 m) lower in the section and only 250 ft (76 m) above the base of the formation. Orlansky's records of *Proteacidites* together with the presence of triporates evidently representing the same palynofloral assemblage are evidence of Coniacian age for the upper part of the Straight Cliffs Formation in the northwestern part of the Kaiparowits Plateau.

Sparse sampling of the upper unit of the formation in the present study accounts for much of the uncertainty that exists in this age determination (only six samples collected at locality D7621, one of which had such poor recovery as to be effectively barren). Remaining uncertainty is attributable to the low relative abundance of specimens of *Proteacidites* in this part of the formation (it is absent from seven of Orlansky's eight samples above its lowest occurrence). However, it should be noted that a Coniacian age determination for this part of the formation based on palynomorphs is consistent with that based on mollusks, as reported by Peterson (1969) and Orlansky (1971).

In the present study, assemblages from the upper unit of the Straight Cliffs Formation in the Markagunt Plateau lack *Plicapollis*, *Pseudoplicapollis*, *Proteacidites*, or other genera of triporate angiosperm pollen. However, only the basal 60 m of the unit was sampled. Thus, although the available palynologic evidence suggests that the age of this limited interval may be pre-Coniacian, most of the (unsampled) upper unit of the formation in the Markagunt Plateau could be the same age as it is in the northwestern Kaiparowits Plateau. Its stratigraphic position beneath the well-dated Kaiparowits(?) Formation in the Markagunt Plateau substantiates this interpretation.

KAIPAROWITS(?) FORMATION

The unit in the Markagunt Plateau referred to as the Kaiparowits(?) Formation, which has been mapped as the lithostratigraphic equivalent of the Kaiparowits Formation of the Kaiparowits Plateau, is determined in the present study to be stratigraphically older than the typical Kaiparowits Formation. The Kaiparowits(?) Formation contains palynomorph species characteristic of the *Proteacidites retusus* Interval Zone, which is Coniacian and Santonian in age, whereas the Kaiparowits Formation in its type area contains species characteristic of rocks of late Campanian age.

All productive samples from the Kaiparowits(?) Formation in the Markagunt Plateau contain pollen of the biostratigraphically important triporate genus *Proteacidites*. As previously noted, this genus is characteristic of Senonian (Coniacian through Maastrichtian) rocks in the Rocky Mountain region. The presence of *Proteacidites* together with the absence of *Aquilapollenites* (or other triprojectate genera) in the Kaiparowits(?) Formation indicates that this unit is Coniacian or Santonian in age. Given the stratigraphic position of this unit—above the Coniacian upper unit of the Straight Cliffs Formation—Santonian age is more likely. A Santonian age determination for the Kaiparowits(?) Formation is also consistent with the relative abundance of *Proteacidites* pollen in this unit.

The stratigraphic relationship of the unit mapped as Kaiparowits(?) Formation in the Markagunt Plateau (Sable and Hereford, 1990) has been a contentious point in regional geologic interpretations. This unit may well be the lithostratigraphic equivalent of the Kaiparowits Formation in its type area, but these units are not chonostratigraphically correlative. Palynological data show that the Kaiparowits(?) Formation of the Markagunt Plateau is Santonian, stratigraphically older than the Campanian Kaiparowits Formation of the Kaiparowits Plateau.

The age of the Kaiparowits Formation in its type area has itself been a source of confusion. As mentioned, the palynoflora of the Kaiparowits Formation in the northwestern Kaiparowits Plateau was described previously by Lohrengel (1969). Most significantly with regard to biostratigraphy, he reported the occurrence of several species of the triprojectate pollen genus *Aquilapollenites*. This genus occurs only in rocks of Campanian and younger age in the Western Interior, and various species of the genus are characteristic of rocks of certain parts of the Campanian and Maastrichtian in the region (Tschudy and Leopold, 1970; Nichols and others, 1982; Nichols, 1994). However, at the time of Lohrengel's (1969) study, the stratigraphic ranges of few palynomorph taxa in the region had been accurately determined, and no palynostratigraphic zonation had been developed. Lohrengel attempted to correlate his entire assemblage statistically, but ultimately relied upon the presence of a few taxa, especially the genus *Aquilapollenites*. He erroneously concluded that his assemblage was late Maastrichtian in age.

Lohrengel (1969) reasoned, on the basis of his interpretation of available palynological data, that the Kaiparowits Formation is late Maastrichtian in age, but this was incorrect. Bowers (1972) discussed palynological data of R.H. Tschudy that indicated a Campanian age for the Kaiparowits Formation. Eaton (1991) reexamined the palynological data presented by Lohrengel (1969) and Bowers (1972), and supplemented this with data from vertebrate paleontology; he concluded that the Kaiparowits Formation is no younger than Campanian. Farabee (1991) concurred with the Campanian ("Judithian") age on the basis of new palynologic data from the type area of the formation.

The age relations of the Kaiparowits Formation in the Kaiparowits Plateau and the Kaiparowits(?) Formation in the Markagunt Plateau can be summarized by reference to palynostratigraphic zones (Nichols, 1994). Rocks of latest Maastrichtian age in the Rocky Mountain region, such as the Lance and Hell Creek Formations of Wyoming and Montana, contain species of pollen (including triprojectates) that are characteristic of the *Wodehouseia spinata* Assemblage Zone. This assemblage is absent from both the Kaiparowits and the Kaiparowits(?) Formations of Utah. The Kaiparowits Formation in its type area in the Kaiparowits Plateau contains triprojectate pollen and other species characteristic of rocks of late Campanian age in the Rocky Mountain region. This assemblage, which is characteristic of the *Aquilapollenites quadrilobus* Interval Zone, is absent from the Kaiparowits(?) Formation of the Markagunt Plateau. The Kaiparowits(?) Formation contains the assemblage of the *Proteacidites retusus* Interval Zone, which is Coniacian and Santonian in age.

OTHER UNITS

Two units having problematic or provocative palynologic age determinations were also investigated in this study. These are the sandstone and conglomerate unit exposed in Parowan Canyon and the sandstone and shale unit of uncertain stratigraphic assignment exposed at locality D7625.

The sandstone and conglomerate unit in Parowan Canyon originally was correlated lithostratigraphically with the Kaiparowits Formation (Gregory, 1950). Goldstrand (1991) considered it to be the basal part of the Tertiary Claron Formation. This unit is now assigned to the Grand Castle Formation of Goldstrand and Mullett (this volume, chapter D); these authors conclude that the Grand Castle Formation may be as young as late Paleocene. No samples were collected from this unit in this study, but Goldstrand and Mullett (this volume) mention a palynological age determination made on a sample from this unit that is Late Cretaceous (possibly Santonian), and cite as the source of information "D.J. Nichols, written commun., 1991." A review of the unpublished report referred to shows that the sample in question came from a bed in what is now the Grand Castle Formation 160 m above the base of the unit in sec. 6, T. 35 S., R. 8 W., Iron County, Utah, and that the palynomorph assemblage it contained is definitively Late Cretaceous in age, probably Santonian. Goldstrand and Mullett (this volume) suggest that these palynomorphs are reworked from Upper Cretaceous rocks and thus are not indicative of the age of the Grand Castle Formation. Reworking of palynomorphs from older to younger rocks is always a possibility, but which Cretaceous unit might have been the source in this case is unclear. The underlying Iron Springs Formation is unlikely because that unit evidently is older than Santonian; a sample from the Iron Springs examined by R.A. Christopher (quoted in Hintze, 1986, p. 18) was determined to be of Cenomanian or Turonian age. The Grand Castle Formation generally lacks lithologies appropriate for palynological analysis, and no other direct palynological evidence of the age of this unit is known.

From field relations, the unit exposed at locality D7625 (sec. 16 and 21, T. 37 S., R. 9 W., Iron County, Utah) appears to be either the Kaiparowits(?) Formation or the Wahweap Formation. Two samples were collected from this unit, one from near the base of the exposed interval and the other from near the top. From palynologic evidence it appears that this unit is the Kaiparowits(?) Formation. That is, the assemblages recovered from these samples are closely comparable with those from the Kaiparowits(?) Formation sampled at other localities in the study area. Most significantly, the pollen of *Proteacidites* is common in the assemblages. However, this age determination presents an interesting alternative to the stratigraphic assignment of the unit mapped as Kaiparowits(?) Formation in the Markagunt Plateau. The unit exposed at locality D7625 includes beds that are lithologically comparable to both the Wahweap Formation and the typical Kaiparowits Formation. Beds comparable to those of the Wahweap Formation predominate (E.G. Sable, oral commun., 1994), and the thickness of this unit exceeds that of the Kaiparowits(?) Formation as mapped elsewhere in the Markagunt Plateau (Sable and Hereford, 1990). These observations suggest that the unit could be assigned to the Wahweap Formation. Nonetheless, the unit also includes lithologies that are similar to or identical with those of both the typical Kaiparowits Formation of the Kaiparowits Plateau and the Kaiparowits(?) Formation elsewhere in the Markagunt Plateau, and its stratigraphic position beneath the Claron Formation argue for its being assigned to the Kaiparowits(?) Formation. The palynological assemblages from the two samples are biostratigraphically indistinguishable from each other. It is evident that the Kaiparowits(?) Formation is a unit that is biostratigraphically uniform but lithologically variable. As noted, the Kaiparowits(?) Formation of the Markagunt Plateau is older than the typical Kaiparowits Formation, and is closer in age to the Wahweap Formation. These results suggest that perhaps the unit known as the Kaiparowits(?) Formation actually is a facies of the Wahweap Formation; as such, perhaps it should have been designated the Wahweap(?) Formation.

CONCLUSIONS

Palynomorphs—including bryophyte and pteridophyte spores, gymnosperm and angiosperm pollen, cysts of freshwater algae, cysts of marine dinoflagellates, and microforams—are present in samples of Cretaceous formations in the Markagunt and northwestern Kaiparowits Plateaus. They provide information on the depositional environments and ages of these units. Units sampled in this study are the Dakota Formation, the lower and upper units of the Straight Cliffs Formation, a unit of uncertain stratigraphic relation to the Kaiparowits Formation in its type area herein designated the Kaiparowits(?) Formation, and a unit of uncertain stratigraphic assignment representing either the Kaiparowits(?) Formation or the Wahweap Formation. The palynoflora of each unit was delineated from a total of more than 60 palynomorph taxa identified in the study area. In most units studied, species of angiosperm pollen have the greatest biostratigraphic value.

The Dakota Formation is Cenomanian in age, as indicated especially by angiosperm pollen of the genus *Nyssapollenites* and the marine dinocyst *Palaeohystrichophora infusorioides*. This age determination is consistent with previously published interpretations based on palynology, as well as on fossil mollusks and vertebrates.

The lower unit of the Straight Cliffs Formation is not well dated on the basis of palynology, but it lies within a palynostratigraphic zone of Cenomanian and Turonian age. Existing data from fossil mollusks indicate a Turonian age for this unit. The upper unit of the Straight Cliffs Formation in the northwestern Kaiparowits Plateau is Coniacian or

younger (Santonian) in age, based on its palynoflora. Biostratigraphically important angiosperm pollen from the upper unit includes species of the triporate genera *Plicapollis*, *Pseudoplicapollis*, and *Proteacidites*. These taxa were not found in samples of the upper unit from the Markagunt Plateau, but only the basal interval of the upper unit was sampled there. The unsampled part of the upper unit of the Straight Cliffs Formation in the Markagunt Plateau probably is the same age as it is in the northwestern Kaiparowits Plateau (Coniacian-Santonian).

The Kaiparowits(?) Formation of the Markagunt Plateau is Coniacian or Santonian in age, and more likely is Santonian. Pollen of *Proteacidites* is common in the palynoflora of this unit, but triprojectate pollen (*Aquilapollenites* and related genera) is absent. The Kaiparowits(?) Formation of the Markagunt Plateau is stratigraphically older than the Kaiparowits Formation in its type area in the Kaiparowits Plateau. As determined previously on the basis of its palynoflora and vertebrate fauna, the typical Kaiparowits is Campanian in age, not Maastrichtian as was originally interpreted on the basis of palynology.

An additional, tentative conclusion may be drawn. A sample from the unit in Parowan Canyon originally correlated with the Kaiparowits Formation of the southern Kaiparowits Plateau by Gregory (1950), but now assigned to the Grand Castle Formation of Goldstrand and Mullett (this volume, chapter D), yielded palynomorphs indicative of a Late Cretaceous, possibly Santonian, age. Barring the possibility that these palynomorphs are reworked, the data indicate that the Grand Castle Formation is in part Cretaceous rather than Paleocene in age.

REFERENCES CITED

Agasie, J.M., 1969, Late Cretaceous palynomorphs from northeastern Arizona: Micropaleontology, v. 15, no. 1, p. 13–30, 4 pls.

am Ende, B.A., 1991, Depositional environments, palynology, and age of the Dakota Formation, south-central Utah, *in* Nations, J.D., and Eaton, J.G., eds., Stratigraphy, depositional environments, and sedimentary tectonics of the western margin, Cretaceous Western Interior seaway: Geological Society of America Special Paper 260, p. 65–83.

Averitt, Paul, and Threet, R.L., 1973, Geologic map of the Cedar City quadrangle, Iron County, Utah: U.S. Geological Survey Geologic Quadrangle Map GQ–1120, scale 1:24,000.

Bowers, W.E., 1972, The Canaan Peak, Pine Hollow, and Wasatch Formations in the Table Cliff region, Garfield County, Utah: U.S. Geological Survey Bulletin 1331–B, 39 p.

Doher, L.I., 1980, Palynomorph preparation procedures currently used in the paleontology and stratigraphy laboratories, U.S. Geological Survey: U.S. Geological Survey Circular 830, 29 p.

Eaton, J.G., 1991, Biostratigraphic framework for the Upper Cretaceous rocks of the Kaiparowits Plateau, southern Utah, *in* Nations, J.D., and Eaton, J.G., eds., Stratigraphy, depositional environments, and sedimentary tectonics of the western margin, Cretaceous Western Interior seaway: Geological Society of America Special Paper 260, p. 47–63.

Farabee, M.J., 1991, Palynology of the upper Kaiparowits Formation (Upper Cretaceous, Campanian) in southcentral Utah [abs.]: Georgia Journal of Science, v. 49, no. 1, p. 34.

Goldstrand, P.M., 1991, Tectonostratigraphy, petrology, and paleogeography of Upper Cretaceous to Eocene rocks of southwest Utah: Reno, Nev., University of Nevada Ph. D. dissertation, 205 p.

Goldstrand, P.M., Trexler, J.H., Jr., Kowallis, B.J., and Eaton, J.G., 1993, Late Cretaceous to early Tertiary tectonostratigraphy of southwestern Utah, *in* Morales, M., ed., Aspects of Mesozoic geology and paleontology of the Colorado Plateau: Museum of Northern Arizona Bulletin 59, p. 181–188.

Gregory, H.E., 1950, Geology of eastern Iron County, Utah: Utah Geological and Mineral Survey Bulletin 37, 153 p.

Gregory, H.E., and Moore, R.C., 1931, The Kaiparowits region, a geographic and geologic reconnaissance of parts of Utah and Arizona: U.S. Geological Survey Professional Paper 164, 161 p.

Gustason, E.R., 1989, Stratigraphy and sedimentology of the middle Cretaceous (Albian-Cenomanian) Dakota Formation, southwestern Utah: Boulder, Colo., University of Colorado Ph. D. dissertation, 376 p.

Hedlund, R.W., 1966, Palynology of the Red Branch Member of the Woodbine Formation (Cenomanian), Bryan County, Oklahoma: Oklahoma Geological Survey Bulletin 112, 69 p., 10 pls.

Hintze, L.F., 1986, Stratigraphy and structure of the Beaver Dam Mountains, southwestern Utah, *in* Thrusting and extensional structures and mineralization in the Beaver Dam Mountains, southwestern Utah: Utah Geological Association Publication 15, p. 1–36.

Lohrengel, C.F., II, 1969, Palynology of the Kaiparowits Formation, Garfield County, Utah: Brigham Young University Geology Studies, v. 16, no. 3, p. 61–180, 12 pls.

May, F.E., 1972, A survey of palynomorphs from several coal-bearing horizons of Utah, *in* Doelling, H.H., ed., Central Utah coal fields; Sevier-Sanpete, Wasatch Plateau, Book Cliffs and Emery: Utah Geological and Mineralogical Survey Monograph 3, p. 497–542, 29 pls.

———1975, *Dichastopollenites reticulatus*, gen. et sp. nov.—Potential Cenomanian guide fossil from southern Utah and northeastern Arizona: Journal of Paleontology, v. 49, no. 3, p. 528–533, 2 pls.

May, F.E., and Traverse, Alfred, 1973, Palynology of the Dakota Sandstone (middle Cretaceous) near Bryce Canyon National Park, southern Utah: Geoscience and Man, v. 3, p. 57–64, 1 pl.

Moir, G.J., 1974, Depositional environments and stratigraphy of the Cretaceous rocks, southwestern Utah: Los Angeles, Calif., University of California Ph. D. dissertation, 316 p.

Nichols, D.J., 1994, A revised palynostratigraphic zonation of the nonmarine Upper Cretaceous, Rocky Mountain region, United States, *in* Caputo, M.V., Peterson, J.A., and Franczyk, K.J., eds., Mesozoic systems of the Rocky Mountain region, USA: Denver, Colo., Rocky Mountain Section SEPM, p. 503–521.

———1995, Palynostratigraphy in relation to sequence stratigraphy, Straight Cliffs Formation (Upper Cretaceous), Kaiparowits Plateau, Utah: U.S. Geological Survey Bulletin 2115–B, 23 p., 1 pl.

Nichols, D.J., and Jacobson, S.R., 1982, Palynostratigraphic framework for the Cretaceous (Albian-Maestrichtian) of the overthrust belt of Utah and Wyoming: Palynology, v. 6, p. 119–147, 4 pls.

Nichols, D.J., Jacobson, S.R., and Tschudy, R.H., 1982 [1983], Cretaceous palynomorph biozones for the central and northern Rocky Mountain region of the United States, *in* Powers, R.B., ed., Geologic studies of the Cordilleran thrust belt: Denver, Colo., Rocky Mountain Association of Geologists, v. 2, p. 721–733, 1 pl.

Orlansky, Ralph, 1971, Palynology of the Upper Cretaceous Straight Cliffs Sandstone, Garfield County, Utah: Utah Geological and Mineralogical Survey Bulletin 89, 57 p., 11 pls.

Peterson, Fred, 1969, Four new members of the Upper Cretaceous Straight Cliffs Formation in the southeastern Kaiparowits region, Kane County, Utah: U.S. Geological Survey Bulletin 1274–J, 28 p.

Peterson, Fred, and Waldrop, H.A., 1965, Jurassic and Cretaceous stratigraphy of south-central Kaiparowits Plateau, Utah: Utah Geological Society and Intermountain Association of Petroleum Geologists, Guidebook to the Geology of Utah 19, p. 47–69.

Robison, R.A., 1966, Geology and coal resources of the Tropic area, Garfield County, Utah: Utah Geological and Mineralogical Survey Special Studies 18, 47 p.

Sable, E.G., and Hereford, Richard, 1990, Preliminary geologic map of the Kanab 30- by 60-minute quadrangle, Utah and Arizona: U.S. Geological Survey Open-File Report 90-542, 1 sheet, map scale 1:100,000.

Singh, Chaitanya, 1983, Cenomanian microfloras of the Peace River area, northwestern Alberta: Alberta Research Council Bulletin 44, 322 p., 62 pls.

Tschudy, B.D., 1973, Palynology of the upper Campanian (Cretaceous) Judith River Formation, north-central Montana: U.S. Geological Survey Professional Paper 770, 42 p., 11 pls.

Tschudy, B.D., and Leopold, E.B., 1970, *Aquilapollenites* (Rouse) Funkhouser—Selected Rocky Mountain taxa and their stratigraphic ranges, *in* Kosanke, R.M., and Cross, A.T., eds., Symposium on palynology of the Late Cretaceous and early Tertiary: Geological Society of America Special Paper 127, p. 113–167.

PLATES 1–4

Contact photographs of the plates in this report are available, at cost, from the U.S. Geological Survey Photographic Library
Federal Center, Denver, Colorado 80225

PLATE 1

[All specimens ×1,000]

Figure 1. *Laevigatosporites* sp., Dakota Formation, D7623-I.
2, 3. *Cyathidites* sp. cf. *C. diaphana.*
2. Straight Cliffs Formation, upper unit, D7621-B.
3. Straight Cliffs Formation, upper unit, D7830-A.
4, 5. *Deltoidospora minor.*
4. Straight Cliffs Formation, upper unit, D7830-A.
5. Straight Cliffs Formation, upper unit, D7830-C.
6. *Lygodiumsporites* sp. 1, Dakota Formation, D7623-F.
7. *Lygodiumsporites* sp. 2, Straight Cliffs Formation, upper unit, D7621-D.
8, 9. *Triporoletes novomexicanus*, Kaiparowits(?) Formation, D7625-B.
8. Proximal view.
9. Distal view.
10. *Triporoletes* sp., Straight Cliffs Formation, upper unit, D7621-E.
11. *Gleicheniidites senonicus*, Dakota Formation, D7621-A.
12–14. *Klukisporites* sp.
12. Straight Cliffs Formation, upper unit, D7830-A.
13, 14. Dakota Formation, D7624-A.

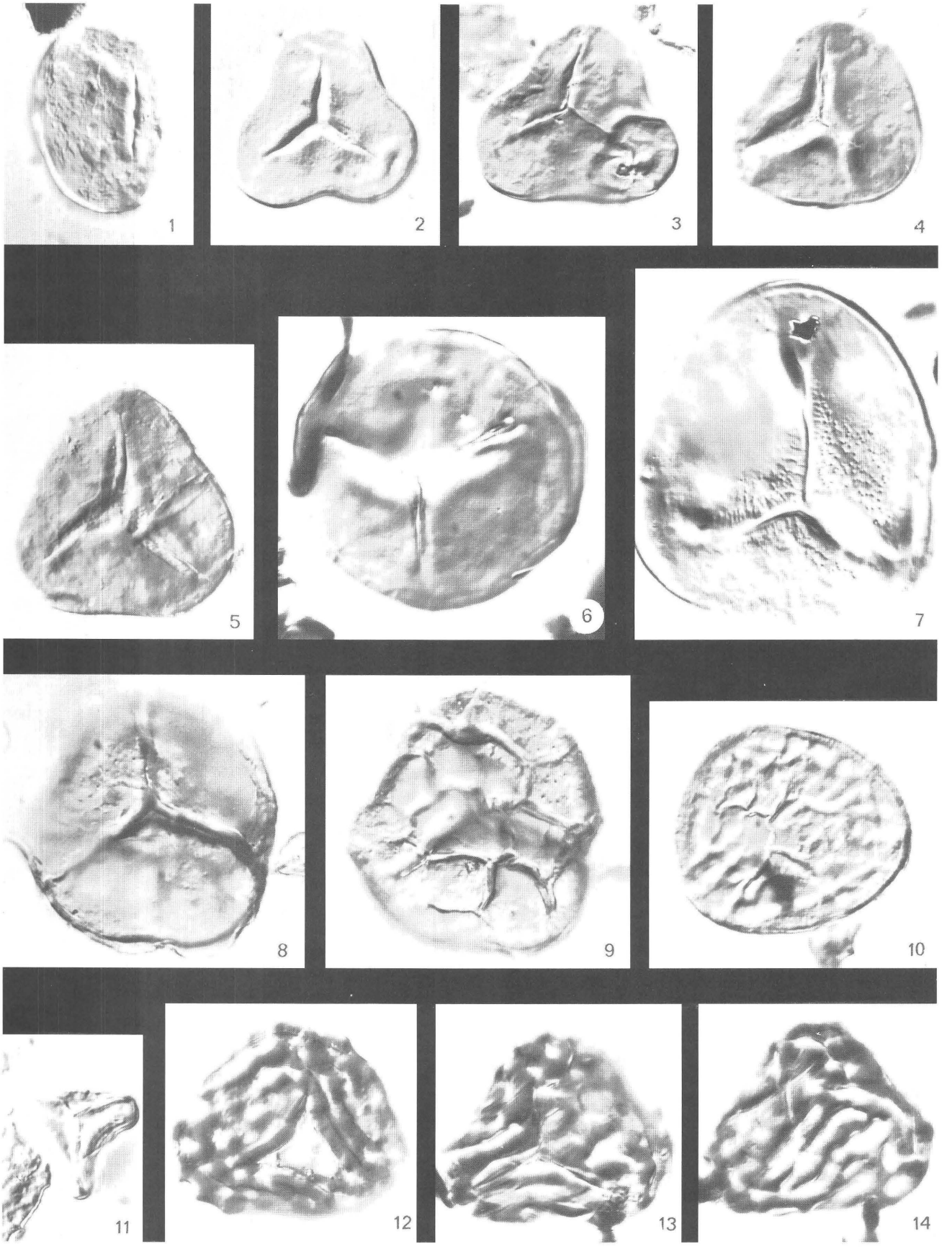

CRETACEOUS SPORES FROM THE MARKAGUNT AND NORTHWESTERN KAIPAROWITS PLATEAUS

PLATE 2

[All specimens ×1,000]

Figure 1. *Appendicisporites potomacensis*, Dakota Formation, D7623-F.
2, 3. *Cicatricosisporites augustus*, Straight Cliffs Formation, upper unit, D7830-A.
2. Proximal view.
3. Distal view.
4. *Cicatricosisporites augustus*, Straight Cliffs Formation, upper unit, D7830-A.
5, 6. *Cicatricosisporites australiensis*, Straight Cliffs Formation, upper unit, D7830-C.
7, 8. *Cicatricosisporites imbricatus*, Straight Cliffs Formation, upper unit, D7621-B.
9. *Cicatricosisporites* sp., Dakota Formation, D7624-A.
10. *Callialasporites dampieri*, Straight Cliffs Formation, upper unit, D7621-F.
11, 12. *Ephedripites* sp. D.
11. Straight Cliffs Formation, upper unit, D7621-C.
12. Straight Cliffs Formation, upper unit, D7830-B.
13. *Araucariacites australis*, Straight Cliffs Formation, upper unit, D7621-E.
14. *Taxodiaceaepollenites hiatus*, Straight Cliffs Formation, upper unit, D7830-A.
15, 16. *Corollina torosa.*
15. Straight Cliffs Formation, upper unit, D7830-B.
16. Straight Cliffs Formation, upper unit, D7830-A.

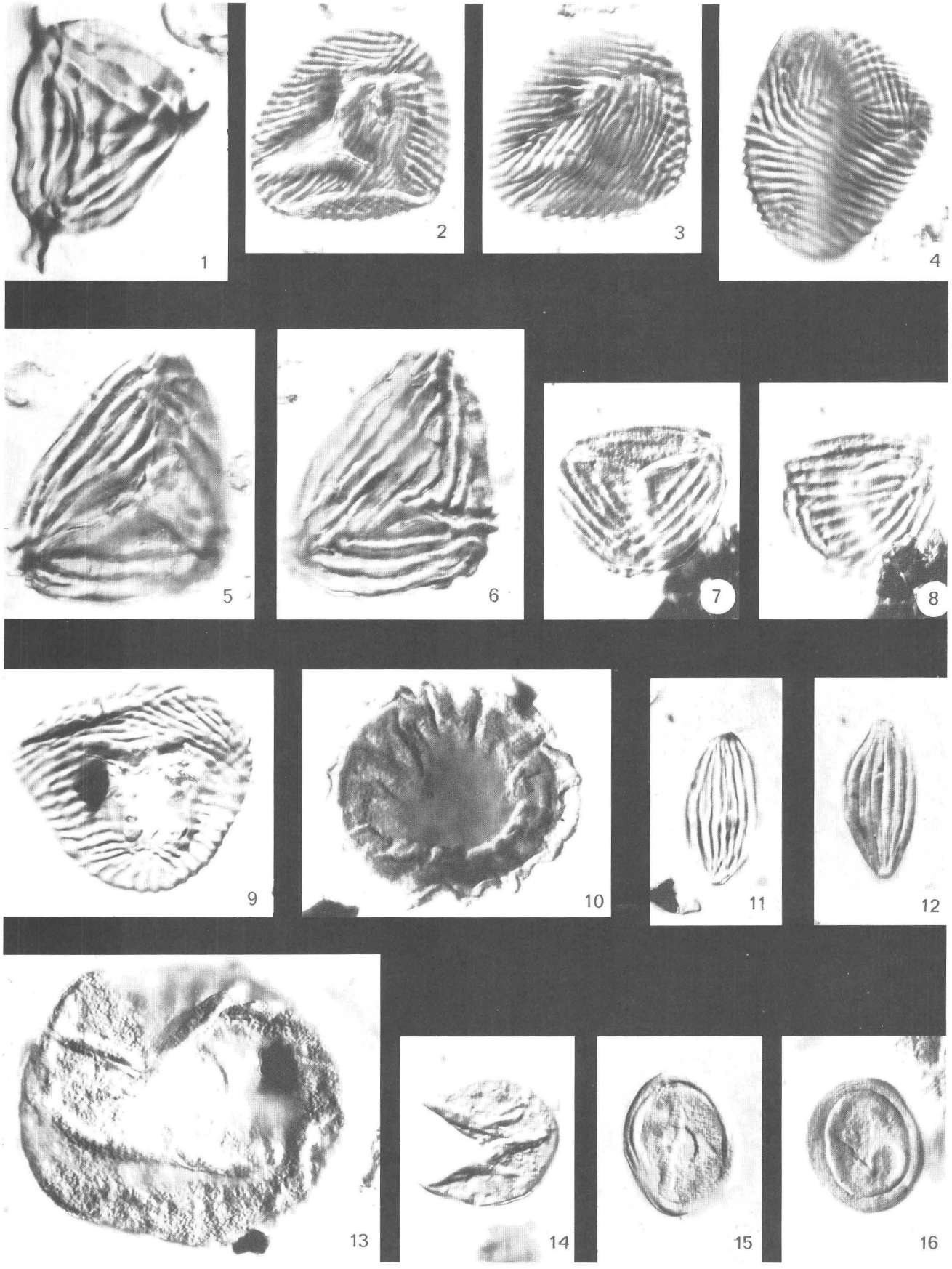

CRETACEOUS SPORES AND GYMNOSPERM POLLEN FROM THE MARKAGUNT AND NORTHWESTERN KAIPAROWITS PLATEAUS

PLATE 3

[All specimens ×1,000]

Figure 1, 2. *Arecipites* sp.
1. Straight Cliffs Formation, upper unit, D7621-E.
2. Straight Cliffs Formation, upper unit, D7621-C.

3. *Liliacidites* sp., Straight Cliffs Formation, upper unit, D7621-D.

4, 5. *Tricolpites* spp.
4. Dakota Formation, D7621-A.
5. Dakota Formation, D7826.

6. *Retitrescolpites* sp., Straight Cliffs Formation, lower unit, D7829.

7–10. *Nyssapollenites* spp.
7. Dakota Formation, D7826.
8. Dakota Formation, D7621-A.
9. Dakota Formation, D7831-B.
10. Dakota Formation, D7831-B.

11. *Nyssapollenites albertensis*, Straight Cliffs Formation, upper unit, D7621-D.

12, 13. *Foveotricolporites* spp.
12. Dakota Formation, D7623-F.
13. Dakota Formation, D7623-I.

14. *Foveotricolporites johnhenryensis,* Straight Cliffs Formation, upper unit, D7621-F.

15, 16. *Rhoipites* sp., Straight Cliffs Formation, upper unit, D7621-E.
15. Mid-focus showing aperture structure.
16. High focus showing sculpture.

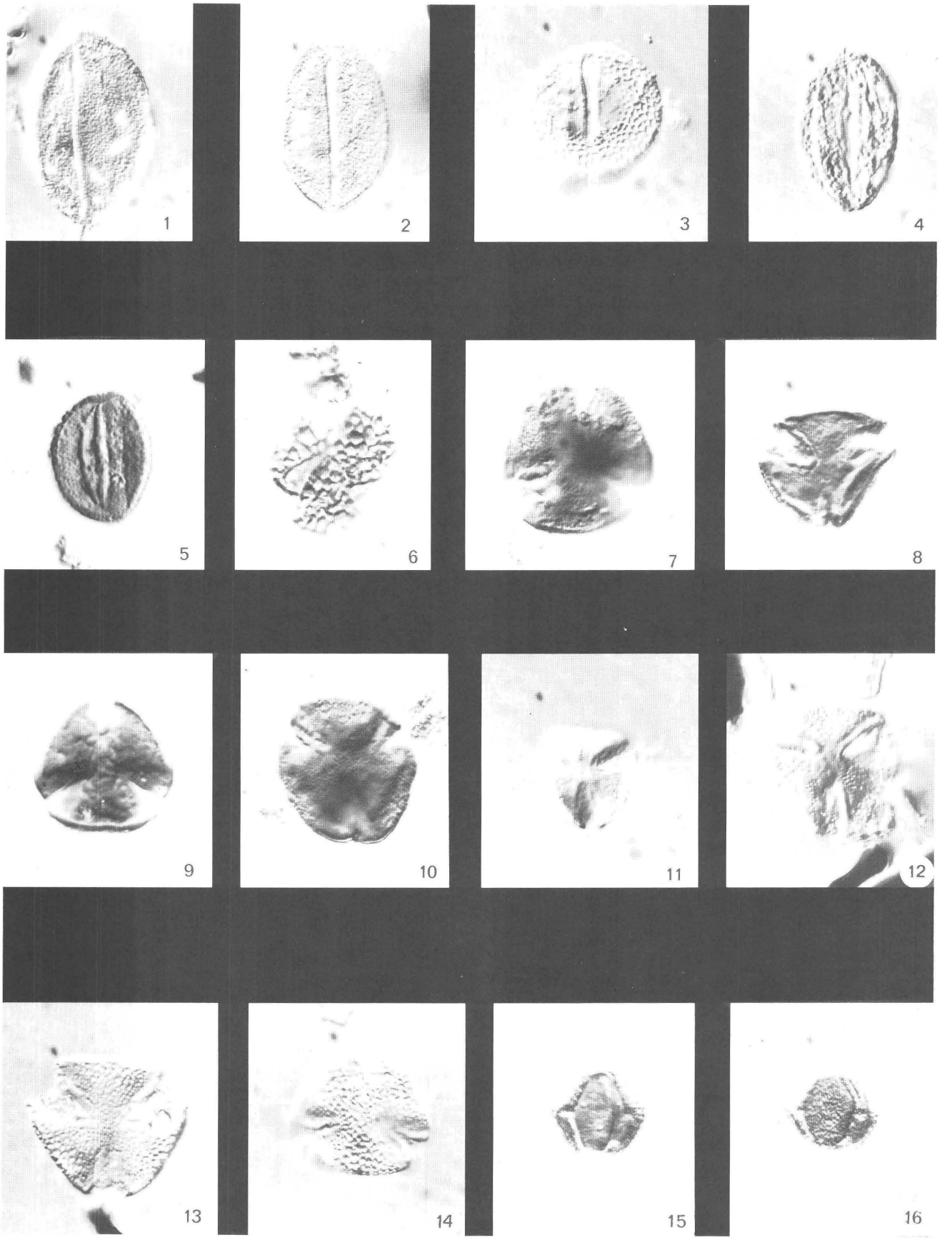

CRETACEOUS ANGIOSPERM POLLEN FROM THE MARKAGUNT AND NORTHWESTERN KAIPAROWITS PLATEAUS

PLATE 4

[All specimens ×1,000]

Figures 1–4. *Proteacidites* spp.
1. Kaiparowits(?) Formation, D7625-A.
2. Kaiparowits(?) Formation, D7625-B.
3. Kaiparowits(?) or Wahweap Formation, D7625.
4. Kaiparowits(?) or Wahweap Formation, D7625.

5, 6. *Pseudoplicapollis triradiata*, Straight Cliffs Formation, upper unit, D7621-F.

7. *Complexiopollis* sp. 1, Straight Cliffs Formation, upper unit, D7621-F.

8. *Palaeohystrichophora infusorioides*, Dakota Formation, D7623-H.

9. *Isabelidinium*? sp., Straight Cliffs Formation, lower unit, D7829.

10. *Alterbidinium* sp., Straight Cliffs Formation, lower unit, D7829.

11. *Palaeohystrichophora infusorioides*, Straight Cliffs Formation, lower unit, D7829.

12. *Oligosphaeridium* sp., Straight Cliffs Formation, lower unit, D7624-C.

13. Microforam, Straight Cliffs Formation, lower unit, D7624-C.

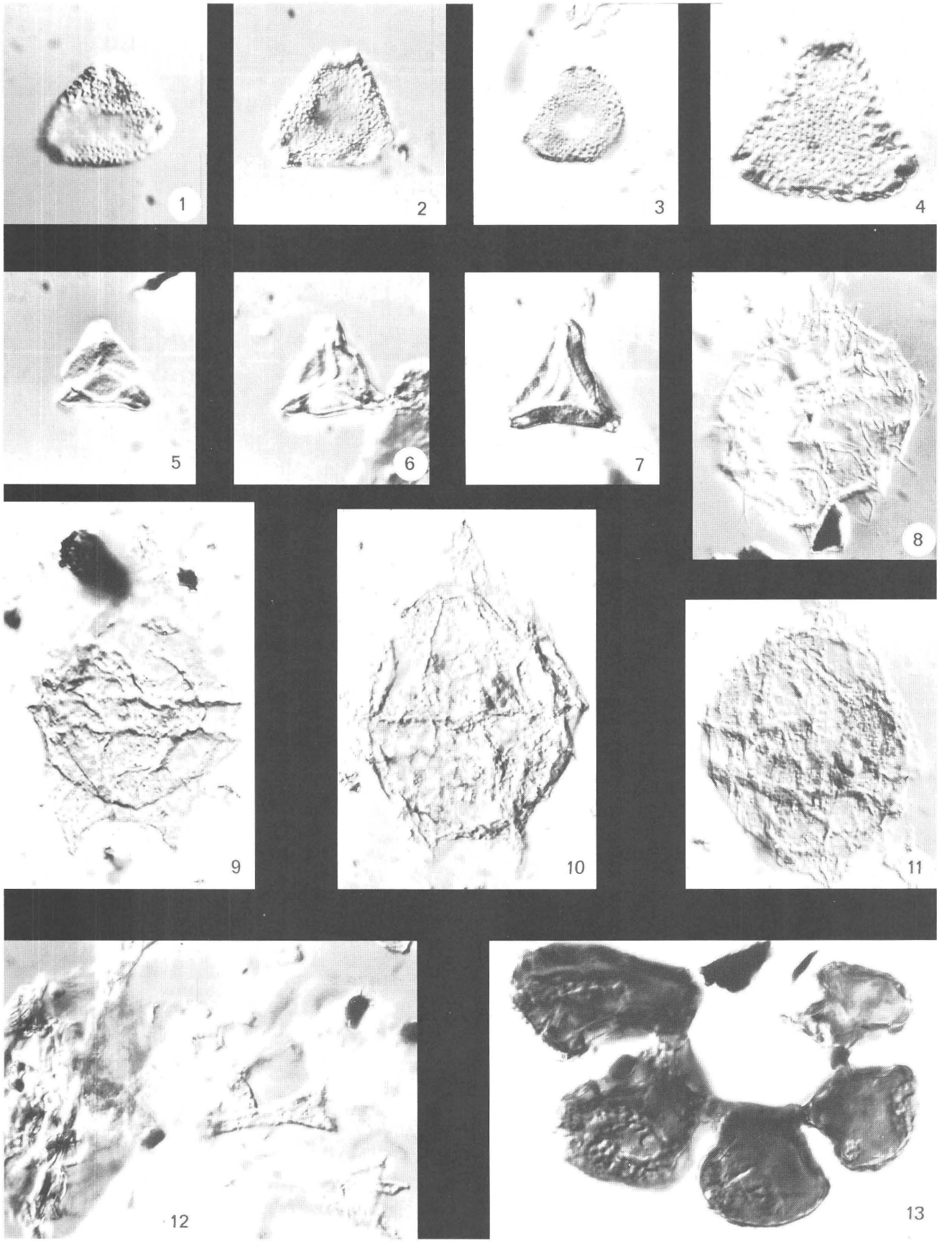

CRETACEOUS ANGIOSPERM POLLEN AND MARINE PALYNOMORPHS FROM THE MARKAGUNT AND NORTHWESTERN KAIPAROWITS PLATEAUS

The Permian Clastic Sedimentary Rocks of Northwestern Arizona

By George H. Billingsley

GEOLOGIC STUDIES IN THE BASIN AND RANGE–COLORADO PLATEAU TRANSITION IN SOUTHEASTERN NEVADA, SOUTHWESTERN UTAH, AND NORTHWESTERN ARIZONA, 1995

U.S. GEOLOGICAL SURVEY BULLETIN 2153–F

UNITED STATES GOVERNMENT PRINTING OFFICE, WASHINGTON : 1997

CONTENTS

PLATES

[Plates are in pocket]

FIGURES

The Permian Clastic Sedimentary Rocks of Northwestern Arizona

By George H. Billingsley

ABSTRACT

The red and white Permian sandstone and siltstone strata in northwestern Arizona, southeastern Nevada, and southwestern Utah overlie carbonate strata of the Pakoon Limestone (Wolfcampian) and underlie carbonate rocks of the Toroweap Formation (Leonardian). In the Gorge of the Virgin River, northwest corner of Arizona, the lower part of the clastic sequence has been called either the Queantoweap Sandstone or the Esplanade Sandstone; the upper part, the Hermit Formation, Hermit Shale, and Coconino(?) Sandstone. When traced northwest into the miogeosyncline of the Basin and Range province of Nevada and Utah, this shelf sequence of the Colorado Plateaus province becomes entirely sandstone, owing to facies and thickness changes. Tracing the clastic sequence south to the Grand Wash Cliffs and Grand Canyon in Arizona has led to a correlation of the lower 140 meters of the strata to the Queantoweap or Esplanade Sandstone, and the upper 300 meters to the Hermit Formation. The Queantoweap is defined as overlying the Pakoon Limestone in western Grand Canyon. Later, the Queantoweap was shown to intertongue with the Pakoon, and the name Esplanade Sandstone was used in the Grand Canyon area. Because this intertonguing is not found in the Gorge of the Virgin River and in southeastern Nevada and southwestern Utah, the name Queantoweap Sandstone should be used for the basal, tan, cliff-forming, high-angle, crossbedded sandstone overlying the Pakoon Limestone. The name Esplanade Sandstone is applied to similar strata along the Grand Wash Cliffs and the Grand Canyon of Arizona where intertonguing does occur.

The thick sequence of red and white, ledge- and slope-forming sandstone and siltstone in the Gorge of the Virgin River overlying the Queantoweap correlates with the Hermit Formation (Shale) in Grand Canyon. This name can be extended to similar Permian strata in southeastern Nevada and northwestern Arizona, but not in southwestern Utah. In southwestern Utah, the entire clastic sequence becomes a white, low-angle, crossbedded sandstone indistinguishable from the Queantoweap Sandstone. All the white, crossbedded sandstone in southwestern Utah should be called the Queantoweap Sandstone (Wolfcampian), with the upper half correlative to the Hermit Formation of Arizona. The Coconino Sandstone does not extend to the Gorge of the Virgin River or into southeastern Nevada and is restricted to northern Arizona.

INTRODUCTION

Detailed mapping during the course of the U.S. Geological Survey BARCO Study Unit in the tri-State area of Nevada, Utah, and Arizona found inconsistencies in correlation of the Permian clastic strata, especially in the Gorge of the Virgin River area. This report attempts to reconcile those inconsistencies with new measured stratigraphic sections of the Permian clastic rocks, together with all available stratigraphic and paleontological references for this tri-State area.

The study area, located in northern Mohave County, northwestern Arizona, covers portions of two physiographic provinces, the Colorado Plateaus and Basin and Range (fig. 1). These two provinces are almost parallel to and between a miogeosyncline in Nevada and the continental shelf area in Arizona. Thus, Paleozoic and Mesozoic strata gradually thicken from southeast to northwest from the Paleozoic continental shelf area of Arizona to the miogeosyncline of Nevada. Numerous facies changes occur within the Permian clastic strata from shelf to basin and are most noticeable at the Gorge of the Virgin River, northwestern Arizona. The Basin and Range strata are locally exposed in folded and faulted terrain (Moore, 1972; Bohannon, 1991; Bohannon and Lucchitta, 1991; Bohannon and others, 1991). Colorado Plateaus strata in northwestern Arizona are exposed as relatively undisturbed bedrock with a regional northeast dip of about 2°–4° (Billingsley, 1993a).

Tertiary and Quaternary erosion has dissected parts of the Colorado Plateaus exposing Paleozoic strata in deep canyons such as the Gorge of the Virgin River and Grand Canyon. Gently dipping to flat-lying Permian strata are exposed along fault scarps of the Hurricane and Grand Wash Cliffs (fig. 1) in northwestern Arizona. These same strata are folded and exposed in the Virgin and Beaver Dam

Mountains and other locations in southeastern Nevada and southwestern Utah. The Permian clastic sequence differs in color, lithology, topographic profile, and thickness in its various exposures in northwestern Arizona, southeastern Nevada, and southwestern Utah because of facies changes over the distances between outcrops. However, the clastic sequence as a whole maintains stratigraphic position between Permian carbonate strata. The facies changes and scarcity of outcrops have caused a nomenclatural dilemma for detailed geologic mapping in the tri-State area. This report suggests descriptive and nomenclatural usage for the Permian clastic sequence in this area.

ACKNOWLEDGMENTS

Special acknowledgment is extended to John D. Hendricks, U.S. Geological Survey, Flagstaff, Ariz., for preparation of illustrations in this report. Acknowledgment is made to the following geologists for their special contribution of geologic data, advice, and careful review of the manuscript: Lehi F. Hintze and J. Keith Rigby, Brigham Young University, Provo, Utah, L. David Nealey, Florian Maldonado, and Lorna Carter, U.S. Geological Survey, Denver, Colo.

PURPOSE AND BACKGROUND

Prior to the 1950's, all Permian redbed strata exposed in this tri-State region were called the Supai Formation, a generalized term proposed by Darton (1910) for Pennsylvanian-Permian redbed exposures at the type section in the vicinity of Supai Village in Havasu (Cataract) Canyon, central Grand Canyon (fig. 1). This was a simple terminology applied to all redbeds in the Grand Canyon between the massive gray Redwall Limestone below and the white Coconino Sandstone above. As shown in figure 2, Noble (1922) redefined the Supai Formation in the Grand Canyon on the basis of erosional breaks within the stratigraphic sequence. Noble introduced the term Hermit Shale for the uppermost slope-forming beds of red shaly siltstone overlying an erosional unconformity, breaking the Hermit out from the original Supai Formation, and retained the term Supai Formation for the lower interbedded sandstone, siltstone, and dolomite sequence above the Redwall Limestone. This division led to uncertainty as to what part of the clastic sequence in Nevada and Utah the Hermit was correlative to because of the lack of an erosional break between the Lower Permian carbonate rocks and the underlying Pennsylvanian Callville Limestone of Longwell (1921). Thus, the term Supai Formation was retained in Nevada and Utah as a general name for all of the red and white sandstone and siltstone strata above the Callville Limestone and upper carbonate strata of Permian age. The term Hermit Shale was restricted to the Grand Canyon area in Arizona.

The first stratigraphic studies and correlations of the Permian sandstones in northwestern Arizona were by McNair (1951). McNair's (1951) nomenclature became the standard usage for the Permian strata in northwestern Arizona and southeastern Nevada, separating Permian strata from the Pennsylvanian Callville Limestone (fig. 2). McNair's work included a measured section at Pakoon Ridge, Ariz., south end of the Virgin Mountains, a section near Hidden Canyon of the Grand Wash Cliffs, Ariz., and a section at Queantoweap Valley (now Whitmore Canyon) in the western Grand Canyon, Ariz. Other measured sections by McNair (1951) were recorded in central Arizona, south of Grand Canyon. McNair proposed the name Queantoweap Sandstone for the Permian red and white, cliff-forming sandstones that formed a topographic platform in the western Grand Canyon area. McNair used the term Hermit Formation for the red, slope-forming siltstone and sandstone overlying the Queantoweap Sandstone; McNair used the term Hermit Formation for what Noble (1922) had called Hermit Shale. McNair also described and proposed the name Pakoon Limestone for the Permian gray, cliff-forming limestone underlying the Queantoweap Sandstone, which firmly established a Permian age for the Queantoweap. However, McNair did not recognize or show the intertonguing relationship between the Queantoweap and Pakoon.

During the 1970's, E.D. McKee conducted a detailed stratigraphic study of the Supai Formation below the Hermit Shale in Grand Canyon and proposed new nomenclature for the Supai Formation based on fossils, lithology, and widespread correlative unconformities. As shown in figure 2, the Supai Formation was raised in rank to the Supai Group and subdivided into four formations, in ascending order, the Pennsylvanian Watahomigi, Manakacha, and Wescogame Formations, and the Permian Esplanade Sandstone (McKee, 1975). By the late 1960's, Queantoweap Canyon was known as Whitmore Canyon on U.S. Geological Survey topographic maps (U.S. Geological Survey, 1967). McKee (1982) demonstrated through several measured sections in western Grand Canyon that the Pakoon Limestone described by McNair (1951) intertongues with the lower half of the Esplanade Sandstone from the Grand Wash Cliffs east to about Whitmore Canyon, Ariz. McNair defined the Queantoweap as overlying the Pakoon Limestone, which it does in the Basin and Range province, but not in Grand Canyon. McKee (1975) raised the Esplanade Sandstone member of the Supai Formation of White (1929) to formation rank in Grand Canyon. The name Esplanade Sandstone is from the Esplanade Platform, a prominent bench originally described by Noble (1914) in the central Grand Canyon area near the type section at Havasupai Village (fig. 1). McKee (1982) stated that the Pakoon Limestone intertongues with the lower Esplanade Sandstone, making the lower part of the Esplanade Sandstone equivalent to the Pakoon Limestone, but kept the Pakoon Limestone as a separate unit within the Esplanade Sandstone (fig. 3). Confusion resulted because

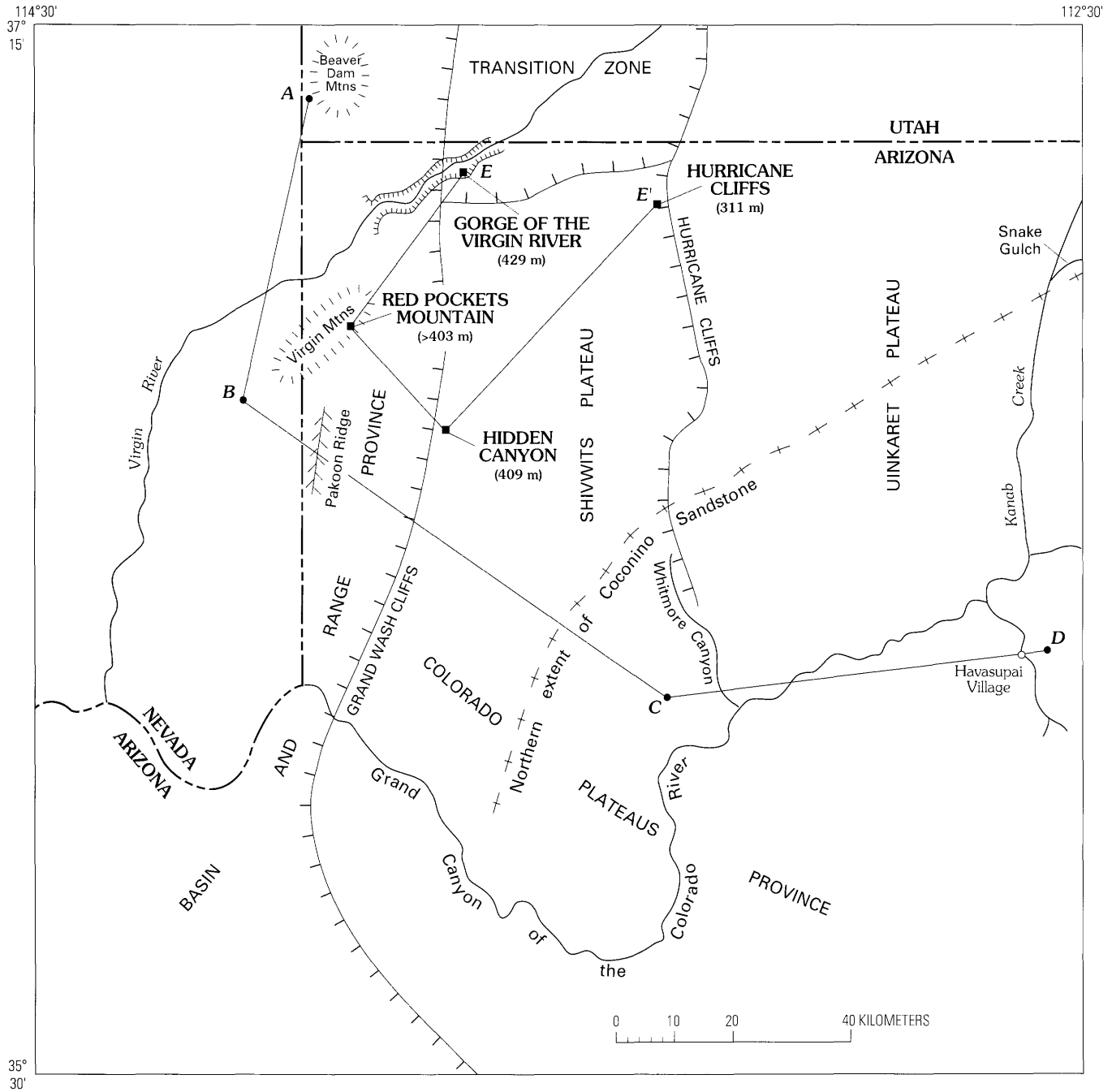

Figure 1. Index map of northwestern Arizona showing geographic and measured section locations (total thicknesses of clastic rocks from sections 1–8). The Grand Wash Cliffs form the boundary between the Colorado Plateaus and Basin and Range physiographic provinces (Peirce, 1984, 1985). *ABCD* shows location of schematic cross section in figure 3. *E-E'* shows location of stratigraphic profiles on plates 1 and 2.

McKee continued to use the term Hermit Shale in western Grand Canyon, even though the term Hermit Formation (McNair, 1951) was well established in the literature and was being used throughout Grand Canyon. The term Hermit Formation is used by present workers in northwestern Arizona and in this report because it refers to two distinct lithologies, sandstone and siltstone.

GORGE OF THE VIRGIN RIVER

During the 1980's, geologic interest in the Gorge of the Virgin River drew considerable attention because it contains the best and most complete exposure of Permian strata in the tri-State region. When Interstate 15 was completed through the gorge in the early 1970's, easy access was made available to numerous geologists.

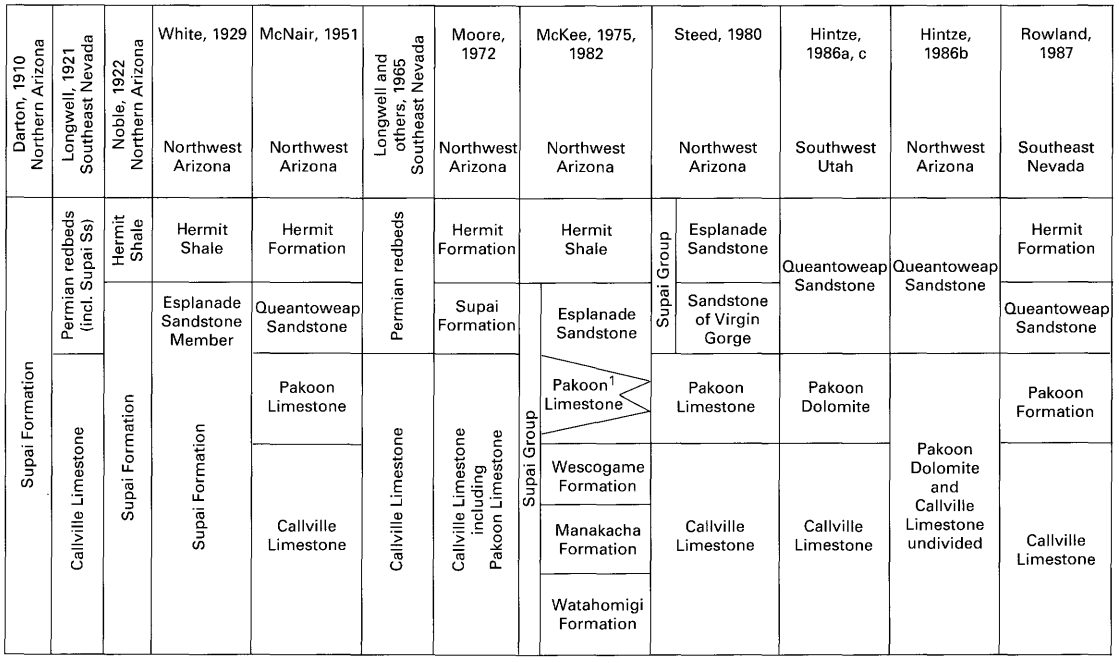

Figure 2 (above and facing page). Nomenclature applied to the Permian clastic strata in northwestern Arizona, southwestern Utah, and southeastern Nevada.

McNair's (1951) Permian nomenclature was used by Hintze (1986a, b, c), Langenheim and Schulmeister (1987), and Rice and Loope (1991) in the Gorge of the Virgin River, and by Rowland (1987) in the Virgin Mountains and other locations of southeastern Nevada (fig. 2). Geologic maps by Bohannon (1991), Bohannon and Lucchitta (1991), Bohannon and others (1991), and Bohannon (1992) use McKee's Permian nomenclature in the Virgin Mountains and Gorge of the Virgin River. A thesis by Steed (1980) also uses McKee's nomenclature in the Gorge of the Virgin River (fig. 2). The Permian correlation from Grand Canyon to the gorge is based on similarity of lithology and stratigraphic position of outcrops along the Grand Wash Cliffs and the Grand Canyon. McNair (1951) mentioned that tracing the Queantoweap northward from Whitmore Canyon in Grand Canyon showed that Queantoweap should be used to name the lower part of the rocks that previously had been called Supai Formation.

As stated by Hintze (1986a), the Beaver Dam Mountains in southwestern Utah and the north rim of the Gorge of the Virgin River (south end of Beaver Dam Mountains) form a no-man's land in relation to rock unit terminology established in Utah, Arizona, and Nevada. Longwell and others (1965) stated that they could not with any confidence correlate the entire red-tinged shale and sandstone sequence in southeastern Nevada and place it into an accurate time frame (or appropriate stage, series), based on comparing its stratigraphic relationships with those of similar appearing units in the distant Colorado Plateaus and using physical evidence only. Because of these uncertainties, Longwell and others (1965) designated the entire redbed sandstone/siltstone sequence as the Permian redbeds. Moore (1972) preferred the usage of broader terms such as Callville Limestone (Moore extended the Callville to include the Pakoon Limestone because the two units could not be distinguished from each other), Supai Formation, and Hermit Formation for all clastic deposits between the Callville and overlying Permian carbonate rocks (fig. 2).

Steed (1980), in his mapping, extended McKee's (1975) Grand Canyon nomenclature to the Gorge of the Virgin River but continued to use the term Supai Group for all the red sandstone and siltstone beds in the Gorge of the Virgin River (fig. 2). Steed introduced the name sandstone of Virgin Gorge for the lower crossbedded sandstone above the Pakoon Limestone. Langenheim and Schulmeister (1987) followed Steed's lead for nomenclature in the Gorge of the Virgin River.

Hintze (1986b) chose to follow McNair's terminology, lumping all 400 m of tan, red, and white sandstone and siltstone in the Gorge of the Virgin River into the Queantoweap Sandstone and, like Steed (1980), did not use the term Hermit Formation. Just north of the Gorge of the Virgin River, the entire clastic sequence becomes a yellow sandstone (Hintze, 1986a).

Nielson (1986) supported the idea that the Hermit Formation and the Coconino Sandstone came to a depositional edge between Grand Canyon and the Gorge of the Virgin River. Like Hintze (1986b), Nielson chose the name Queantoweap Sandstone for all the sandstone/siltstone beds below the Toroweap Formation because his measured

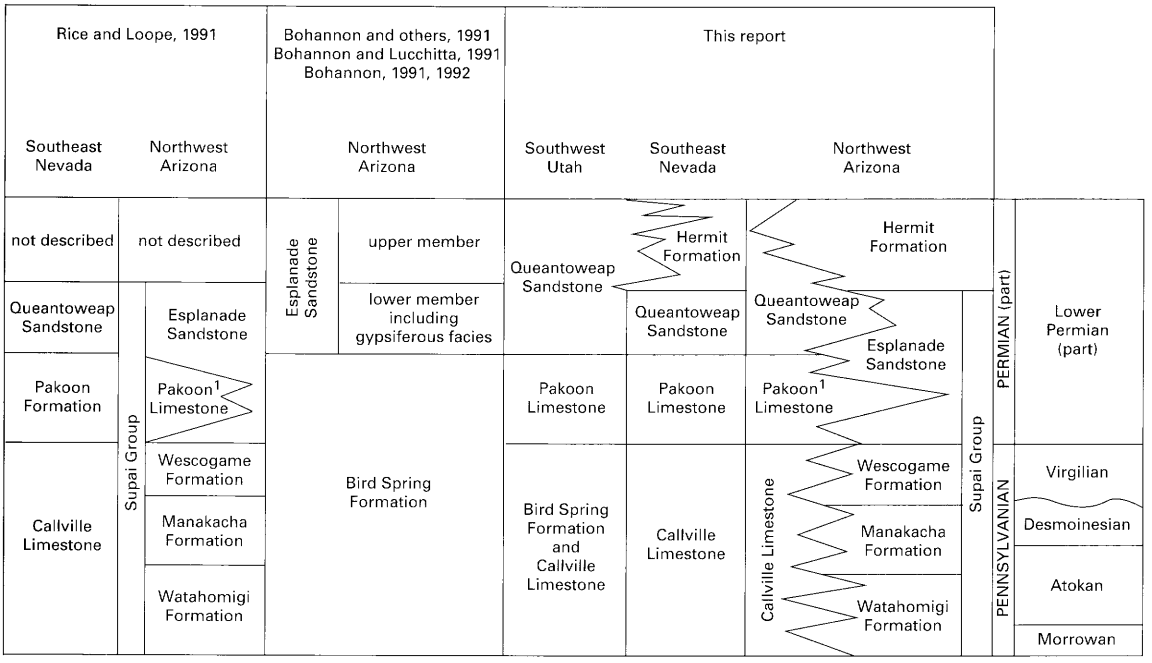

sections were mostly in Utah where the Queantoweap is not readily subdivided.

Bohannon and others (1991) chose the term Esplanade Sandstone for the entire red and white sandstone sequence in the Gorge of the Virgin River and the Virgin Mountains. Bohannon and others (1991) subdivided the Esplanade Sandstone into upper and lower members, the lower member including a gypsiferous facies. Their upper member comprised a red, light-buff, and white nonmarine, slope- and cliff-forming sandstone about 280 m thick; the lower member comprised a light-buff and white, nonmarine, cliff-forming sandstone about 100 m thick. The gypsiferous facies of the lower member, a red-brown, red, gray-brown, and yellow-brown gypsiferous sandstone ranging from a featheredge to about 100 m thick, crops out in the northwest rim area of the Gorge of the Virgin River. Bohannon (1991), Bohannon and others (1991), Bohannon and Lucchitta (1991), and Bohannon (1992) also mapped a highly crossbedded sandstone at the base of the Seligman Member of the Toroweap Formation as the Coconino Sandstone.

THE PERMIAN CLASTIC NOMENCLATURE OF GRAND CANYON

The current nomenclature for the Permian sandstone and siltstone sequence in the western Grand Canyon area is, in ascending order, the Esplanade Sandstone of the Supai Group, which includes the Pakoon Limestone as a separate unit (McKee, 1975, 1982); the Hermit Shale (Noble, 1922; White, 1929) or the Hermit Formation (McNair, 1951); and the Coconino Sandstone (Darton, 1910, studied by McKee, 1934). The Esplanade in its lower part is intertongued with the Pakoon Limestone of McNair (1951). Permian strata that overlie the Grand Canyon clastic sequence are largely marine carbonates and evaporite deposits of the Toroweap and Kaibab Formations (Sorauf and Billingsley, 1991). The Toroweap and Kaibab nomenclature is used throughout the tri-State area of Nevada, Utah, and Arizona. Underlying the Permian siltstone and sandstone sequence in southeastern Nevada, southwestern Utah, and Virgin Mountains and Gorge of the Virgin River of northwestern Arizona are carbonate rocks of the Callville Formation; in other areas of northwestern Arizona (Grand Wash Cliffs), these clastic strata are underlain by Pennsylvanian clastic and carbonate strata of the lower Supai Group.

The Queantoweap Sandstone at Whitmore Canyon, as defined by McNair (1951), is 120 m thick. Thickness of the Esplanade Sandstone at Whitmore Canyon, as defined by McKee (1982), is 111 m. The thickness of the Queantoweap Sandstone near Hidden Canyon, Grand Wash Cliffs, is 197 m as measured by McNair (1951), while the Esplanade Sandstone at the same locality is 174 m as measured by McKee (1982). Thickness of the Esplanade Sandstone at Hidden Canyon measured by the author (section 4) is 158 m. Sections 3 and 4 were measured at the same location as McKee because the author helped McKee measure and describe the Hidden Canyon section in 1967. The discrepancy in thicknesses of measured sections can be attributed to several factors such as technique, method of measuring, slight difference in stratigraphic dip, and weather conditions. But the most significant difference is in placement of the boundary between the Hermit Formation (Shale) and the Esplanade Sandstone.

Erosional channels of considerable depth were cut into the Esplanade Sandstone in many areas of the central and eastern Grand Canyon region. The erosional surface was buried by deposits of the Hermit Formation. However, in the western Grand Canyon and other areas west and north of Arizona, little evidence of an erosional break can be found between the Hermit Formation and the Queantoweap (Esplanade) Sandstone. McKee (1982) interpreted the lack of an erosional surface as the result of a continuous sinking basin north and west of western Grand Canyon with no recognizable interruption in the accumulation of sediment between the Esplanade Sandstone and the Hermit Formation. McKee and McNair both recognized the presence of the Hermit Formation in western Grand Canyon and along the Grand Wash Cliffs separated by an arbitrary boundary from the Esplanade (Queantoweap).

Billingsley and others (1986) suggested that the elusive unconformity does not exist and agreed with McKee's interpretation of continuous deposition. Billingsley and others (1986) estimated the thickness for the Hermit Formation to be 365 m along the Grand Wash Cliffs south of Hidden Canyon. A measured thickness of 251 m was obtained for the Hermit Formation at Hidden Canyon (section 3; pl. 1). At all measured sections of this report, the boundary between the Esplanade (Queantoweap) Sandstone and Hermit Formation is arbitrarily selected on the basis of lithology, color, and cliff/slope profile. A subdued erosional unconformity is probable along the Hurricane and Grand Wash Cliffs (sections 1–4; pls. 1, 2).

NOMENCLATURE FOR THE PERMIAN CLASTIC SEDIMENTARY ROCKS OF NORTHWESTERN ARIZONA, SOUTHEASTERN NEVADA, AND SOUTHWESTERN UTAH

The Permian clastic sedimentary rocks of this tri-State region maintain a general overall color, lithology, thickness, and topographic profile for a considerable distance from the Grand Canyon shelf area (fig. 3). The Permian nomenclature used by McNair (1951) and McKee (1975, 1982) is used in the Virgin Mountains, Beaver Dam Mountains, Gorge of the Virgin River, and the Grand Wash and Hurricane Cliffs based on recent geologic mapping by Huntoon and others (1981, 1982); Wenrich and others (1986, 1987); Hintze (1986b, c); Billingsley and others (1986); Bohannon (1991); Bohannon and Lucchitta (1991); Bohannon and others (1991); Bohannon (1992); and Billingsley (1990a, b, 1991, 1992a, b, c, 1993a, b, 1994).

Based on the measured stratigraphic sections presented herein and profiled on plates 1 and 2, and on recent geologic mapping just mentioned, the name Queantoweap Sandstone should be retained and restricted to the lower, tan, crossbedded, cliff-forming sandstone that overlies Permian carbonate strata of the Pakoon Limestone (fig. 3; pl. 2). The Queantoweap is found in the Virgin Mountains, Beaver Dam Mountains, and Gorge of the Virgin River areas of southeastern Nevada, southwestern Utah, and northwestern Arizona. The Queantoweap Sandstone includes all clastic and evaporite sedimentary rocks between the Pakoon Limestone or Bird Spring Formation, and the Toroweap Formation in the Beaver Dam Mountains of southwestern Utah. Note particularly that the upper part of the Queantoweap Sandstone in the Beaver Dam Mountains area is stratigraphically equivalent to the Hermit Formation in the Gorge of the Virgin River and elsewhere in northwestern Arizona and southeastern Nevada (fig. 3).

The name Esplanade Sandstone is restricted to the Grand Canyon region, including the Grand Wash and Hurricane Cliffs vicinity of the Colorado Plateaus province of northwestern Arizona, because the Esplanade Sandstone and Pakoon Limestone intertongue along the western margin of the Colorado Plateaus, but are separate rock units (fig. 3). The term Esplanade Sandstone should not be used in the Gorge of the Virgin River because of the lack of evidence for intertonguing with the Pakoon Limestone.

The red and white, slope-forming sandstone and siltstone sequence above the cliff-forming Queantoweap or Esplanade Sandstone in northwestern Arizona and southeastern Nevada is correlative to the Hermit Formation of Grand Canyon on the basis of stratigraphic position, some plant fossils, crossbedding, color, and slope profile. An arbitrary boundary is located at or near the topographic change between the cliff of tan Queantoweap or Esplanade Sandstone and the reddish slope of the Hermit Formation.

Within a short distance northwest of the Gorge of the Virgin River, facies changes alter the characteristics of the Hermit Formation within the Gorge of the Virgin River to those of the Queantoweap Sandstone (Hintze, 1986a). The name Hermit Formation cannot with certainty be extended into the Beaver Dam Mountains of southwestern Utah because of a distinctive lack of stratigraphic characteristics and mappable boundaries (fig. 3). Hintze (1986a, b, c) used the name Queantoweap Sandstone in the Beaver Dam Mountains to include all the sandstone beds between the carbonate rocks of his Pakoon Dolomite and Toroweap Formation because the sandstone beds cannot be subdivided on any practical basis. Hintze estimated the Queantoweap Sandstone in the Beaver Dam Mountains to be from 460 to 610 m thick.

The tan, high-angle, crossbedded Coconino Sandstone reported by Steed (1980), Langenheim and Schulmeister (1987), Bohannon and Lucchitta (1991), Bohannon and others (1991), and Bohannon (1992) in the Gorge of the Virgin River and Virgin Mountains is a local crossbedded sandstone within the basal Seligman Member of the Toroweap Formation. This sandstone, at first glance, appears to have the characteristics and stratigraphic position of the Coconino Sandstone. However, close inspection of this sandstone at

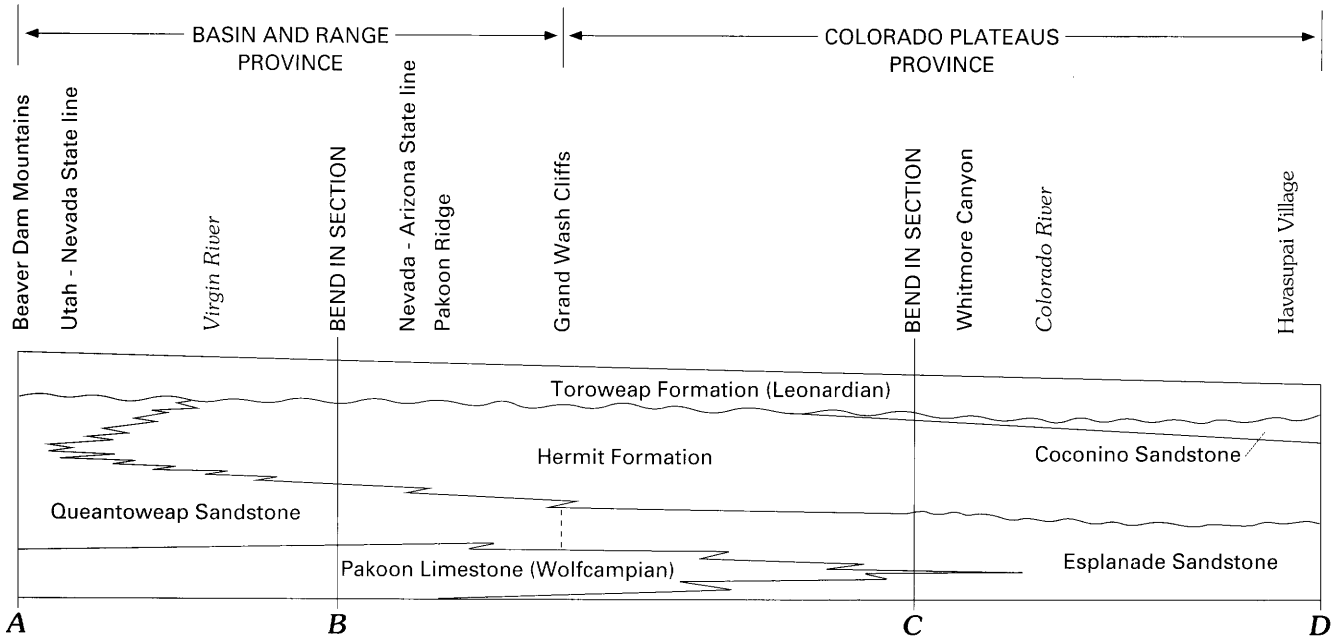

	Gorge of the Virgin River	Red Pockets Mountain	Hidden Canyon	Hurricane Cliffs
Hermit	305	270+	251	137
Esplanade			158	174
Queantoweap	124	133+		
Total	**429**	**403+**	**409**	**311**

Thicknesses (in meters) from sections 1–8

Figure 3. Schematic cross section (*A–D* of fig. 1) showing correlations of Permian clastic rock units from southwestern Utah, through southeastern Nevada, and northwestern Arizona. Thicknesses are relative and approximate. Vertical dashed line, approximate area of nomenclature change for Queantoweap and Esplanade Sandstones.

Hidden Canyon, Gorge of the Virgin River, and Red Pockets Mountain (sections 3, 5, and 7), shows that a sharp unconformable contact is present within the lower sandstone beds of the Seligman Member (Billingsley, 1994). The high-angle, crossbedded sandstone locally pinches out or intertongues laterally into flat sandstone beds within the lower part of the Seligman Member and will form an unconformable contact with the underlying sandstone of the Hermit Formation. The highly crossbedded sandstone locally grades upward into flat-bedded sandstone and gypsum deposits of the basal Seligman Member of the Toroweap Formation. At Red Pockets Mountain (section 5), the crossbedded sandstone is several meters thick, forming an imposing cliff similar to that of the Coconino Sandstone. This sandstone also forms a sharp unconformable contact with the Hermit Formation at some locations in the Gorge of the Virgin River and along parts of the Grand Wash Cliffs (pl. 1).

The highly crossbedded sandstone in the basal Toroweap is mostly absent in the Hurricane Cliffs and locally lenses in and out in the Gorge of the Virgin River. It is nearly a continuous brown sandstone bed in the Hidden Canyon area, and thickens westward to the Red Pockets Mountain area of the Virgin Mountains (pl. 1). The highly crossbedded sandstone is also prominent in the Whitney Ridge area of the southern Virgin Mountains (L. Sue Beard, U.S. Geological Survey, oral commun., 1992).

The Coconino Sandstone is nearly 180 m thick in eastern Grand Canyon but thins to less than 30 m at Whitmore Canyon in the western Grand Canyon (Huntoon and others, 1981; Wenrich and others, 1986). The Coconino pinches out west of Whitmore Canyon in the Green Spring and Twin Spring Canyon areas of the Shivwits Plateau, and thins northward under the Shivwits and Uinkaret Plateaus near Mt. Trumbull (Huntoon and others, 1981, 1982; Wenrich and others, 1987). The Coconino does not extend north of the upper reaches of Whitmore Canyon area along the Hurricane Cliffs (Billingsley, 1993b). The Coconino also does not extend north of Snake Gulch (fig. 1), a tributary of Kanab Canyon (Billingsley, 1992c), and thins to less than 9 m in upper Marble Canyon (Beus and Billingsley, 1989). Therefore, where the Coconino is absent, the contact between the Hermit and Toroweap Formations is expressed as a sharp erosional unconformity (fig. 3) with relief up to 1 m or more in northwestern Arizona. The uppermost Hermit Formation

is a pale-red, flat-bedded sandstone in the western Grand Canyon area, changing to a yellowish-white, low-angle crossbedded sandstone along the Hurricane Cliffs, Grand Wash Cliffs, and Gorge of the Virgin River (pl. 1).

In central and eastern Grand Canyon, the erosional contact between the Coconino Sandstone and Hermit Formation is a sharp, flat, lithologic disconformity (fig. 3). Deep desiccation cracks in the Hermit are filled with Coconino Sandstone, a feature not seen where the Coconino is absent in northwestern Arizona and southeastern Nevada.

REFERENCES CITED

Beus, S.S., and Billingsley, G.H., 1989, Paleozoic strata of the Grand Canyon, Arizona, *in* Elston, D.P., Billingsley, G.H., and Young, R.A., eds., Geology of the Grand Canyon, northern Arizona (with Colorado River guides), 28th International Geological Congress Field Trip Guidebook T115/315, Lees Ferry to Pierce Ferry, Arizona: American Geophysical Union, p. 122–127.

Billingsley, G.H., 1990a, Geologic map of the Purgatory Canyon quadrangle, northern Mohave County, Arizona: U.S. Geological Survey Open-File Report 90-540, scale 1:24,000.

———1990b, Geologic map of the Lizard Point quadrangle, northern Mohave County, Arizona: U.S. Geological Survey Open-File Report 90-643, scale 1:24,000.

———1991, Geologic map of the St. George Canyon quadrangle, northern Mohave County, Arizona: U.S. Geological Survey Open-File Report 91-561, scale 1:24,000.

———1992a, Geologic map of the Gyp Pocket quadrangle, northern Mohave County, Arizona: U.S. Geological Survey Open-File Report 92-412, scale 1:24,000, includes pamphlet, 17 p.

———1992b, Geologic map of the Rock Canyon quadrangle, northern Mohave County, Arizona: U.S. Geological Survey Open-File Report 92-449, scale 1:24,000, includes pamphlet, 17 p.

———1992c, Geologic map of the Jumpup Canyon and Big Springs quadrangles, Mohave and Coconino Counties, Arizona: U.S. Geological Survey Miscellaneous Investigations Series Map I-2290, scale 1:62,500.

———1993a, Geologic map of Wolf Hole Mountain and vicinity, Mohave County, northwestern Arizona: U.S. Geological Survey Miscellaneous Investigations Series Map I–2296, scale 1:31,680.

———1993b, Geologic map of the Russell Spring quadrangle, northern Mohave County, Arizona: U.S. Geological Survey Open-File Report 93-717, scale 1:24,000, includes pamphlet, 17 p.

———1994, Geologic map of the Sullivan Draw and vicinity, Mohave County, northwestern Arizona: U.S. Geological Survey Miscellaneous Investigations Series Map I–2396, scale 1:31,680.

Billingsley, G.H., Antweiler, J.C., Beard, L.S., and Lucchitta, Ivo, 1986, Mineral resource potential map of the Pigeon Canyon, Nevershine Mesa, and Snap Point wilderness study areas, Mohave County, Arizona: U.S. Geological Survey Miscellaneous Field Studies Map MF–1860–A, scale 1:50,000, 10 p.

Bohannon, R.G., 1991, Geologic map of the Jacobs Well and southern part of the Elbow Canyon quadrangles, Mohave County, Arizona: U.S. Geological Survey Miscellaneous Investigations Series Map I–2167, scale 1:24,000.

———1992, Geologic map of the Red Pockets Quadrangle, Mohave County, Arizona: U.S. Geological Survey Miscellaneous Investigations Series Map I–2288, scale 1:24,000.

Bohannon, R.G., and Lucchitta, Ivo, 1991, Geologic map of the Mount Bangs quadrangle, Mohave County, Arizona: U.S. Geological Survey Miscellaneous Investigations Series Map I–2166, scale 1:24,000.

Bohannon, R.G., Lucchitta, Ivo, and Anderson, R.E., 1991, Geologic map of the Mountain Sheep Spring quadrangle, Mohave County, Arizona: U.S. Geological Survey Miscellaneous Investigations Series Map I–2165, scale 1:24,000.

Darton, N.H., 1910, A reconnaissance of part of northwestern New Mexico and northern Arizona: U.S. Geological Survey Bulletin 435, 88 p.

Hintze, L.F., 1980, Geologic map of Utah: Utah Geological and Mineral Survey, Salt Lake City, Utah, scale 1:500,000.

———1986a, Stratigraphy and structure of the Beaver Dam Mountains, southwestern Utah, *in* Griffen, D.T., and Phillips, W.R., eds., Thrusting and extensional structures and mineralization in the Beaver Dam Mountains, southwestern Utah: Annual Field Conference guidebook of the Utah Geological Association, Publication 15, p. 1–36.

———1986b, Geology of the Mountain Sheep Spring Quadrangle, Arizona, *in* Griffen, D.T., and Phillips, W.R., eds., Thrusting and extensional structures and mineralization in the Beaver Dam Mountains, southwestern Utah: Annual Field Conference guidebook of the Utah Geological Association, Publication 15, plate 1.

———1986c, Geologic map of the Beaver Dam Mountains, Washington County, Utah, *in* Griffen, D.T., and Phillips, W.R., eds., Thrusting and extensional structures and mineralization in the Beaver Dam Mountains, southwestern Utah: Annual Field Conference guidebook of the Utah Geological Association, Publication 15, plate 2.

Huntoon, P.W., Billingsley, G.H., and Clark, M.D., 1981, Geologic map of the Hurricane Fault and vicinity, western Grand Canyon, Arizona: Grand Canyon, Ariz., Grand Canyon Natural History Association, scale 1:48,000.

———1982, Geologic map of the Lower Granite Gorge and vicinity, western Grand Canyon, Arizona: Grand Canyon, Ariz., Grand Canyon Natural History Association, scale 1:48,000.

Langenheim, R.L., Jr., and Schulmeister, M.K., 1987, Virgin River Gorge; boundary between the Colorado Plateau and the Great Basin in northwestern Arizona, *in* Hill, M.L., ed., Cordilleran Section of the Geological Society of America Centennial Field Guide, v. 1: p. 43–48.

Longwell, C.R., 1921, Geology of the Muddy Mountains, Nevada, with a section to the Grand Wash Cliffs in western Arizona: American Journal of Science, 5th Ser., v. 1, no. 1, p. 39–62.

Longwell, C.R., Pampeyan, E.H., Bowyer, Ben, and Roberts, R.J., 1965, Geology and mineral deposits of Clark County, Nevada: Nevada Bureau of Mines and Geology Bulletin 62, Mackay School of Mines, University of Nevada/Reno and the U.S. Geological Survey, 218 p.

McKee, E.D., 1934, The Coconino Sandstone—Its history and origin: Carnegie Institution of Washington Publication 440, p. 77–115.

———1975, The Supai Group—Subdivision and nomenclature: U.S. Geological Survey Bulletin 1395-J, p. 1–11.

———1982, The Supai Group of Grand Canyon: U.S. Geological Survey Professional Paper 1173, 503 p.

McNair, A.H., 1951, Paleozoic stratigraphy of part of northwestern Arizona: American Association of Petroleum Geologists Bulletin, v. 35, no. 3, p. 503–541.

Moore, R.T., 1972, Geology of the Virgin and Beaver Dam Mountains, Arizona: Arizona Bureau of Mines Bulletin 186; Tucson, Ariz., University of Arizona, 66 p.

Nielson, R.L., 1986, The Toroweap and Kaibab Formations, southwestern Utah, *in* Griffen, D.T., and Phillips, W.R., eds., Thrusting and extensional structures and mineralization in the Beaver Dam Mountains, southwestern Utah: Annual Field Conference guidebook of the Utah Geological Association, Publication 15, p. 37–54.

Noble, L.F., 1914, The Shinumo Quadrangle, Grand Canyon District, Arizona: U.S. Geological Survey Bulletin 549, 100 p.

———1922, A section of the Paleozoic formations of the Grand Canyon at Bass Trail: U.S. Geological Survey Professional Paper 131–B, p. 23–73.

Peirce, H.W., 1984, The Mogollon Escarpment: Arizona Bureau of Geology and Mineral Technology, Fieldnotes, v. 14, no. 2, p. 8–11.

———1985, Arizona's backbone—The transition zone, Phoenix, Arizona: Arizona Bureau of Geology and Mineral Technology, Fieldnotes, v. 15, no. 3, p. 1–6.

Reynolds, S.J., 1988, Geologic map of Arizona: Arizona Geological Survey, Map 26, scale 1:1,000,000.

Rice, J.A., and Loope, D.B., 1991, Wind-reworked carbonates, Perm-Pennsylvanian of Arizona and Nevada: Geological Society of America Bulletin, v. 103, no. 2, p. 254–267.

Rowland, S.M., 1987, Paleozoic stratigraphy of Frenchman Mountain, Clark County, Nevada, *in* Hill, Mason, ed., Geological Society of America Centennial Field Guide—Cordilleran Section: p. 53–56.

Sorauf, J.E., and Billingsley, G.H., 1991, Members of the Toroweap and Kaibab Formations, Lower Permian, northern Arizona and southwest Utah: Rocky Mountain Geologist, v. 28, no. 1, p. 9–24.

Steed, D.A., 1980, Geology of the Virgin River Gorge, northwest Arizona: Brigham Young University Geology Studies, v. 27, pt. 3, p. 96–115.

Stewart, J.H., and Carlson, J.E., 1978, Geologic map of Nevada: Prepared by the U.S. Geological Survey in cooperation with the Nevada Bureau of Mines and Geology, scale 1:500,000.

U.S. Geological Survey, 1967, Topographic map of the Whitmore Rapids quadrangle, Arizona, 7.5 minute series, scale 1:24,000.

Wenrich, K.J., Billingsley, G.H., and Huntoon, P.W., 1986, Breccia pipe and geologic map of the northeastern Hualapai Indian Reservation and vicinity, Arizona: U.S. Geological Survey Open-File Report 86-458-A, scale 1:48,000, includes pamphlet, 29 p.

———1987, Breccia pipe and geologic map of the northwestern Hualapai Indian Reservation and vicinity, Arizona: U.S. Geological Survey Open-File Report 86–458–C, scale 1:48,000, includes pamphlet, 32 p.

White, David, 1929, Flora of the Hermit Shale, Grand Canyon, Arizona: Carnegie Institution of Washington Publication 405, 221 p.

Wilson, E.D., Moore, R.T., and Cooper, J.R., 1969, Geologic map of the State of Arizona: Arizona Bureau of Mines, University of Arizona, scale 1:500,000.

APPENDIX. MEASURED SECTIONS OF PERMIAN CLASTIC SEDIMENTARY ROCKS OF NORTHWESTERN ARIZONA

Section 1. The Hermit Formation at Hurricane Cliffs, northern Mohave County, northwestern Arizona

Section measured just east of Black Rock Canyon Well, Hurricane Wash, Rock Canyon 7.5-minute quadrangle, Arizona, 1979 (east-central sec. 34, T. 41 N., R. 10 W.; location, fig. 1). Correction for stratigraphic dip 6°–7° east (95° azimuth).

[*Section measured by George Billingsley and Kelly Smith, October 26, 1991*]

Thickness (meters)

Seligman Member of the Toroweap Formation (incomplete, only lowermost bed measured):

10. Gypsiferous sandstone: Calcareous, yellowish-white (weathers tan), very fine grained, thick-bedded. Includes low-angle crossbeds and gypsum and calcite cement. Unconformity truncates underlying white and red, flat-bedded sandstone and siltstone with less than 1 m relief. Forms cliff. Above unit 10 is slope and ledge sequence of alternating thick-bedded gypsiferous siltstone, sandstone, and gypsum 1.8

Unconformity.
Sharp, planar, erosional contact between gray, low-angle, crossbedded sandstone of Seligman Member of Toroweap Formation and white, flat-bedded sandstone and siltstone of Hermit Formation.

Hermit Formation:

9. Sandstone and siltstone: White and light-red sandstone ledges separated by recesses of red siltstone. Sandstone is fine grained, medium bedded 0.3–1.2 m thick. Siltstone is thin bedded, friable. Forms ledgy slope 9.7
8. Siltstone and sandstone: Red and white, very fine grained to medium-grained, thin- to thick-bedded, siltstone beds 0.3–4.6 m thick, sandstone beds 1–1.8 m thick. Sandstone and siltstone beds are bleached yellowish-orange along numerous fractures and bedding planes. Forms slope with ledges 64.0
7. Sandstone: Red and white, fine-grained, thick-bedded, flat-bedded. Forms cliff 11.4
6. Sandstone and siltstone: Red, fine-grained, medium to thick beds as much as 4 m thick, interbedded with red siltstone beds as much as 2 m thick. Includes white sandstone beds. Siltstone beds contain horizontal burrows on bedding planes in lower part. Forms ledgy slope 38.6
5. Sandstone: White, fine-grained, massive bed, thins and thickens in horizontal distance. Forms cliff 1.5
4. Siltstone: Red, very fine grained, thick-bedded. Bleached yellow to orange-yellow in near-vertical fractures and in bedding planes. Forms slope 6.5
3. Sandstone: White, fine-grained, thick-bedded. Forms ledge 2.1

Thickness (meters)

Hermit Formation—Continued

2. Siltstone: Red, thick-bedded to massive. Small irregular contact with underlying white sandstone that thickens and thins in lateral distance. First red siltstone bed at base of Hermit Formation slope 3.5

Total thickness of Hermit Formation 137.3

Unconformity.
Gradational and erosional contact between red siltstone slope of Hermit Formation and white sandstone cliff of Esplanade Sandstone. Shallow depressions with less than 2 m of relief at contact.

Esplanade Sandstone (incomplete, only topmost unit measured):

1. Sandstone and siltstone: White, fine-grained, medium bedded 0.6–3.0 m thick. Sandstone interbedded with red, thick-bedded siltstone. Forms ledgy slope 16.1

Section 2. The Esplanade Sandstone at Hurricane Cliffs, northern Mohave County, northwestern Arizona

Section measured just east of Black Rock Canyon Well, Hurricane Wash, Rock Canyon 7.5-minute quadrangle, Arizona, 1979 (east-central sec. 34, T. 41 N., R. 10 W.; location, fig. 1). Correction for stratigraphic dip is 7° east (95° azimuth).

[*Section measured by George Billingsley and Kelly Smith, October 26, 1991*]

Thickness (meters)

Hermit Formation (incomplete, only lowermost unit measured, continued from Section 1):

16. Siltstone: Red, thick-bedded to massive. Small irregular contact with underlying white sandstone, thickens and thins in lateral distance. First red siltstone bed at base of Hermit Formation slope. Forms slope 3.5

Unconformity.
Gradational and erosional contact between red siltstone slope of Hermit Formation and white sandstone cliff of Esplanade Sandstone. Shallow depressions with less than 2 m relief at contact.

Esplanade Sandstone:

15. Sandstone and siltstone: White, fine-grained, medium-bedded 0.6–3.0 m thick. Includes interbedded red, thick-bedded siltstone. Forms ledgy slope 16.1
14. Sandstone: White (weathers light brown or tan), fine-grained, massive beds 0.6–1.5 m thick. Interbedded with gray or pale-yellow siltstone. Forms ledges in slope 10.3
13. Sandstone: White (weathers tan). Includes several horizontal burrows on bedding planes in lower part. Burrows as much as 1.3 cm in diameter. Forms cliff 9.7
12. Siltstone: Calcareous, light-gray to yellow, thin-bedded, fetid on fresh break. Includes red siltstone beds in lower part. Forms recess in cliff 3.0
11. Sandstone: Slightly calcareous, white (weathers white or tan), fine-grained. Includes limonite stains on quartz grains and large-scale, low-angle, planar crossbeds 1–4 m thick. Forms cliff 13.5
10. Siltstone: Greenish-white. Forms recess in cliff 0.3

Esplanade Sandstone—Continued

		Thickness (meters)
9.	Sandstone: White (weathers tan), fine-grained, thinly laminated to 0.6 m thick. Includes small- and large-scale, low-angle crossbeds. Forms cliff	29.0
8.	Sandstone: Slightly calcareous, white, fine-grained, thin-bedded. Forms slope	5.3
7.	Sandstone: Calcareous, light-yellow to white (weathers pale yellow to white), fine-grained, thin- to medium-bedded 0.3–3.7 m thick. Includes large-scale, low-angle crossbeds with gray siltstone partings between crossbed sets. Forms cliff	35.1
6.	Sandstone: White, fine-grained, thin-bedded. Includes interbedded, red, ripple-laminated siltstone. Forms slope	8.8
5.	Sandstone: White, fine-grained, thin-bedded. Includes large-scale, low-angle crossbeds separated by thin, flat-bedded sandstone. Forms cliff	19.6
4.	Sandstone: White, fine-grained, thinly laminated to thin-bedded. Forms slope	1.5
3.	Sandstone: White, fine-grained, thick-bedded. Includes numerous small-scale, low-angle crossbeds. Forms cliff	4.1
2.	Sandstone: White (weathers tan or light yellow), fine-grained, thin-bedded. Includes low-angle crossbeds 0.3–1 m thick. Forms cliff or ledges	4.1
1.	Sandstone: White, fine-grained, thin-bedded 0.3–1 m thick, flat-bedded to thinly laminated. Bottom of Esplanade Sandstone not exposed by erosion in floor of Hurricane Wash. Unit is close to Pakoon Limestone. Forms cliff or ledges. Contact with Pakoon Limestone not exposed	14.0
	Total Esplanade Sandstone	174.4

Section 3. The Hermit Formation at Hidden Canyon, Grand Wash Cliffs, northern Mohave County, northwestern Arizona

Section measured east of junction of Jump and Hidden Canyons, east wall of Jump Canyon, St. George Canyon 7.5-minute quadrangle, Arizona, 1979 ($NE^1/_4$ sec. 2, T. 36 N., R. 14 W.; location, fig. 1). Correction for stratigraphic dip about 3° north 34° east (34° azimuth).

[*Section measured by George Billingsley and Edwin Pfeifer, May 3, 1992*]

		Thickness (meters)
	Seligman Member of the Toroweap Formation (incomplete, only lowermost unit described, not measured):	
44.	Sandstone: Calcareous. Lower part consists of purplish-red and yellow, medium-grained, thin-bedded sandstone. Includes low-angle crossbed sets. Contains undulating beds with soft sediment slump structures. Upper part consists of yellowish-brown or tan, medium- to coarse-grained, high-angle, crossbedded sandstone. Both parts form sheer cliff as much as 4 m high. Upper unit thickens at expense of lower in lateral distance. Sandstone grades upward into gypsum and siltstone slope above cliff. Unconformity at base of lower part truncates underlying Hermit Formation with trough channels as much as 1.3 m deep	
	Unconformity.	
	Hermit Formation:	
43.	Sandstone: Calcareous, white to pale-red, fine-grained, flat-bedded to massive. Includes few low-angle crossbeds. Forms cliff	2.4
42.	Covered slope: Red, fine-, medium-, and coarse-grained, silty sandstone	8.8
41.	Sandstone: White to pale-red, fine- to medium-grained, thick-bedded 1–2 m. Forms cliff	7.6
40.	Sandstone: Silty, slightly calcareous, pale-red to yellowish-red, flat-bedded, thin-bedded. Forms slope	8.2
39.	Sandstone: Pale-red to pinkish-white, fine- to medium-grained, thick-bedded 1–4 m thick. Includes low-angle crossbeds in upper part and several hematite concretions as much as 7.2 cm in diameter. Slightly calcareous in upper part. Forms cliff	8.8
38.	Siltstone: Dark-red, thin-bedded, friable. Forms slope	0.9
37.	Sandstone: Light-red to pinkish-white, fine- to medium-grained, massive. Forms cliff	1.5
36.	Siltstone: Dark-red, friable. Forms slope	5.3
35.	Covered slope: Contains interbedded red sandstone and dark-red siltstone. Forms slope	15.8
34.	Sandstone and siltstone: Interbedded light-red, fine-grained, flat-bedded, medium- to thick-bedded 1–2.5 m thick sandstone beds with dark-red, thin-bedded, friable, siltstone beds. Several sandstone beds bleached pale-red or white in top part, some siltstone beds bleached white or gray in bottom part. Forms slope with ledges	31.5
33.	Siltstone: Dark-red, extremely friable, may contain clay. Forms slope	1.5
32.	Sandstone: Light-red, fine-grained, flat-bedded and massive. Forms weak ledge	4.1
31.	Siltstone: Dark-red, extremely friable. May contain clay. Includes thin beds of red sandstone as much as 0.3 m thick that lens out laterally. Forms slope	5.9
30.	Sandstone: Silty, dark-red, fine-grained, massive. Includes flat, thin-bedded sandstone. Forms slope	3.5
29.	Siltstone: Dark-red, thin-bedded, friable. Forms slope	0.6
28.	Sandstone: Light-yellowish-red, fine- to medium-grained, massive. Includes small, pea-sized siltstone concretions. Forms cliff	4.4
27.	Sandstone: Silty, light-red, flat-bedded, massive. Forms slope	4.1
26.	Sandstone and siltstone: Contains interbedded white, silty sandstone and dark-red siltstone, thick-bedded 1–2 m, flat-bedded. Forms slope with ledges	15.5
25.	Sandstone: Silty, light-red, fine-grained, massive, flat-bedded. Forms slope	8.8
24.	Sandstone: White, fine- to medium-grained, flat-bedded, massive. Forms cliff	3.5
23.	Siltstone and sandstone: Includes dark-red siltstone and light-red sandstone, thin- to thick-bedded. Forms slope	26.1
22.	Sandstone: White to pale-red, fine-grained, thick-bedded. Forms ledge	0.9
21.	Siltstone and sandstone: Includes dark-red siltstone interbedded with light-red, fine-grained sandstone. Siltstone contains small flakes of rip-up clasts and horizontal burrows. Forms slope	8.8
20.	Sandstone: Light-red, thick-bedded as much as 1.5 m thick. Forms cliff	7.6
19.	Siltstone: Dark-red, thin-bedded, friable. Forms slope	6.7

	Thickness (meters)
Hermit Formation—Continued	
18. Sandstone: Light-orange-red to grayish-white, fine-grained, flat-bedded. Forms cliff	1.8
17. Siltstone and sandstone: Includes dark-red siltstone interbedded with light-red, silty sandstone. Forms slope	7.3
16. Sandstone: Silty, light-red, fine-grained, flat-bedded, medium beds as much as 1 m thick. Forms cliff	3.5
15. Siltstone and sandstone: Includes dark-red siltstone and interbedded light-red silty sandstone. Includes horizontal burrows and pea-size dark-red siltstone rip-up clasts in siltstone beds. Forms slope	18.1
14. Sandstone: Silty, light-red, massive. Forms weak ledge	1.8
13. Siltstone: Dark-red, thin-bedded, platy, friable. Thickens and thins laterally at expense of unit above or below. Forms slope	2.4
12. Sandstone: Light-red, flat-bedded, massive. Forms weak ledge	2.7
11. Siltstone: Dark-red, thin-bedded, friable. Contains horizontal burrows. Forms slope	0.6
10. Sandstone: White, fine-grained, thick bed. Includes horizontal burrows. Forms cliff	0.9
9. Siltstone: Dark-red, very thin bedded. Contains horizontal burrows and possible plant fragments. Forms slope	1.2
8. Sandstone: White, fine-grained, flat-bedded. Includes horizontal burrows less than 1.3 cm in diameter. Forms cliff	1.2
7. Sandstone: White and light-red, fine-grained. Contains low-angle crossbed sets interbedded with light-red, sandy, flat-bedded siltstone. Forms slope	3.8
6. Sandstone: White, fine-grained, thick-bedded, massive. Forms cliff	3.5
5. Siltstone: Dark-red, massive, friable texture on weathered surface. Contains possible trace fossil burrows, and plant fragments. Forms slope	3.5
4. Sandstone: White, fine-grained, massive, mostly flat bedded but contains low-angle crossbeds. Forms cliff	1.2
3. Siltstone: Dark-red, very thin bedded. Contains possible plant fragments and siltstone rip-up clasts. Forms slope	2.4
2. Sandstone and siltstone: Includes red siltstone and interbedded white, fine-grained, medium-bedded sandstone. Includes trace fossils of plants and horizontal burrows. Forms slope	8.5
Total Hermit Formation	251.4

Unconformity.

Unconformity is sharp, planar, erosional contact with relief as much as 1 m. Forms topographic break between red slope of Hermit Formation and white cliff of Esplanade Sandstone.

Esplanade Sandstone (incomplete, only topmost unit measured):

1. Sandstone: White and pinkish-red, fine-grained. Includes numerous, small-scale, low-angle crossbeds. Contains horizontal and vertical burrow traces. Forms cliff	9.1

Section 4. The Esplanade Sandstone at Hidden Canyon, Grand Wash Cliffs, northern Mohave County, northwestern Arizona

Measured section is east of junction of Jump and Hidden Canyons, east wall of Jump Canyon, starting below Hidden Canyon road in Jump Canyon drainage, Cane Springs SE 7.5-minute quadrangle, Arizona, 1979 (SE$^1/_2$ sec. 36, T. 37 N., R. 14 W.; location, fig. 1). Correction for stratigraphic dip about 3° east (34° azimuth).

	Thickness (meters)
[*Section measured by George Billingsley and Edwin Pfeifer, May 3, 1992*]	
Hermit Formation (incomplete, only lowermost unit measured):	
14. Sandstone and siltstone: Red siltstone and interbedded white, fine-grained, medium-bedded sandstone. Includes trace fossils of plants and horizontal burrows. Forms slope	8.5

Unconformity.

Unconformity is sharp, planar, erosional contact with relief as much as 1 m. Forms topographic break between red slope of Hermit Formation and white cliff of Esplanade Sandstone.

Esplanade Sandstone:

13. Sandstone: White and pinkish-red, fine-grained. Includes numerous small-scale, low-angle crossbeds. Contains horizontal and vertical burrow traces. Forms cliff	9.1
12. Sandstone: White, fine-grained, flat-bedded. Includes interbedded silty sandstone. Forms slope with ledges	24.5
11. Sandstone: White, fine- to medium-grained. Includes high-angle and low-angle crossbed sets as much as 6 m thick. Forms cliff	24.5
10. Sandstone: White, fine-grained, flat-bedded. Includes low-angle crossbeds and clusters of burrow tubes. Burrows as much as 19 cm in diameter. Forms cliff	9.4
9. Siltstone and sandstone: Dark-red, thin-bedded. Includes small horizontal burrows. Forms recess in cliff	2.4
8. Sandstone: White and light-red, fine- to medium-grained, thin- to thick-bedded, slightly calcareous in lower part. Contains large, low-angle crossbed sets. Includes clusters of burrows in upper part that radiate out from central or elongate area. Burrow tubes average about 2 cm in diameter. Forms cliff	10.5
7. Sandstone: Calcareous, light-red or pinkish-red, fine- to medium-grained, thin- to thick-bedded. Contains few crossbed sets as much as 1.8 m thick. Alternating sets of low-angle crossbeds and flat beds of sandstone. Forms slope	17.5
6. Sandstone: White to light-brown, fine-grained. Contains high-angle crossbed sets with dips as much as 25°. Forms cliff	1.8
5. Sandstone: Light-brown to white, fine-grained, thin-bedded. Includes numerous low-angle crossbed sets 0.2–0.6 m thick. Partly covered slope	23.7
4. Sandstone: Light-red to white or pinkish-red, fine-grained, thick-bedded. Includes numerous low-angle crossbed sets as much as 1.3 m thick. Some crossbeds dip as much as 15° southeast. Forms cliff	19.3
3. Sandstone and siltstone: Includes interbedded red to light-red, fine-grained, thin-bedded sandstone, siltstone, silty sandstone, and calcareous low-angle crossbed sets. Forms slope	7.0
2. Sandstone: Light-red to white, fine-grained, thick-bedded. Includes calcareous low-angle crossbed sets as much as 1 m thick. Forms cliff	8.2
Total Esplanade Sandstone	158.0

Disconformity.

Sharp planar contact with underlying Pakoon Limestone (Wolfcampian). Cliff-forming white sandstone of Esplanade Sandstone overlies slope and ledges of pink and gray limestone of Pakoon Limestone.

Thickness (meters)

Pakoon Limestone (incomplete, only topmost unit measured):

1. Limestone: Silty, light- to pinkish-gray, fine-grained, thin-bedded 5–14.5 cm thick. No fossils. Forms slope with ledges 2.7

Section 5. The Hermit Formation at Red Pockets Mountain, northern Mohave County, northwestern Arizona

Section measured on northeast side of Red Pockets Mountain, 28 km southeast of Mesquite, Nev., northern Mohave County, Ariz., Red Pockets 7.5-minute quadrangle, Arizona, 1985 ($N^1/_2$ sec. 14, T. 37 N., R. 16 W.; location, fig. 1). Correction for stratigraphic dip is 7° southeast (170° azimuth).

[*Section measured by George Billingsley, Carol Donohoe, and Robert L. Gilbert, March 21, 1992*]

Thickness (meters)

Seligman Member of the Toroweap Formation (incomplete, only lowermost unit measured):

25. Sandstone: Tan to light-yellow (weathers black to light pink), fine-grained. Includes large-scale high-angle crossbed sets that have dips as much as 30° southeast (156° azimuth), estimated as much as 6 m thick. Appears similar to Coconino Sandstone. Grades upward into gypsum and limestone. Forms sheer cliff. Estimated thickness 18–21 m

Unconformity.

Sharp, planar, erosional contact with Hermit Formation. Shallow, erosional trough depressions in lateral distance but mostly flat planar contact.

Hermit Formation (incomplete, base not exposed):

24. Sandstone: Light-red, fine-grained, thick-bedded. Contains low-angle crossbed sets as much as 2 m thick. Forms cliff 17.8
23. Sandstone: Light-red, fine-grained, thin-bedded, small-scale, low-angle crossbed sets as much as 1 m thick. Includes interbedded dark-red, thin-bedded siltstone. Forms cliff 7.0
22. Siltstone: Sandy, dark-red, very fine grained, thin-bedded. Forms slope 4.4
21. Sandstone: Light-red, fine-grained, thin-bedded, small-scale, low-angle crossbeds as much as 1 m thick. Includes interbedded dark-red, thin-bedded siltstone. Forms slope with ledges 7.0
20. Sandstone: Light-red, thin- to medium-bedded 0.3–1 m thick. Includes interbedded dark-red, shaly, thin-bedded siltstone. Sandstone beds have small-scale, low-angle, lenticular crossbeds as much as 1 m thick. Unit is 90 percent sandstone. Forms slope with ledges 52.6
19. Siltstone and sandstone: Interbedded dark-red siltstone and light-red sandstone (weathers to friable, fractured surface), thinly laminated to thin-bedded 0.3–1 m thick. At 17.5 m from base of unit, includes numerous horizontal burrow structures averaging 1.3 cm in diameter. Forms slope 27.2
18. Sandstone: Light-red, fine-grained, thick-bedded. Includes low-angle, small-scale crossbeds as much as 1 m thick. Crossbeds dip less than 7°. Forms cliff 3.8

Thickness (meters)

Hermit Formation—Continued

17. Sandstone and siltstone: Light-red, fine-grained, thick-bedded. Includes low-angle crossbed sets and interbedded dark-red, thin-bedded, friable siltstone and silty sandstone. Forms slope 4.4
16. Sandstone: Pale-orange, fine-grained, thick-bedded. Includes small-scale, low-angle crossbeds as much as 1.2 m thick and interbedded dark-red, thin-bedded, lenticular siltstone and sandy siltstone beds. Forms weak cliff 29.8
15. Sandstone: Light-red, fine-grained, thick to massive, flat-bedded. Includes numerous cluster burrows as much as 0.3 m in diameter. Burrows radiate from central core all directions like tentacles. Burrows commonly 1.2 cm in diameter, most common lower part. Includes lenses of dark-red, friable siltstone 12.3 m up from base of unit forming recess in cliff. Forms prominent cliff 24.5
14. Siltstone: Sandy, dark-red, very fine grained, thin-bedded. Includes mud cracks and horizontal burrows. Forms recess in cliff 0.9
13. Sandstone: Light-red, fine-grained, thick-bedded to massive. Black manganese staining. Forms cliff 2.4
12. Siltstone: Dark-red, thin-bedded. Highly fractured on weathered outcrop, friable. Includes very fine grained, thin-bedded sandstone. Forms slope 5.9
11. Sandstone: Sandy, light-red, fine-grained, thick-bedded. Forms cliff 6.2
10. Siltstone: Sandy, dark-red, very fine grained, thin-bedded. Includes numerous horizontal burrow impressions. Contains interbedded, thin-bedded lenses of sandstone. Forms slope 19.9
9. Sandstone: Light-red, fine-grained, thick-bedded to massive. Forms cliff 7.6
8. Siltstone: Sandy, dark-red, very fine grained, thin-bedded. Forms slope 1.7
7. Sandstone: Light-red, fine-grained, thin- to medium-bedded. Includes low-angle crossbeds as much as 0.6 m thick. Forms weak cliff 6.8
6. Siltstone: Sandy, dark-red, very fine grained, thin-bedded. Forms slope 1.2
5. Sandstone: Light-red, fine-grained, thick-bedded. Forms ledge 4.3
4. Siltstone: Sandy, dark-red, very fine grained, thin-bedded. Includes raindrop impressions, horizontal burrows, plant? impressions, and large root casts or tubelike impressions 5 cm in diameter. Forms slope 5.3
3. Sandstone: Light-red, very fine grained, thin- to medium-bedded, low-angle crossbeds. Includes thin-bedded lenses of dark-red siltstone. Forms cliff 17.5
2. Siltstone: Sandy, shaly, dark-red, very fine grained, thin-bedded. Forms slope 0.6
1. Sandstone: Light-red, fine-grained, thick-bedded. Includes small-scale, low-angle crossbeds in thin sets as much as 1 m thick. Includes minor, black (iron?), rounded to subrounded grains in interbedded dark-red, thin-bedded, siltstone as much as 0.6 m thick. Forms weak cliff 11.1

Hermit Formation (incomplete, base not exposed) 270.0

Contact with Queantoweap Sandstone not exposed. Estimated about 3–5 meters below outcrop.

Section 6. The Queantoweap Sandstone at Red Pockets Mountain, northern Mohave County, northwestern Arizona

Section measured on the northwest flank of Red Pockets Mountain beginning in drainage near Lime Kiln Canyon road, east flank of the Virgin Mountains, northern Mohave County, Ariz. Red Pockets 7.5-minute quadrangle, Arizona, 1985 ($NW^1/_4$ sec. 11, T. 37 N., R. 16 W.; location, fig. 1). Strata dip 7° south (190° azimuth).

[*Measured by George Billingsley, March 31, 1993*]

	Thickness (meters)
Unconformity.	
Contact with Hermit Formation, not exposed, covered slope	
Queantoweap Sandstone (incomplete, top not exposed):	
13. Covered slope: Light-red, flat-bedded, ledge-forming sandstone partly exposed in slope. Red siltstone and sandstone of Hermit Formation exposed and measured about $^1/_4$ km east (Section 7). Estimated thickness about 45–69 m in mostly covered slope	55.0
12. Sandstone: Silty, light-red, fine-grained, mostly flat beds with low-angle crossbeds, partly covered. Forms ledgy slope	23.4
11. Sandstone: Silty, light-red, fine- to medium-grained. Includes high-angle crossbeds in upper part and low-angle crossbeds in lower part. Forms minor cliff	23.1
10. Sandstone: Light-red, fine- to medium-grained. Includes high-angle crossbeds in lower part, mostly flat beds in upper part. Forms cliff	9.1
9. Covered slope	4.0
8. Sandstone: Light-red to white, fine-grained. Includes thinly laminated and low-angle crossbeds 0.3–1.5 m thick. Includes thin beds of red siltstone. Forms ledgy slope	14.0
7. Sandstone: Calcareous in upper part, pinkish-gray to light-red, medium- to coarse-grained, medium beds 1–3 m thick. Contains thinly laminated beds and low-angle crossbeds. Includes high-angle crossbeds in middle part 1.8–3.0 m thick. Forms cliff	31.5
6. Siltstone: Calcareous, light-red, massive bed. Forms cliff	0.9
5. Sandstone: Calcareous, grayish-yellow (weathers light brown), medium-grained. Includes low-angle crossbeds. Forms cliff	10.5
4. Sandstone: Calcareous, light-red, medium-grained, thin-bedded. Forms ledge	3.7
3. Siltstone: Slightly calcareous, dark-red. Includes thin beds of whitish-gray, calcareous sandstone. Forms slope	7.0
2. Sandstone: Calcareous, light-red to grayish-red, fine-grained. Contains low-angle crossbed sets and interbedded red siltstone beds 0.3–1 m thick. Forms ledgy slope	6.2
Queantoweap Sandstone (incomplete, top not exposed)	133.3
Disconformity.	
Contact with Pakoon Limestone, flat, planar, no relief. Contact located at lithologic and color change.	
Pakoon Limestone (incomplete, only topmost bed described, not measured):	
1. Limestone: Light-gray, aphanitic, medium-bedded 0.3–1 m thick. Forms ledges	

Section 7. The Hermit Formation at the Gorge of the Virgin River, northern Mohave County, northwestern Arizona

Section measured on south slope in Gorge of the Virgin River about 0.8 km south of Interstate Highway 15, Purgatory Canyon 7.5-minute quadrangle, Arizona, 1979 ($SE^1/_4$ sec. 8, T. 41 N., R. 13 W.; location, fig. 1). Section begins at Virgin River bottom about 1 km downstream from Interstate 15 bridge. Correction for stratigraphic dip about 4° east (80° azimuth).

[*Section measured by George Billingsley, Carol Donohoe, and Robert L. Gilbert, March 22, 1992*]

	Thickness (meters)
Toroweap Formation, Seligman Member (incomplete, only lower two units measured):	
29. Gypsum and siltstone: Includes gray, thin- to thick-bedded, silty gypsum and interbedded light-red, gypsiferous siltstone. Forms slope	>3
28. Sandstone: Silty, light-yellow and purplish-red, fine- to medium-grained, thin-bedded 0.3–0.6 m thick. Includes small-scale, low-angle, planar-wedge crossbed sets of calcareous sandstone. Contains siltstone, calcite, and gypsum cement. Lower part includes high-angle crossbed sets that pinch out laterally, dips as much as 25°, southeast (170° azimuth). Forms cliff	4.1
Seligman Member	>7.1
Unconformity.	
Sharp, planar, erosional contact between crossbedded sandstone cliff of Seligman Member of Toroweap Formation and flat-bedded sandstone cliff and slope of Hermit Formation.	
Hermit Formation:	
27. Sandstone: Calcareous, light-yellow and light-red, medium-bedded, 1–3 m thick. Includes high-angle crossbeds in upper part, mostly flat bedded. Forms cliff	24.8
26. Sandstone: Silty, calcareous, light-yellowish-red, medium-bedded, flat-bedded sandstone. Includes some low-angle crossbeds and interbedded, flat-bedded siltstone and silty sandstone. Forms weak cliff	31.5
25. Sandstone: Silty, light-red to pale-yellow, fine-grained, medium- to thick-bedded. Includes small-scale, low-angle, concave crossbed sets as much as 1.5 m thick. Forms weak cliff	8.8
24. Sandstone: Silty, white to light-red and pale-yellow, fine-grained, medium- to thick-bedded or massive. Includes small-scale, low-angle crossbed sets as much as 1.8 m thick. Forms weak cliff	33.3
23. Siltstone and sandstone: Light-red, fine-grained, thin-bedded. Forms slope	1.8
22. Sandstone: Light-yellow and light-red, flat, thin-bedded. Includes interbedded, small-scale, low-angle crossbeds and thick to massive sandstone beds. Contains small horizontal burrows on bedding surfaces. Forms cliff	9.7
21. Siltstone and sandstone: Light-red to dark-red, thin-bedded. Forms slope	22.8
20. Sandstone: Light-red, fine-grained, thick-bedded. Includes small-scale, low-angle crossbed sets. Forms cliff	5.3
19. Siltstone: Dark-red, thin-bedded, shaly. Forms slope	3.5

	Thickness (meters)
Hermit Formation—Continued	
18. Sandstone: Light-red, fine-grained, medium- to thick-bedded. Includes vertical burrow structures (root casts?), 1.8 m in length in top part. Forms cliff	19.3
17. Siltstone: Dark-red, thin-bedded. Forms slope	1.7
16. Sandstone: Tan, light-yellow and light-red, fine-grained, thick-bedded. Includes small-scale low-angle crossbed sets as much as 1 m thick. Forms prominent cliff	24.5
15. Siltstone: Dark-red, thin-bedded, and interbedded light-red and tan sandstone. Sandstone beds are lenticular as channel-filling sand in lateral distance. Channels as deep as 1.8 m. Sandstone beds contain giant vertical and horizontal burrows or root? casts as much as 14.4 cm in diameter. Includes small-scale, low-angle, silty, crossbed sets in upper and lower part, friable, shaly. Forms slope	5.3
14. Sandstone: Light-red, massive. Includes small-scale, low-angle crossbed sets as much as 0.6 m thick. Upper part contains clusters of burrows that radiate out from central core area like tentacles, burrows are about 1.2 cm in diameter. Includes dark-red, thin-bedded, interbedded, siltstone beds as much as 0.3 m thick with horizontal burrow casts as much as 4.8 cm in diameter and large-scale mud cracks. Forms cliff	12.3
13. Siltstone: Sandy, dark-red, thin-bedded. Forms recess in cliff	0.9
12. Sandstone: Light-red, thick-bedded. Includes small-scale, low-angle crossbed sets as much as 1 m thick. Forms cliff	7.0
11. Sandstone and siltstone: Includes interbedded light-red sandstone and dark-red siltstone, thin-bedded 15 cm to 3.0 m thick. Some beds bleached to light yellow. Includes light-yellow irregular bands and circular masses. Forms slope with ledges	38.3
10. Sandstone: Light-yellow, tan, and light-red, fine-grained, medium- to thick-bedded, flat-bedded. Includes small-scale, very low angle crossbed sets. Forms ledges in cliff	11.7
9. Sandstone: Light-yellow or tan, fine-grained, massive to thick-bedded. Forms cliff	7.9
8. Siltstone: Sandy, light-red to light-yellow, fine-grained to very fine grained, thin-bedded. Forms recess or slope	1.8
7. Sandstone: Light-yellow, fine-grained, massive to thick-bedded. Includes low-angle crossbed sets as much as 1.3 m thick. Forms cliff	8.8
6. Siltstone and sandstone: Light-red, thin-bedded. Pinches out laterally in several hundred meters. Forms recess in cliff	0.9
5. Sandstone: Light-yellow or tan, fine-grained, massive to thick-bedded. Contains small-scale, very low angle crossbed sets as much as 1 m thick. Forms cliff	19.3
4. Siltstone: Dark-reddish-brown, thin-bedded, shaly. Unit thins and thickens laterally filling small erosional channels. Forms recess in cliff	1.8
3. Sandstone: Tan to light-red, fine-grained, massive. Includes numerous small-scale, very low angle crossbed sets 0.3–0.6 m thick. Forms cliff	1.5
2. Sandstone and siltstone: Light-red, thin-bedded, grades laterally from siltstone to sandstone and back to siltstone. Occupies shallow, lenslike channels, thinning to less than 0.3 m. Forms recess in cliff	1.2
Total Hermit Formation	305.8

	Thickness (meters)
Unconformity.	
Unconformable to gradational contact marked by shallow erosion channels as much as 1.2 m in depth cut into tan or white, high-angle, crossbedded Queantoweap Sandstone and filled with dark-red siltstone and sandstone of the Hermit Formation. Unconformity is not prominent and difficult to place except on cliff exposures.	
Queantoweap Sandstone (incomplete, only topmost unit measured):	
1. Sandstone: Tan to light-yellow (weathers light brown to tan with black manganese staining on some surfaces), fine-grained, thick-bedded. Includes high-angle, planar-wedge crossbed sets 1.8–3.7 m thick; cross-beds dip as much as 16° southeast (155° azimuth). Includes flat-bedded sandstone. Forms cliff	13.8
Virgin River bottom.	

Section 8. The Queantoweap Sandstone at the Gorge of the Virgin River, northern Mohave County, northwestern Arizona

Section measured about 3.2 km down the Virgin River from Interstate Highway 15 bridge, north side of Virgin River in small tributary drainage, Purgatory Canyon 7.5-minute quadrangle, Arizona, 1979 (east-central edge sec. 7, T. 41 N., R. 13 W.; location, fig. 1). Measured section is about 1.6 km west of measured section of Hermit Formation. Strata dip 4° east (105° azimuth).

[*Measured by George H. Billingsley, April 1, 1993*]

	Thickness (meters)
Hermit Formation (incomplete, only lowermost seven units measured):	
13. Siltstone and sandstone: Red. Includes interbedded, low-angle crossbed sandstone sets and flat-bedded siltstone beds 0.3–1.2 m thick. Forms ledgy slope	>2
12. Sandstone: Silty, light-red, fine- to medium-grained, flat-bedded. Forms cliff	10.5
11. Siltstone: Sandy, reddish-brown, friable. Contains yellow bleach spots. Pinches out in short lateral distance. Forms recess or slope beneath cliff of unit 12	0.9
10. Sandstone: Calcareous, light-yellow to yellowish-white, fine- to medium-grained, massive thick bed. Forms slope	5.3
9. Sandstone: Yellowish-white (weathers yellowish brown), fine- to medium-grained. Includes low-angle crossbed sets less than 0.6 m thick. Forms cliff	16.1
8. Siltstone: Light-red to yellow. Forms recess in cliff	0.9
7. Sandstone: Yellowish-white (weathers yellowish brown), fine- to medium-grained. Includes low-angle crossbed sets less than 0.9 m thick. Forms cliff	7.3
6. Siltstone: Red, thick bed. Fills shallow channel. Forms recess in cliff	0.9
Hermit Formation (incomplete)	43.9
Unconformity.	
Erosional shallow channels as much as 1 m in relief at some locations, gradational contact elsewhere.	

	Thickness (meters)
Queantoweap Sandstone:	
5. Sandstone: Silty, calcareous, white to pale-yellow (weathers yellowish brown), fine- to medium-grained. Includes thin, low-angle crossbeds to as much as 0.6 m thick. Forms ledgy slope	16.1
4. Sandstone: Slightly calcareous, white to yellowish-gray (weathers light yellow and brown), fine- to medium-grained, medium to thick beds 1–7.5 m thick. Includes small low-angle crossbeds. Contains many burrows and tracks on flat and rippled bedding surfaces. Forms cliff	37.7
3. Sandstone: Slightly calcareous, white to yellowish-brown (weathers dark gray to brown), fine- to medium-grained. Includes high-angle crossbed sets as much as 22 m thick in lower part. Crossbeds dip as much as 26° southeast (160° azimuth). Contains abundant burrows and similar trace fossils on flat and large-scale rippled bedding surfaces. Forms cliff	63.7
Queantoweap Sandstone—Continued	
2. Sandstone: Calcareous, reddish-yellow to light-brown (weathers brown), fine- to medium-grained. Includes low-angle crossbed sets as much as 1 m thick, mostly flat bedded. Contains numerous red and rusty-yellow liesegang bands in fractured surfaces. Unconformity truncates underlying limestone of unit 1 as much as 1.2 m. Forms ledgy slope	6.5
Total Queantoweap Sandstone	124.0
Unconformity.	
Pakoon Limestone (incomplete, only topmost unit measured):	
1. Limestone: Very sandy, light-gray (weathers yellowish brown), fine-grained. Includes flat and low-angle crossbeds as much as 3 m thick. Includes beds and veins of breccia consisting of subrounded pebbles and boulders of limestone, 5–60 cm in diameter, in light-gray limestone matrix, poorly sorted. Forms cliff	11.4

Cenozoic Low-Angle Faults, Thrust Faults, and Anastomosing High-Angle Faults, Western Markagunt Plateau, Southwestern Utah

By Florian Maldonado, Edward G. Sable, *and* L. David Nealey

GEOLOGIC STUDIES IN THE BASIN AND RANGE–COLORADO PLATEAU TRANSITION IN SOUTHEASTERN NEVADA, SOUTHWESTERN UTAH, AND NORTHWESTERN ARIZONA, 1995

U.S. GEOLOGICAL SURVEY BULLETIN 2153–G

UNITED STATES GOVERNMENT PRINTING OFFICE, WASHINGTON : 1997

CONTENTS

PLATE

[Plate is in pocket]

FIGURES

Cenozoic Low-Angle Faults, Thrust Faults, and Anastomosing High-Angle Faults, Western Markagunt Plateau, Southwestern Utah

By Florian Maldonado, Edward G. Sable, *and* L. David Nealey

ABSTRACT

A complex of Tertiary low-angle faults, thrust faults, and high-angle faults is present along the west edge of the Markagunt Plateau, southwestern Utah, in the transition zone between the Basin and Range and Colorado Plateaus provinces. Most of these structures formed in the Miocene, and some remained active into the Pleistocene and possibly later.

One of the oldest Tertiary structures is the Red Hills low-angle shear zone, interpreted as a shallow structure that decoupled an upper plate, composed of an Oligocene-Miocene ash-flow tuff and volcaniclastic succession, from a lower plate of Tertiary sedimentary rocks. Age of the shear zone is bracketed from field relations at between 22.5 and 20 Ma. The other low-angle faults are younger, probably formed during uplift of the Markagunt Plateau.

Tertiary thrust faults along the western front of the Markagunt Plateau place an upper plate of Upper(?) Cretaceous Iron Springs Formation and Paleocene to Oligocene sedimentary and Oligocene volcanic rocks over a lower plate consisting locally of Oligocene and Miocene volcanic rocks but mostly of Paleocene-Eocene Claron Formation and older rocks. The youngest exposed rock unit in the lower plate is the 22–22.5 Ma Harmony Hills Tuff. These faults may be related to compressional stresses associated with igneous intrusion or to strike-slip faulting along the plateau margin. The thrusts are consistently associated with a monocline, which we interpret as a continuation of the Cedar City–Parowan monocline exposed near Cedar City.

Younger north- to northeast-trending high-angle faults bound a horst and graben system. These faults formed later than about 20 Ma, based on displacement of the 20-Ma Iron Peak laccolith and its associated dikes; some of the faults remained active into the Pleistocene. The faults bounding the horsts and grabens in the central part of this system anastomose in map view and merge toward its southern end. Within the grabens, (1) debris eroded from horst walls forms lobe-shaped deposits, (2) Pleistocene basaltic cinder cones are localized along graben-bounding faults, and (3) local folding of rock units suggests some component of lateral or compressive translation along the bounding faults.

Gravity-slide and landslide blocks form deposits that are common throughout the plateau and probably reflect continuous deformation. Some of the gravity-slide blocks form megabreccia deposits mostly of Miocene age, resulting from formation of the Red Hills shear zone; others were the result of intrusion and volcanism. The landslide blocks form deposits of Pliocene(?)-Pleistocene age along high-angle faults that remained active into the Pleistocene and possibly later.

INTRODUCTION

A structurally complex terrane along the west edge of the Markagunt Plateau, southwestern Utah (fig. 1), straddles the boundary between the Basin and Range province and the High Plateaus subprovince of the Colorado Plateaus province. The High Plateaus is the structural transition zone between the greatly extended terrane in the Basin and Range and the less extended terrane in the Colorado Plateau. The study area is covered by Mesozoic and Tertiary sedimentary rocks, Tertiary volcanic and volcaniclastic sedimentary rocks, Tertiary intrusive rocks, and Quaternary basaltic rocks.

The evolution of ideas about the structural development of the western Markagunt Plateau started with Gregory's (1945, 1949, 1950) stratigraphic and structural studies. The Red Hills area, west of the Markagunt Plateau, was first mapped by Thomas and Taylor (1946) in their ground-water study of Cedar City and Parowan Valleys; that mapping was updated by Threet (1952a) in his dissertation; Rowley and Threet (1976) mapped the southern part of the Red Hills as part of a regional study of volcanic terrane; and the Red Hills were remapped by Maldonado and Williams (1993a, b) as part of a regional compilation. The Mesozoic stratigraphy for the area was established by Averitt (1962) through mapping near Coal Creek, in the southern part of the study area, as part of a coal study; this mapping was later expanded by Averitt and Threet (1973). The general volcanic stratigraphy of the area was developed by Anderson and Rowley (1975) as part of a regional study of the volcanic terrane in the southwestern High Plateaus and adjacent part of the Basin

and Range province. The northern Markagunt Plateau, which includes the northernmost part of the study area, was mapped by J.J. Anderson (1965) as part of his dissertation and by Anderson and others (1987). Anderson's Kent State University students later mapped a large part of the study area as part of their masters' theses; Judy (1974) and Moore (1982) mapped the west-central part of the Markagunt, Iivari (1979) the east-central part, and Spurney (1984) the Iron Peak laccolith. More recent studies include mapping, as part of a regional compilation, by Maldonado and Moore (1993) and unpublished mapping by Maldonado and Sable.

The high-angle faults that bound horsts and grabens have been recognized by previous workers, but the Tertiary low-angle faults and thrust faults are newly proposed. A generalized geologic map (pl. 1) was compiled for the western Markagunt Plateau and adjacent Red Hills from existing maps and from unpublished geologic mapping by the authors. This report describes and interprets the Tertiary structures shown on plate 1.

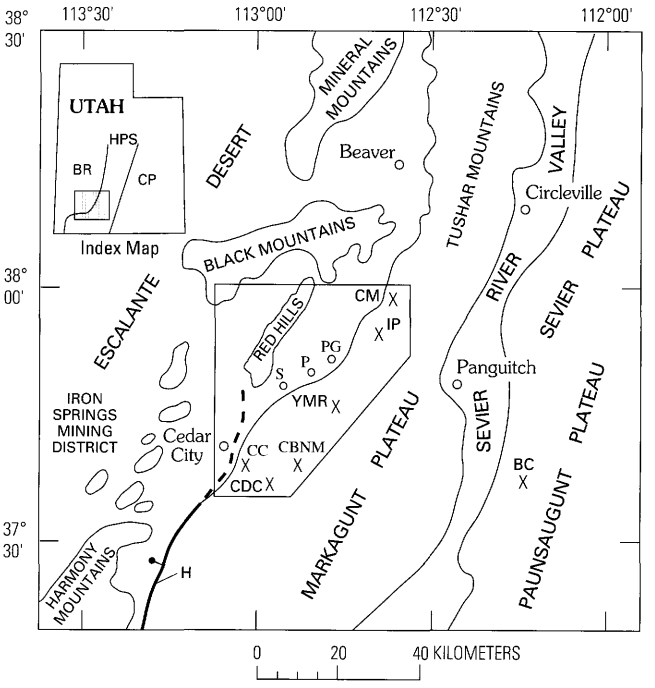

Figure 1. Location map, southwestern Utah. Solid line is outline of plate 1 and figure 10. BC, Bryce Canyon; CBNM, Cedar Breaks National Monument; CDC, Cedar Canyon; CC, Coal Creek; CM, Cottonwood Mountain; H, Hurricane fault; IP, Iron Peak; P, Parowan; PG, Paragonah; S, Summit; YMR, Yankee Meadows Reservoir; BR, Basin and Range province; HPS, High Plateaus subprovince; CP, Colorado Plateaus province.

ACKNOWLEDGMENTS

Discussions with J.J. Anderson, P.D. Rowley, R.E. Anderson, K.F. Fox, Jr., D.W. Moore, D.L. Schmidt, and H.R. Blank, Jr., aided in formulation of ideas presented in this report. We thank D.L. Schleicher, P.D. Rowley, and D.J. Lidke for their review comments.

STRATIGRAPHY

The rock units of the area are Mesozoic and Tertiary sedimentary rocks, Tertiary volcanic and volcaniclastic sedimentary rocks, Tertiary intrusive rocks, and Quaternary basaltic rocks. These rock units are briefly described here and their distribution shown on plate 1.

MESOZOIC SEDIMENTARY ROCKS

The Mesozoic sedimentary rocks are composed of Triassic, Jurassic, and Cretaceous rocks described by Averitt (1962). The Triassic rocks, in ascending order, are the Moenkopi (as much as 575 m thick) and the Chinle (as much as 130 m) Formations—composed mostly of siltstone, mudstone, sandstone, gypsum, and minor limestone. The Jurassic rocks are the Moenave (as much as 155 m) and Kayenta (as much as 350 m) Formations—composed of mudstone and sandstone; the Navajo Sandstone (as much as 520 m thick)—composed almost entirely of sandstone; Temple Cap Sandstone equivalent (about 30 m); and the Carmel Formation undivided (as much as 400 m thick)—composed of limestone, sandstone, mudstone, siltstone, and gypsum. The Cretaceous rocks include the Dakota Formation and the Tropic Shale (combined thickness about 250 m), the Straight Cliffs and Wahweap Formations (combined thickness as much as 850 m), and the Iron Springs Formation (as much as 750 m). These Cretaceous units are generally marine and nonmarine sandstone, siltstone, shale, and conglomerate.

TERTIARY SEDIMENTARY ROCKS

The Tertiary sedimentary rocks, in ascending order, are the Grand Castle, Claron, and Brian Head Formations. The Grand Castle Formation is formalized and described by Goldstrand in this volume (chapter D). He reports it to be of Paleocene age and as much as 275 m thick, and to consist of conglomerate and sandstone. The Claron Formation is upper Paleocene and Eocene (Goldstrand, 1994) and is as much as 435 m thick (Schneider, 1967). Mackin (1960) separated the formation into two informal members—a lower red and an upper white member. The red member consists of poorly to moderately resistant fluvial and lacustrine strata, predominantly sandstone intercalated with mudstone, limestone, and pebble conglomerate. The white member, not present everywhere, is characterized by cliff-forming white limestone, and siltstone, claystone, sandstone, and conglomerate. These two members are very well exposed in the cliffs and hoodoos

at Cedar Breaks National Monument (fig. 1, pl. 1). The original deposits of this formation have been interpreted to have been altered by pedogenic processes (Mullett and others, 1988; Mullett, 1989). The Brian Head Formation, previously abandoned (Threet, 1952b; Anderson, 1971), is formally reinstated and described in more detail (Sable and Maldonado, this volume, chapter A). The formation is late Eocene to middle Oligocene in age, as much as about 300 m thick, and consists mostly of tuffaceous sandstone, sandstone, mudflow breccia, and pebble-to-boulder conglomerate, and lesser limestone, limy shale, and chalcedony lenses, and local ash-flow and ash-fall tuff. The ash-flow tuff, mapped in the Red Hills area, occurs in the upper part of the formation (Maldonado and Williams, 1993b) and is 34 to 33 Ma (Maldonado, 1995).

TERTIARY VOLCANIC AND VOLCANICLASTIC ROCKS

The Tertiary volcanic and volcaniclastic sedimentary rocks include ash-flow tuffs derived from caldera sources in the present Great Basin west of the study area and volcanic and volcaniclastic sedimentary rocks derived from the Marysvale volcanic field north of the area.

The ash-flow tuffs derived from the Great Basin sources include, in ascending order, the Wah Wah Springs and Lund Formations of the Needles Range Group (Mackin, 1960; Best and Grant, 1987), the Blue Meadows (Anderson and Rowley, 1975) and Baldhills Tuff Members of the Isom Formation (Mackin, 1960), and the Quichapa Group here consisting of the Leach Canyon Formation, the Bauers Tuff Member of the Condor Canyon Formation, and the Harmony Hills Tuff. The Wah Wah Springs Formation is a dacitic, moderately welded, simple cooling ash-flow tuff (Anderson and Rowley, 1975) dated at 29.5 Ma (Best and Grant, 1987); it is as much as 120 m thick in the Red Hills (Maldonado and Williams, 1993a) and as much as about 90 m thick on the Markagunt Plateau. The Lund Formation is composed of a dacitic, moderately welded, simple cooling ash-flow tuff unit dated at 27.9 Ma (Best and Grant, 1987). The formation is about 60 m thick in the Red Hills (Maldonado and Williams, 1993a) but has not been recognized on the Markagunt Plateau. The Blue Meadows Tuff Member is a densely welded, simple cooling ash-flow tuff unit about 75 m thick (Judy, 1974) that is restricted to parts of the Markagunt Plateau and is not found west of the plateau (Anderson and Rowley, 1975). The Baldhills Tuff Member is composed of numerous densely welded trachytic ash-flow tuff units dated at about 27 Ma (Best, Christiansen, and Blank, 1989); locally it may be as much as 250 m thick. The Leach Canyon Formation (Williams, 1967) is composed of poorly to partly welded rhyolitic ash-flow tuff dated at 24.7 Ma by Armstrong (1970), but an average age of 24 Ma has been suggested by Rowley and others (1994). The formation is as much as 120 m thick in the Red Hills area (Maldonado and Williams, 1993a) and from about 20 to 50 m thick in the western Markagunt Plateau. The Bauers Tuff Member is composed of densely welded rhyolite ash-flow tuff, dated at 22.8 Ma by Best, Christiansen, and others (1989), but an average age of 22.3 Ma has been suggested by Rowley and others (1994). The member is as much as 15 m thick (Maldonado and Moore, 1993). The Harmony Hills Tuff is composed of moderately welded trachyandesite to andesite ash-flow tuff dated at 22.5–22 Ma (Rowley and others, 1989) and is as much as 15 m thick.

The volcanic and volcaniclastic sedimentary rocks derived from the Marysvale volcanic field include part of the Bear Valley Formation and Mount Dutton Formation. The Bear Valley Formation was described by Anderson (1971) and is composed mostly of crossbedded tuffaceous sandstone; locally it includes intercalated conglomerate, volcanic mud-flow breccia, and tuffs. The tuffaceous sandstones of eolian origin were transported north-northeastward, derived from a south-southwestern source (Anderson, 1971), but the intercalated rocks were probably derived from the Marysvale volcanic field. The unit has been dated at 25–24 Ma (Fleck and others, 1975); it is as much as 190 m thick in the Red Hills area (Maldonado and Williams, 1993b) and about 150 m thick in the northern part of the study area. In the Red Hills it overlies the Baldhills Tuff Member and underlies the Leach Canyon Formation. The Mount Dutton Formation was named by Anderson and Rowley (1975) for stratovolcano deposits that form the southern flank of the Marysvale field north of the study area. There, the tuffs from the Great Basin sources are reported to intertongue locally with the Mount Dutton Formation (Rowley and others, 1994), but that relationship has not been verified in the study area. In the study area, the formation comprises mainly volcanic mudflow breccia and intermediate-composition lava and lava-flow breccia. The formation had been dated at 26–21 Ma (Anderson and Rowley, 1975), but recently Rowley and others (1994) have indicated an age of 34–21 Ma. A unit mapped locally on the Markagunt Plateau by Maldonado and Moore (1993) as "mudflow and lava-flow breccia and tuffaceous sandstone" contains individual blocks as much as 200 m in length of Wah Wah Springs and Isom Formations. This unit overlies the Baldhills Tuff Member and underlies the Bauers Tuff Member; thus it occupies the same stratigraphic position as the Bear Valley and part of Mount Dutton Formations. The mudflow-breccia, however, contains clasts that resemble rocks of the much younger Iron Peak intrusive described in the next section.

TERTIARY INTRUSIVE AND QUATERNARY BASALTIC ROCKS

Tertiary intrusive rocks consist of the Iron Peak laccolith and numerous mafic dikes. The Iron Peak laccolith is gabbroic in composition and was described by Anderson (1965), Judy (1974), and Spurney (1984), and dated at about 20 Ma (Fleck and others, 1975, age corrected for new decay constants of Steiger and Jäger, 1977). It is found in the northeastern part of the study area where it intrudes the Brian Head Formation along the Red Hills shear zone (Maldonado, 1995). The mafic dikes are mostly on the southwest to northwest sides of the Iron Peak laccolith, although some occur on the southeast. The dikes extend out into the country rock several kilometers from the laccolith, where they intrude a northwest-trending fault set mapped by Anderson (1965) and locally crosscut the Red Hills shear zone (Maldonado, 1995). These dikes have been dated at about 20 Ma using the K-Ar method (H.H. Mehnert and R.E. Anderson, written commun., 1988), the similarities in ages and composition of the laccolith and dikes suggesting that they are derived from the same magma.

Basaltic rocks of Pleistocene age occur as lava flows, cinder cones, cinder vents, and dikes and are the youngest volcanic rocks in the area.

STRUCTURAL FEATURES

The western Markagunt Plateau contains the following major Tertiary structures: (1) low-angle faults; (2) a thrust fault associated with a monoclinal fold; and (3) anastomosing high-angle faults bounding horsts and grabens.

LOW-ANGLE FAULTS

We recognize three types of low-angle faults in the study area: (1) an older fault zone, referred to as the Red Hills shear zone; (2) a set of younger faults in Tertiary volcanic and volcaniclastic rocks; and (3) a set of faults inferred to be of Tertiary age in Mesozoic and Tertiary sedimentary rocks.

RED HILLS SHEAR ZONE

The Red Hills shear zone was first described in the Red Hills, about 10 km northwest of Parowan (fig. 1): it is interpreted as a Miocene low-angle fault that extends into the Markagunt Plateau (Maldonado and others, 1989; Maldonado, Sable, and J.J. Anderson, 1992; Maldonado, 1995). The fault zone has detached an upper plate composed of Oligocene and Miocene volcanic and volcaniclastic rocks from an underlying lower plate of Eocene and Oligocene Brian Head Formation and older rocks. In some areas, the top of the shear zone is at the top of the Brian Head Formation; in other areas, the shear zone occurs stratigraphically lower in the upper part of the Brian Head Formation. Because of this complicated relation, the shear zone is shown as a single fault (pl. 1), arbitrarily placed between the Brian Head Formation and the overlying volcanic rocks. The zone appears to be localized in structurally incompetent tuffaceous sandstones of the Brian Head. It is characterized, at least locally, by pulverized rock and by truncation, thinning, or omission of strata both above and below the zone. The detached upper plate has been pervasively fractured and faulted (fig. 2); breakage of the upper plate formed bedding plane faults that emplaced sheets of rocks and (or) high-angle faults that shed blocks from their scarps forming megabreccia deposits.

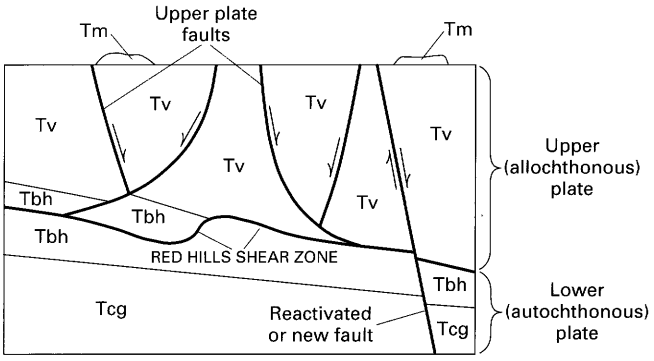

Figure 2. Schematic relationships of gravity-slide blocks (Tm), upper and lower plates, separated by the Red Hills shear zone, and reactivated upper plate faults or new faults. Tv, Tertiary volcanic rocks undivided; Tbh, Brian Head Formation; Tcg, Claron and Grand Castle Formations. Light line, contact; heavy line, fault; barbs show direction of relative movement.

Deformation on the shear zone is bracketed between 22.5 and 20 Ma (Maldonado, 1995): the detached upper plate rocks are as young as 22.5 Ma, and they are intruded by 20-Ma mafic dikes. Possible mechanisms for formation of the shear zone include regional tilting as a consequence of magmatic intrusion and block rotation associated with early regional extension (Maldonado, 1995).

FAULTS IN TERTIARY VOLCANIC AND VOLCANICLASTIC ROCKS

Low-angle faults in Tertiary volcanic rocks are found in three areas: (1) about 4 km south of Parowan along the plateau front; (2) due east of Parowan along the plateau front; and (3) east of the plateau front from 9 to 13 km east and northeast of Cedar City and north of Cedar Canyon.

The low-angle fault south of Parowan underlies an extremely brecciated block approximately 8 km long and 2 km wide. This block is composed of Brian Head Formation and two Tertiary volcanic units—the Isom Formation and a "mudflow and lava-flow breccia and tuffaceous sandstone"

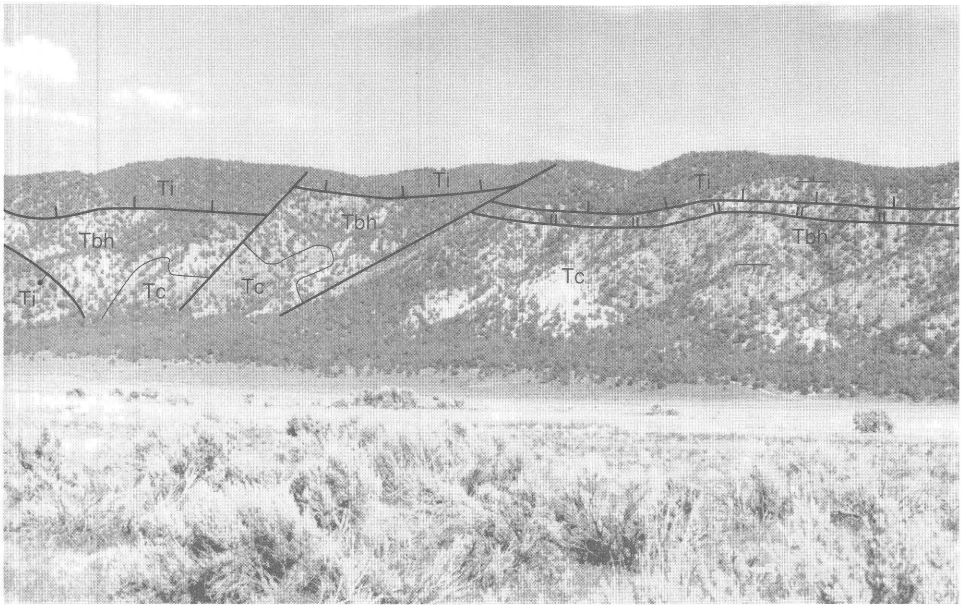

Figure 3. Low-angle faults along western Markagunt Plateau front just east of Parowan. View looking east from Parowan. Ti, Isom Formation; Tc, Claron Formation; Tbh, Brian Head Formation. Dip direction in Tc and Ti shown by strike and dip symbol. Single hachured line, Red Hills shear zone; double hachured line, younger low-angle fault. Bar and ball on downdropped side of normal fault.

unit (Maldonado and Moore, 1993). The block locally contains the Red Hills shear zone and overlies and truncates a thrust fault (described in the section, "Thrust-fault Zone and Monoclinal Fold"). East of this area, the block is downdropped by a younger high angle fault.

The low-angle fault east of Parowan is probably the same age as the one just described. Here, however, the low-angle fault (fig. 3) becomes steeper southward along strike (fig. 4), suggesting rotation of the block containing the fault. This supposition is confirmed by rotation of bedding attitudes. To the east, the block is downdropped by a younger high angle fault, like the block south of Parowan.

Farther south, possible low-angle faults east of the plateau front are present at Dairy Hill, Eagle Peak, and High Mountain (F, G, and H, respectively, on pl. 1). At High Mountain, the strata below the postulated fault are a normal succession of Claron, Brian Head, Needles Range, Isom, and Leach Canyon units; poorly exposed rocks interpreted to be Brian Head strata and Isom Formation overlie this succession. Similar relationships characterize the Eagle Peak (G) and Dairy Hill (F) blocks, but the Dairy Hill strata overlying the postulated fault include the Bauers Tuff Member of the Condor Canyon Formation and the Harmony Hills Tuff. At all three areas, the low-angle relationships are truncated by high-angle faults. The interpretation of low-angle faulting in these three areas is equivocal because of the poor exposures. Another plausible interpretation of these relationships is that the upper unit believed to be the Brian Head Formation may in reality be a younger unit of sedimentary rock and mudflow overlain by, or incorporating, allochthonous Isom Formation rocks. In part, they may also represent graben-fill deposits derived from adjoining horsts.

We postulate that all the low-angle faults in the Tertiary volcanic rocks are slightly younger than 20 Ma. All are older than the high-angle faults, which truncate them. The high-angle faults are younger than about 20 Ma because they cut the 20-Ma Iron Peak laccolith and associated dikes (pl. 1). We interpret the low-angle faults as very slightly younger than the laccolith, because we postulate that some of them may have formed as a consequence of doming due to intrusion of the laccolith.

FAULTS IN MESOZOIC AND TERTIARY SEDIMENTARY ROCKS

In the Coal Creek area, just east of Cedar City (fig. 1), Averitt (1962) and Averitt and Threet (1973) mapped the contact between the Middle Jurassic Carmel Formation and the Upper Cretaceous Dakota Formation as an unconformable contact. We suggest, however, that it may in part be a low-angle fault that decoupled along gypsiferous beds of the Carmel Formation. The suspected fault is probably located within gypsiferous beds of the Carmel Formation, but on plate 1 the fault is arbitrarily shown along the Dakota-Carmel Formation contact. The age of the fault is at least Cretaceous, but a Tertiary age is inferred here because of the abundance of Tertiary low-angle faults in the area. Although

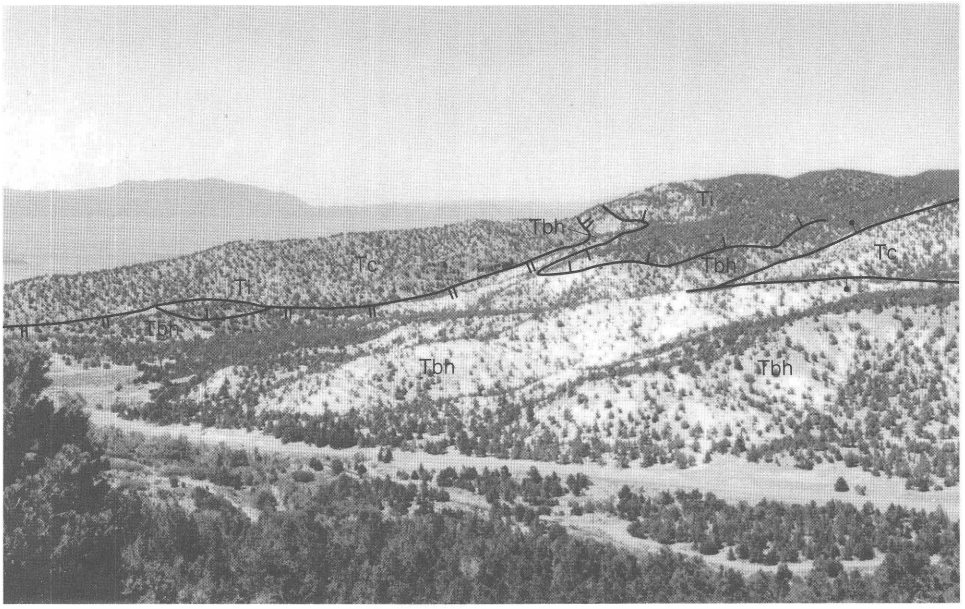

Figure 4. East side of area shown on photograph of figure 3 of the same younger low angle fault and Red Hills shear zone. View northwest from State Highway 143. Ti, Isom Formation; Tc, Claron Formation; Tbh, Brian Head Formation; single hachured line, Red Hills shear zone; double hachured line, younger low-angle fault. Dip attitude of younger low-angle fault steepens in this area. Bar and ball on downdropped side of normal fault.

the suspected fault occurs along or near the stratigraphic contact, numerous folds (fig. 5, pl. 1) in the Jurassic rocks below the suspected fault contrast with the essentially flat lying Cretaceous rocks above. The Cretaceous units do, however, form a northwest-dipping monocline northeast of Coal Creek (see next section). The folds in the Coal Creek area have generally been considered to be of Laramide age; regionally, they are considered part of the Kanarra fold (Gregory and Williams, 1947), which is an anticline partly exposed along the Hurricane Cliffs 15 km south of Cedar City. Threet (1963) interpreted the folds in the Jurassic rocks as disharmonic folds genetically related to the Kanarra fold, but he also stated that some geologists have suggested the folds to be Cenozoic. The relation of these folds to Tertiary structures is discussed in the thrust-fault zone section.

In the eastern part of Cedar Canyon, near the southeast corner of the area of plate 1, we have observed low-angle fault surfaces within the Claron Formation (fig. 6), but we have not shown them on plate 1 because our mapping to 1995 has been cursory there. Brecciated Claron Formation and low-angle faults have also been observed in the upper reaches of the Second Left Hand Canyon area (fig. 7; E on pl. 1). The age of these faults is unknown: whereas some of the low-angle faults described previously displaced stratigraphically younger Tertiary volcanic units, these faults displaced stratigraphically older Tertiary sedimentary units. These low-angle faults may have formed due to intrusion of the Iron Peak laccolith or other unexposed intrusions, as suggested for faults described previously.

THRUST-FAULT ZONE AND MONOCLINAL FOLD

We have mapped three separate thrust faults along the western margin of the Markagunt Plateau as segments of a single zone, herein termed the Parowan thrust-fault zone (Maldonado, Sable, and R.E. Anderson, 1992; Sable and Maldonado, unpub. data, 1991). The northern segment, about 4 km southwest of Parowan (pl. 1), places Cretaceous Iron Springs Formation (fig. 8) and locally Paleocene Grand Castle Formation over the Paleocene-Eocene Claron Formation (fig. 9). The upper plate of this segment contains Cretaceous sedimentary rocks and Tertiary volcanic and sedimentary rocks, and locally includes the Red Hills shear zone. The thrust fault is broken by tear faults, and is characterized by gouge along its plane. In its northern part, it dips about 35°, but it steepens southward, where it is truncated by a high-angle fault. The middle segment, about 3 km southeast of Summit, resembles the northern segment. The southern segment is about 4 km southeast of Enoch. The upper plate of this segment also contains Cretaceous Iron Springs Formation and Tertiary sedimentary rocks, but in contrast to the other segments, the lower plate is composed of Tertiary volcanic rocks (Isom and Leach Canyon Formations, Bauers Tuff Member, and Harmony Hills Tuff) (E.G. Sable, unpub. mapping, 1992) as well as older sedimentary rock units.

The Parowan thrust-fault zone appears to be consistently associated with a monocline, which we interpret as a northeastward continuation of the "Parowan monocline"

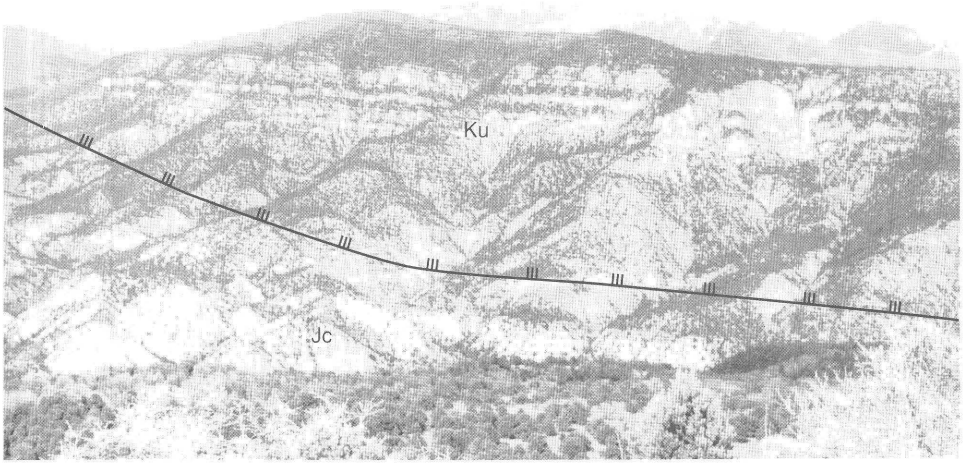

Figure 5. Proposed low-angle fault (hachured line) between flat-lying Cretaceous rocks above and folded Jurassic rocks below, in Coal Creek east of Cedar City. View looking north across Coal Creek. Ku, Cretaceous rocks undivided (see pl. 1 for units); Jc, Carmel Formation.

identified by Threet (1963) near Cedar City. Anderson and Christenson (1989) later called it the "Cedar City–Parowan monocline." At Cedar City, the monocline exhibits at least 300 m of structural relief. Northeast of Cedar City, the monocline is not as apparent, so it is not shown on plate 1; but on the basis of consistent northwest dips there, we infer a northeastward continuation of the monocline along the front of the Markagunt Plateau almost to Parowan, like that shown by Anderson and Christenson (1989, pl. 1). The monocline is in Cretaceous and Tertiary sedimentary rocks and is overlain and masked by volcanic rocks in the upper plate of one of the low-angle faults described previously. (See section *B–B'*, pl. 1.) Threet (1952a, 1963) suggested that the Parowan monocline is a Neogene structural bridge between the Hurricane fault and the Paragonah fault (pl. 1) and may represent unfolding of the Kanarra fold. We agree with Threet (1963) that the monocline is Neogene or younger in age, but suggest that the West Red Hills fault (pl. 1) may actually represent the northern segment of the Hurricane fault because the West Red Hills fault has much greater displacement than the Paragonah fault. This is supported by drill-hole (Hansen and Scoville, 1955) and geophysical data (Blank and Kucks, 1989) that show a deeper graben beneath Cedar Valley relative to Parowan Valley.

A south-vergent thrust-fault system in the Bryce Canyon area about 50 km east of the study area (fig. 1 of this report) involves the same sedimentary rock units as those in the Parowan thrust-fault zone (Davis and Krantz, 1986; Lundin, 1989; Merle and others, 1993). There, the youngest unit in the upper plate is the Claron Formation (Lundin, 1989). In general, the youngest unit in the upper plate in the Parowan thrust-fault zone is the Isom Formation (27 Ma); in its southern segment, the youngest unit in the lower plate is the Harmony Hills Tuff (22.5–22 Ma) (E.G. Sable, unpub. mapping, 1992). In addition, the upper plate of the northern segment contains the Red Hills shear zone (22.5–20 Ma). Thus, the Parowan thrust-fault zone is younger than 22.5 Ma. Merle and others (1993) suggested that the thrusting near Bryce Canyon occurred between 30 and 20 Ma. They and Davis and Rowley (1994) attributed the compressive stresses that formed the thrusts near Bryce Canyon to vertical crustal loading from volcanic rocks extruded from the Marysvale volcanic center, north of Bryce Canyon. Alternatively, they stated that thrusting may be due to southward compressive stresses during emplacement of underlying batholiths.

The faults of the Parowan thrust-fault zone may have formed by plutonic emplacement, as suggested for those faults near Bryce Canyon. Strikes of the faults of the two areas, however, are widely divergent, so it seems unlikely that the compressive stresses generated by intrusion were related to the same intrusive body. However, the presence of a buried intrusion under Parowan Valley that has been suggested (H.R. Blank, Jr., oral commun., 1990; Eppinger and others, 1990, p. 23) could explain the strikes and attitudes of the Parowan thrust faults. A quartz monzonite intrusive body that was penetrated in a drill hole in the southwestern Red Hills (Tompkins and others, 1963) may be part of the intrusive body inferred for the Parowan Valley.

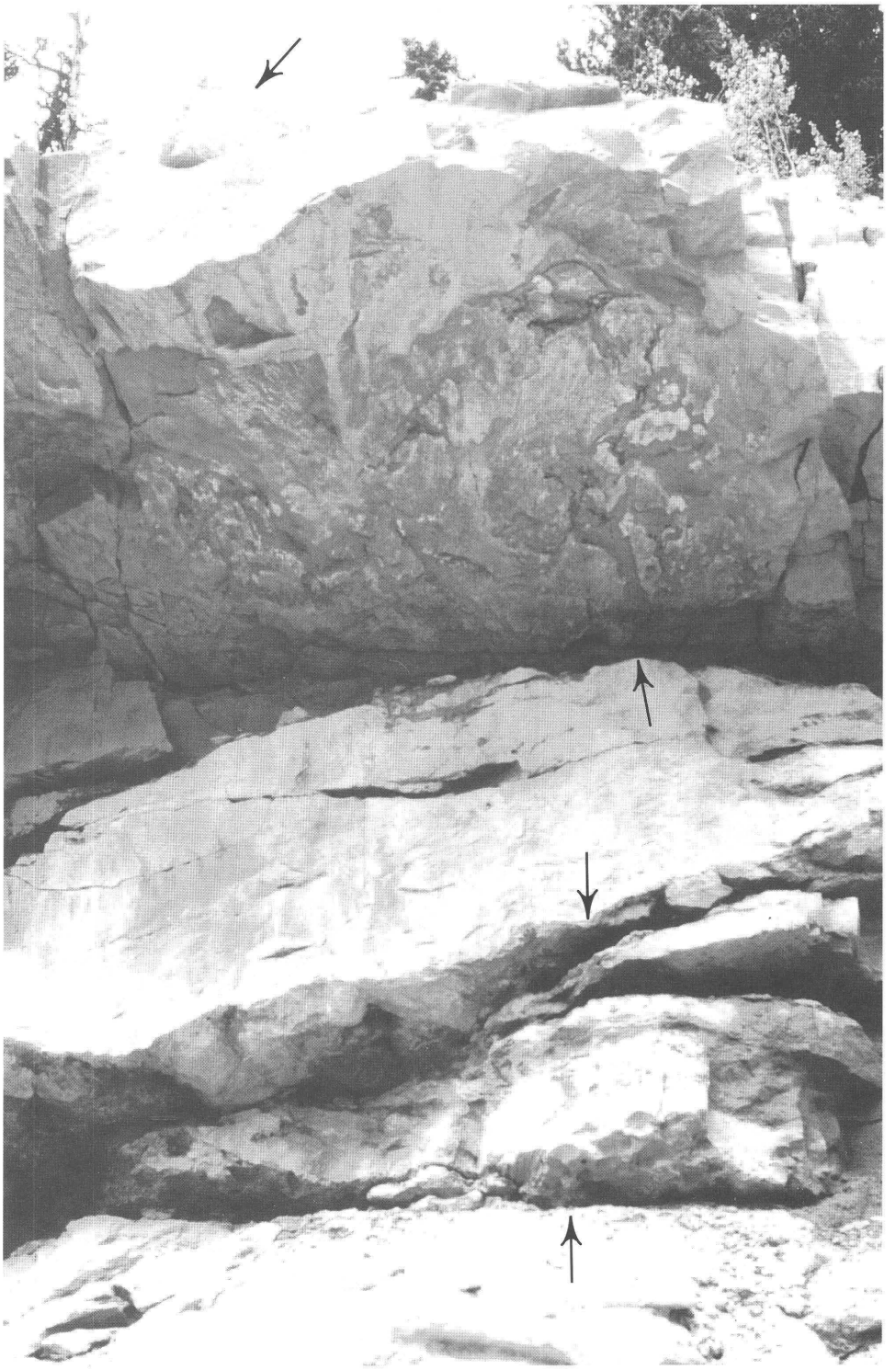

Figure 6. Low-angle faults (shown by arrows) in Claron Formation along north side of State Highway 14 in upper Cedar Canyon near southeast corner of area of plate 1. View looking north. Block at top of photograph (shown by arrow) approximately 1 m high for scale.

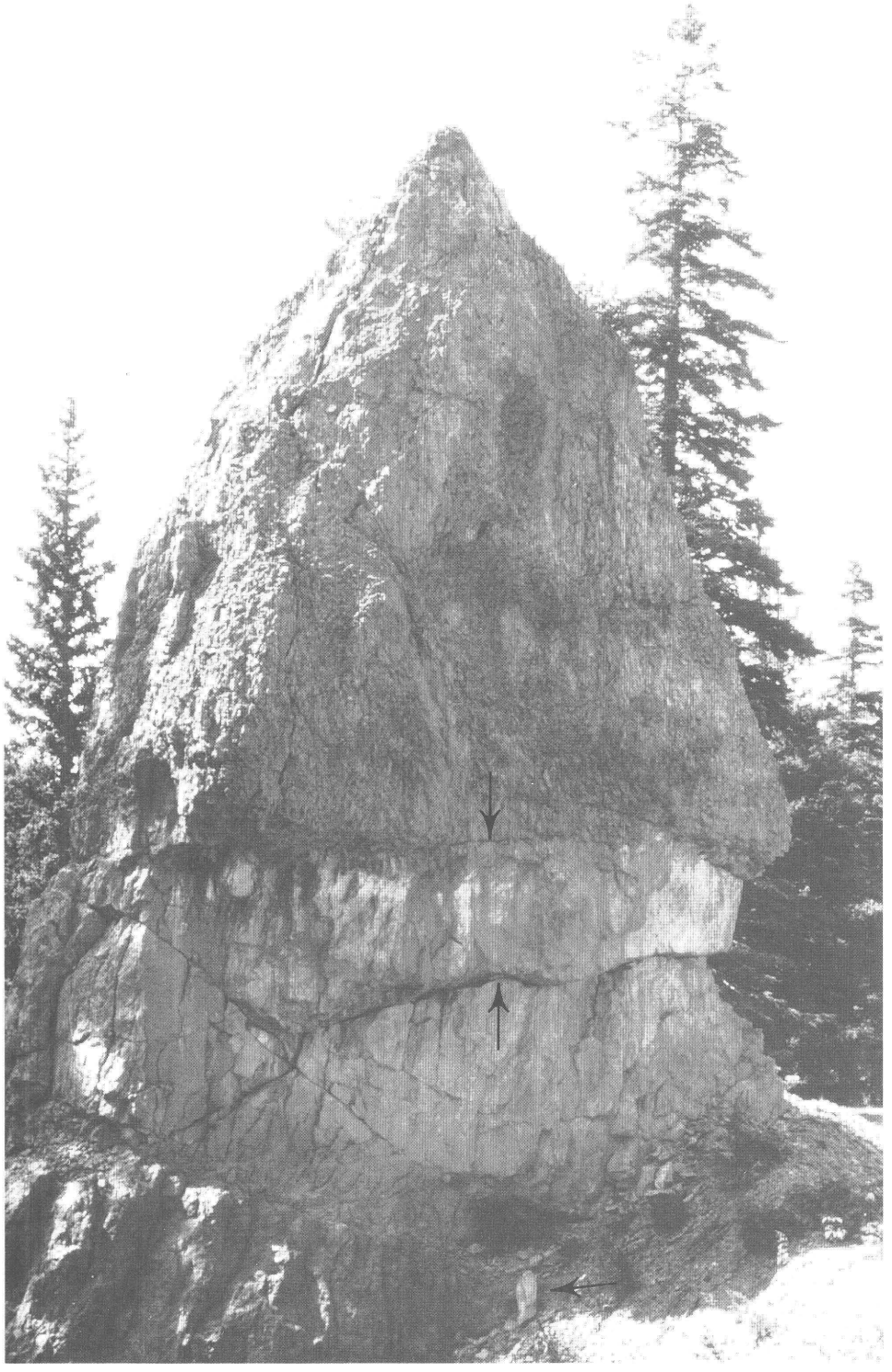

Figure 7. Brecciated Claron Formation with low-angle faults (shown by arrows) in upper reaches of Second Left Hand Canyon (location shown by E on pl. 1). Block at base of exposure (shown by arrow) approximately $^1/_2$ m high for scale.

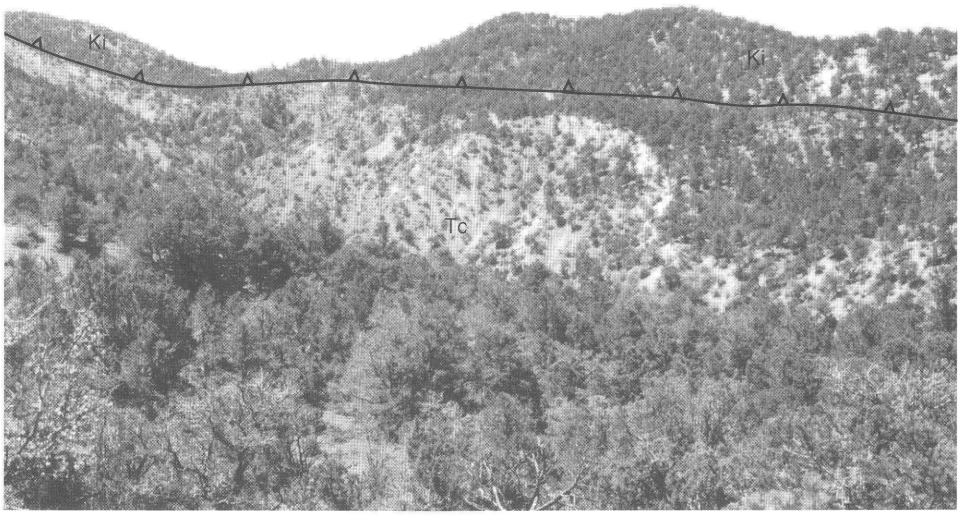

Figure 8. Parowan thrust-fault zone juxtaposing Cretaceous Iron Springs (Ki) over Tertiary Claron Formation (Tc). View looking southwest, from 4 km southwest of Parowan. Sawteeth on upper plate of thrust fault.

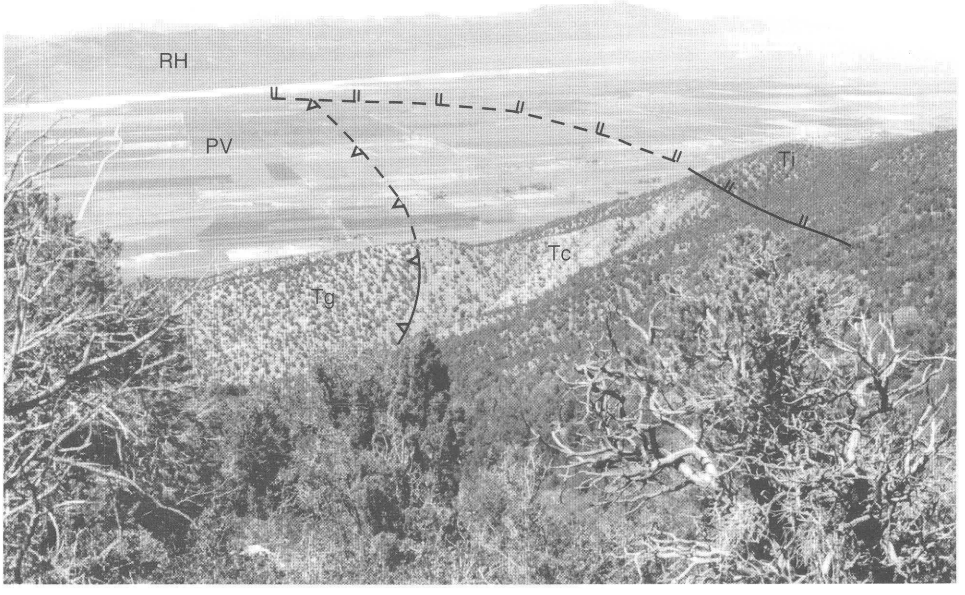

Figure 9. Parowan thrust-fault zone juxtaposing Grand Castle Formation (Tg) over Claron Formation (Tc), southwest of Parowan. Photograph taken north of that of figure 8, looking northwest. Younger low-angle fault to the north truncates thrust fault. Dashes are speculative extensions of faults into eroded area. Sawteeth on upper plate of thrust fault. Hachures on upper plate of low-angle fault. Ti, Isom Formation; PV, Parowan Valley; RH, Red Hills.

We suggest two other compressional models that may explain the Parowan thrust-fault zone. One includes eastward thrusting as an adjunctive effect of strike-slip movement along the plateau's western margin. Such movement has been reported by Anderson and Barnhard (1990) in the central Sevier Valley area, about 40 km northeast of the western Markagunt Plateau. Most of the rarely exposed fault planes in the western Markagunt and south along the Hurricane Cliffs, however, exhibit moderately dipping or vertical dip-slip features, although Anderson and Christenson (1989, p. 20) reported subhorizontal striations in the Braffits Creek area. The other model invokes simple reverse slip related to plateau front deformation on the developing limb of the previously described Cedar City–Parowan monocline.

A gravity-slide model rather than a compressional model may have produced the Parowan thrust-fault zone. Such a model seems unlikely; it would invoke westward horst-to-graben sliding of Cretaceous strata over Tertiary units, and of necessity would result in structural denudation of the Cretaceous rock sections exposed in the horsts along the plateau margin. However, no evidence supports such loss of section; the Cretaceous stratigraphic section is complete in the horsts east of the thrusts and on the main Markagunt Plateau farther east. Thus, eastward-directed stresses most likely resulted in the present structural configuration. A possibility that the blocks slid eastward from the Red Hills also seems unlikely in that the Cretaceous section there too seems complete; however, the Tertiary section is not totally complete in the southern part of the Red Hills.

We prefer a mechanism that confines thrusting to the edge of the plateau. Our provisional conclusion is that the displacement in Cretaceous and early Tertiary rocks in the upper plate of the Parowan thrust-fault zone may be the result of southeasterly-directed compressional stresses, probably resulting from intrusion of a hypabyssal igneous body. Easterly or southeasterly movement of the upper plate is suggested by small-scale shear displacements of some beds. We believe that a detailed search for slip-sense indicators, currently beyond the scope of our mapping, would probably resolve the question of eastward versus westward movement of the upper plate.

ANASTOMOSING HIGH-ANGLE FAULTS

The youngest and most obvious structures in the study area are high-angle faults that bound horsts and grabens and represent extension-related fragmentation of the plateau (fig. 10; pl. 1). In the southernmost part of the area, the faults that bound the grabens strike generally north; elsewhere, they strike more consistently northeast. These faults include both major and subsidiary faults that occur in fault blocks between the major bounding faults (discussed in last paragraphs of this section; fig. 14). The bounding faults have been described as en echelon by previous workers (Anderson, 1965; Moore, 1982), but our mapping suggests that these faults are anastomosing (pl. 1, and figs. 10, 11, 12). The faults localize some Pleistocene basaltic cinder cones, and the horst walls are characterized by lobe-shaped landslides. Within the grabens, Tertiary volcanic units are locally folded (pl. 1), their axes perpendicular to the bounding faults; this suggests some component of lateral translation along the faults.

The anastomosing fault pattern that characterizes the horst-and-graben system extends from the Cottonwood Mountain area in the north to the Coal Creek–Cedar Canyon area in the south (figs. 1, 10) and represents a network of branching and rejoining high-angle fault traces. Vertical displacements along individual faults change drastically within short distances along strike. Measured displacements along sections *A–A′* (Markagunt Plateau part) and *B–B′* (pl. 1) range from about 30 m on the minor faults to about 1,000 m.

In the central part of the horst-and-graben system (near section *B–B′*), many of the anastomosing faults merge towards the south. The faults that bound the Summit Mountain and Iron Peak grabens and the Parowan half graben (fig. 10) exhibit a very well exposed high-angle fault splay of perhaps 70 m displacement (fig. 13), exposed along Utah State Highway 14 in Cedar Canyon (fig. 1). Coal seams in the Upper Cretaceous Tropic Shale or Straight Cliffs Formation have been sheared or drawn out along this fault. The anastomosing fault pattern appears to end abruptly at about Coal Creek. This termination of the anastomosing pattern coincides with the southernmost extent of Oligocene-Miocene volcanic rocks (pl. 1). The southward merging of faults suggests that overall fault displacement decreases southward.

The maximum age of the high-angle faults is constrained by the youngest Tertiary rocks cut by the faults—the 20-Ma Iron Peak laccolith and associated 20-Ma mafic dikes (pl. 1). The dikes fill a north- to northwest-striking fracture system (Anderson, 1965) west of the Iron Peak laccolith (pl. 1) and probably formed during emplacement of the laccolith. The faults cut the laccolith and related dikes and are therefore younger than 20 Ma; some may have remained active into the Pleistocene (Anderson and Christenson, 1989). Anderson (1985, 1988) has presented evidence from the northern Markagunt Plateau that west-northwest-striking faults formed about 26 Ma. These faults are present in the northeastern part of the area (Mortensen Canyon, location B on pl. 1), but they have not been recognized in the horst-and-graben area.

Several hypotheses for the origin of high-angle faults have been proposed. For the Sevier Plateau, east of the study area (fig. 1), Rowley (1968) has proposed (1) late Cenozoic wrench faulting; (2) late Cenozoic strike-slip movement on basement faults; and (3) late Cenozoic torsion. We interpret the faults in the Markagunt Plateau to be minor antithetic and synthetic faults associated with down-to-the-west movement along the three major faults, shown schematically in figure 14. The minor faults are thought to have formed as a result of shallow collapse along the major faults, which are, from east to west, the Black Ledge fault, Paragonah fault, and West Red Hills fault (figs. 10, 14, pl. 1). The major faults bound the widest grabens; the minor faults bound narrower grabens and half grabens (fig. 14). The Black Ledge fault,

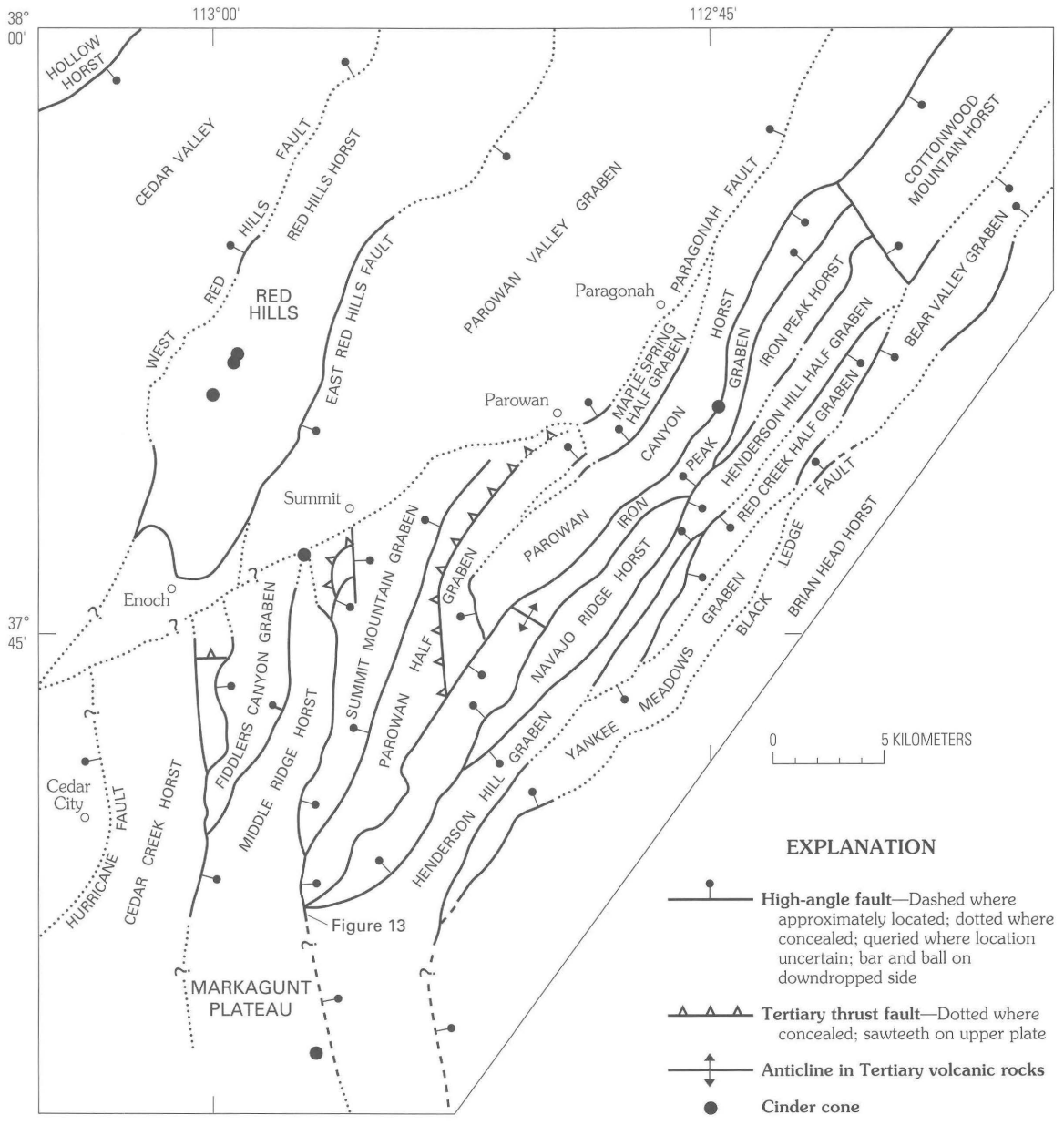

Figure 10. Map showing major faults, horsts and grabens, and half grabens, Red Hills–western Markagunt Plateau.

which bounds the east side of the Yankee Meadows graben in the eastern part of the study area, appears to control this style of deformation there: we attribute the minor faults to downdropping of blocks towards the graben center (fig. 14). East of the Black Ledge fault (east of map area), grabens are present but not as abundant, and the pattern of anastomosing faults has not been observed there. In the western part of the study area, near the edge of the plateau front, the structures are mostly half grabens, and there, the structures may have formed due to movement of the Paragonah fault zone.

We propose two hypotheses that are different from those of Rowley for the origin of the high-angle faults. The horsts and grabens formed as a consequence of movement along two major faults, the Black Ledge fault and Paragonah fault. Within the study area, the West Red Hills fault bounds the horst-and-graben system on the west. The graben-bounding faults may be related not to the Black Ledge fault but rather to the breaking away of the Red Hills from the Markagunt Plateau along the Paragonah fault. This proposed deformation, our preferred hypothesis, formed the Parowan Valley and resulted in loss of lateral support, allowing blocks to extend towards the Parowan Valley, forming horst and graben structures as far east as the Black Ledge fault.

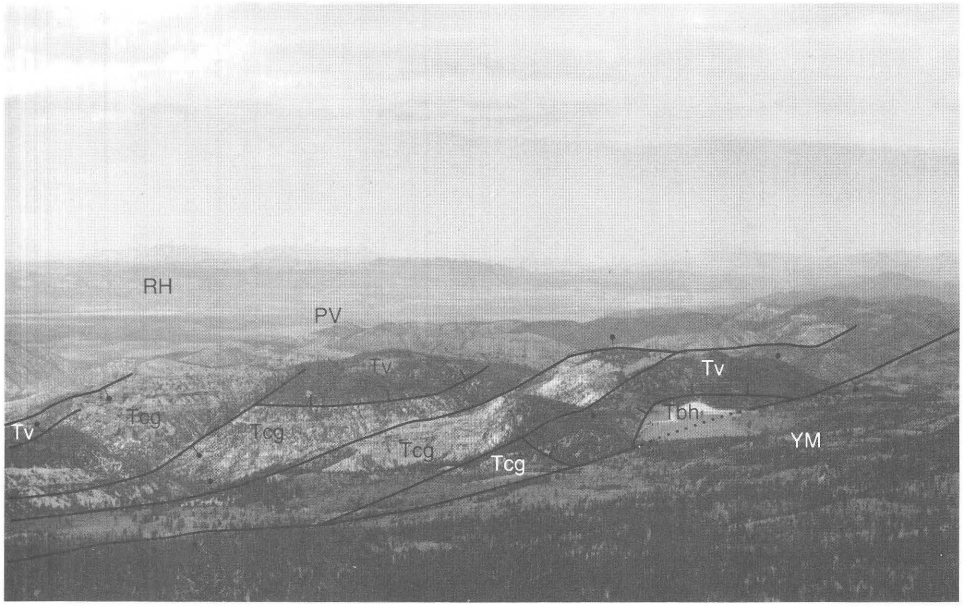

Figure 11. Horst and graben and half graben complex; view looking northwest towards Parowan Valley. Tv, Tertiary volcanic rocks undivided; Tbh, Brian Head Formation; Tcg, Claron and Grand Castle Formations; hachured line, Red Hills shear zone. Bar and ball indicate high-angle fault; dotted where concealed, bar and ball on downdropped side; YM, Yankee Meadows; PV, Parowan Valley; RH, Red Hills.

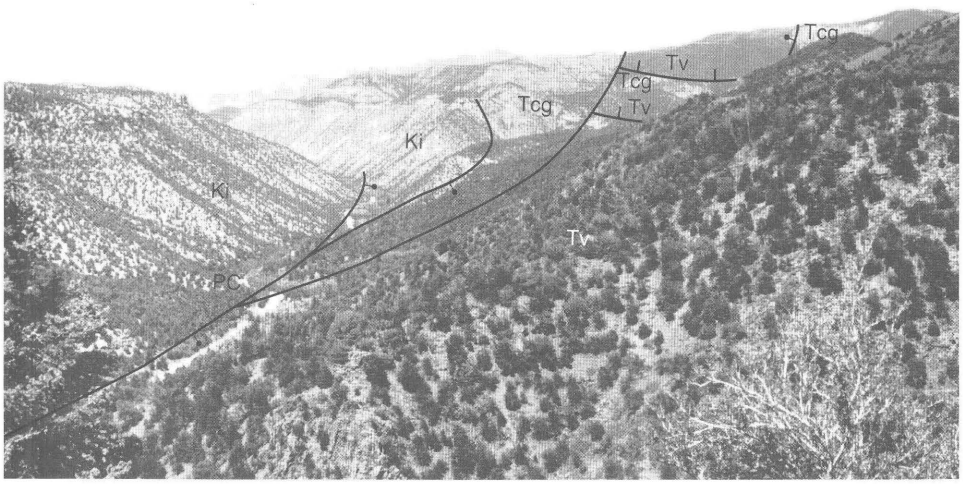

Figure 12. Merging high-angle faults that bound half grabens and graben; view looking north from Parowan Canyon. Tv, Tertiary volcanic rocks undivided; Tcg, Claron and Grand Castle Formations; Ki, Iron Springs Formation; hachured line, Red Hills shear zone. Bar and ball indicate high-angle normal fault; bar and ball on downdropped side. PC, Parowan Canyon.

Figure 13. Fault in Cedar Canyon, east of Cedar City, at intersection of faults that bound Summit Mountain graben, Parowan half graben, and Iron Peak graben to the north (fig. 10). Location of photograph shown on fig. 10. C, coal seam; K, Cretaceous strata of Tropic Shale or Straight Cliffs Formation (E.G. Sable, unpub. data, 1992). Bush (arrow) is approximately $^1/_2$ m high.

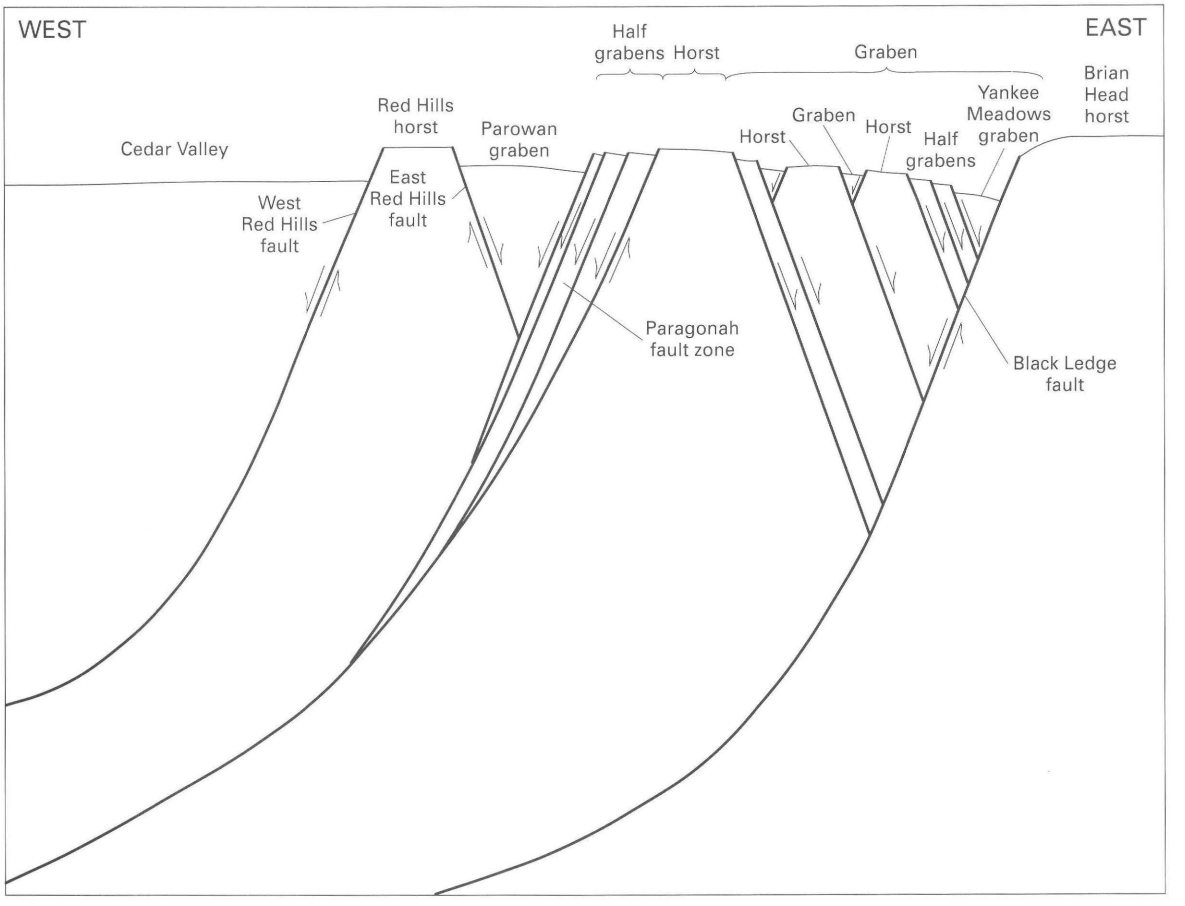

Figure 14. Speculative fault model showing possible propagation of secondary faults above major faults resulting in horsts and grabens and half grabens. Sketch not to scale.

FEATURES RELATED TO STRUCTURAL DEFORMATION

TERTIARY MEGABRECCIA DEPOSITS

Megabreccia deposits in and near the Markagunt Plateau have been described by Judy (1974), Sable and Anderson (1985), Maldonado, Sable, and J.J. Anderson (1992), Maldonado (1995), and in detail, by Anderson (1993), who named them the Markagunt megabreccia. The deposits are widespread (pl. 1) but discontinuous. They are composed of numerous allochthonous blocks of Tertiary volcanic and sedimentary rocks as much as 2.5 km^2 in area and about 100 m thick (Sable and Anderson, 1985), and that occur over an area of more than 1,000 km^2 (E.G. Sable, oral commun., 1993). Some are simple deposits composed of deformed monolithologic blocks; other deposits contain chaotically mixed polylithologic blocks. We interpret many of them to have resulted from gravity-sliding at different times by different mechanisms, but some of them may be the result of low-angle thrust faulting. They are discussed in more detail (Sable and Maldonado, chapter H) elsewhere in this volume. In that report, the authors describe several types of deposits of different origins and ages that have been generally lumped together by previous workers, and present evidence for transport directions of the widespread Markagunt megabreccia. The types of deposits and inferred mechanism for emplaced masses are as follows:

1. Individual blocks and smaller clasts that occur within rock units that are part of the "mudflow and lava-flow breccia and tuffaceous sandstone" unit (Maldonado and Moore, 1993). This type of megabreccia deposit may be related to seismicity during the period of volcanism and sedimentation that resulted in deposition of the unit. The unit is probably Oligocene in age, equivalent in part to the Mount Dutton or the Bear Valley Formations, as it overlies the Isom Formation and locally underlies the Bauers Tuff Member.

2. Deposits associated with the Red Hills shear zone of Maldonado and others (1989) and Maldonado, Sable, and J.J. Anderson (1992). The formation of some of these deposits has been interpreted to be synchronous with movement along the Red Hills shear zone (Maldonado and others, 1989; Maldonado, Sable, and J.J. Anderson, 1992; Maldonado, 1995); breakage of the upper plate formed bedding-plane faults that emplaced sheets of rocks and (or) high-angle faults that shed blocks of rocks from their scarps.

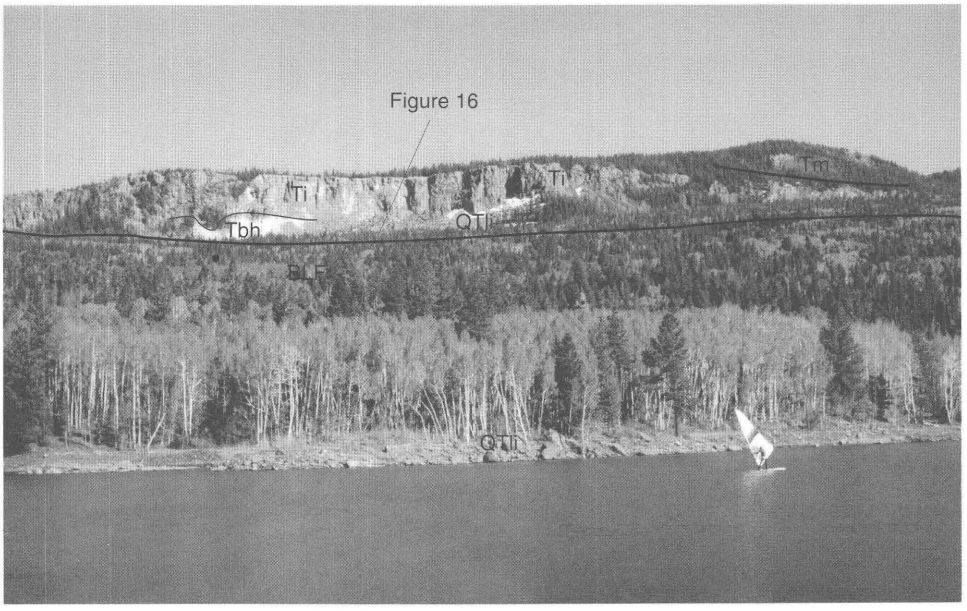

Figure 15. Landslide deposits (QTli) below the Black Ledge (made up mostly of Isom Formation) and mantling the Black Ledge fault (BLF) in Yankee Meadows graben near Yankee Meadows Reservoir. View looking east. Ti, Isom Formation; Tbh, Brian Head Formation; contact between them is shown; Tm, megabreccia deposit. Bar and ball on downdropped side of faults. Location of figure 16 shown. Wind surfer for scale.

Figure 16. Landslide block (QTli) at base of Black Ledge fault east of Yankee Meadows Reservoir. View looking northeast. Ti, Isom Formation; Tbh, Brian Head Formation.

3. Deposits related to high-angle fault scarps.

4. Deposits related to movement away from the Iron Peak laccolith or other Tertiary intrusive bodies that may underlie part of the area (Maldonado, 1995). This type of sliding has been described by Mackin (1960), Rowley and others (1989), and Blank and others (1992) in the Iron Springs mining district west-southwest of the Markagunt Plateau (fig. 1).

TERTIARY(?)-QUATERNARY LANDSLIDE DEPOSITS

Landslide deposits have in part probably resulted from seismic events; they are of two types: those of Pliocene(?) to Pleistocene age that occur in the eastern part of the study area and are composed generally of one type of clast, and those of Pliocene(?) to Pleistocene age that occur along the west edge of the Markagunt Plateau and are composed of multiple clast types. The landslides probably formed during continued deformation of the Markagunt Plateau.

The landslide deposits in the eastern part of the study area (unit QTli, pl. 1) are composed predominantly of the Isom Formation, mostly found just east of Yankee Meadows Reservoir within the Yankee Meadows graben (fig. 15). Similar but smaller landslide deposits are present south of Yankee Meadows and east of Cedar Breaks (Moore, 1992). The Yankee Meadows deposits are as much as 200 m thick and extend as much as 25 km along the graben margin. They formed by landslides that broke away from scarps along the entire length of the Black Ledge fault and along subsidiary parallel faults within the graben. All of these faults are post-20 Ma; some of them probably remained active into the Pleistocene and possibly later. Anderson (1993) included these deposits with the Markagunt megabreccia, but we interpret them as younger landslide blocks that formed along fresh fault scarps (fig. 16).

The landslide deposits that occur locally along the western margin of the Markagunt Plateau (unit QTl, pl. 1) include clasts derived from many rock units. Deposits east and northeast of Parowan (too small to show at the scale of pl. 1) generally exhibit an inverted stratigraphic succession, that is, debris derived from younger units was deposited first near the base of the deposit, and debris from older units was subsequently deposited towards the top. Some of these deposits may be the same as the deposits composed of scallop-shaped blocks bounded by faults that are found along the plateau edge (described in the next section). These allochthonous blocks may reflect continued movement along the Paragonah fault and related faults.

BASALTIC VOLCANIC ROCKS AND THEIR RELATION TO NORMAL FAULTS

The youngest volcanic rocks in the western Markagunt Plateau and Red Hills are Quaternary basaltic rocks that form lava flows, cinder cones, and some dikes. A detailed discussion of their geochemistry and isotopic composition is presented by Nealey and others in this volume. The basaltic rocks are found in the southern Red Hills, Cinder Hill (location C on pl. 1), Water Canyon (location A), and Black Mountain (location I). The most prominent cinder cones in the study area are in the southern part of the Red Hills (Rowley and Threet, 1976; Maldonado and Sable, unpub. mapping, 1991). A single K-Ar date indicates that these cones formed at 1.3 Ma (Best and others, 1980). A cone at Cinder Hill about 2 km southwest of Summit formed between about 1.1 and 0.93 Ma (Anderson and Mehnert, 1979; Anderson and Bucknam, 1979), and the basalt of Water Canyon west of Parowan erupted from a cinder cone (Anderson and Christenson, 1989; Maldonado and Moore, 1993) at about 0.45 Ma (Fleck and others, 1975, age corrected for new decay constants of Steiger and Jäger, 1977). One of the largest cinder cones in the area formed between 0.87 and 0.80 Ma (Best and others, 1980) at Black Mountain, in the southern part of the study area. The K-Ar ages suggest an eastward (younging) migration of basaltic volcanism in Quaternary time, similar to that observed in the western Grand Canyon, San Francisco, and Springerville volcanic fields in southwestern Utah and northern Arizona (Best and Brimhall, 1974; Tanaka and others, 1986; Condit and others, 1989).

The location of some cinder cones is partly controlled by normal faults. Single cinder cones are located on or near high-angle faults on the western Markagunt Plateau, and a three-cone northeast alignment is also present near high-angle faults in the southern Red Hills. A basaltic vent complex composed of breccia and basaltic dikes is exposed in Second Left Hand Canyon (location D on pl. 1; fig. 17) near a high-angle fault. This exposure may be the remnants of a vent breccia with feeder dikes and may represent the lower parts of a cinder cone. In Water Canyon, a single cone and a feeder dike are located along a high-angle fault. The dike is on strike with the fault and probably intruded it (pl. 1).

The distribution of the lava flows indicates several periods of uplift for part of the western Markagunt Plateau. For example, the Water Canyon lavas flowed down a paleovalley (currently, Water Canyon) and out onto Parowan Valley just south of Paragonah (pl. 1). The presence of the lava flows in the paleovalley indicates that the western part of the plateau had already been uplifted when the lava flows were erupted. In addition, as the flows entered Parowan Valley, they flowed over a small scallop-shaped block of Claron Formation (included with unit Tcg on pl. 1) at the plateau edge. These types of blocks are found all along the lower

Figure 17. Basaltic dike and breccia complex in Second Left Hand Canyon that may represent remnants of a vent breccia with feeder dikes. View looking north. Qb, basaltic dike and breccia complex; Tc, Claron Formation; Tg, Grand Castle Formation; Ki, Iron Springs Formation.

parts of the plateau edge (pl. 1) and represent landslides or slide blocks that formed during continued deformation along the plateau edge prior to eruption of the lava flows, although some of these small outcrops do resemble parts of the Parowan thrust-fault zone. Both the block and the lava flows are offset by a fault on their west side (pl. 1), indicating recurrence of movement on the Paragonah fault and continued uplift of the western Markagunt Plateau.

SUMMARY AND CONCLUSIONS

The structures and related features described here represent continuous deformation from the Miocene into the Pleistocene. The history of deformation is summarized as follows:

1. The Red Hills shear zone, the oldest of the low-angle faults, formed 22.5–20 Ma. It may have formed by regional tilting as a consequence of magmatic intrusion and (or) of block rotation associated with early regional extension.

2. The Parowan thrust-fault zone along the western plateau front is younger than about 22.5 Ma and younger than the Red Hills shear zone. Although the zone is about the same age as the thrust complex near Bryce Canyon, we believe it formed by a mechanism that confines thrusting to the edge of the plateau. It may be a thrust fault related to a plutonic body under Parowan Valley and the southwestern Red Hills or to strike-slip faulting that formed thrusts along the plateau margin. We interpret the associated monoclinal fold as a continuation of the Parowan monocline exposed at Cedar City.

3. The low-angle faults displacing Tertiary volcanic and Tertiary and Mesozoic sedimentary rocks are mostly younger than both the Red Hills shear zone and the thrust faults, even though they also probably formed around 20 Ma, approximately coeval with intrusion of the Iron Peak laccolith and its associated dikes. Most of the low-angle faults are slightly younger than 20 Ma but are older than the high-angle faults, which truncate them. The age of the suspected low-angle fault in Mesozoic sedimentary rocks is inferred to be the same age as the low-angle faults in Tertiary volcanic and sedimentary rocks.

4. The high-angle faults that bound the horsts and grabens are the youngest faults in the area; they truncate the Red Hills shear zone, the thrust faults, and the low-angle faults. The high-angle faults are no older than about 20 Ma (they cut the 20-Ma Iron Peak laccolith and associated dikes), but they remained active into the Pleistocene. Most faults are minor antithetic and synthetic faults formed as a result of down-to-the-west movement along three major faults from east to west, the Black Ledge fault, Paragonah fault, and West Red Hills fault. The faults locally control the locations of some Pleistocene basaltic cinder cones.

5. The gravity-slide blocks are megabreccia deposits formed mostly during Miocene deformation. Some are interpreted to be remnants of blocks and (or) sheets from the upper plate of the Red Hills shear zone that separated during or shortly after emplacement of the upper plate. Widespread megabreccias on the Markagunt Plateau were formed during movement of allochthonous rocks away from intrusive bodies such as the Iron Peak laccolith.

6. Some landslides probably remained active into the Pleistocene and possibly later. They are localized along high-angle fault scarps and probably reflect continuing offset along those faults.

The structures in the study area may typify structures in other parts of the transition zone between the Basin and Range and the Colorado Plateaus provinces. The high-angle faults are for the most part minor antithetic and synthetic structures within larger structural blocks bounded by major high-angle faults. The low-angle faults formed in incompetent rocks—tuffaceous sandstones and gypsiferous beds—that served as decoupling horizons. The Red Hills shear zone, the other low-angle faults discussed previously, and the faults that bound gravity-slide blocks are all shallow features.

REFERENCES CITED

Anderson, J.J., 1965, Geology of northern Markagunt Plateau, Utah: Austin, Texas, University of Texas Ph. D. dissertation, 194 p.

———1971, Geology of the southwestern High Plateaus of Utah—Bear Valley Formation, an Oligocene-Miocene volcanic arenite: Geological Society of America Bulletin, v. 82, p. 1179–1205.

———1985, Mid-Tertiary block faulting along west and northwest trends, southern High Plateaus, Utah: Geological Society of America Abstracts with Programs, v. 17, no. 7, p. 513.

———1988, Pre-Basin-Range block faulting along west and northwest trends, southeastern Great Basin and southern High Plateaus: Geological Society of America Abstracts with Programs, v. 20, no. 3, p. 139.

———1993, The Markagunt megabreccia—Miocene gravity slide mantling the northern Markagunt Plateau, southwestern Utah: Utah Geological Survey Miscellaneous Publication 93-2, 37 p.

Anderson, J.J., Iivari, T.A., and Rowley, P.D., 1987, Geologic map of the Little Creek Peak quadrangle, Garfield and Iron Counties, Utah: Utah Geological and Mineral Survey Map 104, scale 1:24,000.

Anderson, J.J., and Rowley, P.D., 1975, Cenozoic stratigraphy of southwestern High Plateaus of Utah, *in* Anderson, J.J., Rowley, P.D., Fleck, R.J., and Nairn, A.E.M., Cenozoic geology of southwestern High Plateaus of Utah: Geological Society of America Special Paper 160, p. 1–51.

Anderson, R.E., and Barnhard, T.P., 1990, Neotectonic framework of the Central Sevier Valley area, Utah and its relationship to seismicity, *in* Gori, P.L., and Hays, W.W., eds. Assessment of regional earthquake hazards and risk along the Wasatch front, Utah: U.S. Geological Survey Bulletin 1500–F, p. F1–F47.

Anderson, R.E., and Bucknam, R.C., 1979, Map of scarps on unconsolidated sediments, Richfield 1°×2° quadrangle, Utah: U.S. Geological Survey Open-File Report 79-1236, 15 p.

Anderson, R.E., and Christenson, G.E., 1989, Quaternary faults, folds, and selected volcanic features in the Cedar City 1°×2° quadrangle, Utah: Utah Geological and Mineral Survey, Utah Department of Natural Resources Miscellaneous Publication 89-6, 29 p.

Anderson, R.E., and Mehnert, Harald, 1979, Reinterpretation of the history of the Hurricane fault in Utah: Rocky Mountain Association of Geologists–Utah Geological Association, 1979, Basin and Range Symposium, p. 145–173.

Armstrong, R.L., 1970, Geochronology of Tertiary igneous rocks, eastern Great Basin and Range Province, western Utah, eastern Nevada, and vicinity, U.S.A.: Geochimica et Cosmochimica Acta, v. 34, p. 203–232.

Averitt, Paul, 1962, Geology and coal resources of the Cedar Mountain quadrangle, Iron County, Utah: U.S. Geological Survey Professional Paper 389, 72 p.

Averitt, Paul, and Threet, R.L., 1973, Geologic map of the Cedar City quadrangle, Iron County, Utah: U.S. Geological Survey Quadrangle Map GQ–1120, scale 1:24,000.

Best, M.G., and Brimhall, W.H., 1974, Late Cenozoic alkalic basaltic magmas in the western Colorado Plateaus and the Basin and Range Transition Zone, U.S.A., and their bearing on mantle dynamics: Geological Society of America Bulletin, v. 85, p. 1677–1690.

Best, M.G., Christiansen, E.H., and Blank, R.H., Jr., 1989, Oligocene caldera complex and calc-alkaline tuffs and lavas of the Indian Peak volcanic field, Nevada and Utah: Geological Society of America Bulletin, v. 101, p. 1076–1090.

Best, M.G., Christiansen, E.H., Deino, A.L., Grommé, C.S., McKee, E.H., and Noble, D.C., 1989, Excursion 3A—Eocene through Miocene volcanism in the Great Basin of the Western United States: New Mexico Bureau of Mines and Mineral Resources Memoir 47, p. 91–133.

Best, M.G., and Grant, S.K., 1987, Stratigraphy of the volcanic Oligocene Needles Range Group in southwestern Utah and eastern Nevada, *in* Oligocene and Miocene volcanic rocks in the central Pioche-Marysvale igneous belt, western Utah and eastern Nevada: U.S. Geological Survey Professional Paper 1433–A, p. 1–28.

Best, M.G., McKee, E.H., and Damon, P.E., 1980, Space-time-composition patterns of late Cenozoic mafic volcanism, southwestern Utah and adjoining areas: American Journal of Science, v. 280, p. 1035–1050.

Blank, H.R., Jr., and Kucks, R.P., 1989, Preliminary aeromagnetic, gravity, and generalized geologic maps of the USGS Basin and Range–Colorado Plateau transition zone study area in southwestern Utah, southeastern Nevada, and northwestern Arizona: U.S. Geological Survey Open-File Report 89-432, 16 p., map scale 1:250,000.

Blank, H.R., Jr., Rowley, P.D., and Hacker, D.B., 1992, Miocene monzonitic intrusions and associated megabreccias of the Iron Axis region, southwestern Utah, *in* Wilson, J.R., ed., Field guide to geologic excursions in Utah and adjacent area of Nevada, Idaho, and Wyoming, Geological Society of America Rocky Mountain Section Meeting: Utah Geological Survey Miscellaneous Publications 92-3, p. 399–420.

Condit, C.D., Crumpler, L.S., Aubele, J.C., and Elston, W.E., 1989, Patterns of volcanism along the southern margin of the Colorado Plateau—The Springerville field: Journal of Geophysical Research, v. 94, p. 7975–7986.

Davis, G.H., and Krantz, R.W., 1986, Post-"Laramide" thrust faults in the Claron Formation, Bryce Canyon National Park, Utah: Geological Society of America Abstracts with Programs, v. 18, p. 98.

Davis, G.H., and Rowley, P.D., 1994, Miocene thrusting, gravity sliding, and near-surface batholithic emplacement, Marysvale volcanic field, southwestern Utah [abs.]: Eos, v. 74, no. 43, p. 647.

Eppinger, R.G., Winkler, G.R., Cookro, T.M., Shubat, M.A., Blank, H.R., Jr., Crowley, J.K., and Jones, J.L., 1990, Preliminary assessment of the mineral resources of the Cedar City 1°×2° quadrangle, Utah: U.S. Geological Survey Open-File Report OF-90-34, 142 p.

Fleck, R.J., Anderson, J.J., and Rowley, P.D., 1975, Chronology of mid-Tertiary volcanism in High Plateaus region of Utah, *in* Anderson, J.J., Rowley, P.D., Fleck, R.J., and Nairn, A.E.M., Cenozoic geology of southwestern High Plateaus of Utah: Geological Society of America Special Paper 160, p. 53–61.

Goldstrand, P.M., 1994, Tectonic development of Upper Cretaceous to Eocene strata of southwestern Utah: Geological Society of America Bulletin, v. 106, p. 145–154.

Gregory, H.E., 1945, Post-Wasatch Tertiary formations in southwestern Utah: Journal of Geology, v. 53, p. 105–115.

———1949, Geologic and geographic reconnaissance of eastern Markagunt Plateau, Utah: Geological Society of America Bulletin, v. 60, p. 969–998.

———1950, Geology of eastern Iron County, Utah: Utah Geological and Mineral Survey Bulletin 37, 153 p.

Gregory, H.E., and Williams, N.C., 1947, Zion National Monument: Geological Society of America Bulletin v. 58, p. 211–244.

Hansen, G.H., and Scoville, H.C., 1955, Drilling records for oil and gas in Utah: Utah Geological and Mineralogical Survey Bulletin 50, 110 p.

Iivari, T.A., 1979, Cenozoic geologic evolution of the east central Markagunt Plateau, Utah: Kent, Ohio, Kent State University M.S. thesis, 154 p.

Judy, J.R., 1974, Cenozoic stratigraphic and structural evolution of the west-central Markagunt Plateau, Utah: Kent, Ohio, Kent State University M.S. thesis, 107 p.

Lundin, E.R., 1989, Thrusting of the Claron Formation, the Bryce Canyon region, Utah: Geological Society of America Bulletin, v. 101, p. 1038–1050.

Mackin, J.H., 1960, Structural significance of Tertiary volcanic rocks in southwestern Utah: American Journal of Science, v. 258, no. 2, p. 81–131.

Maldonado, Florian, 1995, Decoupling of mid-Tertiary rocks, Red Hills–western Markagunt Plateau, southwestern Utah, Chapter I *in* Scott, R.B., and Swadley, W C, eds., Geologic studies in the Basin and Range–Colorado Plateau transition in southeastern Nevada, southwestern Utah, and northwestern Arizona, 1992: U.S. Geological Survey Bulletin 2056, p. 233–254.

Maldonado, Florian, and Moore, R.C., 1993, Preliminary geologic map of the Parowan Quadrangle, Iron County, Utah: U.S. Geological Survey Open-File Report 93-3, scale 1:24,000.

Maldonado, Florian, Sable, E.G., and Anderson, J.J., 1989, Evidence for shallow detachment faulting of mid-Tertiary rocks, Red Hills (Basin and Range), with implications for a more extensive detachment zone in the adjacent Markagunt Plateau (Colorado Plateau), southwest Utah [abs.]: Eos, v. 70, no. 43, p. 1336.

———1992, Evidence for a Tertiary low-angle shear zone, Red Hills, Utah, with implications for a regional shear zone in the adjacent Colorado Plateau, *in* Engineering and environmental geology of southwestern Utah: Utah Geological Association Publication 21, 1992 Field Symposium, p. 315–323.

Maldonado, Florian, Sable, E.G., and Anderson, R.E., 1992, Tertiary thrust(?) faults, Parowan-Summit area, Markagunt Plateau, southwestern Utah [abs.]: Eos, v. 71, no. 43, p. 574–575.

Maldonado, Florian, and Williams, V.S., 1993a, Geologic map of the Parowan Gap quadrangle, Iron County, Utah: U.S. Geological Survey Geologic Quadrangle Map GQ–1712, scale 1:24,000.

———1993b, Geologic map of the Paragonah quadrangle, Iron County, Utah: U.S. Geological Survey Geologic Quadrangle Map GQ–1713, scale 1:24,000.

Merle, O.R., Davis, G.H., Nickelsen, R.P., and Gourlay, P.A., 1993, Relation of thin-skinned thrusting of Colorado Plateau strata in southwestern Utah to Cenozoic magmatism: Geological Society of America Bulletin, v. 105, p. 378–398.

Moore, R.C., 1982, The geology of a portion of the west-central Markagunt Plateau, southwestern Utah: Kent, Ohio, Kent State University M.S. thesis, 72 p.

Moore, D.W., 1992, Origin of breccia of the Isom Formation near Cedar Breaks National Monument, Markagunt Plateau, southwestern Utah: Geological Society of America Abstracts with Programs, v. 24, no. 6, p. 1992.

Mullett, D.J., 1989, Interpreting the early Tertiary Claron Formation of southern Utah: Geological Society of America Abstracts with Programs, v. 2, no. 5, p. 120.

Mullett, D.J., Wells, N.A., and Anderson, J.J., 1988, Unusually intense pedogenic modification of the Paleocene-Eocene Claron Formation of southwestern Utah: Geological Society of America Abstracts with Programs, v. 20, no. 3, p. 217.

Rowley, P.D., 1968, Geology of the southern Sevier Plateau, Utah: Austin, Texas, University of Texas Ph. D. dissertation, 340 p.

Rowley, P.D., McKee, E.H., and Blank, R.H., Jr., 1989, Miocene gravity slides resulting from emplacement of the Iron Mountain Pluton, southern Iron Springs mining district, Iron County, Utah [abs.]: Eos, v. 70, no. 43, p. 1309.

Rowley, P.D., Mehnert, H.H., Naeser, C.W., Snee, L.W., Cunningham, C.G., Steven, T.A., Anderson, J.J., Sable, E.G., and Anderson, R.E., 1994, Isotopic ages and stratigraphy of Cenozoic rocks of the Marysvale volcanic field and adjacent areas, west-central Utah: U.S. Geological Survey Bulletin 2071, 75 p.

Rowley, P.D., and Threet, R.L., 1976, Geologic map of the Enoch quadrangle, Iron County, Utah: U.S. Geological Survey Geologic Quadrangle Map GQ–1296, scale 1:24,000.

Sable, E.G., and Anderson, J.J., 1985, Tertiary tectonic slide megabreccias, Markagunt Plateau, southwestern Utah: Geological Society of America Abstracts with Programs, v. 17, no. 3, p. 263.

Schneider, D.C., 1967, Early Tertiary continental sediments of central and south-central Utah: Brigham Young University Geology Studies, v. 14, p. 143–194.

Spurney, J.C., 1984, Geology of the Iron Peak intrusive, Iron County, Utah: Kent, Ohio, Kent State University M.S. thesis, 84 p.

Steiger, R.H., and Jäger, Emile, 1977, Subcommission on geochronology—Convention on the use of decay constants in geo- and cosmochronology: Earth and Planetary Science Letters, v. 36, p. 359–362.

Tanaka, K.L., Shoemaker, E.M., Ulrich, G.E., and Wolfe, E.W., 1986, Migration of volcanism in the San Francisco volcanic

field, Arizona: Geological Society of America Bulletin, v. 97, p. 129–141.

Thomas, H.E., and Taylor, G.H., 1946, Geology and ground-water resources of Cedar City and Parowan Valleys, Iron County, Utah: U.S. Geological Survey Water-Supply Paper 993, 210 p.

Threet, R.L., 1952a, Geology of the Red Hills area, Iron County, Utah: Seattle, Wash., University of Washington Ph. D. dissertation, 107 p.

———1952b, Some problems of the Brian Head (Tertiary) [abs.]: Geological Society of America Bulletin, v. 63, p. 1386.

———1963, Structure of the Colorado Plateau margin near Cedar City, Utah, *in* Heylmun, E.B., ed., Geology of southwestern Utah: Intermountain Association of Petroleum Geologists Guidebook, 12th Annual Field Conference, p. 109–117.

Tompkins, F.V., Goodwin, J.C., and Malin, W.J., 1963, Cedar City, Utah to Parowan, Utah, via Iron Springs mining district and Parowan Gap, Road log 3, *in* Heylmun, E.B., ed., Geology of southwestern Utah: Intermountain Association of Geologists Guidebook 12th Annual Field Conference, 1963, p. 222–226.

Williams, P.L., 1967, Stratigraphy and petrography of the Quichapa Group, southwestern Utah and southeastern Nevada: Seattle, Wash., University of Washington Ph. D. dissertation, 182 p.

Breccias and Megabreccias, Markagunt Plateau, Southwestern Utah—Origin, Age, and Transport Directions

By Edward G. Sable *and* Florian Maldonado

GEOLOGIC STUDIES IN THE BASIN AND RANGE–COLORADO PLATEAU TRANSITION IN SOUTHEASTERN NEVADA, SOUTHWESTERN UTAH, AND NORTHWESTERN ARIZONA, 1995

U.S. GEOLOGICAL SURVEY BULLETIN 2153–H

UNITED STATES GOVERNMENT PRINTING OFFICE, WASHINGTON : 1997

CONTENTS

FIGURES

TABLE

Breccias and Megabreccias, Markagunt Plateau, Southwestern Utah—Origin, Age, and Transport Directions

By Edward G. Sable *and* Florian Maldonado

ABSTRACT

Although most of the Markagunt Plateau is underlain by autochthonous rocks of generally simple structure, disconnected but extensive areas of the western, central, and northern plateau are covered by chaotic Tertiary rock bodies that have been termed megabreccia. Locally, some bodies are monolithologic, but regionally, they are extremely heterolithologic. Lithologically, the bodies consist of fluvial and lacustrine sedimentary rocks; mudflow, lahar, and lava-flow breccias; and welded ash-flow tuff. They comprise (1) two breccia units coeval with volcanism, of pre- and post-Quichapa Group age consisting of mudflow and lava-flow breccias and fluvial sedimentary rocks containing scattered megaclasts of volcanic rocks; (2) megabreccia associated with high-angle fault blocks; (3) megabreccia associated with the Red Hills shear zone; and (4) the Markagunt megabreccia (restricted), all recognized herein to be separate units. Units 2 and 4 were included in the Markagunt megabreccia of Anderson (1993).

The Markagunt megabreccia is herein restricted to the principal assemblage of allochthonous rocks that covers much of the upland surface of the central and northern "high" Markagunt Plateau. New evidence suggests that the megabreccia was emplaced about 20 Ma by southward low-angle gravity sliding or shallow-depth thrusting. The emplacement is interpreted to have been due to uplift and distension resulting from intrusion of the Iron Peak laccolith or of nearby related intrusive bodies of larger dimensions. Within a belt of observations about 20 km long, slickenlines on the slip surface at the base of the megabreccia form a fan-like pattern that converges on the area of the laccolith. Morphologic forms on the surfaces of overridden rocks, fold-and-fracture features in sedimentary rocks, and shear directions in volcanic rocks within the megabreccia confirm southward movement.

Overburden on the basal slip surface of the Markagunt megabreccia, as reconstructed, was relatively thin, thus supporting the interpretation of a gravity-slide origin for the megabreccia mass. Similarities to south-vergent thrust fault structures near Bryce Canyon, however, suggest the possibility of intrusion-induced horizontal compressive stresses causing emplacement of the megabreccia. Gravity sliding down the surfaces of tilted fault blocks has also been invoked as an explanation for the origin of the Markagunt megabreccia.

INTRODUCTION AND FRAMEWORK

Several terms for chaotically fragmented rock masses are in the geologic literature. The term *megabreccia* was first coined by Landes (1945) for rock that has been brecciated on a very large scale. His type example was the Mackinac Breccia, an Upper Silurian to Middle Devonian unit exposed in northern Michigan, in which blocks as much as 100 m long are inclined within a limited range of relatively low dips. Longwell (1951) used the term for a coarse breccia containing blocks as long as 400 m, developed by gravity sliding along major thrust faults. The term *chaos* was first proposed by Noble (1941), specifically for the Amargosa Chaos (Neogene) in southern California, a gigantic breccia now interpreted to be caused by extensional faulting. All these terms relate to units caused primarily by tectonism, but Longwell allowed for sedimentary origin as well.

Because of their varied character and modes of origin, the megabreccias on the Markagunt Plateau do not fit well in the above definitions; however, we use the term megabreccia for these units. We also retain the name Markagunt megabreccia, coined by Anderson (1993) for all allochthonous bodies of the northern Markagunt Plateau, but we restrict the name to the principal, genetically related allochthonous assemblage exposed in the northern and central Markagunt Plateau.

Large areas of the western, central, and northern Markagunt plateau are capped by allochthonous Tertiary rock assemblages that have been termed chaos or megabreccia. The allochthonous rocks overlie autochthonous rocks of generally simple structure. Those on the plateau have been described by Iivari (1979), Judy (1974), Anderson (1985), Sable and Anderson (1985), Anderson and others (1987), and, in more detail, by Anderson (1993); those in the western Markagunt Plateau and Red Hills were described by Maldonado and others (1994) and Maldonado (1995). The megabreccias are widespread, but not continuously exposed, over an area of more than 500 km^2. Individual megabreccia bodies range from about 50 to perhaps 200 m in thickness. Locally, the rock content ranges from monolithologic blocks to heterolithologic complexes. Regionally, they are extremely heterolithologic: they consist of fluvial and lacustrine sedimentary rocks; mudflow, lahar, and lava-flow breccias; moderately to highly welded ash-flow tuff; minor ash-fall or vent tuff; and lava flows. Specifically, the

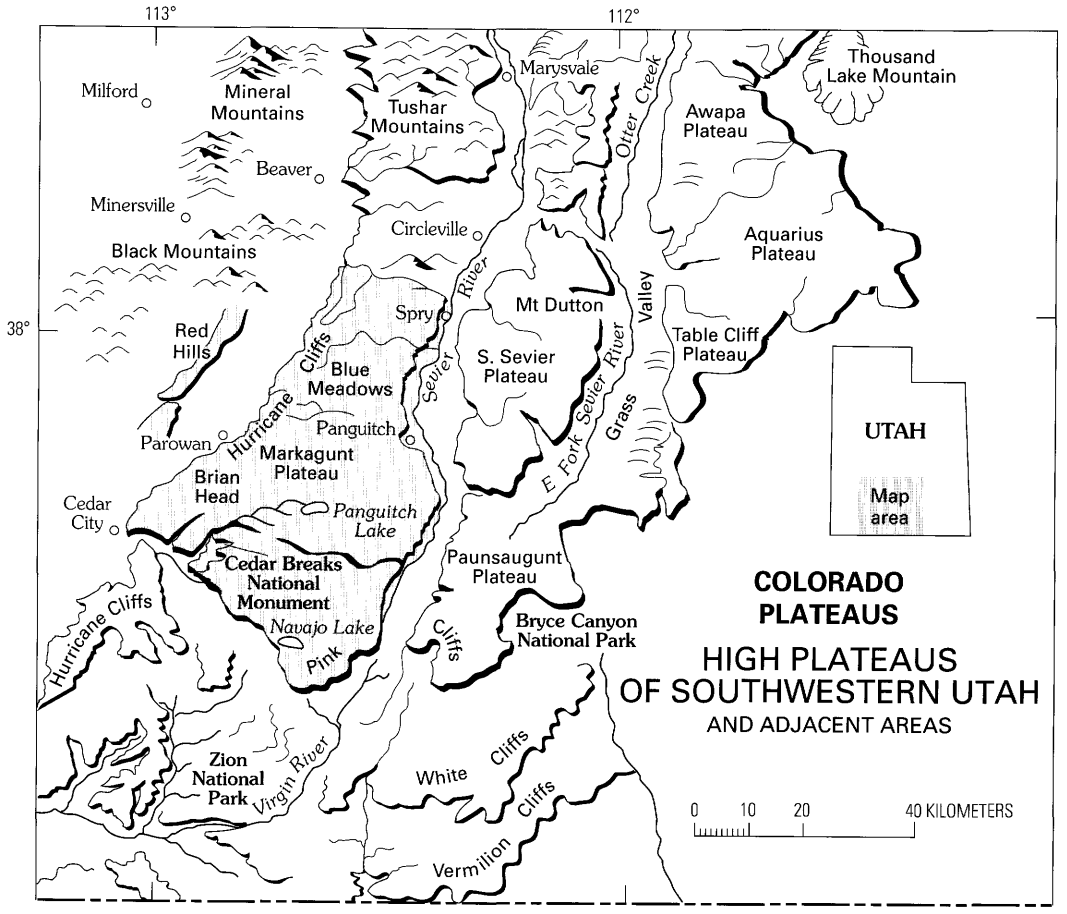

Figure 1. Index map of southwestern Utah (modified from Anderson and Rowley, 1975). Markagunt Plateau and Red Hills shaded.

megabreccias include clasts and megaclasts (greater than 15 m in length or width) of ash-flow tuff of the Needles Range Group, Isom Formation, Buckskin Breccia, Leach Canyon and Condor Canyon Formations, and probably the Harmony Hills Tuff, as well as alluvial facies rocks of the Mount Dutton Formation, sedimentary rocks of the Brian Head and Bear Valley Formations, probably the Haycock Mountain Tuff of Anderson (1993), and rocks of unknown association.

This report focuses on a regional megabreccia mass, the Markagunt megabreccia (restricted), which covers much of the upland surface of the Markagunt Plateau in southwestern Utah. The report also describes the relationships between the Markagunt megabreccia and other megabreccias and breccias in the area. Recent geologic mapping indicates multiple origin and timing for these rock masses, enabling us to build on the heretofore descriptive treatment just cited and on the comprehensive descriptions of Anderson (1993). Secondly, the report presents new evidence for the age of the Markagunt megabreccia (restricted) and for its source and transport directions. Along the southern margin of the megabreccia, directional indicators such as striations on slickensided slip surfaces, morphology of surfaces at the base of the unit, and fold and shear fracture attitudes, as well as the present general surface morphology, are interpreted to indicate southward movement of this allochthonous unit away from the area of the Iron Peak laccolith or nearby areas underlain by a larger intrusion.

The Markagunt Plateau is the southwesternmost of the high plateaus of Utah (fig. 1). Its western boundary lies along the Hurricane Cliffs, which are coextensive with the Hurricane fault zone. This zone marks the western limit of the structural transition zone between the highly extended terrain of the Basin and Range province to the west and the relatively simple structures of the Colorado Plateau to the east. The eastern boundary of the Markagunt Plateau is the Sevier River valley, which approximately coincides with the Sevier fault zone. In the study area the Markagunt Plateau is flanked on the west by the Parowan Valley and the Red Hills; beyond the Sevier River to the east are the Paunsaugunt and Sevier Plateaus. The southern limit of the Markagunt lies roughly along Cedar Canyon, southeast of Cedar City, and the northern border is about lat 38° N. Much of the plateau lies within the Dixie National Forest; Cedar City and Parowan lie along its western margin, Hatch and Panguitch along its eastern margin (fig. 2).

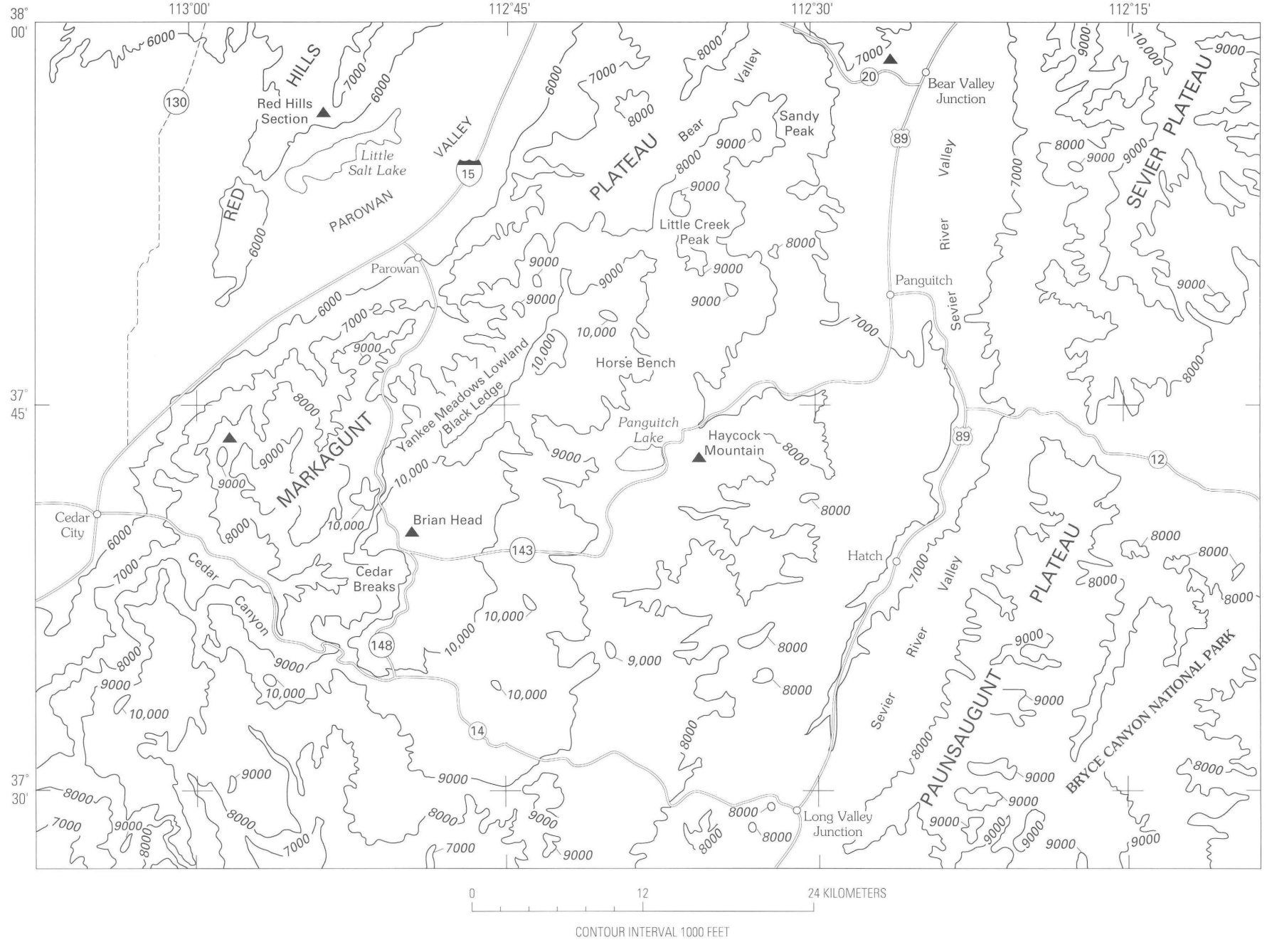

Figure 2. Markagunt Plateau and adjoining areas.

Within the Markagunt Plateau, except for its structurally complex western part (see Maldonado and others, 1994), the regional gentle dips of exposed autochthonous Mesozoic and Tertiary sedimentary and volcanic strata are mostly eastward and northeastward. Tertiary volcanic and sedimentary rocks, aggregating more than 1,000 m thick, constitute the most widespread succession of exposed rocks on the Markagunt and in the adjoining Red Hills (fig. 3), although older rocks are exposed along the western and southern plateau margins. The volcanic rocks are mostly Oligocene and Miocene (30–22 Ma) ash-flow tuffs derived from calderas in the Great Basin to the west; they interfinger with alluvial facies of the 32–21 Ma Mount Dutton Formation. Mudflow breccia, lava flows, and lava-flow breccia of the Mount Dutton Formation were derived from numerous volcanic centers along an east-trending belt, the Blue Ribbon lineament, north and northeast of the plateau (Rowley and others, 1994). Other sedimentary rocks were derived from source areas to the west, northeast, and north. The Tertiary rock units shown in figure 3 are described in publications such as those by Anderson and Rowley (1975), Maldonado and Williams (1993a, b), Anderson (1993), and Rowley and others (1994). Quaternary basalt and andesite lava flows, cinder cones, and shield cones mantle many areas of the plateau surface (Best and others, 1980; Nealey and others, 1994; Rowley and others, 1994).

The main structural elements of autochthonous rocks of the high Markagunt Plateau are the gentle eastward regional dips of less than 5°, a few broad low-amplitude folds, and high-angle faults of small to moderate displacement. Dips of late Tertiary gravel deposits on the high plateau surface reflect the regional tilting and folding, indicating that these structures are relatively young. West of the Black Ledge (fig. 2), structures are considerably more complex, as described by Maldonado and others (1994; this volume, chapter G). There, many high-angle, northeast- to north-trending faults of large displacement bound horst-and-graben blocks, and west-dipping monoclinal structures are present along the western plateau front. We interpret the latter stages of development of these structures, including the regional tilting and low-amplitude folding just mentioned, to be interrelated, and to postdate the Markagunt megabreccia.

The northern part of the plateau is underlain by Tertiary (about 20 Ma) intrusions. A batholithic complex, part of the east-northeast-trending Delamar–Iron Springs igneous belt, is the major intrusive body in the region. It provided magma to several 22–20 Ma (Fleck and others, 1975) exposed and inferred domal intrusions along the belt (Rowley and others, 1994). The extent of the batholith is defined by positive short-wavelength aeromagnetic anomalies of relatively high amplitude, whereas most long-wavelength anomalies farther south are interpreted to reflect either Precambrian basement rock, or to a lesser extent, basaltic vent and flow rocks (Blank and Crowley, 1990, p. 24).

Two intrusive bodies occur in or near the study area: the Iron Peak laccolith (Iron Peak, fig. 2), 14 km northeast of Parowan, and the Spry intrusion, about 25 km north of Panguitch (near the small town of Spry, fig. 1). Erosional remnants of the Iron Peak laccolith (Iron Point intrusion of Anderson and Rowley, 1975), a body of gabbroic to dioritic composition, crop out over 7.4 km^2. Estimated initial relief of the laccolith was interpreted to have been greater than 400 m, emplaced by domal uplift at less than 1,200 m depth (Spurney, 1984). Ages of about 20 Ma for the pluton and probable related mafic dikes are discussed in Rowley and others (1994). The older (provisionally about 25 Ma) monzonitic Spry intrusion (Anderson and Rowley, 1975) is of batholith size. In addition, intrusive rocks have been penetrated in a drill hole in the southwestern Red Hills (Thomas and Taylor, 1946), and a probable intrusive body underlies a dome near Bear Valley Junction, 16 km north of Panguitch. Several small complex domal areas whose presence suggests underlying intrusive bodies lie along an easterly trend between Iron Peak and Bear Valley Junction. Other buried intrusive bodies of large dimensions probably underlie northern parts of and northwest of the plateau, such as under Parowan Valley (Maldonado, 1995, fig. 12), as suggested by the aeromagnetic geophysical anomalies referred to in a preceding paragraph.

ACKNOWLEDGMENTS

Discussions with H.R. Blank, Jr., P.D. Rowley, and J.J. Anderson helped formulate concepts presented here. Concentrated reviews of the manuscript by D.L. Schleicher and D.L. Schmidt resulted in significant improvements in content and presentation. H.H. Mehnert and L.W. Snee kindly provided the K-Ar and $^{40}Ar/^{39}Ar$ age dating results. W.A. Bryant reviewed geologic name usage, and L.M. Carter edited the manuscript for publication. Typing and word processing were done by M.J. Brooke and S.A. Rosema. We much appreciate the considerable time, energy, and dedication given by these individuals during preparation and processing of the manuscript.

BRECCIA AND MEGABRECCIA TYPES OF THE MARKAGUNT PLATEAU

Anderson (1993) included all megabreccia types on the northern "high" Markagunt Plateau in his Markagunt megabreccia unit. He outlined seven separate areas of megabreccia exposure and discussed characteristics of the unit in each area (Anderson, 1993, p. 23–29; fig. 4 of this report). He (1993, p. 15–22) also established a "reference locality" for the Markagunt megabreccia, a belt of well-exposed outcrops along 3 km of Utah State Highway 143 east of Panguitch

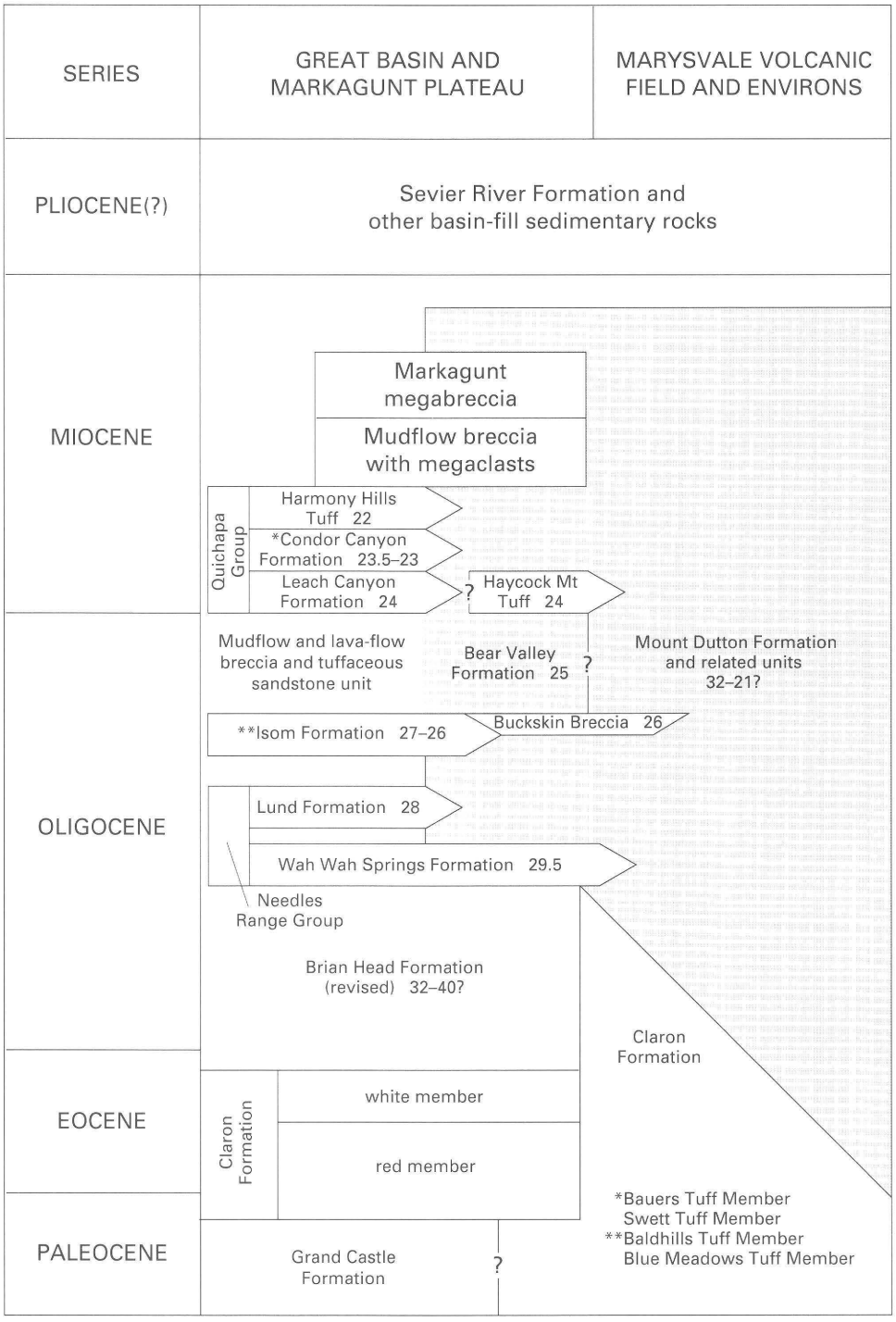

Figure 3. Selected Tertiary units of Markagunt Plateau and adjoining areas. Numbers refer to isotopic ages rounded to nearest half-million years. (Modified from Rowley and others, 1994.) Boundaries or ages queried where uncertain.

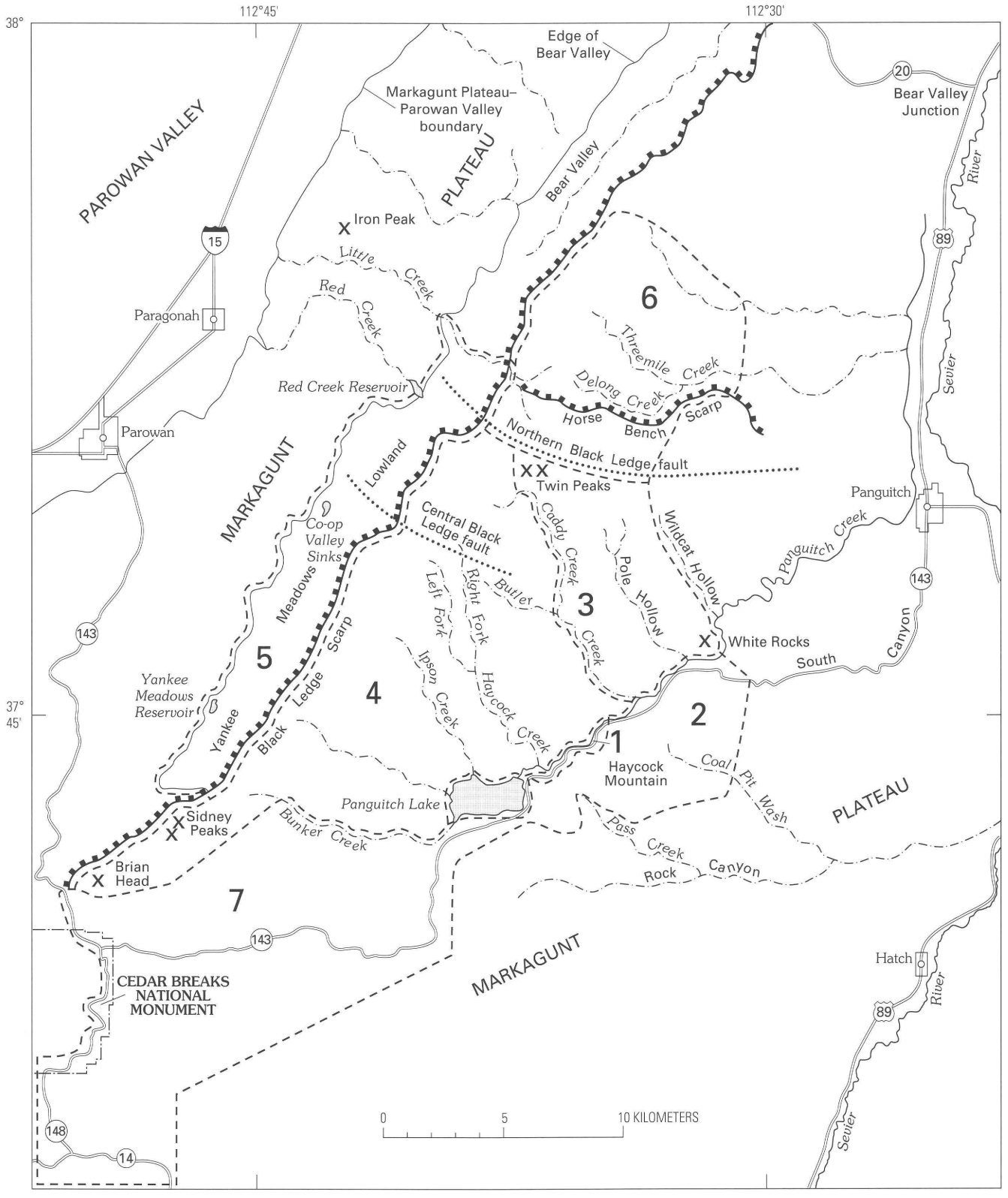

Figure 4. Central and northern Markagunt Plateau showing seven areas of exposure of the Markagunt megabreccia (bounded by short-dashed lines) as defined by Anderson. Modified from Anderson (1993, fig. 23).

Lake. Anderson (1993, p. 29–32) concluded that most of the megabreccia was transported northward by gravity sliding away from uplifts caused by igneous intrusion under the central Markagunt Plateau. He attributed the development of other parts of the megabreccia to seismic shaking along west-northwest-trending high-angle faults that resulted in southward sliding of megabreccia bodies down the dip-slopes of the tilted fault blocks, as well as northward scarp collapse. According to Anderson (1985, 1988, 1993), the west-northwest-trending faults originated in mid-Oligocene time and were active into the Miocene; their topographically prominent fault scarps controlled the distribution and thickness of tuff units such as those of the Needles Range Group and Isom Formation.

Rock units that have been termed megabreccia in the study area include (1) units of primary mudflow and other debris flow *breccias* and fluvial sedimentary rocks coeval with volcanism that contain sand- to boulder-sized clasts and scattered megaclasts of mainly volcanic rocks, (2) megabreccia resulting from high-angle fault scarp collapse and from slide deposits down the tilted fault blocks, (3) megabreccia consisting of fragmented rocks in the allochthonous upper plate of the Red Hills shear zone, and (4) the principal mass of the Markagunt megabreccia that covers large parts of the central and northern Markagunt Plateau. Units 2 and 4 were included in the Markagunt megabreccia by Anderson (1993), but we restrict the term to unit 4.

BRECCIAS COEVAL WITH VOLCANISM

These breccias may in part be related to seismicity during volcanism and contemporaneous sedimentation. They include mudflow, landslide(?), and lava-flow breccias intercalated with tuffaceous sedimentary rocks. They occur between all formally named ash-flow tuff units on the Markagunt Plateau. Volcanic clasts and megaclasts in these deposits include fragments of older units, including those of the Needles Range Group, Isom Formation, and Quichapa Group, tuffs of unknown origin, and mafic lava. Some breccias were incorporated into the Markagunt megabreccia after they were lithified. Two mappable breccia units occur on the western Markagunt Plateau, an older and a younger unit. The older of the two occupies the interval between the Isom Formation below and the Quichapa Group above (fig. 3). It was mapped as "mudflow and lava-flow breccia and tuffaceous sedimentary rocks" by Maldonado and Moore (1995); in Parowan Canyon it is overlain by the Bauers Tuff Member of the Condor Canyon Formation. The unit appears to be persistent in the western Markagunt and is correlated on a lithologic and stratigraphic-position basis with breccia and tuffaceous sedimentary rocks of the Bear Valley Formation at Panguitch Lake. The mudflow breccia contains clasts of mafic to felsic aphanitic rocks, including hornblende- or pyroxene-rich mafic lavas and lesser amounts of Needles Range and Isom tuffs in a matrix of sandy mudstone. The lava-flow breccia is essentially a clast-supported unit that contains clasts of pyroxene-rich mafic rocks. Tuffaceous sandstone beds are similar to those in the Brian Head Formation; in places they contain isolated megaclasts of Needles Range and Isom rocks as much as 200 m long. The older unit ranges from less than 50 to 150 m in thickness; about 40 m, mostly lava flow breccia, is well exposed at Brian Head peak.

The younger breccia, locally more than 180 m thick, is lithologically similar to the older but overlies and incorporates clasts and megaclasts of the Quichapa Group and older tuff units. It is exposed, for example, along the plateau western front 9 km southwest of Parowan, and north and east of Panguitch Lake. The breccia locally overlies strata as young as the Harmony Hills Tuff. In a mudstone matrix, clast sizes are generally bimodal; abundant angular to rounded pebbles to large boulders contrast with scattered angular megaclasts many meters in diameter. Most smaller clasts are aphanitic lava; others are Needles Range and Isom Formation tuffs, tuffs of the Quichapa Group (Leach Canyon and Condor Canyon Formations), and some tuffaceous sedimentary rocks and chalcedony blocks from the Brian Head Formation. Some large boulder-sized clasts, such as those of the Isom and Condor Canyon Formations, are deformed, exhibit polished and "pressure-flaked" surfaces, and are rotated, sheared, and penetrated by mudstone or sandstone matrix; others, especially felsic tuffs of the Needles Range and Leach Canyon units, are in places essentially undeformed and flat-lying; they appear to float in a mudflow breccia matrix. Clasts of red, crystal-poor vitric tuff considered to be of the Blue Meadows Tuff Member of the Isom Formation and possibly in part, of the Bear Valley Formation, are locally common; they increase in size and abundance northward, as north of Panguitch Lake, towards the main outcrop area of the Blue Meadows Tuff Member (Anderson and others, 1987; Anderson, 1993). Anderson (1993) attributed "***small allochthonous masses of the member***to gravity sliding down the flanks of small structural domes***." We suggest that some of these megaclasts, such as those in the Twin Peaks area (fig. 4), were incorporated, perhaps by rockfall, in the mudflows, so that currently, the individual monolithic bodies remain after the softer overlying and flanking mudflow matrix was eroded.

Both the older and the younger breccias are thought to be alluvial facies of the 32–22 Ma Mount Dutton Formation, although the older unit may be from western sources (Anderson and Rowley, 1975). It is at least in part coeval with the Bear Valley Formation (Anderson, 1971). Some of the breccias are probably in their initial emplacement locations; others, after lithification, have moved along low-angle slip surfaces to their present locations as parts of the Markagunt megabreccia.

The mudflow and lava-flow breccias may have originated in volcanic centers situated along the Blue Ribbon lineament, north of the Markagunt Plateau, or from sources within the plateau. The megaclasts of western-source tuffs may have been broken from their outcrops as rockfall or by landslides during volcanism. Some of the huge isolated outcrops of Isom Formation tuff units that overlie younger units, such as those at Sydney Peaks, 5 km northeast of Brian Head peak, could be interpreted to be megaclasts incorporated in the mudflows from which the matrix has been eroded; they are commonly underlain by mudflow breccia. Alternatively, the explanation we favor is that the Isom rocks and underlying mudflow breccia are erosional remnants of the main Markagunt megabreccia sheet. In either case, the huge blocks are allochthonous as evidenced by their older-on-younger relationships and slickenlines on underlying slip-planes.

MEGABRECCIAS ASSOCIATED WITH HIGH-ANGLE FAULT SCARPS

Anderson (1993, p. 26, 31) proposed that some megabreccia deposits in the northern Markagunt Plateau are the result of gravity sliding down tilted fault block surfaces, and from scarp collapse. He included these deposits in the Markagunt megabreccia and related them to seismic shaking along west-northwest-striking high-angle faults in his areas 3 and 5 (fig. 4). These faults, the central and northern Black Ledge faults (not the same as the Black Ledge fault of Maldonado and others (1994), which is the northeast-trending fault along the north face of the Black Ledge scarp) and a fault along the Horse Bench scarp, were initially activated in the Oligocene, contemporaneous with emplacement of the Needles Range and Isom tuff units. We provisionally exclude these megabreccia units from those of the Markagunt megabreccia (restricted) (see section on the Markagunt megabreccia, following). We also suggest two other possibilities for the origin of the deposits below the Horse Bench scarp: (1) that they were transported eastward and southeastward away from an uplifted area to the west, possibly the area of the Iron Peak laccolith or areas of nearby domal uplifts, or (2) that they are relatively local mass-wasting deposits that have slid southeastward down the dip slope of the northeast-trending fault block along the east side of Bear Valley. Linear features in the hummocky topography of these rocks, which consist of Bear Valley Formation and immense rotated blocks mostly of the Baldhills Tuff Member (Anderson and others, 1987), exhibit a generally northeasterly topographic grain parallel to the fault scarp (fig. 5).

Megabreccia deposits in the heavily vegetated Yankee Meadows lowlands northwest of and below the northeast-trending Black Ledge scarp (area 5 of Anderson; fig. 4, this report) are very poorly exposed; they appear to consist mostly of randomly tilted blocks of Brian Head, Needles Range, Isom, and Leach Canyon units. Although Anderson (1993) included the rocks there in his Markagunt megabreccia and attributed them to collapse and sliding along the west-northwest-trending central and northern Black Ledge fault blocks, we consider them to be largely the result of late Tertiary(?)-Quaternary scarp collapse and mass wasting along the Black Ledge scarp, a process that is still currently active. The deposits below this northwest-facing scarp extend as an apparently continuous chaotic assemblage for about 20 km along the scarp and are mapped as Quaternary-Tertiary landslide deposits (Maldonado and others, this volume, chapter G). As Anderson (1993, p. 26) pointed out, Baldhills tuff masses are concentrated along the northern part of this belt, and these may have been controlled by the presence of his projected west-northwest faults. However, unless these faults were active long after their onset in the Oligocene, it seems difficult to reconcile the timing of the megabreccia deposits with these structures. However, J.J. Anderson (oral commun., 1995) has interpreted the west-northwest fault system to "young" southward. If this is true, his central and northern Black Ledge faults may be of Miocene age, contemporaneous with megabreccia formation.

MEGABRECCIA ASSOCIATED WITH THE RED HILLS SHEAR ZONE

This megabreccia resulted from dismemberment of upper plate Tertiary volcanic and sedimentary rock strata during and after movement along the low-angle Red Hills shear zone (Maldonado and others, 1990; 1992; Maldonado, 1995). Evidence for dislocation along the shear zone consists of comminution and shearing along low-angle surfaces of structurally incompetent strata in or at the top of the Brian Head Formation. Cretaceous and Tertiary sedimentary rocks below these strata are essentially undeformed; above the shear zone, huge blocks of structurally competent Needles Range, Isom, and Leach Canyon units are fractured, dismembered, and rotated into locally chaotic assemblages. The known extent of this megabreccia is restricted to the northern Red Hills (fig. 1) and western Markagunt Plateau. Possible regional extent of the shear zone is as yet uncertain, although sheared rocks and brecciated, highly fractured chalcedony with polished surfaces, unlike undeformed chalcedony, are present in the Brian Head Formation as far east as Hatch, more than 50 km southeast from the Red Hills (fig. 2). Shear zone deformation was between 22.5 and 20 Ma (Maldonado, 1995), the younger age being that of mafic dikes, probably related to the Iron Peak laccolith, that intruded the megabreccia overlying the shear zone. Subsequently, the extensional separation (breakaway) of the Red Hills from the plateau took place. If the Markagunt megabreccia is genetically related to emplacement of the Iron Peak laccolith (see section, "Transport Directions"), then the Red Hills shear zone megabreccia is the older of the two, but nearly contemporaneous with the Markagunt megabreccia.

MARKAGUNT MEGABRECCIA (RESTRICTED)

DESCRIPTION AND RELATIONSHIPS

The most extensive megabreccia type described in this report is the Markagunt megabreccia (restricted), exposed in the central and northern Markagunt Plateau (fig. 4, areas 1–4 and 7; this report). Its present bedrock southern limit extends eastward across the north-central Markagunt Plateau from about 5 km northeast of Brian Head (peak) through the Panguitch Lake area to about 30 km east-northeast of the peak (fig. 2); unconsolidated breccia rubble attributed to the former southern extent of the megabreccia occupies much of area 7 (fig. 4). Its northern limit is not well established because geologic mapping has not been completed, and because the thick, youngest units of the Mount Dutton Formation alluvial facies, mostly mudflow breccia, appear to obscure it; the limit may lie near the Iron Peak laccolith and extend eastward across Bear Valley toward the Sevier River valley (fig. 2), where the megabreccia is buried by gravels about 8 km west of Panguitch.

The Markagunt megabreccia is especially well exposed along the excellent reference locality belt established by Anderson (1993, p. 15–22) along Utah Highway 143, east of Panguitch Lake (fig. 4, area 1, this report), which is near the southern limits of the unit. It is also relatively well exposed farther west, both in and west of the Panguitch Lake area. The westernmost bedrock exposures of the Markagunt megabreccia are at Sydney Peaks, 5 km northeast of Brian Head peak (fig. 4, this report; Anderson, 1993, fig. 24). There, isolated klippen-like hills containing rotated megaclasts of the Baldhills Tuff Member of the Isom Formation as much as 500 m in diameter, along with underlying thin mudstone breccia and rubble of Needles Range Group tuff, rest on a low-angle slickenlined surface on tuff of the Leach Canyon Formation. Two to four kilometers farther east, similar relationships with the underlying Baldhills Member

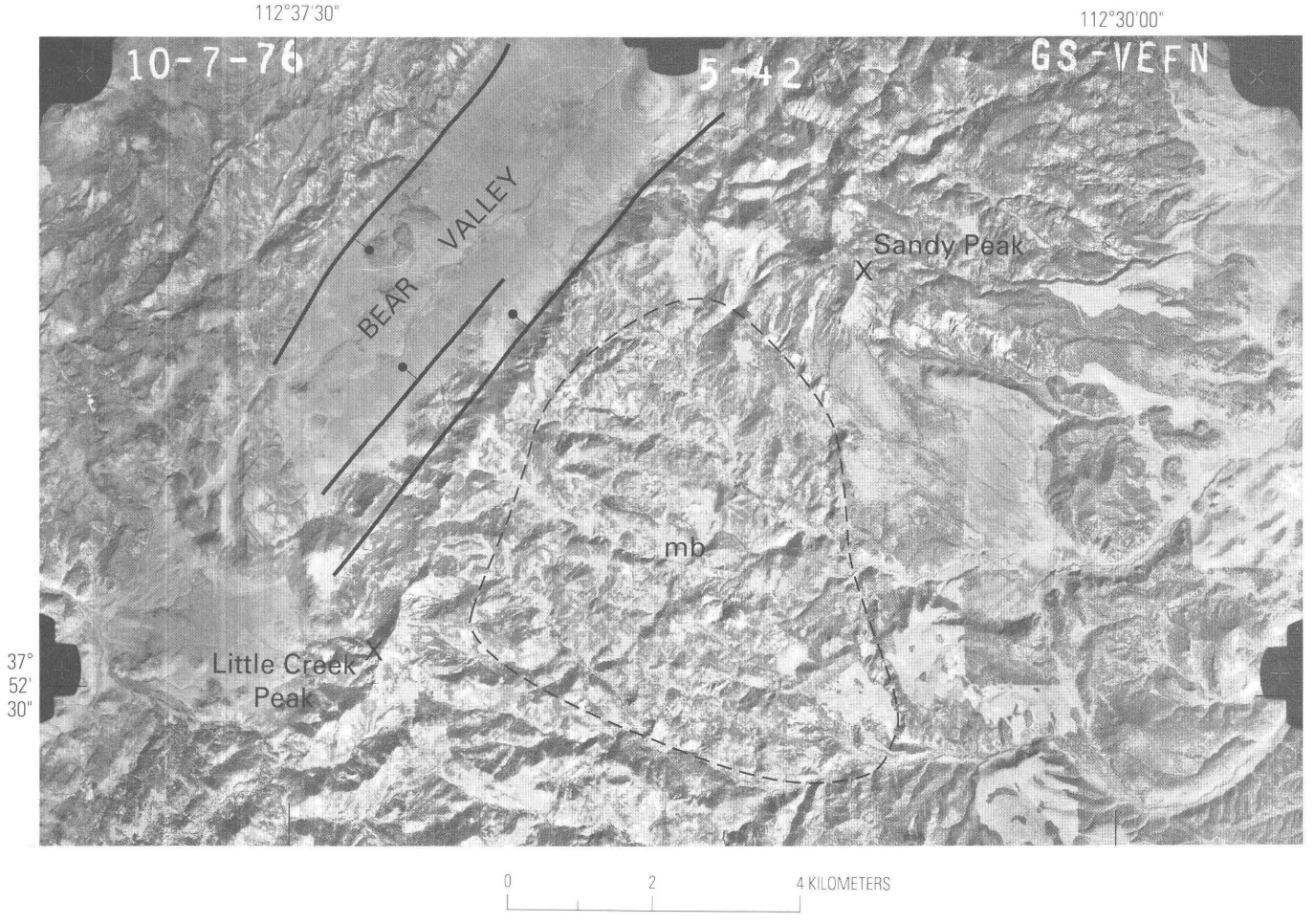

Figure 5. Aerial photograph showing structural grain of hummocky megabreccia topography in Bear Valley Formation and allochthonous tuffs east of Bear Valley. Short dashes outline hummocky topography, occurring in bowl between two high mountains, Little Creek Peak and Sandy Peak. Heavy line, high-angle fault; bar and ball on downthrown side.

(Leach Canyon locally absent) are exposed along the crest of the Black Ledge. The Black Ledge is colinear with a similar scarp along the east side of Bear Valley, both bounded by high-angle faults.

From the Black Ledge east to the Panguitch Lake area, large discontinuous klippen-like hills, composed mostly of Baldhills tuff and mudflow breccia units, rest on either Baldhills or Leach Canyon tuff units. Within the area to 6 km east of Sydney Peaks, most of the hills are elongate at about N. 80° W. trend, normal to slickenline directions in this area. North and east of Panguitch Lake, a more or less continuous sheet of the Markagunt megabreccia containing megaclasts from the Needles Range, Baldhills, Blue Meadows, Bear Valley, and Mount Dutton units overlies a relatively thick but variable autochthonous Baldhills unit (about 5–70 m) that in turn overlies the Brian Head Formation. In many places, such as along the north shore of Panguitch Lake, the slip-surface has cut deeply into the Baldhills Tuff Member, removing the Leach Canyon Formation and the upper part of the Baldhills.

The megabreccia appears to maintain a relatively normal internal stratigraphic succession in and east of the Panguitch Lake area, although intercalated megaclast units vary in thickness and extent in lense-like fashion. The megabreccia also exhibits, near its base, overturned to recumbent folds in sedimentary rocks, shattered and sheared tuff megaclasts, and low-angle shears, well illustrated by Anderson (1993, figs. 14, 16–17, 19–20), that resemble features associated with the toes of thrust sheets. Units incorporated in the megabreccia are cut by numerous closely spaced, moderate- to high-angle antithetic faults of relatively small displacement (less than one to tens of meters) that overprint the earlier megabreccia structures and, in areas of poor exposure, result in bewildering complexity.

North and east of Panguitch Lake (fig. 4, areas 3 and 4) the assemblage above the basal slip-surface of the Markagunt megabreccia is composed mostly of Mount Dutton and Bear Valley mudflow breccia, sandstone, and tuff. These deposits contain mostly small-pebble- to boulder-sized clasts largely of mafic lava. The mudflow breccia is intercalated with large, discontinuous angular and slablike blocks and lenses of Needles Range, Isom, and Quichapa tuffs, tuff that we interpret to be Haycock Mountain (Leach Canyon?) Tuff, tuffs in the Bear Valley Formation, and uncorrelated sedimentary rocks. Although many clasts exhibit random orientations, some tabular ones maintain locally consistent stratigraphic positions in the mudflow breccia. In those places, as 8 km northeast of Panguitch Lake, mudflow breccia strata and intercalated megaclasts dip at shallow angles, and structure appears to be uncomplicated. Because of their simple structure and because the slip-surface of the megabreccia lies in the subsurface in these areas, the exact relationships of these Mount Dutton mudflow breccias to the Markagunt megabreccia are not known—namely, whether or not they are part of the Markagunt megabreccia mass or are in part younger Mount Dutton mudflows unconformably overlying the megabreccia. Farther north, in area 6, nearly horizontal strata of mudflow breccia and lava of the Mount Dutton Formation such as those capping Little Creek Peak appear to overlie disturbed strata of the Bear Valley Formation and older units and thus may represent post-megabreccia deposition.

The thickness of the megabreccia along its southern belt of exposures in and near area 1 (Anderson's reference area) is about 150 m of section. Components of the megabreccia include (generally ascending) discontinuous blocks of the Wah Wah Springs Formation of the Needles Range Group, Baldhills and Blue Meadows(?) Tuff Members of the Isom Formation; the Bear Valley Formation, Mount Dutton mudflow and lahar breccias, and tuffaceous sandstone and conglomerate containing rounded clasts of the Bauers Tuff Member of the Condor Canyon Formation. Also included are ash-fall or vent-facies unwelded felsic tuff and porphyritic pyroxene-phenocryst mafic lava, both of uncertain derivation. We also include the Haycock Mountain Tuff (Anderson, 1993, p. 13–14) as a component of the Markagunt megabreccia, although Anderson interpreted this unit to be a post-megabreccia unit. We, however, suggest that it may not be a new unit, but rather a distal facies of the Leach Canyon Formation (see "Age" discussion). From about 5 to 8 km north of Panguitch Lake, the megabreccia seems to include an increasingly greater thickness of Mount Dutton alluvial facies rocks, some of which may be younger than the megabreccia.

A greater southern extent of the Markagunt megabreccia than that shown by its bedrock distribution is suggested by surficial rubble and poorly consolidated breccia at Cedar Breaks National Monument, below and south of Brian Head peak (Moore, 1992). According to Moore, the deposit is the result of small-volume landsliding and gravitational spreading in and on clay beds of the "uppermost white Claron Formation" (Brian Head Formation of Sable and Maldonado, this volume, chapter A). The unit is almost monolithologic: it consists predominantly of highly resistant clasts of the Baldhills Tuff Member of the Isom Formation and subordinate poorly resistant Brian Head Formation clasts. The Baldhills tuff clasts, from sand-size to many meters in diameter, are characterized by plagioclase phenocrysts in a glassy to devitrified groundmass, whereas the nearest Isom Formation bedrock, underlying the Leach Canyon Formation on Brian Head peak, is an aphanitic, vesicular lava lacking visible phenocrysts, and is not represented in the breccia-rubble below the peak. An alternative explanation is that the surficial unit is largely residual, a lag derived from the Markagunt megabreccia that formerly overlay the Leach Canyon Formation on the peak and has since been eroded. An example of a prior phase in the development of the surficial unit is the klippen-like hills at Sydney Peaks, interpreted to be erosional outliers of the formerly continuous sheet of Markagunt megabreccia that will likely, with continued disaggregation by erosion and gravitational spreading, develop into surficial residual rubble, as suggested by Anderson (1993, p. 28).

TRANSPORT DIRECTIONS

PREVIOUS INTERPRETATIONS

Anderson (1993, p. 30) postulated that most of the Markagunt megabreccia had been transported northward by gravity sliding down the north flank of a batholith "that aeromagnetic data suggest underlies the central Markagunt Plateau or perhaps a cupola on a much larger batholith that may underlie much of southwestern Utah." As discussed previously, he also invoked localized southward gravity sliding down dip slopes of south-tilted fault blocks that were bounded by west-northwest-striking high-angle faults, and the northward collapse of north-facing scarps produced by these faults. Prior to these interpretations, Wagner (1984) and Anderson (1985) had proposed a southward sliding direction for the main Markagunt megabreccia.

Specifically, in the seven areas of exposure of the Markagunt megabreccia (fig. 4) Anderson postulated northward transport in areas 1–4; southward transport for areas 5 and 6; and northward transport (at least in part) for area 7. As evidence for northward transport in areas 1, 2, and 4, Anderson (1993, p. 30–31) cited the generally north-south orientations of striae on slickensided low-angle surfaces (Sable and Anderson, 1985), and postulated that at the time the megabreccia was emplaced, the underlying Baldhills Tuff Member dipped north (as it now does at Haycock Mountain) and thus provided the slope gradient for northward movement. Possibly as further evidence of northward transport, Anderson pointed out that the central part of the Markagunt Plateau is topographically higher than the northern part.

FEATURES INDICATING TRANSPORT DIRECTIONS

Slip surfaces at the base of the Markagunt megabreccia are sporadically exposed across the Markagunt Plateau from 5 km northeast of Brian Head peak to at least Haycock Mountain, 22 km to the east (fig. 4). The surfaces slope both southward and northward at mostly less than 10°. Most surfaces directly underlie the main mass of the Markagunt megabreccia; others underlie now-isolated blocks, like those at Sydney Peaks, that we believe to have been continuous with the main mass. Features on these surfaces define slip lines along which the Markagunt megabreccia was emplaced. The slip lines are mostly striae and broad grooves imposed on ash-flow tuffs of the autochthonous Isom and Leach Canyon Formations. The striae are on the upper surfaces or within these units; in places striated surfaces dipping as much as 50° north cut through the units, suggesting that the structurally competent units were strongly stressed by the overriding megabreccia.

Easily accessible localities where slip lines were observed include the top of the Leach Canyon Formation cliffs just east of Sydney Peaks (fig. 6, loc. 1); the Isom Formation outcrop along the east side of the Panguitch Lake dam (fig. 6, loc. 2; fig. 7); and the small roadcut outcrop of Isom Formation and mudflow breccia along State Highway 143, adjoining the deep canyon cut into contorted Isom Formation layers (fig. 6, loc. 3; fig. 12*A*). Less accessible localities showing asymmetrical features (see second paragraph following) are on the Leach Canyon Formation cliffs on the north side of and high above Bunker Creek (fig. 6, loc. 4; fig. 9) and additional localities on Haycock Mountain (not numbered on fig. 6).

The average strikes of 35 slip line readings on mostly striae, measured at the 10 localities shown in figure 6, is about N. 20° E. in the western part of the study area near Brian Head, and about N. 20° W. at Haycock Mountain, in the eastern part. Several additional but less certain single readings made along this belt closely corresponded to the averages. Locally, the strike varies as much as 15°, but commonly less than 5°–10°. (An anomalous N. 20° E. reading on the south side of Haycock Mountain was observed on the lower surface of a tuff megaclast near the base of the megabreccia; it may be due to rotation during transport.) Although the volume of data may not seem statistically persuasive, we believe the strikes to be valid and significant. Locally, they are consistent and nearly unidirectional. Regionally, within the belt of observations, they form a radial pattern converging on the area of the Iron Peak laccolith, 22 km north of Panguitch Lake (fig. 6).

Larger asymmetrical features interpreted to be prod marks and discontinuous corrugations (roche moutonnée-like features) (figs. 8, 9) are also present on the slip surfaces but are rarely well preserved. Although the evidence is equivocal, we interpret them to indicate southward transport. Structures within the megabreccia also suggest southward-directed stresses, for example, north-dipping shear-planes (fig. 10), and fold and fault attitudes (fig. 11). In addition, many, although not all small fracture displacements in sedimentary rock components of the megabreccia exhibit southward offset and thus tend to confirm southward transport. J.J. Anderson (oral commun., 1995), however, has indicated that a stereonet plot of numerous fracture orientations failed to show preferred directions.

The strikes of the slickenlines indicate that the megabreccia moved either northward or southward, but they do not indicate the actual sense of movement. The outcrop observations of asymmetrical features, fold-and-fracture relationships, and shear features in addition to the radial pattern, however, suggest to us southward movement, contrary to the interpretation of Anderson (1993, p. 30–31). The indicators also suggest movement away from a broad point source.

Further evidence for southward transport of the Markagunt megabreccia lies in the preponderance of north-dipping units within the lower part of the megabreccia near its southern limits. Recumbent folds and low-angle, north-dipping shears in rock components of the megabreccia (Anderson, 1993, figs. 19, 14) are common features above the base of the

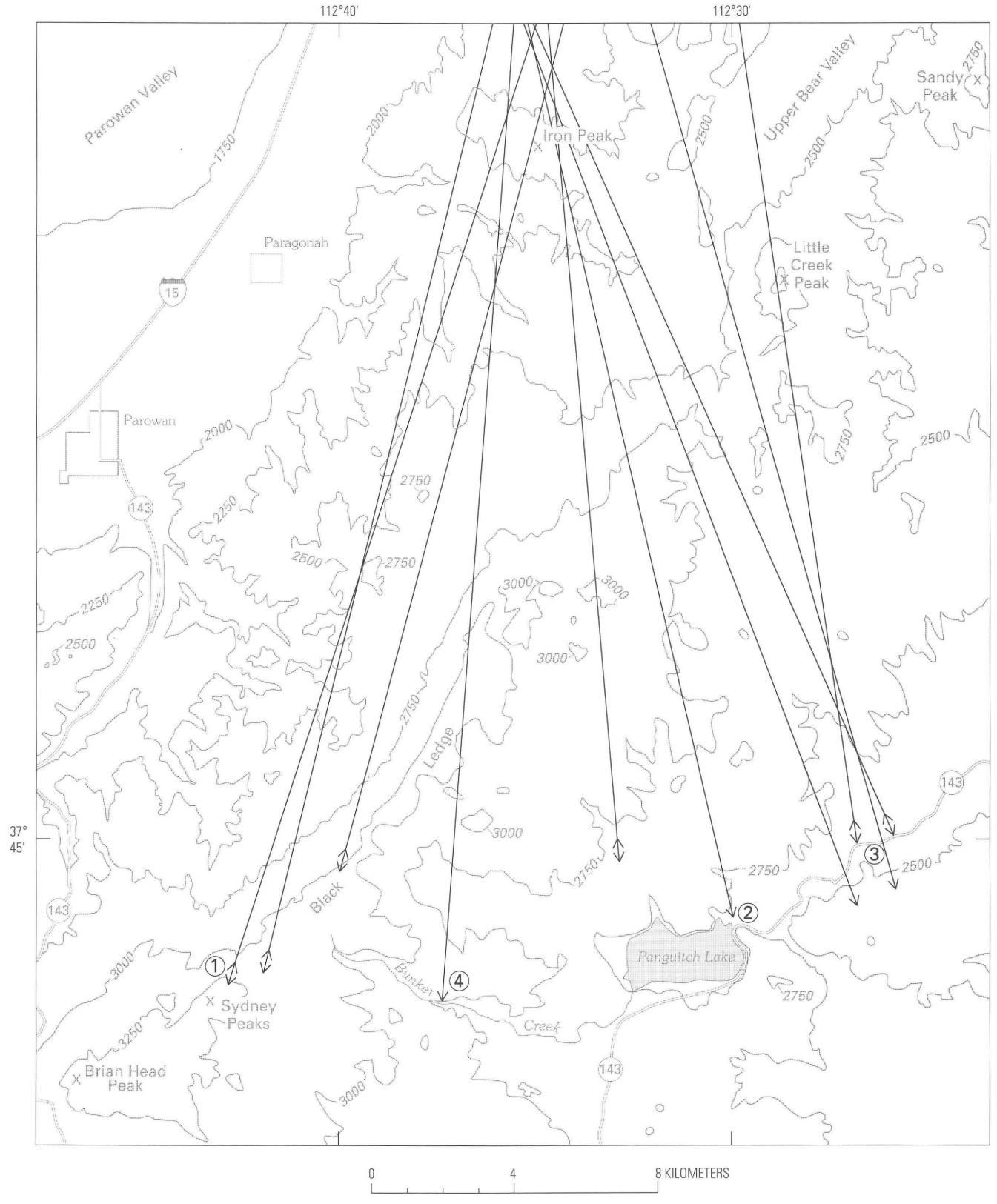

Figure 6. Strikes of transport indicators of Markagunt megabreccia (restricted). Double arrow, directional sense is unknown; single arrow, southward sense of transport. Numbered localities keyed to text. Contour interval 250 m. Base from Panguitch, Utah 30×60-minute quadrangle, 1980.

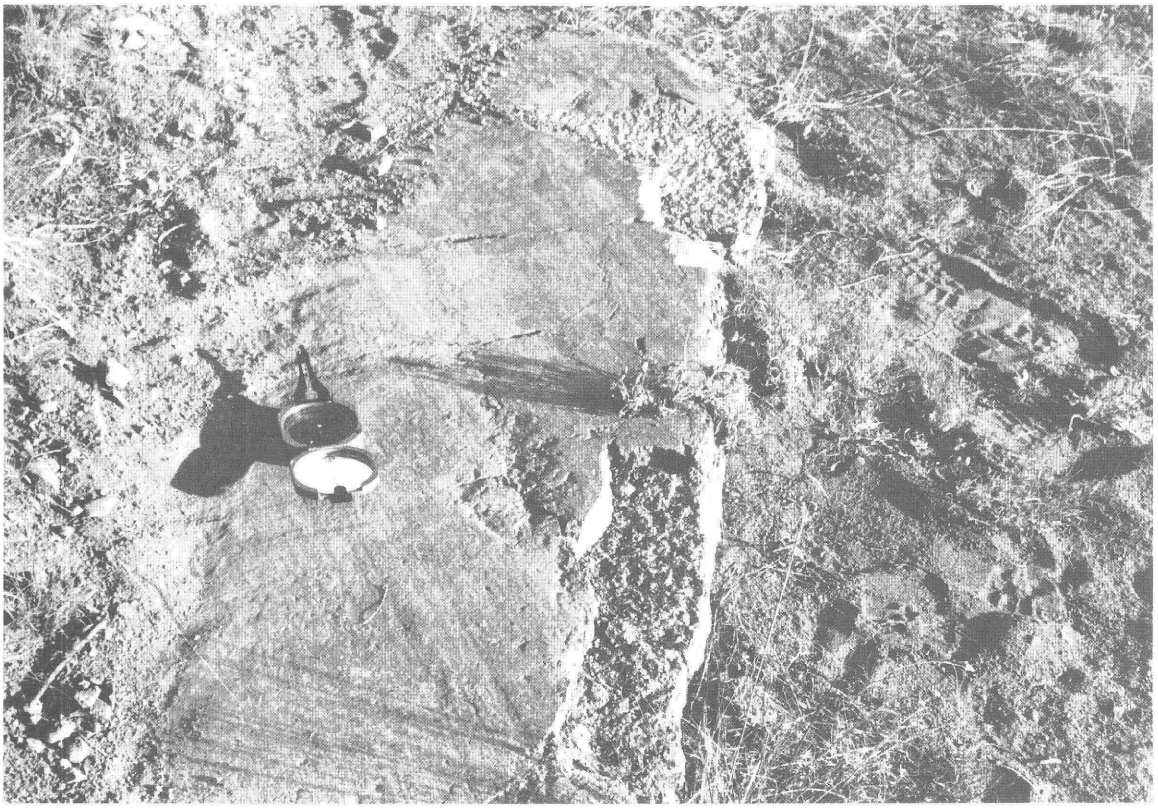

Figure 7. Striated surface on Baldhills Tuff Member of Isom Formation directly beneath Markagunt megabreccia. Striae parallel to compass alignment of N. 16° W. Oblique lines are shadows. East side of Panguitch Creek at Panguitch Lake dam (fig. 6, loc. 2).

megabreccia in the Panguitch Lake area. At the east end of Panguitch Lake, for example, a long roadcut exposes a north-dipping section of mostly Bear Valley Formation cut by several minor antithetic faults. The section lies within 30 m of the projected low-angle base of the megabreccia. Within the section, therefore, beds dip much more steeply than the underlying slip surface at the base of the megabreccia; these northward-dipping beds are interpreted to be rotated and to represent a fold limb due to drag or southward (upward) ramping of strata along that surface.

The slip surface at the base of the Markagunt megabreccia dips variably, less than 10°. North of Panguitch Lake the surface dips southward, but dip reversal along the lake results in north dips near the southern limit of the megabreccia. For the most part, the dip of the slip surface approximates the regional or broadly local dip of the subjacent bedrock. We attribute the present-day dips of the slip surface and the autochthonous underlying bedrock to plateau tilting and associated folding following emplacement of the megabreccia. If our supposition is correct, these present-day dips do not reflect the dip of the slip surface during transport of the megabreccia. Locally the original dip can be inferred from the upper Tertiary gravel valley-fill overlying the megabreccia 3.4 km east of Panguitch Lake (fig. 12), assuming that these strata were deposited as essentially horizontal beds. These valley-fill deposits reflect the post-megabreccia dip of about 5° N. at this location. Below them, the basal slip surface of the megabreccia is generally horizontal. Rotating the valley-fill to horizontal causes the slip surface to exhibit a shallow south dip. Although these relationships are local, this exercise indicates the possibility of a southward gradient for transport of the megabreccia.

AGE

We interpret the age of transport of the Markagunt megabreccia to be about 22–20 Ma. Anderson (1993) suggested that the age of the megabreccia was 23–22 Ma. Constraints on the age of transport of the Markagunt megabreccia are (1) the age of maximum uplift and cooling of the Iron Peak laccolith or other coeval intrusions in that area if the megabreccia is related to that intrusive activity, (2) age of the youngest component of the megabreccia assemblage, and (3) age of autochthonous strata that unconformably overlie the megabreccia.

A

B

Figure 8. Naturally exhumed surface of Baldhills Tuff Member of Isom Formation formerly directly beneath Markagunt megabreccia. Surfaces exhibit asymmetrical "roche moutonnée"-like features and incised depressions interpreted to result from overriding by the megabreccia. *A*, View looking west-southwest; movement interpreted to be right to left; *B*, View looking south-southeast, movement interpreted to be away from observer. North side of Haycock Mountain, near top.

A

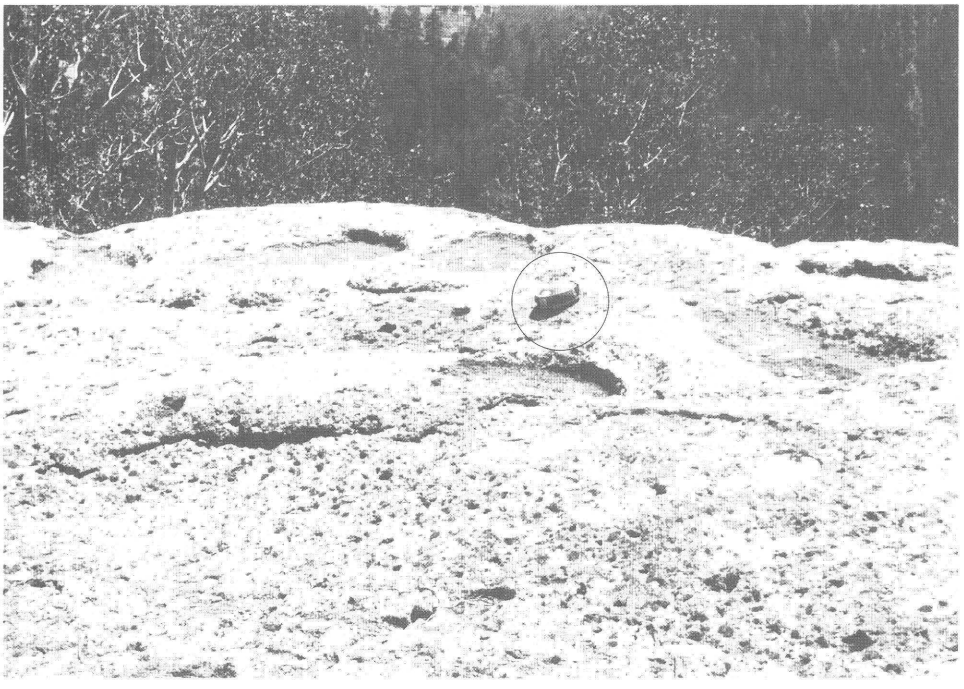

B

Figure 9. Naturally exhumed surfaces of Leach Canyon Formation tuff formerly directly beneath Markagunt megabreccia. Surfaces exhibit asymmetrical "roche moutonnée"-like features and incised depressions interpreted to have resulted from overriding by the megabreccia. *A*, View looking east-southeast; *B*, View looking southeast; movement of megabreccia interpreted to have been from left to right. Circled backpack and canteen for scale. North wall of Bunker Creek.

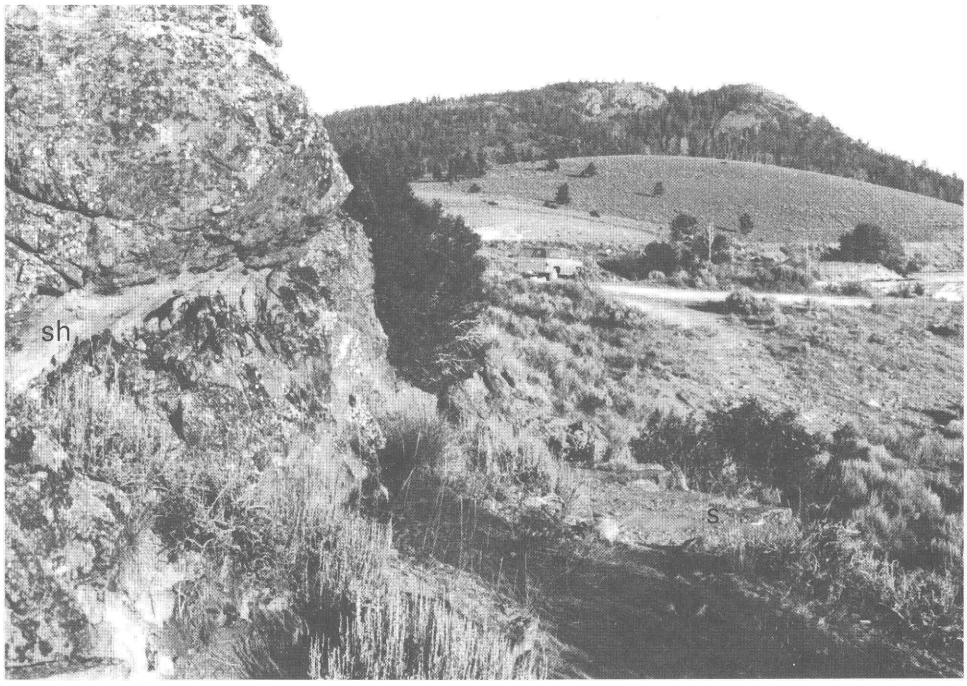

Figure 10. North-dipping shear plane (sh) in allochthonous block of Isom Formation tuff in Markagunt megabreccia overlying slip surface on autochthonous Isom Formation (s) (s is area shown in fig. 7). View looking south-southwest.

K-Ar whole-rock samples from the Iron Peak laccolith, from mafic dikes interpreted to be related to the intrusion, and from nearby lava flows believed to be derived from it, have been dated respectively at 20.2±0.5 Ma, about 20 Ma, and 21.2±0.5 Ma. The reported ages are in some doubt (Rowley and others, 1994, p. 21); the younger dates perhaps most nearly reflect the true age of the intrusion.

The youngest known components of the megabreccia assemblage are tuffaceous sandstone and conglomerate east of Panguitch Lake. Some of these beds contain distinctive tuff clasts that are petrographically identical with tuff of the Bauers Tuff Member of the Condor Canyon Formation, which has been dated by $^{40}Ar/^{39}Ar$ methods at about 22.8 Ma (Rowley and others, 1994, p. 14). If these clasts actually are Bauers Member clasts, the megabreccia obviously postdates that age.

Two rock successions have been interpreted to unconformably overlie the Markagunt megabreccia in its reference locality area along State Highway 143: (1) a succession consisting of thin stream gravels overlain by the Haycock Mountain Tuff (Anderson, 1993, p. 13) or (2) semiconsolidated valley-fill gravel and sand deposits of probable late Tertiary (late Miocene(?)–Pliocene(?)) age that are more than 60 m thick, the upper Tertiary gravels of Anderson (1993, p. 15). We interpret the latter to represent the overlying age constraint, and as discussed next, suggest that, as a possible distal facies of the Leach Canyon Formation, the Haycock Mountain Tuff is a component of the Markagunt megabreccia. Anderson (1993, p. 13–14), on the other hand, defined the Haycock Mountain Tuff as a new unit and postulated that it unconformably overlies the Markagunt megabreccia and thus postdates and constrains the minimum age of the megabreccia.

Several lines of evidence suggest that the Haycock Mountain Tuff may be a distal facies of the Leach Canyon Formation; other evidence supports Anderson's assertion. Because the relationship of the Haycock Mountain Tuff to the Leach Canyon Formation is controversial, the following discussion incorporates data relating to the temporal and spatial relations of these units and of other felsic tuffs in the study area. Correct interpretation of the age of the units and their relationships to the Markagunt megabreccia is of major importance. To this end, comparison of several features of these units is shown in table 1. The discussion following incorporates mostly interpretations by Sable, supporting the possibility that the Haycock Mountain Tuff is a distal facies of the Leach Canyon Formation, and indicating, because of the similarities of many of the features, the difficulties involved in agreement between investigators.

The type section and other outcrops of the Haycock Mountain Tuff, and outcrops of the Leach Canyon Formation on the Markagunt Plateau have been reexamined separately by Sable and P.D. Rowley. Rowley (written commun., March 27, 1995), after field examination of exposures along Utah State Highway 143, the area of Anderson's reference sections of the Markagunt megabreccia, agreed with Anderson's interpretations. Rowley also compared modal compositions and XRF (X-ray fluorescence) analyses of Haycock Mountain Tuff and Leach Canyon Formation samples (see following discussion).

Figure 11. Minor overturned fold and thrust fault in near-basal part of Markagunt megabreccia composed of sandstone, conglomeratic mudstone, and mudstone breccia probably of the Bear Valley Formation. Dashed line, axis of fold; arrows show dip of limbs. Heavy line, fault; dashed where inferred; barb shows direction of relative movement. Red conglomeratic mudstone (rcg) in upper and lower blocks indicates 2–10 m of displacement. Attitude of fault plane N. 80° E., 40° N., indicates south-vergent stress direction from N. 10° W. North side of Utah State Highway 143, about 2 km east of Panguitch Lake.

Age delineation of the Leach Canyon and Haycock Mountain units is of major importance for interpretation of their possible correlation and as a possible constraint for the age of the Markagunt megabreccia. Although earlier K-Ar dates show considerable variation, the $^{40}Ar/^{39}Ar$ dates of the Haycock Mountain Tuff samples, about 24 Ma, are similar to those of both Leach Canyon and Bear Valley Formation tuffs, both of which are older than the megabreccia. Considering age constraints discussed in preceding paragraphs, the 24 Ma dates for the Haycock Mountain Tuff are anomalous, if the Haycock Mountain Tuff is indeed younger than the Markagunt megabreccia, as Anderson stated. Our provisional interpretation is that the Haycock Mountain Tuff is a component of the megabreccia and a distal facies of the Leach Canyon Formation. Further sampling of these disputable units is planned to attempt to clarify their dates.

Further summarizing the data in table 1, the composition of these units is similar although the textures and degrees of welding by devitrification are considerably different. We attribute the unwelded to poorly welded character of the Haycock Mountain Tuff to be the result of distance from western Great Basin sources if this unit is a Leach Canyon facies. Unaltered shards, common in the Haycock Mountain Tuff, are also present in the basal part of the Leach Canyon. The difference in the relative abundance and size of red felsic lithic fragments (vent facies fragments?) and black mafic fragments (locally incorporated?) can also be attributed to distance from source. The modal and chemical XRF data (not in table 1) are also similar, although P.D. Rowley (written commun., March 27, 1995) reported a wider than expected span of XRF data points possibly resulting from the abundance of lithic fragments. Petrographically, there appear to be smaller phenocrysts and less quartz in the Haycock Mountain Tuff samples relative to those of the Leach Canyon. Thickness figures suggest eastward thinning of both the Leach Canyon and Haycock Mountain units, perhaps indicating a western source for both. The differences in structural attitudes and degree of deformation are enigmatic because we interpret the Haycock Mountain Tuff, where undeformed, to rest conformably on relatively undeformed strata within the Markagunt megabreccia but above its highly deformed basal part, whereas Anderson (1993) interpreted the tuff and underlying "gravels" to unconformably overlie units of the Markagunt megabreccia such as sheared Isom Formation tuff. We interpret these undeformed "gravels" to be a fluvial facies of the mafic-clast mudflow breccia (Anderson's "lahar") that elsewhere locally underlies the Haycock Mountain Tuff and overlies undeformed Bear Mountain strata.

Table 1. Comparisons of tuffs of Leach Canyon Formation, Haycock Mountain Tuff, and felsic tuffs in Bear Valley Formation, Markagunt Plateau, southwestern Utah.

DISTINGUISHING FEATURES	LEACH CANYON FORMATION (Narrows Tuff Member) (Anderson, 1965; Judy, 1974; Sable; Rowley, 1995, written commun.)	HAYCOCK MOUNTAIN TUFF (Anderson, 1993; Rowley, 1995, written commun.)	BEAR VALLEY FORMATION (Anderson, 1965, 1971; Wagner, 1984)	
			Welded ash-flow tuff	Unwelded ash-fall (?) or vent facies tuff
LITHOLOGY	Two to three ash-flow cooling units. Vitric-crystal to crystal-vitric. Moderately to densely welded. Light gray, pink, salmon hues. Moderately pumiceous. Prominent lithic fragments—mostly red, minor black and gray. Abundant shards in basal part.	Two ash-flow cooling units. Vitric-crystal to crystal-vitric. Poorly to moderately welded. Light to very light gray, pink, orange hues. Highly pumiceous; uncollapsed fragments. Prominent lithic fragments—mostly black and brown, minor red. Abundant shards.	One(?) cooling unit. Moderately welded. Reddish-brown. Pumiceous. Lithic fragments common.	Unknown number of cooling unit events. Unwelded to poorly welded. Light gray to pinkish gray. Pumiceous; abundant shards.
APPROXIMATE MODAL COMPOSITION (in percent)				
Plagioclase (% of crystals)	32-79	24-60	63-74	21-42
Sanidine do.	3-46	20-66	0-Tr	21-57
Quartz do.	8-57	10-41	0-8	8-27
Biotite do.	2-26	15±	Tr	6-14
Hornblende do.	0-5	<1	Tr	Tr
Pyroxene do.	0-6	<1	7-20	<1-4
Fe-Ti oxides do.	1-3	<1	Tr-4	Tr
Sphene do.	0-1	0	0	0
Apatite do.	0-<1	0	Tr	0
Rock fragments (% of total)	13-42	5-15	3-4	3-7
Pumice do.	Tr-14	5-15	Tr	0-7
Phenocrysts do.	5-23	10-20	10-30	12±
(Tr, trace)				
KNOWN DISTRIBUTION	From west margin of Markagunt Plateau to Panguitch Lake. Fairly continuous and widespread.	Haycock Mountain and Fivemile Ridge 1:24,000 scale quadrangles northeast of Panguitch Lake. Discontinuous exposures.	North-central Plateau. Area of about 500 km^2 east and northeast of Panguitch Lake. Discontinuous.	North-central Plateau. East, northeast, and north of Panguitch Lake. Discontinuous.

THICKNESS (Generally west to east)	West of lower Bear Valley - about 150 m. Summit Canyon - 100 m. Brian Head peak - 20 m; incomplete. Sydney Peaks - 35 m. Bunker Creek - 21 m.	Type section - 13.8 m. 12 kilometers east of type section - 8 to 11 m.	5 to 6 m.	5 to 50 m.
STRUCTURAL ATTITUDE AND DEGREE OF DEFORMATION	Mostly subhorizontal but locally deformed.	Mostly subhorizontal and undeformed but locally tilted.	Mostly subhorizontal and undeformed but locally deformed and sheared.	Mostly subhorizontal or of unknown attitude. Locally deformed.
STRATIGRAPHIC RELATIONSHIPS	At and near Brian Head peak overlies mafic lava-clast conglomeratic sandstone and breccia of "Mudflow and lava-flow breccia and sedimentary rocks" unit of Maldonado and Moore (1993) that overlies Isom Formation. Overlain by allochthonous Markagunt megabreccia components from Brian Head peak area eastward. Overlain by Mount Dutton Formation(?) mudflow breccia or Condor Canyon Formation along Plateau west margin.	At type section, overlies mafic lava-clast conglomeratic sandstone ("gravel" of Anderson (1993)). At most places overlies mafic lava-clast mudflow breccia or sandstone of Bear Valley and/or Mount Dutton Formations. Unconformably overlain by upper Tertiary valley-fill gravels.	Interbedded with Bear Valley Formation sedimentary rocks.	Interbedded with Bear Valley Formation sedimentary rocks.
RADIOMETRIC AGES IN Ma (K-Ar, Potassium Argon; Ar^{40}/Ar^{39},Argon-Argon ZFT, Zircon fission-track) p, plagioclase s, sanidine b, biotite	K-Ar, 24.6 ± 0.5 Ma K-Ar, 26.7 ± 1.0 Ma ZFT, 24.2 ± 2.0 Ma ZFT, 21.6 ± 2.0 Ma Average age 24.0 Ma (Rowley and others, 1994)	K-Ar, 89USa 1a 22.8 ± 1.1 (b) K-Ar, 89USa 1a 24.8 ± 1.0 (s) K-Ar, 89USa 1a 24.3 ± 1.0 (s rerun) K-Ar, 89USa 2a 22.3 ± 1.1 (p) Ar/Ar, 89USa 1a 23.86 ± 0.26 (b) Ar/Ar, 89USa 2a 24.23 ± 0.17 (p) (written communs., H.H. Mehnert, 1992; L.W. Snee, 1994)	K-Ar, 24.5 ± 0.5 Ma (p) (Anderson, 1971)	K-Ar, 24.6 ± 0.4 Ma (b) (Anderson, 1971)
SOURCE	Great Basin	Great Basin (?) Northern Markagunt Plateau (?)	Markagunt Plateau (?)	Markagunt Plateau (?)

Felsic tuffs in the Bear Valley Formation (Anderson, 1965, 1971; Florian Maldonado, unpub. mapping) are of two kinds: moderately welded ash-flow tuff and poorly to nearly unwelded ash-fall or vent facies tuff characterized by abundant shards. Comparison of their features (table 1) with those of the Leach Canyon Formation and Haycock Mountain Tuff shows overlap in mineralogic modes of the unwelded tuff. The welded ash-flow tuff is higher in plagioclase and pyroxene and lower in quartz. Relatively few thin sections of this unit have been reported, however, and some are of uncertain stratigraphic position because of structural complexity within the Markagunt megabreccia.

DISCUSSION

Possible analogs of the Markagunt megabreccia and the megabreccia associated with the Red Hills shear zone are the megabreccias described in the Iron Axis region of the Basin and Range province, about 22 km west and southwest of the Markagunt Plateau (Mackin, 1960; Rowley and others, 1989; Blank and others, 1992). These are associated with monzonitic intrusions of Miocene (22–20 Ma) age, and are attributed mostly to gravity sliding away from rapidly upwelling intrusive bodies. Transport distances of some blocks were as much as 6–9 km. In many respects, the complexity, timing, and relationships of these megabreccias resemble those of the Markagunt megabreccia, but many of the Iron Axis megabreccias are composed of thick, structurally competent, stacked ash-flow tuff units, whereas the Markagunt megabreccia contains a considerable volume of less competent sedimentary rocks, such as those of the Bear Valley and Mount Dutton Formations.

Although the original size of the Iron Peak laccolith was larger than that currently preserved, it is difficult to imagine an intrusive body of its size resulting in movement of a megabreccia as far as 25 km from this point source. If the Markagunt megabreccia was essentially a single south-vergent mass, it may represent movement away from an intrusive body larger than the Iron Peak laccolith, possibly a parent body of that intrusive. Data from aeromagnetic anomalies have suggested to H.R. Blank (oral commun., 1994) that large hypabyssal bodies underlie the Parowan Valley and the area west of the towns of Spry and Panguitch, and thus could have been the main intrusions controlling the emplacement of the megabreccia.

Emplacement of megabreccia units of southwestern Utah has been attributed by most investigators to low-angle gravity sliding during uplift and distension by intrusive doming, but another structural concept for development of some megabreccia units in southwestern Utah is that of low-angle thrusting away from domal intrusive bodies during late stages of emplacement. Low-angle displacement features in the Pine Valley laccolith area, about 45 km southwest of the Markagunt Plateau, appear to be the result of such thrusting (D.B. Hacker, Kent State University, oral commun., May 16, 1992; Blank and others, 1992, p. 408). A similar model, not specifically related to megabreccia formation, has been proposed for thrust faulting on the Paunsaugunt Plateau, east of the Markagunt. There, south-vergent low- to moderate-angle thrust faults involving Upper Cretaceous and Claron Formation (Paleocene and Eocene) strata have been mapped in the Bryce Canyon area, about 40 km east of Panguitch Lake (Davis and Krantz, 1986; Lundin, 1989). The west-trending faults are almost on strike with the southern boundary of the Markagunt megabreccia, and one could interpret both to be thrust-related. Studies by Merle and others (1993) interpret the "Paunsaugunt thrust belt" (Bryce Canyon area faults) to be the result of thin-skinned thrusting by gravity gliding or compressional "push" related to batholithic emplacement, or to vertical loading by the rock column. Nickelsen and Merle (1991) and Nickelsen and others (1993) showed a southward-convex arcuate pattern of kinematic features associated with the thrust faults of the Paunsaugunt thrust belt, and using these directional features such as fractures, slickenlines, small thrusts, and spaced cleavage, also delineated an arcuate radial pattern on the southern Markagunt Plateau south of the southern limits of Markagunt megabreccia. Northward extrapolation of Nickelsen's data, although not an entirely consistent pattern, also converges on or near the Iron Peak area. Whether the southward overriding model presented here for the transport of the Markagunt megabreccia is directly related to the south-vergent thrust model in the Bryce Canyon area is not known. The belt of directional indicators shown in figure 6 and the southern limit of the Markagunt megabreccia are on strike with the Paunsaugunt thrust belt structures. Two similar radial patterns of kinematic directional indicators therefore have been independently documented. If they are related, then the Iron Peak laccolith may represent only part of the plutonic complex of regional dimensions as envisaged by Blank and Crowley (1990), Blank and others (1992), and Rowley and others (1994, p. 8).

Figure 12 (facing page). Markagunt megabreccia components exposed along Utah State Highway 143, 4 km east of Panguitch Lake, showing relationships to underlying and overlying units. Markagunt megabreccia lower contact (lc); upper contact (uc). Autochthonous unit: Baldhills Tuff Member of Isom Formation (Tiba). Allochthonous units: Baldhills Tuff Member of Isom Formation (Tibm), Bear Valley Formation sedimentary rocks (Tbvs), Bear Valley Formation(?) lahar breccia (Tbvl), Haycock Mountain Tuff(?) (Thm). Tertiary valley-fill gravel (Tg) overlies megabreccia components with angular unconformity. Same area as Anderson, 1993, figs. 15–17 and 21. *A*, View looking east; *B*, Close-up of skyline of *A*, view looking south.

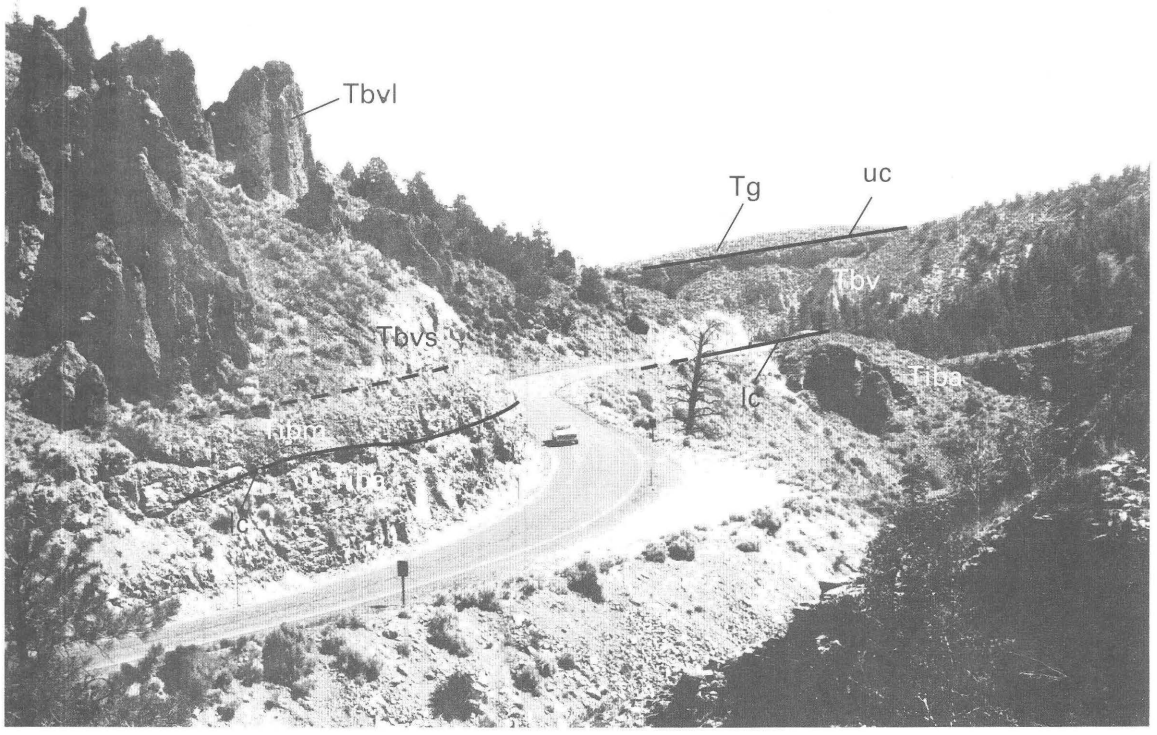

A

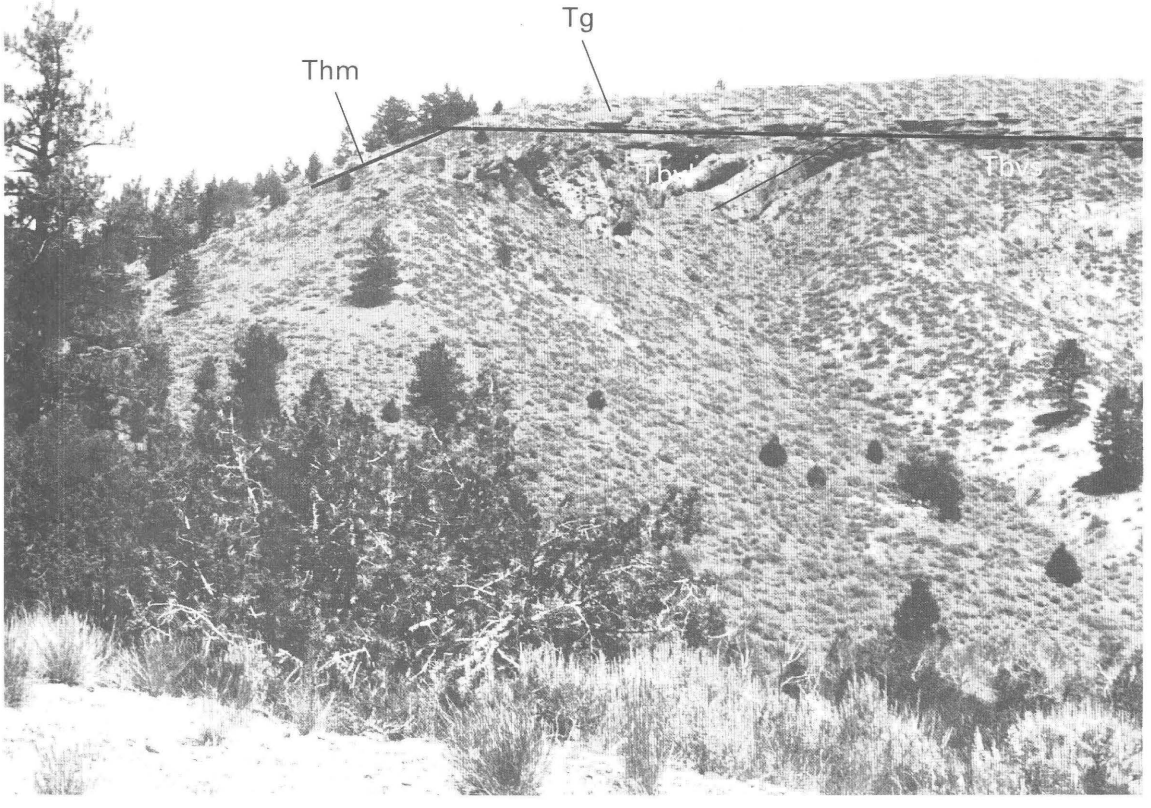

B

Whether transport of the Markagunt megabreccia was by gravity sliding or compressional thrusting can be debated. The mode of transport may simply reflect the original depth of the proximal displacement surface, which is unknown. As shown in figure 6, localities of observed directional features lie along a relatively narrow east-trending belt near the southern limits of the Markagunt megabreccia, where it is thin. Farther north, the widespread Mount Dutton rocks, particularly mudflow breccias that may be post-megabreccia units, obscure relationships of the allochthonous and autochthonous rocks, the actual morphology of the megabreccia mass, and the depth, configuration, and character of the slip surface. Subsurface information such as seismic or drill-hole data has not been studied by us. North of Bryce Canyon National Park, both drill-hole and seismic-reflection data indicate that the south-vergent thin-skinned faults sole in gypsiferous Jurassic rocks at present depths between 1,500 and 2,000 m (Lundin, 1989). Sole depths during faulting were undoubtedly greater. Considering the possible thickness of strata overlying the slip surface (Brian Head Formation into Mount Dutton units) of the Markagunt megabreccia, whether the Markagunt megabreccia is the result of gravity sliding or compressional thrusting, the original maximum depth of the slip surface is estimated to have been less than 1,500 m. Assuming that the stratal overburden above the base of the Markagunt megabreccia during movement was considerably less than that in the Bryce Canyon area, a gravity-sliding model would seem the more likely mode of transport rather than that of low-angle thrusting. A speculation by Davis and Rowley (1993) that the Markagunt megabreccia may represent shallow gravity-slide components transported on an underlying active thrust sheet seems plausible. Both structural types could be related to a common prime mover, the rapid or forceful emplacement of an igneous intrusive with resultant compressive lateral stresses and near-surface distension. The arcuate radial pattern of kinematic indicators of Nickelsen and others (1993) south of the megabreccia may well represent the surface evidence of the distal parts of an underlying thrust sheet.

The Markagunt megabreccia complex can be interpreted to be either one allochthonous mass that moved along a broad front from a broad point source (our interpretation) or as two or more smaller masses that were related or originated separately. If the megabreccia consists of two or more masses, genetic possibilities for megabreccia transport and emplacement other than the intrusion-caused model might apply. The west-northwest-trending high-angle faults of Anderson (1985, 1988, 1993) (the central and northern Black Ledge faults shown in fig. 4) may have provided structural control for a south-southwest direction of megabreccia movement. The S. 20° W. directional elements in the western part of the study area (fig. 6) and the dominant N. 80° W. trends of the klippen-like hills northeast of Brian Head peak are consistent with such tilted fault-block structural interpretation, although it is not the interpretation that Anderson applied to the megabreccia of areas 1, 2, and 4 (fig. 4). In the eastern area of directional observations, the S. 20° E. slip directions (fig. 6) might represent oblique movement of a separate megabreccia mass down a fault block surface, but this seems less likely than the south-southwest direction. The timing of megabreccia transport, which we interpret to be about 20 Ma, is also difficult to reconcile with the timing of formation of the fault blocks, which Anderson interpreted to have begun in middle Oligocene time. Anderson (oral commun., August 1995), however, has stated his belief that the movement on these southernmost faults was as late as Miocene. We prefer to interpret the evidence cited in this report to relate to an integrated pattern of south-vergent movement of a single allochthonous mass away from an intrusive body.

CONCLUSIONS

The Markagunt Plateau contains (1) breccia units coeval with volcanism in which megaclasts of volcanic rocks are embedded, (2) megabreccia associated with high-angle faults, (3) megabreccia associated with the Red Hills shear zone, and (4) the Markagunt megabreccia (restricted), a widespread unit on the upper surface of the plateau. We conclude that emplacement of the Markagunt megabreccia resulted from uplift and radial stresses associated with intrusion of the Iron Peak laccolith or nearby larger hypabyssal bodies. Transport directions of the megabreccia were southward, either by gravity sliding or by low-angle, thin-skinned thrusting away from the intrusion(s). The age of transport is documented to be between about 22 and 20 Ma, roughly coeval with ages of several 22–20 Ma intrusive bodies of the region. If the Markagunt megabreccia is indeed related to the age of maximum intrusive doming of the Iron Peak laccolith or a larger intrusive body, we believe that the age of megabreccia formation was about 20 Ma.

REFERENCES CITED

Anderson, J.J., 1971, Geology of the southwestern High Plateaus of Utah–Bear Valley Formation, an Oligocene-Miocene volcanic arenite: Geological Society of America Bulletin, v. 82, p. 1179–1205.

———1985, Mid-Tertiary block faulting along west and northwest trends, southern High Plateaus, Utah: Geological Society of America Abstracts with Programs, v. 17, no. 7, p. 513.

———1988, Pre-basin-range block faulting along west and northwest trends, southeastern Great Basin and southern High Plateaus: Geological Society of America Abstracts with Programs, v. 20, no. 3, p. 139.

———1993, The Markagunt megabreccia—Large Miocene gravity slides mantling the northern Markagunt Plateau, southwestern Utah: Utah Geological Survey Miscellaneous Publication 93-2, 37 p.

Anderson, J.J., Iivari, T.A., and Rowley, P.D., 1987, Geologic map of the Little Creek Peak quadrangle, Garfield and Iron Counties, Utah: Utah Geological and Mineral Survey Map 104, 11 p., scale 1:24,000.

Anderson, J.J., and Rowley, P.D., 1975, Cenozoic stratigraphy of the southwestern High Plateaus of Utah, *in* Anderson, J.J., Rowley, P.D., Fleck, R.J., and Nairn, A.E.M., Cenozoic geology of southwestern High Plateaus of Utah: Geological Society of America Special Paper 160, p. 1–52.

Berkland, J.O., Raymond, L.A., and Kramer, J.C., 1972, What is Franciscan?: American Association of Petroleum Geologists Bulletin, v. 56, no. 12, p. 2295–2302.

Best, M.G., Christiansen, E.H., Grommé, Sherman, McKee, E.H., and Noble, D.C., 1989, Eocene through Miocene volcanism in the Great Basin of the western United States–Excursion 3A: New Mexico Bureau of Mines and Mineral Resources, Memoir 47, p. 91–133.

Best, M.G., Scott, R.B., Rowley, P.D., Swadley, W C, Anderson, R.E., Grommé, C.S., Harding, A.E., Deino, A.L., Christiansen, E.H., Tingey, D.G., and Sullivan, K.R., 1993, Oligocene-Miocene caldera complexes, ash-flow sheets, and tectonism in the central and southeastern Great Basin, *in* Lahren, M.M., Trexler, J.H., Jr., and Spinosa, Claude, eds., Crustal evolution of the Great Basin and Sierra Nevada: Cordilleran/Rocky Mountain section, Geological Society of America Guidebook, Dept. of Geological Sciences, University of Nevada, Reno, p. 285–311.

Blank, H.R., and Crowley, J.K., 1990, Geophysical studies, *in* Eppinger, R.G., Winkler, G.R., Cookro, T.M., Shubat, M.A., Blank, H.R., Crowley, J.K., and Jones, J.L., Preliminary assessment of the mineral resources of the Cedar City 1°×2° quadrangle, Utah: U.S. Geological Survey Open-File Report 90-34, p. 24–42.

Blank, H.R., Rowley, P.D., and Hacker, D.B., 1992, Miocene monzonitic intrusions and associated megabreccias of the Iron Axis region, southwestern Utah, *in* Wilson, J.R., ed., Field guide to geologic excursions in Utah and adjacent areas of Nevada, Idaho, and Wyoming: Utah Geological Survey Miscellaneous Publication 92-3, p. 399–420.

Davis, G.H., and Krantz, R.W., 1986, Post-"Laramide" thrust faults in the Claron Formation, Bryce Canyon National Park, Utah: Geological Society of America Abstracts with Programs, v. 18, no. 5, p. 98.

Davis, G.H., and Rowley, P.D., 1993, Miocene thrusting, gravity sliding, and near-surface batholithic emplacement, Marysvale volcanic field, southwestern Utah: Eos, v. 74, no. 43, p. 647.

Fleck, R.J., Anderson, J.J., and Rowley, P.D., 1975, Chronology of mid-Tertiary volcanism in High Plateaus region of Utah, *in* Anderson, J.J., Rowley, P.D., Fleck, R.J., and Nairn, A.E.M., Cenozoic geology of southwestern High Plateaus of Utah: Geological Society of American Special Paper 160, p. 53–62.

Iivari, T.A., 1979, Cenozoic geologic evolution of the east central Markagunt Plateau, Utah: Kent, Ohio, Kent State University M.S. thesis, 154 p.

Judy, J.R., 1974, Geologic evolution of the west-central Markagunt Plateau, Utah: Kent, Ohio, Kent State University M.S. thesis, 154 p.

Landes, K.K., 1945, The Mackinac Breccia: Michigan Geological Survey Publication 44, Geological Series 37, chap. 3, p. 123–153.

Longwell, C.R., 1951, Megabreccia developed downslope from large faults: American Journal of Science, v. 249, p. 343–355.

Lundin, E.W., 1989, Thrusting of the Claron Formation, Bryce Canyon region, Utah: Geological Society of America Bulletin, v. 101, p. 1038–1050.

Mackin, J.H., 1960, Structural significance of Tertiary volcanic rocks in southwestern Utah: American Journal of Science, v. 258, p. 81–131.

Maldonado, Florian, 1995, Decoupling of mid-Tertiary rocks, Red Hills-western Markagunt Plateau, southwestern Utah, chapter I *in* Scott, R.B., and Swadley, W C, eds., Geologic studies in the Basin and Range-Colorado Plateau transition in southeastern Nevada, southwestern Utah, and northwestern Arizona, 1992: U.S. Geological Survey Bulletin 2056, p. 233–254.

Maldonado, Florian, and Moore, R.C., 1995, Geology of the Parowan quadrangle, Iron County, Utah: U.S. Geological Survey Geologic Quadrangle Map GQ–1762, scale 1:24,000.

Maldonado, Florian, Sable, E.G., and Anderson, J.J., 1990, Shallow detachment of mid-Tertiary rocks, Red Hills (Basin and Range), with implications for a regional detachment zone in the adjacent Markagunt Plateau (Colorado Plateau), southwest Utah: Geological Society of America Abstracts with Programs, v. 22, no. 3, p. 63.

———1992, Evidence for a Tertiary low-angle shear zone, Red Hills, with implications for a regional shear zone in the adjacent Colorado Plateau, *in* Harty, K.M., ed., Engineering and environmental geology of southwestern Utah: Utah Geological Association Publication 21, p. 315–323.

Maldonado, Florian, Sable, E.G., and Nealey, L.D., 1994, Evolution of Cenozoic structures, western Markagunt Plateau, southwestern Utah: Utah Geological Association Publication 23, p. 105–116.

Maldonado, Florian, and Williams, V.S., 1993a, Geologic map of the Parowan Gap quadrangle, Iron County, Utah: U.S. Geological Survey Geologic Quadrangle Map GQ–1712, scale 1:24,000.

———1993b, Geologic map of the Paragonah quadrangle, Iron County, Utah: U.S. Geological Survey Geologic Quadrangle Map GQ–1713, scale 1:24,000.

Merle, O.R., Davis, G.H., Nickelsen, R.P., and Gourlay, P.A., 1993, Relation of thin-skinned thrusting of Colorado Plateau strata in southwestern Utah to Cenozoic magmatism: Geological Society of America Bulletin, v. 105, p. 387–398.

Moore, D.W., 1992, Origin of breccia of the Isom Formation near Cedar Breaks National Monument, Markagunt Plateau, southwestern Utah: Geological Society of America Abstracts with Programs, v. 24, no. 6, p. 54.

Nealey, D.L., Maldonado, Florian, Unruh, D.M., and Budahn, J.R., 1994, Quaternary volcano-tectonic evolution of the western Markagunt Plateau and Red Hills area, southwestern Utah–Geochronological evidence from young basaltic rocks: Utah Geological Association Publication 23, p. 117–124.

Nickelsen, R.P. and Merle, O., 1991, Structural evolution at the tip line of a mid-Tertiary compressional event in southwestern Utah: Geological Society of America Abstracts with Programs, v. 23, no. 1, p. 109.

Nickelsen, R.P., Merle, O., and Davis, G.H., 1993, Structures of the mid-Tertiary radial compression in the high plateaus of southern Utah in relation to Sevier, Laramide and Basin and Range deformation: Geological Society of America Abstracts with Programs, v. 24, no. 6, p. 55.

Noble, L.F., 1941, Structural features of the Virgin Spring area, Death Valley, California: Geological Society of America Bulletin, v. 52, p. 941–999.

Rowley, P.D., McKee, E.H., and Blank, H.R., Jr., 1989, Miocene gravity slides resulting from emplacement of the Iron Mountain pluton, southern Iron Springs mining district, Iron County, Utah [abs.]: Eos, v. 70, no. 43, p. 1309.

Rowley, P.D, Mehnert, H.H., Naeser, C.W., Snee, L.W., Cunningham, C.G., Steven, T.A., Anderson, J.J., Sable, E.G., and Anderson, R.E., 1994, Isotopic ages and stratigraphy of Cenozoic rocks of the Marysvale volcanic field and adjacent areas, west-central Utah: U.S. Geological Survey Bulletin 2071, 35 p.

Sable, E.G., and Anderson, J.J., 1985, Tertiary tectonic slide megabreccia, Markagunt Plateau, southwestern Utah: Geological Society of America Abstracts with Programs, v. 17, no. 4, p. 263.

Smith, R.L., 1960, Ash flows: Geological Society of America Bulletin, v. 71, no. 6, p. 795–842.

Spurney, J.C., 1984, Geology of the Iron Peak intrusion, Iron County, Utah: Kent, Ohio, Kent State University M.S. thesis, 84 p.

Thomas, H.E., and Taylor, G.H., 1946, Geology and ground-water resources of Cedar City and Panowan Valleys, Iron County, Utah: U.S. Geological Survey Water-Supply Paper 993, 210 p.

Wagner, J.J., 1984, Geology of the Haycock Mountain 7.5 minute quadrangle, western Garfield County, Utah: Kent, Ohio, Kent State University M.S. thesis, 68 p.

Geochemistry and Petrogenesis of Quaternary Basaltic Rocks from the Red Hills and Western Markagunt Plateau, Southwestern Utah

By L. David Nealey, James R. Budahn, Florian Maldonado, *and* Daniel M. Unruh

GEOLOGIC STUDIES IN THE BASIN AND RANGE–COLORADO PLATEAU TRANSITION IN SOUTHEASTERN NEVADA, SOUTHWESTERN UTAH, AND NORTHWESTERN ARIZONA, 1995

U.S. GEOLOGICAL SURVEY BULLETIN 2153–I

UNITED STATES GOVERNMENT PRINTING OFFICE, WASHINGTON : 1997

CONTENTS

FIGURES

TABLE

Geochemistry and Petrogenesis of Quaternary Basaltic Rocks from the Red Hills and Western Markagunt Plateau, Southwestern Utah

By L. David Nealey, James R. Budahn, Florian Maldonado, *and* Daniel M. Unruh

ABSTRACT

Combined elemental and isotopic data for Quaternary mafic rocks from the Red Hills and western Markagunt Plateau, southwestern Utah, suggest that magmas erupted along the western margin of the Colorado Plateau probably originated by an open-system magmatic process involving fractional crystallization and crustal contamination. Magmatism may have tapped two mantle sources in the area, one in the asthenosphere and perhaps one in the lithosphere. Fractionation of these primary magmas appears to have been controlled mainly by the removal of olivine and clinopyroxene. The dominant cause of chemical variations within the magmas, however, appears to have been interaction with lower and upper crust. Chemical variations may also reflect differences in the residence times of magmas within the lithosphere. These processes operated together to produce two magma types: high-Nb (≥38 ppm Nb) and low-Nb (≤20 ppm Nb) mafic rocks. High-Nb mafic rocks have higher Ta, Th, and U contents, and lower Ba/Th and Ba/Nb ratios than the low-Nb rocks. High-Nb rocks also have higher Pb and Nd isotopic compositions than the low-Nb rocks. Overall, mafic volcanic rocks in the Red Hills and western Markagunt Plateau range in composition from basalt to trachybasalt to basaltic andesite. Their silica contents range from 49.9 to 53.6 weight percent SiO_2, and their $^{87}Sr/^{86}Sr$=0.70406 to 0.70587, $^{143}Nd/^{144}Nd$=0.512165 to 0.512333, $^{206}Pb/^{204}Pb$=16.995 to 18.013, $^{207}Pb/^{204}Pb$= 15.421 to 15.513, and $^{208}Pb/^{204}Pb$= 36.683 to 38.169.

Magmatism began about 1.3 Ma and ended about 0.45 Ma. The spatial pattern of ages suggests that magmatism migrated from west to east across the transition zone between the Basin and Range and Colorado Plateaus provinces in southwestern Utah. The migration of magmatism may follow a possible eastward migration of basin-range faulting across the transition zone. Silica content and Sr isotopic compositions decrease overall from west to east, suggesting that residence times were shorter for magmas erupted in the eastern part of the study area.

INTRODUCTION

Studies of basaltic magmas are of fundamental importance to understanding the evolution of the Earth's mantle and crust. Most, if not all, basaltic magmas originate in the upper mantle by partial melting of mantle peridotite. The chemistry of these magmas provides indirect evidence of the composition of mantle peridotite through the behavior of incompatible trace elements (Frey and others, 1978; Allègre and others, 1977; Allègre and Minster, 1978). Variations in the abundance of compatible elements, on the other hand, are controlled mainly by fractionation processes (removal and accumulation of phenocryst phases) that occur during the transport of the magmas to the surface. Following their generation, basaltic magmas may also change in composition due to interaction with the overlying mantle and crust.

The most important control on the bulk composition of basaltic magmas is likely to be the composition of the source materials. However, the source signature may be overprinted by post-melting fractionation and contamination. Uncertainty over the relative effects of fractionation and contamination results in considerable debate in the petrologic community, and two camps have now formed. One camp considers that the source region changes through time as extension causes heating and thinning of the lithospheric mantle (Perry and others, 1987, 1988; Farmer and others, 1989; Bradshaw and others, 1993; Feuerbach and others, 1993). Because the composition of the source materials of basaltic magmas is believed to change, these workers argue that magma compositions also change. The other camp argues that the change in the composition of eruptive products is due mainly to contamination in the lower and upper crust (Glazner and Farmer, 1992; Fitton, 1989; Fitton and others, 1991). Evidence for contamination comes from the presence of crustal xenoliths and xenocrysts in many upper Cenozoic mafic rocks (Nealey and Sheridan, 1989; Nealey and Unruh, 1991; Wendlandt and others, 1993).

Our objectives are: to relate basaltic volcanism between the Basin and Range and Colorado Plateaus provinces to the tectonic evolution of the two provinces in southwestern Utah, and to evaluate the effects of magmatic processes on

the composition of volcanic rocks. We use field studies, K-Ar chronology, major- and trace-element data, and Nd, Sr, Pb isotopic whole-rock data to understand the evolution of a relatively narrow range in magmatic compositions in one of the most interesting parts of the transition zone.

This study follows several previous geologic investigations on mafic rocks in the region. Lowder (1973) reported chemical analyses of a small number of volcanic rocks from the region, and presented the first Sr isotopic data. Everson (1979) reported Pb isotopic data for a lava flow (the Water Canyon flow) in our study area. More recently, chemical and isotopic data for mafic volcanic rocks from throughout the region were described by Kempton and others (1991) and Fitton and others (1991). Although these studies provide insight into the origin of mafic rocks, this report is the first comprehensive geochemical and isotopic study of mafic rocks from the western Markagunt Plateau and Red Hills.

ACKNOWLEDGMENTS

This research was supported by the National Geologic Mapping Program. We thank Robert B. Scott, Peter D. Rowley, Wayne R. Premo, and William D. Johnson, Jr. for critical reviews that helped to focus our thoughts and greatly improved their presentation. J.S. Mee, D.F. Siems, and Judy Kent are thanked for generating the XRF data. Thanks are also given to Harrison Nealey for assistance in the field.

GEOLOGIC SETTING

Volcanic rocks described in this report are part of a broad zone of upper Cenozoic mafic volcanic rocks that surround the Colorado Plateau in Utah, Arizona, New Mexico, and Colorado (fig. 1). This volcanic terrane was subdivided into the northeastern transition zone (NETZ) and the southeastern transition zone (SETZ) provinces by Kempton and others (1991) on the basis of a regional geochemical study. The present study area lies within the NETZ, which extends from northwestern Arizona into central Utah. The study area (fig. 2) contains numerous isolated Quaternary mafic volcanic centers, from which several small volume lava flows were erupted. The rocks described here have been mapped as part of the U.S. Geological Survey's National Geologic Mapping Program (Maldonado and Williams, 1993; Maldonado and Moore, 1993; and Florian Maldonado and E.G. Sable, unpub. mapping), and earlier field studies by the USGS (Averitt and Threet, 1973; Rowley and Threet, 1976).

The Red Hills–western Markagunt Plateau spans the east edge of the Basin and Range province, and lies at the west edge of the transition zone between the Colorado Plateaus and Basin and Range provinces. Near the latitude of the study area, the transition zone of Anderson and Christenson (1989) is 55 km wide and is bounded on the west by the Hurricane fault and on the east by the Paunsaugunt fault. Between the two fault zones, another major fault zone, the Sevier, and numerous minor faults mostly step structural blocks down to the west (figs. 2, 3).

Geologically, the southwestern Utah transition zone is an interesting area because it is adjacent to the widest continental rift in the world. Volcanism in such areas "is generally active as long as the fault[ing] is active, and as fault activity migrates, so too does volcanism" (Ellis and King, 1991). In general, volcanism in and on the margins of the rift is associated with the brittle deformation of the upper crust, and with crustal and lithospheric thinning associated with continental extension. We estimate that the crust in the vicinity of the Red Hills and western Markagunt Plateau was thinned 8–10 km in the Cenozoic, based on the difference between the thickness of the crust near Cedar City and that in the interior of the Colorado Plateau (32–34 km near Cedar City; 40 km in the interior of the Colorado Plateau; Jones and others, 1992). Our method of estimation is the same as that used by McCarthy and Parsons (1994) for calculating crustal thinning in the western Arizona transition zone, an area that has essentially the same structural setting as exists in the transition zone of southwestern Utah. However, for that area, McCarthy and Parsons (1994) estimated a slightly greater amount of crustal thinning (10–15 km), which can be reconciled if Jones and others (1992) underestimated the thickness of the crust beneath the interior of the Colorado Plateau. Other values in the literature range from 45 to more than 50 km for the thickness of the crust beneath the interior of the Colorado Plateau (Warren, 1969; Wong and Humphrey, 1989; Hendricks and Plescia, 1991; McCarthy and Parsons, 1994).

Overall, Cenozoic volcanism in the transition zone and adjacent parts of the Basin and Range and Colorado Plateau in southwestern Utah was long-lived. According to Rowley and others (1979, 1994), calc-alkaline magmatism began in the region about 34 Ma and continued until about 21 Ma. These early magmas erupted from stratovolcanoes and calderas in southwestern Utah and southern Nevada, and were probably fed by shallow batholiths as well as deeper sources (Steven and others, 1984; Blank and others, 1992; Rowley and others, 1994, in press; McKee and others, this volume, chapter L). At about 22 Ma, bimodal magmas (basaltic and rhyolitic) began to be erupted in the High Plateaus of the southwestern Utah transition zone, as rhyolite ash-flow tuff and rhyolite and mafic lava flows (Hausel and Nash, 1977; Lipman and others, 1978; Best and others, 1980; Mattox, 1992, this volume; Coleman and Walker, 1992; Rowley and others, 1994, in press; McKee and others, this volume). After 5 Ma, most of the magmas that were erupted in the Utah transition zone were basaltic (mostly subalkalic) in composition, but andesite erupted locally near Panguitch Lake and Red Canyon in the central Markagunt Plateau (fig. 2), and at the south end of the Escalante Desert near Enterprise, Utah (Lowder, 1973; Hausel and Nash, 1977; Anderson and

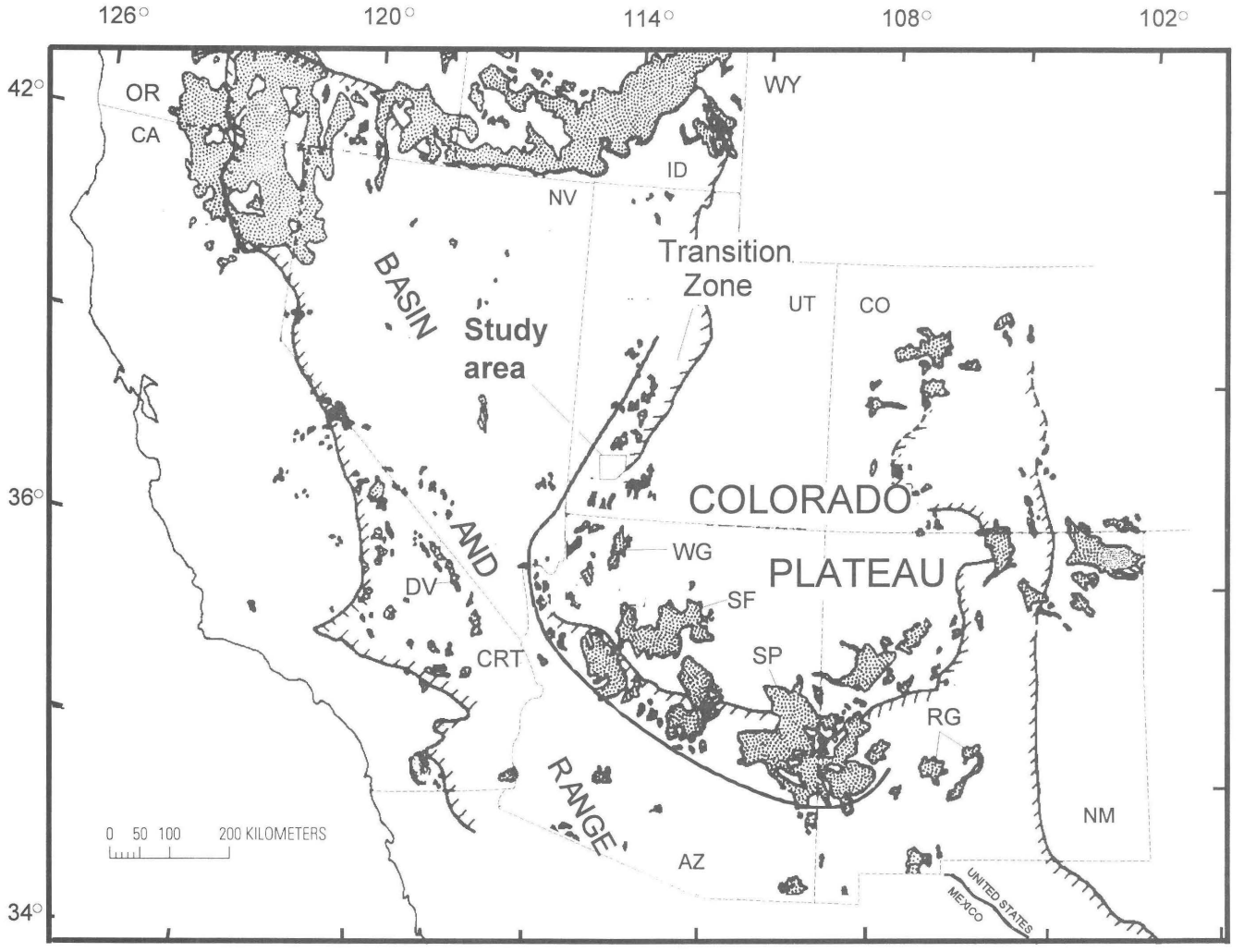

Figure 1. Distribution of upper Cenozoic volcanic rocks (mostly <5 Ma) (patterned) in part of western United States. Transition zone between Basin and Range and Colorado Plateau (Anderson and Christenson, 1989) is area between solid line and hachured line in Utah, Nevada, Arizona, and western New Mexico. Volcanic areas mentioned in text include WG, western Grand Canyon; SF, San Francisco; SP, Springerville; CRT, Colorado River trough, DV, Death Valley; RG, Rio Grande. Modified from Best and Brimhall (1974).

Mehnert, 1979; Best and others, 1980; Nealey and others, unpub. data, 1994). In contrast, post-5 Ma volcanic activity in the eastern Basin and Range, near and in the Mineral Mountains and Black Rock Desert, was bimodal basalt-rhyolite (Lipman and others, 1978; Coleman and Walker, 1992).

In general, volcanism in the Utah transition zone was associated with a long period of complex extensional structural deformation (Anderson and Christenson, 1989; Anderson, 1993; Maldonado and others, this volume, chapter G; Rowley and others, in press). The study area was cut by at least one mid-Tertiary low-angle structures (Maldonado and others, 1992), and by numerous small high-angle normal faults that produced an anastomosing swath of horsts and grabens that extends from the Hurricane fault eastward into the interior of the south-central Markagunt Plateau (fig. 3). Still younger high-angle normal faults cut Quaternary basalt flows and alluvium in different parts of the transition zone (Anderson and Christenson, 1989; Maldonado and Williams, 1993; Maldonado and Moore, 1993; Florian Maldonado and E.G. Sable, unpub. mapping). All these faults probably are basin-range structures that initially began their current episode of movement after 10 Ma (Anderson, 1989; Rowley and others, in press).

DISTRIBUTION OF VENTS

Figure 3 shows the distribution of horsts and grabens, and their bounding faults, in the study area. Several of the vents that erupted Quaternary mafic lavas occur on or near some of the faults, mainly in the horst blocks (fig. 2). In the Red Hills and on the east side of the Paragonah fault, cinder

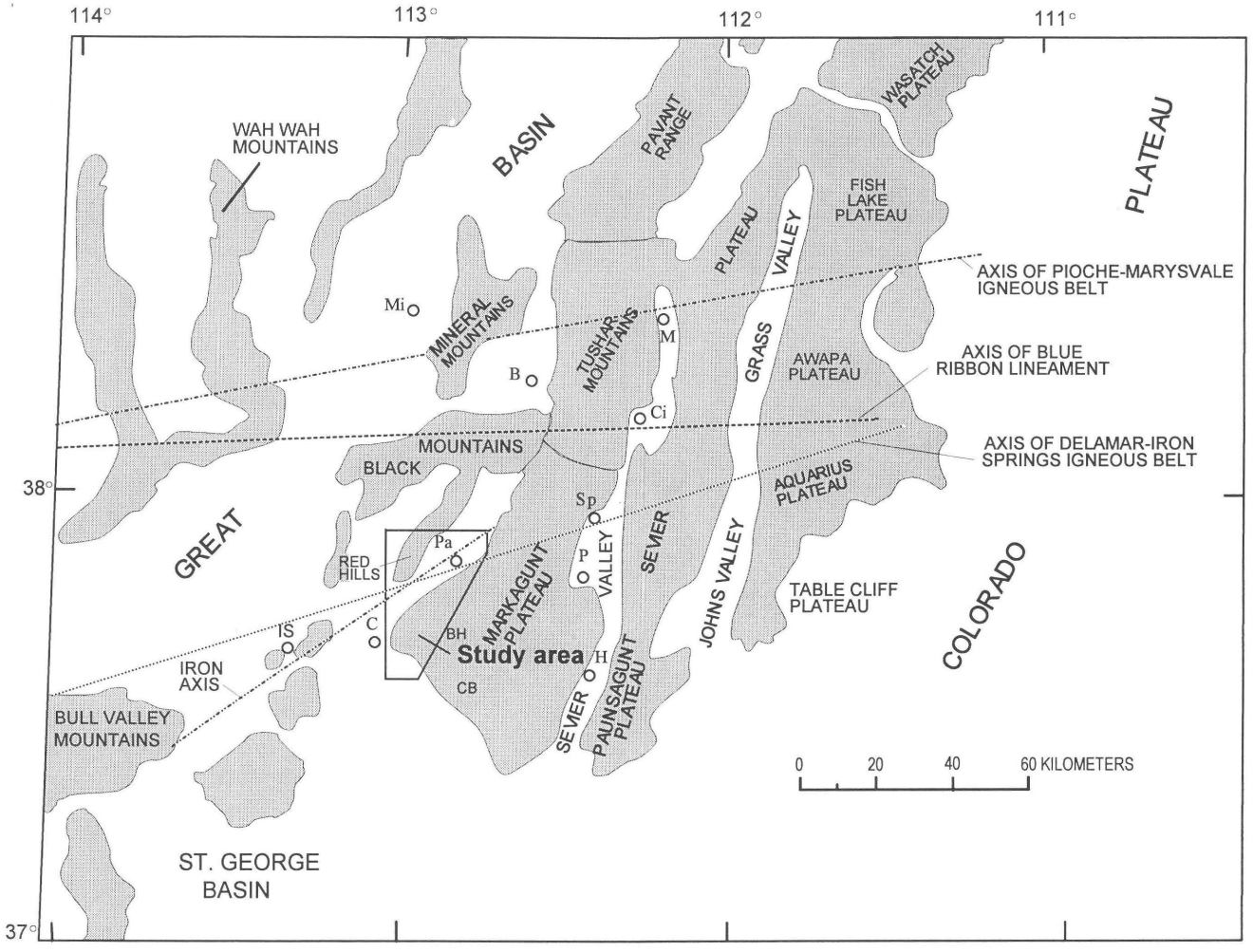

Figure 2. Index map of southwestern Utah. Modified from Rowley and others (1994). B, Beaver; BH, Brian Head; C, Cedar City; CB, Cedar Breaks; H, Hatch; IS, Iron Springs; M, Marysvale; Mi, Milford; P, Panguitch; Pa, Parowan; Sp, Spry; Ci, Circleville.

cones are aligned roughly parallel to faults. We interpret the vent alignments as evidence that volcanism was controlled by the faults or by joints associated with the faults. Similar alignments are very common in the central part of the southern Markagunt Plateau, near Navajo Lake, and in the St. George Basin south of the study area (Thomas and Taylor, 1946; Anderson and Christenson, 1989; Moore and Nealey, 1993). In the central part of the Markagunt Plateau, where some alignments extend for as much as 12 km, vent alignments mostly trend north-northeasterly and northeasterly (Anderson and Christenson, 1989). In contrast, vent alignments east of St. George are northwesterly. The boundary between the generally northeast and northwest trending alignments is near lat 37°10' N., where we suspect a major change takes place in the stress direction surrounding the Colorado Plateau.

AGE AND MIGRATION OF VOLCANISM

The majority of the Quaternary volcanic units in the Red Hills and western Markagunt Plateau have been dated by the K-Ar method. Those dates tell us that volcanism began in the area about 1.3 Ma with the emplacement of basalt and basaltic andesite cinder cones and lava flows in the Red Hills (Best and others, 1980; fig. 3). Activity moved to the east side of Parowan Valley at about 1 Ma (dates are 0.93 and 1.1 Ma; Anderson and Mehnert, 1979; Anderson and Bucknam, 1979), as volcanism became centered on Cinder Hill (fig. 3) and other small vents along the trace of the Paragonah fault (E.G. Sable, oral commun., 1993). Later activity occurred at Black Mountain at about 0.85 Ma (dates are 0.80 and 0.87 Ma; Best and others, 1980; E.G. Sable, oral commun., 1994), creating the largest Quaternary lava flow in the study area. The most recent volcanic activity took place at a vent above Water Canyon at about 0.45 Ma (Fleck and

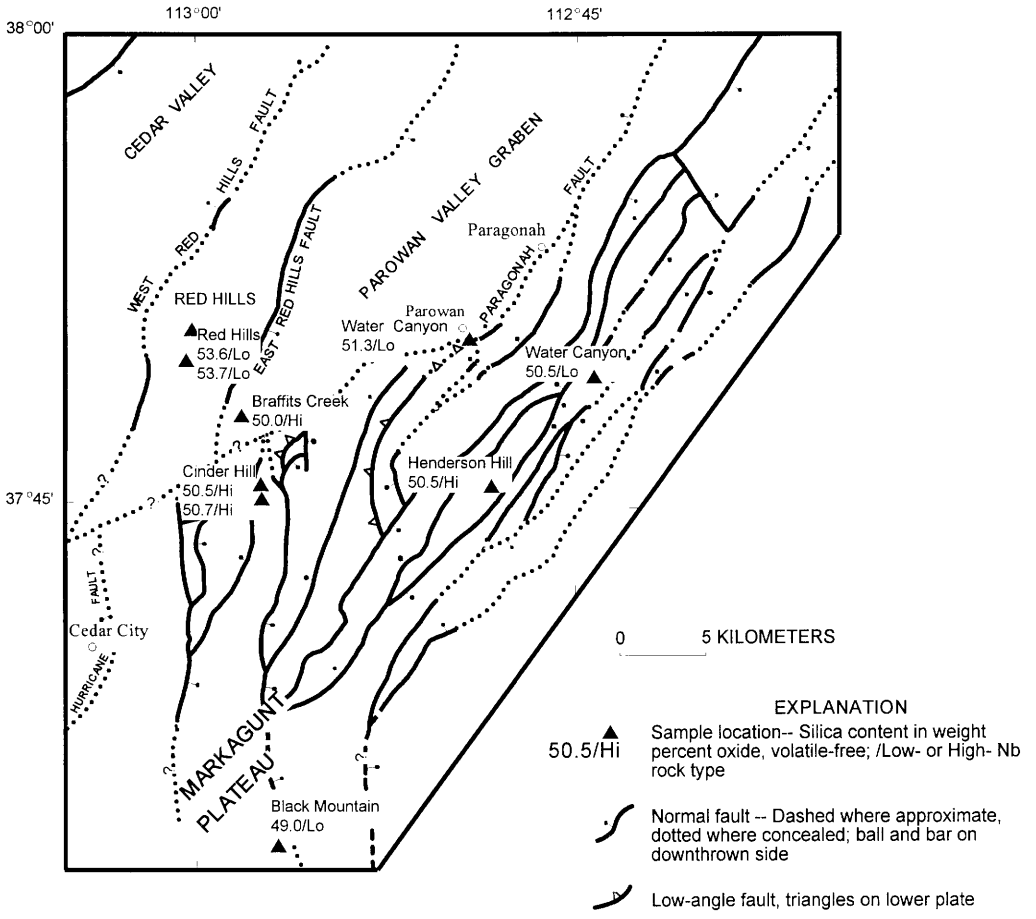

Figure 3. Index map showing relationships of vents and structures in the Red Hills and western Markagunt Plateau study area. Solid triangle, Quaternary volcanic center. Modified from Maldonado and others (this volume, chapter G).

others, 1975). Overall, the dates indicate that volcanism in the Red Hills and western Markagunt Plateau migrated eastward through time.

Late Cenozoic volcanism in the western Grand Canyon, San Francisco, and Springerville volcanic fields in Arizona (fig. 1) shows essentially the same migration pattern as that in the present study area. The similarity of the patterns suggests that volcanism was associated with progressive eastward structural transformation of the margin of the Colorado Plateau into Basin and Range terrain. The eastward and northeastward migration of volcanism in northern Arizona has been related to the relative motion of the North American plate to the Pacific plate (Best and Brimhall, 1974; Tanaka and others, 1986; Condit and others, 1989; Wenrich and others, 1995). However, a global tectonic model such as this is not necessary if the magmatism was the consequence of extension around the margin of the Colorado Plateau, as suggested by Ellis and King (1991).

GEOCHEMISTRY OF IGNEOUS ROCKS

SAMPLING AND ANALYTICAL METHODS

In pursuing our objectives of linking basaltic volcanism to the tectonic evolution of the transition zone, we collected samples from all major flow units in the study area. Analyzed samples are all relatively fresh material, without much evidence of post-emplacement alteration. Three of our samples are from the southern part of the Red Hills; two samples are from Cinder Hill, and two were collected from the Water Canyon flow (fig. 3). Single samples were collected from a dike near Henderson Hill, a flow on the south side of Black Mountain, and a flow near Braffits Creek. Based on location, petrography, and chemistry, the flow near Braffits Creek erupted from Cinder Hill. Macroscopically, all rocks in the study area are olivine basalts. Everson (1979) reported that the Water Canyon flow contains 10 percent olivine as phenocrysts and microphenocrysts, 10 percent augite

Table 1. Chemical analyses and isotopic composition of upper Cenozoic volcanic rocks from Red Hills and western Markagunt Plateau.

[Major-element analyses in weight percent oxide. Trace-element analyses in parts per million. Rock nomenclature modified from LeBas and others (1986). nd, no data, LOI, loss on ignition at 900°C. Analysts: J.S. Mee, D.F. Siems, J. Kent, J.R. Budahn, D.M. Unruh, L.D. Nealey]

Locality	Red Hills			Cinder Hill		Braffits Creek	Water Canyon		Henderson Hill	Black Mountain
Sample No.	**NE4**	**NE29**	**NE30**	**NS7**	**NS8**	**NS5**	**NP9**	**MP152**	**MP115**	**NWF93-1**
Rock type	Basalt	Basaltic Andesite	Basaltic Andesite	Basalt	Basalt	Basalt	Trachy-basalt	Trachybasalt	Basalt	Basalt
					Major element	**(XRF)**				
SiO_2	51.4	53.6	53.5	50.4	50.4	50.0	51.1	49.7	49.9	48.7
Al_2O_3	16.4	15.7	15.8	16.1	16.7	16.4	15.2	14.8	16.1	16.2
FeOT	10.0	9.09	9.1	9.54	9.29	9.43	9.17	9.05	9.87	10.90
MgO	5.80	7.18	7.24	7.57	6.74	7.11	8.27	8.87	7.81	7.66
CaO	9.57	7.51	7.43	9.29	9.34	9.21	8.25	8.85	9.14	8.93
Na_2O	3.17	3.46	3.45	3.54	3.65	3.56	3.5	3.26	3.45	3.31
K_2O	.88	1.47	1.49	1.22	1.21	1.22	1.92	1.86	1.21	1.25
TiO_2	1.29	1.32	1.31	1.36	1.37	1.39	1.37	1.30	1.47	1.67
P_2O_5	.25	.41	.39	.64	.64	.64	.61	.62	.81	.54
MnO	.16	.14	.14	.16	.16	.16	.14	.14	.17	.17
LOI	.44	.02	nd	nd	nd	nd	nd	.83	.04	.44
					Trace element	**(XRF)**				
Nb	11	18	16	38	39	40	9	16	46	6
Rb	23	21	25	26	24	18	28	24	18	18
Sr	410	510	490	740	790	770	1300	1350	870	nd
Zr	168	220	230	235	230	225	225	230	240	210
Y	33	27	26	29	27	26	27	24	24	22
Ba	470	660	690	940	1000	1000	1600	1500	1250	nd
Ce	<30	<30	56	110	87	97	120	122	112	nd
La	<30	<30	43	40	46	61	43	42	51	nd
Cu	59	52	46	50	57	51	39	49	52	46
Ni	63	172	170	112	78	89	194	215	104	100
Zn	71	83	75	71	74	78	71	70	78	66
Cr	144	280	225	260	174	210	255	265	230	182
					Trace element	**(INAA)**				
Ba	453	669	659	921	957	942	1470	1590	1220	796
Sr	466	548	573	876	867	846	1450	1390	867	914
Co	34	36	37	37	33	35	39	41	34	40
Ni	63	143	155	101	94	94	181	222	115	nd
Cr	150	288	261	258	204	227	291	293	251	240
Cs	.17	.30	.29	.17	.16	.04	.27	.20	.47	.17
Hf	3.53	4.59	4.5	4.62	4.50	4.47	4.38	4.11	4.55	3.88
Rb	17	24	22	19	19	18	23	20	16	nd
Sb	.14	.10	.15	.10	.11	.13	.07	.05	.17	.08
Ta	.39	.96	.90	1.87	1.94	1.89	.87	0.83	2.67	1.10
Th	2.25	2.90	2.55	6.47	6.83	6.68	2.74	2.86	10.2	1.88
U	.62	.65	.63	1.58	1.60	1.24	.80	.84	2.05	.35
Zn	77.4	79.7	77.6	76.0	77.5	78.1	74.9	79.2	99.7	nd
Zr	178	198	211	214	210	194	204	196	212	nd
Sc	29.6	24	23.7	27.9	24.6	26.3	23.9	25.2	24.7	nd
La	19.2	29.7	29.2	49.0	50.8	49.7	59.1	60.7	64.8	41.0
Ce	40.8	62.6	60.4	96.4	98.9	95.3	127	125	110	84
Nd	20.6	27.8	27.7	40.6	39.9	40.2	60.5	59.4	45.4	39.9
Sm	4.62	5.73	5.61	7.39	7.21	7.10	9.46	9.44	7.87	7.35
Eu	1.45	1.72	1.69	2.08	2.09	2.08	2.43	2.45	2.25	2.11
Gd	4.80	5.66	5.56	5.79	6.10	5.89	7.09	6.42	6.41	nd
Tb	.76	.79	.76	.82	.85	.83	.86	.83	.91	.83
Tm	.43	.42	.42	.41	.41	.42	.37	.36	nd	nd
Yb	2.70	2.75	2.62	2.57	2.50	2.58	2.28	2.22	2.15	2.43
Lu	.39	.38	.38	.38	.38	.37	.33	.32	.31	.36

Table 1. Chemical analyses and isotopic composition of upper Cenozoic volcanic rocks from Red Hills and western Markagunt Plateau.—*Continued*

				Isotopic	data	(Isotope	Dilution)			
Reference age (Ma)	1.3	1.3	1.3	1.0	1.0	1.0	0.45	0.45	nd	0.8
$^{87}Sr/^{86}Sr$	0.70587	0.70520	nd	0.70453	nd	0.704523	0.704058	nd	0.704577	0.704026
$^{143}Nd/^{144}Nd$	0.51233	0.51223	nd	0.51246	nd	0.512463	0.512165	nd	0.512525	0.512315
ε_{Nd}	-5.9	-5.8	nd	-3.4	nd	-3.4	-9.2	nd	-2.0	-6.3
$^{206}Pb/^{204}Pb$	17.609	17.477	nd	18.013	nd	18.034	16.995	nd	18.275	17.316
$^{207}Pb/^{204}Pb$	15.492	15.499	nd	15.512	nd	15.513	15.421	nd	15.537	15.482
$^{208}Pb/^{204}Pb$	38.169	37.612	nd	37.962	nd	37.983	36.683	nd	38.150	37.138

$\varepsilon_{Nd} = (^{143}Nd/^{144}Nd_{sample}/^{143}Nd/^{144}Nd_{CHUR}-1) \times 10^4$ where CHUR is the equivalent present-day value for a chondritic uniform reservoir (=0.51264)

microphenocrysts, 10 percent groundmass clinopyroxene, 60 percent groundmass plagioclase, 10 percent opaque oxides, and a trace of biotite. Although we have not performed detailed modal analyses of other samples from the study area, macroscopic inspection shows that they are similar petrographically to the Water Canyon flow.

Ten new major- and trace-element analyses of mafic rocks from the western Markagunt Plateau are presented in table 1. Seven of the ten samples were also analyzed for Sr-Nd-Pb isotopic compositions (table 1). All analyses were performed in the laboratories of the U.S. Geological Survey in Denver, Colo., and Menlo Park, Calif. Major-element compositions were determined by wavelength-dispersive X-ray fluorescence (XRF) spectrometry using methods described by Taggart and others (1987). Trace-element compositions were determined by energy-dispersive X-ray fluorescence spectrometry methods described by Johnson and King (1987). Trace-element analyses by instrumental neutron activation analysis (INAA) were obtained using methods similar to those described in Baedecker and McKown (1987). Isotopic analyses were obtained using methods described in Nealey and others (1993). Lead isotope ratios were corrected for mass fractionation by 0.12 ± 0.03 percent per mass based on analyses of NBS standard SRM-982. Measured Nd isotopic ratios were corrected for mass fractionation using $^{146}Nd/^{144}Nd = 0.7219$. Measured Sr ratios were corrected for mass fractionation using $^{86}Sr/^{88}Sr = 0.1194$. The $^{87}Sr/^{86}Sr$ ratios measured for NBS-987 during this study were 0.710255 ± 15. The $^{143}Nd/^{144}Nd$ ratios measured for La Jolla Nd standard were 0.511855±7 (95 percent confidence interval).

MAJOR-ELEMENT GEOCHEMISTRY

Volcanic rocks in the Red Hills and western Markagunt Plateau show a moderate range in major-element composition. Analyzed samples are chemically classified as basalt, trachybasalt, or basaltic andesite, using the IUGS nomenclature scheme for volcanic rocks (fig. 4; LeBas and others, 1986). All the samples have tholeiitic affinities (normative hypersthene and some normative quartz). The most silicic magmas (53.5 weight percent SiO_2) erupted in the Red Hills, near the north end of the Hurricane fault zone, whereas magmas erupted east of the Paragonah fault zone have silica contents less than 52 weight percent SiO_2. Overall, silica and alumina contents increase as potassium and phosphorus contents decrease with decreasing magnesia—regarded here as an index of differentiation (fig. 5). Sodium and titanium contents remain the same in all rock types regardless of their magnesia content. Interestingly, the most silicic samples (NE29 and NE30) have intermediate magnesia contents.

TRACE-ELEMENT GEOCHEMISTRY

Red Hills and western Markagunt Plateau mafic rocks show a wide range in trace-element abundances. Compatible trace elements, that is, those that are preferentially incorporated into mafic phases such as olivine and clinopyroxene, show a large amount of variability: Ni ranges from 22 to 215 ppm, Cr from 65 to 293 ppm, and Co from 34 to 41 ppm. Concentrations of incompatible trace elements, that is, those that are partitioned into the residual melt during fractional crystallization, may also show a significant range in abundance: Rb=15–24 ppm, Yb=0.31–0.41 ppm, Ba=453–1,590 ppm, Sr=410–1,350 ppm, Th=2.5–10.2 ppm, and La=19–64 ppm. On the basis of Nb content, the rocks can be distinguished

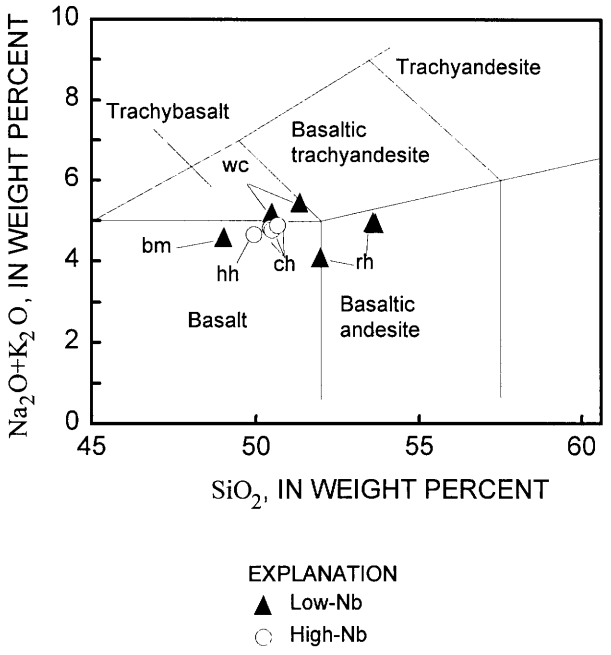

Figure 4. Alkali versus silica variation diagram for Quaternary volcanic rocks from western Markagunt Plateau. Samples are referenced to table 1: ch, Cinder Hill and Braffits Creek; wc, Water Canyon; bm, Black Mountain; rh, Red Hills; hh, Henderson Hill. Rock nomenclature after LeBas and others (1986).

into two magma types: low-Nb magmas containing less than 20 ppm Nb and high-Nb magmas containing more than 37 ppm Nb. High-Nb mafic magmas were erupted from vents in the middle of the study area. The two magma types are also easily distinguished using other incompatible trace elements: high-Nb rocks have high Ta, Th, and U contents compared to the low-Nb rocks (fig. 6). In addition, some incompatible trace- element ratios that have been suggested to have petrologic significance, such as Ba/Th and Ba/Nb (Weaver, 1991), are lower in the high-Nb mafic rocks than they are in the low-Nb rocks (Ba/Th=120–142 in high-Nb versus 201–556 in low-Nb rocks; Ba/Nb= 23.6–26.5 in high-Nb versus 37–163 in low-Nb rocks). Another petrologically important ratio, Ba/La, is also generally lower in the high-Nb rocks than in the low-Nb rocks (Ba/La=18.8–19 in high-Nb versus 19–26 in low-Nb rocks).

All the mafic rocks from the study area are enriched in light rare-earth elements relative to heavy rare-earth elements. Chondrite-normalized La ranges from 61 to 206, and Yb from 10 to 13 times the average chondritic value. Although light to heavy rare-earth element patterns are steep, chondrite-normalized patterns from Tb to Lu are essentially flat (figs. 7, 8). Thus, differences in

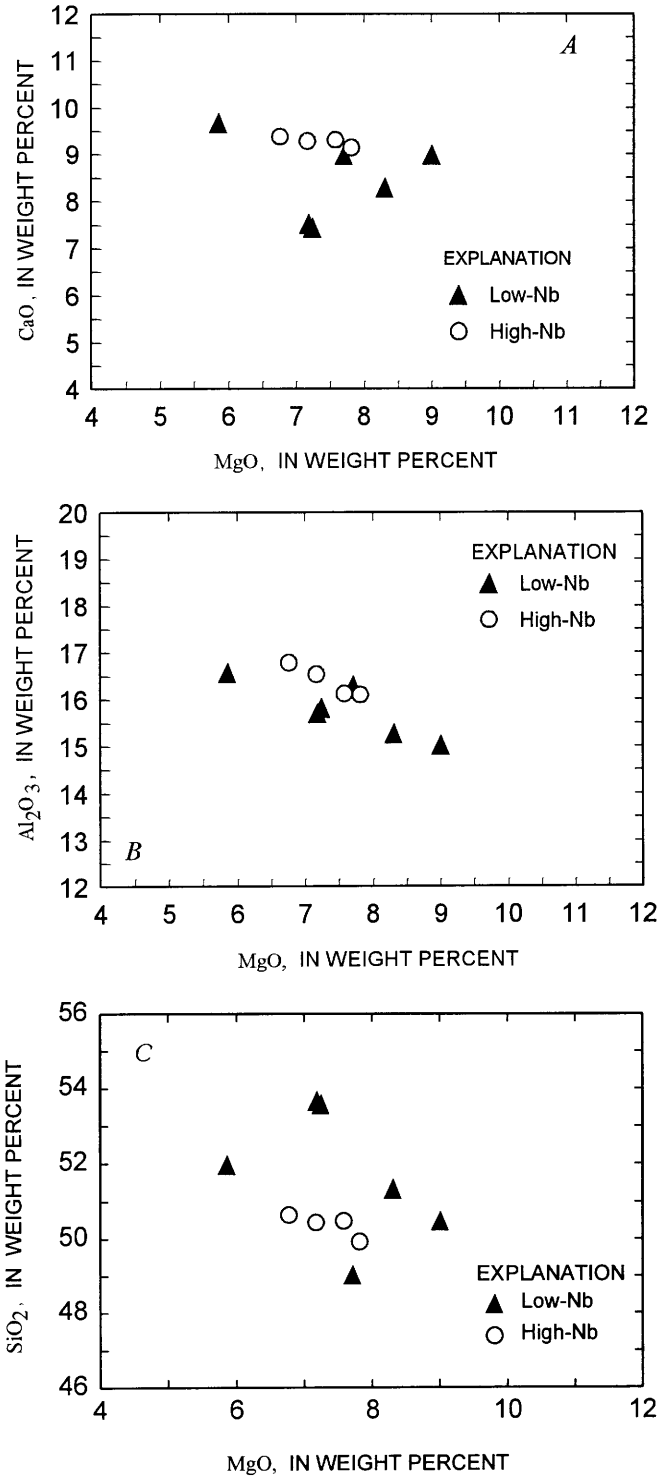

Figure 5 (above and facing page). Magnesia variation diagrams for mafic rocks from Red Hills and western Markagunt Plateau. Oxides plotted on a volatile-free basis. *A*, CaO; *B*, Al_2O_3; *C*, SiO_2; *D*, K_2O; *E*, Na_2O; *F*, TiO_2; *G*, P_2O_5.

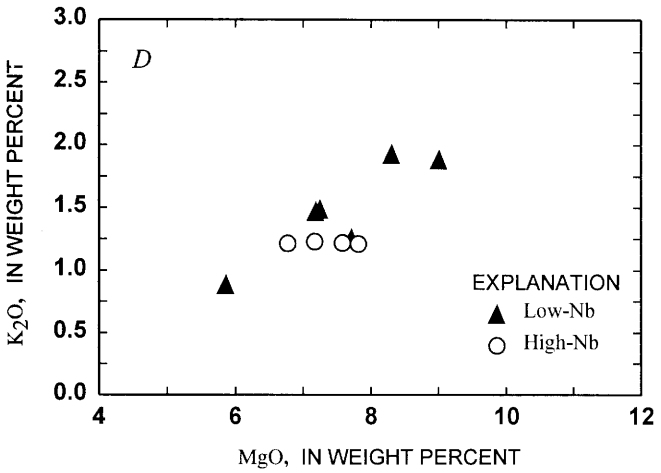

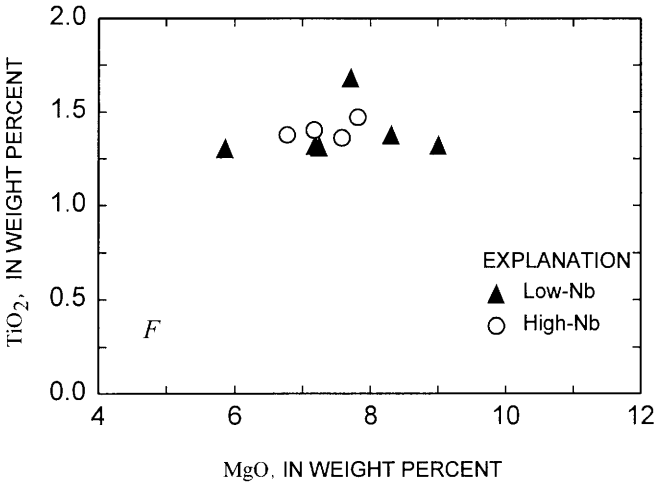

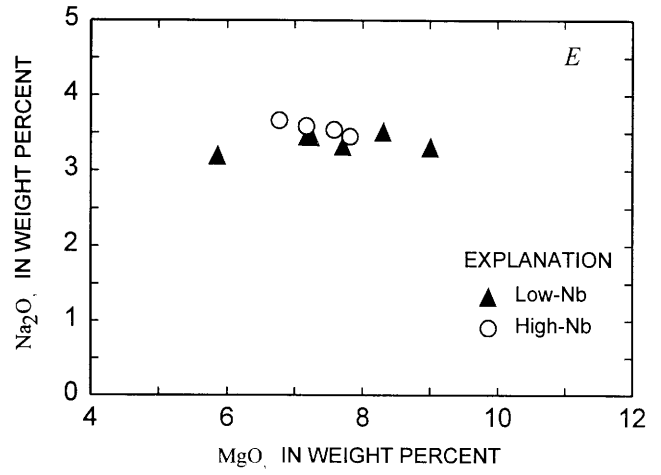

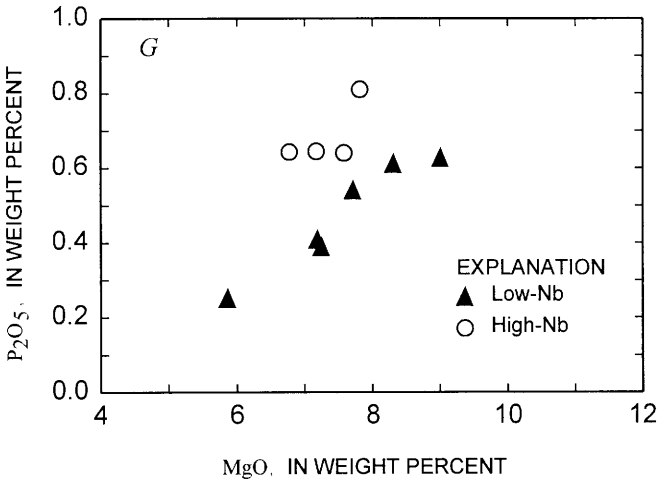

total rare-earth element abundances are due mainly to differences in light rare-earth element abundances. In primitive mantle-normalized spider diagrams, low-Nb rocks show negative anomalies between Ba and La and a large degree of dispersion from La to P (fig. 9). In contrast, high-Nb rocks show only small negative anomalies at K, Hf, and Ti, and almost no dispersion in primitive mantle-normalized spider diagrams (fig. 10). Samples from the same vent area have virtually identical trace-element compositions: normalized patterns for the Water Canyon flow (samples NP9 and MP152), Henderson Hill (NS7, NS8, and NS5), and the two basaltic andesite samples from the Red Hills (NE29 and NE30) are almost indistinguishable. Basalt from the Red Hills is distinguished from basaltic andesite from the same area by lower abundances of most trace elements. Assuming that all low-Nb magmas were related to the same parent magma and that all are related by the fractionation of olivine and clinopyroxene—phases that strongly partition light rare-earth elements into the residual melt—the order of increasing differentiation for the low-Nb magmas is (1) Red Hills basalt, (2) Red Hills basaltic andesite, (3) Black Mountain basalt, and (4) Water Canyon trachybasalt.

ISOTOPIC GEOCHEMISTRY

The isotopic compositions of mafic rocks in the Red Hills and western Markagunt Plateau are similar to those of other upper Cenozoic mafic rocks from the transition zone in southwestern Utah (Kempton and others, 1991; Nealey and others, 1993; Unruh and others, 1994). Measured $^{87}Sr/^{86}Sr$ ranges from 0.704026 to 0.705870 and measured $^{143}Nd/^{144}Nd$ ranges from 0.512165 to 0.512333 (table 1; fig. 11).

Measured $^{206}Pb/^{204}Pb$ ranges from 16.995 to 18.275 as $^{207}Pb/^{204}Pb$ ranges from 15.421 to 15.537, and $^{208}Pb/^{204}Pb$ ranges from 36.683 to 38.169 (table 1; figs. 12 and 13).

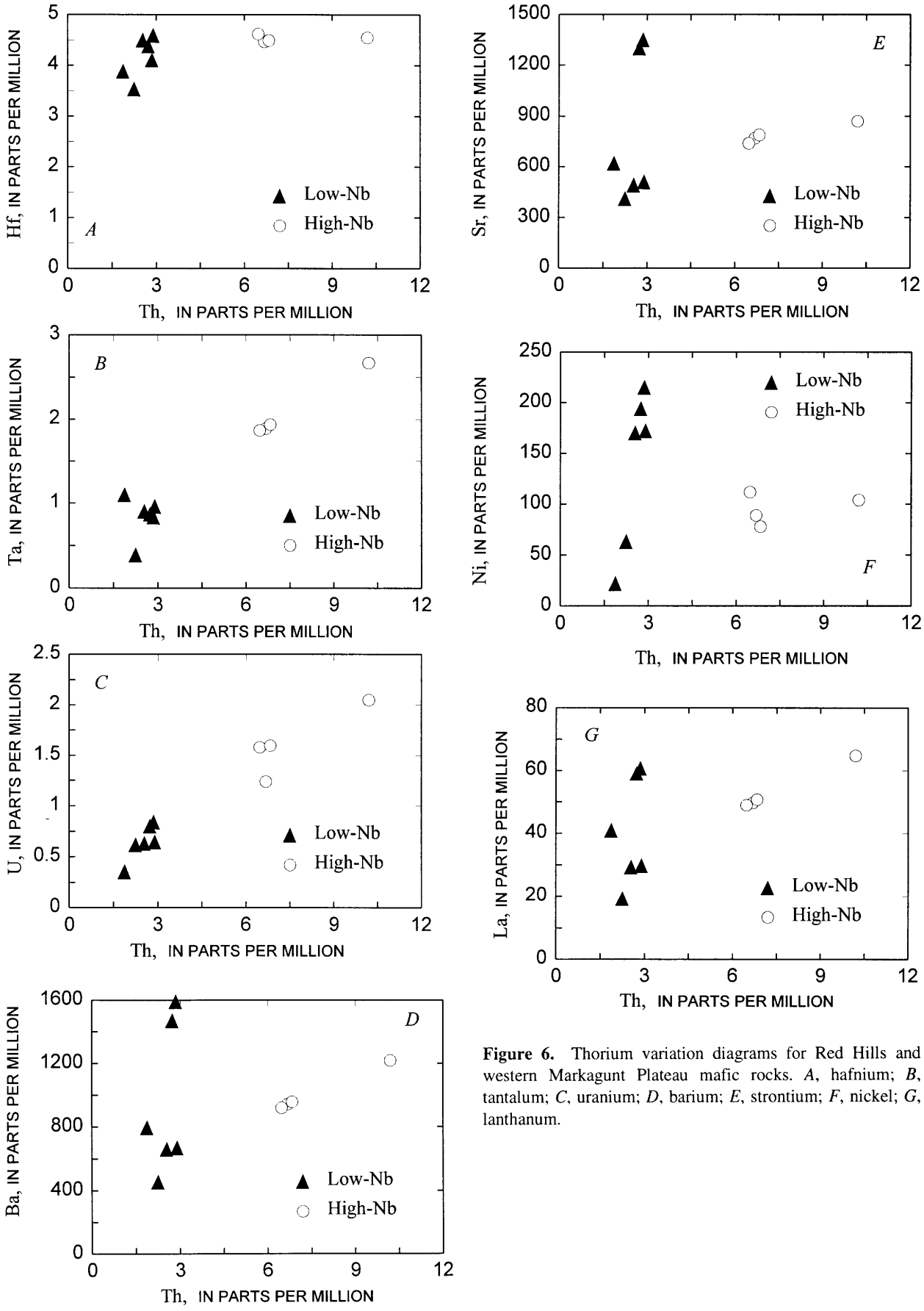

Figure 6. Thorium variation diagrams for Red Hills and western Markagunt Plateau mafic rocks. *A*, hafnium; *B*, tantalum; *C*, uranium; *D*, barium; *E*, strontium; *F*, nickel; *G*, lanthanum.

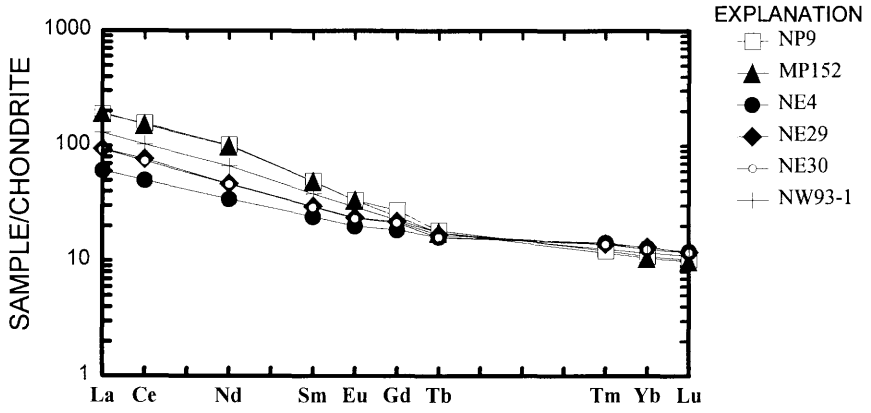

Figure 7. Chondrite-normalized rare-earth element diagram for low-Nb mafic rocks from Red Hills and western Markagunt Plateau. Normalization values from Hanson (1980).

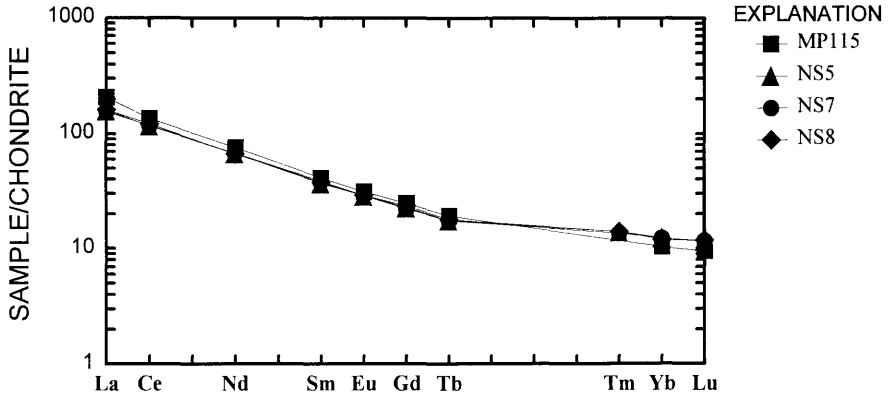

Figure 8. Chondrite-normalized rare-earth element diagram for high-Nb mafic rocks from western Markagunt Plateau. Normalization values from Hanson (1980).

Values of $^{207}Pb/^{204}Pb$ and $^{208}Pb/^{204}Pb$ are strongly correlated with $^{206}Pb/^{204}Pb$ (figs. 12 and 13). The Pb isotopic data plot above the northern hemisphere reference line (Hart, 1984), which is the average Pb isotopic composition of oceanic basalts in the northern hemisphere. The Pb isotopic data also plot generally below the Pb isotopic array of Proterozoic basement rocks from northwestern Arizona (Wooden and DeWitt, 1991), which we consider to represent the upper crust in the region.

High-precision isotopic data like those reported here show promise as a tool for correlating disconnected mafic lava flows. Sample NS7 from Cinder Hill has the same isotopic composition as the sample collected from the lava flow near Braffits Creek, confirming that the lava flow erupted from Cinder Hill.

Isotopically, low-Nb and high-Nb rock types have distinctive signatures. Low-Nb rocks show a wide range in Sr isotopic composition ($^{87}Sr/^{86}Sr$=0.704026 to 0.705870) compared to a very small range for high-Nb rocks ($^{87}Sr/^{86}Sr$=0.7045 ± 0.0001). Similarly, the Nd isotopic composition of low-Nb rocks is much lower than that of the high-Nb rocks ($^{143}Nd/^{144}Nd$=0.512165 to 0.512333 and 0.51246 to 0.512525). High-Nb rocks also have higher Pb isotopic compositions than low-Nb rocks. In general, high-Nb rocks more closely resemble the estimated composition of bulk solid earth and ocean-island basalt than do the low-Nb rocks (fig. 11).

DISCUSSION

Petrologists generally accept that mafic magmas similar in composition to those erupted in the Red Hills and western Markagunt Plateau are generated by partial melting of mantle peridotite. Much of the current literature deals with distinguishing between sources in the asthenosphere and those in the lithosphere. The asthenosphere is defined as that part of the upper mantle that is well stirred by convection, whereas the lithosphere is the rigid part of the upper mantle and the overlying crust (Perry and others, 1987; Fitton, 1989). This distinction is often difficult to establish because lithosphere can be transformed into asthenosphere by rising temperatures, and young lithosphere can show the same chemical signatures as asthenosphere. According to Fitton (1989), the lithosphere represents a long-term repository for

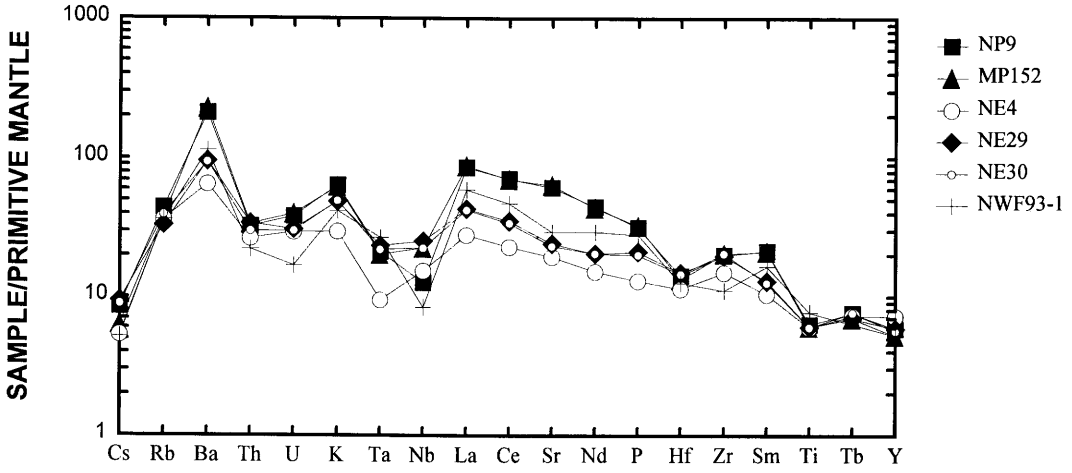

Figure 9. Primitive mantle-normalized spider diagram for low-Nb mafic rocks from Red Hills and western Markagunt Plateau. Primitive mantle values from Sun and McDonough (1989).

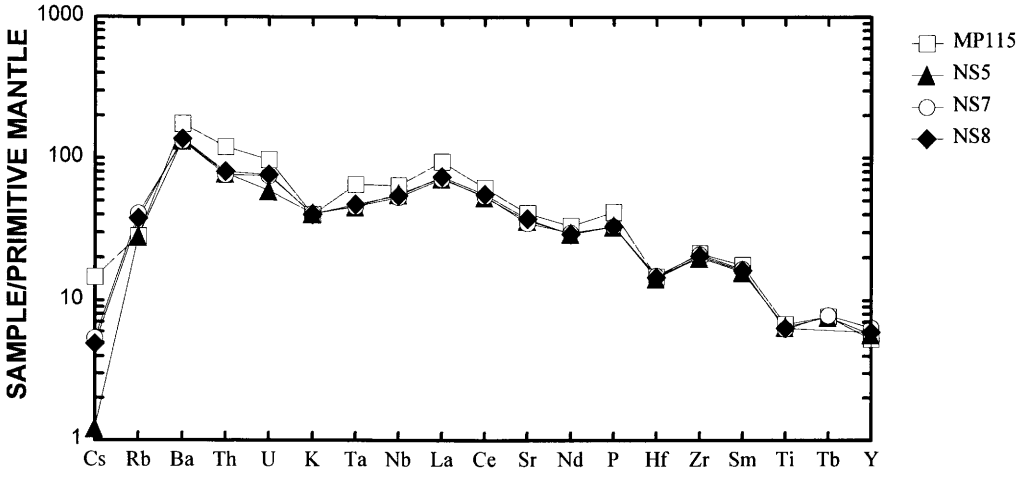

Figure 10. Primitive mantle-normalized spider diagram for high-Nb mafic rocks from western Markagunt Plateau. Chondrite values from Sun and McDonough (1989).

enriched and depleted mantle domains; however, both lithosphere and asthenosphere may contain zones of enriched and depleted mantle peridotite according to Perry and others (1987). Whatever the magma source, silicate melts may undergo extensive differentiation following their generation, as magmas change in composition due to interaction with the lithosphere and undergo crystal fractionation. We attempted to evaluate the effects of these processes on magmas erupted in the study area. We begin by considering the ultimate source of the silicate melts.

SOURCE OF MAGMAS

Trace-element and isotopic data are commonly used to distinguish between asthenospheric and lithospheric mantle sources. The standard for ascribing magmas to an asthenospheric source is ocean-island basalt (OIB), which typically has relatively high Nd ($^{143}Nd/^{144}Nd$=0.5132–0.5124) and low Sr ($^{87}Sr/^{86}Sr$=0.7023–0.706) isotopic compositions (Floyd, 1991). Ocean-island basalt also has $^{206}Pb/^{204}Pb$=17.5–21 and $^{207}Pb/^{204}Pb$=15.4–15.85 (Floyd, 1991). OIB-like asthenosphere has been suggested to exist beneath the Rio Grande rift in New Mexico (Perry and others, 1987), and the Geronimo volcanic field in southeastern Arizona (Kempton and others, 1991), as well as beneath other parts of the western United States. None of the rocks from the Red Hills and western Markagunt Plateau show geochemical signatures of OIB, indicating that they were not derived directly from asthenospheric mantle.

Menzies (1989) and Farmer and others (1989) suggested that enriched lithospheric mantle still exists beneath parts of the western United States. In some areas, the lithosphere is at least 100 km thick (Prodehl, 1979). Although it is possible that Red Hills and Markagunt Plateau magmas

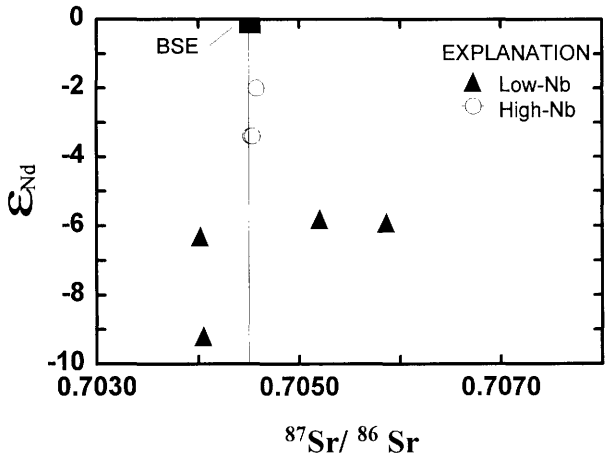

Figure 11. ε_{Nd} versus $^{87}Sr/^{86}Sr$ isotopic variation diagram for mafic volcanic rocks from Red Hills and western Markagunt Plateau. Bulk solid earth (BSE) has the composition $\varepsilon_{Nd}=0$ and $^{87}Sr/^{86}Sr=0.7045$.

could have been derived from enriched lithospheric mantle, the high Nd isotopic composition of mantle xenoliths from the Grand Canyon volcanic field (ε_{Nd}=+14 to +20; Douglas Smith, University of Texas, written commun., 1994) argues strongly against this material being the source of these magmas. Also none of the mafic rocks in the study area have the same isotopic composition as lithospheric mantle presumed to exist beneath the Rio Grande rift (ε_{Nd}=0 to +2; Perry and others, 1987). Additionally, they do not exactly match in composition to lithospheric mantle presumed to exist beneath the Mineral Mountains in southwestern Utah (ε_{Nd} =–5; $^{87}Sr/^{86}Sr$ =0.705: Coleman and Walker, 1992). Thus the preponderance of evidence suggests that Red Hills and western Markagunt Plateau magmas were not derived directly from lithospheric mantle.

CRYSTAL FRACTIONATION

In order to show that crystal fractionation played a role in magma genesis, we tested the efficacy of the fractionation process using various assumed parent magmas. The best evidence that crystal fractionation contributed to chemical variability within the magmas comes from the presence of phenocrysts in analyzed samples. However, none of our samples contains ultramafic xenoliths, so the exact mineral assemblages and proportions involved in fractionation cannot be determined.

We evaluated the role of high-pressure fractionation by assuming that highly incompatible elements like Rb, Th, and La had bulk-partition coefficients of zero. This is a reasonable assumption because partition coefficients for these elements are very small in mineral phases such as olivine and clinopyroxene (D^{Oliv}_{Rb} =0.008–0.011; D^{Cpx}_{Rb} = 0.003–0.018; Bornhorst, 1980; Henderson, 1982). Fractionation of these phases from a parental magma would have significantly increased the abundances of such highly incompatible elements in residual magmas. In our calculations we used the Rayleigh fractionation law:

$$C_L/C_O=F^{(D-1)}$$

where F is the fraction of melt remaining after fractionation and D is the bulk-partition coefficient for minerals fractionated from the parent magma. The variables C_L and C_O represent the concentrations of the elements of interest in the residual magma and in the parent magma, respectively. Thus, if D=0, the amount of fractionation is given by

$$F=C_O/C_L$$

Obviously, the first fractionation tests that should be made are those for magmas erupted from the same volcanic center or alignment, then for magmas within the same petrologic group, and last for magmas from different petrologic groups. The three samples (NS7, NS8, and NS5) from Cinder Hill provide an estimate of the amount of fractionation that may be associated with a single volcanic center. Taking the Braffits Creek sample (sample NS5) as being parental to samples NS7 and NS8, the latter two rocks could have formed by 25–31 percent fractionation using XRF Rb, or about 5 percent fractionation using INAA Rb, assuming that Rb behaved as a perfectly incompatible element. Modeling using Th suggests that these same samples could be related by 3–5 percent fractionation, and modeling using La suggests 1.5–3.5 percent fractionation. The coherence between the calculated amounts of fractionation using Th and La as incompatible elements suggests that the total amount of fractionation associated with the Cinder Hill magma batch is small, probably 3–3.5 percent.

Basalt and basaltic andesite in the Red Hills are petrographically and chemically distinct. Taking Rb as a perfectly incompatible element suggests that these rocks may be related by 8–16 percent fractionation of a parent with the XRF Rb content of sample NE29, which is a basaltic andesite and is therefore unlikely to produce both basalt and another basaltic andesite composition through a simple fractionation process. But, if INAA Rb data are used, the two basaltic andesite samples from the Red Hills can be related to the basalt sample by 22–29 percent fractionation. Modeling using Th suggests that the basaltic andesite samples can be related to the basalt sample by 11–22 percent fractionation. Modeling using La suggests that the basaltic andesite samples can be related to the basalt sample by 34–35 percent fractionation of the parent composition. The discordance here suggests that some process other than simple fractionation is responsible for the chemical variability of rocks in the Red Hills. We suggest then that if magmas erupted in the same general area cannot be related by crystal fractionation, it is extremely unlikely that this process can explain the entire range in elemental and isotopic composition of both the low-Nb and the high-Nb magmas. The most likely explanation for the wide range in trace-element abundances and isotopic composition is crustal contamination.

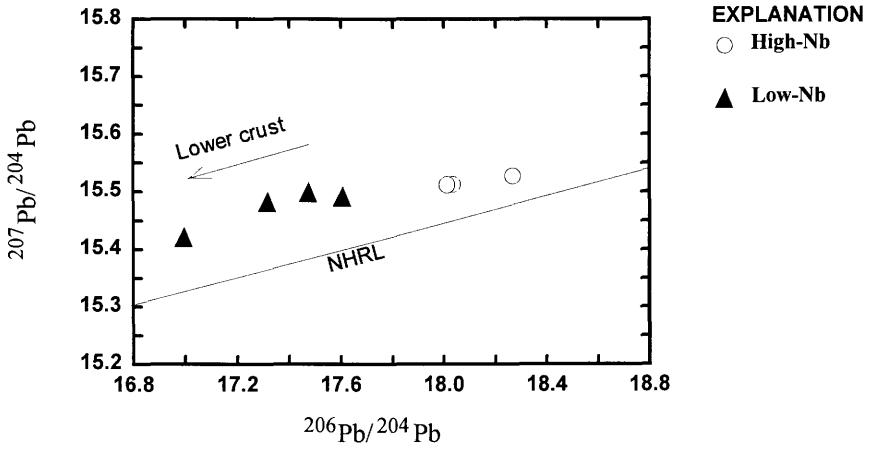

Figure 12. $^{207}Pb/^{204}Pb$ versus $^{206}Pb/^{204}Pb$ isotopic variation diagram for mafic rocks from Red Hills and western Markagunt Plateau. NHRL, northern hemisphere reference line (Hart, 1984).

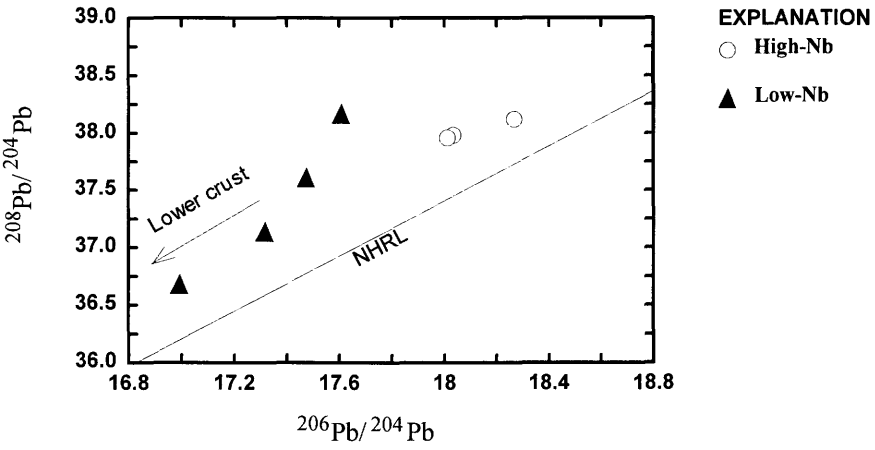

Figure 13. $^{208}Pb/^{204}Pb$ versus $^{206}Pb/^{204}Pb$ isotopic variation diagram for mafic rocks from Red Hills and western Markagunt Plateau. NHRL, northern hemisphere reference line (Hart, 1984).

CRUSTAL CONTAMINATION

According to Fitton and others (1991), asthenosphere-derived magmas may become enriched in Ba, radiogenic Sr, and light rare-earth elements during their residence in the lithosphere. Crustal interaction with silicic rocks would raise the $^{87}Sr/^{86}Sr$ and lower the $^{143}Nd/^{144}Nd$ ratios of hybrid magmas. Exposed basement rocks in the region in fact show a wide range in composition from diabase to granite, and the more silicic varieties have high-Sr, low-Nd, and variable Pb isotopic compositions (Bennett and DePaolo, 1987; Wooden and DeWitt, 1991; Bryant and others, in press), whereas lower crust is probably composed predominantly of mafic and intermediate rock types having low-Sr, Nd, and Pb isotopic compositions (Nealey and Unruh, 1991; McCarthy and Parsons, 1994). Because the range in composition of crustal materials is so large, contamination of asthenosphere-derived magmas by continental crust could result in an extremely wide range of hybrid chemical compositions, depending on which crustal materials and in what proportions they were involved in the contamination process. This is exactly the signature observed in Red Hills and western Markagunt Plateau rocks.

One line of evidence that Red Hills and western Markagunt Plateau magmas were contaminated in the crust comes from high-field-strength element ratios. These ratios are similar to those of mafic magmas erupted in subduction zone environments where crustal contamination has been shown to be a major process. In addition, the low-Nb mafic rocks show large Ta-Nb anomalies in primitive mantle-normalized diagrams, typical of subduction-zone magmas, in contrast to the high-Nb mafic rocks, which lack these anomalies (figs. 9, 10). Thus, low-Nb mafic rocks appear to contain a higher crustal component than high-Nb mafic rocks.

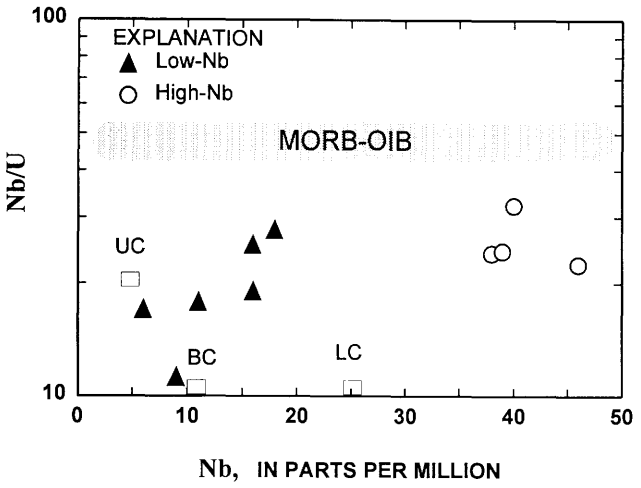

Figure 14. Nb/U versus Nb variation diagram for mafic rocks from Red Hills and western Markagunt Plateau. Shaded area shows composition of mid-ocean ridge (MORB) and ocean-island basalts (OIB), from Hofmann and others (1986). Average upper (UC), lower (LC), and bulk crust (BC), from Taylor and McLennan (1985).

In addition to the evidence shown by the normalized patterns, the low-Nb rocks also show trends in plots of Nb/U versus Nb abundance that are consistent with crustal contamination. With decreasing Nb, the low-Nb rocks show a pattern of decreasing Nb/U (fig. 14). This pattern implies variable amounts of crustal interaction even among the low-Nb rocks as a whole. Not surprisingly, both low- and high-Nb rocks have significantly lower Nb/U values than mid-ocean ridge basalt and ocean-island basalt (Hofmann and others, 1986), implying that neither magma type is uncontaminated.

The second line of evidence that the low-Nb rocks are contaminated comes from their isotopic compositions. All of the low-Nb rocks have lower Nd isotopic compositions than the high-Nb rocks (fig. 11). Although this relation could result from the tapping of different source regions in the mantle, the overall pattern is more consistent with crustal contamination.

The dispersion of data points in the Sr-Nd isotopic diagram (fig. 11) suggests that at least two crustal components may have been involved in the evolution of the low-Nb magmas. Mainly because of differences in Sr isotopic ratios, we suggest that the dominant crustal component in the low-Nb Black Mountain and Water Canyon magmas was lower crust ($^{87}Sr/^{86}Sr< 0.704$) whereas the dominant component in low-Nb Red Hills magmas was upper crust ($^{87}Sr/^{86}Sr> 0.7058$). The lower crustal component in low-Nb magmas also has low Nd and Pb isotopic compositions.

The dominant crustal component in the Black Mountain and Water Canyon magmas may have been similar in composition to mafic deep crustal xenoliths from the San Francisco volcanic field in northern Arizona. The xenoliths have extremely high Ba (612–4,700 ppm Ba), Sr (2,000–6,900 ppm Sr), and light rare-earth element abundances (38–178 ppm La), and low Nd (ε_{Nd}=–16 to –20), Sr ($^{87}Sr/^{86}Sr$=0.7026–0.7029), and Pb ($^{206}Pb/^{204}Pb$=16.9) isotopic compositions (Nealey and Unruh, 1991; Nealey and Unruh, unpub. data, 1993). Assimilation of this material by rising magmas could have lowered the Sr, Nd, and Pb isotopic ratios of the hybrid magmas without significantly affecting their major-element compositions.

The effect of contamination on trace-element abundances is indicated by the primitive mantle-normalized spider diagrams in figure 15. In this diagram, normalized patterns for Water Canyon and Black Mountain magmas show good coherence with the xenoliths, but the patterns of the high-Nb rocks are quite distinct from those of the xenoliths. The troughs at Th-U and Ta-Nb strongly suggest that the low-Nb magmas interacted with lower crust similar in composition to the xenoliths.

The most compelling reason for suggesting that mafic lower crustal material was involved in the evolution of the Water Canyon and Black Mountain magmas is that the assimilation of mafic crust would not significantly affect the major-element composition of the hybrid magmas. The San Francisco field xenoliths that we suggest represent lower crust in this region have silica contents between 49 and 54 weight percent SiO_2 (Nealey and Unruh, 1991). Granulite, garnet amphibolite, and also some paragneiss xenoliths from the interior of the Colorado Plateau have similar mafic compositions (Wendlandt and others, 1993). The low-silica contents of deep crustal materials are crucial to petrologic models of magma genesis in the western United States where continental crust overlies the upper mantle (Glazner and Farmer, 1992).

This kind of crustal contamination is referred to as cryptic contamination because it is difficult to identify the presence of a mafic lower crustal component in mafic magmas. Glazner and Farmer (1992) inferred that cryptic contamination occurs when mantle-derived magmas stagnate in the crust. Recently, cryptic contamination has been suggested as an important petrologic process by Moyer and Esperança (1989), and was later proven by Glazner and Farmer (1992) for Quaternary mafic magmas erupted in southeastern California. Glazner and Farmer (1992) showed that the variation in the Nd isotopic composition of xenolith-bearing basaltic rocks from the Mojave Desert is small (3.8 ε units) and that the Nd isotopic values are generally much higher (ε_{Nd}>5) than those of xenolith-free basalts (11.7 ε units; ε_{Nd}=8.76 to –2.98). The xenolith-bearing rocks have Sr and Nd isotopic compositions that are similar to those of asthenospheric-mantle-derived ocean-island basalt. Although we have found no ultramafic or mafic xenoliths in any of the mafic lava flows in the study area, we suggest that cryptic contamination was an important petrologic process here as well.

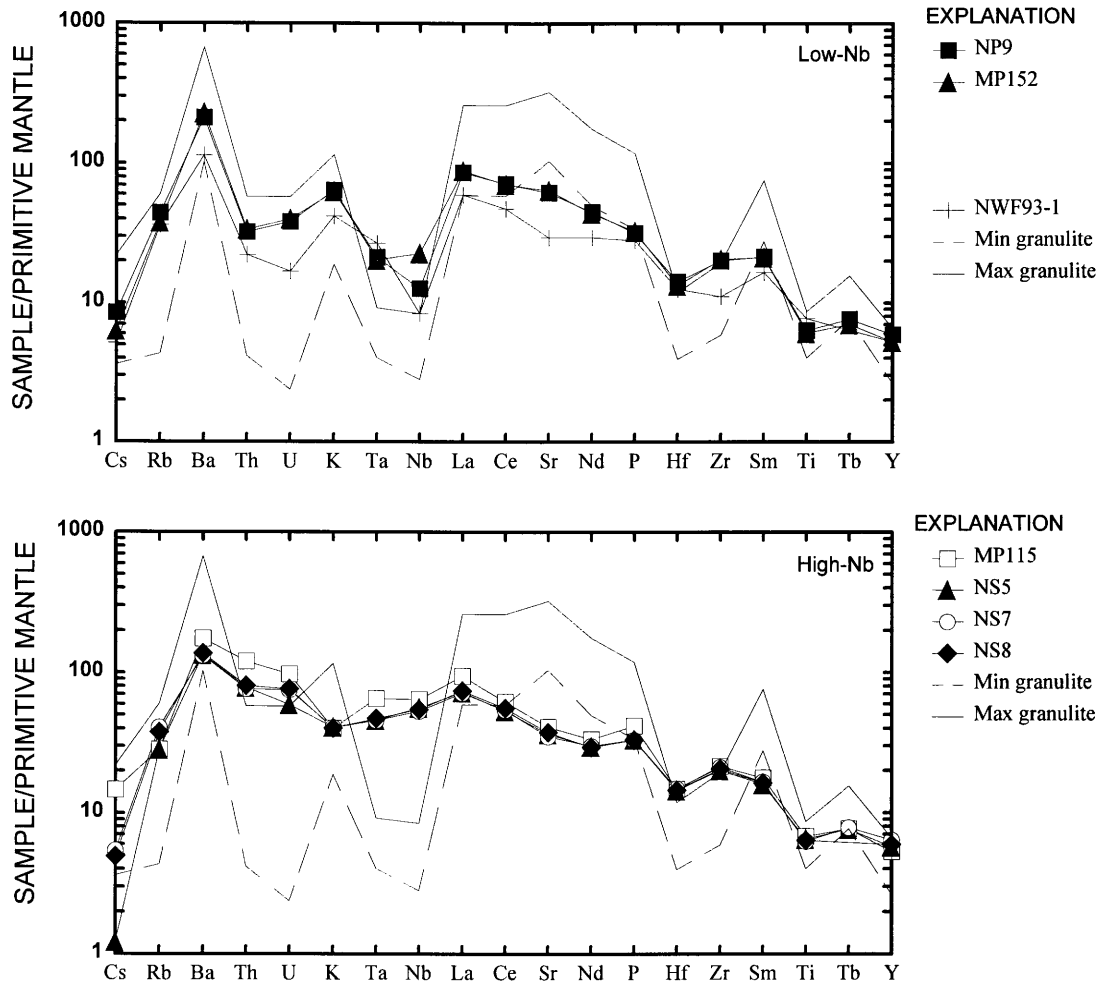

Figure 15. Primitive mantle-normalized spider diagrams comparing high-Nb and selected low-Nb rocks to deep crustal xenoliths from San Francisco volcanic field (data from Nealey and Unruh, 1991).

The generally higher Sr isotopic compositions of Red Hills rocks suggest that the dominant crustal component in these magmas was more evolved than that assimilated by Black Mountain and Water Canyon magmas. This material could be any of a number of crustal rock types that may reside beneath the transition zone in southwestern Utah. The most likely sources of upper crustal contamination would be igneous rocks of Proterozoic to Cenozoic age (Farmer and DePaolo, 1983; Wooden and DeWitt, 1991; Coleman and Walker, 1992; Blank and others, 1992; McKee and others, this volume, chapter L).

Another possible source of crustal contamination is subducted oceanic crust that may have been underplated at the base of the lithosphere in pre-Cenozoic time (Fitton, 1989; Fitton and others, 1991). According to Fitton and his colleagues, this material is likely to have been enriched in Ba and radiogenic Sr. This material would be difficult to distinguish from Proterozoic basement rocks because both would have subduction-zone geochemical signatures.

All this speculation, however, must be tempered by the fact that none of the volcanic rocks in the Red Hills and western Markagunt Plateau contain crustal xenoliths of any composition. Thus although the dispersion of data in the various diagrams is likely due to contamination, this hypothesis cannot be proven. Our working hypothesis is that the low-Nb samples from Water Canyon and Black Mountain assimilated mafic lower crust, whereas low-Nb magmas erupted in the Red Hills mainly assimilated upper crust. We also suggest that the high-Nb magmas contain some amount of a crustal component.

THE PETROLOGIC MODEL

The preceding discussion indicates that neither contamination of a single crustal component nor high-pressure fractionation alone can explain all the chemical variations observed in Red Hills–western Markagunt Plateau magmas.

Isotopic data clearly indicate that two or more crustal components contributed to compositional variations, whereas trace-element modeling indicates that crystal fractionation was involved in some magma batches. We therefore suggest an open-system magmatic model in which primary mantle-derived magmas differentiated by a combined process of crystal fractionation and crustal contamination. The most primitive erupted magmas appear to be represented by the high-Nb mafic rocks. However, based on their relatively low Nd and high Sr isotopic compositions, even this magma type is likely to have been contaminated by crustal materials. Less contaminated magmatic compositions are represented by lava flows in the central part of the Markagunt Plateau, where we have identified more primitive compositions having $^{87}Sr/^{86}Sr=0.704$ and $\varepsilon_{Nd}= 0$ (Nealey and others, 1993). But even these materials probably do not represent primary mantle-derived magma compositions. In addition, covariation of Sr, Nd and Pb isotopic data for regional mafic rocks suggests that two mantle sources may have been tapped by Quaternary magmatism (Nealey and others, 1993; Unruh and others, 1994). Both mantle sources may be asthenospheric mantle, but one source in the lithospheric mantle cannot be ruled out (Nealey and others, 1993). Both mantle sources probably have $^{87}Sr/^{86}Sr<0.703$ and $\varepsilon_{Nd}>0$, but one (asthenospheric) source has $^{206}Pb/^{204}Pb >18.3$ compared with a $^{206}Pb/^{204}Pb$ of ≈ 17.3 in the other mantle source.

TECTONIC IMPLICATIONS

Integrated elemental and isotopic studies of upper Cenozoic mafic magmas erupted in various parts of the western United States commonly show temporal patterns that are interpreted as evidence of rising asthenosphere-lithosphere boundaries attendant to extension (Daley and DePaolo, 1992, Bradshaw and others, 1993; Feuerbach and others, 1993). The exception is the Death Valley magmas, which show the opposite pattern (Asmerom and others, 1994; R.A. Thompson, oral commun., 1994). In most places, magmas erupted during the early stages of extension commonly show lithospheric signatures characterized by low-Nd and high-Sr isotopic compositions (Perry and others, 1987; Daley and DePaolo, 1992; Bradshaw and others, 1993; Feuerbach and others, 1993). Their Nd isotopic compositions are similar to those of some mafic magmas erupted in the Red Hills and western Markagunt Plateau, but their Sr isotopic compositions are not.

In contrast, magmas erupted after the peak periods of extension have high-Nd and low-Sr isotopic compositions similar to those of ocean-island basalts. Mafic rocks from several parts of the western United States show such patterns, including those from the Colorado River trough in Nevada, California, and Arizona, and the Rio Grande rift in New Mexico (fig. 1; Daley and DePaolo, 1992; Feuerbach and others, 1993; Perry and others, 1987; Leat and others, 1988; Bradshaw and others, 1993). If these geochemical patterns are due to rising asthenosphere-lithosphere boundaries, then the isotopic compositions of Quaternary mafic rocks in the Red Hills and western Markagunt Plateau indicate that extension along the margin of the Colorado Plateau in southwestern Utah has not reached its peak and that the asthenosphere-lithosphere boundary is still too deep for the asthenosphere to be tapped as a magma source. The first statement is consistent with the suggestion of Fitton and his colleagues (Fitton, 1989; Fitton and others, 1991) that the transition zone in this region is in the early stages of extension, compared with the interior of the Basin and Range. The statement is also consistent with the geophysical evidence that shows that the crust along the margin of the Colorado Plateau has not been thinned as much as it has in the Basin and Range.

Like previous workers, we suggest that magmas erupted during the early stages of extension interact more effectively with the lithosphere (mantle and crust) as they rise to the surface. Thus a thick crust with cooler ambient temperatures causes more interaction at the crust-mantle boundary and at higher levels within the crust. This causes the final composition of magmas erupted at the surface to be dependent upon the composition of the source, the proportion and composition of overlying lithosphere, and the amount of fractionation that the magmas experience during their residence in the lithosphere.

SUMMARY

The overall range in elemental and isotopic composition of magmas erupted in the Red Hills and western Markagunt Plateau reflects a combination of magmatic processes that operated on primary magmas that originated in the asthenosphere. Based on the isotopic composition of ocean-island basalt, which is derived from asthenospheric mantle, primary magmas generated below the Red Hills–western Markagunt Plateau had much higher Nd and Pb isotopic compositions than those erupted at the surface. Isotopic composition of the Water Canyon lava flow suggests that one lithospheric component (lower crust?) had low-Sr, Nd, and Pb isotopic compositions. Another lithospheric component (middle to upper crust) probably had low Sr and Nd isotopic compositions.

Mafic magmatism in the Red Hills and western Markagunt Plateau migrated eastward in Quaternary time as the margin of the Colorado Plateau was progressively dismembered by lithospheric extension. As magmatism migrated into the Colorado Plateau, the eruptive products changed in composition as lithospheric residence times decreased, and interaction between mantle-derived magmas and lower and upper crust decreased. Rising magmas further differentiated through an open-system magmatic process involving combined fractional crystallization and crustal contamination. These processes produced magmas that range in composition from basalt to basaltic andesite, across a very narrow part of the transition zone between the Colorado Plateaus and Basin and Range provinces in southwestern Utah.

REFERENCES CITED

Allègre, C.J., Hamelin, B., and Dupre, Bernard, 1984, Statistical analysis of isotopic ratios in MORB, The mantle blob cluster model and the convective regime of the mantle: Earth and Planetary Science Letters, v. 71, p. 71–84.

Allègre, C.J., and Minster, J.-F., 1978, Quantitative models of trace element behaviour in magmatic processes: Earth and Planetary Science Letters, v. 38, p. 1–25.

Allègre, C.J., Treuil, Michel, Minster, J.-F., Minster, B., and Albarede, F., 1977, Systematic use of trace elements in igneous processes, Part I, Fractional crystallisation processes in volcanic suites: Contributions to Mineralogy and Petrology, v. 60, p. 57–75.

Anderson, J.J., 1993, The Markagunt megabreccia—Large Miocene gravity slides mantling the northern Markagunt Plateau, southwestern Utah: Utah Geological Survey Miscellaneous Publication 93-2, 37 p.

Anderson, R.E., 1988, Pre-basin-range block faulting along west and northwest trends, southeastern Great Basin and southern High Plateau: Geological Society of America Abstracts with Programs, v. 20, no. 3, p. 139.

———1989, The Intermontane System (Basin and Range, Colorado Plateau, and High Lava Plains), *in* Tectonic evolution, Pakiser, L.C., and Mooney, W.D., eds., Geophysical framework of the continental United States: Geological Society of America Memoir 172, p. 163–176.

Anderson, R.E., and Bucknam, R.C., 1979, Map of scarps on unconsolidated sediments, Richfield 1°×2° quadrangle, Utah: U.S. Geological Survey Open-File Report 79-1236, 15 p.

Anderson, R.E., and Christenson, G.E., 1989, Quaternary faults, folds, and selected volcanic features in the Cedar City 1°×2° quadrangle, Utah: Utah Geological and Mineral Survey Miscellaneous Publication 89-6, 29 p.

Anderson, R.E., and Mehnert, Harald, 1979, Reinterpretation of the history of the Hurricane fault in Utah, *in* Newman, G.W., and Cooke, H.D., eds., 1979 Basin and Range Field Conference: Denver and Salt Lake City, Rocky Mountain Association of Geologists and Utah Geological Association, p. 145–166.

Asmerom, Yemane, Jacobsen, S.B., and Wernicke, B.P., 1994, Variations in magma source regions during continental extension, Death Valley region, western United States: Earth and Planetary Science Letters, v. 125, p. 235–254.

Averitt, Paul, and Threet, R.L., 1973, Geologic map of the Cedar City quadrangle, Iron County, Utah: U.S. Geological Survey Geologic Quadrangle Map GQ–1120, scale 1:24,000.

Baedecker, P.A., and McKown, D.M., 1987, Instrumental neutron activation analysis of geochemical samples, *in* Baedecker, P.A., ed., Methods for geochemical analysis: U.S. Geological Survey Bulletin 1770, p. H1–H14.

Bennett, V.C., and DePaolo, D.J., 1987, Proterozoic crustal history of the western United States as determined by neodymium isotopic mapping: Geological Society of America Bulletin, v. 99, p. 674–685.

Best, M.G., and Brimhall, W.H., 1974, Late Cenozoic alkalic basaltic magmas in the western Colorado Plateau and the Basin and Range Transition Zone, U.S.A., and their bearing on mantle dynamics: Geological Society of America Bulletin, v. 85, p. 1677–1690.

Best, M.G., McKee, E.H., and Damon, P.E., 1980, Space-time-composition patterns of late Cenozoic mafic volcanism, southwestern Utah and adjoining areas: American Journal of Science, v. 280, p. 1035–1050.

Blank, H.R., 1959, Geology of the Bull Valley district, Washington County, Utah: Seattle, Wash., University of Washington Ph. D. thesis, 177 p.

Blank, H.R., Jr., Rowley, P.D., and Hacker, D.B., 1992, Miocene monzonitic intrusions and associated megabreccias of the Iron Axis region, southwestern Utah, *in* Wilson, J.R., ed., Field guide to geologic excursions in Utah and adjacent area of Nevada, Idaho, and Wyoming: Geological Society of America, Rocky Mountain section meeting: Utah Geological Survey Miscellaneous Publications 92-3, p. 399–420.

Bornhorst, T.J., 1980, Major- and trace-element geochemistry and mineralogy of Upper Eocene to Quaternary volcanic rocks of the Mogollon-Datil field, southwestern New Mexico: Albuquerque, N. Mex., University of New Mexico Ph. D. dissertation, 1108 p.

Bradshaw, T.K., Hawkesworth, C.J., and Gallagher, K., 1993, Basaltic volcanism in the southern Basin and Range—No role for a mantle plume: Earth and Planetary Science Letters, v. 116, p. 45–62.

Bryant, Bruce, Wooden, J.L., and Nealey, L.D., in press, Geology, geochronology, geochemistry, and Pb-isotopic compositions of Proterozoic rocks, Poachie region, west-central Arizona—A study of the east boundary of the Proterozoic Mohave crustal province: U.S. Geological Survey Professional Paper.

Coleman, D.S., and Walker, J.D., 1992, Evidence for the generation of juvenile granitic crust during continental extension, Mineral Mountains batholith, Utah: Journal of Geophysical Research, v. 97, p. 11001–11024.

Condit, C.D., Crumpler, L.S., Aubele, J.C., and Elston, W.E., 1989, Patterns of volcanism along the southern margin of the Colorado Plateau—The Springerville field: Journal of Geophysical Research, v. 94, p. 7975–7986.

Daley, E.E., and DePaolo, D.J., 1992, Isotopic evidence for lithospheric thinning during extension—Southeastern Great Basin: Geology, v. 20, p. 104–108.

Ellis, Michael, and King, Geoffrey, 1991, Structural control of flank volcanism in continental rifts: Science, v. 254, p. 839–842.

Everson, J.E., 1979, Regional variations in the lead isotopic characteristics of late Cenozoic basalts from the southwestern United States: Pasadena, Calif., California Institute of Technology Ph. D. dissertation, 454 p.

Farmer, G.L., and DePaolo, D.J., 1983, Origin of Mesozoic and Tertiary granite in the western United States and implications for pre-Mesozoic crustal structure—1, Nd and Sr isotopic studies in the geocline of the northern Great Basin: Journal of Geophysical Research, v. 88, p. 3379–3401.

Farmer, G.L., Perry, F.V., Semken, Stephen, Crowe, Bruce, Curtis, D., and DePaolo, D.J., 1989, Isotopic evidence on the structure and origin of subcontinental lithosphere mantle in southern Nevada: Journal of Geophysical Research, v. 94, p. 7885–7898.

Feuerbach, D.L., Smith, E.I., Walker, J.D., and Tangeman, J.A., 1993, The role of the mantle during crustal extension, constraints from geochemistry of volcanic rocks in the Lake Mead

area, Nevada and Arizona: Geological Society of America Bulletin, v. 105, p. 1561–1575.

Fitton, J.G., 1989, Petrology and geochemistry of late Cenozoic basalt flows, western Grand Canyon, Arizona, *in* Elston, D.P., Billingsley, G.H., and Young, R.A. eds., Geology of Grand Canyon, northern Arizona: American Geophysical Union, Field Trip Guidebook, v. T115/T315, p. 186–189.

Fitton, J.G., James, Dodie, and Leeman, W.P., 1991, Basic magmatism associated with late Cenozoic extension in the western United States—Compositional variations in space and time: Journal of Geophysical Research, v. 96, p. 13693–13711.

Fleck, R.J., Anderson, J.J., and Rowley, P.D., 1975, Chronology of mid-Tertiary volcanism in High Plateau region of Utah, *in* Anderson, J.J., Rowley, P.D., Fleck, R.J., and Nairn, A.E.M., eds., Cenozoic geology of southwestern High Plateau of Utah: Geological Society of America Special Paper 160, p. 53–61.

Floyd, P.A., 1991, Oceanic islands and seamounts, *in* Floyd, P.A., ed., Oceanic basalts: Glasgow, Scotland, Blackie and Son Ltd., p. 174–218.

Frey, F.A., Green, D.H., and Roy, S.D., 1978, Integrated models of basalt petrogenesis, a study of quartz tholeiites to olivine melilitites from southeastern Australia utilizing geochemical and experimental petrological data: Journal of Petrology, v. 19, p. 463–513.

Glazner, A.F., and Farmer, G.L., 1992, Production of isotopic variability in continental basalts as cryptic mafic contamination: Science, v. 255, p. 72–74.

Hanson, G.N., 1980, Rare earth elements in petrogenetic studies of igneous systems: Annual Reviews of Earth and Planetary Sciences, v. 8, p. 371–406.

Hart, S.R., 1984, A large-scale isotope anomaly in the Southern Hemisphere mantle: Nature, v. 309, p. 753–757.

Hausel, W.D., and Nash, W.P., 1977, Petrology of Tertiary and Quaternary volcanic rocks, Washington County, southwestern Utah: Geological Society of America Bulletin, v. 88, p. 1831–1842.

Henderson, Paul, 1982, Inorganic geochemistry: Oxford, Pergamon, 312 p.

Hendricks, J.D., and Plescia, J.B., 1991, A review of the regional geophysics of the Arizona transition zone: Journal of Geophysical Research, v. 96, p. 12351–12373.

Hofmann, A.W., and White, W.M., 1982, Mantle plumes from ancient oceanic crust: Earth and Planetary Science Letters, v. 57, p. 421–436.

Hofmann, A.W., Jochum, K.P., Seufert, H.M., and White, W.M., 1986, Nb and Pb in oceanic basalts–New constraints on mantle evolution: Earth and Planetary Science Letters, v. 79, p. 33–45.

Johnson, R.G., and King, B.-S., 1987, Energy-dispersive X-ray fluorescence spectrometry, *in* Baedecker, P.A., ed., Methods for geochemical analysis: U.S. Geological Survey Bulletin 1770, p. F1–F5.

Jones, C.H., Wernicke, B.P., Farmer, G.L., Walker, J.D., Coleman, D.S., McKenna, L.W., and Perry, F.V., 1992, Variations across and along a major continental rift—An interdisciplinary study of the Basin and Range province, western U.S.A.: Tectonophysics, v. 213, p. 57–96.

Kempton, P.D., Fitton, J.G., Hawkesworth, C.J., and Ormerod, D.S., 1991, Isotopic and trace element constraints on the composition and evolution of the lithosphere beneath the southwestern United States: Journal of Geophysical Research, v. 96, p. 13713–13735.

Leat, P.T., Thompson, R.N., Morrison, M.A., Hendry, G.L., and Dicken, A.P., 1988, Compositionally diverse Miocene-Recent rift related magmatism in NW Colorado—Partial melting, and mixing of 3 different mantle sources: Journal of Petrology Special Lithosphere Issue, p. 351–377.

LeBas, M.J., Le Maitre, R.W., Streckeisen, Albert, and Zanettin, Bruno, 1986, A chemical classification of volcanic rocks based on the total alkali-silica diagram: Journal of Petrology, v. 27, p. 745–750.

Lipman, P.W., Rowley, P.D., Mehnert, H.H., Evans, S.H., Jr., Nash, W.P., and Brown, F.H., 1978, Pleistocene rhyolite of the Mineral Range, Utah—Geothermal and archeological significance: U.S. Geological Survey Journal of Research, v. 6, p. 133–147.

Lowder, G.G. 1973, Late Cenozoic transitional alkali olivine-tholeiitic basalt and andesite from the margin of the Great Basin, southwest Utah: Geological Society of America Bulletin, v. 84, p. 2993–3012.

Maldonado, Florian, and Moore, R.C., 1993, Preliminary geologic map of the Parowan quadrangle, Iron County, Utah: U.S. Geological Survey Open-File Report 93-3, scale 1:24,000.

Maldonado, Florian, Sable, E.G., and Anderson, J.J., 1992, Evidence for a Tertiary low-angle shear zone, Red Hills, with implications for a regional shear zone in the adjacent Colorado Plateau, *in* Engineering and environmental geology of southwestern Utah: Utah Geological Association Publication 21, Field Symposium, p. 315–323.

Maldonado, Florian, and Williams, V.S., 1993, Geologic map of the Parowan Gap quadrangle, Iron County, Utah: U.S. Geological Survey Geologic Quadrangle Map GQ–1713, scale 1:24,000.

Mattox, S.R., 1992, Geochemistry, origin, and tectonic implications of the mid-Teriary and late Tertiary and Quaternary volcanic rocks, southern Marysvale volcanic field, Utah: DeKalb, Ill., Northern Illinois University Ph. D. dissertation, 498 p.

McCarthy, Jill, and Parsons, Tom, 1994, Insights into the kinematic Cenozoic evolution of the Basin and Range–Colorado Plateau transition from coincident seismic refraction and reflection data: Geological Society of America Bulletin, v. 106, p. 747–759.

Menzies, M.A., 1989, Cratonic, circumcratonic and oceanic mantle domains beneath the western United States: Journal of Geophysical Research, v. 94, p. 7899–7915.

Moore, D.M., and Nealey, L.D., 1993, Preliminary geologic map of the Navajo Lake quadrangle, Kane and Iron Counties, Utah: U.S. Geological Survey Open-File Report 93-190, scale 1:24,000.

Moyer, T.C., and Esperança, Sonia, 1989, Petrologic and geochemical variations in basalts associated with bimodal volcanism in the Arizona transition zone—Preliminary results from Kaiser Springs, *in* Continental magmatism abstracts: International Association of Volcanologists and Chemistry of the Earth's Interior, General Assembly, June 25–July 1, 1989, Santa Fe, New Mexico Bureau of Mines and Mineral Resources Bulletin, v. 131, p. 198, 340 p.

Nealey, L.D., and Sheridan, M.F., 1989, Post-Laramide volcanic rocks of Arizona and northern Sonora, Mexico, and their inclusions, *in* Jenney, J.P., and Reynolds, S.J., eds., Geologic

evolution of Arizona: Arizona Geological Society Digest, v. 17, p. 609–647.

Nealey, L.D., and Unruh, D.M., 1991, Geochemistry and isotopic characteristics of deep crustal xenoliths from Tule Tank, San Francisco volcanic field, northern Arizona, *in* Karlstrom, K.E., ed., Proterozoic geology and ore deposits of Arizona: Arizona Geological Society Digest, v. 19, p. 153–163.

Nealey, L.D., Unruh, D.M., and Maldonado, Florian, 1993, Sr-Nd-Pb-isotopic maps of the Panguitch 1:100,000 quadrangle, Utah: U.S. Geological Survey Open-File Report 93-691, scale 1:250,000.

Perry, F.V., Baldridge, W.S., and DePaolo, D.J., 1987, The role of asthenosphere and lithosphere in the genesis of late Cenozoic basaltic rocks from the Rio Grande Rift and adjacent regions of the southwestern United States: Journal of Geophysical Research, v. 92, p. 9193–9213.

———1988, Chemical and isotopic evidence for lithosphere thinning beneath the Rio Grande rift: Nature, v. 332, p. 432–434.

Prodehl, Claus, 1979, Crustal structure of the Western United States: U.S. Geological Survey Professional Paper 1034, 74 p.

Rowley, P.D., Anderson, J.J., Williams, P.L., and Fleck, R.J., 1978, Age of structural differentiation between the Colorado Plateau and Basin and Range provinces in southwestern Utah: Geology, v. 6, p. 51–55.

Rowley, P.D., Cunningham, C.G., Steven, T.A., Mehnert, H.H., and Naeser, C.W., in press, Cenozoic igneous and tectonic setting of the Marysvale volcanic field, and its relation to other igneous centers in Utah and Nevada, *in* Friedman, J.D., and Huffman, A.C., Jr., eds., Laccolith complexes of southeastern Utah—Tectonic control and time of emplacement: U.S. Geological Survey Bulletin 2158.

Rowley, P.D., Mehnert, H.H., Naeser, C.W., Snee, L.W., Cunningham, C.G., Steven, T.A., Anderson, J.J., Sable, E.G., and Anderson, R.E., 1994, Isotopic ages and stratigraphy of Cenozoic rocks of the Marysvale volcanic field and adjacent areas, west-central Utah: U.S. Geological Survey Bulletin 2071, 35 p.

Rowley, P.D., Steven, T.A., Anderson, J.J., and Cunningham, C.G., 1979, Cenozoic stratigraphic and structural framework of southwestern Utah: U.S. Geological Survey Professional Paper 1149, 22 p.

Rowley, P.D., and Threet, R.L., 1976, Geologic map of the Enoch quadrangle, Iron County, Utah: U.S. Geological Survey Geologic Quadrangle Map GQ–1296, scale 1:24,000.

Steven, T.A., Cunningham, G.G., and Anderson, J.J., 1984, Geologic history and uranium potential of the Big John caldera, southern Tushar Mountains, Utah, Chapter B *in* Steven, T.A., ed., Igneous activity and related deposits in the western and southern Tushar Mountains, Marysvale volcanic field, west-central Utah: U.S. Geological Survey Professional Paper 1299, p. 25–33.

Sun, S.s., and McDonough, W.F., 1989, Chemical and isotopic systematics of oceanic basalts–Implications for mantle composition and processes, *in* Saunders, A.D., and Norry, M.J., eds., Magmatism in the ocean basins: Geological Society of London Special Publication, p. 315–345.

Taggart, J.E., Lindsay, J.R., Scott, B.A., Vivit, D.V., Bartel, A.J., and Stewart, K.C., 1987, Analysis of geologic materials by wavelength-dispersive X-ray fluorescence spectrometry, *in* Baedecker, P.A., ed., Methods for geochemical analysis: U.S. Geological Survey Bulletin 1770, p. E1–E19.

Tanaka, K.L., Shoemaker, E.M., Ulrich, G.E., and Wolfe, E.W., 1986, Migration of volcanism in the San Francisco volcanic field, Arizona: Geological Society of America Bulletin, v. 97, p. 129–141.

Taylor, S.M., and McLennan, S.M., 1985, The continental crust; its composition and Evolution: Palo Alto, Calif., Blackwell Scientific Publications, 312 p.

Thomas, H.E., and Taylor, G.H., 1946, Geology and ground-water resources of Cedar City and Parowan Valleys, Iron County, Utah: U.S. Geological Survey Water-Supply Paper 993, 210 p.

Unruh, D.M., Nealey, L.D., Maldonado, Florian, and Nusbaum, R.L., 1994, Sr-Nd-Pb isotopic maps of the St. George 30'×60' quadrangle, southwestern Utah: U.S. Geological Survey Open-File Report 94-11, scale 1:100,000.

Warren, D.H., 1969, A seismic-refraction survey of crustal structure in central Arizona: Geological Society of America Bulletin, v. 80, p. 257–282.

Weaver, B.L., 1991, The origin of ocean island basalt end-member compositions—Trace element and isotopic constraints: Earth and Planetary Science Letters, v. 104, p. 381–397.

Wendlandt, Eric, DePaolo, D.J., and Baldridge, W.S., 1993, Nd and Sr isotope chronostratigraphy of Colorado Plateau lithosphere: implications for magmatic and tectonic underplating of the continental crust: Earth and Planetary Science Letters, v. 116, p. 23–43.

Wenrich, K.J., Billingsley, G.H., and Blackerby, B.A., 1995, Spatial migration and compositional changes of Miocene-Quaternary magmatism in the western Grand Canyon: Journal of Geophysical Research, v. 100, p. 10417–10440.

Wong, I.G., and Humphrey, J.R., 1989, Contemporary seismicity, faulting, and the state of stress in the Colorado Plateau: Geological Society of America Bulletin, v. 101, p. 1127–1146.

Wooden, J.L., and DeWitt, Ed, 1991, Pb isotopic evidence for the boundary between the early Proterozoic Mojave and central Arizona crustal provinces in western Arizona, *in* Karlstrom, K.E., ed., Proterozoic geology and ore deposits of Arizona: Arizona Geological Society Digest, v. 19, p. 27–50.

Geochemistry, Source Characteristics, and Tectonic Implications of Upper Cenozoic Basalts of the Basin and Range–Colorado Plateau Transition Zone, Utah

By Stephen R. Mattox

GEOLOGIC STUDIES IN THE BASIN AND RANGE–COLORADO PLATEAU TRANSITION IN SOUTHEASTERN NEVADA, SOUTHWESTERN UTAH, AND NORTHWESTERN ARIZONA, 1995

U.S. GEOLOGICAL SURVEY BULLETIN 2153–J

UNITED STATES GOVERNMENT PRINTING OFFICE, WASHINGTON : 1997

CONTENTS

FIGURES

TABLES

Geochemistry, Source Characteristics, and Tectonic Implications of Upper Cenozoic Basalts of the Basin and Range–Colorado Plateau Transition Zone, Utah

By Stephen R. Mattox[1]

ABSTRACT

Late Cenozoic basalts (≤16 Ma) in the Utah transition zone vary systematically in the distribution of rock types and in the concentration of major and trace elements. In the transition zone and the adjacent Colorado Plateaus province, all basalts are alkalic; normative nepheline, MgO content, and compatible and incompatible trace-element contents generally increase to the east. Along the west margin of the transition zone and in the adjacent Basin and Range province, all basalts are tholeiitic and, relative to the alkali basalts, less mafic; concentrations of compatible and incompatible trace elements are lower. All basalts have one of the three distinctive trace-element patterns. Alkalic and tholeiitic basalts from the Utah transition zone show overlapping isotopic compositions that occupy a unique position on the Nd-Sr isotopic diagram relative to basalts from other late Cenozoic volcanic provinces in the southwestern United States.

Geochemical data indicate that most of the systematic variation in element concentrations can be accounted for by relatively lower degrees of partial melting at greater depths with increasing distance to the east. All magmas underwent fractional crystallization, but assimilation of crust was limited.

Trace-element patterns provide a genetic link to mafic alkaline dikes that serve as approximations of the compositions of the sources of the basalts. Coupled with the distribution of rock types, the trace-element patterns help to construct a two-layered model for the location of mantle sources in the transition zone.

In contrast to geophysical models, which suggest that the asthenosphere is near the base of the crust near the Basin and Range–Colorado Plateau boundary, limited crustal extension within the transition zone and the Nd isotopic compositions of the basalts indicate that lithospheric mantle is preserved in the Utah transition zone and the adjacent eastern Basin and Range and Colorado Plateaus provinces.

INTRODUCTION

Geochemical data for basaltic rocks provide a means of testing models for the tectonic and magmatic evolution of volcanic fields in the Basin and Range province and along the margin of the Colorado Plateau (Perry and others, 1987; Ormerod and others, 1988; Farmer and others, 1990; Daley and DePaolo, 1992). Studies by Fitton and others (1988, 1991) and Kempton and others (1991) have presented tectonic interpretations of the Utah transition zone based on basalt geochemistry. However, their works were regional in nature and lacked a detailed transect of the transition zone. Early work in Utah (Best and others, 1980) showed interesting space-time-compositional patterns, such as a decline in the potassium content in mantle-generated magmas from 14 to 2 Ma, but was limited by a small number of samples of rocks dated late Cenozoic (< 20 Ma) within the transition zone.

This study presents the geochemical study for 34 basalts erupted during the late Cenozoic. The study (1) describes compositional variation in basalts across the Utah transition zone, (2) identifies the processes that affected magma composition, (3) characterizes their sources, and (4) constrains the tectonic history of the Utah transition zone.

ACKNOWLEDGMENTS

Field work was supported by Northern Illinois University, the Utah Geological Survey, and Sigma Xi Research Society. Analytical support was provided by Drew Coleman, Neil Dickey, Mark Feigenson, Jim Walker, and G. Wandless. Tari Mattox and Jim Walker reviewed an early version of this paper. Constructive reviews by David Clague, Charles G. Cunningham, and L. David Nealey were greatly appreciated.

[1]Northern Illinois University, DeKalb, IL; present address: University of North Dakota, Department of Space Studies, Grand Forks, ND 58202-9008.

GEOLOGIC SETTING AND PREVIOUS WORK

The Utah transition zone shares geologic and geophysical characteristics with the adjacent Basin and Range and Colorado Plateaus provinces and is defined geographically by the boundaries of the High Plateaus subprovince (fig. 1). Like the Basin and Range province to the west, the structure of the transition zone is dominated by north-south-trending uplifts that are separated by intervening alluviated valleys. Sedimentary and volcanic strata in the transition zone are generally subhorizontal or broadly warped, a characteristic of the Colorado Plateau to the east. The Marysvale volcanic field, near the center of the transition zone, is the dominant volcanic terrane. Volcanic rocks of the field cap a sequence of Paleozoic and Mesozoic sedimentary rocks, Tertiary continental sedimentary rocks, and ash-flow tuffs derived from calderas to the west (Mackin, 1960; Steven and others, 1990). The rocks can be divided into an early sequence of calc-alkaline rocks and a late sequence of bimodal basalt-rhyolite rocks.

Calc-alkaline rocks range in age from 35 to 22 Ma. Stratovolcano complexes produced large volumes of intermediate composition lava flows, mudflow breccia and locally derived ash-flow tuffs (Fleck and others, 1975; Rowley and others, 1979; Best and others, 1980; Steven and others, 1990; Cunningham and others, 1991).

About 22 Ma, the composition of the eruptions changed to a bimodal assemblage of silicic alkali rhyolite lava flows and ash-flow tuffs, associated with formation of the Mount Belknap and Red Hills calderas (Cunningham and Steven, 1979), and mafic lava flows (Cunningham and others, 1983; Anderson, 1986; Mattox, 1991a). The change from the 35 to 22 Ma calc-alkaline rocks to the younger than 22 Ma bimodal assemblage coincided with the onset of extension along the eastern margin of the Basin and Range province (Rowley and others, 1978; Cunningham and others, 1991). The earliest mafic rocks (22 to 21 Ma) are potassium rich ($K_2O \geq 3$ weight percent) and erupted from fissures. Younger mafic rocks ($\leq$16 Ma) include alkalic and tholeiitic basalts (Best and others, 1980; Cunningham and others, 1991; Mattox, 1991b, 1992b) that erupted from cinder cones and central vents along the periphery of the volcanic field (Dutton, 1880) and in the adjacent Basin and Range province.

Timing of late Cenozoic magmatism was episodic, and loci of activity shifted between episodes. Small volumes of basalt and basaltic andesite erupted from vents scattered in the Basin and Range and transition zone from 16 to 8 Ma (Best and others, 1980; Mattox, 1991b). From 7 to 4 Ma, volcanism was alkaline and volcanic activity was located in the eastern transition zone, the Sevier and Awapa Plateaus (Rowley and others, 1981; Nelson, 1989; Mattox, 1991b). During this period, mafic alkaline dikes intruded the San Rafael Swell in the Colorado Plateau (Gartner, 1985; Gartner and Delaney, 1988). By 3 Ma, the centers of volcanism shifted to the eastern margin of the Basin and Range province, and compositions of eruptive products were tholeiitic. Tholeiitic volcanism began on the Markagunt Plateau and in the adjacent Basin and Range province, along the west margin of the transition zone, about 1 Ma. The westward shift in volcanism in the Utah transition zone is away from the Colorado Plateau during the last 4 Ma. This shift is opposite to the direction of migration in the transition zone in extreme southwestern Utah and northern Arizona (Best and Hamblin, 1978; Tanaka and others, 1986; Condit and others, 1989).

Previous geochemical studies of volcanic rocks from the Marysvale field were for a limited geographic area (Lowder, 1973), of a reconnaissance nature (Wender, 1976; Wender and Nash, 1979), or part of a regional study (Fitton and others, 1988, 1991; Kempton and others, 1991). Lowder (1973) suggested that alkalic and tholeiitic basalts on the Markagunt Plateau were derived from the same mantle source by differing degrees of partial melting. Wender (1976) and Wender and Nash (1979), whose work preceded complete description of the stratigraphy at Marysvale, sampled numerous units but included only two young basalts ($\leq$ 16 Ma); and Wender and Nash had difficulty in relating rocks by any simple petrogenetic models. Fitton and others (1988) proposed that transition zone basalts were derived from a lithospheric source.

GEOPHYSICAL SETTING

Geophysical methods highlight differences between the Basin and Range and Colorado Plateaus provinces. Extension reduced the thickness of the crust beneath the Basin and Range province from as much as 45 km to 30 km (Allmendinger and others, 1987). The highest heat flow in the southern Basin and Range province is in southwestern Utah (Eaton and others, 1987) where P-wave velocities, electrical resistivity, and gravity data suggest that the asthenosphere is near the base of the crust (Thompson and Zoback, 1979). The crust and lithosphere beneath the Colorado Plateau are approximately 45 and 80 km thick, respectively (Thompson and Zoback, 1979; Allmendinger and others, 1987). Thompson and Zoback (1979) noted that many Basin and Range geophysical characteristics extend inward of the classic plateau physiographic boundary for distances of 50–100 km, which includes the entire transition zone.

Figure 1 (facing page). Index map for Utah transition zone, High Plateaus subprovince, and basalt sample localities. The Fish Lake, Awapa, Aquarius, and Sevier Plateaus are referred to as the eastern transition zone. Most basalts in the eastern transition zone are 7–4 Ma. The Markagunt Plateau is referred to as the western transition zone. Most basalts in the western transition zone are less than 1 Ma. Large-scale map shows basalt sample localities.

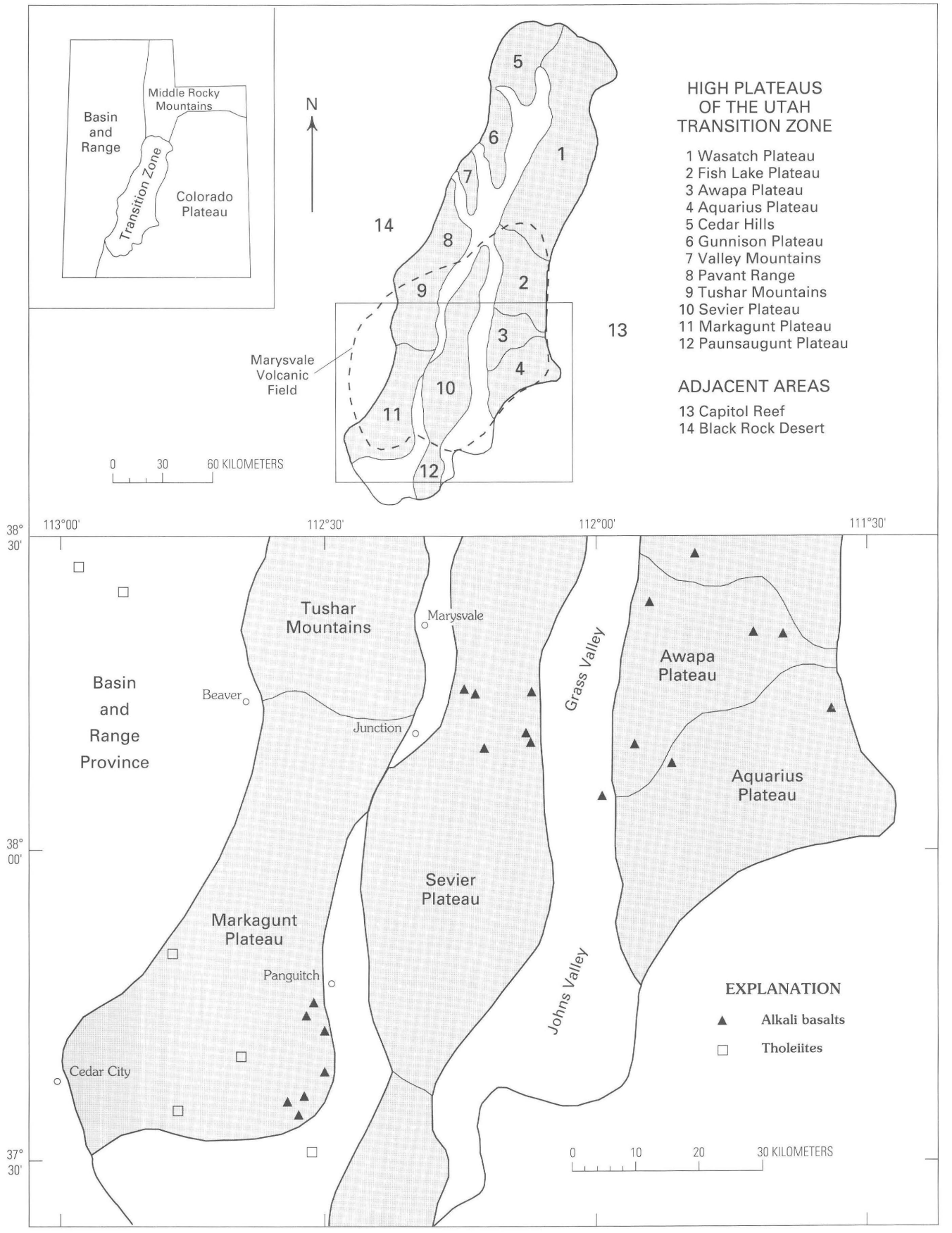
Basin and Range
Middle Rocky Mountains
Transition Zone
Colorado Plateau
N
0 30 60 KILOMETERS
Marysvale Volcanic Field
HIGH PLATEAUS OF THE UTAH TRANSITION ZONE
1 Wasatch Plateau
2 Fish Lake Plateau
3 Awapa Plateau
4 Aquarius Plateau
5 Cedar Hills
6 Gunnison Plateau
7 Valley Mountains
8 Pavant Range
9 Tushar Mountains
10 Sevier Plateau
11 Markagunt Plateau
12 Paunsaugunt Plateau
ADJACENT AREAS
13 Capitol Reef
14 Black Rock Desert
113°00'
112°30'
112°00'
111°30'
38° 30'
38° 00'
37° 30'
Tushar Mountains
Marysvale
Beaver
Junction
Basin and Range Province
Grass Valley
Awapa Plateau
Aquarius Plateau
Sevier Plateau
Markagunt Plateau
Panguitch
Cedar City
Johns Valley
EXPLANATION
Alkali basalts
Tholeiites
0 10 20 30 KILOMETERS

ANALYTICAL METHODS

Thirty-four new whole-rock analyses were obtained for rocks from the transition zone and adjacent Basin and Range and Colorado Plateaus provinces. Major- and trace-element data (table 1) were determined by XRF (X-ray fluorescence) spectrometry at Northern Illinois University using methods described in Mattox (1992a). Samples analyzed by XRF were powdered in a tungsten carbide shatter box. Major-element compositions are plotted on an adjusted volatile-free basis. A subset of 18 samples (table 2) was analyzed by instrumental neutron activation analysis (INAA), using methods described by Baedecker and McKown (1987). Samples analyzed by INAA were powdered in an alumina ball mill. Isotopic data were determined on 10 samples at Rutgers University and the University of Kansas (table 3), using methods described by Carr and others (1990) and Coleman and Walker (1992), respectively. The isotopic composition of basalts is reported and plotted as initial values.

CLASSIFICATION AND PETROGRAPHY

Upper Cenozoic rocks from the Utah transition zone are classified in two ways, the total alkali versus silica diagram (Le Bas and others, 1986) and by normative mineralogy (Irvine and Baragar, 1971). The first method allows the rocks to be divided on broad terms as basalt and trachybasalt. In the total alkali-silica diagram, the rocks plot in the basalt and trachybasalt fields. The second method allows for a more precise petrologic and petrochemical classification and divides the rocks into tholeiitic and alkali basalts. About half the rocks contain normative nepheline; the remainder are hypersthene normative. Nepheline normative rocks plot above the alkaline-subalkaline line of Irvine and Baragar (1971) and are classified as alkali basalts. All the hypersthene normative basalts plot below the alkaline-subalkaline line and are classified as tholeiitic basalts.

The basalts are hypocrystalline or porphyritic and contain phenocrysts of olivine, plagioclase, iron-titanium oxides, and clinopyroxene. Tholeiites have a relatively high modal abundance of plagioclase, olivine, and iron-titanium oxides. Modal abundances of alkali basalts are dominated by olivine and clinopyroxene with less abundant plagioclase and iron-titanium oxides. Olivine crystals are ubiquitous and range in composition from Fo_{90} to Fo_{60} (Mattox, 1991b; Lowder, 1970). Augite occurs as isolated phenocrysts, as glomerocrysts with olivine or plagioclase and hypersthene, or as rims on olivine phenocrysts. Clinopyroxene compositions vary from $Wo_{47}En_{39}$ to $Wo_{40}En_{39}$ (Lowder, 1970). The groundmass is intersertal or, in a few samples, trachytic.

GEOCHEMISTRY

MAJOR-ELEMENT GEOCHEMISTRY

The two basalt types can be distinguished by their MgO content; however, both types include samples with magnesium numbers (Mg/Mg+Fe) in the range suggested for primary basalts. The MgO content of most alkali basalts is greater than 8 weight percent oxide (fig. 2). Most tholeiitic basalts have MgO in the range 6–8 weight percent oxide. Magnesium numbers vary from 0.46 to 0.71 and 0.54 to 0.68 for the alkali basalts and the tholeiites, respectively. Six alkali basalts and one tholeiite have high Mg numbers and probably represent primary mantle magmas. (See section, "Primitive Magmas.") Rocks with high magnesium will be used as the parents of more evolved magmas.

Major-element concentrations show continuous ranges that contain trends for some elements for each of the two basalt types. The concentrations of SiO_2, Al_2O_3, and Na_2O increase and CaO decreases as MgO decreases in the alkali basalts. The concentrations of TiO_2, FeO_T, and P_2O_5, and K_2O remain fairly uniform. For the tholeiites, the contents of TiO_2, Al_2O_3, and FeO_T increase and Na_2O, K_2O, and P_2O_5 decrease as MgO decreases. Calcium content initially increases and then decreases. Relative to the tholeiites, the alkali basalts have higher TiO_2, K_2O, and P_2O_5, and lower Al_2O_3 and FeO_T .

TRACE-ELEMENT GEOCHEMISTRY

Alkali and tholeiitic basalts show fairly distinctive, but slightly overlapping ranges in trace-element contents (fig. 3). The compatible trace elements, Ni and Cr, are higher in most alkali basalts than in tholeiites. Large-ion lithophile elements (Ba, Rb, Sr, and Th) and high-field strength elements (Nb, Hf, and Ta) are also higher in alkali basalts. Chondrite-normalized rare-earth element patterns for alkali basalts are smooth with moderate to high enrichment of light rare-earth elements relative to chondrites (table 2; fig. 4). A tholeiite from the Black Rock Desert, BR9, is characterized by moderate enrichment of light rare-earth elements and a flat, unfractionated pattern for heavy rare-earth elements. The pattern for a tholeiite from the Markagunt Plateau, LC1, resembles the patterns for alkali basalts; however, light rare-earth element abundances in LC1 are slightly lower than those of the alkali basalts.

Basalts become progressively more enriched in light rare-earth elements with increasing distance to the east. Light rare-earth element enrichment is represented by the ratio of La to Eu. BR9, a tholeiite from the eastern margin of the Basin and Range province, has a La/Eu ratio of 15. LC1, a tholeiite from the Markagunt Plateau in the western transition zone, has a La/Eu ratio of 25. The La/Eu of alkali basalt

Table 1. Major-element, trace-element, and normative compositions, and ages of basalts from Utah transition zone.

[Analysts: S.R. Mattox, J.A. Walker; nd, not determined; leaders (---), not present]

Sample	BR1	BR2	BR9	LC1	P13	P32	P36	P42	P22	P35	Mile97	P2
Major-oxide composition												
SiO_2	49.14	48.92	49.35	51.27	52.47	51.87	51.54	48.53	50.04	48.23	48.45	49.79
TiO_2	1.29	1.45	1.74	1.34	1.23	1.35	1.37	1.46	1.29	1.59	1.73	1.36
Al_2O_3	17.15	16.65	16.03	15.57	14.32	16.40	16.30	16.12	16.29	15.54	15.52	15.72
FeO	9.77	9.89	11.93	8.47	8.77	9.05	9.20	11.37	10.07	9.93	8.80	9.67
MnO	.16	.16	.10	.14	.14	.15	.15	.18	.17	.17	.14	.17
MgO	7.80	7.32	6.38	8.36	9.18	6.82	6.80	6.98	7.38	8.13	7.71	8.20
CaO	10.06	10.43	8.62	8.65	7.38	9.11	9.20	9.68	10.66	10.16	8.64	10.02
Na_2O	2.98	2.87	3.13	2.87	3.59	3.43	3.29	3.12	3.10	3.09	3.52	2.93
K_2O	.57	.69	1.11	1.92	1.55	1.06	.99	.35	1.37	1.15	1.78	1.87
P_2O_5	.28	.39	.37	.57	.54	.33	.39	.21	.32	.64	.65	.52
Total	99.20	98.77	98.76	99.16	99.17	99.57	99.23	98.00	100.69	98.63	96.94	100.25
Trace-element composition												
V	200	204	269	166	149	129	141	172	197	159	133	185
Sc	26.1	25.7	29.2	24.9	20.1	21.6	23.3	25.8	29.2	21.9	18.6	23.8
Ba	328	602	463	1,520	1,706	623	633	181	968	841	994	1,592
Cr	168	235	111	343	310	155	150	161	240	215	228	259
Co	74	65	62	43	86	34	42	41	48	43	43	49
Ni	139	132	86	169	275	36	40	48	87	57	143	129
Pb	23.5	8.8	2.0	13.9	22.7	3.0	3.8	0.6	14.9	3.6	9.0	15.2
Th	1.4	0.4	4.9	1.2	3.3	1.8	1.2	1.9	4.5	3.4	3.6	3.6
Rb	9	11	20	18	15	7	7	1	24	6	15	43
Sr	444	523	426	1,315	1,327	387	377	156	605	523	1,127	1,090
Y	33	33	36	26	23	13	13	12	26	13	27	27
Zr	128	157	152	186	173	74	75	63	153	74	241	156
Nb	8	10	17	17	21	6	6	3	15	13	20	25
Normative mineral composition [Based on analyses recalculated to 100 percent water-free oxides]												
Q	----	----	----	----	----	----	----	----	----	----	----	----
or	3.4	4.1	6.6	11.4	9.2	6.3	5.8	2.1	8.1	6.8	10.5	11.1
ab	25.2	24.3	26.5	24.3	30.4	29.0	27.8	26.4	20.7	19.9	24.4	18.6
an	31.7	30.5	26.4	23.9	18.4	26.2	26.8	29.0	26.5	25.1	21.3	24.2
ne	----	----	----	----	----	----	----	----	----	----	----	----
di	13.4	15.4	11.6	12.4	14.9	15.6	15.5	15.8	21.8	20.7	14.2	20.9
hy	4.3	4.7	7.1	9.7	6.3	7.4	9.3	3.3	----	----	----	----
ol	18.1	16.2	16.5	13.6	17.2	12.2	10.9	18.4	17.9	19.0	18.9	19.0
il	2.5	2.8	3.3	2.5	2.3	2.6	2.6	2.8	2.5	3.0	3.3	2.6
ap	0.6	0.9	0.9	1.3	----	----	----	----	----	----	1.5	--
Age (Ma)												
	nd	nd	nd	[1].45	nd	nd	nd	nd	nd	[2].8	[2].5	nd

[1] Age from Fleck and others (1975) and corrected for new decay constants of Steiger and Jäger (1977).
[2] Age from Best and others (1980).

SAMPLE DESCRIPTIONS

BR1 Tholeiite from Black Rock Desert: Black Rock quadrangle at lat 38°42'01" N., long 112°57'12" W.
BR2 Tholeiite from Black Rock Desert: Cinder Crater quadrangle at lat 38°42'44" N., long 112°37'01" W.
BR9 Tholeiite from Black Rock Desert: Pavant Butte North quadrangle at lat 39°07'34" N., long 112°32'12" W.
LC1 Tholeiite from Markagunt Plateau: Parowan quadrangle at lat 37°51'48" N., long 112°46'24" W.
P13 Tholeiite from Markagunt Plateau: Panguitch Lake quadrangle at lat 37°40'10" N., long 112°39'00" W.
P32 Tholeiite from Markagunt Plateau: Henrie Knolls quadrangle at lat 37°38'41" N., long 112°42'14" W.
P36 Tholeiite from Markagunt Plateau: Henrie Knolls quadrangle at lat 37°31'18" N., long 112°44'19" W.
P42 Tholeiite from Markagunt Plateau: Asay Bench quadrangle at lat 37°35'15" N., long 112°36'33" W.
P22 Alkali basalt from Markagunt Plateau: Panguitch Lake quadrangle at lat 37°40'08" N., long 112°40'14" W.
P35 Alkali basalt from Markagunt Plateau: Navajo Lake quadrangle at lat 37°31'49" N., long 112°49'14" W.
Mile97 Alkali basalt from Markagunt Plateau: Glendale Jct. quadrangle at lat 37°25'47" N., long 112°32'10" W.
P2 Alkali basalt from Markagunt Plateau: Panguitch quadrangle at lat 37°46'43" N., long 112°26'33" W.

Table 1. Major-element, trace-element, and normative compositions, and ages of basalts from Utah transition zone.—*Continued*

Sample	P3	P28	P30	P31	P26	EV1	EV4	78164	NS1	OC3	A3
Major-oxide composition											
SiO_2	49.07	49.57	48.81	49.42	49.46	49.95	49.45	47.15	47.40	48.34	49.17
TiO_2	1.32	2.17	2.22	2.14	1.60	1.57	1.56	1.67	1.64	1.74	1.43
Al_2O_3	14.96	15.88	15.58	16.26	15.85	15.77	15.75	15.19	14.48	16.11	16.10
FeO	8.74	9.27	9.07	9.41	8.82	8.72	8.80	9.48	9.26	9.12	9.36
MnO	.15	.15	.15	.16	.16	.15	.15	.16	.16	.15	.16
MgO	9.18	8.17	8.14	7.93	9.44	8.15	7.81	9.20	9.99	7.75	8.61
CaO	9.54	8.21	8.52	8.19	9.36	9.91	8.82	8.44	9.41	8.84	9.33
Na_2O	2.90	3.79	3.63	3.90	3.11	3.31	3.35	3.32	3.80	3.46	3.20
K_2O	1.82	1.79	1.82	1.81	1.95	2.23	2.28	1.76	0.94	1.78	1.90
P_2O_5	.54	.65	.67	.71	.58	.67	.71	.54	.78	.58	.52
Total	98.22	99.65	98.61	99.93	100.33	100.43	98.68	96.91	97.86	97.87	99.78
Trace-element composition											
V	197	131	135	119	153	216	234	186	203	190	211
Sc	23.3	17.6	21.0	15.8	17.6	21.6	23.6	20.4	19.0	25.1	25.9
Ba	1,433	408	407	443	1,156	1,258	1,259	832	1,470	799	1,568
Cr	303	193	200	169	201	277	284	344	391	292	271
Co	52.5	39.1	44.5	37.6	39.4	52.0	56.8	39.3	56.0	52.9	49.8
Ni	180	68	68	84	95	188	196	187	230	146	151
Pb	6.9	4.1	4.5	4.1	3.0	35.3	38.0	8.2	9.3	5.3	21.8
Th	7.7	3.0	3.1	2.2	2.6	5.2	6.3	6.6	10.3	4.7	4.3
Rb	46	10	10	8	22	49	47	46	10	46	43
Sr	936	454	434	515	481	1,115	1,133	889	1,249	838	941
Y	26	14	14	14	14	26	26	27	22	27	26
Zr	150	141	141	141	91	288	195	192	174	186	164
Nb	28	19	20	18	16	28	28	26	30	27	27
Normative mineral composition [Based on analyses recalculated to 100 percent water-free oxides]											
Q	----	----	----	----	----	----	----	----	----	----	----
or	10.8	10.6	10.8	10.7	11.5	13.2	13.5	10.4	5.6	10.5	11.2
ab	21.4	23.3	21.3	22.5	17.9	16.5	19.2	23.7	18.4	19.9	18.0
an	22.4	21.0	20.8	21.5	23.5	21.6	21.2	21.4	19.7	23.2	24.0
ne	1.7	4.7	5.1	5.7	4.6	6.3	5.0	2.4	7.5	5.1	4.9
di	17.4	16.1	17.5	15.6	18.6	22.5	18.5	13.6	22.0	16.9	18.3
ol	20.8	19.1	18.2	19.1	20.6	16.8	17.7	16.6	20.9	18.4	20.2
mt	----	----	----	----	----	----	----	4.5	----	----	----
il	2.5	4.1	4.2	4.1	3.0	3.0	3.0	3.2	3.1	3.3	2.7
ap	1.3	----	----	----	----	----	----	3.2	----	----	----
Age (Ma)											
	nd	[1].5	nd	nd	nd	[1]12.7	[1]12.7	[2]7.8	nd	nd	[1]5.4

[1] Age from Best and others (1980)
[2]Age from Rowley and others (1981)

SAMPLE DESCRIPTION S

P3 Alkali basalt from Markagunt Plateau: Panguitch quadrangle at lat 37°46'08" N.,long 112°27'18" W.
P28 Alkali basalt from Markagunt Plateau: Asay Bench quadrangle at lat 37°31'03" N., long 112°37'15" W.
P30 Alkali basalt from Markagunt Plateau: Asay Bench quadrangle at lat 37°31'03" N., long 112°37'15" W.
P31 Alkali basalt from Markagunt Plateau: Asay Bench quadrangle at lat 37°31'03" N., long 112°37'15" W.
P26 Alkali basalt from Markagunt Plateau: Panguitch quadrangle at lat 37°46'55" N., long 112°23'42" W.
EV1 Alkali basalt from Sevier Plateau: Marysvale quadrangle at lat 38°24'00" N., long 112°09'54" W.
EV4 Alkali basalt from Sevier Plateau: Marysvale quadrangle at lat 38°24'15" N., long 112°09'20" W.
78164 Alkali basalt from Sevier Plateau: Phonolite Hill quadrangle at lat 38°11'52" N., long 112°04'50" W.
NS1 Alkali basalt from Sevier Plateau: Mahustan Peak quadrangle at lat 38°16'18" N., long 112°01'14" W.
OC3 Alkali basalt from Sevier Plateau: Phonolite Hill quadrangle at lat 38°10'28" N.,long 112°01'56" W.
A3 Alkali basalt from Awapa Plateau: Angle quadrangle at lat 38°08'00" N., long 111°57'40" W.

Table 1. Major-element, trace-element, and normative compositions, and ages of basalts from Utah transition zone.—*Continued*

Sample	AP26	AP32	AP45	AP55	AP58	AP107	AP127	AP131	AP133	FV3	CR1
Major-oxide composition											
SiO_2	48.08	47.27	47.56	49.55	48.58	49.12	46.68	48.43	47.04	48.82	47.73
TiO_2	1.23	1.27	1.46	1.30	1.40	1.33	1.49	1.27	1.55	1.30	1.37
Al_2O_3	14.49	13.65	15.36	15.57	14.31	16.58	16.15	15.97	14.73	15.14	15.84
FeO	8.21	8.46	9.07	8.02	9.75	10.23	9.10	10.11	9.11	8.36	7.87
MnO	.15	.15	.17	.14	.17	.18	.17	.17	.17	.16	.14
MgO	9.96	10.09	10.28	6.06	8.99	7.92	9.09	8.76	10.54	8.60	7.81
CaO	9.99	10.35	10.38	10.76	9.13	9.93	9.64	9.61	10.19	8.18	8.54
Na_2O	2.96	2.98	2.55	3.52	2.84	3.16	3.14	2.76	2.69	3.13	3.2
K_2O	1.97	1.88	1.66	2.25	1.95	1.39	2.52	1.40	1.75	2.99	2.69
P_2O_5	.66	.63	.67	.67	.63	.45	.49	.46	.65	.54	.94
Total	97.70	96.73	99.16	97.84	97.75	100.29	98.47	98.94	98.92	97.22	96.25
Trace-element composition											
V	216	203	225	192	186	208	208	177	252	186	203
Sc	28.2	21.1	29.8	22.7	25.0	26.6	23.5	27.8	24.8	23.0	24.3
Ba	1,544	1,277	1,507	1,979	1,302	1,134	2,360	1,128	1,468	2,329	2,539
Cr	513	400	428	238	344	260	271	355	452	371	401
Co	62	50	59	41	49	54	52	50	60	44	40
Ni	237	261	212	63	181	136	146	158	231	169	105
Pb	11.9	9.2	6.0	15.4	9.1	6.6	8.1	7.2	13.8	10.1	24.4
Th	7.2	6.3	3.9	12.4	6.2	5.1	8.3	5.2	7.2	10.9	14.4
Rb	43	41	42	43	50	32	96	31	43	77	69
Sr	1,535	1,261	928	1,660	1,065	882	1,357	892	1,042	868	1,724
Y	23	24	29	25	23	27	31	26	29	24	27
Zr	144	126	183	115	142	130	209	126	174	228	197
Nb	17	18	31	22	24	20	42	19	33	35	37
Normative mineral composition [Based on analyses recalculated to 100 percent water-free oxides]											
or	11.6	11.1	9.8	13.3	10.3	8.2	14.9	8.3	10.3	17.7	15.9
ab	16.3	13.9	12.8	15.7	15.1	19.7	6.4	21.8	11.2	17.1	14.0
an	20.4	18.3	25.6	20.0	21.0	27.0	22.5	27.0	23.0	18.4	20.4
ne	4.7	6.1	4.8	7.6	4.2	3.8	10.9	.9	6.3	5.1	7.6
di	20.1	23.5	21.1	27.4	17.4	18.4	20.6	14.4	22.4	15.2	17.9
hy	----	----	----	----	----	----	----	----	----	----	----
ol	20.6	19.9	21.7	10.6	20.3	20.3	19.8	23.1	21.7	20.0	16.9
il	2.3	2.4	2.8	10.6	2.5	2.5	2.8	2.4	2.9	2.5	2.6
ap	1.5	1.5	----	2.5	----	----	----	1.1	----	1.3	----
Age (Ma)											
	16.4[1]	nd	nd	nd	nd	nd	[1]5.9	nd	nd	nd	[2]4

[1] Age from Mattox (1991b).
[2] Age from Gartner and Delaney (1988).

SAMPLE DESCRIPTIONS

AP26 Alkali basalt from Awapa Plateau: Burrville quadrangle at lat 38°45'05" N., long 111°47'54" W.
AP32 Alkali basalt from Awapa Plateau: Abes Knoll quadrangle at lat 38°26'22" N., long 111°49'27" W.
AP45 Alkali basalt from Awapa Plateau: Flossie Knoll quadrangle at lat 38°12'50" N., long 111°50'11" W.
AP55 Alkali basalt from Awapa Plateau: Flossie Knoll quadrangle at lat 38°11'53" N., long 111°46'48" W.
AP58 Alkali basalt from Awapa Plateau: Flossie Knoll quadrangle at lat 38°14'06" N., long 111°48'22" W.
AP107 Alkali basalt from Awapa Plateau: Moroni Peak quadrangle at lat 38°20'10" N., long 111°41'41" W.
AP127 Alkali basalt from Awapa Plateau: Government Point quadrangle at lat 38°13'48" N., long 111°35'08" W.
AP131 Alkali basalt from Awapa Plateau: Bicknell quadrangle at lat 38°19'22" N., long 111°37'28" W.
AP133 Alkali basalt from Awapa Plateau: Pollywog Lake quadrangle at lat 38°06'18" N., long 111°48'51" W.
FV3 Alkali basalt from Fish Lake Plateau: Geyser Peak quadrangle at lat 38°35'23" N., long 111°28'37" W.
CR1 Alkali basalt from Capitol Reef: Fruita NW quadrangle at lat 38°29'54" N., long 111°28'37" W.

Table 2. Rare-earth element and selected trace-element compositions determined by instrumental neutron activation analysis.

[Analyst: G. Wandless; concentrations given in parts per million; nd, not determined]

Sample	BR9	LC1	P3	P28	EV1	NS1	A3	AP26	AP32	AP127	FV3	CR1
La	28.3	60.3	51.2	45.3	59.3	70.5	48.7	8.5	65.2	76.0	54.3	115.0
Ce	56	122	102	85	115	133	90	157	130	144	99	208
Nd	27.6	54.1	44.7	37.3	51.5	56.8	38.4	64.4	56.0	58.1	43.1	81.0
Sm	6.2	9.4	8.6	7.8	9.5	10.0	7.1	11.4	10.4	9.8	7.6	12.8
Eu	1.9	2.4	2.3	2.2	2.3	2.5	1.9	2.7	2.5	2.5	2.0	3.1
Gd	6.6	7.4	7.6	nd	7.7	8.0	6.0	8.7	7.9	7.6	6.7	9.2
Tb	.9	.9	1.0	1.0	.9	1.0	.9	1.0	1.0	1.0	.9	1.1
Ho	1.4	1.2	1.2	.8	nd	.9	nd	1.6	1.0	1.2	1.0	nd
Tm	.59	.35	.43	nd	.36	.31	.46	.38	.38	.43	.37	.40
Yb	3.20	2.25	2.48	2.34	2.09	1.88	2.58	2.07	2.00	2.50	2.08	2.31
Lu	.48	.30	.33	.33	.27	.25	.38	.26	.28	.35	.31	.30
Sc	28.4	24.1	24.8	24.7	22.6	22.2	28.1	23.6	24.8	28.3	26.1	23.6
Ba	550	1,590	1,220	580	1,290	1,480	1,670	1,490	1,390	2,430	2,460	2,590
Cr	99	299	288	329	307	384	274	511	469	286	389	362
Co	45	40	42	43	40	45	41	41	44	41	37	31
Ni	95	207	174	167	202	244	145	233	261	149	186	124
Zn	114	81	82	78	87	90	83	89	85	81	88	88
Th	2.8	2.8	4.2	3.8	5.2	8.9	4.3	7.1	5.7	6.4	10.1	13.8
Rb	24	20	35	23	45	15	45	47	42	81	79	71
Sr	480	1,520	1,190	980	1,290	1,390	1,120	1,800	1,480	1,500	1,000	1,990
Zr	199	200	198	239	198	154	180	196	210	215	236	213
U	.9	.8	.8	1.0	1.2	1.6	.6	.9	.8	1.6	2.0	2.8
Cs	.3	.3	1.0	.3	1.7	1.5	.7	.9	.8	5.0	5.3	5.0
Hf	3.43	4.33	4.56	5.23	4.55	4.65	3.92	4.27	4.06	5.24	5.95	5.67
Ta	1.02	.93	1.57	2.53	1.60	2.01	1.64	1.08	1.18	2.89	2.88	2.51

NS1 from the Sevier Plateau is 28. CR1, an alkali basalt from the Colorado Plateau, just east of the transition zone, has a La/Eu ratio of 37. The increase in the La/Eu ratio to the east transects the eastern Basin and Range province, the transition zone, and the western Colorado Plateau.

Tholeiitic and alkalic basalts are characterized by small negative europium anomalies of Eu/Eu* =0.89–0.94. The negative europium anomalies may be the result of plagioclase fractionation.

Basalts from the Utah transition zone have one of three distinct patterns on chondrite-normalized spider diagrams (fig. 5). Alkali basalts, represented by CR1, show enrichment of Ba and La, a depletion of Rb, a moderate depletion of Nb and Ta, and moderate light rare-earth element enrichment. A single alkali basalt from the Sevier Plateau, basalt NS1, has a large depletion of Rb and K, no depletion for Nb-Ta, and a small depletion of Zr. Mattox (1992a) analyzed 88 upper Cenozoic rocks, representing nearly every volcanic deposit in the Utah transition zone, and found that only NS1 had these trace-element characteristics. Tholeiitic basalts, represented by basalt BR1, show depletions of more incompatible elements, less pronounced enrichment of Ba and La (and Ce), small depletions of Rb and Nb, and lower light rare-earth element concentrations. None of the basalts from the Utah transition zone have normalized incompatible trace-element patterns with the enrichment in incompatible elements centered at Nb, a characteristic of ocean island basalts or basalts derived from the asthenosphere (fig. 5) (Fitton and others, 1988; Ormerod and others, 1988).

ISOTOPE GEOCHEMISTRY

Alkalic and tholeiitic basalts from the Utah transition zone show overlapping isotopic compositions. Initial $^{87}Sr/^{86}Sr$ of nine alkali basalts ranges from 0.7043 to 0.7046 (fig. 6; table 3). Four analyses of tholeiites define a larger range from initial $^{87}Sr/^{86}Sr$ of 0.7039 to 0.7058. Three tholeiites have initial $^{87}Sr/^{86}Sr$ of 0.7046 or less. The basalts from the Utah transition zone have Sr isotopic compositions similar to the value for bulk earth (0.7045). The value for bulk earth is based on the age of the Earth and the assumption that terrestrial Sr has evolved in a uniform reservoir whose Rb/Sr is equal to that of chondritic meteorites. The tholeiites can be divided into two groups based on isotopic composition and geographic location. Basalts BR1 and BR9, from the Black Rock Desert, plot to the right of bulk earth and are enriched in radiogenic Sr. Enriched isotopic values

Table 3. Sr-Nd-Pb isotopic data for basalts from Utah transition zone.

[$\varepsilon Nd=[^{143}Nd/^{144}Nd_{sample}/^{143}Nd/^{144}Nd_{CHUR}-1]\bullet 10^4$ where $^{143}Nd/^{144}Nd_{CHUR}=0.51264$; nd, not determined]

Sample No.	$^{87}Sr/^{86}Sr_i$	$^{143}Nd/^{144}Nd$	εNd	$^{206}Pb/^{204}Pb$	$^{207}Pb/^{204}Pb$	$^{208}Pb/^{204}Pb$
			Tholeiites			
BR1	.704684±11	.512329±3	-6.1	17.87	15.51	37.69
BR9	.705815±13	.512307±3	-6.5	nd	nd	nd
LC1[1,5]	.704136±21	.512216±8	-8.27	16.982	15.399	36.646
P32[3]	.7043	nd	nd	nd	nd	nd
			Alkali basalts			
NS1[2]	.70448	.512347	-5.7	17.883	15.512	37.845
P3[2]	.70468	.512311	-6.4	17.893	15.509	38.108
AP26[1,6]	.704684±11	.512194±10	-8.7	17.59	15.48	37.52
CR1[1]	.704643±12	.512279±14	-7.0	nd	nd	nd
OC5[2]	.70432	.512325	-6.1	17.739	15.508	37.762
EV1[2]	.70461	.512371	-5.2	18.108	15.532	37.895
P31[3]	.7041	nd	nd	nd	nd	nd
Mile97[4]	.7041	nd	nd	nd	nd	nd

[1]=Sr and Nd isotopic data provided by M. Feigenson, Rutgers University.

[2]=Sr , Nd , and Pb isotopic data provided by D. Coleman, University of Kansas.

[3]=Sr isotopic data from Lowder (1973), P31=Lowder's sample 482.

[4]=Sr isotopic data from sample WPL-8 of Leeman (1970).

[5]=Pb isotopic data from Everson (1979).

[6]=Pb isotopic data provided by R. Ward, Northern Illinois University.

result from basalts with higher Rb/Sr relative to bulk earth. Tholeiite LC1, from the eastern Markagunt Plateau, has lower $^{87}Sr/^{86}Sr$ and plots to the left of bulk earth. The relatively high $^{87}Sr/^{86}Sr$ of BR9 may be the result of contamination by upper crust. (See section, "Crustal Contamination.") Excluding BR9, the alkali basalts and the two remaining tholeiitic samples have similar isotopic compositions.

The initial $^{143}Nd/^{144}Nd$ of the alkali basalts ranges from 0.51219 to 0.51237 (ε_{Nd} = –5.2 to –8.7) and includes the more narrow range of the tholeiites from 0.51221 to 0.51233 (ε_{Nd} = –6.1 to –8.3) (fig. 6; table 3). The Nd isotopic compositions are lower than the value for bulk earth ($^{143}Nd/^{144}Nd=0.51264$, ε_{Nd} = 0) and plot below the mantle array, as defined by mid-ocean ridge and ocean island basalts (White and Hofmann, 1982).

The basalts from the Utah transition zone occupy a unique position on the Nd-Sr isotopic diagram relative to basalts from other late Cenozoic volcanic fields in the southwestern United States (fig. 6 and Kempton and others, 1991). Although the range in Sr isotopic compositions is similar to

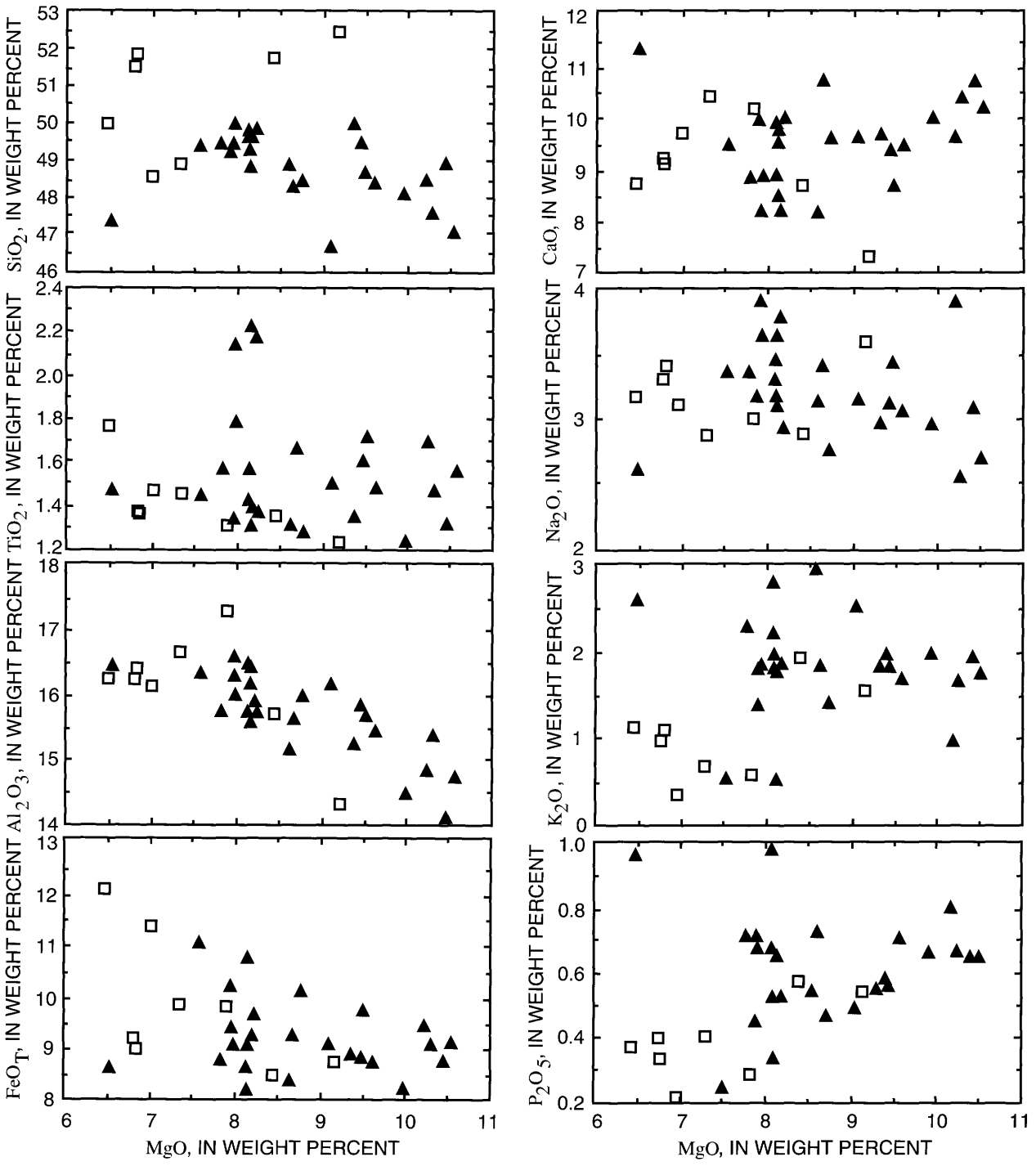

Figure 2. Major-element (in weight percent oxide) variation diagrams for basalts from Utah transition zone. Square, tholeiite; solid triangle, alkali basalt.

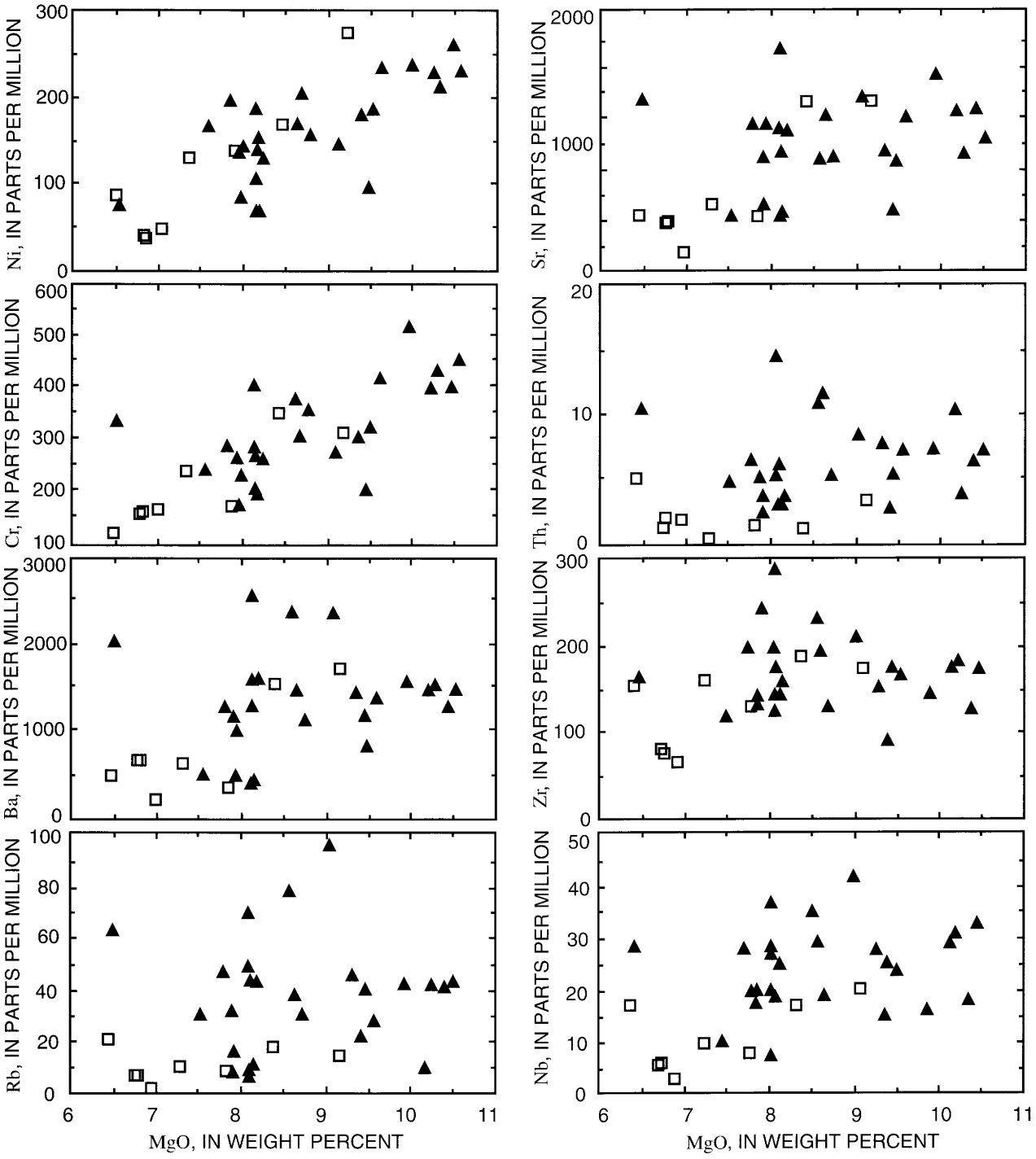

Figure 3. Trace-element variation diagrams for basalts from Utah transition zone. Square, tholeiite; solid triangle, alkali basalt.

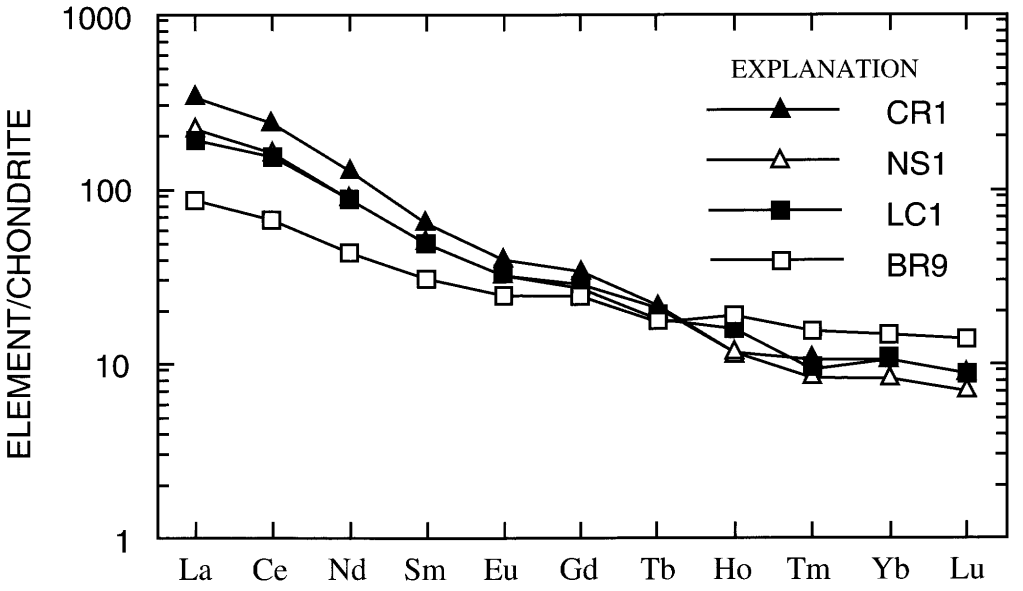

Figure 4. Chondrite-normalized rare-earth element diagram for selected basalts from Utah transition zone. Normalization values from Nakamura (1974). Square, tholeiite; triangle, alkali basalt. Samples are from the western Basin and Range province (BR9), Markagunt Plateau (LC1), Sevier Plateau (NS1), and eastern Colorado Plateau (CR1). Note that light rare-earth element abundances increase with distance to the east.

that of basalts from the Grand Canyon and San Francisco Peaks fields ($^{87}Sr/^{86}Sr$ =0.7032–0.7045, ε_{Nd}= –2.6 to 2.1) (Alibert and others, 1986) and alkali basalts from the Arizona transition zone ($^{87}Sr/^{86}Sr$=0.7049–0.7054, ε_{Nd} = –2.0 to –0.2) (Wittke and others, 1989), basalts from the Utah transition zone are readily distinguished by their less radiogenic Nd isotopic compositions ($\varepsilon_{Nd} \leq -5.2$). None of the analyzed basalts show the more radiogenic Sr isotope compositions found in basalts from southern Nevada ($^{87}Sr/^{86}Sr$=0.7070– 0.7075) (Farmer and others, 1990).

In the "Discussion" section the elemental and isotopic data are used to constrain the origin and evolution of magmas erupted in the Utah transition zone and adjacent provinces. Various magmatic processes will be evaluated to constrain their contribution to the geochemical characteristics of the basalts. Central to this discussion are space-time variation patterns in the composition of the basalts.

DISCUSSION

SPACE-TIME-COMPOSITION PATTERNS

The temporal changes in the location of volcanic centers in the Utah transition zone and adjacent areas are neither simple nor systematic. From 16 to 8 Ma, small volumes of magma erupted from scattered localities in the transition zone and the adjacent Basin and Range province. By 6 Ma, and continuing to about 4 Ma, all activity was located in the eastern transition zone and the adjacent Colorado Plateaus province. After a short lull in volcanism, small volumes of lava erupted in the Black Rock Desert. In the last 1 m.y., all activity has been on the Markagunt Plateau and in the adjacent Basin and Range province. The change in the locus and timing of magmatism, from the eastern transition zone and adjacent Colorado Plateau from 6 to 4 Ma to the western transition zone and adjacent Basin and Range province during the last 1 m.y., defines a westward shift in volcanism that is unique to the Utah transition zone. Furthermore, volcanism in the transition zone did not migrate eastward at uniform rates as observed at other volcanic fields (Best and Brimhall, 1974; Tanaka and others, 1986; Condit and others, 1989) but might be better described as episodic and occurring at different locations.

Basalts from the Utah transition zone define systematic spatial and temporal trends in major-element contents, normative compositions, and trace-element contents (fig. 7) (Best and others, 1980; Mattox and Walker, 1990). From west to east SiO_2, TiO_2, Al_2O_3, and FeO_T decrease and MgO, K_2O, and P_2O_5 increase. Magnesium numbers also increase from west to east from 0.55 to almost 0.71. Basalts from the eastern Basin and Range province and western transition zone are olivine tholeiites, with alkali basalts (average normative nepheline=2.7 percent) first appearing near the center of and along the eastern margin of the Markagunt Plateau (fig. 1). Alkali basalts are abundant near the center of the transition zone (Sevier Plateau; nepheline=6.4 percent) and in the eastern part (Awapa Plateau; nepheline=6.6 percent).

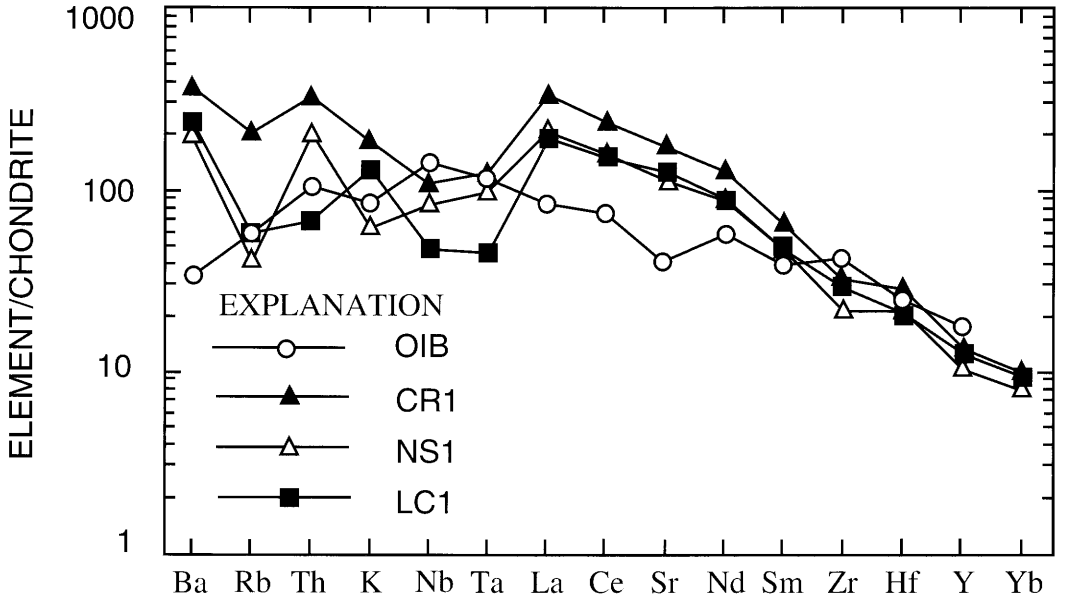

Figure 5. Chondrite-normalized trace-element diagram for selected basalts from Utah transition zone. Normalization values from Nakamura (1974). All basalts from Utah transition zone have one of these three trace-element patterns. Trace-element pattern of an ocean island basalt (OIB) shown for comparison (Thompson and others, 1984).

Farther east, in the Capitol Reef area, all rocks are alkalic (nepheline=7.7 percent). A general trend from subalkaline-to-alkaline compositions in the Basin and Range province to alkaline compositions in the Colorado Plateaus province was recognized earlier by Best and Hamblin (1978). The spatial and temporal trends are most pronounced for the incompatible elements of the most primitive basalts (MgO > 6 weight percent). Concentrations of nearly all compatible and incompatible trace elements increase to the east (fig. 7) except for Zr and Sc.

The overall space-time-composition patterns in the Utah transition zone appear to be as follows: Prior to 10 Ma, small volumes of alkalic and tholeiitic basalts erupted at scattered locations. About 6 Ma, volcanism became localized in the eastern transition zone and adjacent Colorado Plateaus province, increased in volume, and became more alkaline, mafic, and trace element enriched with increasing distance to the east. About 2.5 Ma, tholeiitic volcanism began along the eastern margin of the Basin and Range province. In the last 2 m.y., volcanism has been dominantly tholeiitic and limited to the eastern Basin and Range province and the adjacent Markagunt Plateau. The possible petrogenetic causes of these compositional patterns are discussed next.

PRIMITIVE MAGMAS

Basalts with the characteristics of primitive magmas, if not primary magmas, have erupted on each plateau and during the entire period of late Cenozoic volcanism (16–0 Ma). Characteristics commonly cited for primary magmas include high MgO content (> 10 weight percent), magnesium number (≥0.68), Ni (200–450 ppm), and Cr (170–310 ppm) (Kesson, 1973; Frey and others, 1978; Basaltic Volcanism Special Project, 1981). Six alkalic basalts from the eastern transition zone have characteristics of primary magmas. Two tholeiites and one alkali basalt from the western transition zone have most, but not all of the characteristics of primary magmas. Because these primitive magmas may represent unmodified mantle compositions, they are considered herein as parental magmas and as representatives of different magmatic sources.

Although these chemical features indicate that these basalts may represent primary magmas, the absence of mantle xenoliths coupled with the fact that cryptic contamination cannot be recognized may mean that they are not truly primary magmas. A single, quartz-normative tholeiitic lava flow that contains sedimentary xenoliths (Mattox, 1992a) was not included in this study.

PETROGENESIS

Any model for the genesis of the basalts in the Utah transition zone must explain the distribution of different rock types and the systematic chemical variations. In this section, several geochemical processes are modeled to determine their influence on magma compositions: partial melting, crystal fractionation, and crustal contamination.

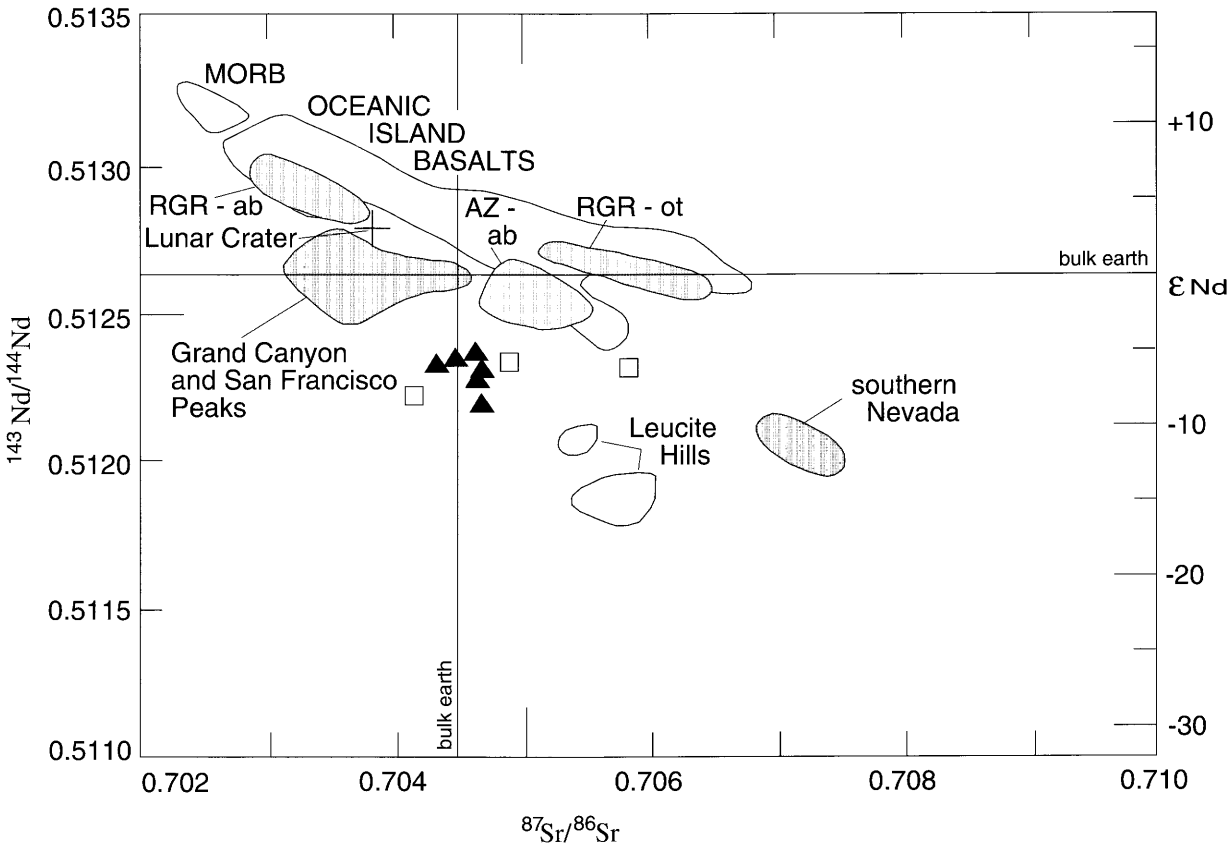

Figure 6. Nd-Sr isotopic composition of Utah transition zone basalts. Square, tholeiite; solid triangle, alkali basalt. Rio Grande Rift (RGR) data for alkali basalts (ab) and olivine tholeiites (ot) are from Perry and others (1987). Grand Canyon and San Francisco Peaks data are from Alibert and others (1986). Arizona alkali basalt (AZ-ab) data are from Wittke and others (1989). Average basalt from Lunar Crater volcanic field shown by cross (Lum and others, 1989). Leucite Hills data are from Vollmer and others (1984). Southern Nevada data are from Farmer and others (1990). Also shown are fields for mid-ocean ridge basalts (MORB) and ocean island basalts from White and Hofmann (1982). Bulk earth values for Nd (0.51264) and Sr (0.7045) isotopic compositions shown by horizontal and vertical lines, respectively.

PARTIAL MELTING

Petrologists universally accept that basaltic magmas similar to those erupted in southwestern Utah are derived by partial melting of upper mantle peridotite. Such magma genesis is modeled as either a batch (equilibrium) or fractional melting process (Allegre and Minister, 1978; Frey and Prinz, 1978). Source materials used in the models are either garnet or spinel peridotites because melting experiments in laboratories have shown that these materials can produce basaltic melts at small degrees of partial melting. The specific compositions of source materials melted to produce magmas in southwestern Utah are unknown, but studies of mantle-derived xenoliths show that both garnet and spinel peridotite compose the upper mantle beneath the southwestern United States (Wilshire and others, 1988; Nealey and Sheridan, 1989).

Batch partial melting calculations can be used to constrain the degree of partial melting required to generate primary magmas as well as the mineralogy of the mantle source. The basic equation for nonmodal equilibrium melting was presented in Allegre and Minister (1978) and takes the form:

$$\frac{C_l}{C_o} = \frac{1}{D_o + F(1\text{-}P)} \qquad (1)$$

where:

C_l = the concentration of the trace element in the partial melt

C_o = the concentration of the trace element in the mantle source

F = the degree of partial melting

D_o = the initial bulk solid-liquid partition coefficient

$= X^a{}_o D^a{}_{a/l} + X^b{}_o D^b{}_{b/l} \ldots$ where a and b are minerals in the source (or melt),

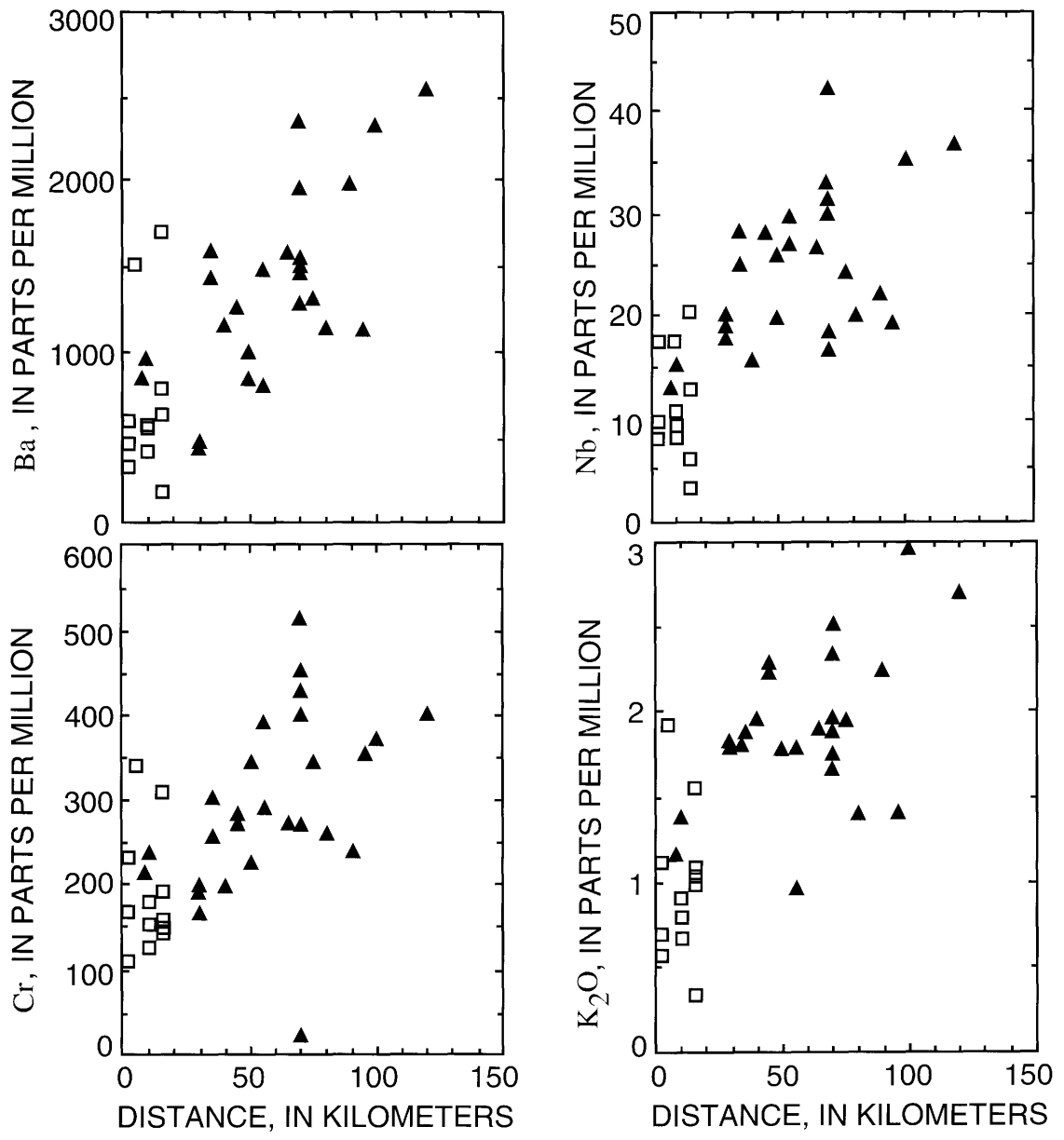

Figure 7. Examples of variation in selected major- and trace-element contents of basalts across Utah transition zone. Square, tholeiite; solid triangle, alkali basalt. Distance is 0 for the Black Rock Desert and increases to the east.

and X^a_o, b_o ... = weight fractions of a, b, ... in the initial source and

D = the mineral-melt partition coefficient, and

$P = p^aKd^{a/l} + p^bKd^{b/l}$ ... where p = fraction of liquid contributed by each phase to the total melt. This model assumes a homogeneous source and constant mineral-melt partition coefficients.

Extensive partial melting calculations using rare-earth element abundances from spinel peridotite xenoliths from the San Carlos volcanic field in Arizona do not produce satisfactory results (Mattox, 1992a). The xenoliths lacked the necessary light rare-earth element enrichments (Frey and Prinz, 1978) to produce transition zone magmas. More importantly, these calculations showed that the primary melts would have high normalized heavy rare-earth element patterns that are not present in patterns in basalts from the Utah transition zone (Mattox, 1992a).

An alternative source for primary basaltic magmas is upper mantle garnet peridotite; rare lherzolite xenoliths from the southwestern United States provide constraints on this possible source material. Partial melting calculations using phlogopite-bearing garnet lherzolite, represented by a xenolith from The Thumb of the Navajo volcanic field (Ehrenberg, 1982), produces the light rare-earth element patterns

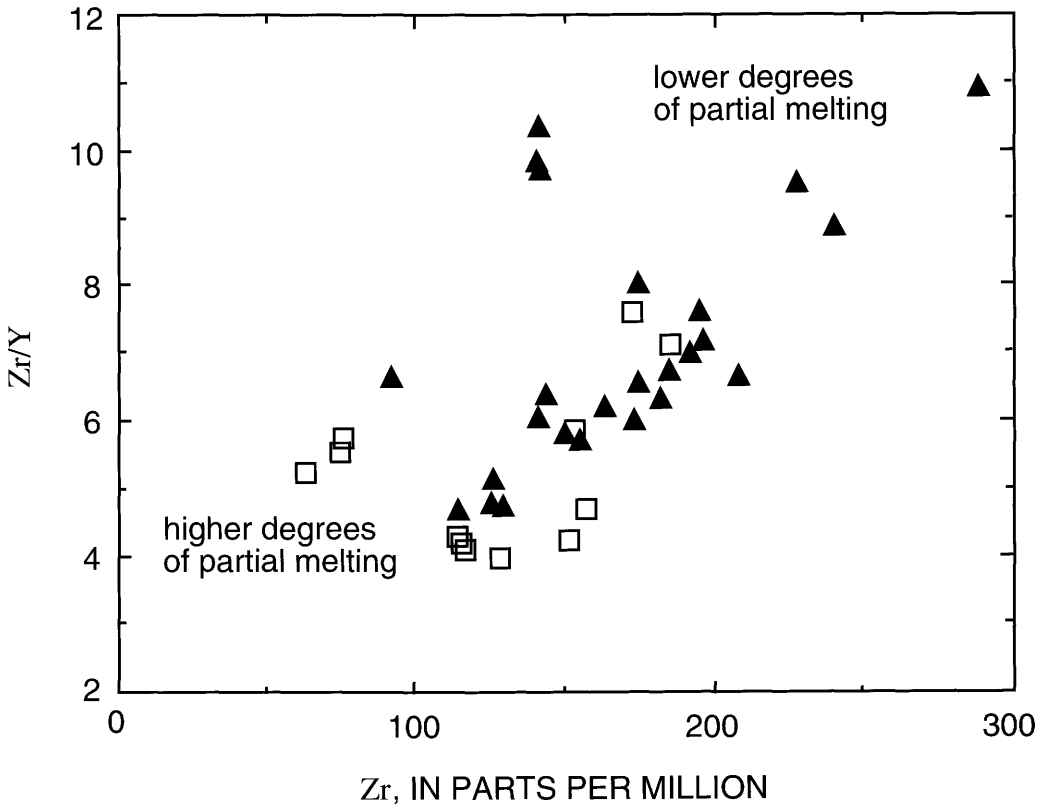

Figure 8. Relative degrees of partial melting for alkali basalts and tholeiites. Alkali basalts (solid triangle) are characterized by high Zr and Zr/Y. Tholeiites (square) are characterized by low Zr and Zr/Y.

similar to those of the Utah basalts, assuming a source contribution to the melt in the proportions of 2:2:4:1:1 for olivine, orthopyroxene, clinopyroxene, garnet, and phlogopite, respectively (Mattox, 1992a). Modeling of this source composition suggests that the primary alkali and tholeiitic basalts of the Markagunt Plateau resulted from ≤5 percent partial melting, with alkalic basalts representing smaller degrees of melting. However, these models fail to produce the higher (7–10 times chondrite) heavy rare-earth element abundances of the Utah transition zone basalts. Additional calculations, including a slightly different source, different proportions of contributing phases in the source, and different degrees of melting also produced unsatisfactory results, suggesting a more complicated source than that proposed by the models (Mattox, 1992a) or a contribution to the geochemical variation of the basalts by a process such as fractional crystallization and (or) contamination.

Trace-element abundances also suggest a continuum in the degree of partial melting. Different amounts of partial melting can be evaluated using a plot of a highly incompatible element versus the ratio of a highly incompatible element and a slightly incompatible element (Allegre and Minister, 1978). Magmas related by partial melting produced a steep, positive trend on such a plot. Alkali basalts and tholeiites produce a steep, positive trend in a plot of Zr versus Zr/Y, with alkali basalts having high Zr contents and Zr/Y ratios relative to tholeiites (fig. 8). This relationship suggests that the basalts are related by variable degrees of partial melting, with alkali basalts resulting from lower degrees of melting relative to tholeiites.

FRACTIONAL CRYSTALLIZATION

The wide range in Ni and Cr concentrations suggests that fractional crystallization of mafic phases greatly influenced the composition of the basalts. Fractional crystallization was modeled using the Rayleigh distillation equation of Allegre and Minister (1978) in the form:

$$\frac{C^i_l}{C^i_o} = F^{(D-1)} \qquad (2)$$

where

C^i_l = trace-element concentration of element i in the liquid

C^i_o = trace-element concentration of element i in the initial liquid

F = weight fraction of residual liquid (or degree of crystallization)

D = bulk partition coefficient for trace element i.

Observed phenocrysts and their modes (Mattox, 1992a) and the partition coefficients compiled by Henderson (1982) were used in the equation. For example, removal of olivine and clinopyroxene from alkali basalt AP26 produces the concentrations of Ni and Th of more differentiated magmas of the Awapa Plateau (fig. 9); the trends can be explained by 5–20 percent crystallization.

The range in Ni and Th concentrations in tholeiites can also be explained by fractional crystallization. The low compatible trace-element contents of some tholeiites on the Markagunt Plateau can be modeled using LC1 as a parental magma and removing 20 percent olivine and pyroxene (fig. 9).

The success of the models indicates that some of the variation in the basalt composition is probably the result of fractional crystallization. Variance from the fractionation curve suggests that some other process operated on parental magmas to produce the chemical variations or that magmas tapped different sources. Because of the likelihood that ascending magmas assimilate crust en route to the surface, crustal contamination is considered next.

CRUSTAL CONTAMINATION

The clustering of isotopic compositions from basalts with diverse major- and trace-element compositions suggests that crustal contamination did not played a major role in the chemical variability of transition zone basalts. In addition, only one of the upper Cenozoic basalts has the elevated initial Sr isotopic compositions ($^{87}Sr/^{86}Sr$ > 0.705–0.708) diagnostic of older andesitic and potassic lava flows that have been contaminated by upper crust (Mattox, 1992a).

Assimilation of crust is modeled using equations that account for concomitant fractional crystallization. The equations were presented by DePaolo (1981). For changes in elemental concentration, the equation takes the form:

$$\frac{C_m}{C^o_m} = F^{-z} + \frac{r}{r-1}\frac{C^a}{zC^o_m}(1-F^{-z}) \qquad (3)$$

where

C_m = concentration of the element in the magma

C^o_m = original concentration of the element in the magma

C^a = concentration of the element in the wallrock

$F = M_m/M^o_m$, where M_m = mass of magma and

M^o_m = the mass of the original magma,

$r = M_a/M_c$, the ratio of mass rate of assimilation to the mass rate of crystal fractionation,

D = bulk partition coefficient of the element for the fractionating assemblage, and

$$z = \frac{r + D - 1}{r - 1}$$

For changes in the isotopic composition of the magma, the equation takes the form:

$$E_m = \frac{\frac{r}{r-1}\frac{C^a}{z}(1-F^{-z})\,E_a + C^o_m F^{-z} E^o_m}{\frac{r}{r-1}\frac{C^a}{z}(1-F^{-z}) + C^o_m F^{-z}} \qquad (4)$$

where

E_m = isotopic ratio of the magma

E^o_m = initial isotopic ratio of the magma

E_a = isotopic ratio of the assimilant

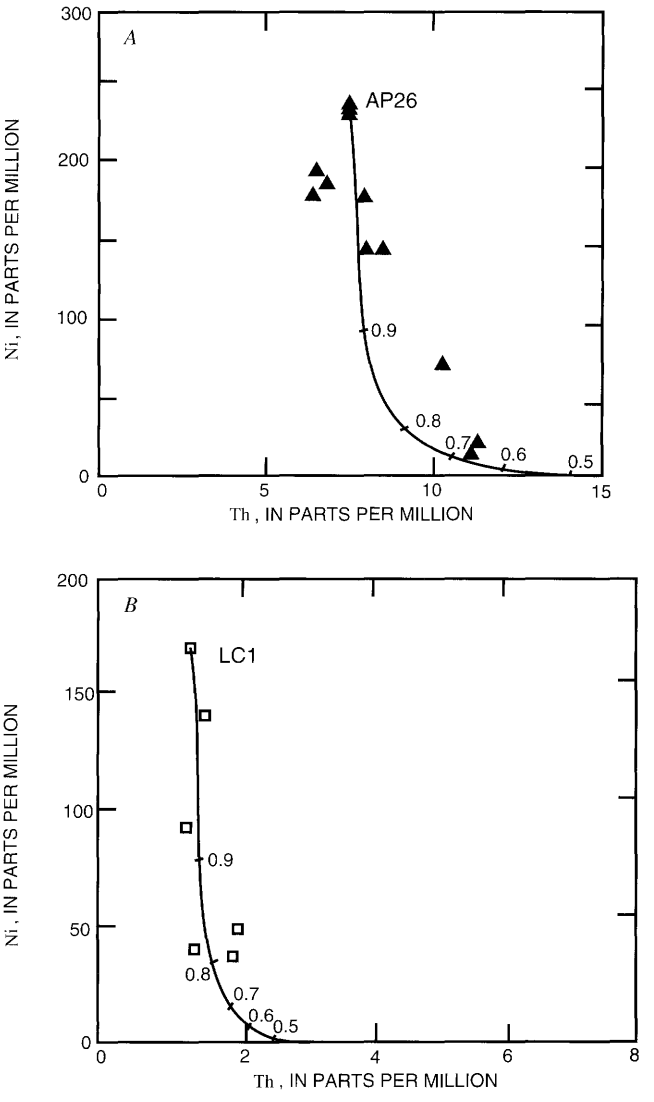

Figure 9. Rayleigh fractionation models for (*A*) Awapa Plateau alkalic and (*B*) Markagunt Plateau tholeiitic magmas. *A*, Derivation of more evolved alkalic magmas by fractional crystallization of olivine and pyroxene. Primitive magma AP26 is the parent. *B*, Derivation of more evolved tholeiitic magmas by fractional crystallization of olivine and pyroxene from parental magma LC1. Bulk partition coefficients for Ni and Th are 8 and 0, respectively.

These equations were used to constrain the magmatic history of a tholeiite from the Black Rock Desert, sample BR9, which has Nd isotopic composition similar to the other basalts but elevated Sr isotopic composition (fig. 6). If basalt BR1, a tholeiite from the Black Rock Desert, is used as the parent, the Sr concentration and isotopic composition of BR9 can be modeled by fractionating only 3 percent olivine plus pyroxene. The bulk distribution coefficient for Sr in the model is $D_{Sr} = 0.5$ and the ratio of the mass assimilated to the initial mass of magma is 0.02. The ratio of mass rate of assimilation to the mass rate of crystal fractionation is 0.5. The model assumes upper crust to be similar in composition to Precambrian gneiss from the nearby Mineral Mountains. The gneiss has the composition SiO_2=74.35 weight percent, Sr=84.8 ppm, and $^{87}Sr/^{86}Sr$=0.8518 (sample MM88-25 of Coleman and Walker, 1992).

The assimilation of lower crust by magmas of the Marysvale volcanic field was modeled by Mattox (1992a) and found to be unlikely. The models assumed lower crust to be chemically similar to mafic xenoliths from the Henry Mountains, 60 km southeast of the transition zone. Although Sr and Nd isotopic compositions of transition zone basalts are similar to those of the xenoliths ($^{87}Sr/^{86}Sr$=0.7032–0.7049 and $^{143}Nd/^{144}Nd$=0.51185– 0.51319; unpub. data of Stephen T. Nelson, University of California at Los Angeles), the Pb isotopic compositions of the basalts (table 3) are substantially less radiogenic compared to the xenoliths ($^{206}Pb/^{204}$ Pb =19.33–20.55, $^{207}Pb/^{204}Pb$=15.65–15.82, $^{208}Pb/^{204}Pb$=38.30–38.88; unpub. data of Stephen T. Nelson). Assimilation of varying amounts of lower crust by different magma bodies during ascent would result in noticeable shifts in the Pb isotopic compositions of the basalts. The observed Pb isotopic compositions of the basalts do not reflect such an event.

DEPTH OF MELTING

Elemental ratios and normative compositions are useful for estimating the depth of mantle melting (Fitton and others, 1988; Ellam, 1992; Kay and others, 1988). Taking the Black Rock Desert as a reference on the western margin of the Utah transition zone, these geochemical data indicate that the depth of melting increases systematically from west to east across the transition zone. Values for CaO/Al_2O_3 and normative diopside increase from west to east from the eastern Basin and Range province, across the transition zone, to Capitol Reef (fig. 10). Fitton and others (1988) interpreted the shift towards higher CaO/Al_2O_3 and higher proportions of normative diopside in Colorado Plateau nephelinites relative to Basin and Range basalts to indicate a higher garnet/clinopyroxene ratio in the mantle source and a greater depth of origin for the Colorado Plateau magmas. The more detailed perspective gained by the most mafic samples from the plateaus in the transition zone supports the hypothesis of Fitton and others (1988).

Trace-element ratios also support a greater depth of magma generation in the eastern transition zone. Because of the higher partition coefficients of heavy rare-earth elements for garnet, the ratio of a light rare-earth element to a heavy rare-earth element can indicate the presence or absence of garnet in the source. Coupled with the change with increasing depth from a spinel lherzolite source to a garnet lherzolite source, magmas with steep rare-earth element patterns and high La/Yb and Ce/Yb can be interpreted as being derived from greater depths (Ellam, 1992). The gradual increase in La/Yb and Ce/Yb from the eastern Basin and Range province, across the transition zone to Capitol Reef, suggests a greater depth of magma generation to the east (fig. 10). Kay and others (1988) interpreted La/Yb of 10–20 to indicate that garnet was minor or absent in the source; ratios of 30–40 indicate that garnet was present. Values for La/Yb for the Utah basalts range from 15 to 50. Furthermore, the ratios mirror the change from abundant tholeiites (shallow source) in the eastern Basin and Range province and western transition zone to abundant alkali basalts (deeper source) in the eastern transition zone and adjacent Colorado Plateau.

In summary, two processes, degree of partial melting and depth of melting, exert the greatest influence on basalt composition. Lower degrees of partial melting at greater depths generate alkali basalts in the eastern transition zone and adjacent Colorado Plateau. Higher degrees of partial melting at shallower depth generate tholeiitic basalts in the western transition zone and the adjacent Basin and Range province. These two processes produce most of the systematic variation in lava chemistries observed across the transition zone (fig. 7). However, these processes alone cannot account for the three distinct trace-element patterns observed for the transition zone basalts (fig. 5), indicating that the chemical composition of the source is also important.

NATURE OF BASALT SOURCE REGIONS

Trace-element patterns of basalts in the Utah transition zone suggest that at least three distinctive source compositions were involved in their generation (fig. 5). To better constrain the nature of these mantle sources, the trace-element patterns of the basalts were compared with patterns from other igneous rocks in the transition zone.

The basalts in the Marysvale region show compositional similarities to mafic alkaline dikes of the Wasatch Plateau in the extreme north of the transition zone (fig. 1). The petrology and geochemistry of these dikes were described by Tingey and others (1991). They classified the dikes as minette and two varieties of melanephelinite. Minette dikes contain phenocrysts of phlogopite and olivine. Melanephelinite dikes contain phenocrysts of diopside and olivine with essential nepheline and trace amounts of phlogopite. Mica melanephelinite dikes contain diopside and olivine and up to 20 percent phlogopite. The major-element composition of each rock type is different. However, all are strongly enriched in compatible and incompatible trace elements (Tingey and others, 1991).

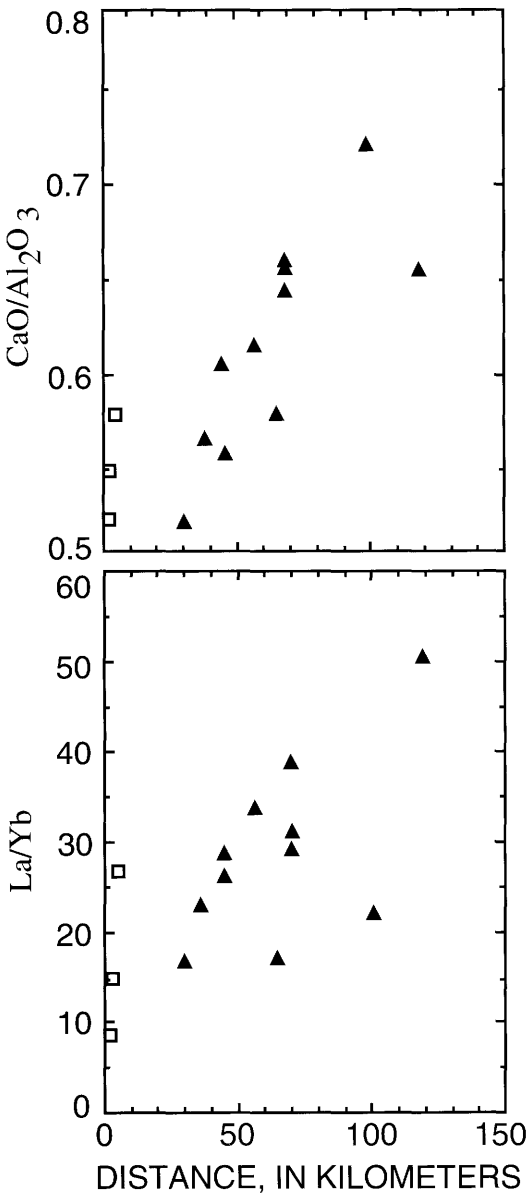

Figure 10. Systematic increase in CaO/Al_2O_3 and La/Yb with increasing distance to the east for the most mafic samples in Utah transition zone and adjacent areas. Square, tholeiite; solid triangle, alkali basalt. Low ratios of La/Yb suggest that garnet is absent or limited in the source. High ratios of La/Yb suggest that garnet is an important phase in the source. Distance is 0 for Black Rock Desert and increases to the east.

The trace-element composition of the transition zone basalts is similar to those of the mafic alkaline dikes. Most of the alkali basalts from the eastern transition zone are similar to mica melanephelinite dikes (fig. 11). A single alkali basalt from the eastern transition zone is similar to the melanephelinite dikes. Both alkali basalts and tholeiites from the western transition zone are similar to minette dikes.

The similarity of the trace-element patterns suggests a genetic relationship between the basalts and the mafic dikes. The basalts may have been derived from mantle veined by dikes similar to those of the Wasatch Plateau. Alternatively, the basalts and the dikes may have been derived from the same three distinct mantle sources and related by high and low degrees of partial melting, respectively. A discussion of source mineralogy and origin of the mafic alkaline dikes appeared in Tingey and others (1991).

LOCATION OF SOURCES

The similarity in compositions of basalts and mafic dikes coupled with depth information gained from the geochemical data can be used to construct a cross section of the lithosphere beneath the Utah transition zone. Elemental ratios and normative compositions indicate that the depth of melting for the basalts in the transition zone increased to the east (fig. 10). This increase in depth of melting correlates with the distribution of the types of basalts, with tholeiitic basalts in the western transition zone and alkalic basalts in the eastern transition zone (fig. 1). Therefore, the source of tholeiitic basalts and dikes of similar composition must be at a shallow depth relative to the source of alkali basalts and dikes of similar composition.

Theoretical and experimental studies also suggest that tholeiites are generated at shallower depths relative to alkali basalts and approximate the depths to the sources of the two types of basalt (Kushiro, 1968; DePaolo, 1979; Jaques and Green, 1980; Presnall and others, 1978; Takahashi, 1980; Takahashi and Kushiro, 1983). The experimental studies of Takahashi (1980) and Takahashi and Kushiro (1983) estimated that alkali basalts, similar to those in the Utah transition zone, originate from depths of about 45–65 km. Since tholeiites are derived from melting at shallower depths, their sources are probably less than 45 km deep. The depths of specific sources can be approximated by these experimental studies.

The vertical distribution of sources in the transition zone can be constrained by basalt type and trace-element patterns. The geochemical compositions of deeper sources are identified by using mafic dikes and alkali basalts with similar chemical affinity. Trace-element patterns of mica melanephelinite, melanephelinite, and minette dikes are similar to those of alkali basalts (fig. 11), placing sources with these geochemical signatures at greater relative depths. The composition of the source at shallow depths is reflected in the composition of mafic dikes and tholeiitic basalts. Trace-element patterns of tholeiites are similar to minette dikes (fig. 11). A source capable of generating these compositions must be present at relatively shallow depths.

The lateral distribution of the sources in the transition zone is reflected in the spatial distribution of basalts with the characteristic trace-element patterns. The presence of a mica

melanephelinite-like source beneath the entire transition zone and the adjacent Colorado Plateau is indicated by trace-element patterns for alkali basalts from the Awapa, Sevier, and Markagunt Plateaus, and Capitol Reef. The lack of alkali basalts in the eastern Basin and Range province precludes the recognition of this source there. A melanephelinite-like source is located, with certainty, only beneath the Sevier Plateau, as indicated by the trace-element pattern of a single alkali basalt. The minette-like source is located beneath the Markagunt Plateau and the adjacent Basin and Range province, as indicated by the trace-element patterns of alkali basalts and tholeiites.

A cross section of the proposed mantle sources beneath the transition zone and the adjacent provinces can be constructed from the depth and spatial information (fig. 12). The cross section represents the known locations of the sources. The nature of the mantle in areas that have not produced basalts, the shallow mantle beneath the eastern transition zone and the deeper mantle beneath the Basin and Range province, remains unknown; the presence of specific sources, that is, minette at shallow levels in the eastern transition zone or mica melanephelinite at deeper levels beneath the Basin and Range province, cannot be excluded. The cross section serves as a model for source regions in the transition zone to be tested in extreme southern Utah and northern Arizona.

TECTONIC SIGNIFICANCE

In contrast with geophysical data (Thompson and Zoback, 1979), which suggest that the asthenosphere is near the base of the crust, the isotopic and trace-element compositions of basalts from the Utah transition zone argue for preservation of lithospheric mantle. The low Nd isotopic compositions of the basalts from the Utah transition zone require a light rare-earth element enrichment event early in the history of the source of these magmas and subsequent long-term isolation from convecting mantle, most likely in the lithospheric mantle. Evolution from lithospheric to asthenospheric sources has been detected elsewhere by a shift in isotopic compositions (Perry and others, 1987; Ormerod and others, 1988; Farmer and others, 1990). The constancy of the isotopic composition of alkali basalts erupted from 16 to 0.5 Ma demonstrates that the asthenosphere has not physically replaced the lithosphere beneath the Utah transition zone.

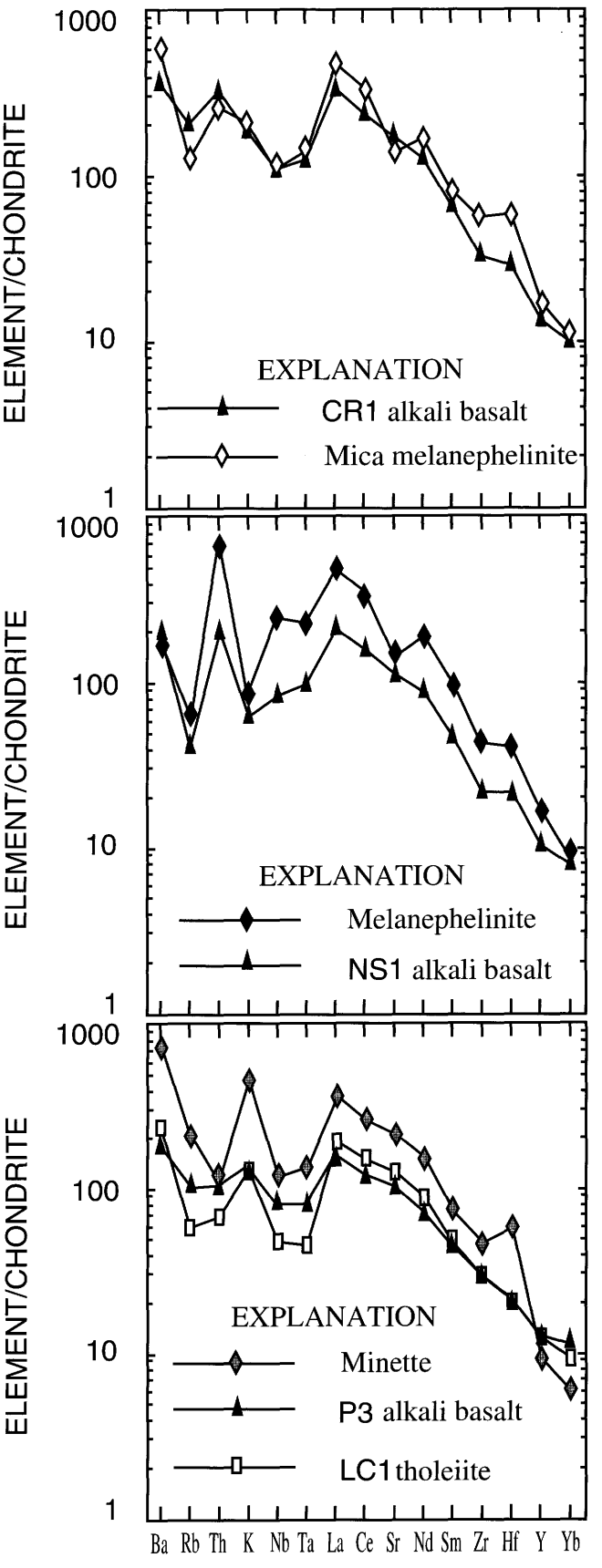

Figure 11. Comparison of trace-element patterns for basalts from Utah transition zone to mica melanephelinite, melanephelinite, and minette dikes of Tingey and others (1991).

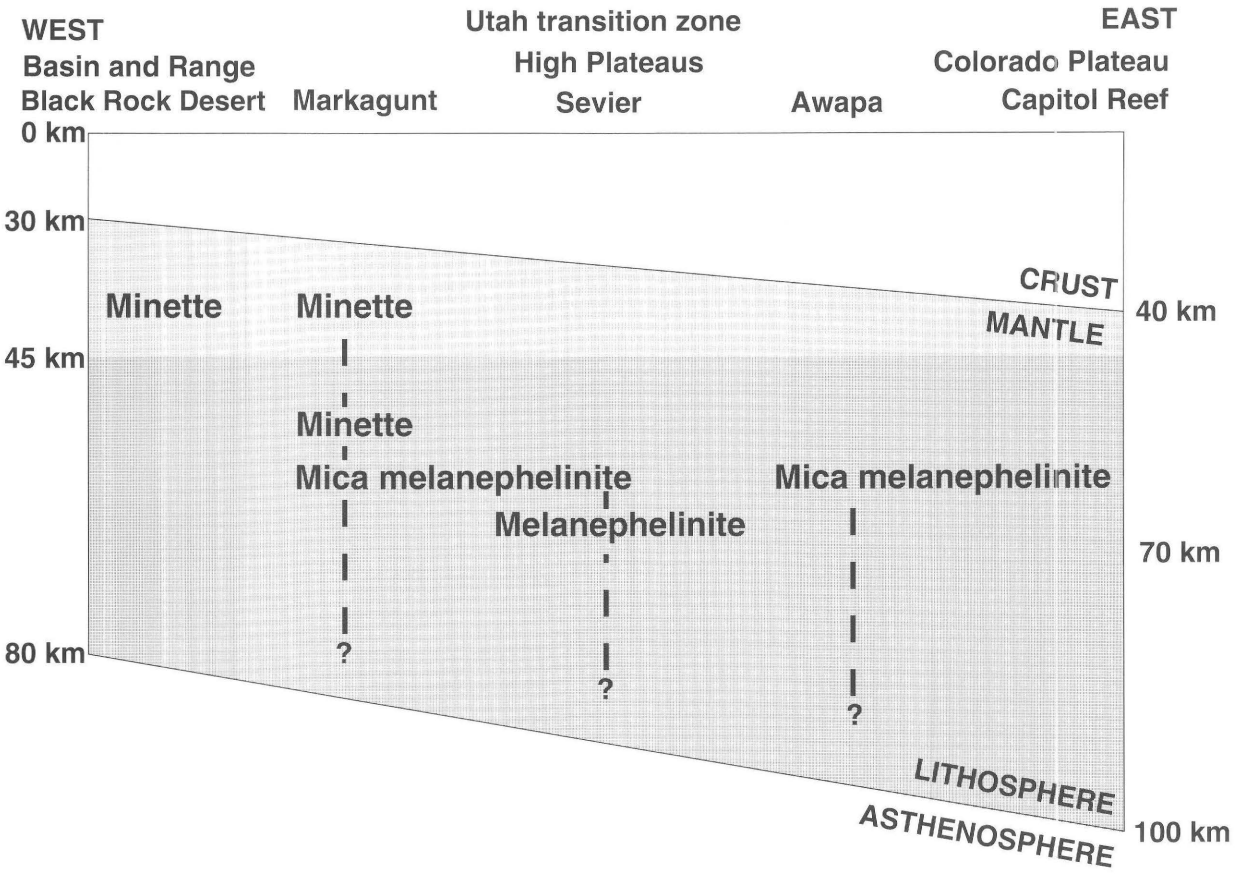

Figure 12. Schematic cross section of the distribution of three trace-element-distinct magma sources beneath Utah transition zone. Theoretical and experimental studies suggest that tholeiites are generated at depths shallower than roughly 45 km. Alkali basalts originate from greater depths. Question marks indicate that exact depth of lithospheric sources is unknown.

The simple structural history of the transition zone, relative to the Basin and Range province, also argues for preservation of the lithosphere. Rowley and others (1979) noted that faults are less abundant in the transition zone and that structural displacement on faults decreases across the transition zone from west to east. Immediately west of the transition zone, the structural history is more complex and includes a west-dipping detachment surface and listric faults (Nielson and others, 1986; Planke and Smith, 1991).

The amount of crustal extension in the Utah transition zone does not support thinning and replacement of the lithosphere. Daley and DePaolo (1992) related the stretching factor ß (where ß = extended length of crust/original length of crust) to the thickness of the lithosphere. In southern Nevada, where isotopic data support replacement of lithosphere by asthenosphere, ß ranges from 2 to 4 (Daley and DePaolo, 1992). In the Utah transition zone, ß is approximately 1.2, based on a summation of the horizontal displacement across faults. ß is approximately 2 for Cenozoic extension along the detachment surface just west of the transition zone (estimated from data in Planke and Smith, 1991). Therefore, the geochemical data of this study are inconsistent with geophysical models that place the asthenosphere in contact with the crust immediately west of the Utah transition zone along the eastern margin of the Basin and Range province.

The tectonic model of Perry and others (1987) may resolve the discordance of the geochemical and geophysical data. Perry and others proposed that mantle lithosphere could be thermally converted to asthenosphere, yet retain the geochemical properties of the lithosphere. Ultimately, the "hot" lithosphere is physically replaced by convecting asthenosphere. The change in magmatic source is reflected in a shift in basalt isotopic composition. The composition of basalts in the Utah transition zone indicate that, although the source may be asthenospheric in physical character, magmas are derived from a source in the lithospheric mantle.

CONCLUSIONS

The distribution of rock types and the composition of the lavas in the Utah transition zone are largely controlled by degree and depth of partial melting. Lower degrees of partial melting at greater depths generate alkali basalts in the eastern transition zone and adjacent Colorado Plateau. Higher degrees of partial melting at shallower depth generate tholeiitic basalts in the western transition zone and the adjacent Basin and Range province. The basalts inherited three distinct trace-element patterns from sources derived from mantle veined by mafic alkaline dikes or from higher degrees of partial melting of the sources for the mafic alkaline dikes. The relationship between the rock types and mafic alkaline dikes indicates that the mantle in the transition zone is layered and that a mica melanephelinite-like source is most common. The Nd isotopic composition of the basalts indicates a source in the lithospheric mantle and long-term stability of the transition zone.

REFERENCES CITED

Alibert, Chantal, Michard, Anne, and Albarede, Francis, 1986, Isotope and trace element geochemistry of Colorado Plateau volcanics: Geochimica et Cosmochimica Acta, v. 50, p. 2735–2750.

Allegre, C.J., and Minister, J.F., 1978, Quantitative models of trace element behaviour in magmatic processes: Earth and Planetary Science Letters, v. 38, p. 1–25.

Allmendinger, R.W., Hauge, T.A., Hauser, E.C., Potter, C.J., Klemperer, S.L., Nelson, K.D., Kneupfer, P.K.L., and Oliver, Jack, 1987, Overview of the COCORP 40°N transect, western United States—The fabric of an orogenic belt: Geological Society of America Bulletin, v. 98, p. 308–319.

Anderson, J.J., 1986, Geologic map of the Circleville Mountain quadrangle, Beaver, Piute, Iron, and Garfield Counties, Utah: Utah Geological and Mineral Survey Map 80, scale 1:24,000.

Baedecker, P.A., and McKown, D.M., 1987, Instrumental neutron activation analysis of geochemical samples, *in* Baedecker, P.A., ed., Methods of geochemical analysis: U.S. Geological Survey Bulletin 1770, p. H1–H14.

Basaltic Volcanism Special Project, 1981, Basaltic volcanism on the terrestrial planets: New York, Pergamon, 1,286 p.

Best, M.G., and Brimhall, H., 1974, Late Cenozoic alkalic basaltic magmas in the western Colorado Plateaus and the Basin and Range transition zone, U.S.A., and their bearing on mantle dynamics: Geological Society of America Bulletin, v. 85, p. 1677–1690.

Best, M.G., and Hamblin, W.K., 1978, Origin of the northern Basin and Range province—Implications from the geology of its eastern boundary, *in* Smith, R.B., and Eaton, G.P., eds., Cenozoic tectonics and geophysics of the western Cordillera: Geological Society of America Memoir 152, p. 313–340.

Best, M.G., McKee, E.H., and Damon, P.E., 1980, Space-time-composition patterns of late Cenozoic mafic volcanism, southwestern Utah and adjoining areas: American Journal of Science, v. 280, p. 1035–1050.

Carr, M.J., Feigenson, M.D., and Bennett, E.A., 1990, Incompatible element and isotopic evidence for tectonic control of source mixing and melt extraction along the Central American arc: Contributions to Mineralogy and Petrology, v. 105, p. 369–380.

Coleman, D.S., and Walker, J.D., 1992, Evidence for generation of juvenile granitic crust during continental extension, Mineral Mountains batholith, Utah: Journal of Geophysical Research, v. 97, p. 11011–11024.

Condit, C.D., Crumpler, L.S., Aubele, J.C., and Elston, W.E., 1989, Patterns of volcanism along the southern margin of the Colorado Plateau—The Springerville field: Journal of Geophysical Research, v. 94, p. 7975–7986.

Cunningham, C.G., Steven, T.A., Rowley, P.D., Hedge, C.E., Mehnert, H.H., and Naeser, C.W., 1991, Geochemical evolution of volcanic rocks associated with ore deposits in the Marysvale volcanic field, Utah: Geological Society of America Abstracts with Programs, v. 23, p. 14.

Cunningham, C.G., and Steven, T.A., 1979, Mount Belknap and Red Hills calderas and associated rocks, Marysvale volcanic field, west-central Utah: U.S. Geological Survey Bulletin 1468, 34 p.

Cunningham, C.G., Steven, T.A., Rowley, P.D., Glassgold, L.B., and Anderson, J.J., 1983, Geologic map of the Tushar Mountains and adjoining areas, Marysvale volcanic field, Utah: U.S. Geological Survey Miscellaneous Investigations Series Map I–1430–A, scale 1:50,000.

Daley, E.E., and DePaolo, D.J., 1992, Isotopic evidence for lithospheric thinning during extension—Southeastern Great Basin: Geology, v. 20, p. 104–108.

DePaolo, D.J., 1979, Estimation of the depth of origin of basic magmas—A modified thermodynamic approach and a comparison with experimental melting studies: Contributions to Mineralogy and Petrology, v. 69, p. 265–278.

———1981, Trace element and isotopic effects of combined wallrock assimilation and fractional crystallization: Earth and Planetary Science Letters, v. 53, p. 189–202.

Dutton, C.E., 1880, Report on the geology of the High Plateaus of Utah with atlas: U.S. Geographical and Geological Survey, Rocky Mountain Region (Powell), 307 p.

Eaton, G.P., Wahl, R.R., Prostka, H.J., Mabey, D.R., and Kleinkopf, M.D., 1987, Regional gravity and tectonic patterns—Their relation to late Cenozoic epeirogeny and lateral spreading of the western Cordillera, *in* Smith, R.B., and Eaton, G.P., eds., Cenozoic tectonics and geophysics of the western Cordillera: Geological Society of America Memoir 152, p. 409–440.

Ehrenberg, S.N., 1982, Rare earth element geochemistry of garnet lherzolite and megacrystalline nodules from minette of the Colorado Plateaus province: Earth and Planetary Science Letters, v. 57, p. 191–210.

Ellam, R.M., 1992, Lithospheric thickness as a control on basalt geochemistry: Geology, v. 20, p. 153–156.

Everson, J.E., 1979, Regional variations in the lead isotopic characteristics of late Cenozoic basalts from the southwestern United States: Pasadena, Calif., California Institute of Technology Ph. D. dissertation, 454 p.

Farmer, G.L., Perry, F.V., Semken, Steve, Crowe, B., Curtis, D., and DePaolo, D.J., 1990, Isotopic evidence on the structure and

origin of subcontinental lithospheric mantle in southern Nevada: Journal of Geophysical Research, v. 94, p. 7885–7898.

Fitton, J.G., James, D., Kempton, P.D., Ormerod, D.S., and Leeman, W.P., 1988, The role of lithospheric mantle in the generation of late Cenozoic basic magmas in the western United States: Journal of Petrology, Special Lithosphere Issue, p. 331-349.

Fitton, J.G., James, Dodie, and Leeman, W.P., 1991, Basic magmatism associated with late Cenozoic extension in the western United States—Compositional variations in space and time: Journal of Geophysical Research, v. 96, p. 13693–13711.

Fleck, R.J., Anderson, J.J., and Rowley, P.D., 1975, Chronology of mid-Tertiary volcanism in High Plateaus region of Utah, *in* Anderson, J.J., Rowley, P.D., Fleck, R.J. and Nairn, A.E.M., eds., Cenozoic geology of southwestern High Plateaus of Utah: Geological Society of America Special Paper 160, p. 53–62.

Frey, F.A., Green, D.H., and Roy, S.D., 1978, Integrated models of basalt petrogenesis, a study of quartz tholeiites to olivine melilitites from southeastern Australia utilizing geochemical and experimental data: Journal of Petrology, v. 19, p. 463–513.

Frey, F.A., and Prinz, Martin, 1978, Ultramafic inclusions from San Carlos, Arizona—Petrologic and geochemical data bearing on their petrogenesis: Earth and Planetary Science Letters, v. 38, p. 129-176.

Gartner, A.E, 1985, Geometry and emplacement history of a basaltic intrusive complex, San Rafael Swell and Capitol Reef areas, Utah: San Jose, Calif., San Jose State University M.S. thesis, 132 p.

Gartner, A.E., and Delaney, P.T., 1988, Geologic map showing a Late Cenozoic basaltic intrusive complex, Emery, Sevier, and Wayne Counties, Utah: U.S. Geological Survey Miscellaneous Field Studies Map MF–2052, scale 1:48,000.

Henderson, Paul, 1982, Inorganic geochemistry: New York, Pergamon, 353 p.

Irvine, T.N., and Baragar, W.R., 1971, A guide to the chemical classification of the common igneous rocks: Canadian Journal of Earth Science, v. 8, p. 523–548.

Jaques, A.L., and Green, D.H., 1980, Anhydrous melting of peridotite at 0–15 Kb pressure and the genesis of tholeiitic basalts: Contributions to Mineralogy and Petrology, v. 73, p. 287–310.

Kay, S.H., Maksaev, V., Moscoso, R., Mpodozis, C., Nasi, C., and Gordillo, C.E., 1988, Tertiary Andean magmatism in Chile and Argentina between 28°S and 33°S: Correlation of magmatic chemistry with a changing Benioff zone: Journal of South American Earth Sciences, v. 1, p. 21–28.

Kempton, P.D., Fitton, J.G., Hawkesworth, C.J., and Ormerod, D.S., 1991, Isotopic and trace element constraints on the composition and evolution of the lithosphere beneath the southwestern United States: Journal of Geophysical Research, v. 96, p. 13713–13735.

Kesson, S.E., 1973, The primary geochemistry of the Monaro alkaline volcanics, southeastern Australia—Evidence for upper mantle heterogeneity: Contributions to Mineralogy and Petrology, v. 42, p. 93–108.

Kushiro, I., 1968, Compositions of magma formed by partial zone melting of the Earth's upper melting: Journal of Geophysical Research, v. 73, p. 619–634.

Le Bas, M.J., Le Maitre, R.W., Streckeisen, Albert, and Zanettin, Bruno, 1986, A chemical classification of volcanic rocks based on the total alkali-silica diagram: Journal of Petrology, v. 27, p. 745–750.

Leeman, W.P., 1970, The isotopic composition of strontium in late Cenozoic basalts from the Basin-Range province, western United States: Geochimica et Cosmochimica Acta, v. 34, p. 857–872.

Lowder, G.G., 1970, Studies in volcanic petrology—I, Talasea, New Guinea; II, Southwest Utah: Berkeley, Calif., University of California Ph. D. dissertation, 194 p.

———1973, Late Cenozoic transitional alkali olivine-tholeiitic basalt and andesite from the margin of the Great Basin, southwest Utah: Geological Society of America Bulletin, v. 84, p. 2993–3012.

Lum, C.C.L., Leeman, W.P., Foland, K.A., Kargel, J.A., and Fitton, J.G., 1989, Isotopic variations in continental basaltic lavas as indicators of mantle heterogeneity—Examples from the western U.S. Cordillera: Journal of Geophysical Research, v. 94, p. 7871–7884.

Mackin, J.H., 1960, Structural significance of Tertiary volcanic rocks in southwestern Utah: American Journal of Science, v. 258, p. 81–131.

Mattox, S.R., 1991a, Origin of potassium-rich mafic lava flows, Marysvale volcanic field, Utah [abs.]: Eos, v. 72, p. 561.

———1991b, Petrology, age, geochemistry, and correlation of the Tertiary volcanic rocks of the Awapa Plateau, Piute, Wayne, and Garfield Counties, Utah: Utah Geological and Mineral Survey Miscellaneous Publication 91-5, 46 p.

———1992a, Geochemistry, origin, and tectonic implications of the mid-Tertiary and late Tertiary and Quaternary volcanic rocks southern Marysvale volcanic field, Utah: DeKalb, Ill., Northern Illinois University Ph. D. dissertation, 498 p.

———1992b, Source and process control of the geochemical variation in late Cenozoic basalts across the Utah transition zone [abs.]: Eos, v. 73, p. 657.

Mattox, S.R., and Walker, J.A., 1990, Late Cenozoic lavas of the Utah transition zone: Geological Society of America Abstracts with Programs, v. 22, p. 65.

Nakamura, N., 1974, Determination of REE, Ba, Fe, Mg, Na, and K in carbonaceous and ordinary chondrites: Geochimica et Cosmochimica Acta, v. 38, p. 757–775.

Nealey, L.D., and Sheridan, M.F., 1989, Post-Laramide rocks of Arizona and northern Sonora, Mexico, and their inclusions, *in* Jenney, J.P., and Reynolds, S.J., eds., Geologic evolution of Arizona: Tucson, Ariz., Arizona Geological Society Digest 17, p. 609–647.

Nelson, S.T., 1989, Geologic map of the Geyser Peak quadrangle, Wayne and Sevier Counties, Utah: Utah Geological and Mineral Survey Map 114, scale 1:24,000.

Nielson, D.L., Evans, S.H., and Sibbett, B.S., 1986, Magmatic, structural, and hydrothermal evolution of the Mineral Mountains intrusive complex, Utah: Geological Society of America Bulletin, v. 97, p. 765–777.

Ormerod, D.S., Hawkesworth, C.J., Rogers, N.W., Leeman, W.P., and Menzies, M.A., 1988, Tectonic and magmatic transitions in the western Great Basin, USA: Nature, v. 333, p. 349–353.

Perry, F.V., Baldridge, W.S., and DePaolo, D.J., 1987, Role of the asthenosphere and lithosphere in the genesis of late Cenozoic basaltic rocks from the Rio Grande Rift and adjacent regions of the southwestern United States: Journal of Geophysical Research, v. 92, p. 9193–9213.

Planke, S., and Smith, R.B., 1991, Cenozoic extension and evolution of the Sevier Desert basin, Utah, from seismic reflection, gravity, and well log data: Tectonics, v. 10, p. 345–365.

Presnall, D.C., Dixon, S.A., Dixon, J.R., O'Donnell, T.H., Brenner, N.L., Schrock, R.L., and Dycus, D.W., 1978, Liquidus phase relations on the join diopside-forsterite-anorthite from 1 atm to 20 kbar—Their bearing on the generation and crystallization of basaltic magma: Contributions to Mineralogy and Petrology, v. 66, p. 203–220.

Rowley, P.D., Anderson, J.J., Williams, P.L., and Fleck, R.J., 1978, Age of structural differentiation between the Colorado Plateau and Basin and Range provinces in southwestern Utah: Geology, v. 6, p. 51–55.

Rowley, P.D., Steven, T.A., Anderson, J.J., and Cunningham, C.G., 1979, Cenozoic stratigraphic and structural framework of southwestern Utah: U.S. Geological Survey Professional Paper 1149, 22 p.

Rowley, P.D., Steven, T.A., and Mehnert, H.H., 1981, Origin and structural implications of upper Miocene rhyolite in Kingston Canyon, Piute County, Utah: Geological Society of America Bulletin, v. 92, pt. 1, p. 590–602.

Steiger, R.H., and Jäger, Emile, 1977, Subcommission on geochronology—Convention on use of decay constants in geo- and cosmochemistry: Earth and Planetary Science Letters, v. 36, p. 359–362.

Steven, T.A., Morris, H.T., and Rowley, P.D., 1990, Geologic map of the Richfield 1°×2°quadrangle, west central Utah: U.S. Geological Survey Miscellaneous Investigations Series Map I–1901, scale 1:250,000.

Takahashi, E., 1980, Melting relations of an alkali-olivine basalt to 30 kbar and their bearing on the origin of alkali basaltic magmas: Carnegie Institution of Washington Year Book 79, p. 271–276.

Takahashi, E., and Kushiro, I., 1983, Melting of dry peridotite at high pressures and basalt magma genesis: American Mineralogist, v. 68, p. 859–879.

Tanaka, K.L., Shoemaker, E.M., Ulrich, G.E., and Wolfe, E.W., 1986, Migration of volcanism in the San Francisco volcanic field, Arizona: Geological Society of America Bulletin, v. 97, p. 129–141.

Thompson, G.A., and Zoback, M.L., 1979, Regional geophysics of the Colorado Plateau: Tectonophysics, v. 61, p. 149–181.

Thompson, R.N., Morrison, M.A., Hendry, G.L., and Parry, S.J., 1984, An assessment of the relative roles of crust and mantle in magma genesis—An elemental approach: Philosophical Transactions of the Royal Society of London, v. 310, p. 549–590.

Tingey, D.G., Christiansen, E.H., Best, M.G., Ruiz, J., and Lux, D.R., 1991, Tertiary minette and melanephelinite dikes, Wasatch Plateau, Utah—Records of mantle heterogeneities and changing tectonics: Journal of Geophysical Research, v. 91, p. 13529–13544.

Vollmer, R., Ogden, Palmer, Schilling, J.G., Kingsley, R.H., and Waggoner, D.H., 1984, Nd and Sr isotopes in ultrapotassic volcanic rocks from the Leucite Hills, Wyoming: Contributions to Mineralogy and Petrology, v. 87, p. 359–368.

Wender, L.E., 1976, Chemical and mineralogical evolution of the Cenozoic volcanics of the Marysvale, Utah area: Salt Lake City, Utah, University of Utah M.S. thesis, 57 p.

Wender, L.E., and Nash, W.P., 1979, Petrology of Oligocene and early Miocene calc-alkaline volcanism in the Marysvale area, Utah: Geological Society of America Bulletin, pt. II, v. 90, p. 34–76.

White, W.M., and Hofmann, A.W., 1982, Sr and Nd isotope geochemistry of oceanic basalts and mantle evolution: Nature, v. 296, p. 821–825.

Wilshire, H.G., Meyer, C.E., Nakata, J.K., Calk, L.C., Shervais, J.W., Nielson, J.E., and Schwarzman, E.C., 1988, Mafic and ultramafic xenoliths from volcanic rocks of the western United States: U.S. Geological Survey Professional Paper 1433, 177 p.

Wittke, J.H., Smith, D., and Wooden, J.L., 1989, Origin of Sr, Nd, and Pb isotopic systematics in high-Sr basalts from central Arizona: Contributions to Mineralogy and Petrology, v. 101, p. 57–68.

The Role of Lithosphere and Asthenosphere in the Genesis of Late Cenozoic Volcanism at Diamond Valley and Veyo Volcano, Southwestern Utah

By Robert L. Nusbaum, Daniel M. Unruh, *and* V.E. Millings, III

GEOLOGIC STUDIES IN THE BASIN AND RANGE–COLORADO PLATEAU TRANSITION IN SOUTHEASTERN NEVADA, SOUTHWESTERN UTAH, AND NORTHWESTERN ARIZONA, 1995

U.S. GEOLOGICAL SURVEY BULLETIN 2153–K

UNITED STATES GOVERNMENT PRINTING OFFICE, WASHINGTON : 1997

CONTENTS

FIGURES

TABLES

The Role of Lithosphere and Asthenosphere in the Genesis of Late Cenozoic Volcanism at Diamond Valley and Veyo Volcano, Southwestern Utah

By Robert L. Nusbaum,[1] Daniel M. Unruh, *and* V.E. Millings, III[1]

ABSTRACT

As part of the U.S. Geological Survey Basin and Range–Colorado Plateau (BARCO) Study Unit, elemental and isotopic compositions were determined for upper Cenozoic basaltic rocks from the Basin and Range–Colorado Plateau transition zone of southwestern Utah. We studied four volcanic units: two which erupted from Veyo Volcano (<0.5 Ma), the Diamond Valley cinder cones, and the Santa Clara flow (≈1 ka). Veyo units exhibit low ε_{Nd} (–8) and $^{206}Pb/^{204}Pb$ (17.5–17.6), but moderately high $^{87}Sr/^{86}Sr$ (0.7052) compared to Diamond Valley–Santa Clara samples (ε_{Nd} = –3.8, $^{206}Pb/^{204}Pb$=18.0–18.3, $^{87}Sr/^{86}Sr$=0.7044). Veyo samples also have higher SiO_2 contents (54–55 percent), LILE abundances, and LILE/HFSE than Diamond Valley–Santa Clara samples. This evidence and the presence of quartz xenocrysts in some Veyo lavas lead us to conclude that the chemical and isotopic characteristics of these samples reflect significant crustal interaction, either by derivation of their parental magmas at the crust-mantle interface or through assimilation-fractional crystallization processes within the lower crust.

The most isotopically enriched volcanic rocks from the Markagunt Plateau also have elevated silica contents (to 58 percent SiO_2), similar low ε_{Nd} and $^{206}Pb/^{204}Pb$, but lower $^{87}Sr/^{86}Sr$, Δ7/4, and Δ8/4 values than Veyo samples. We interpret these data to indicate that the crustal end-members in the two areas were isotopically distinct.

Although the Diamond Valley–Santa Clara samples have a more depleted isotopic signature than Veyo lavas, and have much higher HFSE/LILE abundances (Zr/Ba ≈0.4), their isotopic signature is still more enriched than that normally ascribed to a pure asthenospheric (OIB) source. We suggest that the chemical and isotopic characteristics of these basalts were derived primarily from the lithospheric mantle. Relationships between ε_{Nd}-values and ages for basalts from the St. George area as a whole suggest that lithospheric involvement in the generation of these samples has been increasing over the last ≈4 m.y. The results are consistent with progressive heating of the lithosphere by repeated injection of asthenospheric magmas, and may imply that the rates of extension and volcanism are both currently increasing in the St. George basin.

INTRODUCTION

One of the main objectives of a study of continental basalts is to identify the chemical and physical characteristics of their source regions. In this report, we present chemical and Pb, Sr, and Nd isotopic data for upper Cenozoic volcanic rocks erupted at Diamond Valley and Veyo Volcano, southwestern Utah (fig. 1). These rocks were erupted within the Basin and Range–Colorado Plateau transition zone and provide an opportunity to compare the relationships between magmatism and tectonism in the transition zone with those on the adjacent Colorado Plateau. This type of study is particularly important in the St. George basin because of the rapid population growth in the area, the presence of very young volcanic rocks, and the incidence of significant historic earthquakes. A magnitude 5.5–5.9 earthquake centered approximately 8 km southwest of St. George was recorded in September 1992 (Pearthree and Wallace, 1992). This study is part of the U.S. Geological Survey Basin and Range–Colorado Plateau (BARCO) Study Unit.

The St. George basin lies at the southwest end of an approximately 50 km wide, northeast-trending band of late Tertiary-Quaternary (≈4–0 Ma; Best and others, 1980) basaltic volcanism. This band is bounded on the west by the Gunlock fault and on the east by the Toroweap-Sevier fault, two down-to-the-west high-angle normal faults (Blank and Kucks, 1989). These faults are thought to represent the nominal Basin and Range–transition zone, and transition zone–Colorado Plateau boundaries, respectively. These two faults strike approximately north-south in northwestern Arizona and southwesternmost Utah, but strike northeast-southwest just north of the band of basaltic rocks. The band is bisected by a third similar fault, the Hurricane fault (Blank and Kucks, 1989).

[1]Department of Geology, College of Charleston, Charleston, SC 29424.

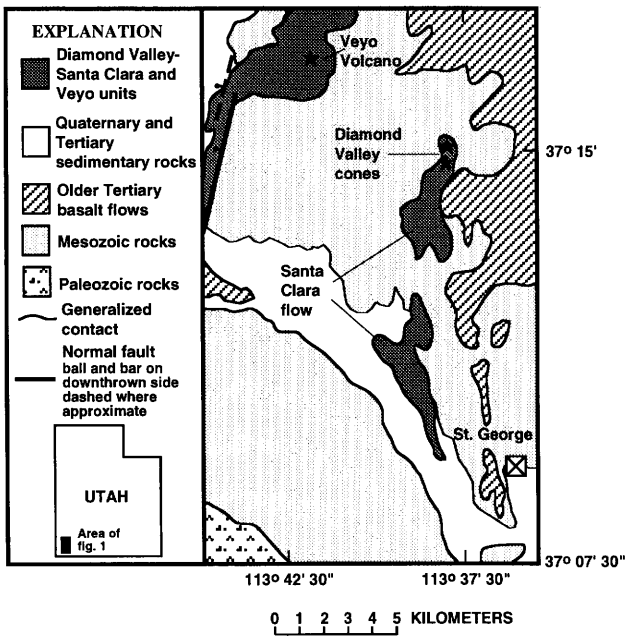

Figure 1. Location map with geology modified from Blank and Kucks (1989). Exact sample locations provided by Unruh and others (in press). Stars represent locations of the Veyo Volcano and Diamond Valley cinder cones.

Older basaltic volcanism (12–6 Ma) occurred only a few kilometers northwest of the Veyo Volcano, but northwest of the Gunlock fault 4–7 Ma basalts are found south of the study area between the Gunlock and Toroweap-Sevier faults and west of the Gunlock fault (Best and others, 1980). Oligocene-Miocene mafic and silicic volcanic rocks are found northwest of the study area, and lower Miocene intermediate to silicic intrusive rocks border the band of basaltic volcanism north of the St. George basin (Blank and Kucks, 1989).

Very little previous work has been conducted on the rocks discussed herein. Hamblin (1987) provided a brief description of the Santa Clara flow and cinder cones in Diamond Valley. The presence of "aa" crust on the upper flow surfaces and the lack of vegetation on the Diamond Valley cinder cones indicate that the units are ≈1,000 years old. Thus, these rocks are among the youngest volcanic features in the southwestern United States and are similar in age to flows associated with Sunset Crater, San Francisco volcanic field near Flagstaff, Ariz. (Hamblin, 1987).

A greater age for the Veyo lava and cinder cone is evident from the lack of "aa" crust and the degree of vegetation on the slopes of the cinder cone. Hamblin (1987) estimated the age of the Veyo units to be less than 0.5 Ma. Consequently, the study of these volcanic units presents an opportunity to study the evolution of the magma source(s) over the last 0.5 m.y., as well as the relationships between magma sources and the chemical composition of the erupted products.

ACKNOWLEDGMENTS

L. David Nealey provided assistance with Sr, Nd, and Pb isotopic analysis and provided geochemical data for samples NSG92 38 and NSG 42. Electron microprobe funding was provided by the Southern Regional Education Board Small Grants Program. Major- and trace-element analysis was supported by a grant from the Department of Geology research fund at the College of Charleston. J. David Green assisted with field work. Mitchell Colgan reviewed an early version of the manuscript. Technical reviews by K. Futa and W.R. Premo and comments by editors L.D. Nealey and Florian Maldonado were also greatly appreciated.

SAMPLES

Seventeen samples were collected for whole-rock major- and trace-element analyses, and 9 were selected for Sr, Nd, and Pb isotopic analyses. Units are informally divided into the following: the Santa Clara flow unit; the Diamond Valley unit, which includes the two cinder cones at Diamond Valley; the Veyo cone unit; and the Veyo lava unit. Field relations indicate that the Veyo lava unit was erupted from Veyo Volcano. The relationship between the Santa Clara flow and Diamond Valley units is less certain; however, the source of the Santa Clara flow is near the north Diamond Valley cone (Hamblin, 1987).

Veyo samples are petrographically distinct from Diamond Valley and Santa Clara. The latter are basaltic and contain only olivine phenocrysts, whereas Veyo samples have plagioclase, olivine, augite, and rare orthopyroxene phenocrysts. Many of the plagioclase phenocrysts are reverse-zoned (An65–An75) and exhibit sieve textures. Quartz xenocrysts were found in some samples of the Veyo lava unit near the cone.

ANALYTICAL PROCEDURES

Whole-rock analyses shown in table 1 were conducted using inductively coupled plasma atomic emission spectrometry (ICP-AES) for major elements and Ba, Rb, Sr, Nb, Zr, and Y. The FeO content was determined using acid decomposition coupled with titration. Samples with K_2O less than 1.5 wt. percent were analyzed by atomic absorption. Analytical errors using ICP-AES are ±5 percent for major elements and ±10 percent for trace elements. Major- and trace-element data for two samples, NSG 9238 and NSG 42, were obtained by XRF (INAA for Ba).

Strontium, Nd, and Pb isotopic ratios were determined at the U.S. Geological Survey using the procedures described by Unruh and others (in press). Powdered samples were dissolved in a mixture of HF and HNO_3 at 70°–90°C in

screw-cap PFA teflon bombs. Lead was separated using anion exchange in 1.2N HBr medium. Strontium and rare-earth elements (REE) were separated by cation exchange in 2.5 and 6.0N HCl. Neodymium was separated from other REE by cation exchange using 0.2M n-methyllactic acid.

Lead and Sr isotopic measurements were performed using a Sector-54, 7-collector mass spectrometer using single Re and oxidized Ta filaments, respectively. Lead isotopic ratios were corrected for mass fractionation of 0.14±0.03 percent per mass based on analyses of NBS Pb standard SRM-982 run at 1,280°–1,400°C. Sr isotopic data were normalized to $^{86}Sr/^{88}Sr=0.1194$. The mean measured $^{87}Sr/^{86}Sr$ value for NBS Sr standard SRM-987 during the course of this study was 0.710258±0.000008 ($2\sigma_m$; 14 analyses).

Neodymium isotopic analyses were made with an Isomass 54R, single-collector mass spectrometer using triple filaments (Re center, Ta sides). Fourteen analyses of the La Jolla Nd standard yielded a mean value of 0.511855±0.000007 ($2\sigma_m$). Single-run precision for Sr and Nd analyses is 0.003–0.004 percent. Uncertainties for Pb isotopic data are essentially those induced by the mass-fractionation corrections.

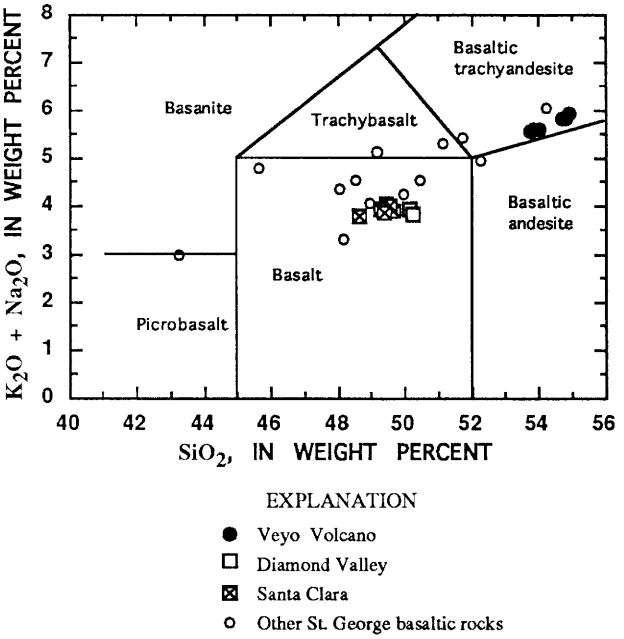

Figure 2. Total-alkali-silica classification (Le Maître and others, 1989) of samples from St. George basin. Data are from table 1 and L.D. Nealey (written commun., 1994).

GEOCHEMISTRY

MAJOR ELEMENTS

Two distinct groups are defined by major-element data for the units (fig. 2; table 1). Diamond Valley and Santa Clara units are basalt on a total alkalies vs. silica (TAS) diagram (LeMaître and others, 1989). Samples of Diamond Valley units, which erupted prior to the Santa Clara flow, have slightly lower Mg# and slightly higher silica than the Santa Clara flow unit. Alkali contents in these samples are slightly lower than in most other basalts from this general area (fig. 2).

Veyo samples are basaltic trachyandesite with lower MgO and CaO contents and slightly lower Mg#, but higher SiO_2, Al_2O_3, P_2O_5, and alkali contents than Diamond Valley and Santa Clara units (fig. 2; table 1). No major-element distinction can be made between Veyo cone samples and the Veyo lava unit. Concentrations of TiO_2 are nearly identical for all units.

TRACE ELEMENTS

Samples of Veyo units also exhibit distinctly different trace element characteristics from those of Diamond Valley and Santa Clara flow samples (table 1). The more evolved Veyo units are strongly enriched in the LIL (large-ion lithophile) elements Rb, Sr, Ba relative to Diamond Valley and Santa Clara units. High field strength elements (HFSE) Zr and Nb are also somewhat enriched in the Veyo units, but not to the extent of the LIL elements. As a result, the ratios of LILE to HFSE are significantly higher for Veyo samples than for Diamond Valley and Santa Clara samples. Diamond Valley and Santa Clara samples have virtually identical trace-element contents, and Y contents are indistinguishable among all units.

ISOTOPIC DATA

Nine samples were analyzed for Pb, Sr, and Nd isotopic compositions: five from Veyo crater, one from the Veyo lava, one from the north cone at Diamond Valley, and two from the Santa Clara flow. One of the Santa Clara samples (92ND6) is from the northern part of the flow; the other (NSG9238) is from the distal end. Measured $^{87}Sr/^{86}Sr$ ratios of samples (table 2) range from 0.70438 to 0.70524. Veyo samples have higher and more uniform values (0.70521 to 0.70524) than Diamond Valley and Santa Clara samples (0.70438 to 0.70454).

Measured $^{143}Nd/^{144}Nd$ values range from 0.51222 to 0.51246 for the nine samples, with ε_{Nd} ranging from –3.7 to –8.1. Samples of the Santa Clara flow and Diamond Valley have identical and higher epsilon values of –3.7 to –3.8. Neodymium isotopic compositions of Veyo samples are distinctly less radiogenic than those of Diamond Valley and Santa Clara with ε_{Nd} =–7.5 to –8.1. The Nd isotopic compositions of Veyo cone and lava samples cannot be distinguished from one another within analytical uncertainty.

Table 1. Major- and trace-element geochemistry of Veyo Volcano, Santa Clara, and Diamond Valley rocks.

[Samples analyzed by ICP-AES except for NSG9238 and NSG42, which were analyzed at the U.S. Geological Survey by XRF (analysts J.S. Mee and D.F. Siems). Barium contents for these two samples were determined by INAA (J. Budahn, analyst). DV, Diamond Valley cinder cones; SCL, Santa Clara lava; VC, Veyo Volcano cinder cone; VL, Veyo lava. Oxides in weight percent, trace-element contents in ppm; leaders (--), not determined]

	92NDC1	92NDC2	92ND6	92ND7	92N1	92N2	92N3	92N4	NSG9238	92VT1	92VT12	92VT14
SiO_2	49.91	49.63	49.15	47.84	48.23	48.07	47.9	48.19	49.5	54.99	54.46	51.91
TiO_2	1.63	1.61	1.59	1.58	1.51	1.48	1.54	1.51	1.49	1.44	1.45	1.66
Al_2O_3	15.89	15.79	15.63	15.67	15.22	14.9	15.15	15.01	15.3	16.93	16.99	17.06
Fe_2O_3	3.64	2.77	2.26	2.37	2.20	2.42	2.96	5.57	13.1	2.71	2.76	3.04
FeO	7.94	8.72	9.42	9.47	9.25	8.88	8.74	6.35	–	4.84	4.77	5.95
MnO	0.17	0.17	0.17	0.17	0.17	0.17	0.17	0.17	0.18	0.13	0.13	0.16
MgO	7.19	7.2	8.27	8.29	7.76	8.07	7.97	8.05	8.3	4.46	4.29	5.56
CaO	8.80	8.86	8.56	8.8	8.59	8.56	8.54	8.55	8.63	6.78	7.57	7.78
Na_2O	3.17	3.16	3.42	3.17	3.26	2.99	3.24	3.2	3.22	3.98	3.9	3.99
K_2O	0.60	0.65	0.57	0.53	0.51	0.86	0.55	0.54	0.57	2.33	2.31	1.77
P_2O_5	0.30	0.30	0.29	0.29	0.28	0.31	0.27	0.27	0.26	0.64	0.65	0.94
Total	99.25	98.87	99.34	98.19	96.99	96.87	97.04	97.42	100.55	99.32	100.30	99.95
LOI	0.01	0.01	0.01	0.01	0.01	0.16	0.01	0.01	0.01	0.09	1.10	0.13
Mg#	55.5	55.0	57.6	57.4	56.5	58.0	57.2	59.1	–	54.7	53.9	55.7
Ba	210	210	200	250	240	250	260	240	269	1220	1200	1570
Rb	<5	<5	<5	<5	6	5	<5	<5	<10	32	27	11
Sr	290	280	280	290	310	310	320	320	320	740	740	920
Nb	20	20	20	10	10	15	15	15	23	35	35	50
Zr	110	100	100	100	–	–	90	90	120	90	90	280
Y	30	30	30	20	–	–	10	10	27	10	10	20
Zr/Ba	0.52	0.48	0.50	0.40	–	–	0.35	0.38	0.45	0.07	0.08	0.18
Ba/Nb	10	11	10	25	24	17	17	16	12	35	34	31
K_2O/TiO_2	0.4	0.4	0.4	0.3	0.3	0.6	0.4	0.4	0.4	1.6	1.6	1.1
Unit[2]	DV	DV	SCL	SCL	SCL	SCL	SCL	SCL	SCL	VC	VL	VL

Measured $^{206}Pb/^{204}Pb$ isotope ratios vary from 17.52 to 18.27; Veyo units exhibit lower ratios (17.52–17.66) than Diamond Valley and Santa Clara samples (17.98–18.27). Lead isotopic compositions of both suites are within the general range of values observed among basalts of this area (fig. 3). The $^{207}Pb/^{204}Pb$ and $^{208}Pb/^{204}Pb$ ratios are highly correlated with $^{206}Pb/^{204}Pb$ (fig. 3) and range from 15.48 to 15.57 and 37.66 to 38.19, respectively. Also shown in table 2 are Δ7/4 and Δ8/4 values. These values, as defined by Hart (1984), represent differences (×100) in $^{207}Pb/^{204}Pb$ and $^{208}Pb/^{204}Pb$ between the sample and average northern-hemisphere ocean island basalts (OIB) with the same $^{206}Pb/^{204}Pb$ (NHRL line in fig. 3). All units have similar Δ7/4 (9–10), but Veyo samples have somewhat higher Δ8/4 (76–92) than Diamond Valley and Santa Clara samples (47–74).

DISCUSSION

Based on field, age, and chemical relationships previously outlined, it is evident that both the Veyo lava and cinder cone may be discussed as a single unit and that the Diamond Valley cinder cones and Santa Clara lava may also be considered to represent a single unit (simply the Diamond Valley unit, hereafter). Consequently, the data will be discussed in terms of two distinct groups in the ensuing discussion.

CONSERVED ELEMENT RATIOS

The K, Ti, and P data from table 1 are plotted as conserved element ratios (elemental ratios that are not affected by fractionation of mafic silicate phases or plagioclase; Pearce, 1968) in figure 4 to test whether the Veyo units were cogenetic with the Diamond Valley unit. Two features of the data are readily apparent: (1) the two units form trends that are distinctly displaced from one another, and (2) the trends exhibited by the data from the two units appear to converge at low Ti/K and P/K. The first of these observations indicates that the two units are not related to one another simply by fractionation of olivine, pyroxene, and (or) plagioclase. Furthermore, the fact that the data for each group form distinct trends rather than tight clusters suggests that some mechanism in addition to olivine-orthopyroxene-plagioclase fractionation was involved.

The second observation suggests that the trends exhibited by each group may reflect contamination from a source, such as Tertiary silicic intrusive rocks of the Pine Valley laccolith (also shown in fig. 4; from Coleman and Walker, 1992), with low Ti/K and P/K. Therefore, the simplest interpretation of these data is that the two units were derived from different sources (or from the same source but under different physiochemical conditions), but share a common crustal contaminant. However, we note that the use of this diagram

Table 1. Major- and trace-element geochemistry of Veyo Volcano, Santa Clara, and Diamond Valley rocks.—*Continued*

92VT20	92VT21	92VT22	92VT23	92VT24	NSG42
54.09	55.46	53.88	55.51	53.93	54.8
1.65	1.49	1.65	1.54	1.63	1.42
17.37	17.49	17.61	17.61	17.49	17.2
4.13	2.86	4.17	2.84	4.03	8.27
4.37	4.76	4.15	4.94	4.29	--
0.14	0.13	0.13	0.13	0.13	0.13
4.53	4.69	4.38	4.54	4.49	4.48
7.38	6.81	7.43	7.04	7.65	6.98
3.82	4.11	3.89	4.10	3.89	3.67
1.76	1.91	1.69	1.84	1.69	2.10
0.61	0.61	0.60	0.65	0.59	0.62
99.93	100.70	99.09	101.1	100.2	99.67
0.08	0.46	0.40	0.37	0.41	0.03
53.5	55.9	53.3	54.49	53.78	--
940	1010	950	1010	1040	1230
21	22	16	22	16	34
680	690	700	690	730	780
40	40	40	40	50	34
250	250	240	260	240	315
30	30	30	30	30	29
0.27	0.25	0.25	0.26	0.23	0.26
24	25	24	25	21	36
1.1	1.3	1.0	1.2	1.0	1.5
VL	VC	VC	VC	VC	VL

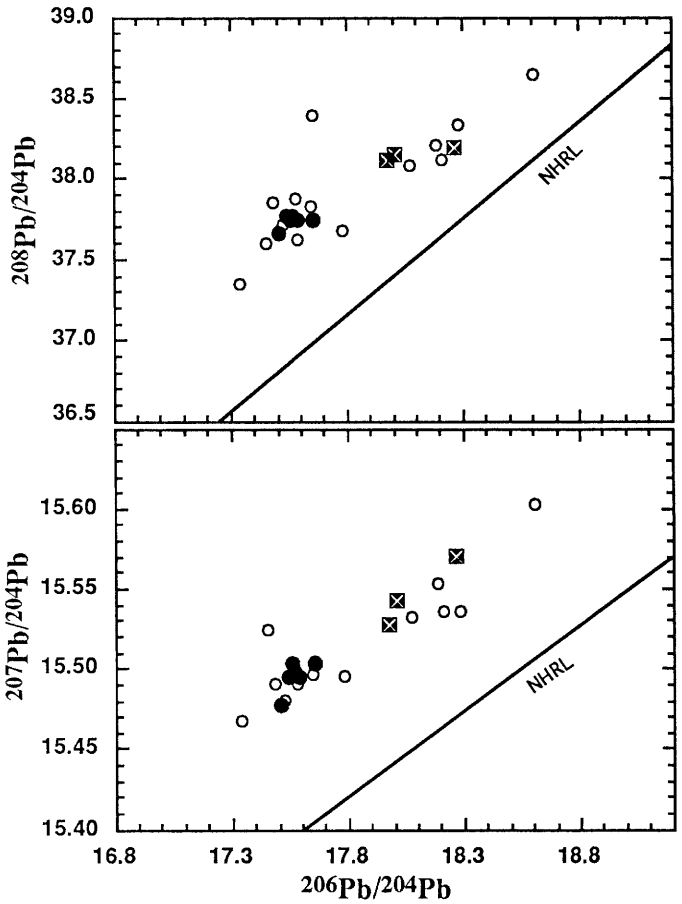

Figure 3. Lead isotopic compositions of Veyo and Diamond Valley–Santa Clara samples. Solid dot, Veyo; crossed square, Diamond Valley–Santa Clara. Also shown (open circles) are data for other basaltic rocks from St. George basin (Unruh and others, in press).

to determine whether or not the two groups share a common source is not valid if one or both magmas were in equilibrium with phases in which Ti, K, and P are not incompatible, such as Fe-Ti oxides or apatite, for example. Furthermore, contamination of the parental magmas at different stages in their evolution can also cause the apparent differences in the two trends observed in figure 4.

TRACE-ELEMENT CONSTRAINTS ON MAGMA SOURCES

Trace-element plots, based on average values for Veyo units and Diamond Valley units (fig. 5), have been constructed in order to further investigate possible relationships between the Veyo and Diamond Valley units. The average data have been both internally normalized and normalized to two other scales, average oceanic island basalt (OIB) and average post-5 Ma transition zone basalt (Fitton and others, 1991), in order to determine possible relationships of these units with potential magma sources as well as with one another.

The trace-element abundance ratios of Veyo to Diamond Valley samples are summarized in figure 5*A*. Veyo samples are enriched relative to Diamond Valley samples by factors of 4–5 in the highly incompatible elements Rb and Ba, and by factors of 2–3 in moderately incompatible elements K, Nb, Sr, P, and Zr; but they show no relative enrichment in Ti and Y. The rather smooth pattern exhibited by the data suggests that the Veyo lavas could have been derived from a source similar to that which produced the Diamond Valley lavas. However, this scenario would require the presence of residual or fractionating clinopyroxene and Fe-Ti oxide phases (Pearce and Norry, 1979) in order to account for the pronounced lack of enrichment of Ti and Y in Veyo samples.

Diamond Valley–Santa Clara units exhibit a relatively flat, OIB-type pattern with depleted Rb and a slight negative Nb anomaly (fig. 5*B*). Fitton and others (1991) concluded that the generally flat patterns, like that of the Diamond Valley–Santa Clara units (fig. 5*B*), are indicative of an asthenospheric mantle source, although the small negative Nb anomaly suggests the presence of a lithospheric component in the source region of these samples.

The Veyo samples have more pronounced negative Nb and TiO_2 anomalies, with enriched Ba and K_2O when compared to mean OIB (fig. 5*B*). Fitton and others (1991)

Table 2. Pb, Sr, and Nd isotopic data for Diamond Valley–Santa Clara and Veyo samples.

[Uncertainties correspond to last significant figures and are $2\sigma_m$. Δ7/4 and Δ8/4 are defined by Hart (1984; the NHRL lines in fig. 3) and represent the absolute differences (×100) between the measured $^{207}Pb/^{204}Pb$ and $^{208}Pb/^{204}Pb$ and average OIB with the same $^{206}Pb/^{204}Pb$]

Sample	$^{206}Pb/^{204}Pb$	$^{207}Pb/^{204}Pb$	$^{208}Pb/^{204}Pb$	Δ7/4	Δ8/4	$^{87}Sr/^{86}Sr$	$^{143}Nd/^{144}Nd$	εNd
Diamond V.								
92NDC2	18.274 ± 11	15.570 ± 14	38.192 ± 46	9.8	47.2	0.704543 ± 22	0.512443 ± 14	-3.8
Santa Clara								
92ND6	17.981 ± 22	15.527 ± 22	38.105 ± 62	8.7	73.9	0.704407 ± 21	0.512445 ± 10	-3.7
NSG 9238	18.020 ± 11	15.542 ± 14	38.146 ± 46	9.8	73.3	0.704384 ± 23	0.512439 ± 15	-3.8
Veyo								
92VT20	17.548 ± 12	15.494 ± 15	37.763 ± 47	10.0	92.0	0.705244 ± 33	0.512231 ± 15	-7.9
92VT21	17.567 ± 11	15.502 ± 15	37.743 ± 45	10.7	87.7	0.705240 ± 23	0.512230 ± 14	-7.9
92VT22	17.662 ± 11	15.502 ± 14	37.738 ± 46	9.6	75.7	0.705206 ± 32	0.512249 ± 13	-7.5
92VT23	17.595 ± 12	15.495 ± 15	37.739 ± 47	9.7	84.0	0.705145 ± 21	0.512246 ± 10	-7.6
92VT24	17.575 ± 12	15.498 ± 15	37.763 ± 47	10.2	88.8	0.705200 ± 25	0.512226 ± 22	-8.0
NSG 42	17.515 ± 13	15.477 ± 15	37.662 ± 48	8.7	85.7	0.705211 ± 25	0.512223 ± 16	-8.1

recognized similar patterns in the post-5 Ma transition zone samples they studied, and argued that crustal assimilation sufficient to elevate Ba/Nb would leave the final product too silicic to be basalt. They proposed an explanation involving enrichment of the lithospheric mantle by subduction-derived fluids, depleted in Nb (for example, pelagic sediment). Although this interpretation could be true for Veyo samples, crustal contamination cannot be ruled out as the cause of the elevated Ba/Nb because Veyo rocks are basaltic trachyandesite, rather than basalt.

Diamond Valley–Santa Clara samples are depleted in incompatible elements, particularly in Rb and Ba, relative to average transition zone basaltic rocks (fig. 5*C*). The Ba depletion relative to high field strength elements (Nb, Zr, Y) suggests that these rocks were derived from a source more similar to those for OIB than for other transition zone basalts. The Zr/Ba for Diamond Valley–Santa Clara units ranges from 0.3 to 0.5 (table 1), and this range represents the highest values yet found in the St. George area (L.D. Nealey and J.R. Budahn, written commun., 1994). Ormerod and others (1988; and see Kempton and others, 1991) proposed that Zr/Ba ratios in excess of ≈0.4 are typical of lavas with an asthenospheric source. This is consistent with K_2O/TiO_2 and Ba/Nb ratios, which are within the range of Hawaiian lavas (Clague and Dalrymple, 1988; Chen and others, 1991).

The trace-element data for Diamond Valley samples are generally consistent with commonly accepted models for basaltic volcanism in the western United States. A common feature of these models is that a lithospheric source for the magmas gives way through time to an asthenospheric source either as a result of thinning of the lithosphere during extension (for example, Perry and others, 1987; Daley and DePaolo, 1992), or depletion of the low-melting components in the lithosphere by previous melt extraction (Fitton and others, 1991). Diamond Valley samples represent one of the youngest episodes of basaltic volcanism in the entire transition zone, and one might therefore expect these magmas to have trace-element abundances similar to OIB.

Veyo samples, normalized to the mean transition zone basalt (fig. 5*C*), show a uniform horizontal trend with a slight negative Sr anomaly and slight depletion in Ti and Y relative to other elements. If one assumes that these samples were derived from a parental magma with trace-element characteristics identical to average transition zone basalts, then the Sr anomaly may reflect plagioclase fractionation and the lowered Ti and Y abundances may reflect fractionation of clinopyroxene and Fe-Ti oxides.

Ormerod and others (1988) suggested that lithospheric mantle is characterized by Zr/Ba of about 0.2 or less. Veyo samples have Zr/Ba ≤0.27 (table 1); thus the predominant source of the trace-element characteristics of the Veyo lavas appears to have been the lithosphere. The parental magma to the Veyo samples was almost certainly generated within the asthenosphere, but it may have interacted extensively with

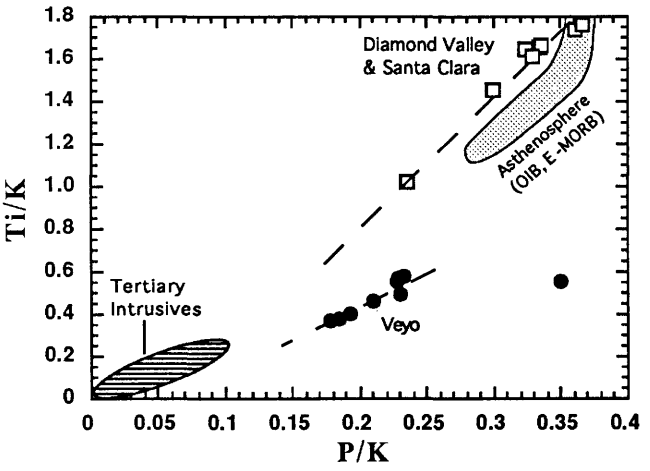

Figure 4. Pearce conserved element ratio diagram for mean Veyo units and mean Diamond Valley–Santa Clara flow units. Shown for reference are fields for OIB and E-MORB (Fitton and others, 1991), and for Tertiary intrusive rocks in southwestern Utah (Coleman and Walker, 1992).

overlying lithospheric mantle to the extent that the magma adopted the trace-element characteristics of the lithospheric mantle. The presence of quartz xenocrysts in some Veyo samples, coupled with the apparent contamination trend observed in figure 4, suggests that crustal interaction also contributed to the chemical characteristics of the Veyo lavas. Conceivably, the lithospheric trace-element signature of the Veyo samples is entirely due to crustal interaction with asthenosphere-derived magmas.

ISOTOPIC DATA AND MAGMA SOURCES

Earlier reports on the Sr isotopic composition of upper Cenozoic volcanic rocks of southwestern Utah include that of Lowder (1973) and Leeman (1982), which demonstrated that the mantle source regions were heterogeneous. The first Pb isotopic data for basaltic rocks in the St. George area were reported by Everson (1979). Kempton and others (1991) were the first to integrate Sr-Nd-Pb isotopic data in an attempt to assess lithosphere contributions to mafic magmatism (<17 Ma) in the southwestern U.S. Their study of the northern part of eastern transition zone (NETZ), which includes southwestern Utah, indicates the following: $^{87}Sr/^{86}Sr$ ranges from 0.7034 to 0.7061; $^{143}Nd/^{144}Nd$ from 0.5121 to 0.5130; and $^{206}Pb/^{204}Pb$ from 17.0 to 18.8. Our isotopic data (table 2) fall within these ranges.

Samples from both Diamond Valley and Veyo exhibit relatively low ε_{Nd} values, high $^{87}Sr/^{86}Sr$, and low $^{206}Pb/^{204}Pb$ compared to basalts from the Great Basin that were apparently derived from uncontaminated asthenosphere ($\varepsilon_{Nd} \geq +4$, $^{87}Sr/^{86}Sr \leq 0.7038$, $^{206}Pb/^{204}Pb \geq 18.9$; Farmer and others, 1989). In addition, several samples from the St. George area (fig. 6) show higher ε_{Nd} and $^{206}Pb/^{204}Pb$ than Diamond Valley samples. Values of $^{206}Pb/^{204}Pb \leq 18.0$ are virtually unknown in OIB (see Hart, 1984 for a summary), but extremely common in Markagunt Plateau and St. George samples (Nealey and others, in press; Unruh and others, in press; also see Everson, 1979; Kempton and others, 1991). These observations in combination with trace-element data previously presented suggest that isotopic characteristics of most samples in this area, including both Veyo and Diamond Valley, were modified by lithospheric (crust or mantle) interaction (for example, Fitton and others, 1991; Kempton and others, 1991).

The Pb, Nd, and Sr isotopic compositions of Veyo and Diamond Valley samples, together with data for other samples from the St. George area (Unruh and others, in press), are summarized as functions of silica content in figure 6. The $^{206}Pb/^{204}Pb$ values show a good negatively correlated trend with silica content (fig. 6*A*). The most mafic samples have $^{206}Pb/^{204}Pb$ of 18.3–18.7, whereas the most silicic samples (including Veyo samples) have $^{206}Pb/^{204}Pb$=17.5–17.8. Diamond Valley samples have intermediate $^{206}Pb/^{204}Pb$ (18.0–18.3) and silica contents. The $\Delta 7/4$ and $\Delta 8/4$ values (not shown) for St. George samples as a group also increase with increasing silica content.

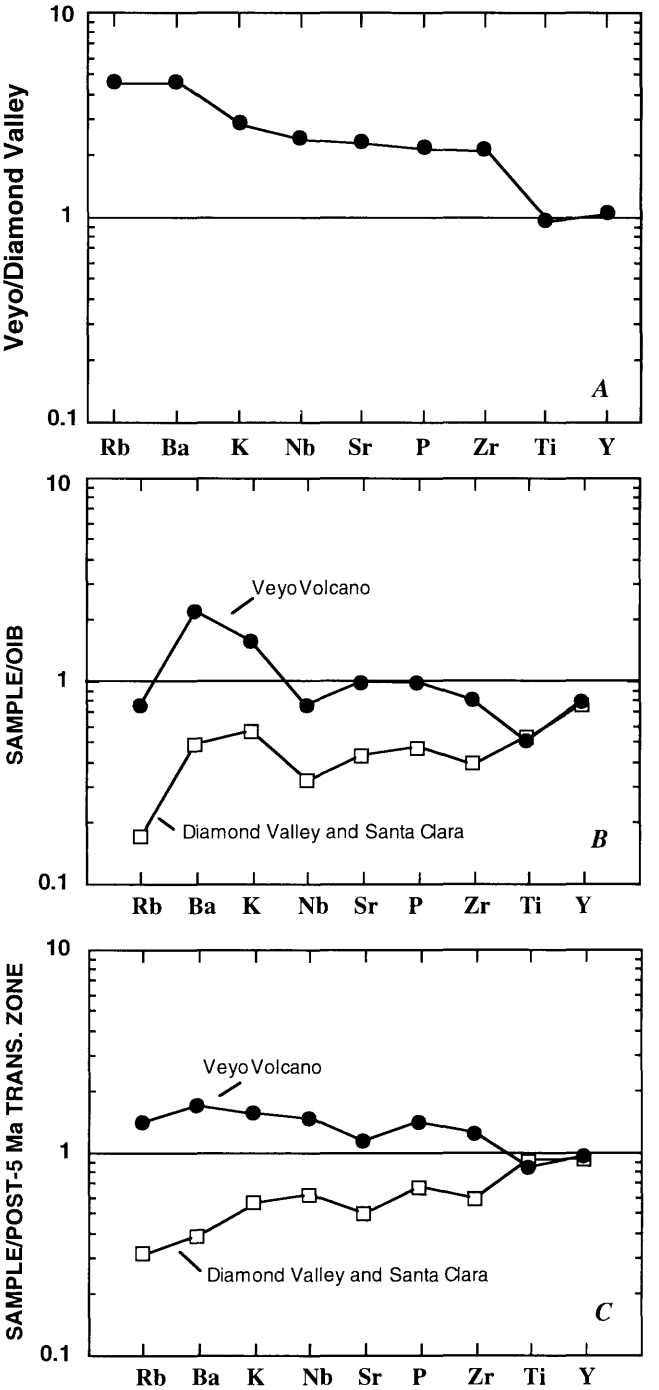

Figure 5. Incompatible element ratio plots. *A*, Internal normalization of Veyo data relative to those for Diamond Valley–Santa Clara samples. *B*, Incompatible elements normalized to mean values of 897 OIB samples. *C*, Incompatible elements normalized to mean values of 137 transition zone rocks <5 Ma. OIB and transition zone normalization from Fitton and others, 1991.

Neodymium isotopic ratios (expressed as ε_{Nd}; fig. 6*B*) show a more scattered but similar trend to the Pb data. The most mafic samples have $\varepsilon_{Nd} = 0$ to -2, whereas Veyo samples have the lowest ε_{Nd} of -7.5 to -8. Diamond Valley samples again have intermediate values ($\varepsilon_{Nd} = -3.8$). Samples

from the Markagunt Plateau (Nealey and others, in press) show trends similar to those of St. George samples in figures 6*A* and 6*B*, and extend the trends to values of $^{206}Pb/^{204}Pb \approx 17.0$ and $\varepsilon_{Nd} \approx -11$ at silica contents of 58–60 percent.

Strontium isotopic data (fig. 6*C*) show a rather poor correlation with silica. However, Veyo samples show among the highest $^{87}Sr/^{86}Sr=0.7052$, and the more mafic samples generally have $^{87}Sr/^{86}Sr < 0.705$. The $^{87}Sr/^{86}Sr$ of Diamond Valley samples is atypically low (0.7044–0.7045) for their silica content when compared to other samples from the area. Markagunt Plateau samples show even less correlation between $^{87}Sr/^{86}Sr$ and silica contents, but have generally lower $^{87}Sr/^{86}Sr$ (0.7038–0.7045) than St. George samples (Nealey and others, in press).

Good correlations between isotopic compositions and silica contents are generally taken as evidence for crustal contamination. If this is indeed the case, then the isotopic composition of the crustal contaminant can be approximated from Veyo samples, which are among the most silicic in this area and plot toward the presumed crustal end-member in figure 6. The contaminant must have $^{87}Sr/^{86}Sr \geq 0.7052$, $^{206}Pb/^{204}Pb \leq 17.55$, $\varepsilon_{Nd} \leq -8$, $\Delta 7/4 \geq +10$, and $\Delta 8/4 \geq +90$ (fig. 6 and table 1). The Pb isotopic characteristics of the apparent contaminant (low $^{206}Pb/^{204}Pb$ and high $\Delta 8/4$) more likely represent lower crust rather than upper crust (for example, Zartman, 1984). The results are consistent with either derivation of the parental magmas at the crust-mantle interface (Johnson, 1991) or assimilation-fractional crystallization processes within the lower crust.

Kempton and others (1991) have suggested that the enriched component in transition zone basalts as a whole more likely represents lithospheric mantle interaction than crustal contamination. Although this interpretation certainly appears valid in many instances, we prefer to interpret the Veyo data in terms of crustal contamination because of petrographic evidence for contamination previously presented, the elevated silica content in Veyo samples, and the correlations between isotopic data and silica content.

The isotopic compositions of the crustal end-member presented in the preceding discussion are both similar to and different from those determined for the isotopically enriched end-member in basaltic rocks from the Markagunt Plateau to the northeast (Nealey and others, in press). This component in Markagunt Plateau basalts is also most apparent in the most silicic samples and is also characterized by low $^{206}Pb/^{204}Pb$ (≤ 17.0) and ε_{Nd} (≤ -11). However, the enriched component in Markagunt Plateau basalts is also characterized by low $^{87}Sr/^{86}Sr$ (≤ 0.7040) and moderately low $\Delta 8/4$ ($\leq +50$).

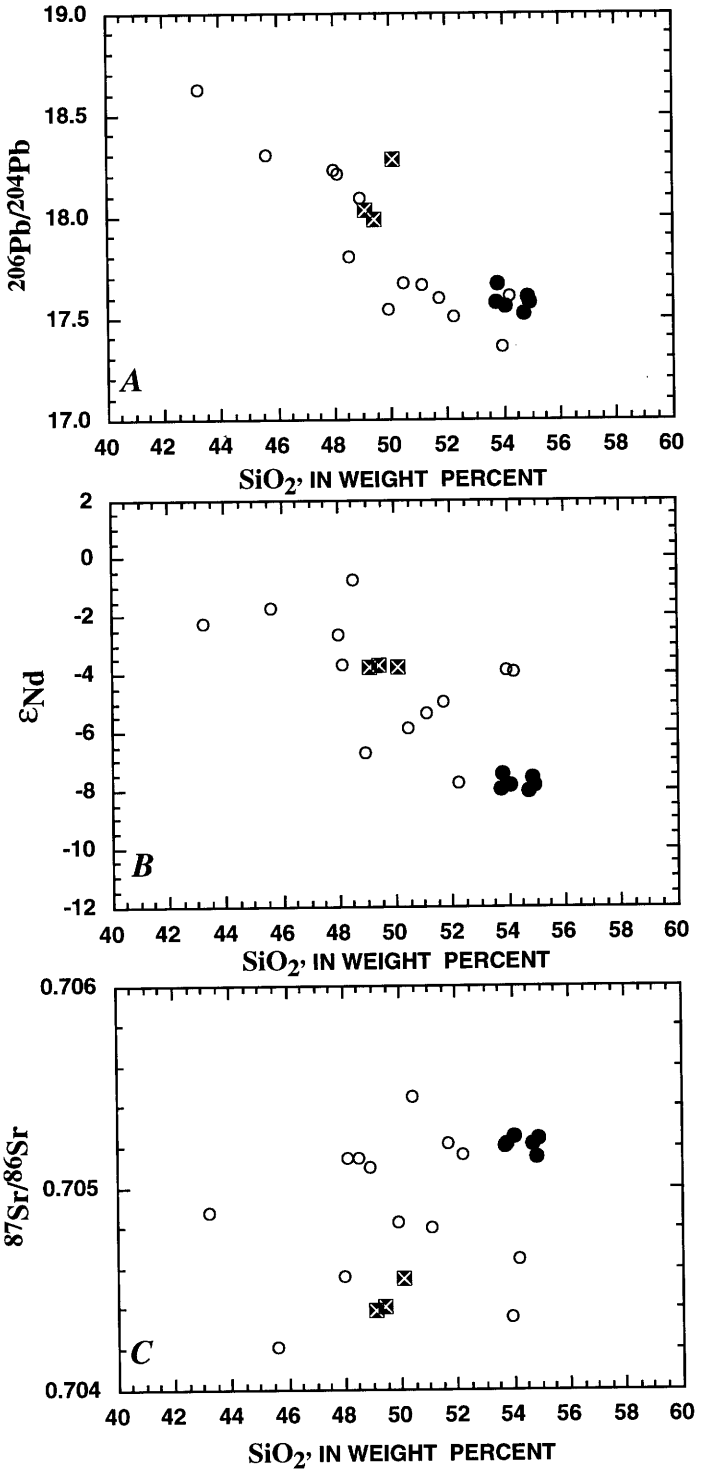

Figure 6. Plots of *A*, $^{206}Pb/^{204}Pb$; *B*, ε_{Nd}; *C*, $^{87}Sr/^{86}Sr$ as functions of silica content for samples from St. George area. Additional data for samples from St. George area are from Unruh and others (in press). Symbols used are the same as in figure 3: solid circle, Veyo; crossed square, Diamond Valley–Santa Clara; open circle, other St. George area basaltic rocks (Unruh and others, in press).

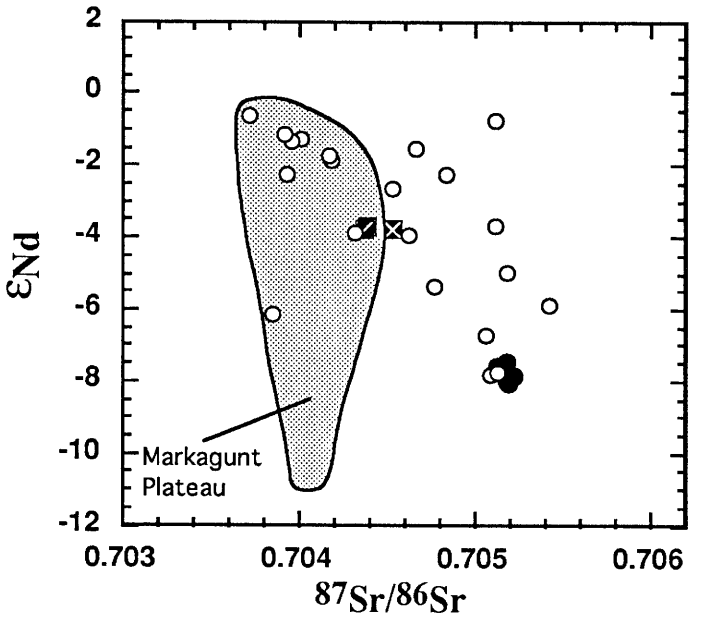

Figure 7. Plot of ε_{Nd} versus $^{87}Sr/^{86}Sr$ for Veyo and Diamond Valley samples. Solid circle, Veyo; crossed square, Diamond Valley–Santa Clara; open circle, other St. George area basaltic rocks (Unruh and others, in press). Data field for Markagunt Plateau samples from Nealey and others (in press).

The chemical and isotopic features of Diamond Valley samples are somewhat enigmatic. Major- and trace-element data for these samples (figs. 3 and 5 and preceding discussion) suggest an OIB-type source for these basalts, with perhaps a small lithospheric component (elevated Ba/Nb; fig. 5*B*). In contrast, the ε_{Nd} values (fig. 6*B*), suggest that there is a relatively large lithospheric component in these samples. The location of the Pb data above the OIB reference line (NHRL) in figure 3 also indicates a significant lithospheric component in these samples.

The isotopic data for St. George basalts as a group form a fairly well defined trend on an ε_{Nd} vs. $^{87}Sr/^{86}Sr$ diagram (fig. 7) that is consistent with mixing between depleted mantle with $^{87}Sr/^{86}Sr \leq 0.7037$ and $\varepsilon_{Nd} \geq 0$ and crust as most apparent in the Veyo data ($^{87}Sr/^{86}Sr \geq 0.7052$, $\varepsilon_{Nd} \leq -8$; the scatter in the trend, toward higher $^{87}Sr/^{86}Sr$, could be attributed to small amounts of upper crustal contamination with very high $^{87}Sr/^{86}Sr$). However, this interpretation for Diamond Valley samples is not consistent with the trace-element data. These samples have higher Zr/Ba and lower Rb and Ba abundances than any other samples (potential parental magmas) or potential contaminants thus far found within the St. George area (L.D. Nealey and J.R. Budahn, written commun., 1994).

Although contamination of asthenospheric magmas with LIL-depleted mafic crust (see Kempton and others, 1991 for a discussion of potential contaminants) cannot be entirely ruled out, we prefer the interpretation that the isotopic characteristics of Diamond Valley basalts were derived from the lithospheric mantle (or a mixed lithosphere-asthenosphere source). The isotopic characteristics of the Diamond Valley basalts are similar to those estimated for the lithospheric mantle in southeastern Nevada during Miocene time ($^{87}Sr/^{86}Sr \approx 0.704$–$0.705$, $\varepsilon_{Nd} \approx -4$ to -5; Scott and others, 1995; Unruh, unpub. data, 1994). This lithospheric source, or in any case the mixed source, was depleted in the typical "subduction-related" component (high Ba/Nb, for example; Fitton and others, 1991), perhaps as a result of prior melt extraction.

TECTONIC SIGNIFICANCE

The relationship between magmatism and tectonism in the southwestern United States is the subject of considerable debate and long-standing interest. In continental rifts such as the Rio Grande rift, there is a tendency for the youngest mafic magmas to have the highest proportion of asthenospheric mantle in their source regions as reflected in their ε_{Nd} values (Perry and others, 1987; Leat and others, 1988; Daley and DePaolo, 1992). The progressive increase in ε_{Nd} values from older to younger lavas observed in these studies has been interpreted to result from progressive replacement of low-ε_{Nd} lithospheric mantle with upwelling asthenospheric material.

During the early stages of extension, particularly in an "off-axis" location (assuming a pure-shear model; see fig. 1 of Farmer and others, 1989) such as is apparently the case in the St. George area, asthenospheric magmas are emplaced within the lithospheric mantle and an inhomogeneous mixture results. The chemical and isotopic characteristics of magmas derived from this mixed mantle are determined by local conditions of mixing and melting (Perry and others, 1987).

The isotopic data for samples from the St. George basin are consistent with expected results from an area in the early stages of extension-related volcanism. Although the Diamond Valley–Santa Clara basalts are the youngest in the basin and have asthenospheric trace-element signatures, the isotopic characteristics of these basalts exhibit a higher lithospheric-mantle component than many of the older basalts in the area. The apparent decoupling of elemental and isotopic data reflects complex mixing and melting processes that occur in a heterogeneous mantle source region.

Limited geochronologic data for samples analyzed for Nd isotopic compositions suggest that the data may follow a trend opposite to those seen in rift environments (fig. 8). Younger basalts in southwesternmost Utah and northernmost Arizona have lower ε_{Nd}, and therefore a more lithospheric source, than older basalts, at least within the last 4 m.y.

Although the apparent trend in figure 8 must be verified by much additional data, we are nonetheless tempted to speculate on its significance. The St. George basin apparently was volcanically inactive from early Miocene time (21 Ma) until about 3–4 Ma (Best and others, 1980). Mafic volcanic rocks of intermediate age (≈6–13 Ma; Best and others, 1980) are found immediately northwest and southwest of the St. George area, but only west of the Gunlock fault. Consequently, the oldest magmas (3–4 Ma) in the area were probably emplaced into relatively cold lithosphere. Those that reached the surface may have done so with minimal lithospheric interaction and may have retained their asthenospheric isotopic signature. As magmatism continued, the lithosphere was progressively heated and more efficiently interacted with the intruding magmas, and basalts with a mixed chemical and isotopic signature, such as the Diamond Valley-Santa Clara basalts, were produced. If this explanation is valid, then one might conclude that the flux of asthenospheric magma in the St. George area has been increasing over the last ≈4 m.y., and that the frequency of basaltic volcanism may also be increasing.

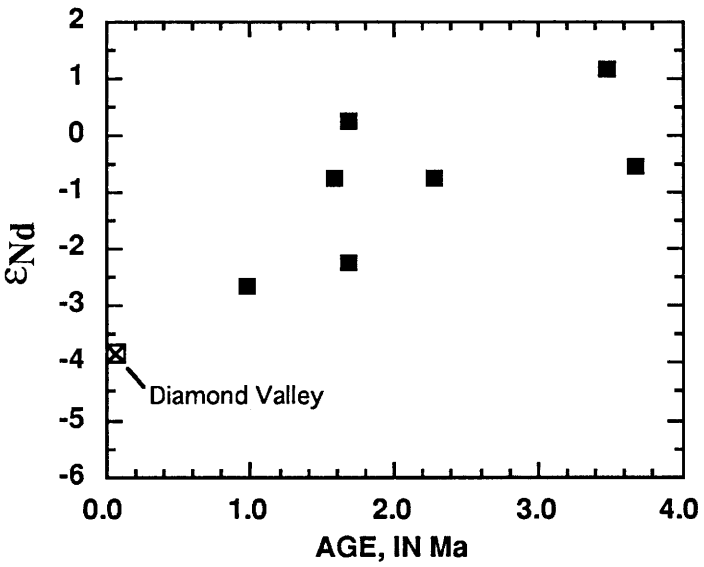

Figure 8. ε_{Nd} versus age for basalts from southwestern Utah and northernmost Arizona. Only those samples that are true basalts (<52 percent SiO_2) with little or no evidence of significant crustal contamination ($^{87}Sr/^{86}Sr \leq 0.7052$) are shown. Nd isotopic data are from this work, Unruh and others (in press), and Wenrich and others (in press). Ages are from Best and others (1980) and Wenrich and others (in press).

SUMMARY AND CONCLUSIONS

The ≈1,000 year old Diamond Valley–Santa Clara units and <0.5 Ma Veyo Volcano units can be distinguished from one another on the basis of mineralogy, major- and trace-element chemistry, and isotopic data. Diamond Valley–Santa Clara samples represent the youngest flows in the St. George area and have the lowest LILE/HFSE abundances. However, their isotopic signature suggests that these basalts were derived, at least in part, from the lithospheric mantle.

Veyo volcanics have lower ε_{Nd} (≈ –8), higher $^{87}Sr/^{86}Sr$ (≈0.7052), and lower $^{206}Pb/^{204}Pb$ (17.5–17.6) than Diamond Valley–Santa Clara samples ($\varepsilon_{Nd} \approx -3.7$, $^{87}Sr/^{86}Sr \approx 0.7044$, $^{206}Pb/^{204}Pb$=18.0–18.3). Veyo samples are also characterized by high silica content, higher LIL-element abundances, and higher LILE/HFSE abundance ratios. This evidence, as well as the presence of quartz xenocrysts in these samples, indicates that the chemical and isotopic characteristics of these magmas were derived in part from the crust, either by direct melting at the crust-mantle interface (Johnson, 1991), or by an assimilation-fractional crystallization process, or both.

When compared to the most isotopically enriched Markagunt Plateau volcanic rocks, the Veyo samples have similar low ε_{Nd} and $^{206}Pb/^{204}Pb$, but higher $^{87}Sr/^{86}Sr$, Δ7/4 and Δ8/4 values. We interpret these data as an indication that the crustal end-members in the two areas were isotopically distinct. The apparent low $^{206}Pb/^{204}Pb$ values and the lack of strongly elevated $^{87}Sr/^{86}Sr$ in the most silicic samples suggest that the contamination from the lower crust was more significant than that from "typical" upper crust.

Although based on an extremely limited data set, ε_{Nd}-age relationships for basalts ≤ 4 Ma in this area suggest that this area is in the initial stages of extension-related volcanism and that magmatism, and presumably volcanism, in the St. George area are both currently increasing.

REFERENCES CITED

Best, M.G., McKee, E.H., and Damon, P.E., 1980, Space-time-composition patterns of late Cenozoic mafic volcanism, southwestern Utah and adjoining areas: American Journal of Science, v. 280, p. 1035–1050.

Blank, H.R., and Kucks, R.P., 1989, Generalized geologic map of the USGS "BARCO" Project area, southwestern Utah, southeastern Nevada, and northwestern Arizona: U.S. Geological Survey Open-File Report 89-432, plate 3.

Chen, C.-Y., Frey, F.A., Garcia, M.O., Dalrymple, G.B., and Hart, S.R., 1991, The tholeiite to alkalic basalt transition at Haleakala Volcano, Maui, Hawaii: Contributions to Mineralogy and Petrology, v. 106, p. 183–200.

Clague, D.A., and Dalrymple, G.B., 1988, Age and petrology of alkalic post shield and rejuvenated-stage lava from Kauai, Hawaii: Contributions to Mineralogy and Petrology, v. 99, p. 202–218.

Coleman, D.S., and Walker, J.D., 1992, Evidence for the generation of juvenile granitic crust during continental extension, Mineral Mountains Batholith, Utah: Journal of Geophysical Research, v. 97, p. 11011–11024.

Daley, E.E., and DePaolo, D.J., 1992, Isotopic evidence for lithospheric thinning during extension—Southeastern Great Basin: Geology, v. 20, p. 104–108.

Everson, J.E., 1979, Regional variations in the lead isotopic characteristics of late Cenozoic basalts from the southwestern United States: Pasadena, Calif., California Institute of Technology Ph. D. dissertation, 454 p.

Farmer, G.L., Perry, F.V., Semken, S., Crowe, B., Curtis, D., and DePaolo, D.J., 1989, Isotopic evidence on the structure and origin of subcontinental lithosphere mantle in southern Nevada: Journal of Geophysical Research, v. 94, p. 7885–7898.

Fitton, J.G., James, D., and Leeman, W.P., 1991, Basic magmatism associated with late Cenozoic extension in the western United States—Compositional variations in space and time: Journal of Geophysical Research, v. 96, no. B8, p. 13693–13711.

Hamblin, W.K., 1987, Late Cenozoic volcanism in the St. George basin, Utah, *in* Geological Society of America Centennial Field Guide, Rocky Mountain Section: p. 291–294.

Hart, S.R., 1984, A large-scale isotope anomaly in the southern hemisphere mantle: Nature, v. 309, p. 753–757.

Johnson, C.M., 1991, Large-scale crust formation and lithosphere modification beneath middle to late Cenozoic calderas and volcanic fields, western North America: Journal of Geophysical Research, v. 96, p. 13485–13507.

Kempton, P.D., Fitton, J.G., Hawkesworth, C.J., and Ormerod, D.S., 1991, Isotopic and trace element constraints on the composition and evolution of the lithosphere beneath the southwestern United States: Journal of Geophysical Research, v. 96, p. 13713–13735.

Leat, P.T., Thompson, R.N., Morrison, M.A., Hendry, G.L., and Dickin, A.P., 1988, Compositionally-diverse Miocene-Recent rift-related magmatism in NW Colorado—Partial melting, and mixing of 3 different mantle sources: Journal of Petrology, Special Lithosphere Issue, p. 351–377.

Leeman, W.P., 1982, Tectonic and magmatic significance of strontium isotopic variations in Cenozoic volcanic rocks from the western United States: Geological Society of America Bulletin, v. 93, p. 487–503.

Le Maître, R.W., Bateman, P., Dudek, A., Keller, J., Lameyre, J., Le Bas, M.J., Sabine, P.A., Schmid, R., Sorensen, H. Streckeisen, A., Woodley, A.R., and Zanettin, B., 1989, A classification of igneous rocks and glossary of terms: Oxford, Blackwell, 193 p.

Lowder, G.G., 1973, Late Cenozoic transitional alkali olivine-tholeiitic basalt and andesite from the margin of the Great Basin, southwest Utah: Geological Society of America Bulletin, v. 84, p. 2993–3012.

Nealey, L.D., Unruh, D.M., and Maldonado, F., in press, Sr-Nd-Pb isotopic maps of the Panguitch 1:100,000 quadrangle: U.S. Geological Survey Open-File Report 93-691, scale 1:250,000.

Ormerod, D.S., Hawkesworth, C.J., Rogers, N.W., Leeman, W.P., and Menzies, M.A., 1988, Tectonic and magmatic transitions in the western Great Basin, USA: Nature, v. 333, p. 349–353.

Pearce, J.A. and Norry, M.J., 1979, Petrogenetic implications of Ti, Zr, Y, and Nb variations in volcanic rocks: Contributions to Mineralogy and Petrology, v. 69, p. 33–47.

Pearce, T.H., 1968, A contribution to the theory of variation diagrams: Contributions to Mineralogy and Petrology, v. 19, p. 142–157.

Pearthree, P.A., and Wallace, T.C., 1992, The St. George earthquake of September 2, 1992: Arizona Geology, v. 22, p. 7–8.

Perry, F.V., Baldridge, W.S., and DePaolo, D.J., 1987, Role of asthenosphere and lithosphere in genesis of late Cenozoic basaltic rocks from the Rio Grande rift and adjacent regions of the southwestern United States: Journal of Geophysical Research, v. 92, p. 9193–9213.

Scott, R.B., Unruh, D.M., Snee, L.W., Harding, A.E., Nealey, L.D., Blank, H.R., Budahn, J.R., and Mehnert, H.H., 1995, Relation of peralkaline magmatism to heterogeneous extension during middle Miocene, southeastern Nevada: Journal of Geophysical Research, v. 100, p. 10381–10401.

Unruh, D.M., Nealey, L.D., Maldonado, Florian, and Nusbaum, R.L., in press, Sr-Nd-Pb isotopic maps of late Cenozoic volcanic rocks of the St. George 30'×60' quadrangle, southwestern Utah: U.S. Geological Survey Open-File Report 94-11, scale 1:250,000, with accompanying text.

Wenrich, K.J., Billingsley, G.H., and Blackerby, B.A., in press, Spatial migration and composition changes of Miocene-Quaternary magmatism in the western Grand Canyon: Journal of Geophysical Research.

Zartman, R.E., 1984, Lead, strontium, and neodymium isotopic characterization of mineral deposits relative to their geologic environments: Proceedings of the 27th International Geologic Congress, v. 12, p. 83–106.

Potassium-Argon Ages of Tertiary Igneous Rocks in the Eastern Bull Valley Mountains and Pine Valley Mountains, Southwestern Utah

By Edwin H. McKee, H. Richard Blank, *and* Peter D. Rowley

GEOLOGIC STUDIES IN THE BASIN AND RANGE–COLORADO PLATEAU TRANSITION IN SOUTHEASTERN NEVADA, SOUTHWESTERN UTAH, AND NORTHWESTERN ARIZONA, 1995

U.S. GEOLOGICAL SURVEY BULLETIN 2153–L

UNITED STATES GOVERNMENT PRINTING OFFICE, WASHINGTON : 1997

CONTENTS

FIGURES

TABLE

Potassium-Argon Ages of Tertiary Igneous Rocks in the Eastern Bull Valley Mountains and Pine Valley Mountains, Southwestern Utah

By Edwin H. McKee, H. Richard Blank, *and* Peter D. Rowley

ABSTRACT

The eastern Bull Valley Mountains and Pine Valley Mountains of the Basin and Range province in southwestern Utah were the sites of extensive Tertiary volcanism and plutonism. The older (Oligocene and Miocene) exposed igneous rocks consist mostly of regional ash-flow sheets derived from sources outside the area. Most of the younger (Miocene and Pliocene) igneous rocks consist of locally derived ash-flow tuffs and lava flows that erupted from a major batholith complex, which underlies the eastern Bull Valley Mountains and Pine Valley Mountains and large areas to the north. At least a dozen discrete intrusions (cupolas) rose from the roof of the batholith, localized along a northeast-striking Sevier-age thrust fault zone. This northeast-trending line of intrusions is called the Iron Axis, so named because iron-ore deposits occur along the margins of those intrusions in the Iron Springs mining district north of the study area and in the Bull Valley mining district in the eastern Bull Valley Mountains. Fourteen K-Ar dates published herein constrain the ages of some of the igneous rocks, especially the younger, locally derived units. Isotopic ages were determined for three intrusions along the Iron Axis: 21.5 Ma for the Stoddard Mountain intrusion, 22.8 Ma for the Bull Valley intrusion, and 20.9 Ma for the Pine Valley laccolith. Two cooling units from the Rencher Formation, an ash-flow sheet derived from the Bull Valley intrusion, provided isotopic ages of 21.8 Ma (lower) and 21.5 Ma (upper). After consolidation of the batholith, local rhyolite and dacite volcanic domes erupted in the northern Bull Valley Mountains. Isotopic ages of these domes are 15.3–14.3 Ma for the rhyolite of Cow Hollow, 12.0 Ma for the rhyolite of Little Pine Creek, 12.0 Ma for the dacite of the Hogback, and 4.9 Ma for the rhyolite of Shinbone Creek.

INTRODUCTION

The Bull Valley and Pine Valley Mountains are in the Basin and Range province, just west of the Colorado Plateaus province in southwestern Utah (fig. 1). Most of the rocks in the Bull Valley and Pine Valley Mountains consist of volcanic rocks that range in age from Oligocene to Pliocene. The older part of the volcanic sequence consists mostly of regional ash-flow sheets, derived from outside the area, whose stratigraphy and age are well known. Most of the younger part of the sequence, however, consists of locally derived ash-flow tuffs, lava flows, flow breccia, and volcanic mudflow breccia that were erupted and emplaced above a major batholith complex, but the stratigraphy and ages of these rocks are relatively poorly known. Also poorly known are still younger but volumetrically minor local volcanic units. The regional geologic framework of the eastern Bull Valley Mountains was established by Blank (1959), whereas that of the Pine Valley Mountains was established by Cook (1957). K-Ar dating of some stratigraphically significant units in the two ranges and adjacent areas were made in the 1970's by E.H. McKee, but the analytical data were never published, although Hausel and Nash (1977, fig. 2) mentioned most of the dates, and Rowley and others (1989) mentioned two of them. Recently the eastern Bull Valley Mountains and Pine Valley Mountains have become the focus of new detailed mapping, by Blank (1993) in the Bull Valley Mountains and by D.B. Hacker of Kent State University in the Pine Valley Mountains, and the overall area was discussed and visited during a recent field trip (Blank and others, 1992). In conjunction with this new mapping, we herein publish the dates and their analytical data (table 1) of mapped igneous rocks.

The K-Ar age determinations follow the method described by Evernden and Curtis (1965). Analyses were done at the U.S. Geological Survey isotope geology laboratory in Menlo Park, Calif. Potassium (K) analyses were made by flame photometer using a lithium internal standard. Argon (Ar) analyses were done by standard isotope dilution

techniques on a Nier-type 6-inch 60°-sector mass spectrometer operated in the static mode. The analytical precision at the 68 percent confidence level (one sigma) of the calculated ages, owing to uncertainties in the argon and potassium analyses, in the isotopic composition and concentration of the Ar^{38} tracer, and in the flame photometer standards, is from 3 to 5 percent. The new dates reported here, and where necessary other dates cited, were recalculated using the IUGS (International Union of Geological Sciences) decay constants (Steiger and Jäger, 1977). Classifications of volcanic and intrusive rocks are those of IUGS (Le Bas and others, 1986, and Streckeisen, 1976, respectively).

ACKNOWLEDGMENTS

We thank D.B. Hacker for unpublished information based on his Ph. D. study in progress, and M.G. Best and A.L. Deino for unpublished data on their argon dating in progress. For many years of help in our understanding and interpreting many other concepts presented here, we are grateful to P.L. Williams, J.J. Anderson, D.S. Barker, M.G. Best, and the late J.H. Mackin. We thank J.M. O'Neill and R.B. Scott for good, constructive technical reviews of the manuscript.

GEOLOGIC SETTING

The volcanic rocks in the eastern Bull Valley Mountains and the Pine Valley Mountains rest on, or are interbedded near the top of, fluvial and lacustrine rocks of the Paleocene and Eocene Claron Formation and the upper Eocene and Oligocene Brian Head Formation (Rowley and others, 1994; Sable and Maldonado, this volume, chapter A). The Claron, in turn, rests unconformably on the Upper Cretaceous Iron Springs Formation, and that unit unconformably overlies the Middle Jurassic Carmel Formation and Temple Cap Sandstone. The sequence extending from the Temple Cap upward through the volcanic rocks is similar to the stratigraphy in the Iron Springs mining district to the north (fig. 1), initially described by Mackin (1947, 1954). Sevier-age thrust faults cut rocks older than the Claron Formation in the Iron Springs district and the southern flank of the eastern Bull Valley Mountains. In the Beaver Dam Mountains and other areas to the south, these thrusts cut a thick pre-Temple Cap sequence as well (Hintze, 1986, among others).

The oldest volcanic rocks in the eastern Bull Valley Mountains and Pine Valley Mountains consist largely of regional calc-alkaline andesite to rhyolite ash-flow tuffs that were deposited over large parts of southwestern Utah and southeastern Nevada, ranging from the Oligocene Wah Wah Springs Formation (>29.5 Ma) at the base, to the Miocene Condor Canyon Formation (about 23 Ma) in the upper part (fig. 2). Locally the tuffs are intertongued with andesitic and dacitic lava flows erupted from the Bull Valley Mountains centers. The regional stratigraphy of the tuffs was summarized by Blank (1959, 1993), Mackin (1960), Cook (1965), Anderson and Rowley (1975), Rowley and others (1979, 1994, 1995), Siders and Shubat (1986), Best, Christiansen, and others (1989), Best and others (1993), Blank and others (1992), and Scott and others (1995). Most of the older tuffs were derived from outside the study area, notably the Indian Peak caldera complex (Best, Christiansen, and Blank, 1989) north of the Bull Valley Mountains and the Caliente caldera complex (Williams, 1967; Noble and McKee, 1972; Ekren and others, 1977; Rowley and others, 1992) in and west of the Bull Valley Mountains (fig. 1). Isotopic dates of the tuffs have been reported by many workers, notably Armstrong (1970), Noble and McKee (1972), Fleck and others (1975), Best and Grant (1987), Best, Christiansen, and others (1989), and Rowley and others (1994).

At about 23–22 Ma, voluminous calc-alkaline volcanism began in the eastern Bull Valley Mountains and Pine Valley Mountains above an inferred major batholith complex that not only underlay much of these areas but also extended north under the Iron Springs mining district (Mackin, 1947; Blank and Mackin, 1967; Blank and Kucks, 1989) and parts of the Escalante Desert (Grant and Proctor, 1988; Williams, in press), and from there northeast beneath the northern Markagunt Plateau and areas east of that, all in the Colorado Plateau transition zone (Blank and others, in press; Rowley and others, in press). Parts of the roof of the batholith complex were intruded along a northeast-striking Sevier-age thrust fault zone that extends from the eastern Bull Valley Mountains, through the Iron Springs district, to the Red Hills 15 km northeast of The Three Peaks intrusion; it apparently reaches to the Markagunt Plateau of the Colorado Plateau 35 km east-northeast of The Three Peaks intrusion (fig. 1). More than a dozen intrusions are thus aligned northeast, and those extending from the Bull Valley Mountains through the Iron Springs district were referred to as the Iron Axis by Tobey (1976) and Blank and others (1992) because extensive iron-ore deposits were derived from, and occur along the margins of, many of these plutons (fig. 1). Rowley and others (1994) extended the Iron Axis farther northeast so that it includes plutons of the same trend that contain no commercial iron deposits.

The volcanic rocks in the eastern Bull Valley Mountains and the Pine Valley Mountains that are known or inferred to have been derived from the common batholithic source make up a thick younger sequence (fig. 2), the oldest of which are the andesite of Little Creek, the product of a local volcano, and the Harmony Hills Tuff (Mackin, 1960), a regional ash-flow sheet that spread over much of southwestern Utah and southeastern Nevada. In the eastern Bull Valley Mountains, Blank (1959) mapped a thick sequence of locally derived lava flows and ash-flow tuffs that blanket much of the area. In the Pine Valley Mountains, Cook (1957) demonstrated that voluminous lava flows, which he termed the Pine Valley Latite, were

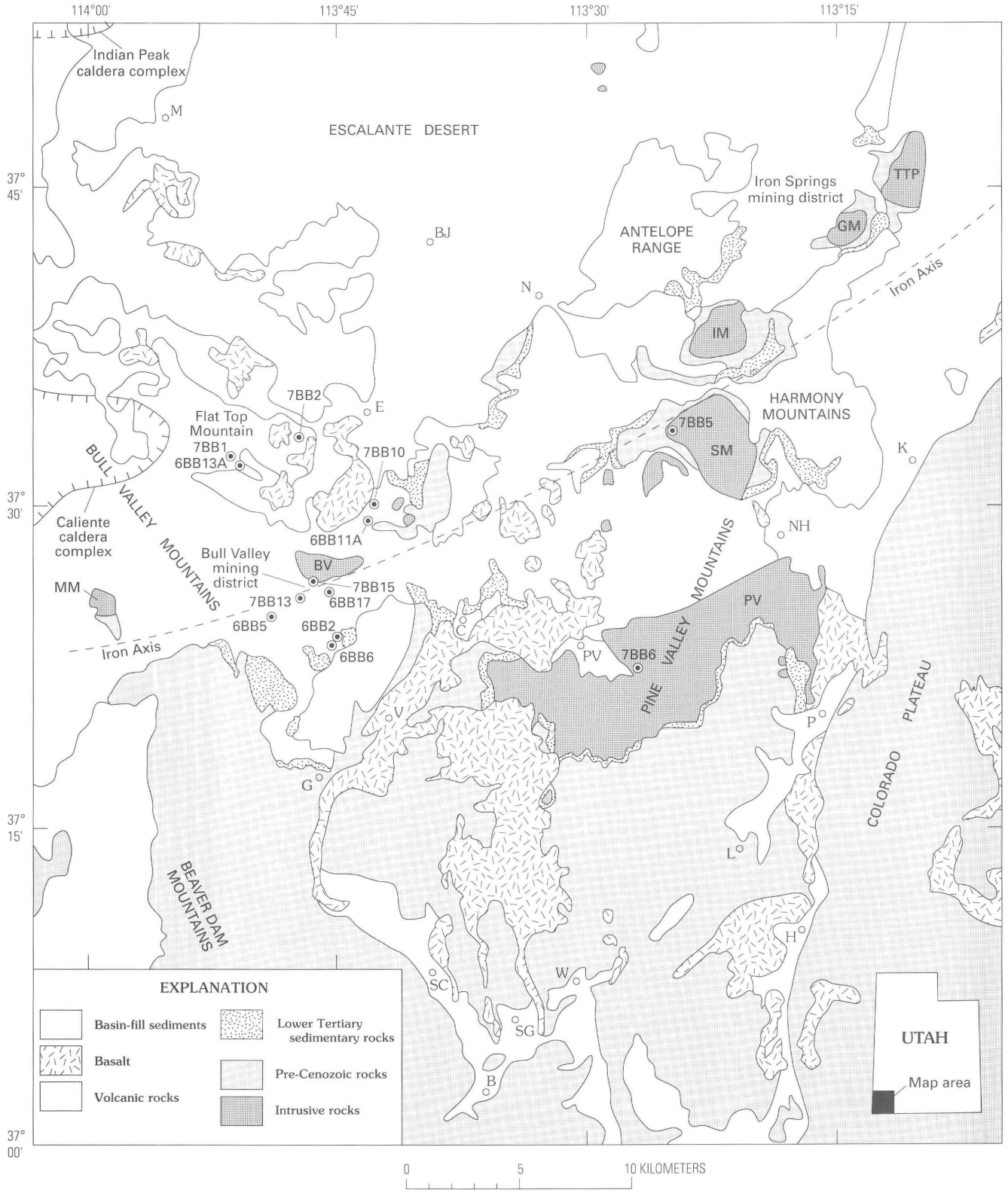

Figure 1. Generalized geologic map of Bull Valley and Pine Valley Mountains and adjacent areas, Utah, showing locality of samples whose ages and analytical data are reported here. Map modified from Hintze (1980). B, Bloomington; BJ, Beryl Junction; C, Central; E, Enterprise; G, Gunlock; H, Hurricane; K, Kanarraville; L, Leeds; M, Modena; N, Newcastle; NH, New Harmony; P, Pintura; PV, Pine Valley; SC, Santa Clara; SG, St. George; V, Veyo; W, Washington. Intrusions of the Iron Axis: BV, Bull Valley; GM, Granite Mountain; IM, Iron Mountain; MM, Mineral Mountain; PV, Pine Valley; SM, Stoddard Mountain; TTP, The Three Peaks. Hachured line, edge of caldera complex.

Table 1. Analytical data for K–Ar ages, Bull Valley and Pine Valley Mountains, Utah.

Rock unit, sample No. mineral analyzed[1]	$^{2}K_2O$ (percent)	$^{*40}Ar(10^{-10}$ moles/gram)	$^{*40}Ar$ (percent)	Age in m.y.±1σ
Rhyolite of Shinbone Creek				
7BB10; S	10.12, 10.17	0.68	63.4	4.7±0.2
6BB11A; S	10.54, 10.59	0.75	81.8	5.0±0.2
Dacite of the Hogback				
7BB1; H	0.86, 0.87	0.15	33.4	12.0±0.5
Rhyolite of Little Pine Creek				
6BB13A; S	6.28, 6.33	0.11	63.0	12.0±0.4
Rhyolite of Cow Hollow				
7BB2; S	9.16, 9.15	0.19	89.4	14.3±0.4
7BB2; S	9.16, 9.15	2.02	77.2	15.3±0.4
Pine Valley laccolith				
7BB6; B	7.64, 7.74	2.32	69.1	20.9±0.6
Rencher Formation, upper member				
6BB5; B	8.28, 8.23	2.57	80.1	21.5±0.6
Rencher Formation, middle member				
6BB2; B	8.70, 8.74	2.75	64.1	21.8±0.7
Rencher Formation, lower member				
6BB6; B	8.48	2.90	70.8	23.6±0.7
Bull Valley intrusion				
7BB15; B	6.21, 6.20	2.05	65.4	22.8±0.7
Stoddard Mountain intrusion				
7BB5; B and H	3.81, 3.95	1.21	52.6	21.5±0.9
Condor Canyon Formation, Bauers Tuff Member				
6BB17; B	7.08, 7.14	2.33	73.2	22.6±0.6
Wah Wah Springs Formation				
7BB13; B	6.49, 6.41	2.76	80.6	29.5±0.9

[1]Constants: $^{40}K\lambda_\varepsilon=0.581x10^{-10}yr^{-1}$, $\lambda_\beta=4.962x10^{-10}yr^{-1}$, $^{40}K/K=1.67x10^{-4}$; mineral analyzed: B, biotite; H, hornblende; S, sanidine.

[2]Determined by flame photometer.

derived from breaching the roof of the huge Pine Valley laccolith. Major extensional faulting in the region began at the same time (about 23–22 Ma) as large-scale magmatism took place (Mackin, 1960; Siders and Shubat, 1986; Siders and others, 1990), but the present topography was not established until the inception of the regional basin-range episode of extensional faulting, at about 10 Ma (Rowley and others, 1979; Siders and others, 1990). Just before and after the inception, and after solidification of the batholith complex, local rhyolite and dacite domes formed in the northern Bull Valley Mountains (Rowley and others, 1979). These domes are part of the bimodal (dominantly basaltic and rhyolitic) volcanism that characterized the basin-range faulting regime, which continued into the Holocene.

DATED IGNEOUS UNITS

The rock units that we have dated are discussed briefly herein, from oldest to youngest. We use informal stratigraphic names for local rhyolite and dacite dome complexes, until current mapping by H.R. Blank is completed. The new dates, analytical data, and descriptions of sample sites are given in table 1. Sample sites are shown in figure 1, and stratigraphic relationships of volcanic and sedimentary rocks are given in figure 2.

Table 1. Analytical data for K–Ar ages, Bull Valley and Pine Valley Mountains, Utah.—*Continued*

SAMPLE DESCRIPTIONS

7BB10. Flow-layered rhyolite from along Shinbone Creek, 0.2 km south of Bullrush Spring and about 6.5 km south of Enterprise, W½ sec. 1, T. 38 S., R. 17 W.; lat 37° 30′ 37″ N., long 113° 42′ 49 ″ W.

6BB11A. Rhyolite tuff-lava from ridge 0.3 km east of Bullrush Creek at outlet of Ox Valley, SE¼SW¼ sec. 11, T. 38 S., R. 17 W.; lat 37° 29′ 33″ N., long 113° 43′ 31″ W.

7BB1. Flow-layered dacite lava flow from 0.4 km west of Veyo-Shoal Creek road and about 1 km north of spillway of Lower Enterprise Reservoir, SE¼ sec. 27, T. 37 S., R. 18 W.; lat 37° 32′ 06″ N., long 113° 51′ 00″ W.

6BB13A. Rhyolite lava flow from just east of Veyo-Shoal Creek road in upper Little Pine Creek, 0.4 km north of spillway of Lower Enterprise Reservoir, NE¼ sec. 34, T. 37 S., R. 18 W.; lat 37° 31′ 46″ N., long 113° 50′ 54″ W.

7BB2. Rhyolite lava flow from pack trail in Cow Hollow, about 1.2 km south of paved road leading west from Enterprise along Shoal Creek, SW¼NE¼ sec. 20, T. 37 S., R. 17 W.; lat 37° 33′ 19″ N., long 113° 46′ 44″ W.

7BB6. Quartz monzonite porphyry from Pine Valley campground area, about 5 km east-southeast of town of Pine Valley; lat 37° 22′ 13″ N., long 113° 27′ 21″ W.

6BB5. Poorly welded tuff from matrix of block-flow breccia exposed on ridgecrest along pack trail about 0.5 km west of summit of Cove Mountain and about 5.5 km southwest of Bull Mountain, S½SW¼ sec. 12, T. 39 S., R. 18 W.; lat 37° 24′ 21″ N., 113° 49′ 10″ W.

6BB2. Poorly welded ash-flow tuff from upper of two cooling units exposed just east of Veyo-Shoal Creek road, 0.5 km south of Cove Wash and about 3.2 km south of Bull Mountain, NE¼ sec. 16, T. 39 S., R. 17 W.; lat 37° 23′ 57″ N., long 113° 45′ 17″ W.

6BB6. Poorly welded ash-flow tuff from lower of two cooling units exposed just east of Veyo-Shoal Creek road, 0.6 km south of Cove Wash and about 3.4 km south of Bull Mountain, NE¼ sec. 16, T. 39 S., R. 17 W.; lat 37° 23′ 52″ N., long 113° 45′ 20″ W.

7BB15. Quartz monzonite porphyry from north side of Moody Wash, 0.7 km upstream from confluence with Pilot Creek (Racer Canyon), E½NE¼ sec. 32, T. 38 S., R. 17 W.; lat 37° 26′ 32″ N., long 113° 46′ 19″ W.

7BB5. Quartz monzonite porphyry from roadcut about 100 m northeast of Page Ranch, SE¼ NE¼ sec. 21, T. 37 S., R. 14 W.; lat 37° 34′ 05″ N., long 113° 25′ 17″ W.

6BB17. Densely welded ash-flow tuff from north side of Bull Mountain, 0.2 km south of Moody Wash and 0.2 km downstream from confluence of Moody Wash and Pilot Creek (Racer Canyon), SE¼NW¼ sec. 33, T. 38 S., R. 17 W.; lat 37° 26′ 27″ N., long 113° 45′ 43″ W.

7BB13. Poorly welded ash-flow tuff from just west of a jeep trail about 1.5 km west of Bull Mountain and 1 km south of Moody Wash, SW¼ SW¼ sec. 32, T. 38 S., R. 17 W.; lat 37° 26′ 06″ N., long 113° 47′ 10″ W.

WAH WAH SPRINGS FORMATION

The Oligocene Wah Wah Springs Formation of the Needles Range Group (Mackin, 1960; Best and Grant, 1987) is one of the largest and most widespread ash-flow sheets in the world. It is a moderately welded, crystal-rich, dacitic ash-flow tuff derived from the huge Indian Peak caldera complex straddling the Nevada-Utah State line north of Modena (fig. 1) (Best, Christiansen, and Blank, 1989). The tuff generally rests on, but locally is interbedded in, the upper part of rocks mapped as the Claron Formation; these mapped rocks, however, may correlate with the Brian Head Formation, as defined by Sable and Maldonado (this volume, chapter A). The average K-Ar age of the Wah Wah Springs Formation is 29.5 Ma (Best, Christiansen, and Blank, 1989), but unpublished $^{40}Ar/^{39}Ar$ dates indicate that the current best estimate of the age is closer to 30 Ma (M.G. Best, written commun., 1993). The new date (sample 7BB13) on biotite from the eastern Bull Valley Mountains is 29.5±0.9 Ma (table 1), within analytical error of the probable age of the unit calculated by Best and his colleagues.

BAUERS TUFF MEMBER OF THE CONDOR CANYON FORMATION

The Bauers Tuff Member of the Miocene Condor Canyon Formation of the Quichapa Group (Mackin, 1960; Cook, 1965; Williams, 1967; Anderson and Rowley, 1975)

is a widespread ash-flow sheet in southwestern Utah and southeastern Nevada. It is a densely welded, crystal-poor, rhyolite ash-flow tuff derived from the Clover Creek caldera of Nevada, in the northern part of the central Caliente caldera complex (Rowley and Siders, 1988; Rowley and others, 1992; Rowley and others, 1995). Best, Christiansen, and others (1989, table B3, no analytical data published) determined two $^{40}Ar/^{39}Ar$ dates on the unit that average 22.8 Ma. The new date (sample 6BB17) on biotite from the eastern Bull Valley Mountains is 22.6±0.6 Ma, very close to the argon dates.

STODDARD MOUNTAIN INTRUSION

The Stoddard Mountain intrusion, which underlies the Stoddard Mountain area just north of the Pine Valley Mountains, is one of the intrusions of quartz monzonite porphyry of the Iron Axis. It is similar in its lithology and most field relations to intrusions in the Iron Springs mining district (Mackin, 1947, 1954, 1960, 1968; Blank and Mackin, 1967; Mackin and Rowley, 1976; Mackin and others, 1976; Rowley and Barker, 1978; Barker, 1982, 1991; Van Kooten, 1988). It differs from all the others, except the Pine Valley laccolith (see p. 249), however, in that it intruded to a higher structural level (the Upper Cretaceous Iron Springs Formation), its roof is largely discordant, and it is barren of iron deposits (Cook, 1957, 1960; Mackin, 1960; Blank and Mackin, 1967; Barker, 1982, 1991). The new date (sample 7BB5) on the intrusion, the first to be published on it, is 21.5±0.9 Ma on impure biotite, similar to the dates on intrusions in the Iron Springs district.

Previously published isotopic dates, some clearly discordant, on intrusions of the Iron Axis range from 24.6 to 20.2 Ma (Jaffe and others, 1959; Armstrong, 1966, 1970; Fleck and others, 1975). All intrusions must postdate the Harmony Hills Tuff of the Quichapa Group because the tuff was deformed by the intrusions (Mackin, 1960; Anderson and Rowley, 1975). Although several lines of evidence suggest that the Harmony Hills Tuff was erupted from the Bull Valley intrusion (Blank, 1959), its exact source has not been discovered. Six K-Ar dates (Armstrong, 1970; Noble and McKee, 1972) on the tuff average 21.6 Ma but have a wide range of values (24.4–20.3 Ma), so the true age of the Harmony Hills is not well constrained. Except for the Iron Peak intrusion (20.2 Ma; Fleck and others, 1975) in the Markagunt Plateau and the Pine Valley laccolith (see p. 249), which appear to be distinctly younger, the age of most intrusions of the Iron Axis is probably about 22–21.5 Ma (Rowley and others, 1989), coeval with the emplacement of the Stoddard Mountain intrusion.

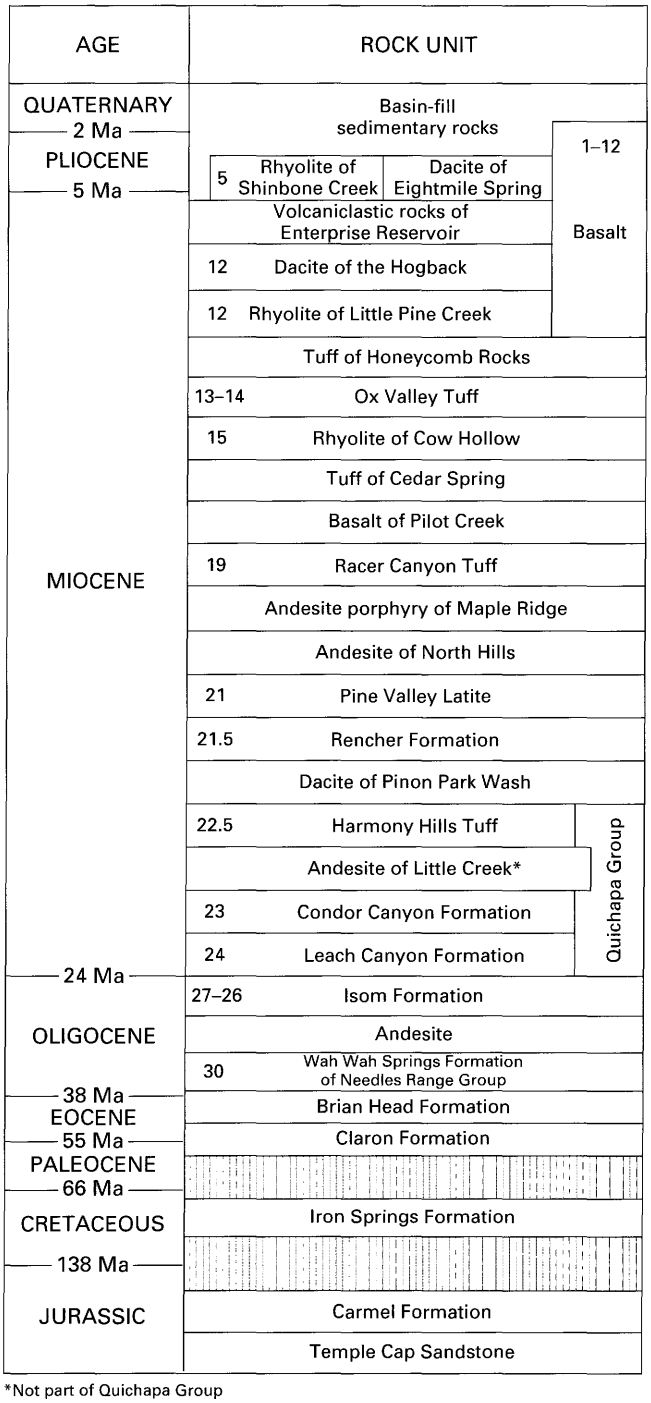

Figure 2. Composite stratigraphic column of volcanic and sedimentary rocks in eastern Bull Valley Mountains and Pine Valley Mountains, Utah, modified from Blank (1959, 1993) and Blank and others (1992). Numbers refer to isotopic ages of volcanic rocks, rounded to nearest half million years. Major hiatus in deposition shown by vertical lines, but local unconformities not shown.

BULL VALLEY INTRUSION

The Bull Valley intrusion, in the eastern Bull Valley Mountains, is another mass of quartz monzonite porphyry of the Iron Axis. It has been mapped and described by Blank (1959), Tobey (1976), and Blank and others (1992), who found that it was emplaced rapidly and created a topographic high that shed gravity slides to the north, south, and east. Its roof is mostly concordant against the Middle Jurassic Temple Cap Sandstone and overlying Carmel Formation, as with most other intrusions in the Iron Springs mining district. It vented a sequence of ash-flow tuff (the Rencher Formation, described next) and lava flows (Blank, 1959; Blank and others, 1992). It is the source of vein iron and relatively minor replacement iron-ore deposits of the Bull Valley mining district. The new date (sample 7BB15) on the Bull Valley intrusion, the first to be published on the body, is 22.8±0.7 Ma on biotite. This date is numerically older than, but within analytical error of, dates on the Harmony Hills Tuff, Rencher Formation (see next), and most other intrusions in the Iron Axis. Moreover, field relations indicate that the Stoddard Mountain intrusion is older than the Bull Valley intrusion (D.B. Hacker, oral commun., 1993).

RENCHER FORMATION

The Rencher Formation (Cook, 1957) is a composite ash-flow sheet of moderate regional extent and volume exposed in the eastern Bull Valley Mountains, northern Pine Valley Mountains, and southern Iron Springs district. It consists mainly of poorly to moderately welded, crystal-rich, andesitic to dacitic ash-flow tuff derived from the Bull Valley intrusion (Blank, 1959). In the Bull Valley Mountains, two cooling units and an overlying tuff-breccia flow have been recognized. Biotite from each unit is dated here. The dates are 23.6±0.7 Ma on the lowest unit (sample 6BB6), 21.8±0.7 Ma on the middle unit (sample 6BB2), and 21.5±0.6 Ma on the top unit (sample 6BB5). The date on the lower unit is discordant with the others and is numerically older than the probable age of the underlying Harmony Hills Tuff, so it is rejected; perhaps the sample was contaminated with lithic material derived from older rocks over which the tuff spread. The other two isotopic dates, which were first mentioned by Rowley and others (1989) but without their analytical data, are believed to more accurately represent the time of eruption of the Rencher and numerically may better represent the age of the Bull Valley intrusion, from which they were derived.

PINE VALLEY LACCOLITH

The Pine Valley laccolith, one of the largest bodies of this form in the world, consists of quartz monzonite porphyry of the Iron Axis suite. It was intruded to a still higher structural level than other laccoliths of the suite, within the Paleocene to Eocene Claron Formation, and it breached its thin roof on its north side and erupted thick dacitic lava flows, the Pine Valley Latite (Cook, 1957). An abrupt topographic high was formed by emplacement of the laccolith, and gravity slides were shed to the west off this high (Blank and others, 1992; D.B. Hacker, unpub. data, 1993). The floor of the laccolith is well exposed, with monzonite resting directly on the lower part of the Claron, and the laccolith, now almost completely deroofed by erosion, is about 1,000 m thick. Because it was intruded to such a shallow level, it is difficult to distinguish intrusive from extrusive rock in the field, and thus Mattison (1972) interpreted the whole laccolith as volcanic rock, and Grant (1991) interpreted the upper half of the laccolith as volcanic. Mapping by D.B. Hacker (oral commun., 1993), however, favors the interpretation of Cook that most of it is intrusive rock except for more finely flow-foliated Pine Valley Latite on its northern top. The new date (sample 7BB6), the first to be determined on the intrusion, is 20.9±0.6 Ma, on biotite from a sample collected in the lower part of the laccolith; it and the date on the Iron Peak laccolith indicate distinctly younger ages for some intrusions of the Iron Axis.

RHYOLITE OF COW HOLLOW

The rhyolite of Cow Hollow is one of four small local tholoidal eruptive sequences in the northeastern Bull Valley Mountains that were dated in this study. The unit consists of crystal-poor, high-silica rhyolite lava flows and feeders confined to the Flat Top Mountain area, west-southwest of Enterprise. The dated sample was collected from Cow Hollow, on the east side of the mountain. Blank (1959) noted that the unit is petrographically similar to, and is overlain by, the Ox Valley Tuff, a regional ash-flow sheet whose age is about 14–13 Ma (Rowley and others, 1995). The unit was informally called the Cow Creek rhyolite of the Flattop Mountain suite by Blank (1959); the name Flattop Mountain Suite was formalized by Cook (1960). We prefer, however, to use the informal name rhyolite of Cow Hollow (applying the new topographic name proposed when the quadrangle map of the area was published in 1972). Two new dates, determined on splits of sanidine from the same sample (sample 7BB2), are 15.3±0.4 Ma, and 14.3±0.4 Ma. We cannot choose which of these slightly discordant dates best approximates the age of the rhyolite of Cow Hollow, and we suggest that the best estimated age is their average, 14.8 Ma.

RHYOLITE OF LITTLE PINE CREEK

The rhyolite of Little Pine Creek consists of crystal-poor rhyolite that occurs as small domoform intrusive masses exposed at low elevations along upper Little Pine

Creek and at Upper and Lower Enterprise Reservoirs. The occurrence of macroscopically similar lava flows and flow breccia several kilometers west of Little Pine Creek suggests that the volcanic domes may be exogenous, as with the rhyolite of Cow Hollow. Both the lithology and geologic environment of the two map units are similar. The unit was informally called the Little Pine Creek rhyolite of the Flattop Mountain suite by Blank (1959), but we prefer to use the informal name rhyolite of Little Pine Creek. The new date (sample 6BB13A) on sanidine is 12.0±0.4 Ma.

DACITE OF THE HOGBACK

The dacite of the Hogback is a local eruptive sequence of dacitic to rhyodacitic lava flows and feeders of moderately low phenocryst content exposed west and east of the rhyolite of Cow Hollow, in the area north of Lower Enterprise Reservoir occupied by high, broad-topped ridges called the Hogback. Feeders of the dacite apparently intruded the rhyolite of Little Pine Creek. The unit was informally called the Hogs Back formation of the Flattop Mountain suite by Blank (1959), but we prefer to use the informal name dacite of the Hogback (applying the name published on the Hebron 7.5-minute topographic quadrangle). The new date (sample 7BB1) on hornblende is 12.0±0.5 Ma, the same age as the rhyolite of Little Pine Creek.

RHYOLITE OF SHINBONE CREEK

The rhyolite of Shinbone Creek is a rhyolite to rhyodacite rock of a local eruptive sequence of crystal-poor rhyolitic lava flows, tuff-lava, and inferred intrusive rock exposed along Shinbone Creek and on the northeastern flanks of adjacent Ox Valley, east of the rhyolite of Cow Hollow and south of Enterprise. The unit, interpreted to be an exogenous dome containing highly vesiculated margins, was informally called Shinbone rhyolite of the Flattop Mountain suite by Blank (1959), but we prefer to use the informal name rhyolite of Shinbone Creek. Two new concordant dates on sanidine from different rocks were determined, one on tuff-lava (sample 6BB11A) on the northeastern side of Ox Valley of 5.0±0.2 Ma, and the other on dense rock (sample 7BB10) interpreted to be the main vent, to the north along Shinbone Creek, of 4.7±0.2 Ma. Their average, 4.9 Ma, is our best estimate of the age of the rhyolite mass.

CONCLUSIONS

A large batholith complex underlies the Bull Valley and Pine Valley Mountains of southwestern Utah, and it also extends north to underlie the Iron Springs mining district and eastern Escalante Desert. From there the complex may extend northeast to underlie the northern Markagunt Plateau of the Colorado Plateau transition zone and probably other areas farther east (Rowley and others, 1994; Blank and others, in press; Rowley and others, in press). Many cupolas on the roof of the batholith complex are exposed along the Iron Axis, which extends northeast from the central Bull Valley Mountains to the western edge of the Markagunt Plateau and which was controlled by a Sevier-age thrust fault that strikes northeast.

The batholith complex was the source of volcanic rocks that erupted from numerous vents, some of them along the Iron Axis. K-Ar dates published here constrain the age of the intrusions and their ash-flow products. Field relationships show that the oldest dated intrusion from the Iron Axis is the Stoddard Mountain intrusion, which has an age of 21.5 Ma. Although field relations prove that the Bull Valley intrusion of the Iron Axis is younger than the Stoddard Mountain intrusion, the Bull Valley intrusion has a K-Ar date of 22.8 Ma. This intrusion erupted the Rencher Formation, an ash-flow tuff that is dated at 21.8 and 21.5 Ma. The Pine Valley laccolith, southeast of the Iron Axis and part of the overall batholith complex, is younger (20.9 Ma) than the Stoddard Mountain and Bull Valley intrusions.

After solidification of the batholith complex, local rhyolite and dacite volcanic domes erupted from small centers in the northern Bull Valley Mountains. These include the rhyolite of Cow Hollow (14.8 Ma), the rhyolite of Little Pine Creek (12.0 Ma), the dacite of the Hogback (12.0 Ma), and the rhyolite of Shinbone Creek (4.9 Ma).

REFERENCES CITED

Anderson, J.J., and Rowley, P.D., 1975, Cenozoic stratigraphy of the southwestern High Plateaus of Utah, *in* Anderson, J.J., Rowley, P.D., Fleck, R.J., and Nairn, A.E.M., Cenozoic geology of southwestern High Plateaus of Utah: Geological Society of America Special Paper 160, p. 1–52.

Armstrong, R.L., 1966, K-Ar dating using neutron activation for Ar analysis—Granitic plutons of the eastern Great Basin, Nevada and Utah: Geochimica et Cosmochimica Acta, v. 30, p. 565–600.

———1970, Geochronology of Tertiary igneous rocks, eastern Basin and Range province, western Utah, eastern Nevada, and vicinity, U.S.A.: Geochimica et Cosmochimica Acta, v. 34, p. 203–232.

Barker, D.S., 1982, Magnetite-apatite veins in quartz monzonite, Iron Springs district, Utah—A revised model: Geological Society of America Abstracts with Programs, v. 14, no. 7, p. 439.

———1991, Quartz monzonite and associated iron deposits, Iron Springs, Utah: Geological Society of America Abstracts with Programs, v. 23, no. 5, p. 388.

Best, M.G., Christiansen, E.H., and Blank, R.H., Jr., 1989, Oligocene caldera complex and calc-alkaline tuffs and lavas of the Indian Peak volcanic field, Nevada and Utah: Geological Society of America Bulletin, v. 101, p. 1076–1090.

Best, M.G., Christiansen, E.H., Deino, A.L., Grommé, C.S., McKee, E.H., and Noble, D.C., 1989, Excursion 3A—Eocene through Miocene volcanism in the Great Basin of the western United States: New Mexico Bureau of Mines and Mineral Resources Memoir 47, p. 91–133.

Best, M.G., and Grant, S.K., 1987, Stratigraphy of the volcanic Oligocene Needles Range Group in southwestern Utah and eastern Nevada: U.S. Geological Survey Professional Paper 1433–A, 28 p.

Best, M.G., Scott, R.B., Rowley, P.D., Swadley, W C, Anderson, R.E., Grommé, C.S., Harding, A.E., Deino, A.L., Christiansen, E.H., Tingey, D.G., and Sullivan, K.R., 1993, Oligocene-Miocene caldera complexes, ash-flow sheets, and tectonism in the central and southeastern Great Basin, *in* Lahren, M.M., Trexler, J.H., Jr., and Spinosa, Claude, eds., Crustal evolution of the Great Basin and Sierra Nevada: Cordilleran/Rocky Mountain section, Geological Society of America Guidebook, Department of Geological Sciences, University of Nevada, Reno, p. 285–311.

Blank, H.R., 1993, Preliminary geologic map of the Enterprise quadrangle, Washington and Iron Counties, Utah: U.S. Geological Survey Open-File Report 93-203, 55 p., scale 1:24,000.

Blank, H.R., Jr., 1959, Geology of the Bull Valley district, Washington County, Utah: Seattle, Wash., University of Washington Ph. D. dissertation, 177 p.

Blank, H.R., Butler, W.C., and Saltus, R.W., in press, Residual gravity and aeromagnetic anomaly fields of the northern Colorado Plateau and environs, *in* Friedman, J.D., and Huffman, A.C., eds., Laccolith complexes of southeastern Utah—Time of emplacement and tectonic setting: U.S. Geological Survey Bulletin 2158.

Blank, H.R., and Kucks, R.P., 1989, Preliminary aeromagnetic, gravity, and generalized geologic maps of the USGS Basin and Range–Colorado Plateau transition zone study area in southwestern Utah, southeastern Nevada, and northwestern Arizona (the "BARCO" project): U.S. Geological Survey Open-File Report 89-432, 16 p., scale 1:250,000.

Blank, H.R., Jr., and Mackin, J.H., 1967, Geologic interpretation of an aeromagnetic survey of the Iron Springs district, Utah: U.S. Geological Survey Professional Paper 516–B, 14 p., scale 1:48,000.

Blank, H.R., Rowley, P.D., and Hacker, D.B., 1992, Miocene monzonitic intrusions and associated megabreccias of the Iron Axis region, southwestern Utah, *in* Wilson, J.R., ed., Field guide to geologic excursions in Utah and adjacent areas of Nevada, Idaho, and Wyoming, Rocky Mountain section, Geological Society of America Guidebook: Utah Geological Survey Miscellaneous Publication 92-3, p. 399–420.

Cook, E.F., 1957, Geology of the Pine Valley Mountains, Utah: Utah Geological and Mineralogical Survey Bulletin 58, 111 p.

———1960, Geologic atlas of Utah, Washington County: Utah Geological and Mineralogical Survey Bulletin 70, 119 p.

———1965, Stratigraphy of Tertiary volcanic rocks in eastern Nevada: Nevada Bureau of Mines Report 11, 61 p.

Ekren, E.B., Orkild, P.P., Sargent, K.A., and Dixon, G.L., 1977, Geologic map of Tertiary rocks, Lincoln County, Nevada: U.S. Geological Survey Miscellaneous Investigations Series Map I–1041, scale 1:250,000.

Evernden, J.F., and Curtis, G.H., 1965, The present status of potassium-argon dating of Tertiary and Quaternary rocks: International Association of Quaternary Research, 6th Congress, Warsaw, 1961, Report, v. 1, p. 643–651.

Fleck, R.J., Anderson, J.J., and Rowley, P.D., 1975, Chronology of mid-Tertiary volcanism in High Plateaus region of Utah, *in* Anderson, J.J., Rowley, P.D., Fleck, R.J., and Nairn, A.E.M., Cenozoic geology of southwestern High Plateaus of Utah: Geological Society of America Special Paper 160, p. 53–62.

Grant, S.K., 1991, Geologic map of the New Harmony quadrangle, Washington County, Utah: Utah Geological and Mineral Survey Open-File Report 206, 32 p., scale 1:24,000.

Grant, S.K., and Proctor, P.D., 1988, Geologic map of the Antelope Peak quadrangle, Iron County, Utah: Utah Geological and Mineral Survey Open-File Report 130, 20 p., scale 1:24,000.

Hausel, W.D., and Nash, W.P., 1977, Petrology of Tertiary and Quaternary volcanic rocks, Washington County, southwestern Utah: Geological Society of America Bulletin, v. 88, p. 1831–1842.

Hintze, L.F., 1980, Geologic map of Utah: Utah Geological and Mineral Survey, scale 1:500,000.

———1986, Stratigraphy and structure of the Beaver Dam Mountains, southwestern Utah, *in* Griffen, D.T., and Phillips, W.R., eds., Thrusting and extensional structures and mineralization in the Beaver Dam Mountains, southwestern Utah: Utah Geological Association Publication 15, p. 1–36.

Jaffe, H.W., Gottfried, David, Waring, C.L., and Worthing, H.W., 1959, Lead-alpha age determinations of accessory minerals of igneous rocks (1953–1957): U.S. Geological Survey Bulletin 1097–B, p. 65–148.

Le Bas, M.J., Le Maître, R.W., Streckeisen, A., and Zanettin, B., 1986, A chemical classification of volcanic rocks based on the total alkali-silica diagram: Journal of Petrology, v. 27, pt. 3, p. 745–750.

Mackin, J.H., 1947, Some structural features of the intrusions in the Iron Springs district: Utah Geological Society, Guidebook to the geology of Utah, no. 2, 62 p.

———1954, Geology and iron ore deposits of the Granite Mountain area, Iron County, Utah: U.S. Geological Survey Mineral Investigations Field Studies Map MF–14, scale 1:12,000.

———1960, Structural significance of Tertiary volcanic rocks in southwestern Utah: American Journal of Science, v. 258, no. 2, p. 81–131.

———1968, Iron ore deposits of the Iron Springs district, southwestern Utah, *in* Ore deposits of the United States, 1933–1967 (Graton-Sales Volume), Volume 2: American Institute of Mining, Metallurgical, and Petroleum Engineers, p. 992–1019.

Mackin, J.H., Nelson, W.H., and Rowley, P.D., 1976, Geologic map of the Cedar City NW quadrangle, Iron County, Utah: U.S. Geological Survey Geologic Quadrangle Map GQ–1295, scale 1:24,000.

Mackin, J.H., and Rowley, P.D., 1976, Geologic map of The Three Peaks quadrangle, Iron County, Utah: U.S. Geological Survey Geologic Quadrangle Map GQ–1297, scale 1:24,000.

Mattison, G.D., 1972, The chemistry, mineralogy and petrography of the Pine Valley Mountains, southwestern Utah: University Park, Pa., The Pennsylvania State University Ph. D. dissertation, 141 p.

Noble, D.C., and McKee, E.H., 1972, Description and K-Ar ages of volcanic units of the Caliente volcanic field, Lincoln County, Nevada, and Washington County, Utah: Isochron/West, no. 5, p. 17–24.

Rowley, P.D., and Barker, D.S., 1978, Geology of the Iron Springs mining district, Utah, *in* Shawe, D.R., and Rowley, P.D., eds., International Association on Genesis of Ore Deposits, Guidebook to mineral deposits of southwestern Utah: Utah Geological Association Publication 7, p. 49–58.

Rowley, P.D., Cunningham, C.G., Steven, T.A., Mehnert, H.H., and Naeser, C.W., in press, Cenozoic igneous and tectonic setting of the Marysvale volcanic field, and its relation to other igneous centers in Utah and Nevada, *in* Friedman, J.D., and Huffman, A.C., eds., Laccolith complexes of southeastern Utah—Time of emplacement and tectonic setting: U.S. Geological Survey Bulletin 2158.

Rowley, P.D., McKee, E.H., and Blank, H.R., Jr., 1989, Miocene gravity slides resulting from emplacement of the Iron Mountains pluton, southern Iron Springs mining district, Iron County, Utah [abs.]: Eos, v. 70, no. 43, p. 1309.

Rowley, P.D., Mehnert, H.H., Naeser, C.W., Snee, L.W., Cunningham, C.G., Steven; T.A., Anderson, J.J., Sable, E.G., and Anderson, R.E., 1994, Isotopic ages and stratigraphy of Cenozoic rocks of the Marysvale volcanic field and adjacent areas, west-central Utah: U.S. Geological Survey Bulletin 2071, 35 p.

Rowley, P.D., Nealey, L.D., Unruh, D.M., Snee, L.W., Mehnert, H.H., Anderson, R.E., and Grommé, C.S., 1995, Stratigraphy of Miocene ash-flow tuffs in and near the Caliente caldera complex, southeastern Nevada and southwestern Utah, Chapter B *in* Scott, R.B., and Swadley, W C, eds., Geologic studies in the Basin and Range–Colorado Plateau transition in southeastern Nevada, southwestern Utah, and northwestern Arizona, 1992: U.S. Geological Survey Bulletin 2056, p. 43–88.

Rowley, P.D., and Siders, M.A., 1988, Miocene calderas of the Caliente caldera complex, Nevada-Utah [abs.]: Eos, v. 69, no. 4, p. 1508.

Rowley, P.D., Snee, L.W., Mehnert, H.H., Anderson, R.E., Axen, G.J., Burke, K.J., Simonds, F.W., Shroba, R.R., and Olmore, S.D., 1992, Structural setting of the Chief mining district, eastern Chief Range, Lincoln County, Nevada, chapter H *in* Thorman, C.H., ed., Application of structural geology to mineral and energy resources of the central and western United States: U.S. Geological Survey Bulletin 2012, p. H1–H17.

Rowley, P.D., Steven, T.A., Anderson, J.J., and Cunningham, C.G., 1979, Cenozoic stratigraphic and structural framework of southwestern Utah: U.S. Geological Survey Professional Paper 1149, 22 p.

Scott, R.B., Grommé, C.S., Best, M.G., Rosenbaum, J.G., and Hudson, M.R., 1995, Stratigraphic relationships of Tertiary volcanic rocks in central Lincoln County, southeastern Nevada, Chapter A *in* Scott, R.B., and Swadley, W C, eds., Geologic studies in the Basin and Range–Colorado Plateau transition in southeastern Nevada, southwestern Utah, and northwestern Arizona, 1992: U.S. Geological Survey Bulletin 2056, p. 5–42.

Siders, M.A., Rowley, P.D., Shubat, M.A., Christenson, G.E., and Galyardt, G.L., 1990, Geologic map of the Newcastle quadrangle, Iron County, Utah: U.S. Geological Survey Geologic Quadrangle Map GQ–1690, scale 1:24,000.

Siders, M.A., and Shubat, M.A., 1986, Stratigraphy and structure of the northern Bull Valley Mountains and Antelope Range, Iron County, Utah, *in* Griffen, D.T., and Phillips, W.R., eds., Thrusting and extensional structures and mineralization in the Beaver Dam Mountains, southwestern Utah: Utah Geological Association Publication 15, p. 87–102.

Steiger, R.H., and Jäger, Emile, 1977, Subcommission on geochronology—Convention on the use of decay constants in geo- and cosmochronology: Earth and Planetary Science Letters, v. 36, p. 359–362.

Streckeisen, A., 1976, To each plutonic rock its proper name: Earth Science Reviews, v. 12, p. 1-33.

Tobey, E.F., 1976, Geology of the Bull Valley intrusive-extrusive complex and genesis of the associated iron deposits: Eugene, Oreg., University of Oregon Ph. D. dissertation, 244 p.

Van Kooten, G.K., 1988, Structure and hydrocarbon potential beneath the Iron Springs laccolith, southwestern Utah: Geological Society of America Bulletin, v. 100, no. 11, p. 1533–1540.

Williams, P.L., 1967, Stratigraphy and petrography of the Quichapa Group, southwestern Utah and southeastern Nevada: Seattle, Wash., University of Washington Ph. D. dissertation, 182 p.

Williams, V.S., in press, Geologic map of the central Escalante Desert area, Iron County, Utah: U.S. Geological Survey Miscellaneous Investigations Map I–2547, scale 1:50,000.

Local Contraction Along the Pahranagat Shear System, Southeastern Nevada

By Barbara Byron

GEOLOGIC STUDIES IN THE BASIN AND RANGE–COLORADO PLATEAU TRANSITION IN SOUTHEASTERN NEVADA, SOUTHWESTERN UTAH, AND NORTHWESTERN ARIZONA, 1995

U.S. GEOLOGICAL SURVEY BULLETIN 2153–M

UNITED STATES GOVERNMENT PRINTING OFFICE, WASHINGTON : 1997

CONTENTS

FIGURES

TABLE

Local Contraction Along the Pahranagat Shear System, Southeastern Nevada

By Barbara Byron[1]

ABSTRACT

New geologic mapping near a conspicuous overhanging fault scarp on a splay of the left-lateral Maynard Lake fault zone, one of three major fault zones composing the Pahranagat shear system of southeastern Nevada, has identified contraction coeval with regional Cenozoic extension. Left-lateral strike-slip movement along the northeast-striking Maynard Lake fault zone generally accommodates differential extension. The study area along an east-striking splay fault zone that branches from a major strand of the Maynard Lake fault zone, however, contains structures that accommodate contraction. These structures are found in Miocene ash-flow tuffs and in upper Tertiary to lower Quaternary basin-fill deposits. A gently plunging upright close syncline is present in the eastern map area and a gently plunging upright close anticline and syncline are present in the western map area. The southern limb of the western syncline is overturned and cut by three east-striking high-angle faults—a northern, middle, and southern fault. Shear-sense indicators on the northern fault recorded reverse movement, while those on the middle fault recorded left-lateral strike-slip movement. The southern fault experienced oblique movement with both left-lateral and high-angle reverse components of slip. Computer analyses of fault-slip data indicate a normal faulting stress regime with an east-west extension direction.

INTRODUCTION

Contractional deformation is not expected in the classic extensional terrain of the Basin and Range. This study, however, describes contractional structures found during new geologic mapping near a conspicuous overhanging fault scarp (fig. 1) within the Pahranagat shear system, in the Basin and Range province of southeastern Nevada, and proposes an explanation for their occurrence. The fault scarp is one of three closely spaced high-angle faults constituting an east-striking splay fault zone that branches from the main strand of the northeast-striking Maynard Lake fault zone. The study area lies along the Maynard Lake fault zone at the south end of the Hiko Range, 22 km southeast of Alamo and 4 km east of Pahranagat National Wildlife Refuge in Lincoln County, Nev. (fig. 2). Recent geologic mapping is of an 8 km^2 area in the northeast corner of the Lower Pahranagat Lake 7.5-minute quadrangle (Barbara Byron and R.B. Scott, unpub. data, 1991) (fig. 3). Fault-slip data were collected from this area and then compiled and analyzed to determine paleostress orientations.

The Pahranagat shear system was previously mapped in two regional 1:250,000-scale maps of Lincoln County, one of the pre-Cenozoic units by Tschanz and Pampeyan (1970) and the other of Cenozoic units by Ekren and others (1977). More recently, an unpublished geologic synthesis of the Pahranagat 1°×30' quadrangle at a scale of 1:100,000 (A.S. Jayko, written commun., 1992) includes the study area but does not reveal the contractional structures found by the larger scale mapping (1:24,000) of this study. The adjoining Delamar 3 NW 7.5-minute quadrangle to the east was mapped (1:24,000) by Scott and others (1990).

ACKNOWLEDGMENTS

I am grateful to R.B. Scott for introducing me to the conspicuous overhanging scarp and for valuable field instruction and discussion while I was a volunteer field assistant in the U.S. Geological Survey Volunteer for Science Program. I thank R.B. Scott, M.R. Hudson, and P.D. Rowley for painstaking, helpful reviews of earlier versions of this paper.

GEOLOGIC SETTING

The Pahranagat shear system was first described by Tschanz and Pampeyan (1970) as a set of three parallel northeast-striking post-Miocene left-lateral strike-slip fault zones. The southernmost of these is the Maynard Lake fault zone (fig. 2). Following Wright and Troxel's proposal

[1]2456 West 3rd Avenue, Durango, CO 81301.

(1970) that right-lateral offset on the northwest-striking northern Death Valley/Furnace Creek fault was due to marked differences in extension along opposite sides of the fault, subsequent studies throughout the Basin and Range have utilized differential extension to explain strike-slip movement. (See, among others, Anderson, 1973; Davis and Burchfiel, 1973; Lawrence, 1976; Bohannon, 1979; Guth, 1981; Wernicke and others, 1982; Cemen and others, 1985; Clayton, 1988; Weber and Smith, 1987.) The Pahranagat shear system formed to accommodate differential extension (Tschanz and Pampeyan, 1970; Liggett and Ehrenspeck, 1974; Davis, 1979; Jayko, 1990) between more highly extended areas to the northwest and less extended areas to the southeast. Left-lateral offset across the fault system was synchronous with normal offset on faults on either side of the shear system.

In the broad region surrounding the Pahranagat shear system, Tertiary clastic and volcanic rocks unconformably overlie Paleozoic miogeoclinal strata that were folded and faulted during the Late Cretaceous Sevier orogeny, but only Miocene volcanic rocks and late Tertiary and Quaternary alluvial and colluvial sediments are exposed in the study area. The volcanic rocks consist of five major ash-flow tuffs and a basalt lava flow. The 18.6 Ma Hiko Tuff (sanidine $^{40}Ar/^{39}Ar$ dating, Taylor and others, 1989) is a rhyolitic ash-flow tuff and the oldest unit exposed in the map area. A 15.5 Ma olivine basalt flow (Novak, 1984) separates the older calc-alkalic Hiko Tuff and four younger, more alkaline ash-flow tuffs. The 15.6 Ma Delamar Lake Tuff and the 14.7 Ma Sunflower Mountain Tuff are metaluminous rhyolites (Scott and others, 1995). The two youngest tuffs in the map area have been redefined as members of the Kane Wash Tuff (Scott and others, 1995). The older Grapevine Spring Member is a metaluminous rhyolite dated at 14.67 Ma (Scott and others, 1995) and the younger Gregerson Basin Member is a 14.55 Ma peralkaline comendite (Scott and others, 1995). Further description and discussion of these units are found in a field trip summary by Best and others (1993) and in stratigraphic summaries by Ekren and others (1977), Novak (1984), Rowley and others (1995), and Scott and others (1995). Tertiary and Quaternary sediments are summarized by Scott and others (1990).

METHODS

Geologic mapping on stereopairs of 1:31,250-scale, color aerial photographs was transferred to a 1:24,000-scale topographic base map (Lower Pahranagat Lake 7.5-minute quadrangle). At each of 27 slickenlined surfaces in the study area, the following data were recorded: (1) strike and dip of fault plane, (2) rake of slickenlines, (3) sense of displacement on the slickenlines, (4) orientation of compaction foliation in the ash-flow tuffs, and (5) location on aerial photo.

Sense of slip was determined stratigraphically where possible. Commonly, however, faults were found in homogeneous rock, and the opposing surface of the exposed fault plane was missing. Slip could not, therefore, be determined from the offset of geologic structures or stratigraphic units. These circumstances necessitated using certain fault-plane features (shear-sense indicators) to determine sense of displacement (Angelier and others, 1985; Petit, 1987). Frequent use was made of Riedel shears, tension fractures, and asymmetric grooves.

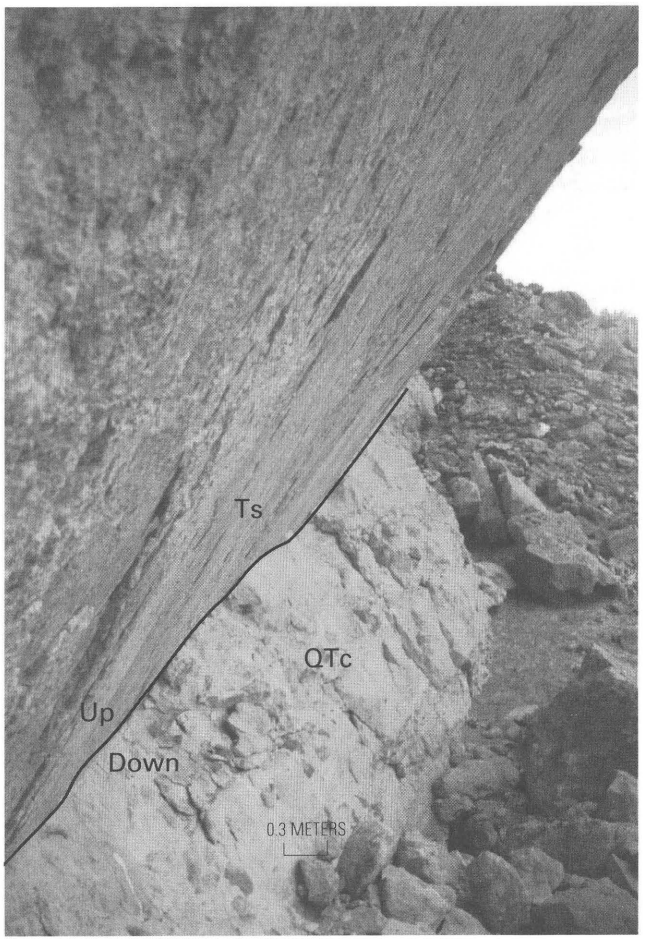

Figure 1. Conspicuous overhanging fault scarp (N. 85° E., 52° NW.) in splay fault zone of Maynard Lake fault zone, juxtaposing Miocene Sunflower Mountain Tuff (Ts) in hanging wall against younger Tertiary-Quaternary conglomerate (QTc) in footwall.

Paleostress orientations were determined using the method of Reches (1987). His computer software requires input of (1) fault dip, (2) direction of fault dip, (3) plunge of slickenline (slip axis), and (4) trend of slickenline (see appendix). Rakes measured in the field were converted to trend and plunge using two trigonometric equations:

$$\tan \beta = \tan r \cos \sigma \quad (1)$$

$$\cos p = \cos r / \cos \beta \quad (2)$$

where β is the angle between the strike of the fault plane and the trend of the slickenline, r is the rake of the slickenline, σ is the dip of the fault plane, and p is the plunge of the slickenline. Calculations of trend and plunge were confirmed by stereographic determinations.

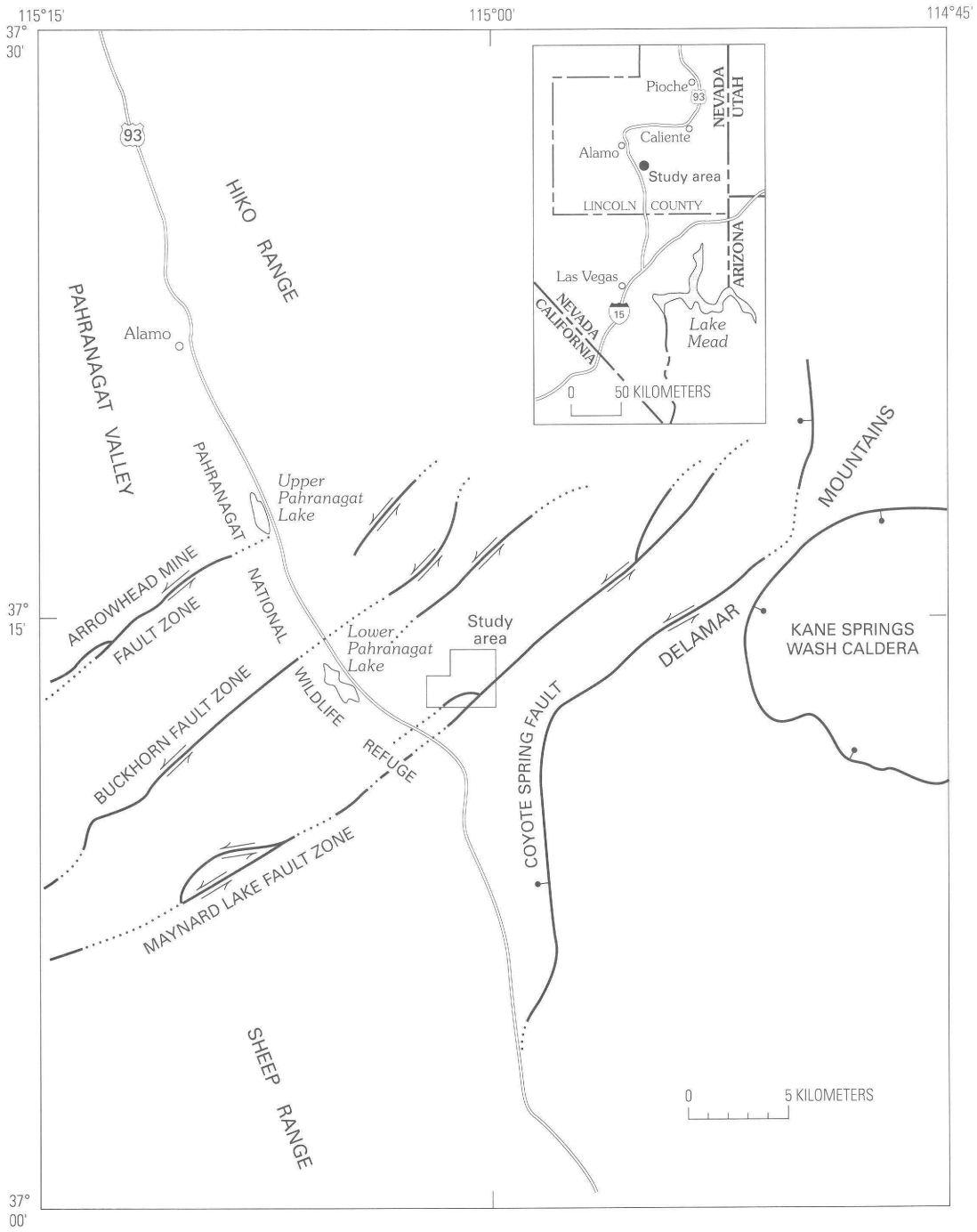

Figure 2. Map showing location of the study area and the three left-lateral fault zones composing the Pahranagat shear system (modified from Ekren and others, 1977, and Scott and others, 1990). The splay of the Maynard Lake fault zone that is the subject of this study is shown branching into the study area. Normal faults shown with bar and ball on downthrown side. Strike-slip faults shown with opposed arrows. Faults dotted where concealed.

RESULTS

Middle to late Tertiary contractional deformation is unexpected in the Basin and Range province of Nevada, for this region is considered to have been affected by generally east west extension at this time (Zoback and others, 1981; Wernicke and others, 1988). In the study area, however, several such contractional structures were mapped. The simplest of these, in the eastern part of the mapped area, is a gently east plunging upright close syncline whose axial trace trends N. 86° E. (parallel to the east-striking splay fault zone) (fig. 3). Rocks are even more deformed (about 40

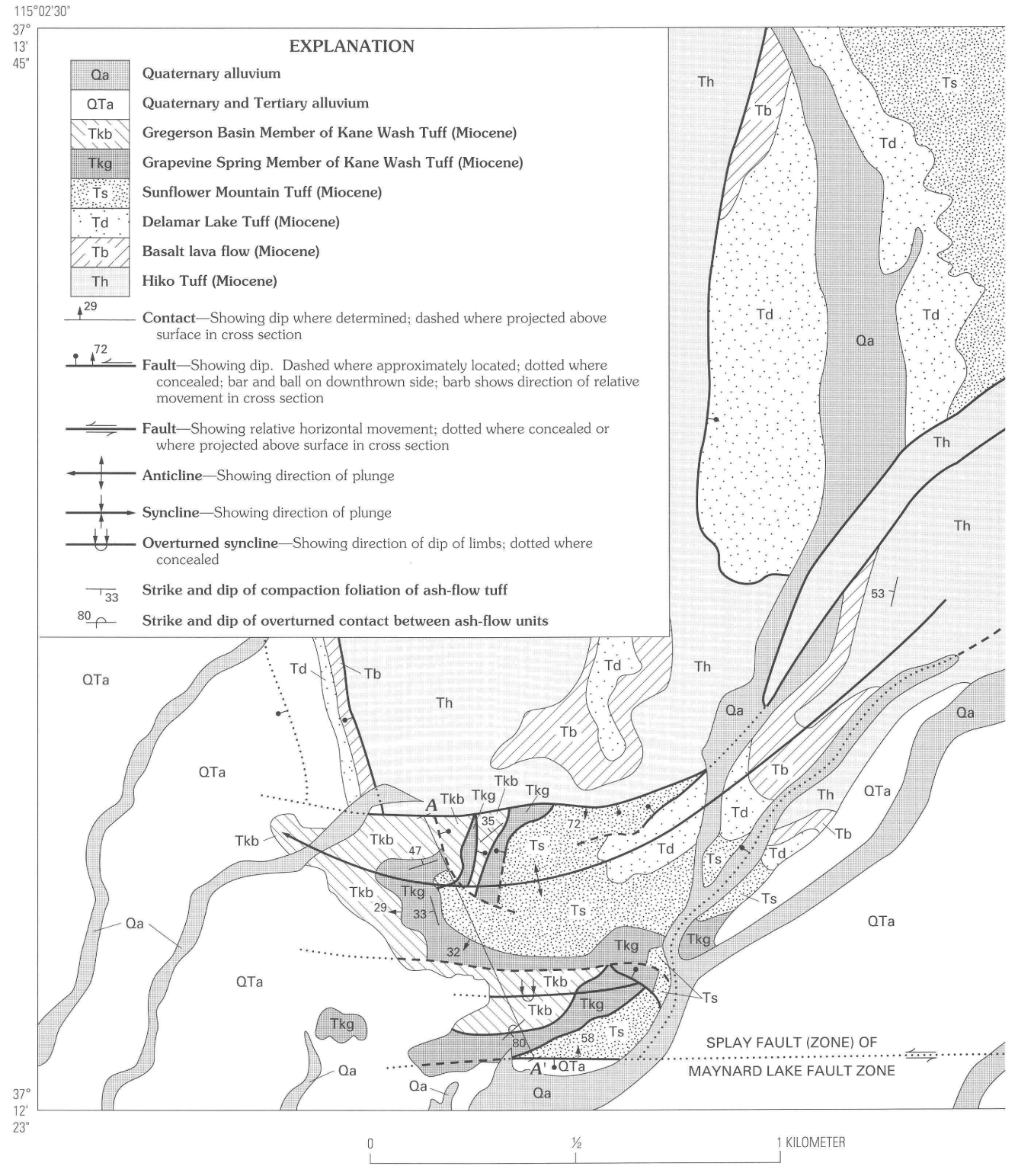

Figure 3 (above and facing page). Geologic map of study area (scale 1:12,000) along splay fault zone of Maynard Lake fault zone. Geology mapped by Barbara Byron and R.B. Scott, 1991. Cross sections show western anticline and overturned syncline along *A–A′* and eastern syncline along *B–B′*.

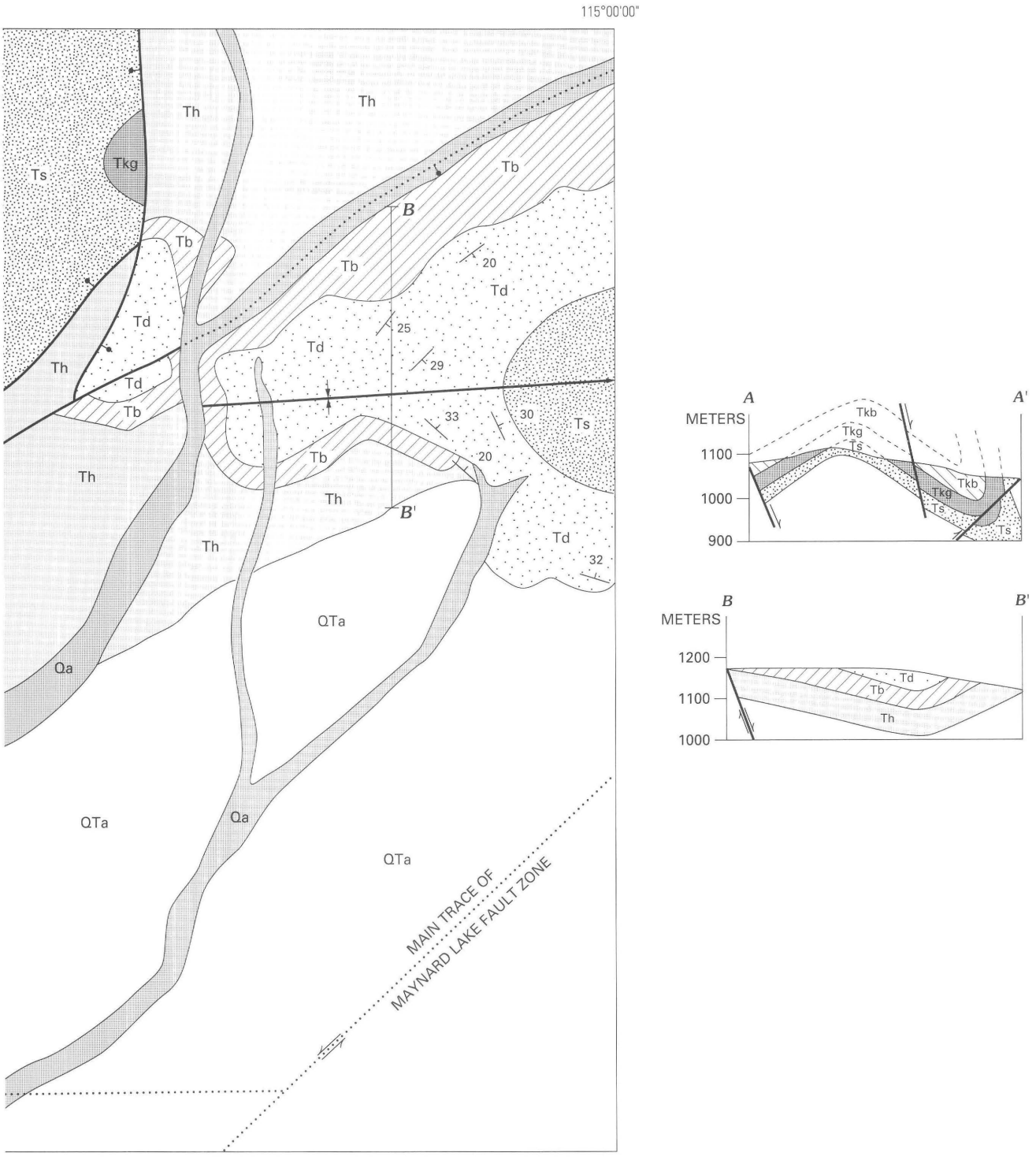
115°00'00"
Th
Th
Ts
Tkg
Tb
B
Tb
Tb
20
Td
Td
25
Td
Th
29
Td
Tb
33
30
Ts
Tb
20
Th
Th
B'
Th
Td
32
QTa
Qa
QTa
Qa
QTa
MAIN TRACE OF
MAYNARD LAKE FAULT ZONE
A
A'
METERS
1100
1000
900
Tkb
Tkg
Ts
Tkb
Tkg
Ts
Ts
B
B'
METERS
1200
1100
1000
Td
Tb
Th

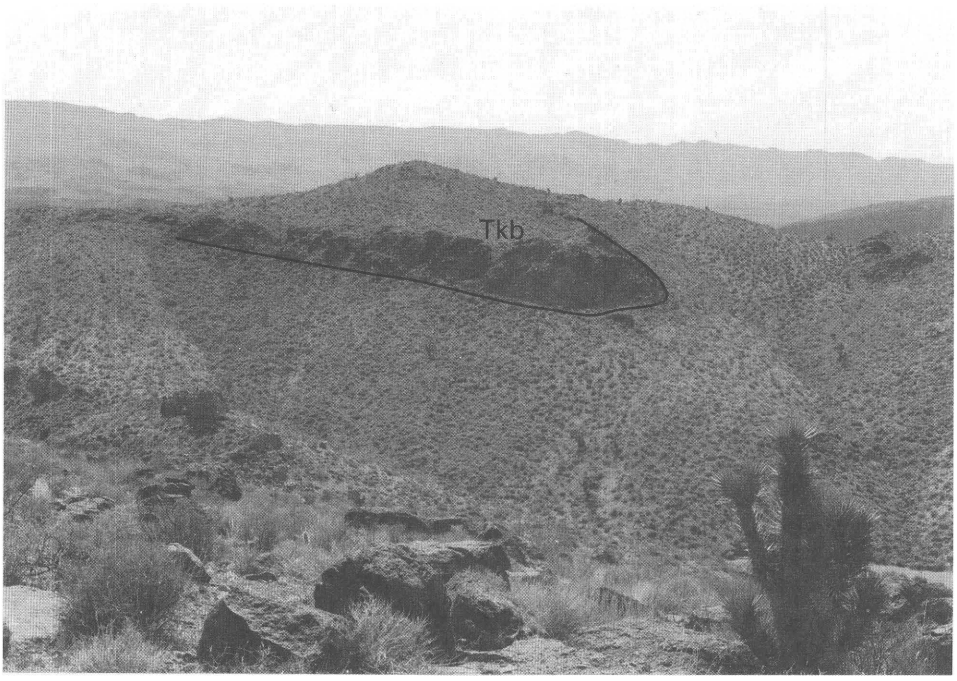

Figure 4. West-northwest-plunging upright close anticline exposed in western map area. Dark unit is the Gregerson Basin Member of the Kane Wash Tuff (Tkb). View toward southeast.

percent north-south shortening) in the western part of the mapped area, where an anticline and overturned syncline are well exposed (fig. 3). The axial trace of the gently west plunging upright close anticline (fig. 4) is curved and changes from trending west-northwest to trending northeast. The anticline is transversely cut by several steeply dipping faults. The southern limb of the western syncline is nearly vertical. At one location the stratigraphic contact between the middle and basal zones of the 14.55 Ma Gregerson Basin Member of the Kane Wash Tuff strikes N. 50° E. and dips 80° SE. Here the stratigraphy is overturned; the densely welded, partly devitrified middle zone of the Gregerson Basin Member is overlain by its partially welded orange base, which is overlain by the older (14.67 Ma) Grapevine Spring Member of the Kane Wash Tuff. This overturned limb is intensely fractured, brecciated, and weathered.

The overturned limb is cut by three subparallel, high-angle, east-west-striking, curviplanar faults referred to as northern, middle, and southern faults. These closely spaced faults are separated in a north-south direction by only a few meters and cannot be shown at map scale, but they clearly demonstrate that the east-west splay (fig. 3) is a fault zone approximately 10 m wide. The splay shown on the map represents the combined lengths of the traces of these three closely spaced subparallel faults.

The attitude of the northern fault is N. 85° E., 83° SE. Several steeply raking grooves on the footwall contain small rock fragments at their upper end. Riedel shears intersect the surface at acute angles and dip southward. These shear-sense indicators indicate reverse movement.

The middle fault, just a few meters south of the northern fault, has an attitude of N. 80° W., 84° NE, and its slickenlines rake from 5° to 10° to the west. Acute angles between the strikes of tension fractures on the hanging wall and the strike of the slickensided fault surface open eastward. Several aligned crescentic fractures on the hanging wall are oriented with their horns pointing eastward. These shear-sense indicators indicate sinistral movement.

The southern fault forms a conspicuous overhang approximately 100 m long by 3 m high. The fault places Miocene Sunflower Mountain Tuff in the hanging wall above younger but undated Tertiary-Quaternary alluvium in the footwall (fig. 1). The average attitude of the fault is N. 85° E., 52° NW. Its surface is partly coated with cemented fault gouge. A few polished (slickensided) surfaces are preserved. Rakes of slickenlines range from 24° to 84° to both east and west. Sets of superposed oblique-slip and dip-slip striations also were observed, but the relative age of the striations was not determined. The footwall conglomerate contains clasts of Tertiary volcanic units that crop out in the area, and several large clasts (as much as 40 cm long) are truncated by the fault.

Fault-slip data from nearly half of the faults in the already small data set are rejected because of large misfit angles (Reches, 1987). Analysis of slip data from the remaining 14 faults (fig. 5; table 1) indicates a nearly horizontal minimum principal stress trending N. 85° E. and a nearly vertical maximum principal stress.

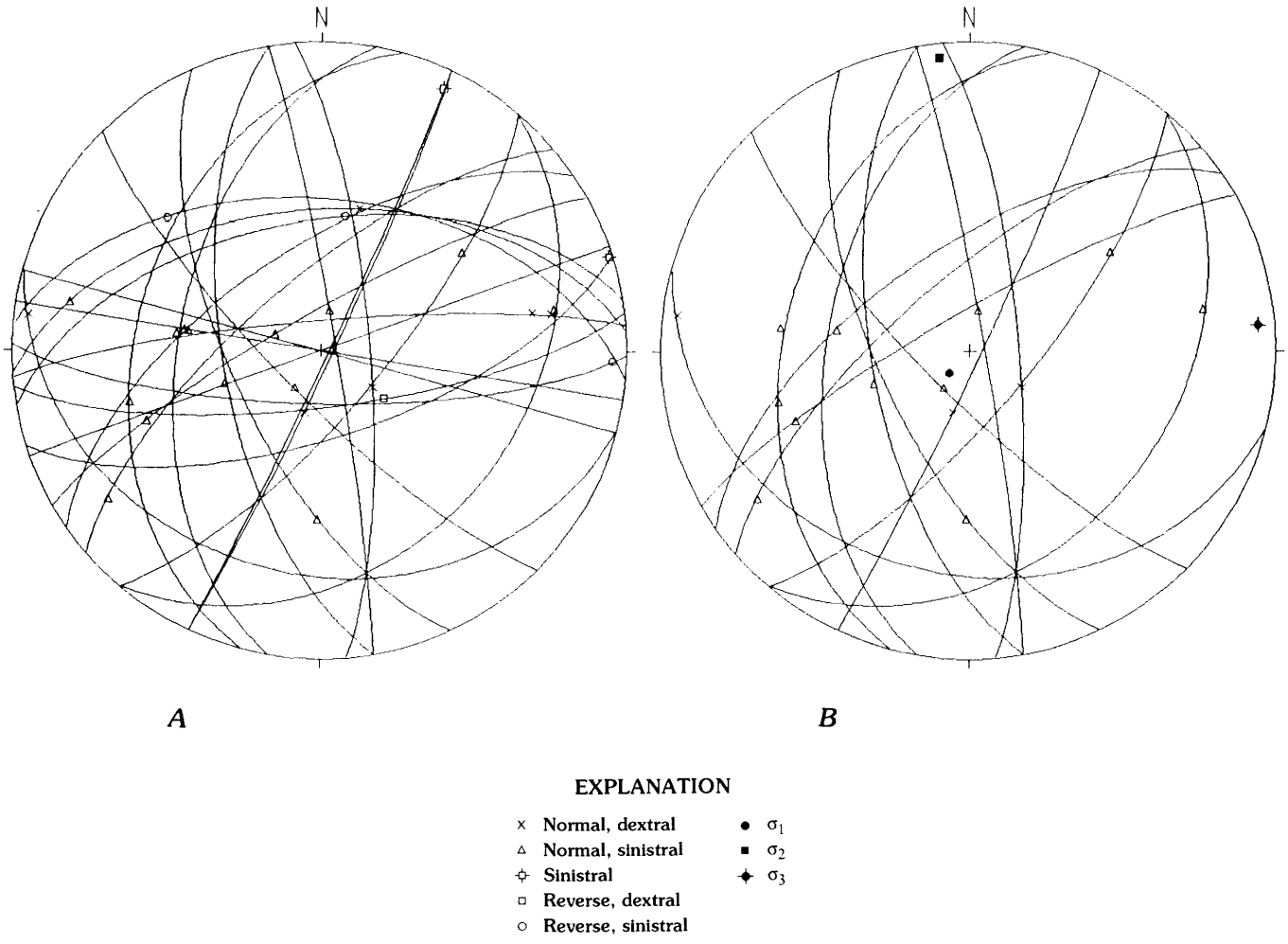

Figure 5. Lower hemisphere equal-area projection of *A*, all faults and fault striae measured; and *B*, selected faults yielding a paleostress solution of a nearly vertical maximum principal stress, σ_1; a nearly horizontal intermediate principal stress, σ_2, trending 354°; and a nearly horizontal minimum principal stress, σ_3, trending 85°.

INTERPRETATION OF RESULTS

Shear-sense indicators on the three high-angle faults that cut the overturned limb of the western syncline indicate mixed modes of faulting. The northern fault had high-angle reverse movement. The middle fault had left-lateral strike-slip movement. The conspicuous overhanging southern fault had oblique movement with both left-lateral and reverse components of slip. Stratigraphic offset verifies the sense of slip on the southern fault. Juxtaposition of the Sunflower Mountain Tuff in the hanging wall against the younger Tertiary-Quaternary conglomerate in the footwall indicates reverse movement on the fault. Several clasts in the conglomerate are truncated by the fault, providing evidence that the conglomerate was indeed involved in the faulting and was not subsequently deposited against the hanging wall. The presence of superposed striae suggests that this fault experienced multiple episodes of movement.

Jayko (1990) reported that the prominent folds within the Pahranagat shear system are drape folds formed in cover rocks over deeper seated, blind normal faults. Most are northeast trending and plunging, but a few trend north-northwest (subparallel to the dominant strike of the normal faults). These folds are generally broad open structures. Folds along the splay in the study area are not of this orientation or geometry.

The three east-striking faults that cut the southern overturned limb of the western syncline are interpreted as a splay fault zone branching from the main northeast strand of the Maynard Lake fault zone. In the adjacent Delamar 3 NW 7.5-minute quadrangle to the east, Scott and others (1990) mapped the main strand of the Maynard Lake fault zone striking N. 40°–50° E. Ekren and others (1977) and Jayko (1990) mapped that main strand as a throughgoing fault to the south of the study area. Strike-slip movement along this main fault strand is constricted by the splay fault zone, and

the fault intersection is an area of local convergence characterized by local contraction. The resulting contractional structures are not unlike those resulting from the buildup of horizontal stresses associated with restraining bends (fig. 6) (Crowell, 1974; Aydin and Page, 1984; Christie-Blick and Biddle, 1985; Ramsey and Huber, 1987; Sylvester, 1988) and compressive stepovers (Aydin and Nur, 1985; Campagna and Aydin, 1991).

Additional work in this area remains. Horizontal slickenlines were noticed on the major east-west fault that cuts the northern limb of the western anticline, but shear sense was not determined. As this fault parallels the subject splay fault, then angles to the northeast to parallel the main trace of the Maynard Lake fault zone (fig. 3), it is quite possible that further shear-sense investigation will reveal left-lateral movement, thus making the splay fault zone much wider than described in this report.

Paleostress analysis depicts a normal faulting stress regime with nearly vertical σ_1 and nearly horizontal σ_2 and σ_3. The least principal stress orientation, N. 85° E., represents an approximately east-west extension direction. Despite the small number of selected faults, the data set shows geometric variability, and the resulting extension direction is consistent with the modern stress field characterizing the Basin and Range province (Zoback and others, 1981; Zoback, 1989).

CONCLUSIONS

1. Several contractional structures are present in a zone of local convergence where an east-striking splay fault zone diverges from a major northeast-striking strand of the left-lateral Maynard Lake fault zone.

2. Local paleostress orientations indicate a normal faulting stress regime with an east-west extension direction.

3. Local contraction along the splay of the Maynard Lake fault zone is coeval with strike-slip faulting and normal faulting.

Table 1. Results of analyses of fault-slip data from 14 selected faults depicted in figure 6*B*.

[Stress ratio, $\phi = (\sigma_2-\sigma_3) / (\sigma_1-\sigma_3) = 0.24$]

Principal stress	Plunge/Trend	Magnitude*
σ_1 (maximum)	82°/222°	1.01
σ_2 (intermediate).	4°/354°	0.33
σ_3 (minimum)	5°/ 85°	0.11

*Normalized by the vertical stress.

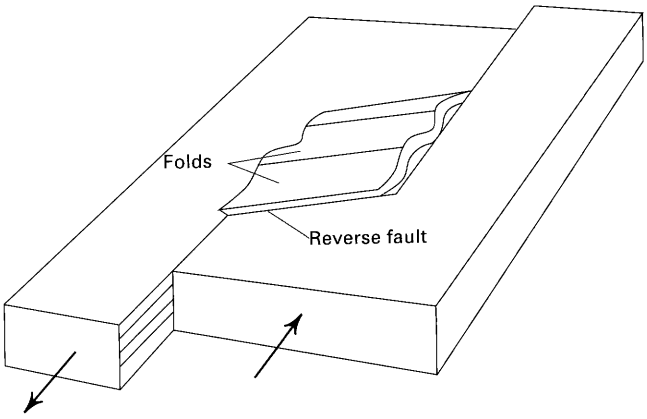

Figure 6. Contractional structures associated with a right-hand bend along a left-lateral strike-slip fault. (From Ramsay and Huber, 1987, with permission of the publisher, Academic Press Ltd., London.)

REFERENCES CITED

Anderson, R.E., 1973, Large-magnitude late Tertiary strike-slip faulting north of Lake Mead, Nevada: U.S. Geological Survey Professional Paper 794, 18 p.

Angelier, Jacques, Colletta, Bernard, and Anderson, R.E., 1985, Neogene paleostress changes in the Basin and Range—A case study at Hoover Dam, Nevada-Arizona: Geological Society of America Bulletin, v. 96, p. 347–361.

Aydin, Atilla, and Nur, Amos, 1985, The types and role of stepovers in strike-slip tectonics, *in* Biddle, K.T., and Christie-Blick, Nicholas, eds., Strike-slip deformation, basin formation, and sedimentation: Society of Economic Paleontologists and Mineralogists Special Publication 37, p. 35–44.

Aydin, Atilla, and Page, B.M., 1984, Diverse Pliocene-Quaternary tectonics in a transform environment, San Francisco Bay region, California: Geological Society of America Bulletin, v. 95, p. 1303–1317.

Best, M.G., Scott, R.B., Rowley, P.D., Swadley, W C, Anderson, R.E., Grommé, C.S., Harding, A.E., Deino, A.L., Christiansen, E.H., Tingey, D.G., and Sullivan, K.R., 1993, Oligocene-Miocene caldera complexes, ash-flow sheets, and tectonism in the central and southeastern Great Basin, *in* Lahren, M.M., Trexler, J.H., Jr., and Spinosa, C., eds., Crustal evolution of the Great Basin and Sierra Nevada: Cordilleran/Rocky Mountain Section, Geological Society of America Guidebook, Department of Geological Sciences, University of Nevada, Reno, p. 285–311.

Bohannon, R.G., 1979, Strike-slip faults of the Lake Mead region of southern Nevada, *in* Armentrout, J.M., Cole, M.R., and ter Best, H., eds., Cenozoic paleogeography of the Western United States-Pacific Coast Paleogeography Symposium 3: Los Angeles, Pacific Section, Society for Economic Paleontologists and Mineralogists, p. 129–139.

Campagna, D.J., and Aydin, Atilla, 1991, Tertiary uplift and shortening in the Basin and Range; the Echo Hills, southeastern Nevada: Geology, v. 19, p. 485–488.

Cemen, Ibrahim, Wright, L.A., Drake, R.E., and Johnson, F.C., 1985, Cenozoic sedimentation and sequence of deformational

events at the southeastern end of the Furnace Creek strike-slip fault zone, Death Valley region, California, *in* Biddle, K.T., and Christie-Blick, Nicholas, eds., Strike-slip deformation, basin formation, and sedimentation: Society of Economic Paleontologists and Mineralogists Special Publication 37, p. 127–141.

Christie-Blick, Nicholas, and Biddle, K.T., 1985, Deformation and basin formation along strike-slip faults, *in* Biddle, K.T., and Christie-Blick, Nicholas, eds., Strike-slip deformation, basin formation, and sedimentation: Society of Economic Paleontologists and Mineralogists Special Publication 37, p. 1–29.

Clayton, R.W., 1988, Fault kinematics and paleostress determined from slickenlines in an area of unusual fault patterns, southwestern Utah: Brigham Young University Geology Studies, v. 35, p. 63–79.

Crowell, J.C., 1974, Origin of Late Cenozoic basins in southern California, *in* Dickinson, W.R., ed., Tectonics and sedimentation: Society of Economic Paleontologists and Mineralogists Special Publication 22, p. 190–204.

Davis, G.A., 1979, Problems of intraplate extensional tectonics, western United States, with special emphasis on the Great Basin *in* Rocky Mountain Association of Geologists–Utah Geological Society 1979 Basin and Range Symposium: p. 41–53.

Davis, G.A., and Burchfiel, B.C., 1973, Garlock Fault—An intracontinental transform structure, southern California: Geological Society of America Bulletin, v. 84, p. 1407–1422.

Ekren, E.B., Orkild, P.P., Sargent, K.A., and Dixon, G.L., 1977, Geologic map of Tertiary rocks, Lincoln County, Nevada: U.S. Geological Survey Miscellaneous Investigations Series Map I–1041, scale 1:250,000.

Guth, P.L., 1981, Tertiary extension north of the Las Vegas Valley shear zone, Sheep and Desert Ranges, Clark County, Nevada: Geological Society of America Bulletin, v. 92, p. 763–777.

Jayko, A.S., 1990, Shallow crustal deformation in the Pahranagat area, southern Nevada, *in* Wernicke, B.P., ed., Basin and Range extensional tectonics near the latitude of Las Vegas, Nevada: Geological Society of America Memoir 176, p. 213–237.

Lawrence, R.D., 1976, Strike-slip faulting terminates the Basin and Range province in Oregon: Geological Society of America Bulletin, v. 87, p. 846–850.

Liggett, M.A., and Ehrenspeck, H.E., 1974, Pahranagat shear system, Lincoln County, Nevada: U.S. National Aeronautics and Space Administration Report CR–136388, 10 p.

Novak, S.W., 1984, Eruptive history of the rhyolitic Kane Springs Wash volcanic center, Nevada: Journal of Geophysical Research, v. 89, p. 8603–8615.

Petit, J.P., 1987, Criteria for the sense of movement on fault surfaces in brittle rocks: Journal of Structural Geology, v. 9, no. 5/6, p. 597–608.

Ramsay, J.G., and Huber, M.I., 1987, The techniques of modern structural geology, Volume 2, Folds and fractures: New York, Academic Press, 529 p.

Reches, Z., 1987, Determination of the tectonic stress tensor from slip along faults that obey the Coulomb yield condition: Tectonics, v. 6, no. 6, p. 849–861.

Rowley, P.D., Nealey, L.D., Unruh, D.M., Snee, L.W., Mehnert, H.H., Anderson, R.E., and Grommé, C.S., 1995, Stratigraphy of Oligocene and Miocene ash-flow tuffs in and near the Caliente caldera complex, southeastern Nevada and southwestern Utah, chapter B *in* Scott, R.B., and Swadley, W C, eds., Geologic studies in the Basin and Range–Colorado Plateau transition in southeastern Nevada, southwestern Utah, and northwestern Arizona, 1992: U.S. Geological Survey Bulletin 2056, p. 43–88.

Scott, R.B., Grommé, C.S., Best, M.G., Rosenbaum, J.G., and Hudson, M.R., 1995, Stratigraphic relationships of Tertiary volcanic rocks in central Lincoln County, southeastern Nevada, chapter A *in* Scott, R.B., and Swadley, W C, eds., Geologic studies in the Basin and Range–Colorado Plateau transition in southeastern Nevada, southwestern Utah, and northwestern Arizona, 1992: U.S. Geological Survey Bulletin 2056, p. 5–42.

Scott, R.B., Page, W.R., and Swadley, W C, 1990, Preliminary geologic map of the Delamar 3 NW quadrangle, Lincoln County, Nevada: U.S. Geological Survey Open-File Report 90-405, scale 1:24,000.

Sylvester, A.G., 1988, Strike-slip faults: Geological Society of America Bulletin, v. 100, p. 1666–1703.

Taylor, W.J., Bartley, J.M., Lux, D.R., and Axen, G.J., 1989, Timing of Tertiary extension in the Railroad Valley–Pioche transect, Nevada—Constraints from $^{40}Ar/^{39}Ar$ ages of volcanic rocks: Journal of Geophysical Research, v. 94, p. 7757–7774.

Tschanz, C.M., and Pampeyan, E.H., 1970, Geology and mineral deposits of Lincoln County, Nevada: Nevada Bureau of Mines and Geology Bulletin 73, 187 p.

Weber, M.E., and Smith, E.I., 1987, Structural and geochemical constraints on the reassembly of disrupted mid-Miocene volcanoes in the Lake Mead–Eldorado Valley area of southern Nevada: Geology, v. 15, p. 553–556.

Wernicke, B.P., Axen, G.J., and Snow, J.K., 1988, Basin and Range extensional tectonics at the latitude of Las Vegas, Nevada: Geological Society of America Bulletin, v. 100, p. 1738–1757.

Wernicke, B.P., Spencer, J.E., Burchfiel, B.C., and Guth, P.L., 1982, Magnitude of crustal extension in the southern Great Basin: Geology, v. 10, p. 499–502.

Wright, L.A., and Troxel, B.W., 1970, Right-lateral displacement in the western Great Basin: Geological Society of America Bulletin, v. 81, p. 2167–2173.

Zoback, M.L., 1989, State of stress and modern deformation of the northern Basin and Range province: Journal of Geophysical Research, v. 94, p. 7105–7128.

Zoback, M.L., Anderson, R.E., and Thompson, G.A., 1981, Cainozoic evolution of the state of stress and style of tectonism of the Basin and Range province of the western United States: Philosophical Transactions of the Royal Society of London, series A, v. 300, p. 407–434.

APPENDIX. DATA USED FOR COMPUTER DETERMINATION OF PALEOSTRESS ORIENTATION

Slip axis is slip direction of hanging block. A negative plunge indicates reverse slip. Asterisk (*) denotes the 14 selected faults yielding an extension direction of N. 85° E./S. 85° W.

Azimuth of dip direction of fault plane	Amount of dip of fault plane	Azimuth of trend of slip axis	Plunge of slip axis
356	52	15	–50
181	76	90	5
350	55	190	–53
162	67	72	0
*325	63	279	54
5	49	311	–34
355	82	81	24
355	82	80	30
9	89	284	53
173	75	127	–69
*130	33	80	23
*195	28	278	4
*245	66	181	44
115	88	25	5
*130	74	55	43
*85	77	125	73
15	89	290	77
160	89	88	87
*80	86	12	79
*225	78	215	78
*319	71	235	17
*115	87	195	73
*260	64	251	63
*285	40	255	36
*280	52	277	51
*330	80	248	39
356	52	281	–21

Structural Geometry Resulting from Episodic Extension in the Northern Chief Range Area, Eastern Nevada

By Kelly J. Burke *and* Gary J. Axen

GEOLOGIC STUDIES IN THE BASIN AND RANGE–COLORADO PLATEAU TRANSITION IN SOUTHEASTERN NEVADA, SOUTHWESTERN UTAH, AND NORTHWESTERN ARIZONA, 1995

U.S. GEOLOGICAL SURVEY BULLETIN 2153–N

UNITED STATES GOVERNMENT PRINTING OFFICE, WASHINGTON : 1997

CONTENTS

FIGURES

Structural Geometry Resulting From Episodic Extension in the Northern Chief Range Area, Eastern Nevada

By Kelly J. Burke[1] *and* Gary J. Axen[2]

ABSTRACT

Tertiary extension repeatedly faulted and rotated Late Proterozoic to Middle Cambrian and Oligocene to Miocene strata in eastern Nevada. Extension was episodic and accommodated by regionally continuous systems of low-angle normal faults and associated steeper normal faults. These faults dipped both east and west in the northern Chief Range area and produced the present geometry of complexly overprinted and rotated fault sets. The structural complexity resulted from major prevolcanic, possible minor synvolcanic, and major late synvolcanic to early postvolcanic episodes of faulting, followed by faulting that produced the present basin-and-range topography.

The earliest of the four episodes of extensional faulting produced the Stampede detachment system, comprising bedding-parallel, low-angle east-dipping faults, and upper plate planar and listric faults. In the hanging wall of the Stampede detachment fault, closely spaced northeast- to northwest-striking faults cut and are cut by transversely oriented dip-slip and strike-slip faults. Bedding dips in the hanging wall, consistent with a faulted syncline-anticline pair in the upper plate, may reflect a local ramp in the basal fault of the Stampede detachment system.

During the second major episode of extension, the low-angle (7°–15°) west-dipping Highland detachment fault formed. Fault displacement opened a syntectonic basin where Miocene McCullough Formation, containing fault scarp facies fanglomerate and landslide breccia and local thin ashfall tuff, was deposited. The hanging wall of the Highland detachment fault was extended on subparallel, moderately to steeply west dipping planar and listric faults. In the footwall of the Highland detachment fault, the moderately east dipping Prospect fault zone offsets the Stampede detachment fault. This same relation is inferred in the hanging wall of the Highland detachment fault west of the map area. The Prospect fault is thus younger than or related to the Stampede detachment fault and older than the Highland detachment fault.

The most recent major episode of extension is represented by the moderately to steeply east dipping Bennett fault. We consider the Bennett fault to be part of the Arizona fault zone, which cuts the Highland detachment fault north of the study area. The Bennett fault also offsets the hanging wall of the Stampede detachment fault, juxtaposing two different structural styles and stratigraphic levels in present exposures. The Burnt Springs Range fault zone, near the southern boundary of the area, obliquely crosscuts the Highland detachment fault and is interpreted there to be a northwest-dipping normal fault rather than a left-lateral strike-slip fault as previously proposed.

The timing of faulting is constrained by dates on volcanic rocks within a transect from Railroad Valley to Pioche. The Stampede detachment fault and probably the Prospect fault are prevolcanic (pre-31.5 Ma) and the Highland detachment fault is late synvolcanic to early postvolcanic (post 18.2–post 15.3 Ma). Early synvolcanic (27–24 Ma) unconformities and minor faults, exposed immediately west of the mapped area, may indicate the additional minor extensional episode. The Bennett fault is probably related to range-bounding faults on the margins of Meadow Valley. If so, it may have been active as recently as 3.5 Ma. Timing of the Burnt Springs Range fault is uncertain but its most recent activity is probably postvolcanic.

The Stampede detachment fault is proposed to be part of a set of east-directed faults of prevolcanic age extending south from the northern Snake Range. The magnitude of this prevolcanic faulting is interpreted to decrease southward. This would explain the relatively small offset on the Stampede detachment fault and the lack of ductile deformation or metamorphism in the northern Chief Range area. In the Mormon Mountains, about 100 kilometers south of the northern Chief Range area, the oldest extensional faults have the same movement sense and are close in age to the west-directed mid-Miocene Highland detachment fault. However, the Caliente caldera complex forms a barrier across which the

[1]USGS volunteer, U.S. Geological Survey, 2255 Gemini Dr., Flagstaff, AZ 86011.

[2] USGS volunteer, University of California, Los Angeles, Box 951567, Los Angeles, CA 90095-1567.

Highland detachment fault cannot be directly correlated to faults in the Mormon Mountains. In general, extension in the northern Chief Range area is accommodated along low-angle basal detachment faults where removal of the hanging wall is compensated by syntectonic sedimentation, possible slight footwall flexure, and collapse of the hanging wall through listric and planar rotational and nonrotational faulting.

INTRODUCTION

Early field observations in the Basin and Range province revealed puzzling relations of younger rocks overlying older rocks along shallowly dipping faults. These fault geometries were generally attributed to Mesozoic to early Tertiary thrust-related deformation (Westgate and Knopf, 1932; Longwell, 1945). The formation of sets of tilt-blocks, bounded by normal faults and detached from an underlying ductilely deformed metamorphic complex, was also assigned to this tectonic episode (Ransome and others, 1910). Other workers explained what Langenheim and others (1969) called "the problem of younger-over-older thrusting" by invoking surficial gravity-sliding (Drewes, 1958) or again, Sevier hinterland attenuation faulting (Hintze, 1978). The latter interpretation reappeared as "omissional faulting" in a paper by Jansma and Speed (1990).

Anderson (1971) and Armstrong (1972) documented normal-sense displacement and late Tertiary movement for a number of low-angle faults. Subsequent geologic field research in the Basin and Range province has led to provocative and partially conflicting interpretations of modes of regional continental extension. Gently dipping Tertiary normal faults and ductile shear zones are now widely believed to accommodate tens of kilometers of horizontal extensional strain (Hamilton and Meyers, 1966; Davis and others, 1980; Davis, 1983; Miller and others, 1983; Wernicke and others, 1988). Disagreement continues over the orientation of these faults during their movement and the amount of displacement across many low-angle extensional faults (detachment faults). In general, the kinematics of low-angle normal fault systems and the nature of driving mechanisms that localize and initiate extension remain controversial.

This study focuses on the geometry and timing of regionally extensive low-angle normal fault systems mapped in the northern Chief and southernmost Highland Ranges (the northern Chief Range area) near Pioche in southeastern Nevada (fig. 1). The northern Chief Range area provides important opportunities for evaluating geometric variations in low-angle extensional faults. Interacting fault networks in the area are well exposed in laterally continuous miogeoclinal strata and well-dated Tertiary volcanic units. These low-angle normal fault systems tilted and displaced strata in several ways rather than by a single end-member process such as domino-style faulting or listric normal faulting. Additionally, end-member models in which (1) extension facilitates magmatism or (2) magmatism drives extension (Sonder and others, 1987; Wernicke and others, 1987; Gans, 1987, 1990, among others) do not account for the variety of geographic and temporal relations between magmatism and extension observed in the northern Chief and nearby ranges (Bartley and others, 1988; Taylor and others, 1989; Axen and others, 1993).

The northern Chief Range area was originally mapped at 1:62,500 scale by Westgate and Knopf (1932). Their map was compiled on the Lincoln County geologic map by Tschanz and Pampeyan (1970). A detailed (1:12,000) geologic map of the Pioche Hills by Park, Gemmil, and Tschanz was published in 1958. In 1977, Ekren and others subdivided and remapped the Tertiary units at a scale of 1:250,000. These maps identified some of the major faults in and near the field area and provided the framework for detailed structural analysis.

ACKNOWLEDGMENTS

We heartily acknowledge P.D. Rowley for many discussions and good company in the field. We thank K.E. Karlstrom and W.J. Taylor for much assistance during this research and L.S. Beard, W.R. Page, and P.D. Rowley for very helpful technical reviews. The study was partly supported by grants from the Sigma Xi Scientific Society, Mobil Oil Corporation, Marathon Oil Corporation, Texaco, and Northern Arizona University.

REGIONAL GEOLOGIC SETTING

Armstrong (1968) and Wernicke and Burchfiel (1982) emphasized that a variety of structural levels are exposed in the Basin and Range province. This variety results from differences in the age of extension or magnitude of extension, or both, across the province. Tectonic models constructed in one region of the province are testable in other regions that represent higher or lower structural levels. Similarly, models relating magmatism to extension must be able to explain variations in volume and age of magmatism. The application of this approach to the northern Chief Range area requires an understanding of temporal and geographic variations in extensional geometries and magmatic histories in surrounding regions.

Well-studied east-west transects to the north and south of the northern Chief Range area (fig. 2) exhibit the results of contrasting magnitudes of extension, different magmatic and extensional histories, and different deformational styles. The northern transect crosses the Snake, Schell Creek, and Egan Ranges (Miller and others, 1983). The southern transect crosses the Mormon Mountains and is referred to as the Lake Mead extensional belt (Wernicke and others, 1984). The study area lies at the east end of a central transect

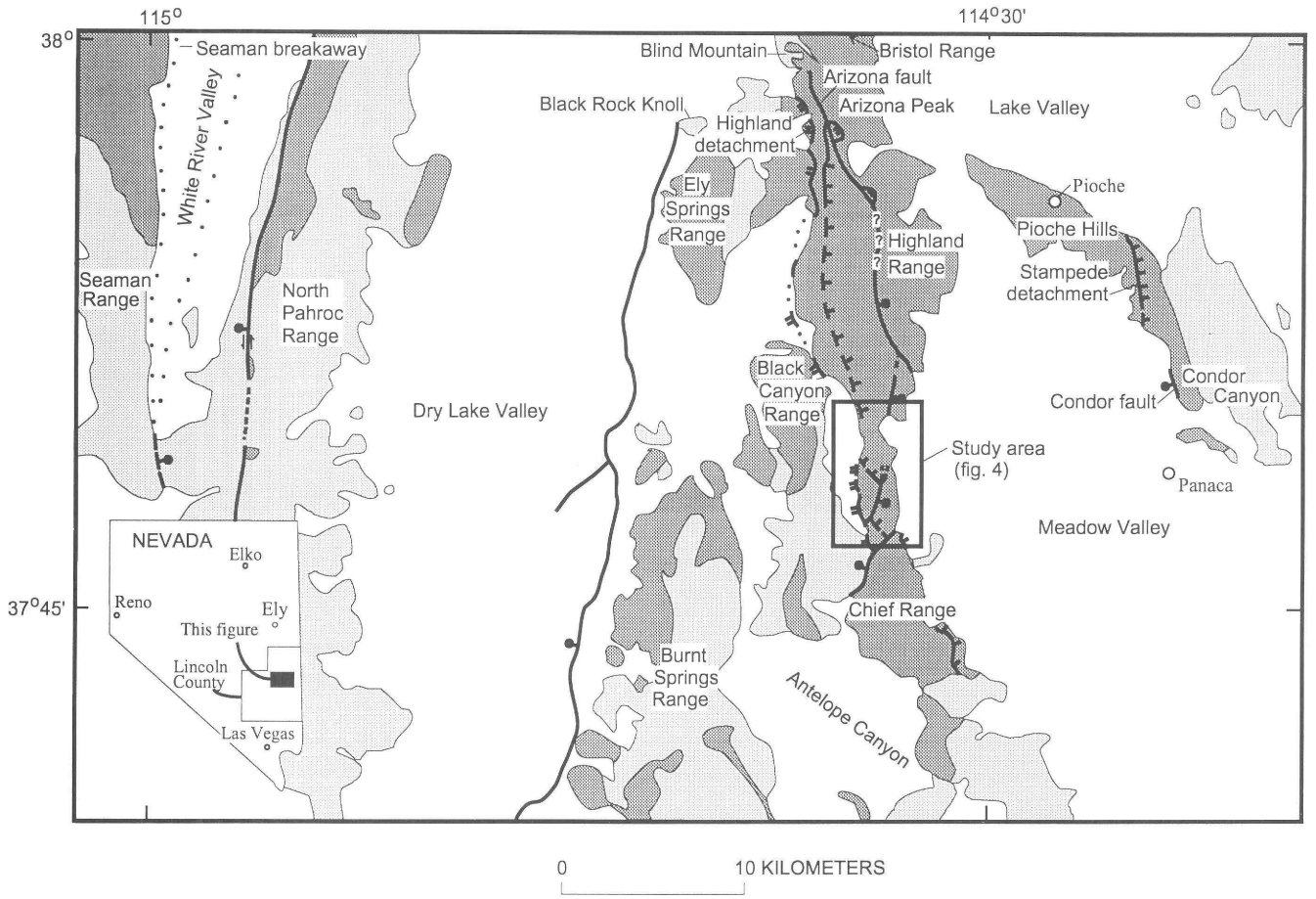

EXPLANATION

Quaternary rocks
Tertiary rocks
Pre-Tertiary rocks

Approximate contact

Oblique slip fault—Dashed where approximate; bar and ball on downthrown side; barbs show direction of relative movement

High-angle normal fault—Dashed where approximate; dotted where concealed; queried where inferred; bar and ball on downthrown side

Highland detachment fault—Dashed where approximate; dotted where concealed; hachures on downthrown side

Stampede detachment fault—Dashed where approximate; dotted where concealed; hachures on downthrown side

Figure 1. Simplified geologic map showing major structural features of northern Chief Range area and adjacent areas around Dry Lake Valley.

at lat 38° N. (fig. 2) (Bartley and others, 1988) that crosses the Grant–Quinn Canyon, Seaman, and Highland–northern Chief Ranges. The ranges in the three transects generally contain uplifted, faulted, and rotated strata of the Cordilleran miogeocline. The sequence exposed in the eastern third of the central transect contains a thick basal clastic section of Late Proterozoic to Early Cambrian age, overlain by a thick, primarily shallow-water carbonate sequence representing Cambrian to Permian sedimentation.

The Sevier orogenic belt runs obliquely northeast-southwest through eastern Nevada (fig. 2), and from north to south, the frontal fold-and-thrust belt is progressively more involved in Tertiary extension (Burchfiel and Davis, 1972; Burchfiel 1975, 1979). Sevier(?) thrusts and folds occur west of the study area, in the Grant and Quinn Canyon Ranges and locally in the Seaman Range and Golden Gate Range area (fig. 2) (Bartley and others, 1988; Bartley and Gleason, 1990). East of the central transect, the structurally highest major frontal thrust of the Sevier belt crops out in the Wah Wah Mountains of western Utah (Hintze, 1980). The Chief and Highland Ranges are in the upper plate of this thrust and in the lower plate of the thrust system exposed in the Grant and Quinn Canyon Ranges.

Metamorphic terranes of several ages crop out in the Grant, Snake, and Egan Ranges. These ranges represent examples of the metamorphic core complexes that form a sinuous belt, part of the eastern Cordilleran metamorphic belt (see for example, Coney, 1980; Haxel and others, 1984). This belt roughly parallels the Sevier frontal thrusts, which lie approximately 400 km or less to the east. Tertiary ages of uplift and latest ductile deformation have been established for most of the core complexes in the belt (Crittenden and others, 1980; Davis, 1977; Davis and others, 1980; Miller and others, 1983). Several major Tertiary calderas formed in or near the central transect (fig. 2). Thick sequences of tuffs and flows are exposed in the central transect, but Tertiary volcanic rocks are less voluminous in the Snake Range (northern) transect and sparse in the Lake Mead extensional belt.

NORTHERN TRANSECT

In the Snake Range, extension along an east-dipping, low-angle normal fault system of Oligocene age unroofed a metamorphic core complex. Faults related to this extensional episode may continue southward into the study area (Taylor and Bartley, 1992). In the northern Snake Range, extension occurred along the northern Snake Range decollement (fig. 2) (Gans, 1982; Miller and others, 1983; Miller and others, 1988), beginning about 30 Ma (Lee, 1993). This earliest extensional system involved top-to-the-east-southeast extension of about 250 percent (Miller and others, 1983) that accumulated episodically but mainly in middle Miocene time (Lee, 1995).

The upper plate of the northern Snake Range decollement was brittlely thinned by two generations of top-to-the-east, rotational, domino-style normal faults formed in Middle Cambrian and younger Paleozoic carbonates. Lower plate rocks, chiefly the Late Proterozoic and Lower Cambrian Prospect Mountain Quartzite and Lower and Middle Cambrian Pioche Shale at present exposure levels, were ductilely deformed, metamorphosed, and intruded by granitoid magmas during Jurassic, Cretaceous, and Tertiary tectonic events (Miller and others, 1988). Miller and others (1983) interpreted the northern Snake Range decollement to be the uplifted brittle-ductile transition. Alternatively, Lee (1993, 1995) interpreted thermal history data to be consistent with domino-style faulting or with a rolling hinge detachment fault model (Wernicke and Axen, 1988).

The southern Snake Range decollement was treated independently from the northern Snake Range decollement (Miller and others, 1988) despite similarities in structural level, timing, and transport direction. An alternate interpretation is that the southern Snake Range decollement represents the southward continuation of the northern Snake Range decollement (Bartley and Wernicke, 1984; Taylor and others, 1989; McGrew, 1993). Also, metamorphic grade decreases southward through the southern Snake Range, where Precambrian McCoy Creek Group rocks underlie the Prospect Mountain Quartzite (Miller and others, 1988; McGrew, 1993). Calderas of the Indian Peak caldera complex (fig. 2) (Best, Christiansen, and Blank, 1989; Best, Christiansen, and others, 1989), the westernmost of which is in the Wilson Creek Range, separate the southern Snake Range from the Chief and Highland Ranges to the south.

SOUTHERN TRANSECT

In contrast to the northern transect, the Lake Mead extensional belt of southern Nevada (fig. 2) exhibits a top-to-the-west episode of extension. Extension in the belt began later, between 17–19 Ma and 8.5 Ma, and continued locally through Quaternary time (Bohannon, 1984; Wernicke and others, 1985, 1989). Faulting probably began in the southern transect when top-to-the-west mid-Miocene faults were active in the northern Chief Range area. The Cretaceous Sevier foreland fold-and-thrust belt, well exposed in the Lake Mead extensional belt, was dismembered there by normal faults, some of which reactivated parts of the thrusts (Wernicke and others, 1985; Smith and others, 1987; Axen and others, 1990; Axen, 1993). In contrast, exposures of Sevier-related structures in the study area are lacking. Also, Tertiary metamorphism and ductile deformation did not affect the southern transect (Wernicke and others, 1985).

Figure 2 (facing page). Location map and geologic setting of eastern Nevada, southwestern Utah, and northwestern Arizona. White boxes show the three transects discussed in text.

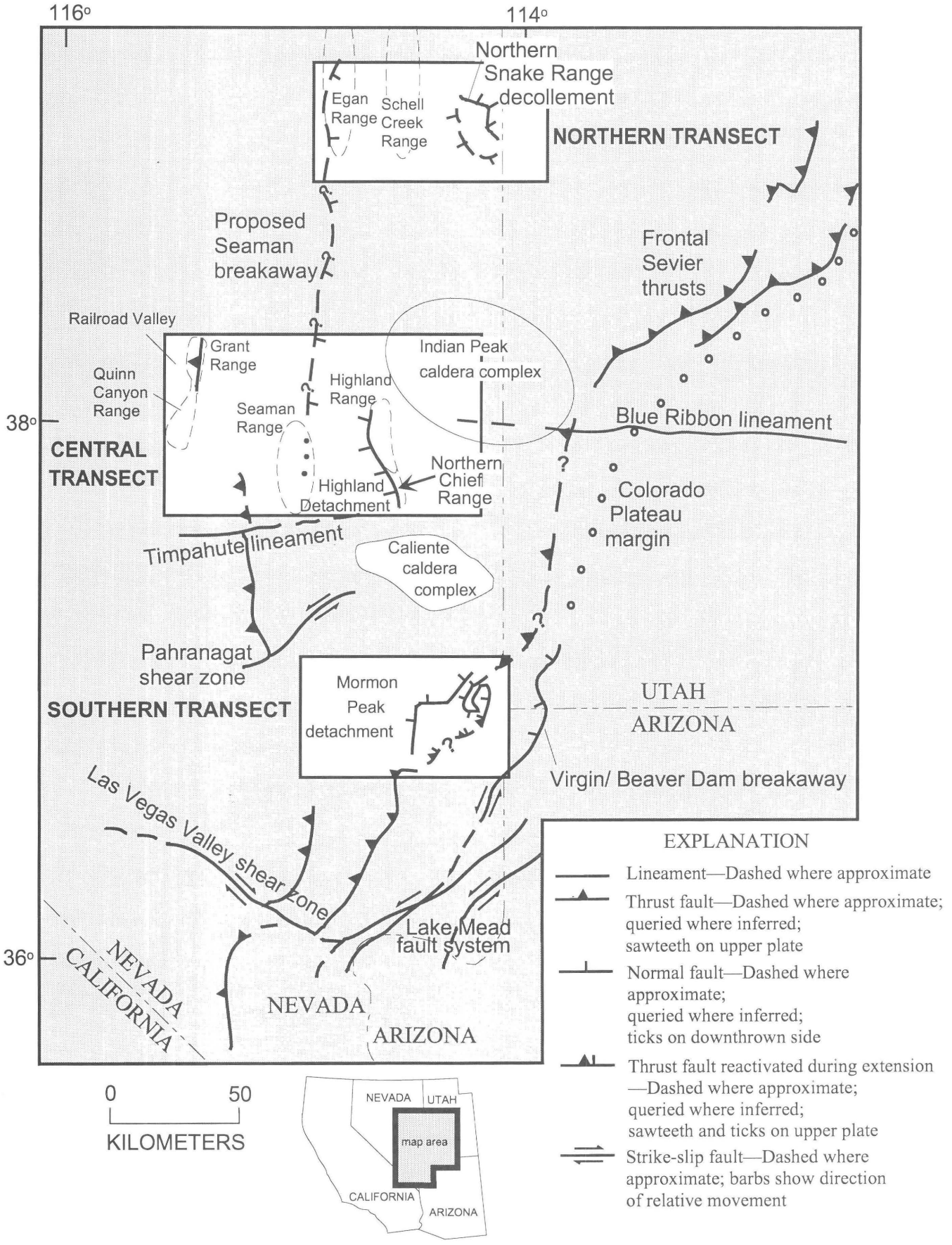
116°
114°
38°
36°
Northern Snake Range decollement
Egan Range
Schell Creek Range
NORTHERN TRANSECT
Proposed Seaman breakaway
Frontal Sevier thrusts
Railroad Valley
Grant Range
Quinn Canyon Range
Seaman Range
Highland Range
Indian Peak caldera complex
Blue Ribbon lineament
CENTRAL TRANSECT
Highland Detachment
Northern Chief Range
Colorado Plateau margin
Timpahute lineament
Caliente caldera complex
Pahranagat shear zone
SOUTHERN TRANSECT
Mormon Peak detachment
UTAH
ARIZONA
Virgin/ Beaver Dam breakaway
Las Vegas Valley shear zone
Lake Mead fault system
NEVADA
CALIFORNIA
NEVADA
ARIZONA
0
50
KILOMETERS
NEVADA
UTAH
map area
CALIFORNIA
ARIZONA
EXPLANATION
Lineament—Dashed where approximate
Thrust fault—Dashed where approximate; queried where inferred; sawteeth on upper plate
Normal fault—Dashed where approximate; queried where inferred; ticks on downthrown side
Thrust fault reactivated during extension —Dashed where approximate; queried where inferred; sawteeth and ticks on upper plate
Strike-slip fault—Dashed where approximate; barbs show direction of relative movement

Wernicke and others (1988) interpreted detachment fault systems in the southern transect to have accommodated west-southwest extension of about 100 percent, and presented evidence for footwall uplift by isostatic rebound. The hanging walls of the faults are internally extended along high- and low-angle brittle faults that flatten into or are truncated by the detachment faults. Alternatively, Anderson and Barnhard (1993a,b) and Anderson and Bohannon (1993) proposed that footwall blocks are uplifted and tilted below concave-down faults and that the uplift was accommodated by overlying discontinuous gently dipping attenuation zones.

Relatively small volumes of Tertiary volcanic rocks were deposited in the area of the southern transect. The Caliente caldera complex (Rowley and others, 1992) forms the northern geologic boundary of the Lake Mead extensional belt (fig. 2) (Wernicke and others, 1989). Eruptions from the Caliente caldera complex, from about 26–18.2 Ma and prior to the onset of extension to the south, deposited a thick sequence of ash-flow tuffs across the central transect (Best, Christiansen, and Blank, 1989; Best, Christiansen, and others, 1989; McKee and others, 1993; Rowley and others, 1995; Scott and others, 1995).

CENTRAL TRANSECT

These differences in timing and orientation of faulting, between the northern and southern transects, make the central transect a key area for understanding the transition from north to south. The central transect is characterized by (1) extensive volcanism; (2) episodic extension that is pre-, syn-, and postvolcanic; (3) complex overprinting of variably oriented fault sets, basal detachment faults, and accommodation structures such as transfer faults; (4) brittle deformation and general absence of metamorphism; and (5) faults that generally do not reactivate preexisting structures (Bartley and others, 1988).

A thick sequence of Tertiary volcanic units in the central transect records the longest continuous volcanism among the three transects. Most of the ash-flow tuffs and lava flows are well dated by K/Ar and $^{40}Ar/^{39}Ar$ methods. The ash-flow tuffs are particularly useful structural markers because of their lateral continuity and relatively instantaneous emplacement.

Bartley and others (1988) and Taylor and others (1989) documented four periods of extension in the 130-km-long central transect (fig. 2): prevolcanic (pre-32 Ma), early synvolcanic (30–27 Ma), late syn- to early postvolcanic (about 18.2–14 Ma), and Pliocene to Quaternary. Rowley and others (1992), however, found no evidence for the early synvolcanic episode. Bartley and others (1988) divided the transect into three areas that differ in magnitude of Tertiary extension and degree of Mesozoic disruption. From east to west these are (1) the Dry Lake Valley area, highly extended in Cenozoic time (including the Chief, Highland, Pahroc, and other ranges), (2) the Seaman and Golden Gate Range area, containing Mesozoic thrusts and folds overprinted by minor Tertiary extension, and (3) the Grant and Quinn Canyon Range area, exhibiting substantial Tertiary extension superimposed on Mesozoic folds, thrusts, small intrusions, and local metamorphic rocks (figs. 1, 2).

The first period of extension affected only the Dry Lake Valley area. The Stampede detachment fault (Bartley and others, 1988) and the Seaman breakaway (Taylor and Bartley, 1992; fig. 1) constitute a prevolcanic, top-to-the-east normal fault system. This fault system is probably Oligocene in age (Taylor and Bartley, 1992) but could be older (see discussion of similar faults in Utah, in Nutt and Thorman, 1992). Minor faults and unconformities within the 30–27 Ma volcanic rocks and possibly, the low-angle Troy Peak fault in the Grant Range may represent extension during the second (synvolcanic) period that, along with all younger faulting episodes, affected the entire transect (Bartley and others, 1988).

The gently west dipping Highland detachment fault (Axen, 1986), originally mapped as a thrust fault (Westgate and Knopf, 1932; Langenheim and others, 1969; Tschanz and Pampeyan, 1970) (fig. 1) is a major structure active during the third extensional period. It formed north-trending synextensional basins where fanglomerate and breccia of the Miocene McCullough Formation were deposited (Axen, Lewis, and others, 1988). Most of the high-angle, generally oblique slip faults in the Chief Range and southward formed during this period (Rowley and others, 1992). Recent faults in Railroad Valley may have been active in mid-Miocene time also, and west-dipping faults in the Grant and Quinn Canyon Ranges are interpreted to be similar in age and orientation to the Highland detachment fault (Bartley and others, 1988).

The youngest faults in the transect are exemplified by the Condor fault (fig. 1) (Axen, Burke, and Fletcher, 1988). The Miocene and Pliocene Panaca Formation is cut by the Condor fault and overlaps it. The range-bounding faults on both sides of Meadow Valley are interpreted to be coeval with the Condor fault and the Arizona fault, which cuts the Highland detachment fault near Arizona Peak (fig. 1). Quaternary faults are exposed along the east edges of Dry Lake Valley and Railroad Valley (Bartley and others, 1988).

A probable piercing point formed by an offset granitic body in the Highland Range (Axen, Lewis, and others, 1988) indicates west-southwest extension of the transect, at least during Highland detachment fault activity. This orientation agrees with extension directions documented to the south in Rainbow Canyon (Bowman, 1985; Michel-Noël and others, 1990) and in the Lake Mead extensional belt (Wernicke and others, 1984, 1985; Smith and others, 1987). The magnitude of extension across the transect is not presently well constrained, but local areas record 30–110 percent extension (Axen, 1986; Lewis, 1987; Sleeper, 1989; Burke, 1991).

Throughout the central transect, high- and low-angle planar and curviplanar faults brittlely extended the upper plates of gently dipping detachment faults above less deformed lower plates. Current mapping in and near the Caliente caldera complex (Rowley and Shroba, 1991; Rowley and others, 1994; Swadley and Rowley, 1994) has reinterpreted some of the extensional deformation in the transect to be accommodated by a heterogeneous combination of high- and low-angle faults with normal, oblique and strike-slip motion. Younger faults in the transect have generally not reactivated either older Tertiary extensional faults or Mesozoic thrusts, but tend to cut discordantly across older structures, even opposing previous orientation; for example, the west-dipping Highland detachment fault cuts the east-dipping Stampede detachment fault.

LITHOLOGIC UNITS IN THE NORTHERN CHIEF RANGE AREA

Tertiary extensional faults in the northern Chief and southernmost Highland Ranges disrupted miogeoclinal clastic and carbonate strata, and the overlying Tertiary volcanic and sedimentary sequence. In ascending order (fig. 3), the Precambrian and Paleozoic stratigraphy in the study area includes the latest Proterozoic to Lower Cambrian Prospect Mountain Quartzite, the Lower and Middle Cambrian Pioche Shale, Middle Cambrian Lyndon Limestone and Chisholm Shale, and the Middle and Upper Cambrian Highland Peak Formation (Westgate and Knopf, 1932; Wheeler, 1940; Merriam, 1964; Tschanz and Pampeyan, 1970). These units have been correlated with those in the southern Great Basin (fig. 3) (Stewart, 1974). The upper Highland Peak Formation corresponds to the Banded Mountain Member of the Bonanza King Formation in southern Nevada (Tschanz and Pampeyan, 1970). Recognition of mappable members in the Highland Peak Formation (fig. 3) (Westgate and Knopf, 1932; Merriam, 1964; Burke, 1991) was essential to detailed mapping of faults and offsets in this study.

Regionally extensive outflow sheets of Tertiary ashflow tuffs and local Tertiary lava flows and sedimentary rocks (figs. 3, 4) overlie the Paleozoic units with angular unconformity. Limited exposures of volcanic rocks in the southwest part of the mapped area project into a more continuous section mapped to the south (Rowley and others, 1994). The Tertiary section has been described by Best, Christiansen, and Blank (1989), Best, Christiansen, and others (1989), McKee and others (1993), Rowley and others (1995), and Scott and others (1995). The ash-flow tuffs include, from base to top, the Lund Formation (27.9 Ma) of the Needles Range Group; the Isom Formation (27 Ma; Best, Christiansen, and Blank, 1989; Best, Christiansen, and others, 1989); the Leach Canyon Formation (24 Ma); the Swett Tuff and Bauers Tuff Members (23 Ma) of the Condor Canyon Formation, and the Harmony Hills Tuff (22 Ma) of the Quichapa Group (Anderson and Rowley, 1975); the Pahranagat Formation (23 Ma; Scott and others, 1995); and the Hiko Tuff (18.2 Ma; Rowley and others, 1995). Andesitic flow rocks are interlayered with the Harmony Hills and Hiko Tuffs. Unnamed rhyolite tuffs locally overlying the Hiko Tuff were mapped with the Hiko. The Miocene McCullough Formation, comprising fanglomerate, landslide breccia sheets, tuffaceous sandstone, and thin ashfall tuff, overlies the volcanic rocks.

STRUCTURAL ANALYSIS

Mapping during this study revealed that the stratigraphic section was cut and rotated during at least three and possibly four episodes of normal faulting that can be correlated with the four regional extensional periods in the central transect. Faulting occurred along five main structural features exposed in the map area: (1) the north-northwest-striking, east-dipping Stampede detachment fault (Axen, Lewis, and others, 1988), (2) the north-striking, east-dipping Prospect fault, (3) the north-striking, west-dipping Highland detachment fault (Westgate and Knopf, 1932; Langenheim and others, 1969; Tschanz and Pampeyan, 1970; Axen, 1986), (4) the north-striking, east-dipping Bennett fault, and (5) the northeast-striking Burnt Springs Range fault zone (Tschanz and Pampeyan, 1970; Ekren and others, 1977) (fig. 4). The geometry and timing of structures related to the four episodes of faulting are presented below. Absolute timing constraints are derived from areas elsewhere in the central transect, but relative age constraints from crosscutting and overlap relationships in the study area are consistent (Bartley and others, 1988; Taylor and others, 1989).

STAMPEDE DETACHMENT FAULT SYSTEM AND PROSPECT FAULT—PREVOLCANIC EXTENSION

The east-dipping Stampede detachment fault was mapped as part of the Highland "thrust" (Tschanz and Pampeyan, 1970). Axen, Lewis, and others (1988) named the fault for exposures in Stampede Gap and mapped the fault southward along the Highland Range (fig. 4). The fault extends through the northern Chief Range area (Burke, 1991) and south to Antelope Canyon, just north of Caliente, Nev. (Callaghan, 1936; Rowley and others, 1994). It is also exposed in the Bristol Range (fig. 1), north of the Highland Range (W.R. Page, written commun., 1995).

In the Ely Springs Range (fig. 1), west of the Highland Range, east-dipping normal faults interpreted to lie in the hanging wall of the Stampede detachment fault are overlapped by a 31.5 Ma ashflow tuff (Axen, Lewis, and others, 1988; Taylor and others, 1989). Near Gray Cone, in the

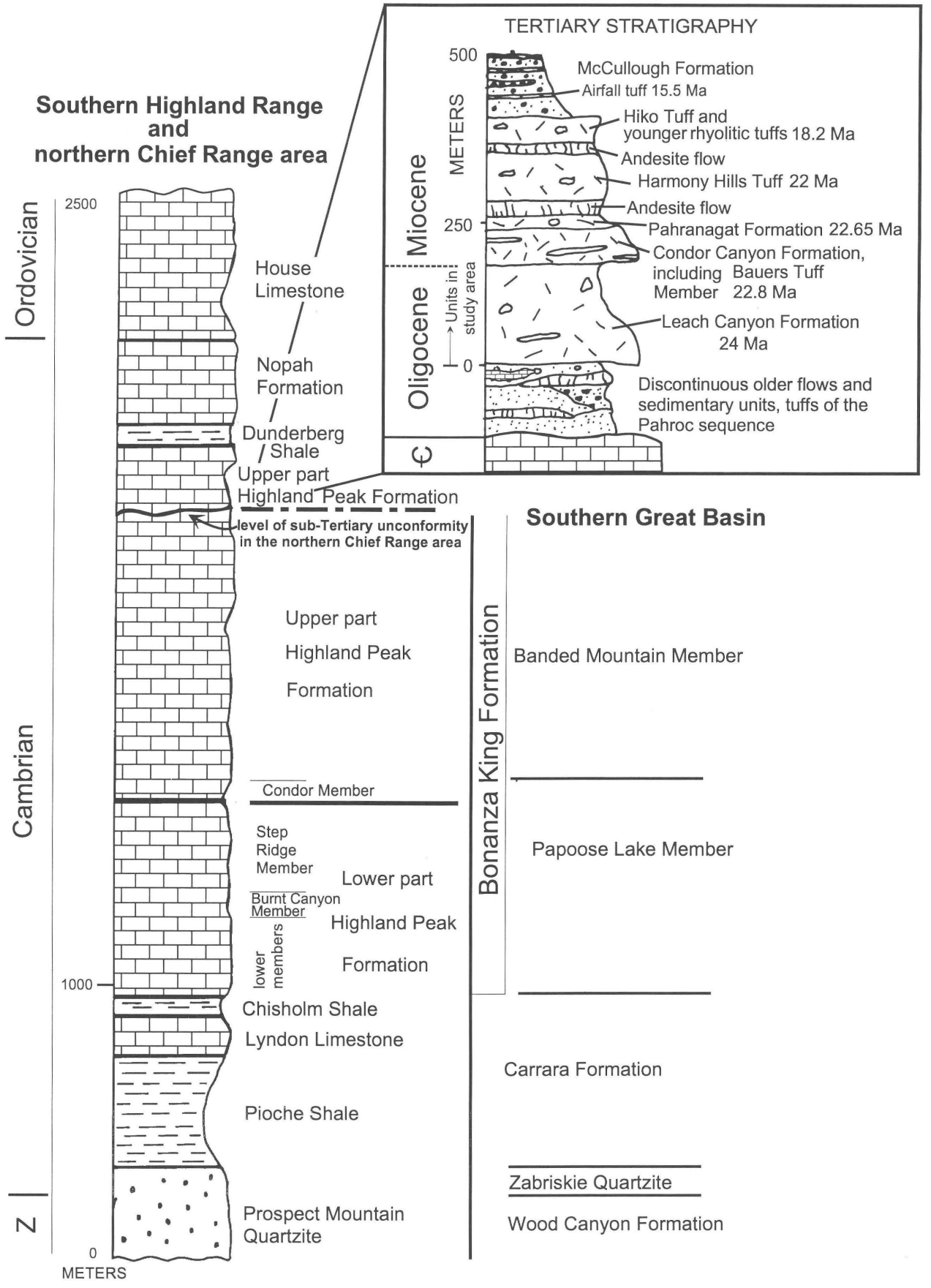
TERTIARY STRATIGRAPHY
500
250
0
METERS
Miocene
Oligocene
Units in study area
McCullough Formation
Airfall tuff 15.5 Ma
Hiko Tuff and younger rhyolitic tuffs 18.2 Ma
Andesite flow
Harmony Hills Tuff 22 Ma
Andesite flow
Pahranagat Formation 22.65 Ma
Condor Canyon Formation, including Bauers Tuff Member 22.8 Ma
Leach Canyon Formation 24 Ma
Discontinuous older flows and sedimentary units, tuffs of the Pahroc sequence
Southern Highland Range and northern Chief Range area
Ordovician
Cambrian
Z
2500
1000
0
METERS
House Limestone
Nopah Formation
Dunderberg Shale
Upper part Highland Peak Formation
level of sub-Tertiary unconformity in the northern Chief Range area
Upper part Highland Peak Formation
Condor Member
Step Ridge Member
Lower part Highland Peak Formation
Burnt Canyon Member
lower members
Chisholm Shale
Lyndon Limestone
Pioche Shale
Prospect Mountain Quartzite
Southern Great Basin
Bonanza King Formation
Banded Mountain Member
Papoose Lake Member
Carrara Formation
Zabriskie Quartzite
Wood Canyon Formation

Pioche Hills just east of Pioche, transfer faults in the hanging wall of the Stampede detachment fault are also clearly overlapped by the lowest Tertiary volcanic units (Axen, Lewis, and others, 1988). Thus, the Stampede detachment fault system is prevolcanic.

Evidence for prevolcanic extension continues west of Dry Lake Valley, to between the Seaman and North Pahroc ranges, where Taylor and Bartley (1992) inferred a buried east-dipping breakaway (fig. 1) for the Stampede detachment. West of this Seaman breakaway no evidence of prevolcanic extension exists (Bartley and others, 1988). Taylor and Bartley (1992) projected this breakaway northward to the Snake Range area.

In the northern Chief Range area, the Stampede detachment fault system consists of bedding-parallel faults that disrupted the lower part of the Highland Peak Formation, particularly the interval between the Chisholm Shale and the Condor Member of the Highland Peak Formation (fig. 3). Exposed fault planes dip between 16° and 20° east (Burke, 1991), and the low-angle faults attenuated bedding dramatically. South of Bennett Pass (fig. 4), domino-style faults cutting the hanging wall of the Stampede detachment fault are well exposed and terminate at the basal detachment fault. Offset on the Stampede detachment fault is difficult to constrain. The moderately dipping upper plate faults typically have offsets between 10 and 200 m. These faults are spaced at about 150-m intervals (Burke, 1991). Fault spacing is obscured in the Step Ridge Member of the Highland Peak Formation (fig. 3) by massive oolitic and fine-grained limestone. However, the presence of abundant breccia and discontinuous dolomitized zones in this member suggests that it is also intensely faulted.

The geometry of stratigraphic units disrupted by faults of the Stampede detachment fault system varies along the length of the map area. The best exposures of the system are in the south end of the Highland Range, where it is a complex zone of moderately to steeply east and west dipping faults, which sole into east-dipping low-angle normal faults (Burke, 1991). This area also contains high-angle transversely oriented faults (some having strike-slip offset). The structural complexity is summarized in figure 5.

Exposures of the hanging wall of the Stampede detachment fault in the south end of the Highland Range are divided into two zones (fig. 5). The Bennett fault and a narrow, structurally complex transitional area immediately west of the fault separate the two zones. The Bennett fault is interpreted to be much younger than the Stampede detachment fault (see section on the Bennett fault). Upper and lower Highland Peak Formation rocks in the transitional area are intensely brittlely deformed and dip both east and west. The zone east of the Bennett fault consists of east-dipping upper Highland Peak Formation rocks cut by widely spaced, moderately to steeply east dipping faults. In the zone west of the fault and transitional area, lower Highland Peak Formation rocks dip west and are cut by closely spaced faults of various orientations.

The contrast in spacing of faults cutting the upper versus lower Highland Peak Formation indicates that hanging-wall faults of the Stampede detachment fault system may splay downward to accommodate space problems, much like brecciation processes. This interpretation is based on the prior one, that the eastern and western zones are respectively higher and lower structural levels of the Stampede detachment fault system juxtaposed by offset on the Bennett fault. Downward splaying faults are mapped further south in the northern Chief Range area and can also be observed in the models of McClay and Ellis (their fig. 4, 1987).

In cross section *A–A′* (fig. 6), the Stampede detachment fault could not be projected to depth at a constant dip and maintain normal offset. Projection downward of the stratigraphy of upper plate blocks forced the detachment fault to be drawn steepening eastward between locations A and B in the cross section and then flattening between locations B and C. This maintains normal displacement on the detachment fault rather than thrust displacement (for which no surface evidence is found). The stratigraphic position of the detachment fault in the Condor Canyon area (fig. 1), about 40 km to the east, is above the Prospect Mountain Formation. Therefore, the Stampede detachment fault is projected flattening eastward from location C into a position near the top of the Prospect Mountain Formation. The resulting geometry of the basal detachment fault is flat-ramp-flat.

Bedding dips above the Stampede detachment fault define a syncline-anticline pair also suggestive of a ramp at depth. On the west end of section *A–A′* (fig. 6) the western zone units dip west, the eastern zone rocks dip east, and in the southern Highland Range immediately east of the study area (G.J. Axen, unpub. mapping, 1988), the bedding again dips west. This geometry is similar to that produced in the sand model experiments of McClay and Ellis (1987), although their models also produced reverse faults. Wernicke and Burchfiel (1982) and Gibbs (1984) also suggested that fault-bend folding would be expected above a ramp in a low-angle normal fault, analogous to that above thrust ramps. In the southern Highland Range, the syncline-anticline pair has apparently been produced through a combination of faulting and bedding rotations. Some of the bedding rotations are too large to be explained by applying a listric

Figure 3 (facing page). Precambrian (Z), Paleozoic, and Tertiary stratigraphy of northern Chief Range area and correlation with southern Great Basin Paleozoic stratigraphy. Dot pattern, quartzite; dash pattern, shale; block pattern, limestone. Contacts of mappable members were used to constrain fault offsets in Highland Peak Formation. Correlations based on Tschanz and Pampeyan (1970), Lewis (1987), Stewart (1974, 1978), and Rowley and others (1992). Ages are from Taylor and others (1989), Rowley and others (1995), and Scott and others (1995).

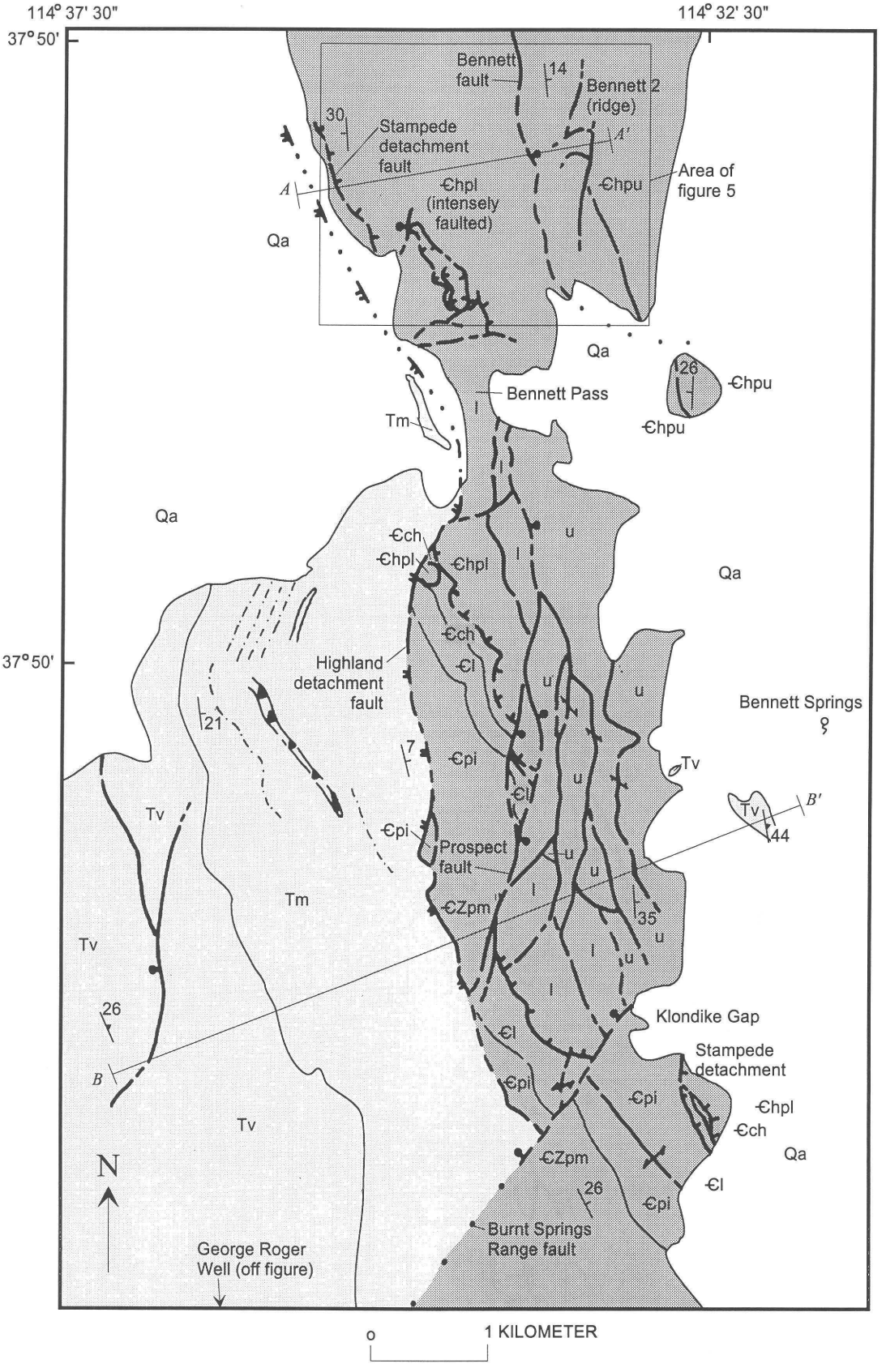

Figure 4 (above and facing page). Generalized geology of northern Chief Range area. *A–A'* and *B–B'*, cross section locations (figs. 6, 7). Attitudes in Tertiary volcanic rocks from eutaxitic foliation. Short dash-dot lines in McCullough Formation show thin airfall tuffs.

EXPLANATION

Qa Quaternary alluvium

Tertiary rocks

Tm McCullough Formation

Tv Volcanic rocks, undivided

Paleozoic rocks

Chpu (u) Highland Peak Formation (upper)

Chpl (l) Highland Peak Formation (lower)

Cch Chisholm Shale

Cl Lyndon Limestone

Cpi Pioche Shale

CZpm Prospect Mountain Quartzite

Contact

High-angle normal fault—Dashed where approximately located; dotted where concealed; queried where uncertain; bar and ball on downthrown side

Highland detachment fault—Dashed where approximately located; dotted where concealed

Stampede detachment fault—Dashed where approximately located

Marker bed—Thin ashfall tuff or distinctive thin debris flow (?) deposit containing Tertiary volcanic clasts

Landslide breccia

7 Strike and dip

26 Volcanic foliation attitude

Tie line—Indicates same lithology on both sides of fault

geometry to small offset faults, so these rotations more likely are the result of folding or distortion of blocks by shearing and bedding-parallel slip. The proximity of the syncline-anticline pair to the ramp suggests relatively small magnitude transport (about 1 km or less) along the Stampede detachment fault.

The Stampede detachment fault and bedding in its footwall, as projected in the west end of section *A–A′* at D, form a very open fold. This geometry may reflect slight uplift of the footwall of the Highland detachment fault in response to the removal of the hanging wall. Furthermore, when the folding is removed, the beds in the hanging wall of the Stampede detachment fault restore to a steeper west dip and the faults restore to a shallower east dip. The dip of these faults is then more consistent with the dip of the domino-style faults in the hanging wall of the Stampede detachment fault south of Bennett Pass (fig. 4).

In the northern Chief Range, north of Klondike Gap, the Prospect fault offsets the prevolcanic Stampede detachment fault and is truncated by the Highland detachment fault (figs. 4, 7*A*). The Prospect fault places Prospect Mountain Quartzite against lower Highland Peak Formation. It dips steeply east and at the south end of the map has a stratigraphic separation of about 500 m. In cross section *B–B′* (fig. 7*A*) the Prospect fault is inferred to lie in the hanging wall of the Highland detachment fault and to offset the Stampede detachment fault and Paleozoic rocks underlying the Tertiary volcanics. This part of the cross section corresponds to an area between the Burnt Springs Range (fig. 1) and the northern Chief Range.

The crosscutting relations indicate that the Prospect fault formed in the interval between major movement on the Highland and the Stampede detachment faults. The Prospect fault splays northward into several faults with smaller offsets (fig. 4), apparently losing displacement northward. Near Bennett Pass (fig. 4), steeply to moderately east dipping faults may be splays of the Prospect fault or hanging-wall structures related to the Stampede detachment fault. The similarity in structural style and orientation of the Prospect fault zone and faults of the Stampede detachment system suggests that the Prospect fault may be related to and may have begun activity late in Stampede detachment fault time.

MINOR FAULTS AND UNCONFORMITIES—EARLY SYNVOLCANIC EXTENSION(?)

Air photo and field reconnaissance of the volcanic outcrops just beyond the western boundary of the study area indicates that units underlying the Leach Canyon Formation are discontinuous due either to small fault displacements or to unconformities within the section. Rowley and others (1994) attributed these discontinuities to syntectonic sedimentation and small volcanic dome building. However, similar faults and unconformities are observed in this stratigraphic interval elsewhere in the central transect, particularly near Condor Canyon (Bartley and others, 1988; Axen, Burke, and Fletcher, 1988). We interpret these features to be part of a regional expression of tectonic activity during the time of deposition of these volcanic rocks. In the mapped areas around Dry Lake Valley where only Paleozoic units are exposed, faults representing this proposed synvolcanic extensional episode would not be distinguishable from prevolcanic and late synvolcanic to postvolcanic faults.

HIGHLAND DETACHMENT FAULT—LATE SYNVOLCANIC TO EARLY POSTVOLCANIC EXTENSION

The Highland detachment fault cuts through the Bristol Range (fig. 1) (Page and Ekren, 1995) and bounds the western margin of the Highland and northern Chief Ranges (G.J. Axen, unpub. mapping, 1988; Burke, 1991). It juxtaposes a footwall of complexly faulted Cambrian units against a hanging wall of gently east dipping Tertiary volcanic units cut by widely spaced moderately to steeply west dipping normal faults (fig. 4). Some of these faults exhibit a listric geometry and are interpreted to sole into the Highland detachment fault. The trace of the Highland detachment fault is sinuous and well located on the map despite the absence of exposures (fig. 8). Three point calculations where the fault trace crosses topography yield westerly dips of 7°–15° (Burke, 1991) similar to dips of 5°–30° calculated to the north (Sleeper, 1989; Axen, Lewis, and others, 1988).

The Highland detachment fault formed an east-tilted synorogenic basin filled with the McCullough Formation, which includes fault-scarp facies breccia and fanglomerate and thin interbedded ashfall tuffs (fig. 4). The McCullough Formation was defined to the north between the Highland and the Ely Springs Ranges (fig. 1) (Axen, Lewis, and others, 1988), where included clasts record a progressive unroofing of rock units in the footwall of the Highland detachment fault. Exposures in the study area suggest a similar history. Landslide breccia composed of lower Highland Peak Formation units dominates the east side of the basin, adjacent to the detachment fault. On the western margin clasts are primarily volcanic. In the middle of the basin, deposits contain a mix of volcanic and carbonate clasts.

Small horizontal-axis rotations of McCullough Formation strata resulted from movement on the detachment fault. The east dip of tuffaceous fluvial layers within the McCullough Formation gradually shallows from west to east, from about 25°–30° to 5°–7° (near the trace of the Highland detachment fault) reflecting a growth fault geometry (fig. 4) (Burke, 1991). In summary, as the hanging wall of the Highland detachment fault moved westward, the void created was filled by deposition of Miocene McCullough tuffs and sediments and by collapse of the hanging wall along the listric and planar west-dipping faults.

In the map area, the McCullough Formation overlies dacitic to andesitic lava flows that in turn overlie thin unnamed rhyolite tuffs mapped with the Hiko Tuff. A thin, local ashfall tuff intercalated with McCullough Formation strata east of the Ely Springs Range yielded a $^{40}Ar/^{39}Ar$ age of 15.3 Ma (Taylor and others, 1989). The age of the Hiko Tuff at the top of the Caliente caldera sequence is 18.2 Ma (Rowley and others, 1995), so the Highland detachment fault is post-18.2 Ma and probably active at and after 15.3 Ma. Movement of the Highland detachment fault began after the major volcanic activity in the Caliente caldera complex.

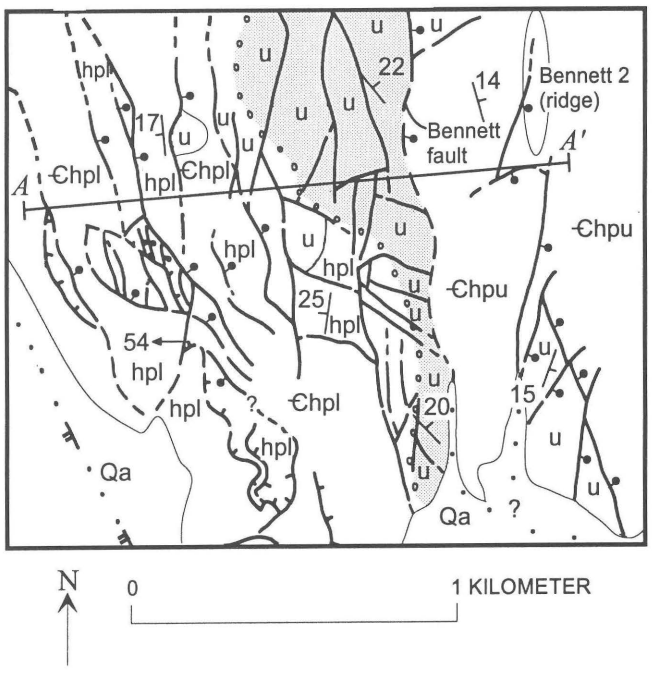

EXPLANATION

Qa	Quaternary alluvium
Chpu (u)	Highland Peak Formation (upper) (Cambrian)
Chpl (hpl)	Highland Peak Formation (lower)
———	Approximate contact
——•——	High-angle fault—Dashed where approximately located; dotted where concealed; queried where uncertain; bar and ball on downthrown side
———	Highland detachment fault—Dotted where concealed
———	Stampede detachment fault (and minor low-angle faults)—Dashed where approximately located; queried where uncertain
15	Strike and dip
o o o o	Approximate west limit of 'transition zone'

Figure 5. Detailed geology of southernmost Highland Range. Location, figure 4. Shaded area bounded by line of small circles and Bennett fault is transitional area between zones of hanging-wall exposures along Stampede detachment fault.

Axen, Lewis, and others (1988) calculated a slip vector of about 10 km west-southwest for the Highland detachment fault, by restoring the displacement between granitic intrusions in the hanging wall (Blind Mountain) and footwall (Black Rock Knoll) (fig. 1). Although slickenside data are

lacking from the volcanic units, the orientations of hanging-wall faults and rotated beds agree with west-southwest slip indicated by the proposed piercing point. Restoration of cross section *B–B'* (fig. 7), drawn parallel to the inferred extension direction, indicates about 3.7 km or 80 percent extension across the Highland detachment fault. This compares with 5.1 km and as much as 110 percent extension calculated by Sleeper (1989) and Lewis (1987) respectively.

BENNETT FAULT AND BURNT SPRINGS RANGE FAULT—PLIOCENE(?) TO QUATERNARY(?) EXTENSION

The youngest generation of faulting in the map area disrupts the Highland detachment fault system. The Bennett fault (fig. 4) is interpreted to be part of the Arizona fault zone which, north of the map area (fig. 1), offsets the Highland Peak detachment fault down-to-the-east (G.J. Axen, unpub. mapping, 1988; Axen, Lewis, and others, 1988). Like the Arizona fault zone, the Bennett fault is long, straight, continuous, and east dipping (stratigraphic separation about 200 m). The Arizona fault zone can be projected along strike into a range-bounding position along the eastern front of the northern Chief Range. The location of the Bennett fault south of the Bennett Pass area is uncertain. It most likely bends eastward to separate the east-dipping toe of the ridge containing Bennett 2 (the peak) from the west-dipping outlier of upper Highland Peak rocks at Hill 5871 (fig. 4). The Bennett fault is probably coeval with the Condor fault (fig. 1) and other faults along the east edge of Meadow Valley which have a similar orientation and also control topography. The Condor fault moved during Pliocene time (Axen, Burke, and Fletcher, 1988).

The small-displacement down-to-the-east faults in the hanging wall of the Bennett fault may either accommodate extension in its hanging wall or be older and related to the Stampede detachment fault. In cross section *A–A'* they are inferred to be part of the Stampede detachment fault system. The Bennett fault is inferred to cut the Highland detachment fault above the surface and the Stampede detachment fault at depth.

Another major fault cutting the Highland detachment fault is the northeast-striking Burnt Springs Range fault (Ekren and others, 1977), which truncates the Highland detachment fault at Klondike Gap (fig. 4). The Pioche Shale is offset across the Burnt Springs Range fault about 1,200 m in an apparently sinistral sense. However, the trace of the Highland detachment fault exposed directly west of the Pioche Shale, northwest of the Burnt Springs Range fault, does not reappear in that position southeast of the fault. This observation counters the interpretation of strike-slip movement along the Burnt Springs Range fault as proposed by Ekren and others (1977).

Mapping by Rowley and others (1994) instead suggests that the Highland detachment fault crops out on the high point of the Chief Range just south of the northern Chief Range area and is therefore downfaulted to the north. Thus, the Burnt Springs Range fault can be confidently interpreted as younger than the Highland detachment fault. Rowley and others (1994) indicated that the Burnt Springs Range fault is a steeply northwest dipping fault with mostly normal slip and minor left-lateral slip. The McCullough Formation does not reappear southeast of the Burnt Springs Range fault (Rowley and others, 1994), although it may be present in the subsurface.

The Burnt Springs Range fault branches northeastward through Klondike Gap into a zone of several moderately to steeply northwest dipping normal faults (not shown on simplified map of fig. 4) and like the Bennett fault, may be coeval with range-bounding faults in Meadow Valley. The southwestward continuation of the Burnt Springs Range fault abruptly cuts off the western volcanic strike ridge near George Roger Well (fig. 4). The fault was interpreted by Tschanz and Pampeyan (1970) and Ekren and others (1977) to extend southwest to Dry Lake Valley at the south end of the Burnt Springs Range (fig. 2). Rowley and others (1992) however, confined the fault to the northwest and west side of the Chief Range.

CROSS SECTION *B–B'*

Fault geometries in the northern Chief Range area are summarized in cross section *B–B'* (fig. 7). Data from outside the study area are from Tschanz and Pampeyan (1970) and Lewis (1987). The section is balanced by the line-length method (Woodward and others, 1985) in separate segments, because only Tertiary rocks are present at the surface in the hanging wall of the Highland detachment fault whereas mainly Cambrian rocks are exposed in the footwall block.

When offset along the Highland detachment fault is restored and Tertiary ashflow tuffs are rotated back to horizontal on the cross section, the inferred pre-Highland detachment fault configuration is shown (fig. 7*B*). Rotation of the footwall of the Highland detachment fault is somewhat uncertain. First, the contact between upper Highland Peak Formation and Tertiary volcanic units on the east side of the northern Chief Range is not exposed (Burke, 1991). However, it is inferred to be unconformable based on mapping immediately south of the map area (Rowley and others, 1994). Second, the Condor Canyon Formation in the outlier at the east end of *B–B'* dips about 15° steeper than the same tuffs in the hanging wall of the Highland detachment fault (fig. 4) (Burke, 1991). This suggests that the hanging wall has rotated less than the footwall. The Highland detachment may be concave down, but the fanned dips in the McCullough Formation in the hanging wall suggest

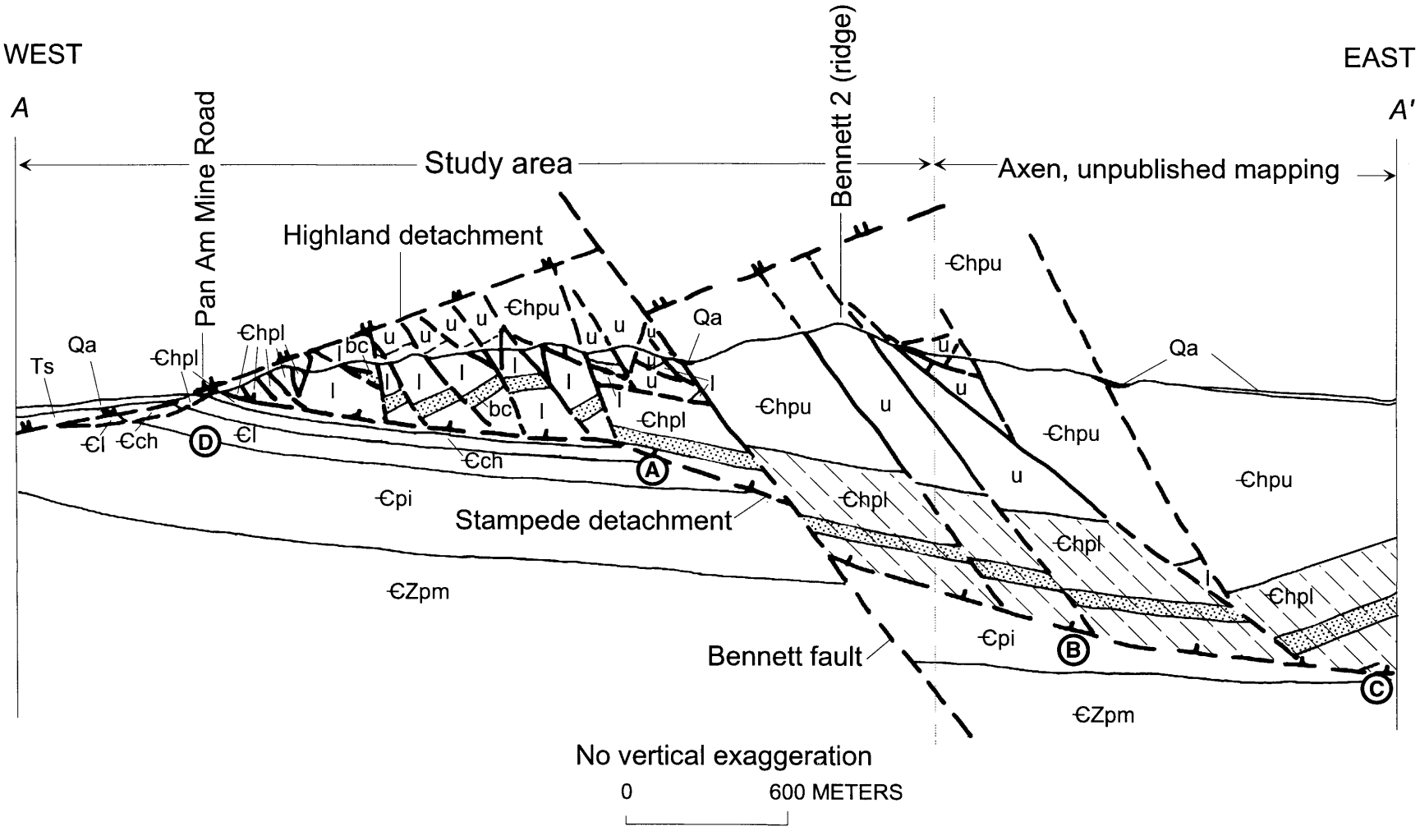
WEST
EAST
A
A′
Pan Am Mine Road
Study area
Bennett 2 (ridge)
Axen, unpublished mapping
Highland detachment
Stampede detachment
Bennett fault
Ts
Qa
Chpl
Chpu
bc
u
l
Cl
Cch
Cpi
CZpm
D
A
B
C
No vertical exaggeration
0
600 METERS

EXPLANATION

Qa Quaternary alluvium

Ts Tertiary sediment

Cambrian rocks

Ꞓhpu (u) Highland Peak Formation (upper)

Ꞓhpl (l) Highland Peak Formation (lower)

bc Burnt Canyon Member (marker bed)

Ꞓch Chisholm Shale

Ꞓl Lyndon Limestone

Ꞓpi Pioche Shale

Cambrian and Precambrian rocks

ꞒZpm Prospect Mountain Quartzite

Contact

High-angle normal fault—Dashed where approximately located or projected above present ground surface; barbs show direction of relative movement

Highland detachment fault—Dashed where approximately located or projected above present ground surface; queried where inferred; barbs show direction of relative movement

Stampede detachment fault—Dashed where approximately located; barbs show direction of relative movement

A Location discussed in text

Zone of complex faulting

Figure 6 (above and facing page). Geologic cross section *A–A'*, southernmost Highland Range. See text for explanation at locations A–D. Cross section is drawn from the detailed geologic map (1:24,000 scale) of Burke (1991, pl. 1); location shown in figures 4 and 5. Scale is greatly enlarged from figures 4 and 5. Highland Peak Formation is subdivided into upper and lower members and includes the Burnt Canyon Member, which is used as a marker bed to show relative offsets.

that the Highland detachment fault is listric. Instead, the extra rotation of the footwall tuffs may be due to later faulting associated with the range-front faults. In *B–B'*, a small east-dipping fault at A is inferred to be a splay from a range-front fault that is younger than the Highland detachment fault. The Tertiary tuffs are then rotated in a small fault-bounded sliver. Rocks within the sliver may have been faulted, brecciated, or thinned to accommodate the rotation. After restoring this small fault, the Highland detachment fault can be restored to an initial 35°-40° west dip based on an average east dip of 25° for the Tertiary volcanic units on both sides of the range.

In the restored *B–B'* section (fig. 7*B*), some of the faults in the hanging wall of the Highland detachment fault are actually hanging-wall faults to the older Stampede detachment fault that have been offset, whereas others are related to the Highland detachment fault itself. The faults were restored based on the generalization that faults of the Stampede detachment fault system dip east and faults of the Highland detachment fault system dip west, even though these relations are not always observed in the field.

The Stampede detachment fault, after restoration of the Highland detachment fault, dips about 5°–10° west, which contradicts the evidence for top-to-the-east movement. However, if in *B–B'* the Prospect fault is restored and the Highland Peak Formation rotated back to horizontal, the Stampede detachment fault rotates to a gentle east dip. The initial orientation of the Highland Peak Formation before the formation of the Prospect fault is not known.

CONCLUSIONS

The northern Chief Range area exhibits prevolcanic, synvolcanic, and postvolcanic extensional deformation (fig. 9). Prevolcanic (Stampede detachment fault), late synvolcanic to postvolcanic (Highland detachment fault), and Pliocene(?) to Quaternary(?) faults mapped previously in the Highland Range (Axen, Lewis, and others, 1988) continue through the northern Chief Range area into the Chief Range. Rowley and others (1994) recently mapped faults of these three episodes south from the Chief Range to the boundary of the Caliente caldera complex. In addition, possible early synvolcanic deformation is represented by minor faults and low-angle unconformities in Tertiary volcanic and sedimentary rocks (fig. 9) exposed immediately west of the northern Chief Range area. Faults of this episode could be present but not distinguishable within the study area.

Prevolcanic extension represented by the Stampede detachment fault is proposed to correlate with extension in the Snake Range area in terms of timing, transport direction, and stratigraphic level (fig. 9). However, in contrast to the

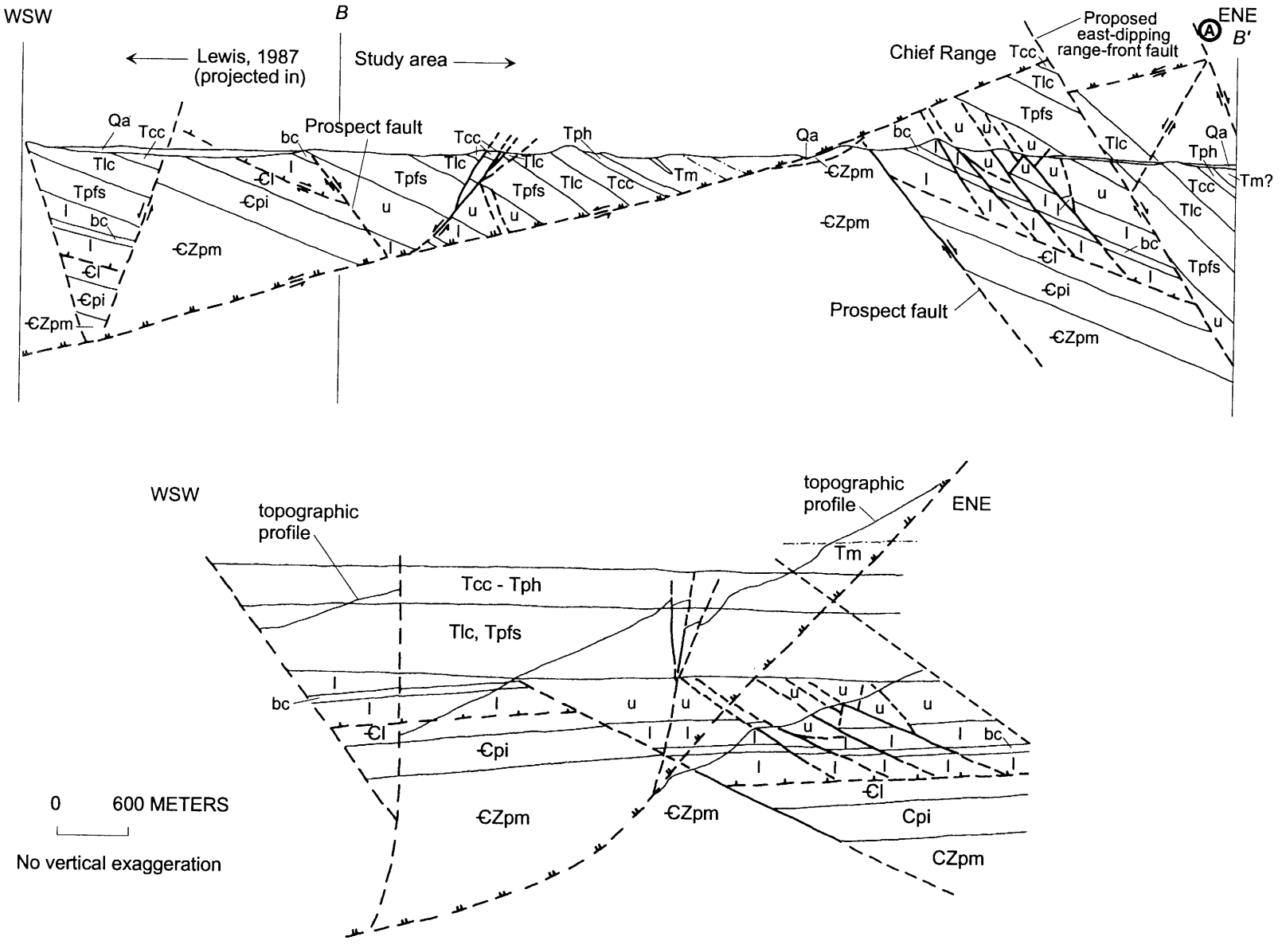
WSW
B
Lewis, 1987
(projected in)
Study area
Qa
Tcc
bc
Prospect fault
Tlc
Tpfs
Cl
Cpi
u
l
CZpm
Tph
Tm
Chief Range
Proposed
east-dipping
range-front fault
A
ENE
B'
Tm?
topographic
profile
Tcc - Tph
Tlc, Tpfs
Cpi
CZpm
0
600 METERS
No vertical exaggeration

EXPLANATION

Qa Quaternary alluvium

Tertiary rocks

Tm McCullough Formation

Tph Pahranagat Formation to Hiko Tuff

Tcc Condor Canyon Formation

Tlc Leach Canyon Formation

Tpfs Pahroc sequence and Tertiary flows and sediments

Cambrian rocks

u Highland Peak Formation (upper)

l Highland Peak Formation (lower)

bc Burnt Canyon Member (marker bed)

Cl Lyndon Limestone

Cpi Pioche Shale

Cambrian and Precambrian rocks

CZpm Prospect Mountain Quartzite

Contact

High-angle normal fault—Dashed where approximately located or projected above present ground surface; arrows show direction of relative movement

Highland detachment fault—Dashed where approximately located or projected above present ground surface; arrows show direction of relative movement

Stampede detachment fault—Dashed where approximately located

Ⓐ Location discussed in text

Figure 7 (facing page and above). Present and restored geologic cross section *B-B'*, northern Chief Range. See text for discussion. Cross section is drawn from the detailed geologic map (1:24,000 scale) of Burke (1991, pl. 1); location is shown in figure 4. Scale is greatly enlarged from figure 4. Highland Peak Formation is subdivided into upper and lower members and includes the Burnt Canyon Member, which is used as a marker bed to show relative offsets.

Snake Range, the footwall of the Stampede detachment fault in the northern Chief Range area is not ductilely deformed or metamorphosed. Displacement on the prevolcanic east-dipping fault system may be decreasing southward from the Snake Range area. Evidence of the prevolcanic extension has not been found south of the Caliente caldera complex (Wernicke and others, 1985; Axen and others, 1990; Axen, 1993; P.D. Rowley, mapping in progress) and is absent from the Lake Mead extensional belt of southern Nevada.

The Stampede detachment fault is interpreted to have a ramp that cuts downsection eastward in its footwall in the south end of the Highland Range, which produced a complexly faulted syncline-anticline pair in the upper plate. This type of geometry has been previously proposed as analogous to thrust fault ramps (Gibbs, 1984; McClay and Ellis, 1987) and recognized elsewhere in the Basin and Range province (such as in Death Valley; Wernicke and others, 1989). This geometry may roughly constrain offset on the Stampede detachment fault to be about 1 km.

The west-dipping Highland detachment fault (fig. 9) of mid-Miocene age represents late synvolcanic to postvolcanic extension of similar orientation and age as the earliest extension in the Mormon Mountains area. Fanning of dips within the mid-Miocene McCullough Formation records progressive rotation along the Highland detachment fault. This structural evidence, along with inverted stratigraphy in clast contents, supports the interpretation of the formation as syntectonic (Axen, Lewis, and others, 1988). Structures correlative with the Highland detachment fault system have not been documented in the northern Snake Range. Instead, a younger top-to-the-east fault system overprints the northern Snake Range decollement.

The Bennett fault and the Burnt Springs Range fault represent the youngest extensional episode in the northern Chief Range area. The northeast-striking Burnt Springs Range fault (fig. 9) transversely cuts the Highland detachment fault and was previously mapped as a left-lateral strike-slip fault. We reinterpret it here to be a young, steeply northwest dipping dominantly normal fault (compare Rowley and others, 1994). The fault juxtaposes two blocks representing different structural levels of the Highland detachment and Stampede detachment faults (Burke, 1991; Rowley and others, 1994). The Burnt Springs Range fault partly defines the northwest side of the Chief Range. It may have had an extended history, but the most recent movement could be as young as the Pliocene(?)-Quaternary(?) range-bounding faults in Meadow Valley. The Bennett fault is also interpreted to be related to these faults and to the Arizona fault zone.

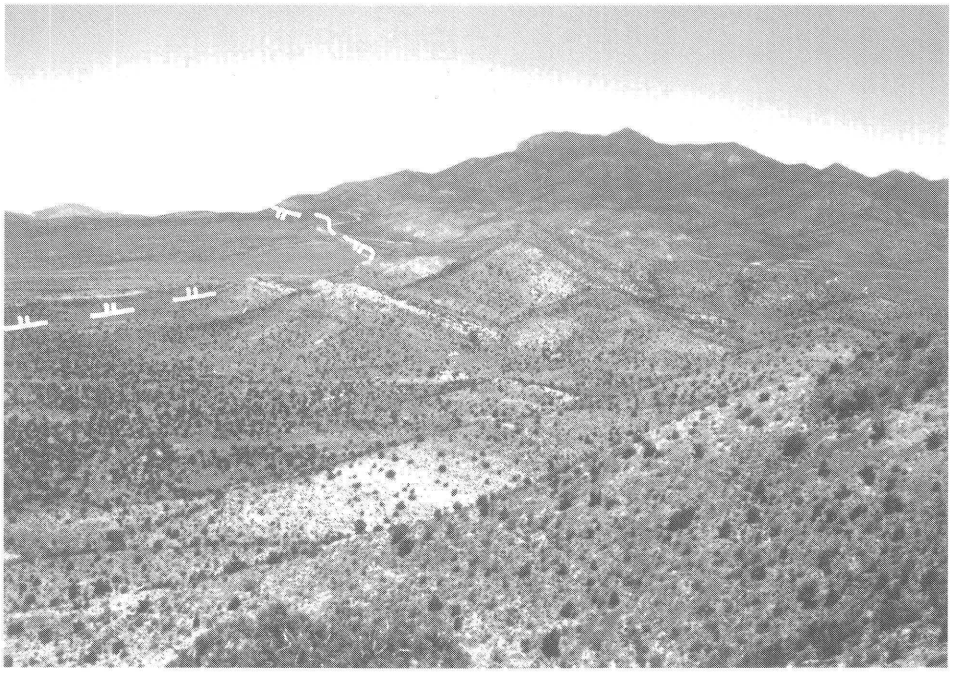

Figure 8. Southern Highland Range with northern Chief Range in the nearground. Note sinuous trace of Highland detachment fault (double-hachured line) bounding west edge of resistant outcrops of Paleozoic rocks in both ranges.

In summary, mapping in the northern Chief Range area supports the interpretation of episodic extension along low-angle detachment faults across the central transect. This study expands the known area in which these detachment fault systems dominate, an area on the scale of several hundred square kilometers (Taylor and others, 1989). The lack of metamorphic rocks in the footwalls of these major detachment faults indicates they are not the uplifted brittle-ductile transition. At the structural levels exposed in the northern Chief Range, the master detachment faults are single fault surfaces or narrow fault zones. Also, as seen in cross section, the older detachment fault is nearly bedding parallel and the younger detachment fault cuts bedding at a moderate angle. Metamorphic core complexes apparently result from larger fault displacements and possibly more Tertiary plutonism, inputting heat and facilitating ductile deformation, than affected the northern Chief Range area.

No evidence exists in the northern Chief Range area for extensional faults having reactivated older structures, and large-volume volcanic deposition has occurred without contemporaneous extensional faulting (fig. 9). The ideas of synextensional volcanism and fault reactivation have often contributed to the construction of models for continental extension (compare Gans, 1987, and discussion in Wernicke and others, 1985), but this study indicates that they do not apply universally in the Basin and Range province (see Taylor, 1990, and Axen and others, 1993).

Models for extension in the Basin and Range province in general are often necessarily simplistic, in the sense of limiting the number of variables involved. The northern Chief Range area provides an example of the complexity of overprinted geometries produced during low- to high-angle, listric and planar, rotational and nonrotational faulting of multiple episodes. Penetrative deformation including bedding-parallel slip, brecciation and dolomitization, and possible downward splaying of faults accommodated the shape changes that developed during faulting and rotation. The removal of the hanging wall of a major detachment fault also resulted in possible slight footwall flexure, fault-bend folding, and syntectonic sedimentation.

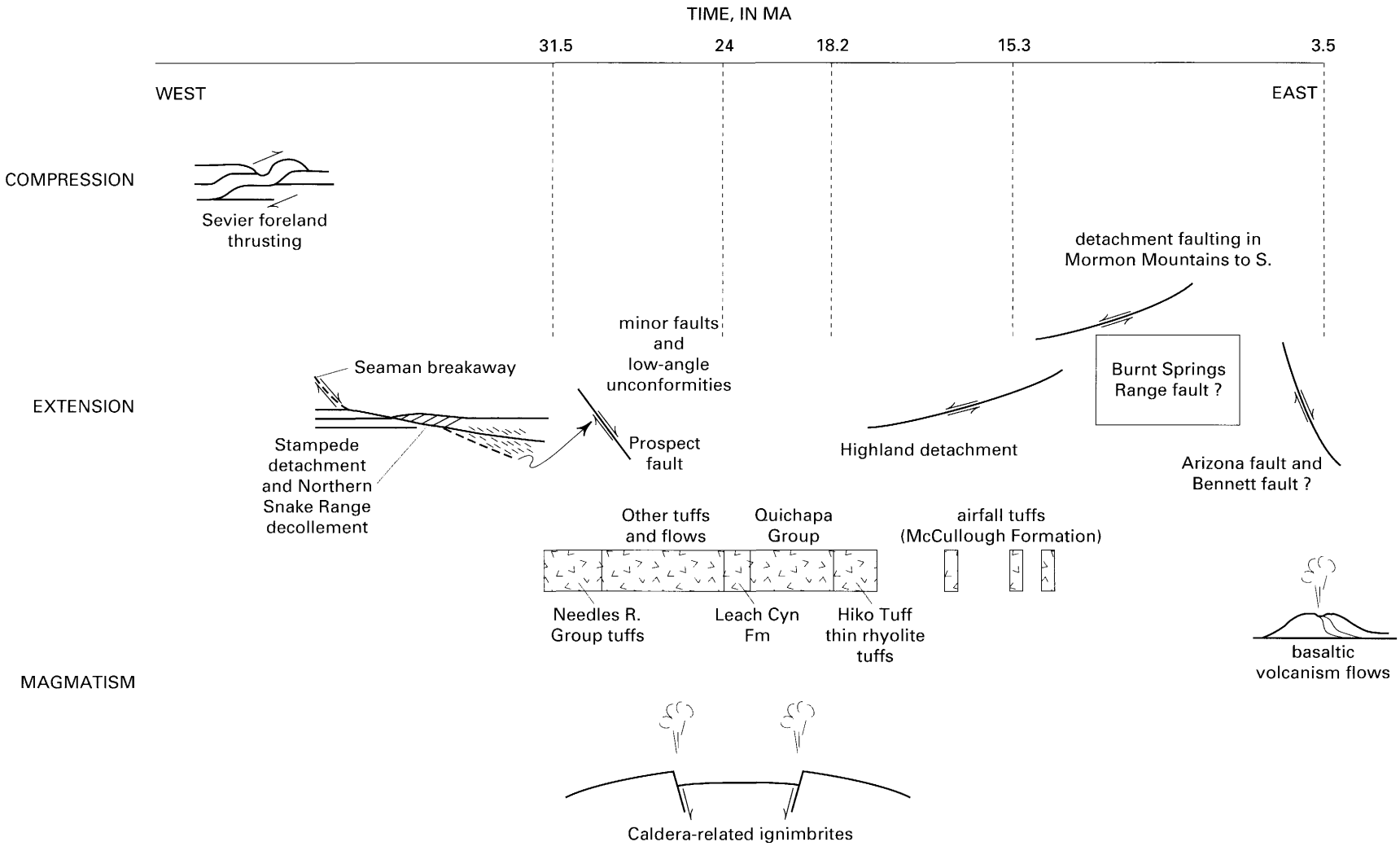

Figure 9. Schematic summary diagram of timing and orientation of compression and extension, and timing of magmatism in eastern Nevada. Barbs give movement sense on faults. See figure 3 for ages of volcanic units.

REFERENCES CITED

Anderson, R.E., 1971, Thin skin distension in Tertiary rocks of southern Nevada: Geological Society of America Bulletin, v. 82, p. 43–58.

Anderson, R.E., and Barnhard, T., 1993a, Heterogeneous Neogene strain and its bearing on horizontal extension and horizontal and vertical contraction at the margin of the extensional orogen, Mormon Mountains area, Nevada and Utah: U.S. Geological Survey Bulletin 2011, 43 p.

———1993b, Aspects of three-dimensional strain at the margin of the extensional orogen, Virgin River depression area, Nevada, Utah, and Arizona: Geological Society of America Bulletin, v. 105, p. 1019–1052.

Anderson, R.E., and Bohannon, R.G., 1993, Three-dimensional aspects of the Neogene strain field, Nevada-Utah-Arizona tricorner area, *in* Lahren, M.M., Trexler, J.H., Jr., and Spinosa, C., eds., Crustal evolution of the Great Basin and the Sierra Nevada: Cordilleran/Rocky Mountain Section Meeting, Geological Society of America Guidebook, p. 167–196.

Anderson, J.J., and Rowley, P.D., 1975, Cenozoic stratigraphy of the southwestern High Plateaus of Utah, *in* Anderson, J.J., Rowley, P.D., Fleck, R.J., and Nairn, A.E.M., eds., Cenozoic geology of the southwestern High Plateaus of Utah: Geological Society of America Special Paper 160, p. 1–52.

Armstrong, R.L., 1968, Sevier orogenic belt in Nevada and Utah: Geological Society of America Bulletin, v. 79, p. 429–458.

———1972, Low-angle (denudation) faults, hinterland of the Sevier orogenic belt, eastern Nevada and western Utah: Geological Society of America Bulletin, v. 83, p. 1729–1754.

Axen, G.J., 1986, Superposed normal faults of the Ely Springs Range, Nevada—Estimates of extension: Journal of Structural Geology, v. 8, p. 711–713.

———1993, Ramp-flat detachment faulting and low-angle normal reactivation of the Tule Springs thrust, southern Nevada: Geological Society of America Bulletin, v. 105, p. 1076–1090.

Axen, G.J., Burke, K.J., and Fletcher, J.M., 1988, Tertiary extensional and volcanic history of the Condor Canyon area, Lincoln County, Nevada: Geological Society of America Abstracts with Programs, v. 20, p. 140.

Axen, G.J., Lewis, P.R., Burke, K.J., Sleeper, K.G., and Fletcher, J.M., 1988, Tertiary extension in the Pioche area, Lincoln County, Nevada, *in* Bartley, J.M., Axen, G.J., Taylor, W.J., and Fryxell, J.E., 1988, Cenozoic tectonics of a transect through eastern Nevada near 38° N latitude, *in* Weide, D.L., and Faber, M.L., eds., This extended land—Geological journeys in the southern Basin and Range: Geological Society of America, Cordilleran Section, Field Trip Guidebook, p. 3–5.

Axen, G.J., Taylor, W.J., and Bartley, J.M., 1993, Space-time patterns and tectonic controls of Tertiary extension and magmatism in the Great Basin of the western United States: Geological Society of America Bulletin, v. 105, p. 56–76.

Axen, G., Wernicke, Brian, Skelly, M., and Taylor, W., 1990, Mesozoic and Cenozoic tectonics of the Sevier thrust belt in the Virgin Valley area, southern Nevada, *in* Wernicke, B.P., ed., Basin and Range extensional tectonics near the latitude of Las Vegas, Nevada: Geological Society of America Memoir 176, p. 123–154.

Bartley, J.M., Axen, G.J., Taylor, W.J., Fryxell, J.E., 1988, Cenozoic tectonics of a transect through eastern Nevada near 38°N latitude, *in* Weide, D.L., and Faber, M.L., eds., This extended land—Geological journeys in the southern Basin and Range: Geological Society of America, Cordilleran Section, Field Trip Guidebook, p. 1–20.

Bartley, J.M., and Gleason, G., 1990, Tertiary normal faults superimposed on Mesozoic thrusts, Quinn Canyon and Grant Ranges, Nye County, Nevada, *in* Wernicke, B.P., ed., Basin and Range extensional tectonics near the latitude of Las Vegas, Nevada: Geological Society of America Memoir 176, p. 195–212.

Bartley, J.M., and Wernicke, B.P., 1984, The Snake Range decollement interpreted as a major extensional shear zone: Tectonics, v. 3, p. 647–657.

Best, M.G., Christiansen, E.H., and Blank, R.H., 1989, Oligocene caldera complex and calc-alkaline tuffs and lavas of the Indian Peak volcanic field, Nevada and Utah: Geological Society of America Bulletin, v. 101, p. 1076–1090.

Best, M.G., Christiansen, E.H., Deino, A.L., Grommé, C.S., McKee, E.H., and Noble, D.C., 1989, Excursion 3A—Eocene through Miocene volcanism in the Great Basin of the western United States: New Mexico Bureau of Mines and Mineral Resources Memoir 47, p. 91–133.

Bohannon, R.G., 1984, Nonmarine sedimentary rocks of Tertiary age in the Lake Mead region, southeastern Nevada and northwestern Arizona: U.S. Geological Survey Professional Paper 1259, 72 p.

Bowman, S.A., 1985, Miocene extension and volcanism in the Caliente Caldera Complex, Lincoln County, Nevada: Golden, Colo., Colorado School of Mines M.S. thesis, 143 p.

Burchfiel, B.C., 1975, Nature and controls of Cordilleran orogenesis, western United States—Extensions of an earlier synthesis: American Journal of Science, v. 275, p. 363–396.

———1979, Geologic history of the central western United States *in* Ridge, J.D., ed., Papers on mineral deposits of western North America: Nevada Bureau of Mines and Geology, Report 33, pages unknown.

Burchfiel, B.C., and Davis, G.A., 1972, Structural framework and evolution of the southern part of the Cordilleran orogen, western United States: American Journal of Science, v. 272, p. 97–118.

Burke, K.J., 1991, Tertiary extensional tectonism in the northern Chief and southernmost Highland Ranges, Lincoln County, Nevada: Flagstaff, Ariz., Northern Arizona University M.S. thesis, 91 p.

Burke, K.J., and Axen, G.J., 1990, Structural geometry and timing of deformation in the northern Chief and southernmost Highland Ranges near Pioche, Nevada: Geological Society of America Abstracts with Programs, v. 22, no. 3, p. 11.

Callaghan, Eugene, 1936, Geology of the Chief district, Lincoln County, Nevada: University of Nevada Bulletin, v. 31, no. 2 (Nevada Bureau of Mines Bulletin 26), 29 p.

Coney, P.J., 1980, Cordilleran metamorphic core complexes—An overview, *in* Crittenden, M.D., Coney, P.J., and Davis, G.H., eds., Cordilleran metamorphic core complexes: Geological Society of America Memoir 153, p. 7–34.

Crittenden, M.D., Coney, P.J., and Davis, G.H., eds., 1980, Cordilleran metamorphic core complexes: Geological Society of America Memoir 153, 490 p.

Davis, G.H., 1977, Characteristics of metamorphic core complexes, southern Arizona: Geological Society of America Abstracts with Programs, v. 9, p. 944.

———1983, Shear zone model for the origin of metamorphic core complexes: Geology, v. 11, p. 342–347.

Davis, G.H., Anderson, J.L., Frost, E.G., and Shackelford, T.J., 1980, Mylonitization and detachment faulting in the Whipple–Buckskin–Rawhide Mountains Terrain, southeastern California and western Arizona, *in* Crittenden, M.D., Coney, P.J., and Davis, G.H. 1980, Cordilleran metamorphic core complexes: Geological Society of America Memoir 153, p. 79–130.

Drewes, H.D., 1958, Structural geology of the southern Snake Range, Nevada: Geological Society of America Bulletin, v. 60, p. 221–240.

Ekren, E.B., Orkild, P.P., Sargent, K.A., and Dixon, G.L., 1977, Geologic map of Tertiary rocks, Lincoln County, Nevada: U.S. Geological Survey Miscellaneous Investigations Series Map I–1041, scale 1:250,000.

Gans, P.B., 1982, Geometry of Tertiary extensional faulting, northern Egan Range, east-central Nevada: Geological Society of America Abstracts with Programs, v. 14, p. 165.

———1987, An open-system, two-layer crustal stretching model for the eastern Great Basin: Tectonics, v. 6, no. 1, p. 112.

———1990, Space-time patterns of N-S extension, N-S shortening, E-W extension, and magmatism in the Basin and Range province; evidence for active rifting: Geological Society of America Abstracts with Programs, v. 22, p. 24.

Gibbs, A.D., 1984, Structural evolution of extensional basin margins: Geological Society of London Quarterly Journal, v. 141, p. 609–620.

Hamilton, W.B., and Meyers, W.B., 1966, Cenozoic tectonics of the western United States: Reviews of Geophysics, v. 4, p. 509–549.

Haxel, G.B., Tosdal, R.M., May D.J., and Wright, J.E., 1984, Latest Cretaceous and early Tertiary orogenesis in south-central Arizona—Thrust faulting, regional metamorphism, and granite plutonism: Geological Society of America Bulletin, v. 94, p. 632–653.

Hintze, L.F., 1978, Sevier orogenic attenuation faulting in the Fish Springs and House Ranges, western Utah: Brigham Young University Geological Studies, v. 25, p. 11–24.

———1980, Geologic map of Utah: Salt Lake City, Utah Geological and Mineral Survey, scale 1:250,000.

Jansma, P.E., and Speed, R.C., 1990, Omissional faulting during Mesozoic regional contraction at Carlin Canyon, Nevada: Geological Society of America Bulletin, v. 102, p. 417–427.

Langenheim, R.L., Jr., Lamport, M.B., and Winter, J.K., 1969, Geology, stratigraphy, and structure of the West Range, Lincoln County, Nevada: Wyoming Geological Association Earth Science Bulletin, Sept. 1969, p. 27–36.

Lee, J., 1993, Rapid uplift and rotation of mylonitic rocks from beneath detachment faults: insight from K-feldspar $^{40}Ar/^{39}Ar$ thermochronology, northern Snake Range, Nevada: Geological Society of America Abstracts with Programs, v. 25, no. 6, p. A-411.

———1995, Rapid uplift and rotation of mylonitic rocks from beneath detachment faults: insight from K-feldspar $^{40}Ar/^{39}Ar$ thermochronology, northern Snake Range, Nevada: Tectonics, v. 14, p. 54–77.

Lewis, P.R., 1987, Structural geology of the northern Burnt Springs Range and Robber Roost Hills, Lincoln County, Nevada: Flagstaff, Ariz., Northern Arizona University M.S. thesis, 90 p.

Longwell, C.R., 1945, Low-angle normal faults in the Basin and Range province: American Geophysical Union Transactions, v. 26, p. 107–118.

McClay, K.R., and Ellis, P.G., 1987, Geometries of extensional fault systems developed in model experiments: Geology, v. 15, p. 341–344.

McGrew, A.J., 1993, The origin and evolution of the southern Snake Range decollement, east central Nevada: Tectonics, v. 12, p. 21–34.

McKee, E.H., Best, M.G., Barr, D.L., and Tingey, D.G., 1993, Potassium-argon ages of mafic and intermediate-composition lava flows in the Great Basin of Nevada and Utah: Isochron/West, no. 60, p. 15–18.

Merriam, C.W., 1964, Cambrian rocks of the Pioche mining district, Nevada: U.S. Geological Survey Professional Paper 469, 59 p.

Michel-Noël, G., Anderson, R.E., and Angelier, Jacques, 1990, Fault kinematics and estimates of strain partitioning of a Neogene extensional fault system in southeastern Nevada, chapter 7 *in* Wernicke, B.P., ed., Basin and Range extensional tectonics near the latitude of Las Vegas, Nevada: Geological Society of America Memoir 176, p. 155–180.

Miller, E.L., Gans, P.B., and Garing, J., 1983, The Snake Range decollement—An exhumed mid-Tertiary brittle-ductile transition: Tectonics, v. 2, p. 239–263.

Miller, E.L., Gans, P.B., Wright, J.E., and Sutter, J.F., 1988, Metamorphic history of the east-central Basin and Range province—Tectonic setting and relationship to magmatism, *in* Ernst, W.G., ed., Metamorphism and crustal evolution of the western United States (Rubey Volume 7): New York, Prentice-Hall, p. 649–682.

Nutt, C.J., and Thorman, C.H., 1992, Pre-late Eocene structures and their control of gold ore at the Drum Mine, west-central Utah, *in* Thorman, C.H., ed., Application of structural geology to mineral and energy resources of the central and western United States: U.S. Geological Survey Bulletin 2012, p. F1–F7.

Page, W.R., and Ekren, E.B., 1995, Preliminary geologic map of the Bristol Well Quadrangle, Lincoln County, Nevada: U.S. Geological Survey Open-File Report 95-580, scale 1:24,000, 26 p.

Park, C.F., Jr., Gemmil, P., and Tschanz, C.M., 1958, Geologic map and sections of the Pioche Hills, Lincoln County, Nevada: U.S. Geological Survey Map MF-136, scale 1:12,000.

Ransome, F.L., Emmons, W.H., and Garrey, G.H., 1910, Geology and ore deposits of the Bullfrog district, Nevada: U.S. Geological Survey Bulletin 407, 130 p.

Rowley, P.D., Nealey, L.D., Unruh, D.M., Snee, L.W., Mehnert, H.H., Anderson, R.E., and Grommé, C.S., 1995, Stratigraphy of Miocene ash-flow tuffs in and near the Caliente caldera complex, southeastern Nevada and southwestern Utah, chapter B *in* Scott, R.B., and Swadley, W C, eds., Geologic studies in the Basin and Range–Colorado Plateau transition in southeastern Nevada, southwestern Utah, and northwestern Arizona, 1992: U.S. Geological Survey Bulletin 2056, p. 43–88.

Rowley, P.D., and Shroba, R.R., 1991, Geologic map of the Indian Cove quadrangle, Lincoln County, Nevada: U.S. Geological Survey Geologic Quadrangle Map GQ–1701, scale 1:24,000.

Rowley, P.D., Shroba, R.R., Simonds, F.W., Burke, K.J., Axen, G.J., and Olmore, S.D., 1994, Geologic map of the Chief Mountain quadrangle, Lincoln County, Nevada: U.S. Geological Survey Geologic Quadrangle Map GQ–1731, scale 1:24,000.

Rowley, P.D., Snee, L.W., Mehnert, H.H., Anderson, R.E., Axen, G.J., Burke, K.J., Simonds, F.W., Shroba, R.R., and Olmore, S.D., 1992, Structural setting of the Chief Mining district, eastern Chief Range, Lincoln County, Nevada, chapter H *in* Thorman, C.H., ed., Application of structural geology to mineral and energy resources of the Central and Western United States: U.S. Geological Survey Bulletin 2012, p. H1–H17.

Scott, R.B., Grommé, C.S., Best, M.G., Rosenbaum, J.G., and Hudson, M.R., 1995, Stratigraphic relationships of Tertiary volcanic rocks in central Lincoln County, southeastern Nevada, chapter A *in* Scott, R.B., and Swadley, W C, eds., Geologic studies in the Basin and Range–Colorado Plateau transition in southeastern Nevada, southwestern Utah, and northwestern Arizona, 1992: U.S. Geological Survey Bulletin 2056, p. 5–42.

Sleeper, K.G., 1989, Structural geology of the Black Canyon Range, the Bluffs, and southwestern Highland Range, Lincoln County, Nevada: Flagstaff, Ariz., Northern Arizona University M.S. thesis, 113 p.

Smith, E.I., Anderson, R.E., Bohannon, R., and Axen, G.J., 1987, Miocene extension, volcanism, and sedimentation in the eastern Basin and Range province, southern Nevada, *in* Davis, G.H., and Vandenholder, E.M., eds., Geologic diversity of Arizona and its margins—Excursions to choice areas: Arizona Bureau of Geology and Mineral Technology, Geological Survey Branch, Special Paper 5, p. 383–397.

Sonder, L.J., England, P.C., Wernicke, B.P., and Christiansen, R.L., 1987, A physical model for Cenozoic extension of western North America, *in* Coward, M.P., and others, eds., Continental extensional tectonics: Geological Society of London Special Publication 28, p. 187–201.

Stewart, J. H., 1974, Correlation of uppermost Precambrian and Lower Cambrian strata from southern to east-central Nevada: U.S. Geological Survey Journal of Research, v. 2, p. 609–618.

———1978, Basin-range structure in western North America—A review, *in* Smith, R.B., and Eaton, G.P., Cenozoic tectonics and regional geophysics of the western Cordillera: Geological Society of America Memoir 152, p. 1–32.

Swadley, W C, and Rowley, P.D., 1994, Geologic map of the Pahroc Spring SE quadrangle, Lincoln County, Nevada: U.S. Geological Survey Geologic Quadrangle Map GQ–1752, 37 p., scale 1:24,000.

Taylor, W.J., 1990, Spatial and temporal relations of Cenozoic volcanism and extension in the North Pahroc and Seaman Ranges, eastern Nevada, *in* Wernicke, B.P., ed., Basin and Range extensional tectonics at the latitude of Las Vegas, Nevada: Geological Society of America Memoir 176, p. 181–194.

Taylor, W.J., and Bartley, J.M., 1992, Prevolcanic extensional Seaman breakaway fault and its geologic implications for eastern Nevada and western Utah: Geological Society of America Bulletin, v.104, p. 255–266.

Taylor, W.J., Bartley, J.M., Lux, D.R., and Axen, G.J., 1989, Timing of Tertiary extension in the Railroad Valley-Pioche transect, Nevada—Constraints from $^{40}Ar/^{39}Ar$ ages of volcanic rocks: Journal of Geophysical Research, v. 94, p. 7757–7774.

Tschanz, C.M., and Pampeyan, E.H., 1970, Geology and mineral deposits of Lincoln County, Nevada: Nevada Bureau of Mines Bulletin 73, 188 p.

Wernicke, B.P., and Axen, G.J., 1988, On the role of isostasy in the evolution of normal fault systems: Geology, v. 16, no. 9, p. 848–851.

Wernicke, B.P., Axen, G.J., and Snow, J.K., 1988, Basin and Range extensional tectonics at the latitude of Las Vegas, Nevada: Geological Society of America Bulletin, v. 100, p. 1738–1757.

Wernicke, B.P., and Burchfiel, B.C., 1982, Modes of extensional tectonics: Journal of Structural Geology, v. 4, p. 105–115.

Wernicke, B.P., Christiansen, R.L., England, P.C., and Sonder, L.J., 1987, Tectonomagmatic evolution of Cenozoic extension in the North American Cordillera, *in* Coward, M.P., and others, eds., Continental extensional tectonics: Geological Society of America Special Publication 28, p. 203–221.

Wernicke, B.P., Guth, P.L., and Axen, G.J., 1984, Tertiary extensional tectonics in the Sevier thrust belt of Southern Nevada, *in* Lintz, J., Jr., ed., Western geological excursions, Volume 4 (Guidebook for 1984 Annual Meeting of the Geological Society of America): Reno, Nev., Mackay School of Mines, p. 473–510.

Wernicke, B.P., Snow, J.K., Axen, G.J., Burchfiel, B.C., Hodges, K.V., Walker, J.D., and Guth, P.L., 1989, Extensional tectonics in the Basin and Range province between the southern Sierra Nevada and the Colorado Plateau: American Geophysical Union 28th International Geological Congress Field Trip Guide, 80 p.

Wernicke, B.P., Walker, J.D., and Beaufait, M.S., 1985, Structural discordance between Neogene detachment faults and frontal Sevier thrusts, central Mormon Mountains, southern Nevada: Tectonics, v. 4, p. 213–246.

Westgate, L.G., and Knopf, A., 1932, Geology and ore deposits of the Pioche district, Nevada: U.S. Geological Survey Professional Paper 171, 77 p.

Wheeler, H.E., 1940, Revisions in the Cambrian stratigraphy of the Pioche district, Nevada: Nevada University Bulletin, v. 34, no. 8, 40 p.

Woodward, N.B., Boyer, S.E., and Suppe, J., 1985, An outline of balanced cross-sections: University of Tennessee, Department of Geological Sciences Studies in Geology, v. 11, 2nd ed., 170 p.

☆ U.S. GOVERNMENT PRINTING OFFICE: 1997 - 573-046 / 20067 REGION NO. 8